

UNIVERSITA' DEGLI STUDI DELLA TUSCIA DI VITERBO

DIPARTIMENTO DI SCIENZE ECOLOGICHE E BIOLOGICHE

**DOTTORATO DI RICERCA IN GENETICA E BIOLOGIA CELLULARE
XXV CICLO**



**Red blood cell ageing in vivo and in vitro:
the Integrated omics perspective**

Settore scientific disciplinare: BIO/11

Candidato

Angelo D'Alessandro

Coordinatore del corso

Prof. Giorgio Prantera

Tutor

Prof. Lello Zolla

“We are only what we know, and I wished to be so much more than I was, sorely.”

David Mitchell

I would like to dedicate this thesis to my friends and colleagues. I could not ever be able to even scratch the surface of red blood cell biology without the invaluable contribution and the team work of my friends and colleagues, Barbara Blasi, Federica Gevi, Gian Maria D’Amici, Maria Giulia Egidi, Valentina Longo, Cristina Marrocco, Cristiana Mirasole, Leonardo Murgiano Valeria Pallotta, Sara Rinalducci, Anna Maria Timperio, Valerio Zolla (strictly in alphabetical order!!!). I love you, nakamas! With you I shared my hopes and my despair, my will and desires. Wish you all the best!

I would also like to dedicate this thesis to Dr. Grazzini and the Italian National Blood Centre, since they believed in me when I was but a M.Sc. graduate, full of hopes and void of the rest. They filled that void with the passion for red blood cells, and that is why I owe you so much.

I would like to dedicate this thesis to my parents. In a country where social ladders have been abated, a worker and a housewife never stopped fueling my hopes and pointing straight towards the dream of a “three years old” boy, now closer to realization than ever before. I dedicate this to their sacrifices and their silent suffering, constantly by my side.

I am grateful to destiny for allowing me to meet a handful of people that changed my life.

My friends, Marco, Giansante and Alessandro. You taught me that happiness can be found in the smallest things, as Trilussa wrote: “C’è un’ape che si posa su un bottone di rosa: lo succhia e se ne va. Tutto sommato, la felicità è una piccola cosa”

My “father in science”, Prof. Lello Zolla. I hope I repaid your bet on me. Together we traveled, we invested, we planned, we worked hard. Very hard. You guided and protected me. Looking up on you I found the example to follow. What I learned from you, paraphrasing Rabelais, could be summarized as follows: “Science sans *“passion”*, n’est que ruine de l’âme!”

Last but not least, I dedicate this thesis to the one who helped me the most, my soulmate. This is for you:

“Souls cross ages like clouds cross skies, an' tho' a cloud's shape nor hue nor size don't stay the same, it's still a cloud an' so is a soul. Who can say where the cloud's blowed from or who the soul'll be 'morrow? ... Our lives are not our own. We are bound to others, past and present, and by each crime and every kindness, we birth our future.” *David Mitchell*

Chapter 1: Introduction

Contents

-
- 1.1 Introduction to Red Blood Cell storage: the clinical/biological question about storage quality and compromised safety and efficacy of long-stored erythrocyte concentrates
 - 1.2 Introduction to the field of “Integrated Omics”: Proteomics, Metabolomics, Lipidomics and Interactomics and their application to Transfusion Medicine and Red Blood cell Biology relevant issues
-

The contents of this chapter represent a critical and updated re-elaboration of the following publications of the candidate:

1. D'Alessandro A, Liumbruno G, Grazzini G, Zolla L.
Red blood cell storage: the story so far.
Blood Transfus. 2010;8(2):82-8.
 2. Zolla L, D'Alessandro A. **Proteomic Investigations on Stored Red Blood Cells.** In *Chemistry and Biochemistry of Oxygen Therapeutics: From Transfusion to Artificial Blood*. 2010; Mozzarelli A. Editor; John Wiley and Sons Ltd The Atrium, Southern Gate Chichester, West Sussex, PO19 8SQ
 3. Liumbruno G, D'Alessandro A, Grazzini G, Zolla L.
Blood-related proteomics.
J Proteomics. 2010;73(3):483-507.
 4. D'Alessandro A, Zolla L.
Proteomics for quality-control processes in transfusion medicine.
Anal Bioanal Chem. 2010;398(1):111-24.
 5. Liumbruno G, D'Alessandro A, Grazzini G, Zolla L.
How has proteomics informed transfusion biology so far?
Crit Rev Oncol Hematol. 2010;76(3):153-72.
 6. D'Alessandro A, Zolla L.
Pharmacoproteomics: a chess game on a protein field.
Drug Discov Today. 2010;15(23-24):1015-23.
 7. D'Alessandro A, Zolla L.
The SODyssey: superoxide dismutases from biochemistry, through proteomics, to oxidative stress, aging and nutraceuticals.
Expert Rev Proteomics. 2011;8(3):405-21.
 8. Zolla L, D'Alessandro.
Shaking hands with the future through Omics application in Transfusion Medicine and Clinical Biochemistry. Preface
Blood Transfusion 2012; 10 Suppl 2:s1-3.
 9. D'Alessandro A, Gevi F, Timperio AM, Giardina B, Zolla L.
Clinical Metabolomics: the next stage of clinical biochemistry
Blood Transfusion 2012; 10 Suppl 2:s19-24.
 10. D'Alessandro A, Zolla L.
Metabolomics and cancer drug discovery: let the cells do the talking
Drug Discov Today 2012; 17(1-2):3-9.
 11. Zolla L, D'Alessandro A.
Preface to the Special Issue Integrated Omics.
J Proteomics 2012; doi: 10.1016/j.jprot.2012.10.007
-

1. Introduction to Red Blood Cell storage: the clinical/biological question about storage quality and compromised safety and efficacy of long stored erythrocyte concentrates

Overview of this section

At the dawn of the RBC biopreservation-research era, the donor and the recipient were forced to lay side by side. A sequence of fundamental achievements, from storage solutions to plastic bags and additive solutions have lead to increase the shelf-life of stored RBCs. Cold liquid storage, enabling a 42 –day storage of RBCs, was early paralleled by long-term frozen storage, which potentially allows RBCs to be stored for more than three decades. Notwithstanding this, frozen storage has not hitherto found a broad diffusion due to its elevated costs for required facilities and trained personnel.

Accumulating data over the years showed how the storage processes negatively affect the quality of RBCs, ultimately causing risks to the recipients. These risks are stressed on the critically ill patients.

Strikingly, one entire unit out of four meeting International criteria is rapidly removed from the circulation of the recipient only after 24 hours, owing to the senescent/apoptotic-like process which RBCs undergo during storage. Therefore, notwithstanding its long history, red blood cell storage is still a “work in progress”. Indeed, recent clinical retrospective non randomized trials have stressed the likely harmful potential and the reduced safety and effectiveness of long-stored red blood cells. However, conclusive data from prospective randomized studies are still missing and, although smoke could be seen on the horizons, it is still impossible to draw an unbiased conclusion on the presence of a burning fire nearby.

On the other hand, a growing body of molecular studies has been recently built which underlines the dramatic changes red blood cells undergo during prolonged storage. Although some are reversible (such as pH drop, 2,3-DPG and ATP consumption), other events such as fragmentation and aggregation occur, triggered by many factors, including oxidative damage. These changes irreversibly compromise the erythrocyte physiology and thus its functionality, survival and immunogenic/pro-inflammatory potential upon reinfusion to the recipients.

In this chapter, we summarize the recent past of the RBC biopreservation research, by focusing on a few milestones and pointing out future perspectives.

Moreover, RBC storage lesions will be briefly listed out. All these notions will contribute to depict a well-rounded portrait of the happenings at the molecular levels during RBC storage. In particular, reactive oxygen species seem to be the eligible trigger for these lesions and the main contributor to the final quality loss (both at the macroscopic and microscopic levels) of RBCs. Hereby we describe alternative storage protocols which have been proposed in order to overpass these hurdles, such as RBC anaerobic storage.

For the foreseeable future, the “quality issue” should become a top priority in the RBC biopreservation field and early attempts to prevent storage lesions appear to be a preferable option. Definitive clinical evidence is awaited to resume these whole observations under a unique question: the need for a new storage protocol. Whether this will become a priority, alternative storage strategies could represent a clue for a not-yet definitely posed question.

At the end of this thesis, upon evaluating currently allowed (either hypothermic and cryostorage) and recently proposed storage strategies (i.e. anaerobic storage), we will outline the necessity to wonder whether researchers should continue to pursue a longer storage or start focusing on a protocol to ensure a better one. In this view, we will also mention in this chapter the “antioxidant additive solution” perspective, which will be tested as well through Omics technologies within the framework of this PhD thesis project.

Keywords: red blood cell; storage lesion; blood transfusion; adverse effect; oxidative stress;

Red blood cell storage: the story so far

Red blood cells (RBCs) are still the most widely transfused blood component worldwide and their story is intimately intertwined with the history of transfusion medicine and the changes in the collection and storage of blood (Hess, 2006; Zimrin and Hess, 2009).

At present, the most widely used protocol for the storage of RBCs (for up to 42 days) is the collection of blood into anticoagulant solutions (typically citrate-dextrose-phosphate); red cell concentrates are prepared by the removal of plasma and, in some cases, also leukoreduction. The product is stored at $4 \pm 2^\circ \text{C}$ in a slightly hypertonic additive solution, generally SAGM (sodium, adenine, glucose, mannitol, 376 mOsm/L).

Despite this, a definitive protocol that reconciles long-term storage on the one hand and safety and efficacy of the transfusion therapy on the other is still the subject of intense debate and discussion. In fact, although the organisation of the blood system, through the achievement of self-sufficiency, currently enables ordinary requests of the transfusion 'market' to be met, in the case of a calamity, disaster, or emerging infections (Tinmouth and Chin-Yee, 2001; Liumbruno et al., 2008; Hess, 2009), or in particular periods of the year, local reserves can sometimes face a temporary shortage. There is still an underlying concern about the real need to store blood components for as long as possible in order to obtain a gradual increase in the interval between the donation and the transfusion, and how much this elastic time span can be prolonged without definitively compromising the quality of the product and, in the end, the recipients' health (Zimrin and Hess, 2009). Indeed, although the transfusion establishment initially pursued both objectives (product quality and prolongation of the storage period), recent retrospective studies (whose results are, therefore, weakened by all the statistical limitations of this type of analysis) (Tinmouth and Chin-Yee, 2001; Adamson, 2008; Steiner and Stowell, 2009; Zolla et al., 2009; Lelubre et al., 2009; Flegel, 2012; Grazzini and Vaglio, 2012;) have indicated the apparent irreconcilability of the two aims. These studies seem to suggest that the quality (in terms of safety and efficiency) of RBCs decreases in proportion to the time the storage period is prolonged. However, considerations about shortening the storage period have to be pondered in the light of the evident pitfalls on availability of erythrocyte concentrates (Flegel, 2012; Grazzini and Vaglio, 2012). Besides, it should be considered that although 92% of all RBC units that met release criteria actually find a recipient (Hess, 2006), the demand from organizations for longer and better storage has recently increased. Moreover, although the modern blood banking establishment keeps the pace with the current ordinary demand, it is nevertheless not tailored to meet the need for massive RBC supplies and rare blood-group units under extraordinary circumstances, such as in a calamity or a disaster (Tinmouth and Chin-Yee, 2001; Ramsey, 2008).

On the other hand, there is extremely convincing molecular evidence (Bennett-Guerrero et al., 2007; Bosman et al., 2008) which, together with the results of clinical studies (Wasser et al. 1989; Marik and Sibbald, 1993; Purdy et al., 1997; van de Edna and Bjerkeset, 1998; Zallen et al., 1999; Vamvakas et al., 1999; Vamvakas et al., 2000; Mynster and Nielsen, 2000; Mynster and Nielsen, 2001; Offner et al., 2002; Keller et al., 2002; Fernandes et al., 2001; Leal-Noval et al., 2003; Murrel et al., 2005; Hébert et al., 2005; Watering et al., 2006; Basran et al., 2006; Sakr et al., 2007; Koch et al., 2008; Yap et al., 2008; Leal-Noval et al., 2008; Weinberg et al., 2008), appears to confirm the preliminary conclusions regarding the likely poorer quality of red blood cells stored for a long time. However, the

statistical validity and methodological rigour, in terms of evidence-based medicine, of the clinical studies have recently been challenged, highlighting the need for prospective, double-blind, randomized studies, in like fashion to the one carried out by Walsh et al. (2004), which led the authors to conclude "the data did not support the hypothesis that transfusing red blood cells stored for a long time has detrimental effects on tissue oxygenation in critically ill, anaemic, euvolumaemic patients without active bleeding". The international scientific community now seems much more convinced of the need of prospective studies, since such studies, on large cohorts of subjects, are currently underway, including the Age of Blood Evaluation (ABLE) Study, the Age of Red Blood Cells in Premature Infants (ARIP) Study, Red Cell Storage and Outcomes in Cardiac Surgery Trial, the Red Cell Storage and Duration Study (RECESS) (US Public Health Service, 2008; Lacroix, 2008; Koch, 2009; Bennet-Guerrero et al., 2009; Fergusson, 2010; Assmann, 2010).

The key point of the problem is probably the lack of universally accepted standard criteria that closely reflect the dramatic molecular changes that occur during prolonged storage of RBCs and which, simply put, would enable 'good' blood to be distinguished from 'no longer sufficiently good' blood (Cluitmans et al., 2012; Sparrow, 2012).

The current standard requirements for patenting new additive solutions in the USA, and also suggested in the recommendations of the European Council, are essentially based on two parameters: the level of haemolysis (below the threshold of 0.8% at the end of the storage period, following the introduction of the "95/95" rule – Council of Europe, 2008; Hess et al., 2009) and a survival rate of the transfused cells of more than 75% at 24 hours after transfusion. This latter parameter can be assessed by measuring the half-life of RBCs labeled with ⁵¹chromium and/or ⁹⁹technetium prior to transfusion (Peters et al., 1986). These parameters are, however, fairly general and easily affected by the considerable biological variability between donors, given that it is known that blood from some donors resists storage better than that from other donors (Moroff et al., 1984).

Haemolysis is an easier parameter to monitor. Typically, between 0.2 and 0.4% of RBCs stored in the presence of standard additive solutions are haemolysed after 5-6 weeks of storage, while prestorage leukoreduction halves the incidence of this phenomenon (Hess, 2002). These widely accepted and well established parameters do not, however, reflect the profound molecular changes that affect RBCs during their storage.

A brief list of the elements of the so-called "red blood cell storage lesion" includes (Bennet-Guerrero et al., 2007; D'Alessandro et al., 2010; Zolla and D'Alessandro, 2010):

- (i) morphological changes,
- (ii) slowed metabolism with a decrease in the concentration of adenosine triphosphate (ATP),
- (iii) acidosis,
- (iv) decrease in the concentration of 2,3-diphosphoglycerate (2,3-DPG),
- (v) loss of function (usually transient) of cation pumps and consequent loss of intracellular potassium and accumulation of sodium within the cytoplasm,
- (vi) oxidative damage with changes to the structure of band 3 (Karon et al., 2009)
- (vii) and lipid peroxidation,
- (viii) apoptotic changes with racemisation of membrane phospholipids and loss of parts of the membrane through vesiculation (Bosman et al., 2008).

Some of these changes occur within the first few hours of storage, for example, the decrease in pH or the increases in potassium and lactate; others, however, take days or weeks (Bennet-Guerrero et al., 2007). Together, these events risk compromising the safety and efficacy of long-stored RBCs, reducing their capacity to carry and release oxygen, promoting the release of potentially toxic intermediates (for example, free haemoglobin can act as a source of reactive oxygen species) and negatively influencing physiological rheology (through the increased capacity of the RBCs to adhere to the endothelium (Annis et al., 2005; Koshkaryev et al., 2009) or through their enhanced thrombogenic (Sweeney et al., 2009) or pro-inflammatory (McFaul et al., 2009) potential).

These observations at a molecular level were supported by the results of a series of clinical studies (albeit retrospective and not randomised). These studies appeared to show a relationship between the duration of storage and a proportional increase in adverse events in the transfused patients, although the data available are preliminary and the statistically more reliable studies that conform more closely with the gold standard criteria represented by evidence-based medicine are considered necessary by many (Hess, 2009) and are, indeed, underway (reviewed in Grazzini and Vaglio, 2012).

Clinical evidence of adverse effects following the transfusion of RBCs stored for prolonged periods

Numerous clinical studies have been carried out throughout the world to identify a possible relationship between the duration of storage of RBCs, the changes observed at a molecular level and side effects in the transfused patients, in order to determine whether and, if so, to what extent RBCs stored for a long time lose safety and efficacy (Bennett-Guerrero et al., 2007; Bosman et al., 2008) which, together with the results of clinical studies (Wasser et al. 1989; Marik and Sibbald, 1993; Purdy et al., 1997; van de Edna and Bjerkeset, 1998; Zallen et al., 1999; Vamvakas et al., 1999; Vamvakas et al., 2000; Mynster and Nielsen, 2000; Mynster and Nielsen, 2001; Offner et al., 2002; Keller et al., 2002; Fernandes et al., 2001; Leal-Noval et al., 2003; Murrell et al., 2005; Hébert et al., 2005; Watering et al., 2006; Basran et al., 2006; Sakr et al., 2007; Koch et al., 2008; Yap et al., 2008; Leal-Noval et al., 2008; Weinberg et al., 2008). In 2009, Zimrin and Hess and Lelubre et al. conducted meticulous elaborations of the data from the studies published so far. Despite the intrinsic statistical limitations of retrospective, non-randomised studies, the results of such studies are undeniably useful if they are considered as a warning bell, albeit debatable, but not to be ignored, of a potential increase in the negative effects of the transfusion of RBCs in proportion to the duration of storage of the blood product in certain groups of patients such as those in intensive care (Marik et al., 1993; Purdy et al., 1997; Fernandes et al., 2001; Hébert et al., 2005; Taylor et al., 2006; Sakr et al., 2007), those undergoing cardiac Interventions (Wasser et al., 1989; Vamvakas and Carven, 1999; Vamvakas and Carven, 2000; Leal-Noval et al. 2003; van de Watering et al., 2006; Basran et al., 2006; Koch et al., 2008; Yap et al., 2008), those submitted to colorectal surgery (Edna and Bjerkeset, 1998; Mynster and Nielse, 2000; Mynster and Nielse, 2001), or traumatized patients (Zallen et al., 1999; Offner et al., 2002; Keller et al., 2002; Murrell et al., 2005; Leal-Noval et al., 2008; Weinberg et al., 2008).

The side effects described in these groups of patients following multiple transfusions of 'old' red cells are very varied, ranging from a decrease in gastric pH (Marik et al., 1993) to an increase in mortality rate (Purdy et al., 1997), from multiorgan failure (Zallen et al., 1999) to an increased incidence of pneumonia in patients transfused following aorto-coronary artery bypass (Vamvakas and Carven 2000 and 2001; van de Watering et al., 2006), from an increased susceptibility to infections (Offner et al., 2002) to major complications following heart surgery (Hébert et al., 2005; Basran et al., 2006; Koch et al., 2008), and from an increase in the duration of hospital admissions (Keller et al., 2002; Murrell et al., 2005) to the development of complications such as transfusion-related acute lung injury (TRALI) (Silliman et al., 2005; Gajic et al., 2007).

It is, however, worth stating that given the current lack of irrefutable statistical proof, it cannot yet be concluded "there's no smoke without fire", to mention Steiner and Stowell (2009). In fact, it is worthwhile to mention that a few years ago a series of retrospective, non-randomised clinical studies suggested a correlation between reduced efficacy of transfusions and lack of leukoreduction; the subsequent prospective, randomised studies did not, however, fully confirm these observations (Vamvakas and Blacjchman, 2001 and 2007).

The storage of RBCs, however, until 2009 had not been the focus of prospective, randomised studies similar to those needed to market a new drug (Spiess, 2007). For this reason, although it has now been ascertained and widely accepted that something more or less irreparable occurs during prolonged storage of RBCs, it is currently impossible to conclude objectively and without preconceptions that these changes are accompanied by decreased efficacy and safety of the blood component.

Current research suggests that the RBC hypothermic storage lesions significantly influence the efficacy of transfusion since they are related to a worsened prognosis, increased oxygen affinity ultimately resulting in a reduced oxygen delivery capacity in tissues, proinflammatory and immunomodulatory effects, increased infections, multiple organ system failure, and ultimately, increased morbidity and mortality (Scott and Lecay, 2005). Indeed, while it is long known that storage has a negative effect on RBC oxygen delivery capacity (Valtis and Kennedy, 1954) there is a growing awareness around the potential hazards of allogenic RBC infusion, which may actually harm some recipients (Munoz et al., 2004; Rao et al., 2004; Rawn, 2008). On the oxygen delivery issue, a particularly telling experiment has been performed by Tsai and coworkers, who showed that when 25 percent of the circulating RBCs were replaced by RBCs stored for 28 days, microvascular flow was reduced by 63% and oxygen partial pressure in tissues was 3.5 mmHg against 14.4 mmHg when the RBCs were fresh (Tsai et al., 2004). Notably, systematic reviews of multiple randomized trials invited to reconsider and minimise the routine use of blood transfusion to maintain arbitrary hematocrit levels in stable patients with ischemic heart disease (Rao et al., 2004; Charles et al., 2006). The risk of serious complications dramatically rises when dealing with patients who are undergoing cardiac surgery (Koch et al., 2008).

Recent evidence supports an inflammatory mechanism in the development of atrial fibrillation which involves c-reactive protein inflammatory mediation (Anderson et al., 2004; Lo et al., 2005; Aviles et al., 2003). RBC transfusion modulates the inflammatory response to cardiac surgery by changing plasma concentrations of inflammatory mediators and augmenting the inflammatory response (Fransen et al., 1999).

One of the eligible criteria for a blood unit to be transfused is that RBC survival rate after re-infusion should be over the 75% threshold. This means that, at the end of the 42-day shelf life, a good-quality transfused RBC unit will contain up to 25% non-functional RBCs, whose removal by RES might be a basis for at least a transient immune depression (Kendall et al., 2000). It is striking that a patient receiving 4 full-term stored RBC units will benefit only of 3 of them while, statistically, an entire blood unit will end up to participate to the total reinfused volume though only providing inexorably and irreversibly damaged RBCs. Moreover, it is a fact that 70% of the re-infused RBCs are rapidly removed from circulation in the recipient after 3 days from the treatment, which definitely represents an alarming datum (Bratosin et al., 2002).

Contaminating WBCs and their by products present in the storage medium may affect and induce changes in RBCs, directly by consuming glucose needed by the RBC or indirectly by releasing bioreactive substances in the storage medium, which could endanger RBC integrity and functionality (Blajchman, 2006). Thus, besides clinical complication deriving from alterations on RBCs, many other clinical complications are related to bioreactive substances released by leukocytes in the storage medium of non-leukoreduced units, such as histamine, lipids, and cytokines, which may exert direct effects on the recipients. Cytokines known to increase during storage of RBC or platelets include interleukin (IL) 1 beta, tumor necrosis factor alpha (TNF α) and IL8. Both TNF α and IL8 are derived from WBCs and can potentially activate neutrophils. Several of the cytokines generated during storage including TNF α , IL1b, and IL8 have potent pyrogenic activity, can recruit neutrophils from the bone marrow and cause further release of cytokines 4. The effect of cytokines may account for some febrile transfusion reactions (Dwyre and Holland, 2008).

An increase in haemolysis and potassium leakage resulting from altered membrane permeability during storage has been also attributed to leukocyte enzymes such as elastase, collagenase and cathepsin G and/or activated neutrophils liberating toxic O₂ species (Kriebardis et al., 2007). Enzymes and eicosanoids released by degenerating leukocytes and platelets may be damaging to stored erythrocytes (Bell et al., 2000). Greenwalt et al. (1991) found that leukodepleted units of RBCs were significantly better preserved after 56 days of storage with a remarkable reduction of potassium, haemolysis and total vesicle membrane-protein shed and higher morphology scores in comparison to non-leukodepleted RBCs in the supernatant. Leukoreduction tends to reduce storage haemolysis by about 50% (Hess et al., 2002). In one situation where RBC recovery was compared directly between leukoreduced and non leukoreduced RBC stored in the same system, leukoreduction increased RBC recovery by 4% and reduced haemolysis from about 0.40% to 0.25% at 6 weeks (AuBuchon et al., 2006).

For these reasons, as previously mentioned, the removal of WBCs from RBC concentrates is now universally practiced in several European countries and Canada, and is widely used in the USA.

Until recently the clinical milieu and the academic setting have walked together through the trodden path of cold and frozen RBC storage, while few approaches have contemporary addressed the “quality deal”. It has been hitherto unclear whether what we could now do in terms of prolonged storage should be definitely done. In this chapter, we will try to shed light on this debated issue as well, by referring to the molecular changes at the membrane and metabolic level which RBCs undergo over storage duration (which will be further addressed through Omics

technologies in the present PhD thesis project. In order to better understand storage-associated changes to RBCs, it is worthwhile to describe the role and biochemistry of RBCs *in vivo*, a topic that will be indeed further addressed through Omics technologies inside this PhD thesis.

RBC ageing and metabolism *in vivo*

RBCs play a pivotal role in gas transport (i.e. oxygen and carbon dioxide) and a minor, but not less important, role in a range of other functions, such as transfer of GPI-linked proteins (Shichishima et al., 1993; Kooyman et al., 1995; Civenni et al., 1998) and transport of iC3b/C3b-carrying immune complexes (Schifferli et al., 1989).

In humans, the circulating mature RBC is the end stage of a developmental process which starts in the bone marrow, as hematopoietic stem cells differentiate to enucleated reticulocytes (Palis, 2008). After extrusion of nuclei and degradation of internal organelles and endoplasmic reticulum, reticulocytes emerge in the circulation, where they rapidly develop into mature RBCs (Koury et al., 2002; Pasini et al., 2006). Until the end of its life span of 120 ± 4 days, with 120 miles of travel and $1.7 \cdot 10^5$ circulatory cycles, the human RBC has successfully coped with a number of dangers, such as passages across narrow capillaries and splenic slits, periodic high turbulences and high shear stresses, along with extremely hypertonic conditions. Owing to its constant cytoskeleton rearrangement, RBCs are able to traverse passage ways as narrow as $1 \mu\text{m}$ in diameter, by changing their shape from a biconcave disc of $8 \mu\text{m}$ diameter to a cigar shape (Goodman et al., 2007). During the last decades, a plethora of studies sought to fathom the depths of the two dimensional meshwork of proteins called the spectrin membrane skeleton (Bennet, 1990; Bennet and Lambert, 1991; Lux, 1979; Marchesi, 1983; Agre, 1992; Agre and Cartron, 1991). These proteins lie on the cytoplasmic surface of the plasma membrane and give the RBC its properties of deformability (i.e. elasticity and flexibility) which represent the foundation of their successful journey. Spectrin, ankyrin, actin, band 4.1 and anion exchanger band 3 are the major protein actors of RBC deformability. The lack of internal organelles and nuclei intuitively eases protein complexity of RBCs (Goodman et al., 2007), making them an eligible target for early biochemical studies and for proteomic investigations, the latter recently gaining momentum (reviewed in D'Alessandro et al., 2010 and detailed in the next Chapter 2 of the Introduction).

Circulating RBCs undergo metabolic and physical changes associated with the process of senescence, viz membrane vesiculation, decrease in cell size, increase of cell density, alteration of cytoskeleton, enzymatic desilylation, and phosphatidylserine (PS) exposure just to mention few (Tannert et al., 1977; Clark and Shohet, 1985; Shinozuka, 1994). At the end of their life span, senescent RBCs are recognized and removed by the resident macrophages in the reticuloendothelial system (RES), mainly by Kupffer cells in the liver. It has been estimated that 5 million RBCs per second each day are endocytosed by RES macrophages (Bratosin et al., 1998).

More than one cause participates to the senescent/ageing process. Membrane and cytosolic proteins of RBCs are continuously stressed by oxygen radical attacks, which cause aminoacid modifications. Morphology, function and metabolism of RBCs suffer from continuous alterations matching with the cell winding its way through the circulatory system. Basically due to the lack of protein synthesis and inability to regenerate effete protein molecules, most notably enzymes, a multitude of alterations accumulate as the end of the RBC life span approaches. Neoantigens form from membrane proteins, especially through clustering of anion exchanger band 3 (Kay, 1993)

and haemoglobin (Hb) denaturation (Low et al., 1989). Both proteins are closely-related to gas transport (Hamasaki et al., 1996; De Rosa et al., 2007), cell homeostasis and shape (Jay, 1996), or to glycolytic metabolism (Low et al., 1993). Thus, physiologically fundamental proteins fail to fulfil their biological goal. Furthermore, these senescent antigens that appear on oxidatively-damaged old cells, radically accelerate RBC removal from blood flux through the activation of life-span immunoregulation mechanisms, via triggering macrophage erythrophagocytosis, complement deposition and Immunoglobulin G (Ig G) binding (Bosman and Kay, 1988; Turrini et al., 1991; Kay, 2005). Antibody binding induces major alterations in membrane organization as well as vesicle formation (Head et al., 2004; Head et al., 2005). Kupffer cells also remove RBC vesicles, with a major role for exposure of PS (Bosman et al., 2005). Taken together, all this data suggest more than a superficial resemblance between RBC ageing and apoptosis (Bosman et al., 2005). Particularly telling is the term “eryptosis”, coined by Lang’s group to identify that special form of apoptosis typical for the anucleated RBCs (Lang et al., 2008). Eryptosis is characterized by PS exposure, cellular shrinkage, membrane blebbing, ceramide formation, opening of cation channels, increase of intracellular Ca^{2+} activity, and activation of intracellular proteases such as μ -calpain, in the absence of hemolysis but ensuing into phagocytic recognition of exposed PS by a scavenger receptor on the macrophage (Lang et al., 2008). This mechanism is possibly a parallel pathway leading to RBC removal without passing through the Ig G mediation (Bosman and Kay, 1988; Turrini et al., 1991; Kay, 2005).

To counteract oxidative damages, the anucleated RBC, which is unable to synthesize new proteins, is equipped with protective enzymes fully adequate to sustain even excessive oxidative stress for limited time periods (D’Alessandro and Zolla, 2011). Indeed, it is not a coincidence that Goodman and Colleagues (2007), in their thorough review article mapping the RBC interactome, could point out a central core of proteins. They named it the Repair and Destroy Box after the activity of its protein constituents, which are involved in nascent protein folding or re-folding of denatured proteins (e.g. chaperonines, heat shock proteins, anti-oxidant proteins such as peroxiredoxins, catalases, glutathione peroxidases, superoxide dismutases).

Together with membrane and cytoskeleton alterations, senescence also provokes metabolic anomalies in RBCs. Similarly, the energy-less RBC is inevitably lost (van Wijk and van Solinge, 2005). Because of the lack of nuclei and mitochondria, mature RBCs are incapable of generating energy via the (oxidative) Krebs cycle. Nonetheless, there are 4 RBC metabolic pathways (**Figure 1**): the Embden-Meyerhof pathway (glycolysis), in which most of the RBC adenosine triphosphate (ATP) is generated through the anaerobic breakdown of glucose; the hexose monophosphate shunt (HMS), which produces NADPH to protect RBCs from oxidative injury; the Rapoport-Lubering shunt, responsible for the production of 2,3-diphosphoglycerate (DPG) for the control of Hb oxygen affinity; and finally, the methemoglobin (met-Hb) reduction pathway, which reduces ferric heme iron to the ferrous form to prevent Hb denaturation (Wiback and Palson, 2002; Schmaier et al., 2003). Glucose, the only fuel utilized by mature RBCs, is primarily metabolized via anaerobic glycolysis. Following facilitated diffusion, glucose is immediately converted to glucose-6 phosphate. Glucose can be transformed to lactate via glycolysis, or to ribulose-5-phosphate via the oxidative section of HMS. Ribulose-5-phosphate can re-enter glycolysis via the nonoxidative section of HMS. Under normal steady-state conditions, 92% of glucose is metabolized along glycolysis and 8% along HMS. Under oxidant conditions up to 90% of glucose can be metabolized along HMS. Net output of

glycolysis is 2 moles of ATP per mole of glucose metabolized. The main glycolytic pathway has two branching points: in the first one, the product of hexokinase, glucose-6-phosphate can be diverted to the HMS by glucose-6-phosphate dehydrogenase (G6PD). In the second branching point, 1,3-DPG can be diverted by DPG-mutase to produce 2,3-DPG.

Maintenance of the RBC membrane system and Hb function is dependent on energy generation through RBC metabolic pathways.

Five metabolic intermediates are particularly important in RBCs: ATP, DPG, NADH, NADPH and glutathione (GSH).

- ATP, the primary energy intermediate is essential to maintain electrolyte balance by powering sodium-potassium cationic pumps, which are necessary to preserve the cytoplasmic ionic milieu thus preventing colloidal osmotic lysis and, ultimately, conserving RBC shape and flexibility (Card, 1988); RBCs have an intrinsic program of cell death that is held in check by normal concentrations of RBC ATP. Normal ATP concentrations are necessary to prevent calcium-induced membrane loss by microvesiculation and for active transport of negatively charged phospholipids, specifically PS, from the outer to the inner leaflet of the RBC membrane to prevent RBC clearance from the circulation by macrophages (Kamp et al., 2001). ATP is an essential resource for other focal physiological activities: the synthesis of GSH and other metabolites; purine and pyrimidine metabolism; the maintenance of Hb iron in its functional, reduced, ferrous state; the protection of metabolic enzymes, such as Hb and membrane proteins, from oxidative denaturation; and the preservation of membrane phospholipid asymmetry (van Wijk et al., 2005).

- DPG, in association with pH and $\text{HCO}_3^-/\text{CO}_2$ modulates position and shape of the oxygen dissociation curve (Rouault, 1973; Salhany et al., 1973; meldon et al., 1983). When arterial blood arrives in peripheral capillaries, RBCs pass through the narrow capillaries one by one, CO_2 is rapidly hydrated to H_2CO_3 inside RBCs by carbonic anhydrase, and the H_2CO_3 promptly dissociates into H^+ and HCO_3^- . Band 3 protein, the major integral membrane protein of RBCs, exchanges the cellular HCO_3^- with Cl^- in plasma, a process that is conventionally known as the 'chloride shift'. As the result of the anion exchange, the weak acid H_2CO_3 is converted to the strong acid HCl, and consequently the intracellular pH of RBCs is rendered acidic. This acidification is the trigger for the dissociation of O_2 from oxyhemoglobin (HbO_2), and the dissociated O_2 is supplied to tissues that metabolically produce CO_2 . Protons formed in RBCs are accepted by the groups of deoxyhemoglobin (HbH^+) participating in the 'Bohr Effect', and the pH within the RBCs is restored in order to prevent further dissociation of oxygen from HbO_2 . By means of the transient acidification triggered by the anion exchange activity, tissues producing more CO_2 are supplied with more O_2 from HbO_2 (Hamasaki and Okubo, 1996). The rapid disappearance of 2,3-DPG from preserved blood has not been of high concern because RBCs regain the ability to synthesize 2,3-DPG after transfusion. However, the restoration of 2,3-DPG in vivo requires up to 48 hours, and this period of altered oxygen affinity may be significant in certain clinical conditions (Valeri et al., 1971). Preserving RBC 2,3-DPG levels is therefore an essential element in maintaining the ex vivo quality of hypothermically stored RBCs. Inorganic phosphate is also added to the storage medium to act both as a buffer to the continuously decreasing pH and as a substrate for the synthesis of 2,3-DPG.

- The ferrous iron of Hb is exposed continuously to high concentrations of oxygen and, thereby, is oxidized slowly to met-Hb, a protein unable to carry oxygen. To restore Hb function, met-Hb (methemoglobin also known as

ferrihemoglobin) must be reduced to Hb (ferrohemoglobin) (Salhany et al., 1973). Under physiological conditions, met-Hb reduction is accomplished mainly by red cell NADH-dependent cytochrome b5 reductase (NADH-methemoglobin reductase) so efficiently that there are insignificant amounts of methemoglobin in the circulating blood (Abe et al., 1979; Borgese et al., 1993; Mansouri et al., 1993).

- Under oxidative stress, Hb could be oxidized to met-Hb (as it regards its heme iron) and to hemichromes, a variant of Hb in which cystein thiol groups have been dangerously oxidized to form denatured Hb-aggregates precipitating in inclusion bodies within RBCs, also known as “Heinz bodies”. GSH is the main protector of thiol groups, scavenger of oxides, peroxides, oxidant radicals and detoxicant of foreign compounds. Glutathione cycling from oxidized glutathione (GSSG) to the reduced form (GSH) is dependent upon NADPH generation, during the first two reactions of HMS, by via G6PD and 6-phosphogluconate dehydrogenase (6-PGD). NADPH is the substrate for GSH-reductase to regenerate glutathion after oxidant insults and protect catalase from inactivation (Untucht-Grau et al., 1981).

Oxidized glutathione (GSSG) + 2 NADPH + H⁺ → 2 GSH + 2 NADP⁺

- In concomitance with GSH-reductase, glutathione-S-Transferase, peroxidases (namely peroxiredoxins and glutathione peroxidases) and superoxide dismutase, catalase is believed to be very important in cellular antioxidant defence and therefore prolongs RBC life-span in mammals (Kurata et al., 1993). NADPH is also a protector of peroxiredoxin and catalase efficiency and an insufficient concentration of NADPH causes an impairment of the catalase-dependent detoxication route (Winterbourn, 1990).

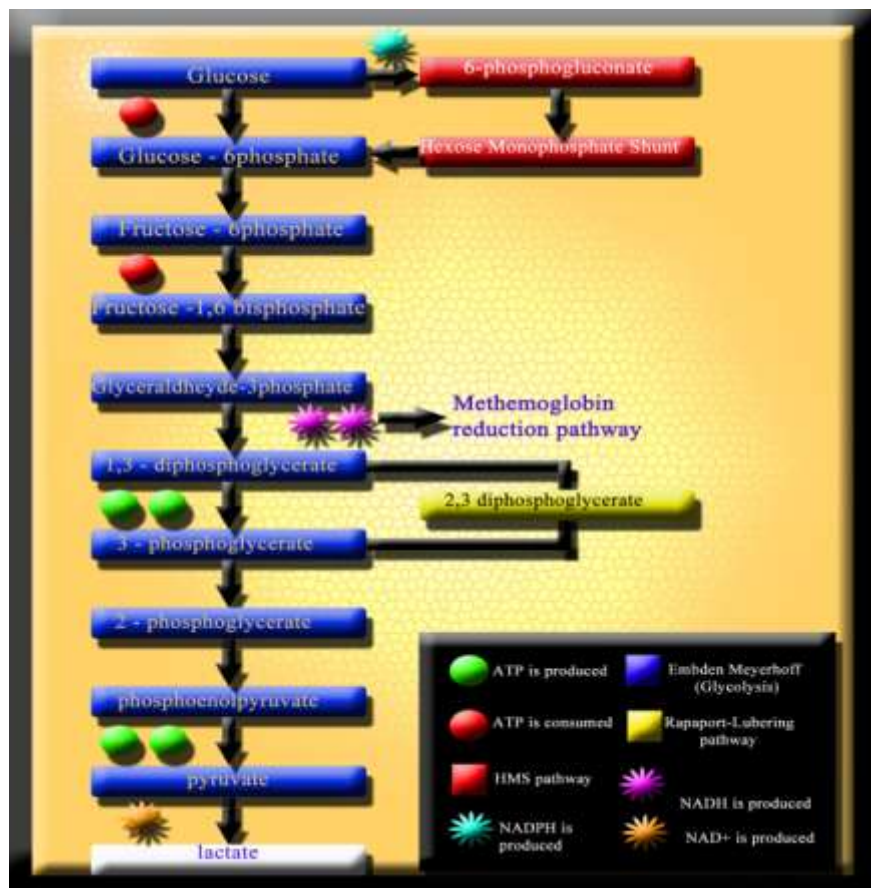


FIGURE 1 RBC metabolism mainly gravitates towards four main pathways: the Embden-Meyerhoff glycolytic pathway (for ATP production), the methemoglobin reduction pathway, the Rapaport-Luberling pathway for 1,3-DPG conversion to 2,3-DPG and the Hexose Monophosphate Shunt (HMS) pathway (for NADPH generation). Whether NADH is not fully oxidized back to NAD⁺ through the methemoglobin reduction pathway, lactate is produced from pyruvate as a byproduct of anaerobic glycolysis.

Current storage protocols

Erythrocyte biopreservation (Bp) is the ability to preserve the integrity of RBCs outside the native environment for extended periods. Its main end is to provide viable and functional RBCs for patients requiring a blood transfusion. The data provided in this section should contribute to help the readers glean insight of RBC physiology, which is essential to assess the effectiveness of a Bp approach, as well as the in vitro and in vivo quality of transfused RBCs. While at the dawn of the transfusion era donors and recipients were forced to lay side by side, owing to the practice of Bp in transfusion medicine they could be today separated in space and time (Hess, 2006). The development of effective RBC Bp-techniques that maintain ex vivo RBC viability and function has been experimented since the beginning of the 20th century (Rous and Turner, 1916) and paved the way for modern blood banking. Present approaches in RBC Bp will be described in this section, while their shortcomings and contraindications will be dealt with in the next one.

Current European and American guidelines for transfusable-RBC acceptability criteria (Council of Europe, 2008) primarily focus on the volume of blood collected and the proportion of viable RBCs present at the time of transfusion. These standards specify 450-mL collections and a mean 24-hour in vivo survival of at least 75% of the re-infused RBCs. In vivo survival of RBCs after reinfusion has been investigated since 1947, when radiolabeling experiments on erythrocytes were carried out for this purpose (Ross et al., 1947). However, it was only in 1985 that ⁵¹Chromium was introduced as a standard protocol for the follow-up of transfused RBCs (Ebaugh et al., 1985). Other criteria include a threshold limit to the measured haemolysis value, which indicates the amount of free Hb, commonly not exceeding 1.0 percent of the RBC mass (Hogman and Meryman, 2006). Leukoreduction of white blood cells (WBCs) by centrifugation or filtration has become quite a routine practice in transfusion medicine almost worldwide [87-88]. In a comparative study between leukoreduced and non-leukoreduced RBC units, leukoreduction increased RBC recovery by 4% and reduced haemolysis from about 0.40% to 0.25% at 6 weeks (Heaton et al., 1994).

Leukodepleted RBCs should not contain more than 1×10^6 WBCs per unit. A unit of RBCs should contain at least 45 g of RBC Hb and at least 40 g when leukoreduced. The European recommendations state that no more than 13% of a donor's blood volume should be collected at one session.

Liquid storage of RBCs, usually referred to as cold or hypothermic storage, should be performed at approximately 4°C, a temperature definitely lower than the normal physiological temperature but higher than the freezing point of the storage solution (Council of Europe, 2008). Hypothermic preservation of RBCs is based on the principle that biochemical events and molecular reactions can be suppressed by a reduction in temperature (thermodynamically speaking, low temperature parallels a diminution of the free energy function). It has been estimated that storage temperatures ranging between 1 and 6°C minimize RBC degradation through an intense reduction of RBC metabolism, in the order of about 40 times (Hogman, 1998). Moreover, most bacterial organisms do not survive in the cold storage conditions, though a few such as *Serratia marcescens*, *Yersinia enterocolitica*, and *Aeromonas* species can grow at refrigerator temperatures (Brecher, 2005). Whereas they tend to grow slowly in cold blood, dividing about once a day, in approximately 27 days a single organism grows exponentially to generate up to 108 organisms, an overwhelming army at the cellular-scale which could be responsible of acute infections or endotoxic

shock. Many attempts have been performed to sterilely preserve RBCs, including heat sterilization, and plastic bags (Artz et al., 1954). The latter were seen as advantageous for military logistics because of their lighter weight and resistance to breakage. The ability to manufacture connected sets of bags enabled the design of a sterilized closed-collection system that decreased the rate of bacterial contamination from experimental surfaces. By the time they became approved commercial products in the 1960s, their vein-to-bag unitary construction, their ability to exclude air bubbles reducing the chance of air embolism during pressure infusion, small volume in refrigerator storage and optical clarity were all recognized as distinct advantages. In the field of plastic bags, the main improvement was the introduction of diethylhexyl phthalate (DEHP), the plasticizer used with polyvinyl chloride (PVC). DEHP plastic bags have been proven to reduce haemolysis by four fold at each weekly measurement (Hill et al., 2001), although the molecular mechanisms are yet to be uncovered.

Notably, the subsequent history of RBC storage has been characterized by slowly-progressing distinct cycles, each one needing roughly a decade to become well-rounded and finally encounter a widespread diffusion. Storage solutions and plastic bags are just two of the earlier but still most relevant steps (Hess, 2006).

Concerning the former, acid citrate dextrose (ACD) heat sterilizable solutions were introduced in the 1940s and enabled 3 weeks storage of RBCs (Loutit and Mollison, 1943). Citrate phosphate dextrose (CPD) solution, with 16 mM/l phosphate, increased the fraction of RBC recovered after 3 weeks of storage from $\approx 75\%$ with ACD to $> 79\%$, in the 1950s (Orlina and Josephson, 1969). In the first 2 weeks of storage, the 2,3-DPG is demolished to furnish the phosphate indispensable for the synthesis of ATP energetic tokens (Gibson et al., 1957; Hess et al., 2002). However, when all the 2,3-DPG is consumed, RBCs have no physiological way to contrast the energetic debacle. CPD solution was observed to replenish the phosphate supplies of stored RBCs.

In 1968 citrate phosphate dextrose adenine (CPDA-1) solution was developed and shown to permit a whole-blood extended storage for 5 weeks (Shields, 1969). CPDA solutions slowed adenine and adenosine lost due to deamination reactions while they improved osmotic fragility and recovery of RBCs (Simon et al., 1962). The main concern was about the safety of adenine, which was thought to lead to the formation of uric acid stones. That was the reason why CPDA solution licensure in the USA was delayed until 11 years later (Hess, 2006). Whole blood storage for 5 weeks yielded an average survival rate at 24h of $\approx 81\%$, while packed RBCs have a slight lower recovery percentage (72%) (Zuck et al., 1977). It was concluded that the tighter the stored cells were packed, the more rapidly they ran out of glucose. However the addition of glucose dangerously raised the hematocrit and hampered a readily suitability of the unit for the administration to the recipient. Therefore, additive solutions (ASs) were engineered in order to provide additional volume and nutrients for longer storage and better flow of packed RBCs (Moore et al., 1980).

The first AS, saline, adenine and glucose (SAG) dramatically ameliorated and overpassed the high hematocrit and viscosity hurdles (Hogman et al., 1978). SAG with the addition of mannitol (SAGM), chronologically the second AS, is now the standard AS used in Europe and in the USA, where two modestly differing variants are available (AS-1 and AS-5) (Hess, 2006). Mannitol works as a free radical scavenger, but also as a membrane stabilizer. In this respect, there is a significant likelihood that mannitol hampers haemolysis by preventing the osmotic swelling of RBCs that might otherwise increase their volume beyond their critical hemolytic volume (Beutler et al., 1988).

The third AS is AS-3. It is exclusively used in Canada, though being licensed in the USA. Again, it is based on SAG but also contains citrate and phosphate and a higher dose of dextrose. The citrate appears to serve the same membrane-protective and osmotic pressure-balancing function that mannitol serves in SAGM (Jarvis et al., 2003). AS-3 allows 6 weeks of storage and is associated with 78–84% recovery and 0.4% haemolysis.

Other ASs are adopted in some other countries (e.g. Circle Pack in Australia (Lovric, 1986) and MAP in Japan (Tanemoto et al., 1994)) and depend on a higher dextrose version of the primary and aforementioned CPD anticoagulant, thus they are called CP2D. Despite this, none of these ASs appears to markedly ameliorate the overall statistics regarding RBCs after storage when compared to the others (Hess, 2006).

All currently licensed ASs support the minimal 75%, 24-hour in vitro survival and 0.8% hemolysis standard criteria set by the American Association of Blood Banks and Council of Europe for up to 42 days of hypothermic storage at 1 to 6 °C (Hess et al., 2011). Notwithstanding this, current storage criteria are too general to depict a fully-detailed portrait of RBCs upon storage.

The pH conditions, which are also strongly associated with the RBC storage lesion, are affected by the volume and osmolality of the storage solution, as well as by the gas permeability of the storage container. Moreover, glycolysis slows as pH falls. As pH decreases and metabolism slows, RBC ATP concentrations reach a maximum higher and later than usual, resulting in a prolonged conservation of ATP levels exceeding the critical values that are necessary to suppress microvesiculation and PS exposure. The acidic pH of current ASs maintains ATP levels, but is detrimental to 2,3-DPG levels, which fall below 10% of the initial value by 3 weeks of storage (Valeri et al., 1971). Bicarbonate buffering is effective for the maintenance of acidic pH and ATP levels by driving the diffusion of carbon dioxide from PVC bags (Hogman, 1998). Some authors determined the effects on storage quality of ASs pH and volume, as well as of phosphate, sodium chloride and mannitol concentrations (Hess et al., 2001; Hess et al., 2003). The most complicated task is to find a delicate balance of the pH, which should not be too high in order to contrast 2,3-DPG generation with a consequent ATP depletion and, conversely, not too low, in order to prevent glycolysis to completely stop and hamper new ATP generation. ASs have an important part in this piece and ultimately contribute to the pH fine tuning.

For example, collecting whole blood into acidic CPD normally reduces its pH from ≈ 7.35 to ≈ 7.1 (Hess et al., 2002). Adding an acidic AS further reduces the pH to ≈ 7.0 . However, if the pH of the AS is raised to 8.5 by adding disodium phosphate, then the resulting pH of the RBC suspending fluid can be raised to ≥ 7.2 at the beginning of storage. A pH of 7.2 at the beginning of storage means that the ATP production will suffice for several weeks (Hess, 2006). On the contrary, if the pH is raised above 7.2, then DPG is produced and consumes all of the intracellular phosphate, leading to a decrease in the ATP content that limits storage time and RBC quality.

Hogman and Meryman (Hogman and Meryman, 1999) proposed several practical procedures to extend the maintenance of RBC 2,3-DPG levels during hypothermic storage, including elevating the pH of ASs, increasing the volume of the additives, using hypotonic additives, and cooling the RBCs to room temperature after collection. Accordingly, several recent publications describe high pH storage solutions that preserve DPG content for many weeks (Hogman et al., 2002; Kurup et al., 2003; Murrell et al., 2005). Normally, the storage life of RBC is determined by the length of time it takes the cells to produce enough lactic acid and protons to reduce the pH to 6.5,

with a consequent low ATP production which no longer supports cell viability. This time is largely determined by the rate of production of protons and the buffer capacity of the suspension. Clearly, this buffer capacity can be increased by adding sodium bicarbonate to the additive solution. In solution, bicarbonate combines with a proton to produce carbonic acid, which is converted to CO₂ and water by RBC carbonic anhydrase. The CO₂ then diffuses out through the plastic bag, effectively removing protons from the solution and slowing the rate of pH fall (Murrell et al., 2005). The combination of using alkaline additive solutions and bicarbonate buffering can effectively double the metabolic capacity of the storage system and allow RBC to be stored for longer and under better conditions (Hess et al., 2005).

ASs prospect a new deal in RBC storage and will hopefully integrate actual cold liquid storage protocols. Indeed, although hypothermic liquid storage drastically fades RBC metabolism, ageing and senescence seem to be exacerbated by the storage process, since a series of lesions accumulate as the erythrocytes sail across the cold and troublesome waters of their 42day hypothermic-storage odyssey. 4 RBC storage lesions

Storage lesions

While from a clinical standpoint there is only preliminary evidence, still to be confirmed, from the molecular point of view, the observations of changes that accumulate in red cells in proportion to the duration of their storage are numerous and indisputable, as described here. Although the average half-life of RBCs in the circulation is 120 ± 4 days (Palis, 2008), the standard maximum duration of storage of RCC is 42 days. This is because stored/transfused red cells seem to have a notably shorter half-life. In fact, 25% of the cell components are removed from the recipient's circulation within 24 hours of transfusion; in other words, of four units of red cells transfused, one is completely eliminated by the body already the day after the transfusion. There are probably two causes for this. The first, which is easily deducible, is that at the time of being donated, the unit of blood contains a percentage of already aged RBCs which, during storage, do nothing other than complete their aging process and are too old by the time of transfusion.

The second cause depends on the storage conditions, which are far from being normal, physiological conditions and which represent a greater and more long-lasting stress than the RBCs are able to counteract, despite their well-supplied protein machinery *ab origine*. In fact, although RBCs are anucleated and, therefore, are devoid of an actual genome and consequently protein synthesis, they do have their own armamentarium of proteins devoted to protecting and maintaining pre-existing protein functions through a "central core" of chaperone proteins, heat shock proteins and proteins involved in the detoxification of free radicals (peroxiredoxins, catalases, glutathione peroxidases) whose role is critical in the economy of the RBC proteome (the protein complement of the genome) and interactome (the system of protein-protein interactions) (D'Alessandro et al., 2010).

The most evident changes affecting RBCs during the storage period are alterations of the cell phenotype, which varies from a smooth discoid shape to a phenotype characterised by various membrane protrusions or spicula (echinocyte) and finally to a spheroid-shaped cell (spherocochinocyte) (Holme, 2005). The reversibility of these changes is inversely proportional to the duration of storage.

At the macroscopic level, RBC cold liquid storage induces a series of evident changes in the RBC shape (Berezina et al., 2007; Bosman et al., 2008) (**Figure 2**). During storage the erythrocyte shape visibly changes from a deformable discoid to a reversibly-deformed echinocyte to an irreversibly-deformed spheroechinocytes (Berezina et al., 2007). These changes are triggered by the irreversible loss of membrane through the formation of vesicles, which is the likely cause of an increased osmotic fragility, a reduced deformability and poor function after

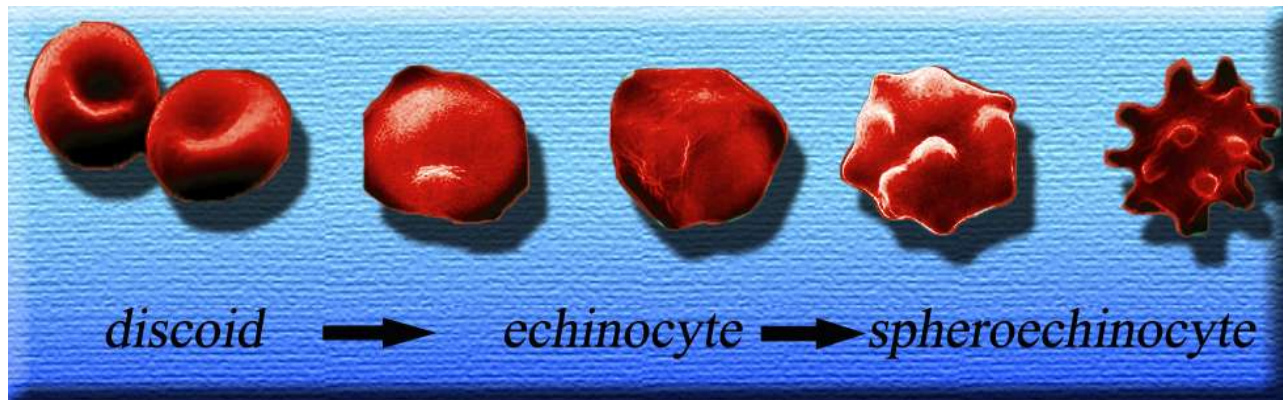


FIGURE 2 Main phases of the macroscopic changes of RBC shape during storage: from a discoid shape to echinocyte and spheroechinocytes.

transfusion. Vesicles are commonly grouped under two distinct categories: microvesicles and nanovesicles. The former have a mean diameter of approximately 180 nm, while the latter have an approximate diameter of 80 nm (Salzer et al., 2002). Though deriving from the shedding membranes, microvesicles display a particular protein composition in that they contain a low number of membrane proteins, a high number of metabolic enzymes, and an elevated content of Hb (Bosman et al., 2008). These vesicles contain almost no integral membrane proteins or cytoskeletal components, with the exception of band 3 and actin. The protein composition of the nanovesicles is quite different from that of the microvesicles and of the RBC membrane, with a conspicuous large number of complement and immunoglobulin proteins (Rensing et al., 2001). Raft formation may be involved in vesicle formation (Salzer et al., 2002) and RBC storage has recently been shown to be associated with changes in the concentration of raft-associated proteins of the membrane fraction (Bosman et al., 2008). When examining the presence of the raft-associated proteins flotillin-1, flotillin-2 and stomatin Bosman et al. (2008) found out that, during storage, the RBC membrane content of flotillins and stomatin decreases, whereas the microvesicles become strongly (10-fold) enriched in stomatin, and that upon prolonged storage, the nanovesicles become 20-fold depleted of flotillins. These main changes are accompanied by a wide range of biochemical and molecular alterations.

By a mere biochemical point of view, cooling below normal physiological temperatures inhibits metabolic processes and partially contrasts both the depletion of critical cellular metabolites and the accumulation of oxidative injuries. However, these benefits are counteracted by three effects: (I) the rate of met-Hb reduction by cytochrome b5 reductase is slowed; (II) met-Hb may be more prone to denaturation as suggested by lower thermodynamic stability of metmyoglobin at 4°C; and (III) the solubility of oxygen is doubled at 4°C. As a result, oxidative damage can accumulate with refrigerated red cell liquid storage (Zolla and D'Alessandro, 2011).

The storage lesion also involves the fluxes of sodium ions (massive entry into the cell) and potassium ions (exit from the cell), since the Na^+/K^+ pump is inactive at 4°C (Bennet-Guerrero et al., 2007). Although this is a reversible process (it takes 24 hours to restore the physiological gradients for sodium, and up to 4 days for potassium (Hogman and Meryman, 1999)), this phenomenon means that blood stored for a prolonged period should not be used for neonates or paediatric patients, unless first washed or the potassium removed from the storage medium (Klein et al., 2007).

Another biochemical effect is a clear decrease in the levels of 2,3-DPG (which is consumed already within the first week), translating into increased affinity of haemoglobin for oxygen and, consequently, decreased capacity of the RBCs to release oxygen according to local metabolic needs. The decrease in 2,3-DPG levels is also a reversible event, and completely normal levels can be restored within 3 days after the transfusion (Beutler et al., 1969).

Contrary to senescent process, upon storage RBCs lose potassium, DPG, ATP and calcium stores. Moreover, RBCs undergo several changes including alterations in cellular membrane, shape changes, phospholipid content, phospholipid asymmetry and antigenic markers, while they become more rigid and demonstrate reduced oxygen off-loading (Rensing, 2001). RBCs become more acidotic and the suspending fluid has higher concentrations of free Hb and biologically active lipids and contains greater quantities of negatively charged microvesicles with pro-inflammatory and pro-thrombotic activity (Greenwalt et al., 1991; Ho et al., 2003; Bessos and Segatchian, 2005). The potassium loss is a consequence of the altered metabolic activity upon cooling, while the loss of DPG and reduced glycolytic activity provoke a decrease in pH levels. DPG is typically gone by the 10th day of RBC storage, whereas ATP concentrations initially increase, due to preox DPG breakdown, or are stable during the first 2 to 4 weeks of storage, with generally declining concentrations thereafter. New experimental solutions, such as CPD and other phosphate-containing ASs, are aimed to further delay the total ATP consumption (Hess, 2006). It is noteworthy that, at the end of the RBC life-span, its enzyme activities, ATP and other crucial metabolites are still present in sufficient amounts and do not justify RBC death. On the contrary, upon storage ATP and DPG are almost fully depleted and most of the membrane proteins are oxidized as well as lipids, while the cytosolic enzymes are only in part damaged.

The experimental evidence on the role of S-nitrosothiol-haemoglobin is, on the other hand, controversial. It was thought that reduced levels of this form of haemoglobin would be related to 'old' blood having a lesser vasodilatory effect in recipients (Bonaventura et al., 2007); however, recent molecular biology studies seem to suggest that this is not the case (Reynolds et al., 2007; Isbell et al., 2008).

Erythrocytes also undergo other irreversible damage, as exemplified by the haemolysis in the second half of the actual maximal blood bank storage period. Determination of the degree of haemolysis is currently based on the amount of extracellular Hb. Nonetheless, the detection of extracellular Hb is not the foremost and reliable criterion, since up to 50% of the extracellular Hb is contained within vesicles and could not be detected with routine approaches (Greenwalt et al., 1991).

HbO_2 is potentially harmful as it promotes the generation of reactive oxygen species (ROS), putatively $\text{OH}\cdot$, after Fenton's reaction involving its haeme iron. During RBC storage, Hb becomes associated with the membrane fraction, mainly with the cytoplasmic domain of band 3 (Zhang et al., 2000), partially in a non-reducible, cross-

linked form (Wolfe et al., 1986). This association has been speculated to induce the generation of neoantigens that trigger immune recognition and removal of aged and/or damaged RBCs (Kriebardis et al., 2007).

Regarding membrane protein damages, it is well known that the etiology of lesions in RBC membranes is multifactorial, involving both ROS and proteolytic enzyme activity. Recently, in order to gather information on the time course of storage lesions, investigations on the relative contributions of oxidation and enzyme cleavage to this process and the fragmentation of RBC membranes have been documented by mapping the proteome changes over storage time.

Alongside these reversible changes, various irreversible events occur during the storage process, including fragmentation and aggregation of proteins and lipids, activated by radical species generated by prolonged, continuous oxidative stress (Wolfe, 1989; Racek et al., 1997; Sharifi et al., 2000). In this way oxygen constantly leaves one molecule of haemoglobin to bind to another. It is known that, occasionally, an oxygen leaving the haemoglobin molecule carries with it an electron, forming a superoxide ion (O_2^-) and (ferric) methaemoglobin.

Normally, the methaemoglobin is reduced by cytochrome b5 reductase (Abe et al., 1979) and the superoxide is dismutated without consequences. However, during prolonged storage, the superoxide ion can interact with iron and water in a Fenton reaction, resulting in the formation of hydroxyl radicals capable of attacking and damaging both proteins and lipids, leading to their fragmentation and the formation of aggregates. For example, haemoglobin can be converted into hemichromes (haemoglobin whose cysteine residues have been oxidised, leading to the formation of aggregates). Eligible targets of the radical species generated in a cascade from the hydroxyl radical are membrane phospholipids (with the formation of lysophospholipids and malondialdehyde (Dumaswala et al., 1999)), and proteins within (or closely related to) the cell membrane, such as the band 3 ion exchanger (Kaon et al., 2009) (which plays a fundamental role in maintaining the oxygen transport function of RBCs (Hamasaki et al., 1996) and acts as an anchor for a series of key glycolytic enzymes (Low et al., 1993; Weber et al., 2004)) and spectrin. These membrane alterations end up causing the previously-described echinocyte or spherocytocyte phenotypes. Finally, it is known that the cell activates a process of vesiculation, in order to eliminate proteins and lipids that have been altered by oxidative stress, as to protect the cell from a further chain reaction of stress and consequent removal from the circulation (Willekenes et al., 2008). In fact, aggregates of band 3 appear at the membrane during both *in vivo* and *in vitro* aging (Willekenes et al., 2008; Karon et al., 2009), constituting membrane signals to "remove" the cell, through IgG- or complement-mediated phagocytosis by the recipients' Kupffer cells. These membrane neoantigens, by stimulating the immune system, seem to be related to the onset of proinflammatory events, which are often harmful if not fatal in critically ill patients undergoing transfusion therapy (Tinnmouth et al., 2001; Lelube et al., 2009). Alongside these signals, which are particular to red cell aging, a series of other markers appear; these markers are common in other physiological phenomena associated with programmed cell death or apoptosis, such as exposure of phosphatidylserine on the external leaflet of the lipid bilayer of the cell membranes, whose presence in microvesicles increases in proportion to the duration of storage (Bosman et al., 2005). This very same phenomenon of vesiculation through membrane protrusions (blebs) has contributed to strengthening the parallels between the processes of red blood cell aging and apoptosis (Bosman et al., 2008), leading Lang and colleagues (2006) to coin the term "eryptosis" to describe this physiological phenomenon, which is exacerbated during the

storage of the RBCs. The increase in the number of vesicles (0.5 μm) with the duration of storage is noteworthy, as is the increased content of proteins (band 3 and ankyrin) and lipids (stomatins), again proportional to the duration of storage. In contrast, the variability in proteins in the red cell cytoplasm and membrane decreases gradually (Pasini et al., 2006; D'Amici et al., 2007; Bosman et al., 2008).

Most of these irreversible events seem to be favoured by prolonged oxidative stress arising under non-physiological conditions of storage in the blood bank (Wolfe et al., 1989; Racek et al., 1997; Sharifi et al., 2000). However, as far as proteins are concerned, the first signs of fragmentation and aggregation begin to appear in the third week of storage, at least in non-leukofiltered concentrates (D'Amici et al., 2007), while this research project is focused in complementing proteomics information also on the leukofiltered concentrates. A comparative study of stored (at 0, 7, 14 and 42 days of storage) and fresh non-leukoreduced RBCs (D'Amici et al., 2007) was performed with 2-dimensional-gel electrophoresis, followed by in-gel digestion and electrospray ionization-tandem mass spectrometry. The former analysis showed a diminished staining intensity of some spots over storage time, whereas other spots resulted to suffer of a decreased electrophoretic mobility. These phenomena are usually observed when proteins are exposed to ROS (Sheehan et al., 2006). In fact, the presence of smearing, mobility shifts of intrinsic protein bands, aggregate formation and also protein fragmentation could all be caused by ROS generated during storage, which attack proteins in the cytoskeleton. Mainly ROS produced prevalently from HbO_2 and hemichromes, the final oxidized variant of denatured Hb, are likely to constitute the leading cause of the well known morphologic, biochemical and metabolic changes in RBCs during storage, through an initial oxidation of amino acid residues with consequent protein fragmentation and/or aggregation phenomena. Consistent with this, most of the affected proteins investigated in the report from Zolla's group were located in the cytoskeleton and oxidation occurred systematically after 10 days of storage (Annis et al., 2005; Kriebardis et al., 2006). During the first 7 days of storage oxidative degradation was observed prevalently in band 4.2, to a minor extent in bands 4.1 and 3 and in spectrin. Indeed, the most important RBC membrane protein, band 3, was found to decrease in the 75 kDa fraction while it increased its presence in the 150kDa one, as aggregation occurred during storage (Bosman et al., 2008; Kriebardis et al., 2007). A band 3-centric process was therefore suggested to be the most relevant in complement activation and, ultimately, RBC removal of senescent cells or re-infused RBCs in the recipient (Arese et al., 2004). Indeed antibodies which have too weak affinities to bind to band 3 monovalently would avidly react with band 3 aggregates (bivalent interaction). These clusters show an enhanced affinity (more than 3 orders of magnitude) for normally circulating anti-band 3 antibodies, which in turn activate the complement system. It has been shown that less than 1% oligomerized band 3 was sufficient to elicit deposition of autologous anti-band 3 IgG. These few molecules were able to induce generation of large amounts of complement fragments via activation of the alternative pathway (Lutz, 2004).

After 14 days, in non-leukofiltered erythrocyte membranes new fragments appeared from beta-actin, G3PD, band 4.9 and ankyrin, among others, as a clear symptom of fragmentation. Preliminary protein-protein cross-linked products, involving alpha and beta spectrin, were also detected. The cross-linked products continued to increase over time (D'Amici et al., 2007).

ROS attack the protein fraction at the membrane levels, but also initiate lipid peroxidation reactions that lead to loss of membrane integrity and cell death (Baynes, 2005). For example, malondialdehyde (MDA), a highly reactive bifunctional molecule, is an end product of membrane lipid peroxidation. Lipid derivatives of oxidant attack, most notably malondialdehyde, exert a number of detrimental effects on RBCs. MDA has been shown to cross-link erythrocyte phospholipids and proteins. MDA accumulation can affect the anion transport and function of the band 3 associated enzymes, i.e. G3PD and phosphofructokinase (Dumaswala et al., 1999). MDA can damage the membrane structure via a series of cascade events: the formation of membrane pores, which increase potassium leakage and alter water permeability; the polymerization of membrane components and a decreased cell deformability; cross-linkage of membrane proteins; enhanced IgG binding and complement activation; finally, an enhanced exposure of PS on the outer cell surface (Kuypers et al., 1998). We have already emphasised the role of PS exposure as an alternative mechanism to explain RBC removal and, in general, as an apoptotic marker (for review, see Lang et al., 2005; Pantaleo et al., 2008; Foller et al., 2008). CD47 has been shown to decrease in membranes over storage (Annis and Sparrow, 2002; Stewart et al., 2005) and the likely mechanism seems to be vesiculation (Bosman et al., 2008).

Proteomics changes arising upon the second week of storage represents a remarkable temporal synchronisation with the findings reported by retrospective, albeit in non-randomised, clinical studies, about adverse effects of RBCs stored for more than 2 weeks in patients undergoing heart surgery (Koch et al., 2007), and with the onset of conformational changes of band 3 (Karon et al., 2009). It does, therefore, seem wise to prevent this type of irreversible lesion in the early period of storage, rather than intervening a posteriori (for example, through the adoption of alternative storage strategies, such as the addition of rejuvenation solutions (Valei et al., 2000), oxygen removal (Yoshida et al., 2007 and 2008; Dumont et al., 2009) or the formulation of alternative additive solutions).

Within the framework of this thesis project I will focus on the determination of the major biochemical changes arising during RBC storage under blood banking conditions, or rather upon the introduction of alternative storage strategies such as anaerobic storage and alternative additive solution formulations, such as those including antioxidants (e.g. Vitamin C and N-acetylcysteine).

Alternative methods in RBC storage: rejuvenation solutions, cryopreservation and anaerobic storage

Notwithstanding the aforementioned drawbacks of long-term storage of RBCs, during the last 2 decades the bet of RBC Bp research has been placed on lengthening the RBC hypothermic storage beyond the current 42-day boundary.

To this end, even unorthodox solutions have been experimented, such as the addition of ammonia, which turned out to enhance ATP maintenance and longer preserve RBCs (for 9 weeks or slightly longer), though at the expenses of an actual clinical application (Greenwalt et al., 1997).

More realistically, solutions allowing 7-week hypothermic storage, such as ErythroSol, MAP, and PAGGS-S/M have been developed for clinical use (Walker et al., 1990; Hogman, 1999). Besides, several rejuvenation solutions have been elaborated that regenerate ATP and 2,3-DPG levels of hypothermically stored RBCs near or post-outdating (Valeri et al., 2000). Rejuvesol is currently the only solution approved by the American Food and Drug

Administration. It adds 2-3 more weeks to the life-span of the stored RBCs, by providing the effete cells with adenine, inosine, phosphate and pyruvate (Hess, 2006). However, the high costs of the time-consuming rejuvenation process have hitherto hindered the way of its large-scale diffusion.

In alternative, more than a decade ago the addition of phosphoenolpyruvate was proposed for rejuvenation of preserved blood, yielding a considerable increase of 1,3-DPG, the precursor of 2,3-DPG and therefore, a potentially extended storage period without toxic consequences to the recipient (Matsuyama et al., 1989). Nonetheless, phosphoenolpyruvate has not so far encountered the favour of the specialists in this endeavour.

Among the strategies which have been proposed to lengthen the storage suitability of RBCs, cryopreservation appeared to be the most promising since when it was demonstrated a protective action of glycerol against the freezing injuries to RBCs in 1950 (Smith, 1950). RBCs can be frozen in glycerol solutions and stored for as long as 37 years (Valeri et al., 2000). In clinical practice, units of RBC are frozen using either low- or high-glycerol methods.

Formation of crystalline ice in a biologic fluid leaves the salts behind, creating osmotic forces, which disrupt cell membranes. Glycerol slows the rate of ice crystal formation and allows the RBC suspension to freeze as a glass (Pert et al., 1965). Low, 15–20%, concentrations of glycerol are sufficient to limit rates of crystal growth during rapid cooling, that is to say when cooling with liquid nitrogen at -170°C ($-100^{\circ}\text{C min}^{-1}$). High, 40–50%, glycerol is necessary to slow crystal growth even more when rates of cooling are slower ($-1^{\circ}\text{C min}^{-1}$) in mechanical -80°C freezers (Hess, 2004). Glycerolization and deglycerolization are two key steps, since RBC must be rapidly frozen after the former and rapidly deglycerolized after thawing. There is a reduced likelihood of a potential break in sterility caused by opening the blood bag to transfer RBC and glycerol to the freezing container as bacteria do not grow at the temperatures of frozen RBC storage. However, the freeze-thaw-wash procedure yields the inexorable loss of 4-20% of the original stored RBCs, diminishing the efficiency of the transfused unit. Furthermore, two more shortcomings must be faced when dealing with RBC cryopreservation. First of all, the elevated costs for maintenance, ranging from 2 to 20 as much as liquid hypothermic storage (Hess, 2004). The time consuming procedures of glycerolization and deglycerolization (25 and 40 minutes respectively) hamper a readily suitability of frozen units in dramatic and urgent circumstances. These obstacles have so far dampened the enthusiasms around RBC cryopreservation, whose distribution is nowadays limited to the military setting (Ramsey, 2007).

Notwithstanding these hurdles, the American Food and Drug Administration has licensed this system for 2-week, post-thaw, 4°C storage of RBC collected into CPDA-1 and frozen with sterile process within 6 days. The system has 88% freeze–thaw–wash recovery and 77% *in vivo* recovery at 14 days in the licensure study (Valeri et al., 2001).

Whether the costs of automated devices to process the cells, bench space, freezers, air conditioning, electricity and trained technical staff will be amortized and in-depth investigations, such as proteomic analyses (still missing in this field), will prove that RBC cryopreservation advantages offset its drawbacks is still a matter of debate. For the foreseeable future, skepticism has already spread through the main personalities of the RBC Bp field (Hess, 2004).

In order to cut the costs for the aforementioned procedures, it has been a desideratum to obtain a method for the storage of RBCs which was not dependent on the maintenance of specific storage temperatures or other storage conditions. Lyophilization has been proposed as an option. Lyophilization (freeze-drying) involves the removal of

most unbound water from biologic materials through controlled freezing followed by the sublimation of ice under vacuum (Scott et al., 2005). However, it has not so far found a proper collocation in clinical practice due to several non-secondary issues affecting RBCs during this process (such as extreme membrane fragility after rehydration and Hb unfolding in the dried solid, which facilitates the rate of methHb formation, even after rehydration) (Scott et al., 2005).

A totally different approach has been recently proposed. When dealing with RBC storage lesions, recent literature focuses on the fulcrum role of ROS. Therefore, it was a matter of time that RBC Bp research tried to reduce the oxidative stress by adding antioxidants to the storage solution and reducing the main oxidative stress trigger, oxygen. Intuitively, while the former approach counteracts ROS negative action while delaying but not stopping oxidative cascades, the latter represents a sort of “renversement de rôle” in RBC Bp where the effects are no longer elicited as the centre of the study, being dethroned by the likely cause. Though being fascinating, the effectiveness of this approach is still under assessment. Early attempts were oriented to reduce the oxidative damage to red cells during storage through storing under carbon monoxide to stabilize haemoglobin and prevent oxygen diffusion into the bag during storage (Hogman et al., 1986; Wolfe et al., 1987). Unfortunately, high concentrations of carbon monoxide in RBCs also bind to the haeme of other key regulator proteins and stop glycolysis (Hess, 2007). Alternatively, noble gases such as argon or helium have been used to reduce oxygen saturation of Hb under a 4% threshold (Yoshida et al., 2007 and 2008; Dumont et al., 2009). Anaerobic storage in presence of AS-3 solution allowed RBCs to be stored for up to 9-weeks (Yoshida et al, 2007). Additional weeks, up to 120 days, could be added to the stored RBC life-span when adding rejuvenation solutions at day 63 (Yoshida et al., 2008). Rejuvesol restores ATP and 2,3-DPG levels in anaerobically stored RBCs, by replenishing the RBC reserve reaching a minimum around day 60.

Moreover, anaerobic storage reduces the PS exposure on RBC membranes. Therefore, although the anaerobic strategy does not allow to dreadfully prolong the shelf-life of stored RBCs, preliminary evidence suggested that the quality of RBCs which were stored with this protocol was ameliorated. In order to assess this first impressions, D’Amici and co-workers (2007) performed a comparative investigation with proteomic tools between refrigerated liquid stored non-leukofiltered RBCs stored either in presence or absence of oxygen. 2dimensional-gel electrophoresis maps of RBCs under aerobic and anaerobic storage conditions were performed, the former displaying a considerable number of new spots over time, especially after ten days of storage. Fragmentation and aggregation events were individuated as the likely early cause of these phenomena, since the sequences of those spots matched with the mass fingerprints of higher or lower molecular-weight proteins. Furthermore, a second experiment adopted protease inhibitors in order to reveal that only few fragments were produced by proteases. Nonetheless, anaerobic conditions slowed protease activity as the climax of protease-induced fragmentation was observed under aerobic storage, in agreement with several proteases, such as caspases 2 and 3 being activated by oxygen presence or oxygen induced-stresses (Mandal et al., 2002; Matarrese et al., 2005).

However, among the above mentioned fragments, band 3-, G3PD- and band 4.1-derived fragments were the firsts and utterly more abundant to be individuated. Contrarily, it was evidenced that, under anaerobic conditions, fragmentation and aggregation rates were relevantly reduced and definitely procrastinated, even in absence of

protease inhibitors. Therefore, anaerobic storage has been proposed for further evaluation as a valid alternative to classic hypothermic storage, since it represented an alternative way to prevent RBC storage lesions, rather than attempting to reconstitute their physiological conditions, as ASs have been thought for.

Taken together, the data reported in the various sections of this review article appear to support the hypothesis that most of the storage-induced lesions under aerobic hypothermic storage could be the result of a cascade of events, primarily induced by oxidative processes (**Figure 3**). These processes are triggered by a domino effect: being stored in an oxygen-stressed environment for a prolonged period, oxy-hemoglobin is oxidized to methemoglobin and, finally, hemichromes are generated. Oxygen radicals are subsequently released and attack a series of key proteins, among which an eligible target seems to be the cytosolic fraction of band 3. Thus the nearby proteins (cytoskeletal proteins - e.g. ankyrin) and enzymes are compromised after radical exposure. Another likely mechanism could be the transport/binding of denatured proteins to the membrane fraction, such as for membrane-bound Hb in consequence of oxidative injury [179]. In consequence, neoantigens are exposed from the membrane, RBC physiology and structure are impaired and, parallelly, glycolysis fades off. Thereon, the no-more functional re-infused RBCs are rapidly removed from the bloodstream or are likely to cause untoward effects in the recipients.

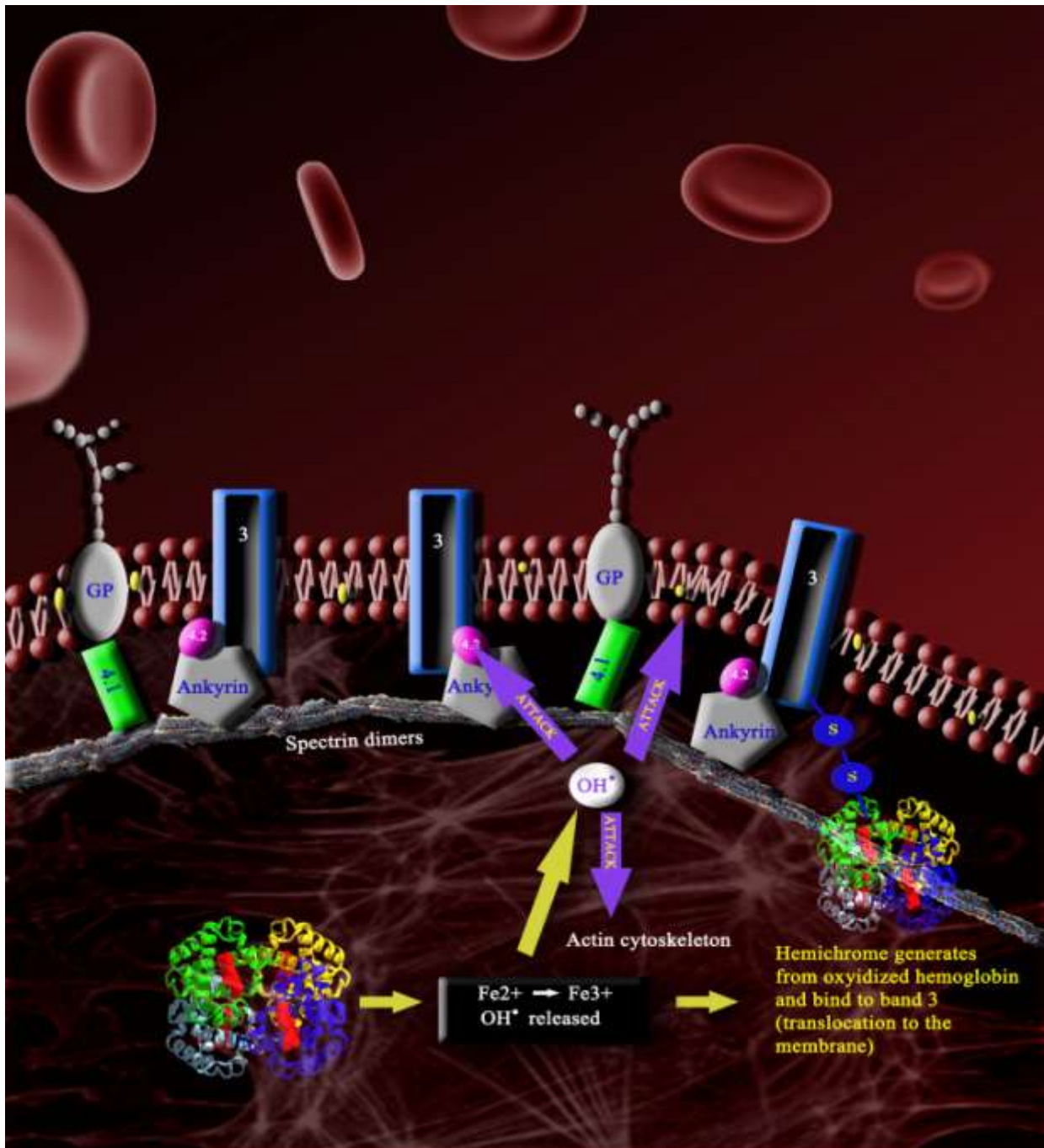


FIGURE 3 A domino of events appears to be responsible of RBC storage lesions. Being stored in oxidative environment, hemoglobin is slowly oxidized to methemoglobin and, utterly, a low percentage of hemichrome aggregates form through disulfide bonds. In the meanwhile, haeme iron is reduced from a ferrous to a ferric state via a Fenton's reaction, which produces OH[•] radicals. Thereon, a cascade of oxidative events takes place due to the spreading of reactive oxygen species (ROS). These events involve ROS attack to the cytoskeleton and membrane (either lipid or protein) fraction, whose a particular eligible target appears to be the anion exchanger band 3 and the proteins nearby its cytosolic portion (band 4.2, ankyrin and several enzymes such as glyceraldehyde-3-phospho-dehydrogenase). Although RBCs are dramatically equipped for high-oxidative stresses, prolonged storage periods end up to exacerbate the oxidative phenomena, thus the outcome is a no-longer functional or vital RBC. Furthermore, the oxidative environment rapidly switches the metabolic trigger from the classic glycolytic pathway to the HMS pathway, with the result to lead the RBC to a final ATP total depletion. When re-infused, the long-stored effete RBC is rapidly removed from the bloodstream or contributes to the promotion of untoward responses in the recipient.

Conclusion

Molecular and retrospective clinical studies have recently compelled the international scientific community to reconsider the validity of the current protocols for RBCs storage. Randomised, prospective studies of unquestionable statistical rigour, are, however, yet to be completed (reviewed in Grazzini and Vaglio, 2012). If, however, future data confirm the numerous already available retrospective clinical observations, research and new storage strategies will need to be focused on avoiding the possible side effects of prolonged storage.

Furthermore, ad hoc studies will have to be carried out on the impact that a change in the duration of storage of red cells could have on the self-sufficiency of the blood system.

From a molecular standpoint, most of the changes occurring during storage are already well known (summarized in **Figure 4**). Some of the changes are reversible, through the addition of new additive solutions (Hess, 2006) or rejuvenating solutions (Valeri et al., 2000), while others are irreversible and must, therefore, simply be prevented. The former changes include alterations in the levels of small molecules, such as ATP and 2,3-DPG, pH, sodium and potassium, while the latter changes include irreparable denaturation of proteins following fragmentation and aggregation catalysed by free radicals.

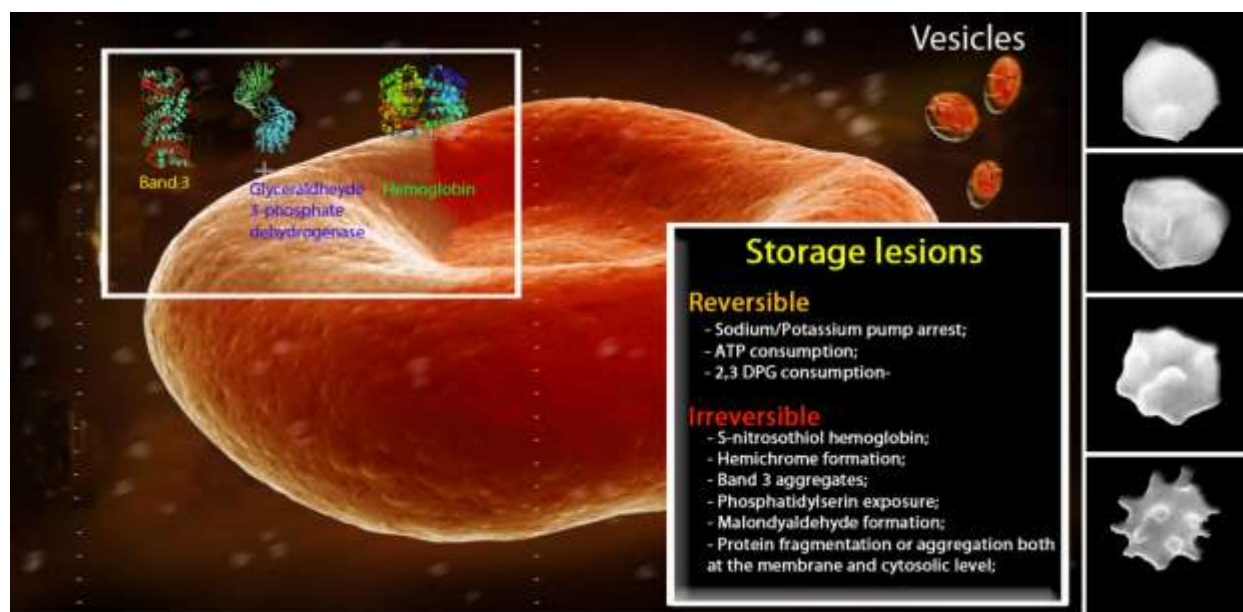


FIGURE 4 Red blood cell storage causes a series of alterations at the macroscopic level leading to echinocyte phenotype and vesiculation processes (right side), and on the molecular level (Storage lesions box). Although some are reversible, there are numerous irreversible fragmentation and aggregation events which involve pivotal proteins, such as anion exchanger band 3, glyceraldehyde 3-phosphate dehydrogenase and hemoglobin (top left), and thus hamper fully functional recovery of the erythrocyte even upon transfusion. Thus, the damaged red blood cell is rapidly removed from the bloodstream of the recipient.

The underlying cause of these phenomena is the prolonged oxidative stress to which the RBCs are exposed during storage (Wolfe, 1989; Racek et al., 1997; Sharifi et al., 2000). To contrast this oxidative stress, it was proposed, in the past, to treat donors with antioxidants (vitamins E and C, beta-carotene (Racek et al., 1997)), although this type

of treatment tends to limit oxidative stress rather than to prevent it. Yoshida's group (Yoshida et al, 2007 and 2008; Dumont et al., 2009), however, suggested a storage protocol that tackled the problem at its source.

They proposed storing blood directly in an atmosphere of inert gas at a $pO_2 < 4\%$, using a method that they patented (WO/1996/039026). The clinical outcome of this protocol has been tested with respect to the classical standards (haemolysis and RBC survival at 24 hours post-transfusion) with positive results; slowing in the decreases of 2,3-DPG and ATP was also observed. Furthermore, Yoshida's group showed that addition of a standard rejuvenation solution at day 63 of storage restored the levels of 2,3-DPG and ATP, making storage for as long as 120 days theoretically possible (Yoshida et al., 2008). In support to this strategy, but independently, Zolla's group (D'Amici et al., 2007) also analysed a model of anaerobic storage, using classical proteomic methods to compare the total protein profile of non-leukoreduced RBCs stored using this protocol with that of control units stored according to a standard protocol. No signs of fragmentation or aggregation were found in the blood stored in inert gas in the medium term (during the first 2 weeks); these phenomena began to be seen, albeit to a reduced extent, towards the end of the storage period (42 days), thus, from a molecular point of view, the blood provided to recipients was of better quality. It should, however, be appreciated that these results are drawn from preliminary studies and further investigations, both clinical and molecular, were mandatory and hereby addressed throughout the experimental workplan of this PhD thesis.

In conclusion, given that anaerobic storage can prevent the above-described irreversible phenomena of fragmentation and/or aggregation, as well as slower the decreases in 2,3-DPG and ATP levels (Yoshida et al., 2007) (although these latter processes can be reversed in any case by the addition of rejuvenating solutions (Valeri et al., 2000), such a form of storage could be an excellent solution to the clinical problems observed in the preliminary retrospective studies on the efficacy and safety of the current protocols of blood storage, while awaiting the definitive clinical data, which will be provided by prospective, methodologically incontrovertible studies. The task remaining is to bridge the gap between basic research and large scale application of its results, a goal that current translational research must meet in order that anaerobic storage can be adopted in daily transfusion practice.

1.2.1. Introduction to the field of “Integrated Omics”: Proteomics, Metabolomics, Lipidomics and Interactomics and their application to Transfusion Medicine and Red Blood cell Biology relevant issues

Overview of this section

Since the genomic era has not fully kept its promises, studies addressing the protein and metabolic complement to the genome (i.e. the proteome and metabolome) have been recently gaining momentum. Blood-related proteomics and metabolomics are emerging fields, recently gaining momentum. Indeed, a wealth of data is now available and a plethora of groups have contributed to add pieces to the jigsaw puzzle of protein and metabolic complexity within plasma and blood cells, especially erythrocytes. In this chapter, we purposed to sail across the *mare magnum* of the actual knowledge in these research endeavours, with the aim to highlight the major applications and technological features of blood (and in particular, of red blood cell)-related proteomics and metabolomics. The main strides in proteomic and metabolomics investigations on red blood cells will be hereby presented in a chronological order. Besides, a glance will be given at those branches of proteomics and metabolomics that promise to expand existing knowledge while providing translational clues, including the analyses of lipid species (lipidomics). Finally, the next stage of the evolution of the so called “omics” disciplines is represented by the field of Integrated Omics, and its mathematical interpretation within the framework of Systems Biology.

Omics investigations could be indeed potentially used from bench to bedside, in order to test the quality of collected blood components prior to or during storage. In parallel, Integrated Omics could be used to verify the effects of the production and pathogen reduction processes of plasma derivatives and blood components on the protein fractions, or to reduce the effects of storage lesions. Another area of interest is represented by the discovery of peculiar biomarkers (either at the protein, *in silico*, metabolic or lipid level) readily adoptable for targeted evaluation of blood-component integrity or functionality.

Integrated Omics technologies have recently proven their worth in shifting the focus of attention from the end product to its provider, the donor, in a sort of Kantian “Copernican revolution”. A well-rounded portrait of the usefulness of Integrated Omics in blood-related research is accurately given, including the analysis of blood-banking production processes (a comparison of collection methods, pathogen inactivation techniques, storage protocols). Thus Omics disciplines have been recently transformed from mere basic-research extremely-expensive (mass spectrometry-based) toys into dramatically-sensitive and efficient eye-lenses to either delve into the depths of the molecular mechanisms of blood and blood components or to establish quality parameters in the blood-banking production chain totally anew.

Introducing Omics technologies and their application to the field of RBC biology

In this section of Chapter 1: Introduction, we will introduce the recent advancements in the field of Integrated Omics applications to blood and blood cells, with a particular focus on red blood cells (RBCs). An overview will be given of the main Omics technologies which found recent, albeit widespread application, as basic science and translational tools in the field of RBC biology and transfusion medicine. The reader will be guided through a point by point description of proteomics (including gel-based and chromatography-based proteomics, mass spectrometry, quantitative proteomics, PTMs, native and *in silico* approaches), metabolomics (the study of the low MW < 1.5 kDa complement to the proteome), lipidomics, and their intertwined elaboration in the fields of Integrated Omics and Systems Biology.

Blood-related Proteomics: an introduction

A decade has almost passed since the real turning point of the genomic era, the completion of the Human Genome Project, which utterly delivered us a fundamental dataset of over 20,000/25,000 confirmed genes (Stein, 2004). From thereon, clinicians and researchers started auspicing a new deal in the biomedical field. Forthwith, both the scientific and the academic milieu began to dream of new generations of genetically-targeted pharmaceuticals, though they still remain unachieved or under development (Evans et al., 2004; Shah, 2005). Therefore, initial enthusiasms have been recently tempered (Nebert et al., 2008), since mere genomic approaches have not hitherto lived up to expectations and failed to be self-sufficient in exhaustively depicting what actually happens within biological systems at the nanoscale. Indeed, the complexity of a cell (not to mention the complexity of a whole organism) lies on a whole different level, since it is not only influenced by the initial informational patrimony (its genome), but also by the “when and how” (spatio-temporal and causal principles) of its actual transformation into bioactive products, that is to say, into proteins (Wasinger et al., 1995; Kitano, 2003). Proteomics (Wasinger et al., 1995) represents a step forward towards a better understanding of the molecular biological events, since an approximate estimation of the human proteins outnumbers the 20,000/25,000 gene threshold by 3 or 4 orders of magnitude (Marko-Varga et al., 2004). However, also the proteome (the protein complement to the genome) is a dynamic entity which responds to a series of fluctuations (e.g. quantitative variability and post-translational modifications – PTMs) under altered conditions (disease, stress, sport, pregnancy and so on). Taken together, all these variables likely influence the experimental outcome.

Shifting the focus of attention from the genome to the proteome is an inevitable step when dealing with transfusion medicine (TM). One of the main purposes of TM is to ensure safety, efficiency and effectiveness of blood components (BCs) and raw materials for biopharmaceutical fractionation (Atallah et al., 2006) (**Figure 1**).

Three main BCs are routinely used in the TM endeavour: erythrocyte concentrates, platelet concentrates (PCs) and fresh frozen plasma (FFP) (Queloz et al., 2006). Being enucleated, erythrocytes or red blood cells (RBCs) and platelets (PLTs) display a meager amount of mRNA, as a limited heritage from their reticulocyte (Pasini et al., 2006) and megakaryocyte (McRedmond et al., 2004) ancestors. It should be also considered that mRNA levels do not often strictly correlate to protein ones, thus transcriptomic investigations should at least be used to complement proteomic analyses and vice versa (Anders and Seilhamer, 1997; Anderson and Anderson, 1998; Cristea et al.,

2004; de Hoog and Mann, 2004). It is thus small wonder that early investigations on BCs elgibly addressed the protein fraction (Tiselius, 1937). Nonetheless, the analysis of the protein fractions of blood and BCs still represents a challenging task. Blood and BCs display an extremely rich spectrum of proteins, which are involved in the most different activities (coagulation, transport, immune system, cell signaling), and their proteomes harbor byproducts of cellular damage and foreign proteins as well (Page et al., 2006).

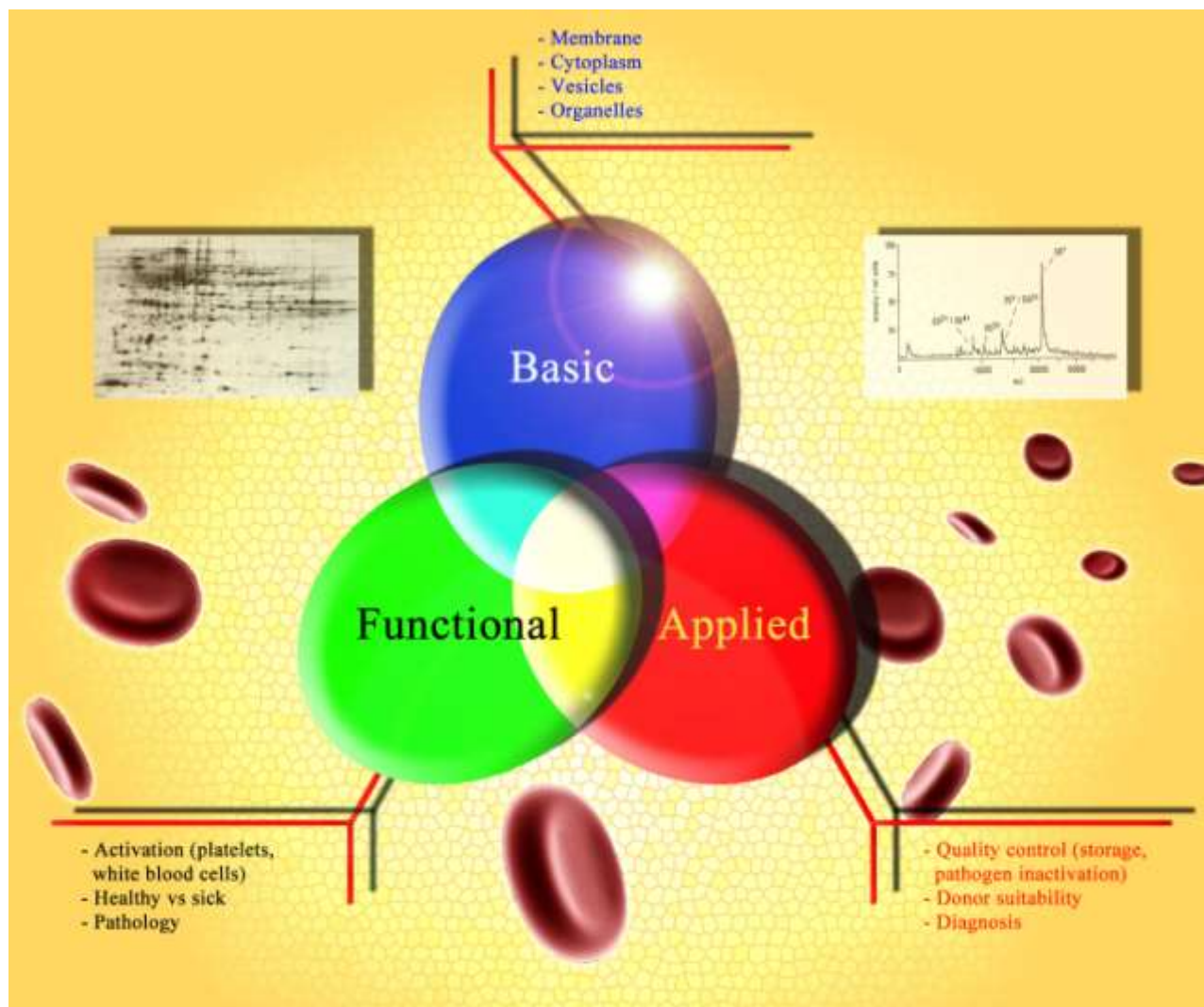


FIGURE 1 Proteomic techniques could be adopted for basic research, though recently there is a new trend towards functional and applied proteomics

Most importantly, in blood plasma there is an extreme dynamic range of protein concentrations (10 orders of magnitude), which spans from picogram to tens of milligram quantities per milliliter (Anderson and Anderson, 2002). At present, no technology exists to simultaneously study proteins throughout this entire dynamic spread. Therefore, one of the main inconveniences that proteomicists have to cope with is the elevated heterogeneity of the protein fractions within the sample. For example, erythrocytes contain large amounts of hemoglobin while more than 90% of the plasma proteome is represented by less than 10 different proteins, albumin being the most abundant

(Anderson and Anderson, 2002). As a rule of thumb, there is an elevated risk of low-abundant protein loss. This technical obstacle ultimately hinders detection of a whole “hidden proteome”. In order to overpass this hurdle, several strategies have been proposed with the goal to reduce sample complexity by splitting it (electrophoresis pre-fractionation (Pieper et al., 2003)) or by lowering the “analytical noise” through the removal of high-abundant species. As far as the latter approach is concerned, immunoaffinity depletion (Pieper et al., 2003; Echan et al., 2005), alone or in combination with electrophoretic pre-fractionation (Echan et al., 2005; Boschetti and Righetti, 2009), and combinatorial ligand libraries (Boschetti and Righetti, 2009) have been recently gaining momentum. Nevertheless, the removal of high-abundant proteins has some considerable detrimental pitfalls, since proteins such as albumin can frequently function as carriers through binding of protein fragments of biological interest (Zolla, 2005). These technical shortcomings have hitherto hampered a comprehensive analysis of the most complex proteomes by altering the outcomes with minor, albeit inevitable, losses of information (Yocum et al., 2005). Notwithstanding these relevant issues, blood-related proteomics is an emerging field with recent past and considerable future perspectives. Indeed, the burgeoning literature around this topic is tangible evidence (Reddy and Perrotta, 2004; Unwin et al., 2004; Greinacher and Warkentin, 2005; Thaddikkaran et al., 2005; Calvo et al., 2005; Page et al., 2006; Unwin and Whetton, 2007; Thiele et al., 2007; Liumbruno et al., 2008; Liumbruno et al., 2008).

Transfusion Medicine, haematology and proteomics: an introduction

Recent strides in analytical strategies have made hematology evolve from a descriptive medical discipline based on microscopic evaluation of red blood cells (RBCs), leukocytes, and platelets (PLTs), towards a dynamic science at the crossroads of genomics and proteomics (Thaddikkaran et al., 2005). PCR-based analyses have radically changed the study of chromosomal translocation products (Braziel et al., 2003). New technologies, such as DNA microarray allow a direct analysis of the transcriptome, the mRNA pool, which is the intermediate product of gene expression (Wiltgen et al., 2007). However, changes in the expression pattern at the mRNA level do not necessarily correlate with changes at the protein level (Anderson and Seilhamer, 1997). Furthermore, It is worthwhile to recall that among the most relevant blood components for transfusion purposes there are RBCs and PLTs, which are enucleated, thus they lack of a proper genome, although they inherit meager amounts of mRNAs from their nucleated precursors. Therefore proteomic investigations in hematology and transfusion medicine (TM) have been lately attracting a great deal of attention (Reddy and Perrotta, 2004; Unwin et al., 2004; Greinacher and Warkentin, 2005; Thaddikkaran et al., 2005; Calvo et al., 2005; Page et al., 2006; Unwin and Whetton, 2007; Thiele et al., 2007; Liumbruno et al., 2008; Liumbruno et al., 2008).

Proteomics tries to determine the whole protein profile of a specific sample under analysis. Proteomics analyses of blood and blood components definitely represent a challenging task. Blood and blood components display an extremely rich spectrum of proteins, which are involved in the most different activities (coagulation, transport, immune system, cell signaling), as well as byproducts of cellular damage and proteins from other tissues (Page et al., 2006). Most importantly, the range of protein concentrations in blood plasma spans from picogram to tens of milligram quantities per milliliter (a dynamic range of 10 orders of magnitude) (Anderson and Anderson, 2002). At present, no technology exists to simultaneously study proteins throughout this entire dynamic spread. For

example, erythrocytes contain large amounts of hemoglobin while more than 90% of the plasma proteome is represented by less than 10 different proteins, albumin being the most abundant (Anderson and Anderson, 2002). As a rule of thumb, there is an elevated risk of low-abundant protein loss, which ultimately hinders detection of a whole “hidden proteome”. In order to overpass this hurdle, Several approaches have been proposed with the goal to either reduce sample complexity - by splitting protein fractions (electrophoresis pre-fractionation (Righetti et al., 2005)) - or to lower the “analytical noise”, through the removal of high-abundant species. As far as the latter approach is concerned, immunoaffinity depletion (Pieper et al., 2003; Echan et al., 2005), alone or in combination with electrophoretic prefractionation (Heller et al., 2005), and combinatorial ligand libraries (Boschetti and Righetti, 2009) have been recently gaining momentum. Nevertheless, the removal of high-abundant proteins has some considerable detrimental pitfalls, since proteins such as albumin frequently also function as carriers for protein fragments of biological interest (Zhou et al., 2004; Granger et al., 2005). These technical obstacles have hitherto hampered a comprehensive analysis of the most complex proteomes by altering the outcomes with minor, albeit inevitable, loss of information (Yocum et al., 2005).

The proteomics workflow

Proteomics analysis actually begins at the end of the sample preparation (**Figure 2**). Protein species undergo an analytic step which separates them on the basis of their biochemical/physical properties (e.g. molecular weight, isoelectric point, mass/charge ratio). This analytic phase mainly relies on gel-based approaches (mono- or bi-dimensional electrophoresis) and chromatographic methods (Liumbruno et al., 2009). Separated protein spots are then cut from the gels and trypsinized (thus cleaved into peptides) or directly chromatographically eluted to a mass spectrometer for protein/peptide identification (also known as peptide mass fingerprinting). The protein from which these peptides were derived is determined upon mass spectrometric identification by comparing the obtained sequence with theoretical mass predictions of “known” protein sequences from the database.

In detail, a mass spectrometer roughly includes an ionization source, a mass analyzer, and a detector. The ionization source produces gaseous ions from molecules in either a solution or solid phase. The mass analyzer measures the mass-to-charge ratio of these ionized molecules (Liumbruno et al., 2009). The most common mass analyzer (time of flight or TOF) determines the mass-to-charge ratio by measuring the time required for the ions to pass through a charged field. To further increase the resolving power of the system, tandem mass spectrometers contain two mass analyzers in a row.

Huge amounts of data are produced by mass spectrometers at the end of the analyses. Thus it has been necessary to introduce informatic platforms for elaboration of the obtained data, in order to compare them against online databases (for example MASCOT). This is perhaps the most delicate phase of the whole proteomics analysis, along with the preliminary sample preparation steps. Data analyses and elaborations should be interpreted in the light of technical and biological variability. This is probably the main reason why, although serving its role as a powerful and highly-sensitive research tool, proteomics has not hitherto found a proper collocation in routine clinical practice.

Biological complexity of proteins from blood and blood components is increased by a series of post-translational modification (PTM) events, such as phosphorylations and glycosylations, which are closely related to

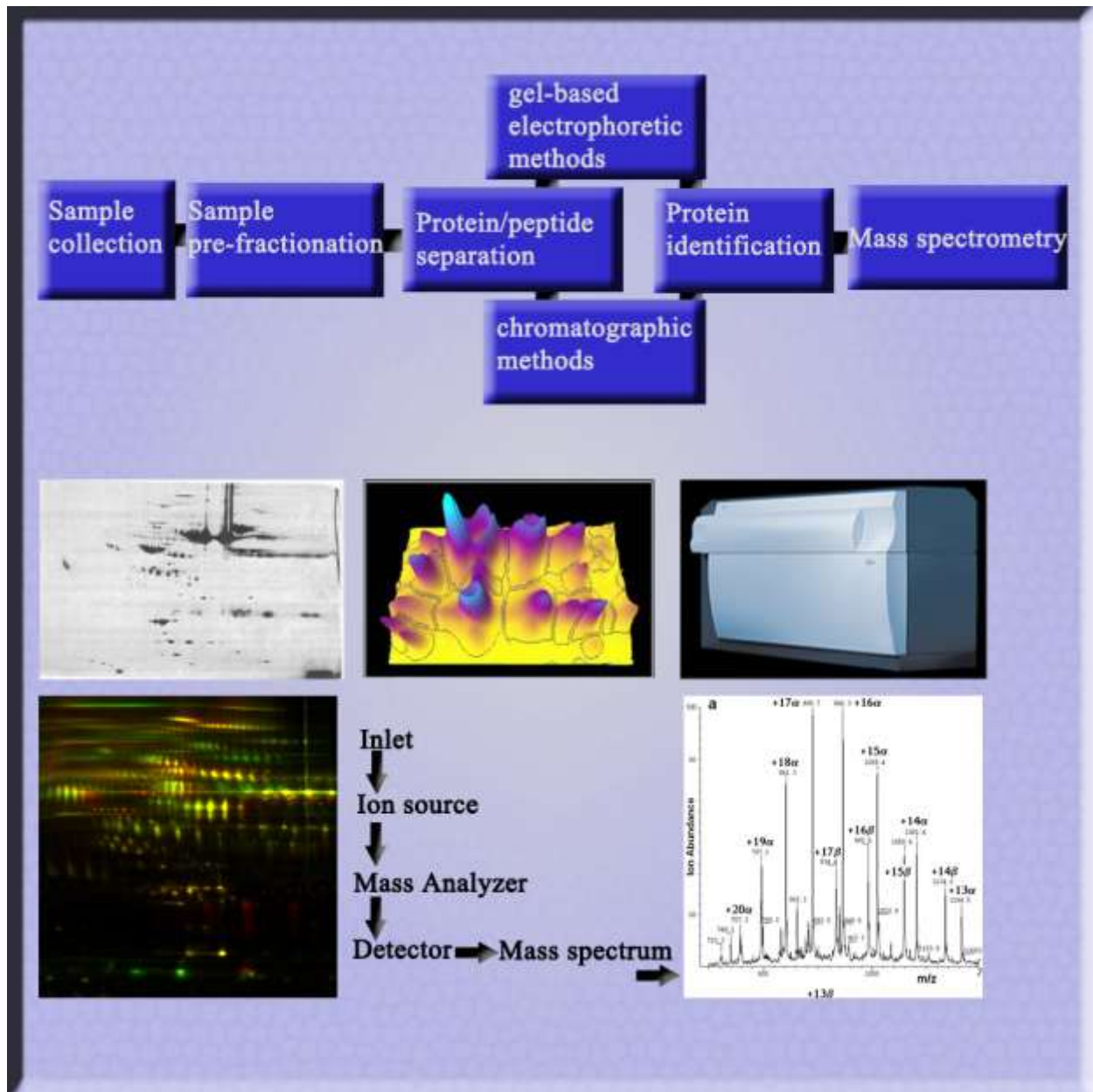


FIGURE 2 The proteomics workflow. As reported in the text, upon sample collection it is possible to perform pre-fractionation techniques in order to normalize the relative quantities of protein species within blood-derived samples. This is particularly necessary in those samples with high dynamic ranges of protein concentrations such as plasma and red blood cells. Proteins or peptides could be addressed with complementary approaches, mainly relying on gel-based techniques such as electrophoresis (first two images on the left) or chromatography. These analytical techniques allow separation of the protein/peptide species by exploiting their biochemical/physical characteristics (molecular weight, mass/charge ratio, isoelectric point, etc.). Separated species are subsequently identified with mass spectrometric tools (right column images). Each protein/peptide is characterized by a unique amino acid sequence which represents its specific molecular fingerprint. Informatic elaboration of the obtained sequences is performed through comparison against online international databases. A score is attributed to each

physiological events (e.g. the composition of sugar moieties of a protein and protein aging in vivo). PTMs exacerbate the variability of the proteome framework and nullify the efforts to individuate a standard proteomic profile of healthy (and pathological) cells.

The interactome, the record of protein-protein interactions, could be of interest in order to understand the interactions among the proteins individuated experimentally. In fact, half of the 300 proteins identified in plasma until 2002 are smaller than the 45-kDa cutoff limit for kidney filtration, thus they must exist as protein complexes not to be cleared from the bloodstream (Anderson and Anderson, 2002). If not standardized, technical caveats behind different proteomics approaches could end up influencing the experimental outcome (Petricoin et al., 2006). This is relevant when considering proteomics applications to transfusion medicine (TM).

One of the main goals of TM is to ensure safety, efficiency and effectiveness of blood components and raw materials for biopharmaceutical fractionation (Atallah et al., 2006). The three mainly transfused blood product types are erythrocyte concentrates, platelet concentrates (PCs) and fresh frozen plasma (FFP) (Atallah et al., 2006). In the last few years, TM units have started to be committed with the collection, storage, banking, manipulation and reinfusion of peripheral blood stem cells either for autologous or for homologous transplantation. Granulocytes or lymphocytes can be collected as well, the former being usually transfused into neutropenic recipients with uncontrolled infectious complications (Peters et al., 2009).

All the procedures performed at blood banks, from collection, processing, testing, production to storage and delivery of blood components, are strictly regulated by laws and/or directives issued by State or government agencies. Previous efforts in TM research, as a heritage of reductionist biology, have been so far aimed to identify single biomarkers to be adopted as diagnostic factors in ordinary clinical analysis (Page et al., 2006). Proteomics instead allows a comprehensive study of protein modifications, yields qualitative and quantitative information and high-throughput protein identification with unprecedented specificity and sensitivity. Therefore proteomics potentially enables a global assessment of processing, pathogen reduction and storage methods, as well as of possible contaminants and neoantigens which may influence the immunogenic capacity of blood-derived therapeutics (Liumbruno et al., 2008). There still remains in TM an ambitious agenda which includes the determination of thorough proteomic profiles to associate with healthy/pathological phenotypes, or as a consequence of the blood bank or industrial manufacturing processes (Allain et al., 2005).

For further details on blood-related proteomics and the technical caveats related to the application of the proteomics workflow to the study of blood-derived therapeutics, the interested reader is referred to the following publications by the candidate:

1. Liumbruno G, D'Alessandro A, Grazzini G, Zolla L.
Blood-related proteomics.
J Proteomics. 2010;73(3):483-507.
2. D'Alessandro A, Zolla L.
Proteomics for quality-control processes in transfusion medicine.
Anal Bioanal Chem. 2010;398(1):111-24.
3. Liumbruno G, D'Alessandro A, Grazzini G, Zolla L.
How has proteomics informed transfusion biology so far?
Crit Rev Oncol Hematol. 2010;76(3):153-72.
4. D'Alessandro A, Zolla L.
Pharmacoproteomics: a chess game on a protein field.
Drug Discov Today. 2010;15(23-24):1015-23.

Red blood cell (RBC) Proteomics

Table 1 summarizes the main proteomic papers on RBCs. In 1982, Rosenblum and co-workers firstly pioneered the RBC membrane proteome by means of 2-DE in normal adults, neonates and patients with erythrocyte membrane disorders (Rosenblum et al., 1982). More than 10 years later, a second proteomic paper was published dealing with 2-DE of RBCs as a model for aging (Aminoff et al., 1992). More in-depth proteomic studies on RBC membranes strictly followed: in 2002 Low and colleagues individuated overall 102 proteins (59 distinct polypeptides, 43 isoforms) by means of 2-DE and MALDI-TOF analysis (Low et al., 2002). Further 1-DE (SDS-PAGE) analysis revealed 25 additional proteins.

In 2004, Kakhniashvili investigated the RBC proteome by means of an IT-MS/MS coupled on-line with a rp-LC. A preliminary pre-fractionation step allowed the separation of membrane and cytoplasmic fractions, which were subsequently further divided into 21 subfractions. MS/MS analyses yielded identification of 182 unique protein sequences, equally distributed either in the membrane fractions (91 proteins) or in the cytoplasmic ones (91 proteins) (Kakhniashvili et al., 2004). Several proteins were reliably identified and catalogued as membrane skeleton proteins, metabolic enzymes, transporters and channel proteins, adhesion proteins, hemoglobins, cellular defense proteins, proteins of the ubiquitin-proteasome system, G-proteins of the Ras family, kinases and chaperone proteins. By contrast, few RBC specific antigens were characterized.

In 2005, Körbel and colleagues investigated the phosphoproteome profile of erythropoietin induced cascades (Korbel et al., 2005). They took advantage of two complementary approaches: the first one included both 2-DE and MALDI-TOF analyses, while the second LC-ESI-MS/MS. Notably, only the latter yielded valid results. This study showed how proteomics can offer the potential to address functional studies of complex signaling processes.

In a recent and interesting study, Tyan and colleagues adopted a special proteolytic chip, consisting of 11-mercaptoundecanoic acid bonded on self-assembled monolayers of alkanethiols onto gold surfaces (Tyan et al., 2005). 2D-nano-HPLC and MS/MS analyses enabled the identification of 272 proteins from erythrocyte protein samples.

In 2005, Bruschi and co-workers individuated 500 spots with soft immobiline GE (Bruschi et al., 2005), among which noteworthy was the presence of high levels of filamentous proteins, such as alpha-spectrin and ankyrins, or integral membrane proteins, such as band 3, band 4.1 and 4.2. Both classes of proteins are not usually displayed or barely present in maps exploiting immobilized pH gradients in the first dimension, while they were revealed through this alternative approach. Indeed, several drawbacks limit the use of 2-DE for proteomic research. Although 2-DE has many benefits, the technique does not lend itself to large-scale, high-throughput proteomic analyses for several reasons. First, not all types of proteins are well resolved in this system. Proteins bearing extremes of size, hydrophobicity, or charge fail to enter the gel and are not represented (Page et al., 2006). Soft immobiline replacing IPG strips in the first dimension of 2-DE allowed to partially overcome these obstacles, especially as far as it regarded high molecular weight (MW) proteins.

Table 1 – Relevant RBC proteomic studies

Authors	Ref	Year	Methods	Proteins individuated	Annotations
Rosenblum	[35]	1982	2-DE (IEF-SDS)	More than 600 spots	A proteomic survey on RBC membrane proteins of adults, neonates and patients with erythrocyte membrane disorders.
Aminoff et al	[36]	1992	2-DE (IEF-SDS)	First evidences of profile changes over aging	First study on aging of RBCs.
Messana et al	[59]	2000	1-DE (SDS)	Band 3 progressive loss during storage	Storage conditions with SAGM and after rejuvenation solution addition pointed out a progressive loss of membrane proteins and, in particular, of band 3. These effects are not restored after addition of the rejuvenation solution.
Low et al	[37]	2002	1-DE or 2-DE (IEF-SDS), MALDI-TOF	102 overall proteins (59 distinct polypeptides, 43 isoforms)	First in-depth study of RBC membrane proteins.
Jiang et al	[44]	2003	2-DE, in-gel digestion, MALDI-TOF	27 spots up-regulated and 15 spots down-regulated	A comparative study between normal RBCs and RBCs from patients affected by type-2 diabetes (a lipid raft protein increased: i.e. flotilin). Synthaxin (target-membrane fusion protein) reduction in diseased patients could explain the alterations in glucose transport mechanisms.
Brand et al	[45]	2004	ICAT (quantitative MS)	Target protein: MafK	Quantitative proteomic studies on murine erythroleukemia (MEL) cell lines revealed that MafK worked as functional switch in erythroid differentiation process by changing its dimerization partner from Batch-1 to NF-E2p45.
Kakhniashvili et al	[47]	2004	rp-HPLC, IT-MS/MS; Gel filtration – LC-MS/MS	181 unique proteins (91 membrane proteins, 91 cytosolic proteins)	Glycophorins. At first, proteasomal subunits were attributed to a small contamination of reticulocytes. Western blot and immune-assays demonstrated that these proteins are expressed by mature RBCs too.
Florens et al	[46]	2004	Biotinylated membrane proteins purification with streptavidin affinity chromatography, trypsin digestion, MudPIT (SCX+rp-HPLC) – MS/MS	PIEP 1 (154 kD) and 2 (49 kD) were characterized (knob-like protrusions on the surface of the parasite infected RBCs)	Analysis of RBCs from malaria infected patients. Two proteins were individuated on the surface of infected erythrocytes (PIEP).
Körbel et al	[39]	2005	2-DE, MALDI-TOF; 1D-LC-ESI-MS/MS	49 proteins identified with 1D-SDS LC-MS/MS	A phosphoprotein profile of RBCs upon erythropoietin receptor activation.
Annis et al	[60]	2005	2-DE (IEF-SDS), in-gel digestion, nanoLC-MS	Leukofiltered supernatants showed a lower number of proteins (thioredoxin peroxidase). Standard non-leukofiltered supernatants displayed more proteins (especially attachment proteins and potentially bioactive proteins).	Analysis of the proteins in the supernatant. Samples were collected fortnightly from day 1 until expiration date (42 days after collection). Supernatants from standard non-leukofiltered RBCs prior to storage displayed a greater number of RBC regulatory proteins.
Kakhniashvili et al	[38]	2005	2D-DIGE, in-gel digestion, nanoLC-ESI-MS/MS	22 unique proteins out of 44 spots (38 spots increased and 11 decreased in diseased patients when compared to control patients)	A comparison between patients affected by sickle cell anemia and control patients. Oxygen scavengers (peroxiredoxins, catalases), proteasome components, heat shock proteins were highly abundant in diseased patients. Lipid raft components (flotilin and stomatin) decreased in sickle cell anemia-affected patients.
Tyan et al	[40]	2005	Gold enzyme chip for tryptic digestion of proteins, MudPIT (SCX+rp-HPLC, ESI-MS/MS analysis)	272 proteins (but only 30 by 2 unique peptides)	This manuscript introduces a novel technology for preliminary sample treatment.
Bruschi et al	[41]	2005	2-DE (Immobiline gels instead of IPG strips + SDS) + MALDI-TOF	500 spots (but only a few new proteins)	Many filamentous proteins (spectrins and ankyrins) were detected.
Chou et al	[48]	2006	ICAT, nanoLC-ESI-IT/MS	19.7% variation ratio between samples	A comparative study between sickle cell anemia-affected patients versus controls.
Pasini et al	[11]	2006	1-DE (SDS), in-gel digestion, LC-ESI-MS/MS (either Q-TOF and LTQ-FT MS)	566 (340 membrane proteins and 252 soluble proteins)	RBCs from control donors were analyzed after 72 and 96 hours of storage. Thirty-nine proteins were found to anomalously migrate and displayed altered MW (degradation or incorrect maturation were proposed as the likely causes).
Prabakaran et al	[49]	2007	2D-DIGE	1200 overall protein spots (49 spots differed between the two groups)	A comparative study between schizophrenic patients versus control patients: RBCs from schizophrenic patients suffered of an increased oxidative stress. Indeed alterations were observed for several ROS quenchers such as selenium binding protein 1, thioredoxin and glutathione reductase.
Goodman et al	[42]	2007	<i>In silico</i> analysis of yet existing databases	751 (review resuming previous studies and depicting a preliminary interactome)	Protein-protein interactions were graphed. The “Repair or destroy” (ROD) box was the fulcrum of the protein network. ROD was made up of chaperonines, heat shock proteins and proteasomal subunits. Being anucleated, erythrocytes almost do not synthesize new proteins. Thus ROD proteins may operate a pivotal role in refolding damaged ones.
D’Amici et al	[58]	2007	2-DE (IEF-SDS), in-gel digestion, nano-rp-HPLC-ESI-MS/MS (IT, Q-TOF)	392 (day 0) 487 (day 14) 447 (day 42)	Erythrocytes were analyzed after 0, 7, 14 or 42 days of 4°C storage under aerobic or anaerobic (under helium) conditions, in presence or absence of protease inhibitors. Changes in spot numbers and electrophoretic mobilities were attributed to oxidative processes. Band 4.1, 4.2, 3 and spectrin were the main targets of these ROS-induced reactions. Total number of spots increased (protein fragmentation) when GSH concentration decreased. Proteases (such as caspases 2 and 3) were absent under anaerobic conditions. Although being more expensive than N ₂ , helium is preferable for oxygen removal since it does not create further radical species (such as nitric oxide).
Roux-Dalvai et al	[66]	2008	Combinatorial Ligand Libraries (CLL) – ProteoMiner – 2-DE (IEF-SDS), nanoLC-ESI-MS/MS	1578 proteins in the cytoplasmic fraction	Peptide ligand libraries allowed in-depth proteomic analysis of RBCs and revealed a whole hidden proteome.
Bosman et al	[61]	2008	1D-GE (SDS), in-gel digestion, nanoHPLC-ESI-	257 (from membrane and vesicles during storage)	Storage reduced membrane-protein variability (less band 3, small G proteins, chaperones and components of the proteasome were observed)

Q/IT-FTICR; semi-quantification with emPAI method (spectral counting exponentially modified protein abundance index)

while increased the total number of microvesicle-isolated proteins (especially as it regarded Hb, band 3, CD47, complement proteins and metabolic enzymes); glucose transporter was found to increase in the membrane fraction of stored RBCs, suggestive of RBC resistance to storage lesions.

In 2006, Pasini et al. carried out a thorough proteomic analysis of RBCs, which consisted of 1-DE (SDS-PAGE) followed by in-gel digestion and LC-ESI-MS/MS (either Q-TOF and FTICR) (Pasini et al., 2006). Experimental observations revealed 340 membrane and 252 soluble proteins. Thirty-nine proteins were found to anomalously migrate, resulting in an unexpected perceived molecular-weight. This was attributed either to co-migration phenomena with ubiquitins, as a result of partial degradation, or to the outcome of incorrect maturation events, as a remainder from reticulocytes.

In 2007, Goodman and colleagues elaborated an *in silico* analysis of the interactome of RBCs basing on a summary of overall 751 proteins from previously published studies. The “interactome” scheme orbited around a central fulcrum of expressed proteins. This central core of expression encompassed a series of proteins involved in physiological responses to oxidative stress and unfolding (e.g. peroxiredoxins, catalases, chaperonins, heat shock proteins and proteasomal subunits). Thus, the authors named it the Repair or Destroy (ROD) box after the biological role of these classes of proteins (Goodman et al., 2007). These findings highlight the molecular behavior of RBCs, which are enucleated and base their survival on the maintenance of the damaged proteome instead of on the synthesis of new proteins.

A recent paper described the peculiar adoption of combinatorial ligand libraries of hexapeptides (sequences of 6 aminoacids) as a powerful tool for sample pre-fractionation. Hexapeptides were packed in the stationary phase of chromatographic affinity columns, although each column only contained one species of aminoacids. Aminoacids were named “petit catchers” and “grand catchers” after their capacity to interact and retain peptides in the pre-fractionation steps (**Figure 3**).

This protocol allowed the individuation of approximately 800 proteins upon 2-DE (SDS-IEF) and by nanoLC-ESI-MS/MS (Simò et al., 2008). Being repeatedly eluted from each one of the 16 affinity columns, a group of 72 proteins represented the “minimum common denominator”. It is worthwhile to underline that better outcomes were obtained with hydrophobic aminoacids, as polarity seemed to be a negative interaction-factor.

Proteomic approaches could be used either for basic or applied research. An example of the latter is the study performed in 2003 by Jiang and colleagues, who showed protein dysregulation in the RBC membrane of type-2 diabetic patients (Jiang et al., 2003). RBCs from healthy subjects and from patients suffering from type-2 diabetes were analyzed with 2-DE and identified with MALDI-TOF. Analyses evidenced up-regulation of 27 spots (for example: flotilin, a lipid-raft protein) and down-regulation of 15 proteins in diseased RBCs. Particularly telling was

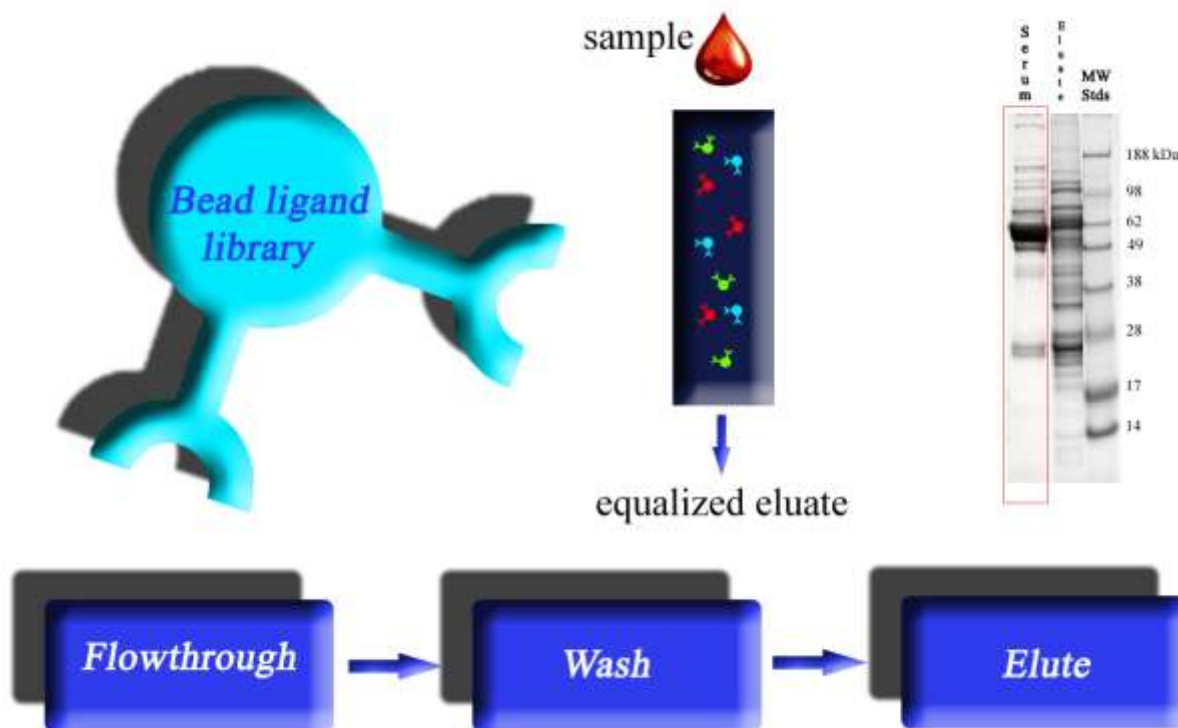


FIGURE 3 Recently, pre-fractionation methods have been referred to as a panacea to complex samples analysis. Of all the procedures, combinatorial ligand libraries appear to be the most appealing solution. Hexapeptide ligand libraries could be packed into the stationary phase of affinity chromatography columns. Complex samples, such as plasma or serum, are introduced in the column. High and low abundant proteins both interact with different and specific libraries and are retained in the stationary phase. However, high abundant proteins rapidly saturate their targeted bead ligand libraries, thus they readily flow through the column. Multiple wash steps could be performed in order to clean the column from unbound components. In the end, elution is performed. In the eluted fraction, high-abundant species result to be drastically reduced (but not absent), while low-abundant species have been now concentrated. As a result of equalization, new proteins are now perceivable through classic proteomic analyses (e.g. 1D-SDS-PAGE), enabling detection of the “hidden proteome”.

the diminished expression of syntaxin, which was indicated to be involved in the misregulation of glucose transport (Jiang et al., 2003).

In 2004, quantitative MS studies (isotope coded affinity tagging - ICAT (Brand et al., 2004)) on murine-erythroleukemia cell lines revealed that Mafk worked as a functional switch for erythroid differentiation processes by changing its dimerization partner from Batch-1 to NF-E2p45.

High-throughput proteomic approaches could be used to discriminate between healthy RBC populations and erythrocytes infected by *Plasmodium falciparum* (Florens et al., 2004). After a preliminary biotinylation step, Florens et al. performed a purification of membrane proteins by means of streptavidin affinity chromatography. These proteins were further analyzed with multidimensional protein identification technology (MudPIT), which

included 2D-HPLC (SCX, rp-HPLC) online with a MS/MS analysis. Two proteins were characterized from knob-like protrusions on the surface of parasite infected RBCs, namely PIEP1 (154 kD) and 2 (49 kD).

In 2005, Goodman's group performed a thorough study on RBCs from patients affected by sickle-cell anemia (Kakhniashvili et al., 2005). Tandem MS analysis utterly identified 22 unique proteins out of 44 electrophoretic spots. The authors found that anomalous RBCs highly expressed oxygen scavengers (peroxiredoxins, catalases), proteasome components and heat shock proteins in comparison to healthy controls. Lipid raft components (flotilin and stomatin) decreased in sickle cell anemia-affected patients. An analogue study with shared authors was performed in 2006, this time by means of ICAT and nanoLC-ESI-IT-MS (Chou et al., 2006). No significant variations were observed in sickle cell anaemia RBCs versus healthy cells as it concerned the core skeleton proteins (alpha spectrin, beta spectrin, band 4.1 and actin). On the other hand, changes in proteins related to oxidative stress were detected, though not as easily as in the aforementioned study (Kakhniashvili et al., 2005). This was attributed by some intrinsic limitations of the ICAT approach, which was hereby suggested to be used in parallel to classic gel-based approaches.

Indirectly, RBC alterations could correlate with non-properly blood-related pathologies, such as schizophrenia. Accumulating evidence has recently suggested for a peripheral component to schizophrenia (Prabakaran et al., 2007). This is what emerged from a recent study which addressed a pool of healthy and schizophrenic patients. Prabakaran et al. adopted 2-DE to separate 1200 spots, 49 of which were differentially expressed when comparing these groups. As a result, RBCs from schizophrenic patients turned out to suffer from an increased oxidative stress, since profound alterations were observed for several ROS quenchers, such as selenium binding protein 1, thioredoxin and glutathion reductase.

A functional proteomic approach could be hopefully adopted to address both the donor and the final product (see the study of Jiang and colleagues from type-2 diabetes-affected subjects (Jiang et al., 2003)), but also to test the effectiveness and efficiency of the various stages of the blood-banking production chain. Storage of RBCs is undoubtedly one of these topic and long-debated steps. Erythrocyte concentrates can be actually stored in PVC bags in presence of anticoagulants at 1-6°C for a maximum of 42 days; in vivo recovery 24 hours after re-infusion must be over the 75% threshold (Council of Europe, 2008). The time of storage has been linked to an increased risk of untoward effects after reinfusion to the recipients, although data are not coming from randomized prospective clinical trials (reviewed in Grazzini and Vaglio, 2012). This is mainly due to the lesions which accumulate during storage of RBCs. Several interventions have been proposed in order to overpass these hurdles, such as the addition of additive or rejuvenation solutions () or the adoption of alternative storage protocols such as frozen [56] or anaerobic (Yoshida et al., 2007) storage. Proteomics tools have been used to glean insight of the proteome variability in all these circumstances (Messana et al., 2000; Annis et al., 2005; D'Amici et al., 2007; Bosman et al., 2008).

So far, the quality of stored RBCs has been tested with routinely clinical tools. A few parameters have been so far addressed: in vivo recovery after 24 hours from reinfusion, which is followed by means of ⁵¹C isotope; pO₂ - from which sO₂ could be derived - that is measured by specific oxygen sensors; haemolysis values, glucose, DPG and ATP levels as well as pH, by means of standard biochemical approaches. As far as it regards the sensitivity and

specificity parameters, proteomic tools are currently unrivaled and will hopefully integrate or substitute the above-mentioned routine criteria.

The first proteomic study of stored RBCs addressed metabolic alterations of erythrocytes during storage (Messana et al., 2000). Messana et al. (2000) collected samples fortnightly until unit expiry prior to the analytical phase with SDS-PAGE. Oxygen-dependent metabolic modulation resulted to be progressively altered during storage and even an addition of rejuvenation solutions at day 21 did not contribute to restore it. Band 3 was identified as a crucial factor in mediating RBC storage lesions.

Annis and colleagues performed a proteomic analysis (2-DE, nanoLC-MS) of the proteins that accumulate in the supernatant of leukoreduced and non-leukoreduced stored samples (Annis et al., 2005). Much lower amounts of proteins were present in the supernatants of leukofiltered RBCs and, although the majority of proteins identified by MS were common to both types of RBC concentrates, transthyretin (a transport/binding protein), Ig k-light chain (Igk), serum amyloid P (SAP), and connective tissue activating peptide III (CTAP-III) accumulated predominantly in non-leukoreduced RBCs, whereas cytosolic enzymes, such as carbonic anhydrase I and thioredoxin peroxidase B, were found to accumulate in leukofiltered RBCs. The unexpected increase of serum proteins, such as transthyretin, Igk, and SAP, was explained basing on the fact that they are physiologically absorbed on the cell surface and then released during storage (Queloz et al., 2006). These findings have been linked to the importance of white blood cell (WBC)-reduction prior to storage in the abrogation of the pro-inflammatory response elicited by supernatants from stored RBCs (Annis et al., 2006). Therefore, the presence of WBCs could represent a burden in increasing the number and strength of RBC adhesion to vascular endothelium (Sparrow et al., 2004). The accumulation of cytosolic proteins in the supernatant of leukofiltered RBCs is instead explained with storage-related haemolysis (Annis et al., 2006).

A recent article by Zolla's group examined the changes of RBC cytoskeleton during storage of SAGM-preserved non-leukodepleted RBC units either under anaerobic or aerobic conditions (D'Amici et al., 2007). Leukoreduction was not performed, in order to include any contribution of leukocytes to proteolytic cleavage and ROS production. The authors used 2-DE to evaluate RBC membrane changes over storage, either under atmospheric oxygen or helium, in the presence or absence of protease inhibitors. Indeed, the etiology of lesions in RBC membranes involves both ROS and proteolytic enzyme activity (Valeri et al., 2000; Hogman and Meryman, 2006; Hess, 2006; Klein et al., 2007). The authors observed a gradual increase in the number of protein spots on gel-maps over the first 14 days of storage. Oxygen exacerbated cytoskeleton protein attack by ROS, whereas only a small number of changes were related to proteolytic cleavage, which seemed to play a minor role in storage lesions in comparison to protein oxidization. During the first 7 days of storage, oxidative damage was observed prevalently in band 4.2, to a minor extent in bands 4.1 and 3, and in spectrin. All those factors may contribute to stress the formation of neoantigens and the accumulation of storage lesions in blood units. Protein degradation was greatly reduced in the absence of oxygen, when blood was stored under helium. In agreement with data from Yoshida and his group (Yoshida et al., 2007; Yoshida et al., 2008; Dumont et al., 2009), this study confirmed that any action to improve storage conditions should be carried out in the first weeks in order to prevent damages of the membrane-

cytoskeleton network and, to this end, oxygen removal is a more effective way of limiting RBC storage lesions than any chemical addition.

An emphasis should be put on the possible role of the micro- and nano-vesicles as diagnostic and investigative tools. RBCs lose membrane, both *in vivo* and during *ex vivo* storage, by the blebbing of vesicles from the tips of echinocytic spicules. Vesicles shed by RBCs *in vivo* are rapidly removed by the reticuloendothelial system. During storage, this loss of membrane contributes to the storage lesion and the accumulation of the vesicles are believed to be thrombogenic and, thus, to be clinically important. From a recent study it emerged that storage reduced membrane-protein variability and increased the number of proteins individuated in blebbing micro- and nano-vesicles (Bosman et al., 2008). Bosman and colleagues (2008) investigated the proteome of RBC membranes and of these vesicles. The authors identified a total of 257 proteins with 1-DE (SDS-PAGE) followed by in-gel digestion, nanoHPLC-ESI-MS/MS (Q and FTICR) and partially quantified with semi-quantitative method emPAI (exponentially modified protein abundance index). Micro-vesicles contained almost no integral membrane proteins or cytoskeletal components, with the exception of band 3 and actin. The protein composition of the nanovesicles differed from the protein content of microvesicles and RBC membranes, in that nanovesicles contained a conspicuous number of complement and immunoglobulin proteins. Storage reduced membrane protein variability (lower levels of expression of band 3, small G proteins, chaperones and components of the proteasome) while it increased the total number of microvesicle-isolated proteins (Hb, band 3, CD47 and metabolic enzymes) [61]. The authors concluded that storage is likely to disturb/accelerate physiological processes such as cellular aging, and the accelerated appearance of physiological removal signals in the RBC membrane (for example, neoantigens from band 3) might have a role in determining the survival of RBC after reinfusion.

To conclude this section, RBCs have been one of the eligible targets for proteomic investigations due to their importance in TM, and the relative simplicity of their protein profiles as a consequence of their enucleated nature. Prospective proteomic studies, taking advantage of the actual basic knowledge, will probably focus on the metabolic and post-translational modification/quantitative changes of *in vivo* and *ex vivo* (stored) RBCs. In this view, new proteomic techniques have recently expressed their detection potential (1578 proteins) in a fast (ORBITRAP MS) and high-throughput way (Roux-Dalvai et al., 2008). Indeed, removal of haemoglobin, which quantitatively represents the 98% of the RBC proteome, has recently opened a completely new scenario by conveying a portrait of RBCs by far more detailed and exhaustive than ever before.

Proteomics and Red Blood cells: Conclusions

In this section we purported to sail through the mare magnum of proteomic investigations in merit of RBCs (at least providing the background from which the elaboration of this thesis project moved its first steps forward).

In a close future, proteomic investigations could be used from bench to bedside in order to test the quality of collected blood components prior to or during storage, to verify the effects of the production processes of blood components and plasma derivatives on the protein fractions, to reduce the effects of the storage lesions or to discover peculiar biomarkers readily adoptable for early diagnosis or targeted evaluation of blood therapeutics integrity, functionality or immunogenic potential, as well as to assess proliferation capacity of hematopoietic stem

cells for therapeutic treatments. In addition, functional proteomic approaches have recently shifted the focus of attention from the final product to the provider (donor), thus proteomics could represent the fulcrum of this sort of Copernican revolution in TM (**Figure 4**). Until recent years, several key aspects in the blood-banking production processes have been completely ignored, such as those related to peptide and protein changes in blood products. Emerging concepts from recent blood-related proteomics have strengthened the belief about the importance of leukoreduction procedures prior to storage in order to reduce side-effects in blood transfusion recipients.

The Sherlock Holmes of the third millennium ought to make the tough choice and find a compromise between the cheapest, quickest and most sensitive technique for the question being posed. Undoubtedly, every technique has its advantages and drawbacks, such as for 2-DE (SDS-IEF) and BN-GE, when handling high-molecular weight or hydrophobic membrane proteins. In like fashion to Kant's critical philosophy, in which the position of the knower of the world in general is not only taken into account, but also has a determinant impact on the structure of his/her known world, the choice of the most suitable method to adopt in each circumstance will reflect into a different result (for example, protein-centric versus peptide-centric approaches).

To conclude, proteomics has sculptured the figure of the modern scientist, who is now endowed with detection instruments of unprecedented sensitivity and specificity.

Many strides have been made in the field of blood-related proteomics and many others appear to be at hand. Quantitative proteomics and post-translational modifications are the declared next goal.



FIGURE 4 Recent functional proteomic approaches have shifted the focus of attention from the end-product to the suitability of the donor.

Metabolomics: red blood cells, transfusion medicine and clinical biochemistry

Metabolomics is the lesser-known cousin to genomics and proteomics. Embracing the “omics” philosophy, this discipline seeks to measure the concentrations of nominally all of the [small molecular weight (MW) – below 1.5 kDa] metabolites in a particular system, for example, a body fluid such as serum or a pool of cells (Dunn and Ellis, 2005; D’Alessandro et al., 2011). However, a more restricted subset is measured in practice. This is mainly due to the huge chemical diversity of metabolic compounds, especially in terms of polarity (Kell et al., 2006). The number of human metabolites estimated via genomics (approximately 3000) and the number measured experimentally are rapidly converging over the last few years (Kell et al., 2006). Nevertheless, the measured metabolome is greater than that encoded by the genome, as it will include molecules acquired exogenously as drugs, foods or food additives, and will also include molecules derived from the microflora of the host (Kell et al., 2006).

Directly profiling metabolites (metabolic profiling or metabolomics) has distinct advantages over other “omics” approaches in efficiently building knowledge of biological status. Biologically relevant information includes the genesis of metabolic biomarkers, the progress of a disease, and the modes of action, efficacy, off-target effects and toxicity of pharmaceutical drugs, storage solutions for blood components and storage quality control (Kell et al., 2006).

Indeed, intermediary metabolism is proximal to phenotype, and the possibility to measure metabolites quantitatively and semi-comprehensively allows for almost immediate screening of biological matrices, which is often difficult to obtain with other “omics” approaches (Morris and Watkins, 2005).

At the same time, metabolomics is also clinical biochemistry “on steroids” (Wishart, 2008). In clinical chemistry, most metabolites are typically identified and quantified using colorimetric chemical assays. In metabolomics, large numbers (tens to hundreds) of metabolites are measured within minutes using non-chemical, non-colorimetric methods such as chromatography - mass spectrometry and Nuclear Magnetic Resonance (NMR) (Wishart, 2008). The close relation to clinical biochemistry, which is routinely used in everyday screening of patients worldwide, might allow easier translation of novel findings from discovery science, this being a critical step for all of the other “omics” so far. In clinical practice, the extension of actual protocols to those biomarkers discovered through genomics and proteomics has not hitherto taken proportional advantage of the wealth of data available. For example, in the United States the rate of introduction of protein tests approved by the Food and Drug Administration has declined to less than one new protein diagnostic marker per year (Anderson and Anderson, 2002).

Advancements in metabolomics

In the late 1940s Williams introduced the concept that individuals might be characterized by a unique “metabolic profile” (the composition of their biological fluids) that could reflect their health condition (Williams et al., 1951). However, it was only upon the optimization of extraction methods (Bligh and Dyer, 1959) and the introduction of more sensitive analytical platforms, such as novel NMR and mass spectrometers (MS) that metabolomics began to flourish.

Earliest approaches to metabolomic investigations mainly relied on NMR, which was favoured by machine accessibility, established data handling, and the nondestructive nature of the analysis (Nicholson et al., 1999). Nonetheless, NMR has been gradually complemented by MS, as both technologies hold several advantages.

A brief list of the “pros” of the former includes easy sample preparation, no derivatization necessary, safe metabolite identification and quantification, non-destructive nature of the analysis (both on intact tissue and biofluids), easy sample automation, and the possibility to translate applications to ex vivo or in vivo samples.

The latter has higher sensitivity, improved metabolite discrimination, coverage of the metabolome space, and is characterized by modularity to perform compound-class-specific analyses, other than to a dramatically reduced demand for starting material necessary to perform an extensive analysis (Griffiths et al., 2010).

Both NMR- and MS-based metabolomics have some limitations as well, including the timing or temporal relationship of biological intermediates, the rapidity of enzymatic kinetics and variability across individuals (biological variability).

MS is often coupled to pre-analytical approaches, such as gas chromatography, liquid chromatography and capillary electrophoresis. Gas chromatography is dampened by the poor discrimination against large intermediates such as nucleotides, flavines, and coenzyme A derivatives. Liquid chromatography holds several advantages, viz widespread coverage, sensitivity, ease-of-use, robustness to matrix, and robustness in routine operation. Capillary electrophoresis is equivalent to liquid chromatography in terms of separation and sensitivity, although it lacks in robustness, which is pivotal for routine analysis of biological extracts (Buescher et al., 2009).

Recent advances are not only inherent to the analysis itself, but also include the creation of ad hoc freely available databases (such as METLIN – Smith et al., 2005 – or MAVEN – Clasquin et al., 2012) or the introduction of specific bioinformatic tools. Software advancements now enable the production (and computer-readable encoding as SBML) of metabolic network models reconstructed from genome sequences, as well as experimental measurements of much of the metabolome (Kell et al., 2006). In like fashion to functional enrichment of proteomics data (pathway analyses, gene ontology term enrichment, protein-protein interaction modeling (D’Alessandro and Zolla, 2010)), metabolic modeling exploits metabolic networks or logical graphs, and resources such as Kyoto Encyclopedia of Genes and Genomes (KEGG) (Kanehisa et al., 2006).

As in proteomics, one of the main challenges in metabolomics is to cope with the very diverse range of metabolites found within the cell (either hydrophilic or lipophilic), in conjunction with the large dynamic range of metabolite concentrations (Griffin, 2006).

Conversely, unlike signalling pathways (Kell et al., 2006), metabolic networks are subject to strict stoichiometric constraints. In other terms, slight changes at the protein level might be amplified at the metabolite level both in theory (Mendes et al., 1996) and in practice (Urbanczyk-Wochniak et al., 2003).

Besides, changes at the metabolic level might be occasioned by disease or pharmaceutical intervention (Harrigan and Goodacre, 2003).

MS-based metabolomics also offers the potential to perform targeted analyses, through selection, isolation and fragmentation of precursor ions and subsequent isolation of the product ions (features) of interest. This “targeted”

metabolomics strategy is known as Selected/Multiple Reaction Monitoring (SRM or MRM) (D'Alessandro et al., 2011).

However, in discovery-science metabolomics only 'untargeted' strategies allow individuating molecules whose concentrations are unexpectedly fluctuating in the experimental matrix under investigation.

As an extension of clinical biochemistry, the metabolome is chemical pathology writ large. Therefore, it is realistic enough to assume that measuring small molecule concentrations in biofluids will prove out to be of significant utility in various kinds of diagnosis, with obvious consequences in the fields of haematology, transfusion medicine (D'Alessandro et al., 2012), drug design, development and testing (Harrigan and Goodacre, 2003).

Metabolomics and clinical biochemistry: towards blood (and red blood cell) testing

Centuries of scientific advancements have paved the way for the relatively recent great strides in clinical biochemistry, a field which mainly relies upon biochemical analyses of various body fluids, prime amongst which are urine¹, blood and cerebrospinal fluid (Olukoga et al., 1997). Technological innovation, through the introduction of cutting edge instrumentation has enabled decades of substantial improvements in the field of standard analytical chemistry in the clinical setting.

At its dawn, clinical biochemistry relied on rudimental approaches, such as in the case of Richard Bright's (1789-1858) test for proteinuria in cases of suspected renal disease, in which a candle flame was used to heat urine in a tablespoon (Bright, 1836).

Only minor technological improvements could date back to the early twentieth century. As reported by Olukoga et al. (1858), the equipment of a clinical pathology laboratory within a 200-bedded American hospital in 1920 listed "a centrifuge, a urinometer, two monocular microscopes, two small substage microscope lights, a Bunsen burner, a Dubosq colorimeter, a basal metabolic rate machine, an electro-cardiograph, a microtome, a knife, a paraffin bath, a few antisera and an assortment of test tubes, beakers and pipettes".

The dawn of blood collection

Other than testing, collection of blood samples was challenging as well, since only small blood volumes could be obtained by finger prick or either collected by 'cut-down' to expose the vein, with subsequent venesection and cupping⁶. Indeed, the first hypodermic needle was created in 1840s by Francis Rynd for local injection of opiate in the treatment of neuralgia (Winsten, 1969): it was made of steel and accompanied by a hard rubber hub. Subsequent strides in the field of blood collection are to be attributed to the introduction of new syringe materials for the collection tube, since the rubber was replaced with glass to allow syringes to be reused. Finally, the Luer-Lok syringe provided a convenient method of attaching and removing the hypodermic needle from the glass syringe⁴.

Collection tubes containing small volumes of additives (e.g. anticoagulants) have represented a standard in blood collection procedures since their first appearance in the 1950s. Along the last fifty years, manufacturers have introduced only minor modifications to collection tubes, including the use of plastic as the primary tube component, and the addition of polymer gel or clot activator (Bowen et al., 2010).

Early analytical methods

In the history of clinical chemistry, separation technologies held a key role, with the centrifuge being invented in 1883 by the Swedish engineer Carl Gustav Patrik de Laval (1845-1913) (Lines, 1977).

Further advancements in analytical chemistry were then due to the theoretical and practical foundation of emission spectroscopy (a technique could be used to identify elements by means of the characteristic spectra of their free atoms), which dates back to the 1820s when John Frederick William Herschel (1792-1871) and Talbot.^{10,11} However, it was only in 1860 that this phenomenon could be fully explained by Robert Bunsen and Gustav Robert Kirchoff (1824-1887). Therefore, early strides in analytical methods in clinical biochemistry mostly stem from the brilliant work of Robert Wilhelm Bunsen (1811-1899), who introduced spectroanalysis and the concept of coefficient of extinction and, thereby, spectroscopy, which allowed detecting the various spectrogenic pigments in blood (Lines, 1977).

Analytical application of emission spectroscopy can be attributed to the work of Henrik Gunnar Lundgardh (1888-1969), who introduced the flame photometer for a direct estimation of the concentrations of specific elements. The rudimentary version of the photometer was based on a mixture of air and acetylene (energy source), while the emitted light was dispersed by a quartz prism and captured on a photographic plate (Olukoga et al., 1997). This instrument was used to perform electrolyte determinations in body fluids, overcoming the cumbersome titrimetric or colorimetric assays which had hitherto represented the traditional approach. Nevertheless, it was only in 1955 that the technique was applied in a clinical setting for quantitative elemental analysis (Walsh, 1955).

Other than spectroscopy, electrophoresis is one of the most widely diffused methods to investigate proteins in the clinical setting. The first electrophoresis apparatus was devised in 1937 by Arne Wilhelm Tiselius (1902-1971) (Tiselius, 1937).

Finally, chromatography was introduced by the Russian botanist Mikhail Tsvett (1872-1919) who described the absorption chromatography in 1906 in the frame of a research based upon the separation of plant pigments into their constituent parts (De Benedetti, Tsvet, 1956).

Despite analytical methods were available decades before, it was only with the introduction of automation by Leonard Skeggs (1957) that clinical chemistry started taking actual advantage of these analytical approaches. As reviewed by Rocks and Riley,¹⁶ the AutoAnalyzer was characterized by a single-channel, continuous flow, batch analyser that provided one result per analyte for each specimen at a rate of 40-60 specimens per hour (Skeggs, 1957; Rocks and Riley, 1986).

However, greater number of samples increase the complexity of the data handling process (collection, validation and interpretation) in the clinical setting, which represented a challenge until the introduction of computers and *ad hoc* software into laboratory work. In recent times (last two decades), the capillarity of internet connections has thus allowed further easing centralization and distribution of clinical data.

Despite the above mentioned implementations in the field of clinical chemistry, the introduction of novel technologies, such as metabolomics will likely enough add up to the analytical strategies currently at disposal of clinical experts.

Metabolomics

One of the main analytical advancements over the last decades has been represented by the introduction of Omics disciplines, that is to say those disciplines which investigate only certain classes of biomolecules in their entirety in biological matrices. Omic-oriented strategies have been designed as to delve into biological complexity as a whole (e.g. proteins in proteomics, mRNAs in transcriptomics), rather than dissecting biological samples through targeted analysis of single molecules.¹⁷ While at the beginning of the third millennium genomics (investigating the whole genome compartment) represented perhaps the leading science, during the last ten years it has been possible to observe the dramatic expansion of the fields of proteomics (proteins), lipidomics (lipids) and metabolomics (metabolites) (Nicholson et al., 2008; Roux et al., 2011; Serkova et al., 2011; Christians et al., 2011; Kortz et al., 2011; D'Alessandro et al., 2012; Krisp et al., 2012; Himmelsbach, 2012; Rhee and Gerszten, 2012).

Metabolomics investigates the metabolome within a specific biological matrix (biological fluid, tissue, cells), that is to say the molecular complement to the genome and proteome below the 1.5 kDa range (Nicholson et al., 2008). Being closer to the phenotype than any other omics discipline, metabolomics and metabolic patterns have been in depth investigated in many fields of basic and applied research, including toxicology (Robertson et al., 2011), pharmaceutical research (Pichini et al., 1996; Lindon et al., 2004; Nicholson et al., 2011; Wei, 2011) and fertility research (Singh and Sinclair, 2007; Bromer and Seli, 2008; D'Alessandro et al., 2012; Nel-Themaat et al., 2011). More recently, a role has been proposed for metabolomics in clinical biochemistry and personalized medicine (Lindon et al., 2003; Holmes and Nicholson, 2007; Mayr, 2008; Gowda et al., 2008; Giovane et al., 2008; Kaddurah-Dakou et al., 2008; Lane et al., 2009; Koulman et al., 2009; Bowen and Northen, 2010; Vinayavekhin et al., 2010; McNiven et al., 2011; Robertson et al., 2011; Holmes et al., 2011) in that whether an experimental connection will emerge between metabolome profiles and specific diseases, metabolomics could soon become a reliable and robust analytical approach in predictive medicine. Indeed, the origins of metabolomics share consistent traits with clinical biochemistry, which has historically pursued determination of standard and anomalous parameters (i.e. absolute concentration, relative abundance, etc.) of small molecular compounds in blood and its components (plasma/serum and cellular fractions).

Metabolomics: historical perspectives and future directions

Citing Roux et al. (2011), “biochemists have long been doing metabolomics, just like the Bourgeois Gentilhomme was speaking prose without knowing it” (Molière – Bourgeois Gentilhomme II. 4).

Despite early applications in 1960's, it was only in 1971 that Pauling, Robinson et al. conceived the core concept of modern metabolomics, which posits that “information-rich data reflecting the functional status of a complex biological system resides in the quantitative and qualitative pattern of metabolites in body fluids” (Pauling et al., 1971).

The metabolome is also referred to as the set of small molecular mass organic compounds found in a given biological media, which includes endogenous compounds (all organic substances naturally occurring from the metabolism of the studied living organism), and xenobiotics (and their catabolic products). Metabolic analyses at first relied upon nuclear magnetic resonance (NMR), although recent improvement in the field of mass spectrometry (MS) made available two complementary methods which allow detecting from a few hundreds to thousands of

signals related to both genetic and environmental contributions. Each technique holds specific advantages over the other: while NMR was favoured by (i) machine accessibility; (ii) established data handling; and (iii) the nondestructive nature of the analysis; MS has gradually complemented NMR owing to its (i) higher sensitivity; (ii) improved metabolite discrimination; (iii) coverage of the metabolome space; and (iv) modularity to perform compound-class-specific analyses; other than to (v) a dramatically reduced demand for starting material necessary to perform an extensive analysis (Sana et al., 2008; Buescher et al., 2010). MS also allows to perform (vi) targeted analyses, through monitoring of one (or a handful) of metabolites through isolation and fragmentation of precursor ion and subsequent isolation of the fragmented transitions, a workflow which is known as selected/multiple reaction monitoring (SRM or MRM) (D'Alessandro et al., 2011). Direct monitoring of specific metabolites allows quantitation throughout a wide spread range of linear concentrations (from mM to nM, down to picomole quantities, depending on the characteristics of the MS instruments) and results in less demanding requirements for analyte volumes (0.5 μ l as in the case of blastocoele fluid (D'Alessandro et al., 2012)).

The recent improvements in the field of metabolomics are not only to be attributed to technical advancements, but also to the creation of specific software and databases which now allow mapping and interpreting metabolic fluctuations with relative ease (Ekins et al., 2007; Jamshidi and Palsson, 2008; Wishart et al., 2010). These improvements have opened brand new scenarios in the field of red blood cell investigations (basic science systems biology (Jamshidi et al., 2001; Price et al., 2003; Jamshidi and Palsson, 2006), red blood cell cold liquid (D'Alessandro et al., 2012)-or cryo- storage (Pallotta et al., 2012) for transfusion purposes), being erythrocyte both one of the simplest biological cell models and a unique treasure trove of either direct or indirect biological signatures (biomarkers) for most various diseases and pathological conditions.

Integrated Omics and Clinical Chemistry - the four paths of the new couple or the guidelines for a happy marriage

One main goal in the ambitious agenda of both metabolomics (or “omics”, in general) researchers and clinician experts is to rapidly configure a *rendez-vous* point and propose future directions which deserves further joint explorations. Hereby we propose four main objectives (**Figure 5**) that are already technically feasible and could be at hand within the next few years.

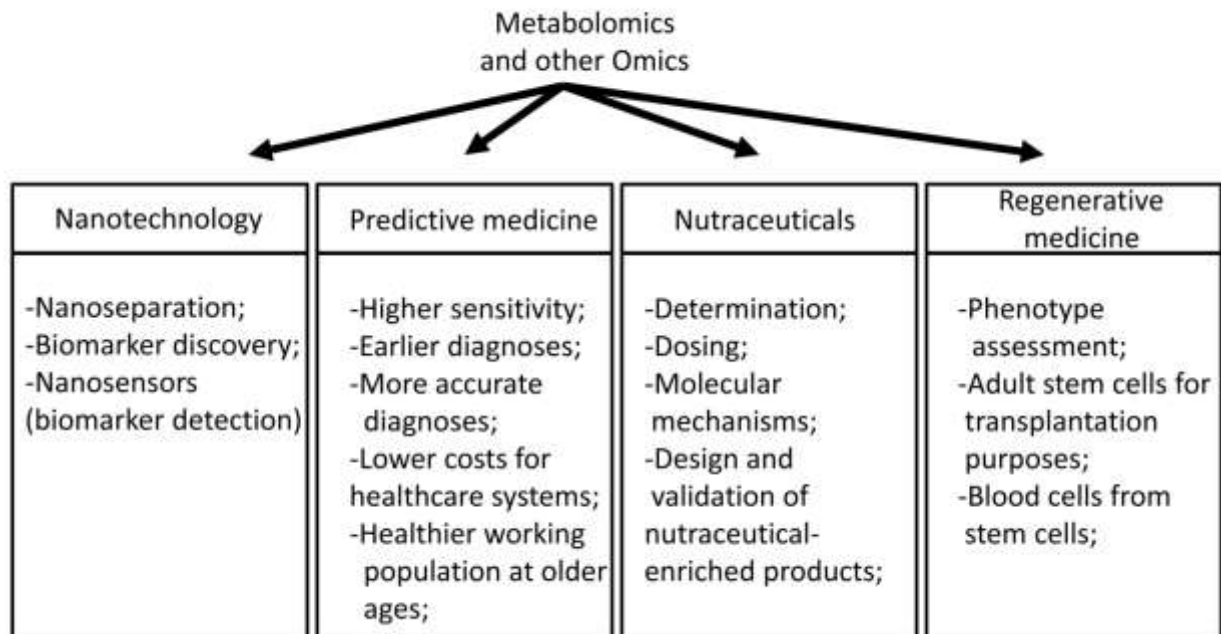


FIGURE 5 – An overview of the likely applications of metabolomics and other omics disciplines in the future of clinical chemistry and transfusion medicine.

Nano-HPLC and nanosensors for targeted detection of metabolites

Theoretical and technical improvements have recently allowed separation of biological compounds at the nanoscale. Rapid resolution HPLC approaches of nano-fluxes and MS instruments with over 1×10^6 resolving power (Nicolardi et al., 2011) have boosted Omics disciplines, including metabolomics, which could soon be elicited as investigative approaches indicating biomarkers to implement nanosensors (Cullum and Vo-Dinh, 2000) to most various biological compounds (in like fashion to glucose nanosensors for diabetes (Jeffery, 2011)), thus dramatically enhancing the sensitivity of clinical chemistry assays.

Predictive medicine

Enhanced sensitivity and improved metabolite coverage also translates into faster and more accurate predictive capacity. In a society where ageing is rapidly becoming the main challenge of 21st century both in western and rapidly developing countries, it is becoming mandatory to tackle the life-long quality issue. In this frame, prevention and therefore predictive medicine have been erected as the watch-tower in the strive to guarantee a better quality life for a longer period to the greatest possible portion of the population worldwide. Early diagnoses indeed result in more effective therapies and lower costs for the whole healthcare systems, and could pave the way for a healthier (other than older) working population.

Metabolomics: Red blood cells and Clinical Biochemistry - Conclusions

In the next few years, we will testify a big stride in the field of metabolomics and clinical chemistry, since the valuable expertise accumulated in laboratory science (mostly in the field of “omics” disciplines, such as metabolomics, and their integration in “Systems biology” – Nicholson and Lindon, 2008) will endow clinicians with

new and powerful analytical technologies. In this ambitious agenda, the four yet undisclosed paths hereby proposed (nanotechnology, predictive medicine, nutraceuticals and regenerative medicine) will likely become the pillars of a new era, the next stage of clinical chemistry. Within this framework, metabolomics promises to contribute great strides in the field of transfusion medicine, especially in the amelioration of storage conditions for RBC concentrates (Sparrow, 2012; Cluitmans et al., 2012; Whitsett et al., 2012).

Lipidomics: a branch of metabolomics focusing on lipid species

Recent developments in mass spectrometry (MS) have enabled fast and sensitive detection of lipid species in different biological matrices.

Lipidomics is the systematic identification of the lipid molecular species of a biological matrix (either a cell, organelle, globule, or whole organism) with emphasis on the relative quantitation of composition changes in response to a perturbation, such as ageing or drug treatments (Alex Brown, 2012). While the term “lipidomics” dates back to a decade ago, investigations of the lipid content of specific biological matrices was an already consolidated field of research over the last fifty years (Philips et al., 1959). In particular, this holds true for those matrices that are largely available and display limited biological complexity, such as anucleated cells and, in particular red blood cells (RBCs) (Hanahan et al., 1960; Farquar et al., 1963; Ways et al., 1964; Dodge et al., 1967; Dougherty et al., 1987; Han and Gross, 1994; Beermann et al., 2005; Skeaff et al., 2006; Rise et al., 2007; Kabagambe et al., 2008; Novgorodtseva et al., 2011).

Indeed, RBCs are also devoid of organelles and of any *de novo* lipid synthesis capacity, which makes their lipidome rather stable in comparison to other cell types. Indeed, phospholipid synthesis is known to be active in reticulocytes and suppressed in mature RBCs (Percy et al., 1973). Nonetheless, alteration of lipid homeostasis is strictly tied to membrane reorganization during RBC ageing *in vivo* and *in vitro* (RBC storage), mainly owing to lipid peroxidation phenomena which promote membrane shape alterations through the progressive loss of lipids (and membrane-associated proteins) via vesiculation (D'Alessandro et al., 2012). Therefore, it is small wonder that the RBC lipidome has long attracted a great deal of interest over the last five decades.

Yet in 1959, Phillips and Roome (1959) provided a preliminary portrait of the human RBC phospholipidome]. However, it was only in 1960 that Hanahan and colleagues described a more complex scenario, also by including species-specific differences between human and bovine RBCs (Hanahan et al., 1960). Four years later, Ways and Hanahan reported a detailed lipid class composition of normal human RBCs, indicating the following percentages: cholesterol 25%, choline glycerophosphatides 30%, sphingomyelin 24%, ethanolamine glycerophosphatides 26%, and serine glycerophosphatides 15% (Ways and Hanahan, 1964). Meanwhile, Farquhar and Ahrens (1963) had showed that 67% of the PE, 8% of the PS, and 10% of the lecithin of human RBCs are in the plasmalogen form, with a vinyl ether linkage at the sn-1 and an ester linkage at the sn-2 position. In 1967, Dodge and Philips described a silicic acid thin-layer chromatography strategy to investigate the phospholipid and phospholipid fatty acids and aldehydes in human RBCs (Dodge and Philips, 1967). Thirty-three fatty acids and five aldehydes were separated and tentatively classified into lipid classes, including phosphatidyl ethanolamine (PE), phosphatidyl serine (PS), lecithin, and sphingomyelin (SM) 24:0 and 24:1, while fatty acid moieties were tentatively attributed. Of note, the

values reported by Dodge and Philips (1967) were consistent with those by Ways and Hanahan (1964). Interesting results were obtained also as far as it concerned the composition in fatty acid moieties of the different lipid classes. About 37% of the total fatty acid in PS was 18:0, while only about 3% was 16:0; in PE and lecithin, 16:0 was the major saturated fatty acid, with the level in lecithin being over twice that in PE. The relative amount of 18:1 was also much lower in PS than in PE and lecithin. The fatty acid distribution of sphingomyelin differed markedly from that of the glycerophospholipids (GP), in particular in the greater degree of saturation (Dodge and Philips, 1967). Only about 33% of the fatty acids were unsaturated; in addition, less than 6% of the fatty acids appeared to have more than one double bond and less than 3% more than two double bonds. The 16:0, 24:0, and 24:1 made up almost 7% of the total fatty acids. Essentially all of the 24:0 and most of the 24:1 of the human RBC phospholipids appeared to reside in sphingomyelin.

Different instrumentations and techniques have been tested for the improvement of lipid analysis. During the last two decades, big technological strides have prompted the dissemination of chromatography separation and mass spectrometry-based lipidomics studies of RBCs (Han and Gross, 1994; Beermann et al., 2005; Skeaff et al., 2006; Rise et al., 2007; Ivanova et al., 2010; Dinkla et al., 2012; Bicalho et al., 2013). At the dawn of the mass spectrometry-based lipidomics era the complexity of the lipidome did not enable comprehensive studies like the ones performed with thin layer chromatography (TLC) or gas chromatography (GC) described in the previous paragraphs (Philips and Roome, 1959; Farquar et al., 1963; Ways and Hanahan, 1964; Dodge and Philips, 1967; Owen et al., 1982). The expensive instrumentation and the lack of bioinformatic tools to handle the high-throughput amount of data collected via the mass spectrometry-based workflow hampered at first its diffusion in the field (Alex Brown, 2012). More recently, the introduction of highly accurate and less expensive instruments (in comparison to the ones available decades ago) was also paralleled by consistent improvements in the field of bioinformatic elaboration of the raw mass spectra. The acquired expertise have helped laboratories worldwide to cope with the intrinsic difficulties related to lipid mass attribution and fueled new efforts to bring about the systematic classification of lipid species and structures (Fahy et al., 2005; Clasquin et al., 2012). The current burgeoning of OMICS disciplines has thus given new verve to the field of lipidomics research, while enabling further steps forward. Regarding RBC lipid homeostasis, as premised by Farquhar and Ahrens (1963), lipid composition of human RBCs is largely influenced by the diet. In this view, Dougherty and colleagues performed an extensive investigation to relate region specific diets to the lipid content of plasma, platelets and RBCs (1987). By comparing RBCs of individuals from rural areas in Finland, Italy (province of Viterbo) and the United States, the Authors demonstrated how diets largely relying on fish and olive oil consumption (in Finland and Italy, respectively), resulted in a significant decrease (in comparison to the US counterparts) in the levels of polyunsaturated fatty acids (PUFA), which they relate to the potential production of unhealthy prostaglandins (thromboxane and prostacyclins) byproducts. Finally, the Authors also noted that in all plasma and RBC glycerolphospholipids, the monounsaturated fatty acids (especially oleic acid 16:1 and palmitic acid, 16:0) were highest in the Italian and the saturated fatty acids were highest in the Finnish samples. In this frame, we exploit novel databases such as LIPID MAPS and ad hoc software suites for mass spectrometry-based metabolomics analyses (such as MAVEN – Clasquin et al., 2012) to address the key biological issue of the RBC lipidome.

Conclusion: Integrated Omics

The field of Omics disciplines applied to blood and blood components is but a mirror reflecting the rapidly evolving scenario filled with technological innovations (new mass spec instruments), bioinformatic tools (enriched and updated compound class-specific databases) and pragmatic issues in the clinical setting. Indeed, while proteomics is a rather young research endeavor in comparison to transfusion medicine and clinical biochemistry, encouraging results have prompted reconsidering the figures of proteomics researchers either in the role of supporting experts or leading innovators.

Nevertheless, it is not to be forgotten that, given their older origin, transfusion medicine and clinical chemistry have already found their proper collocation in the healthcare system, while a definitive role for proteomics is still matter of debate (at least in Italy). In order to avoid any pre-emptive ostracism toward new technologies with no immediate applications, proteomics experts have strived to find themselves a niche where their expertise was supportive or expansive in relation to clinicians, rather than in opposition to them. The integration of Omics approaches and the introduction of mathematical models, as in the case of Systems biology (Paglia et al., 2012), will soon help further bridging the gap between observational studies and applied research.

The interested reader is referred to the Special Issue of Journal of Proteomics (Volume 76, December 5, 2012) devoted to Integrated Omics – guest edited by Prof. Lello Zolla and Angelo D’Alessandro (PhD candidate).

References

- Abe K, Sugita Y. Properties of cytochrome b5 and methemoglobin reduction in human erythrocytes. *Eur J Biochem* 1979; 101: 423-8.
- Adamson JW. New blood, old blood, or no blood? *N Engl J Med*. 2008;358(12):1295-6.
- Agre P, Cartron JP. Molecular biology of the Rh antigens. *Blood* 1991;78:551-63
- Agre P. Clinical relevance of basic research on red cell membranes. *Clin Res* 1992;40:176-86.
- Alex Brown H. Lipidomics: when apocrypha becomes canonical. *Curr Opin Chem Biol*. 2012;16(1-2):221-6.
- Allain JP, Bianco C, Blajchman MA, Brecher ME, Busch M, Leiby D, et al. Protecting the blood supply from emerging pathogens: the role of pathogen inactivation. *Transfus Med Rev* 2005;19(2):110–26.
- Aminoff D, Rolfes-Curl A, Supina E. Molecular biomarkers of aging: The red cell as a model. *Arch Gerontol Geriatr* 1992;15 (1):7–15.
- Anderson JL, Maycock CA, Lappe DL. Frequency of elevation of C-reactive protein in atrial fibrillation. *Am J Cardiol* 2004;94:1255–9.
- Anderson L, Seilhamer J. A comparison of selected mRNA and protein abundances in human liver. *Electrophoresis* 1997;18(3–4):533–7.
- Anderson NL, Anderson NG. Proteome and proteomics: new technologies, new concepts, and new words. *Electrophoresis* 1998;19(11):1853–61.
- Anderson NL, Anderson NG. The human plasma proteome: history, character, and diagnostic prospects. *Mol Cell Proteomics* 2002;1:845–67.
- Annis AM, Glenister KM, Killian JJ, Sparrow RL. Proteomic analysis of supernatants of stored red blood cell products. *Transfusion* 2005; 45(9):1426-33.
- Antonucci R, Atzori L, Barberini L, Fanos V. Metabolomics: the "new clinical chemistry" for personalized neonatal medicine. *Minerva Pediatr* 2010; 62 (3Suppl 1): 145-8.
- Arese P, Turrini F, Schwarzer E. Band 3/complement-mediated recognition and removal of normally senescent and pathological human erythrocytes. *Cell Physiol Biochem* 2005;16:133-46.
- Artz CP, Howard JM, Davis JH, Scott R Jr. Plastic bags for intravenous infusions: observations in Korea with saline, dextran and blood; in Howard JM (eds): *Battle Casualties in Korea: Studies of the Surgical Research Team*, vol 2. Army Medical Service Graduate School, Washington, DC. 1954; 219–24.
- Assmann SF. The Red Cell Storage Duration Study (RECESS) 2010. Available from: <http://clinicaltrials.gov/>. Last access on 16/05/2012.
- Atallah E, Schiffer CA. Granulocyte transfusion. *Curr Opin Hematol* 2006;13(1):45–9.
- AuBuchon JP, Cancelas JA, Herschel L, Roger J, Rugg N, Pratt PG, et al. In vitro and in vivo evaluation of LEUKOSEP HRC-600-C leukoreduction filtration system for red cells. *Transfusion* 2006;46(8):1311-5.
- Aviles RJ, Martin DO, Apperson-Hansen C. Inflammation as a risk factor for atrial fibrillation. *Circulation* 2003;108:3006 –10.
- Basran S, Frumento RJ, Cohen A, et al. The association between duration of storage of transfused red blood cells and morbidity and mortality after reoperative cardiac surgery. *Anesth Analg* 2006; 103: 15-20.

- Baynes JW. Oxygen and life. In: Baynes JW, Domoniczak MH, editors. *Medical Biochemistry*. Philadelphia: Elsevier 2005;497–506.
- Beermann C, Mobius M, Winterling N et al. sn-position determination of phospholipid-linked fatty acids derived from erythrocytes by liquid chromatography electrospray ionization ion-trap mass spectrometry. *Lipids* 2005 February;40(2):211-8.
- Bell JG, Sargent JR, Tocher DR, Dick JR. Red blood cell fatty acid compositions in a patient with autistic spectrum disorder: a characteristic abnormality in neurodevelopmental disorders? *Prostaglandins Leukot Essent Fatty Acids* 2000;63(1-2):21-5.
- Bennet-Guerrero E, Stafford-Smith M, Waweru PM, et al. A prospective double-blind, randomized clinical feasibility trial of controlling the storage age of red blood cells for transfusion in cardiac surgical patients. *Transfusion* 2009; 49: 1375-83.
- Bennett V, Lambert S. The spectrin skeleton: from red cells to brain. *J Clin Invest* 1991;87:1483-9.
- Bennett V. Spectrin-based membrane skeleton: a multipotential adaptor between plasma membrane and cytoplasm. *Physiol Rev* 1990;70:1029-65.
- Bennett-Guerrero E, Veldman TH, Doctor A, et al. Evolution of adverse changes in stored RBCs. *Proc Nat Acad Sci USA* 2007; 104: 17063-8.
- Berezina TL, Zaets SB, Morgan C, Spillert CR, Kamiyama M, Spolarics Z, et al. Influence of storage on red blood cell rheo-logical properties. *J Surg Res* 2002; 102(1):6–12.
- Bessos H, Seghatchian J. Red cell storage lesion: the potential impact of storage-induced CD47 decline on immunomodulation and the survival of leucofiltered red cells. *Transfus Apher Sci* 2005;32(2):227-32.
- Beutler E, Kuhl W. Volume control of erythrocytes during storage. The role of mannitol. *Transfusion* 1988;28:353–7.
- Beutler E, Wood L. In vivo regeneration of red cell 2,3 diphosphoglyceric acid (DPG) after transfusion of stored blood. *J Lab Clin Med* 1969; 74: 300.
- Bicalho B, Holovati JL, Acker JP. Phospholipidomics reveals differences in glycerophosphoserine profiles of hypothermically stored red blood cells and microvesicles. *Biochim Biophys Acta*. 2013;1828(2):317-26.
- Blajchman MA. The clinical benefits of the leukoreduction of blood products. *J Trauma* 2006;60(6):83-90.
- Bligh EG and Dyer WJ. A rapid method of total lipid extraction and purification. *Can. J. Biochem. Physiol.* 1959; 37, 911-917.
- Bonaventura J. Clinical implications of the loss of vasoactive nitric oxide during red blood cell storage. *Proc Natl Acad Sci USA* 2007;104:19165-6.
- Borgese N, D'Arrigo A, De Silvestris M, Pietrini G. NADH-cytochrome b5 reductase and cytochrome b5 isoforms as models for the study of post-translational targeting to the endoplasmic reticulum. *FEBS Lett* 1993;325(1-2):70-5.
- Boschetti E, Righetti PG. The art of observing rare protein species in proteomes with peptide ligand libraries. *Proteomics* 2009, doi:10.1002/pmic.200800389.

- Bosman GJ, Kay MM. Erythrocyte aging: a comparison of model systems for simulating cellular aging in vitro. *Blood Cells* 1988;14:19-46.
- Bosman GJ, Lasonder E, Luten M, Roerdinkholder-Stoelwinder B, Novotný VM, et al. The proteome of red cell membranes and vesicles during storage in blood bank conditions. *Transfusion* 2008; 48(5):827-35.
- Bosman GJ, Werre JM, Willekens FL, Novotný VM. Erythrocyte ageing in vivo and in vitro: structural aspects and implications for transfusion. *Transfus Med* 2008; 18: 335-47.
- Bosman GJ, Willekens FL, Werre JM. Erythrocyte aging: a more than superficial resemblance to apoptosis? *Cell Physiol Biochem* 2005;16(1-3):1-8.
- Bosman GJCGM, Lasonder E, Luten M, et al. The proteome of red cell membranes and vesicles during storage in blood bank conditions. *Transfusion* 2008; 48: 827-35.
- Bowen BP, Northen TR. Dealing with the unknown: metabolomics and metabolite atlases. *J Am Soc Mass Spectrom* 2010; 21(9): 1471-6.
- Bowen RA, Hortin GL, Csako G, et al. Impact of blood collection devices on clinical chemistry assays. *Clin Biochem*. 2010; 43(1-2): 4-25.
- Brand M, Ranish JA, Kummer NT, Hamilton J, Igarashi K, Francastel C, et al. Dynamic changes in transcription factor complexes during erythroid differentiation revealed by quantitative proteomics. *Nat Struct Mol Biol* 2004;11:73–80.
- Bratosin D, Estaquier J, Ameisen JC, Montreuil J. Molecular and cellular mechanisms of erythrocyte programmed cell death: Impact on blood transfusion. *Vox Sang* 2002; 83(1):307–10.
- Bratosin D, Mazurier J, Tissier JP, Estaquier J, Huart JJ, Ameisen JC, et al. Cellular and molecular mechanisms of senescent erythrocyte phagocytosis by macrophages. A review. *Biochimie* 1998;80(2):173-95.
- Brazier RM, Shipp MA, Feldman AL, et al. Molecular diagnostics. *Hematol Am Soc Hematol Educ Program* 2003;1:279–93.
- Brecher ME, Hay SN. Bacterial contamination of blood components. *Clin Microbiol Rev* 2005;18:195–204.
- Bright R. Cases and observation illustrative of renal disease accompanied with secretion of albuminous urine. *Guys Hosp Rep* 1836; 1: 338.
- Bromer JG, Seli E. Assessment of embryo viability in assisted reproductive technology: shortcomings of current approaches and the emerging role of metabolomics. *Curr Opin Obstet Gynecol* 2008; 20(3): 234-41.
- Bruschi M, Seppi C, Arena S, Musante L, Santucci L, Balduini C, et al. Proteomic analysis of erythrocyte membranes by soft Immobiline gels combined with differential protein extraction. *J Proteome Res* 2005;4(4):1304–9.
- Buescher JM, Moco S, Sauer U, Zamboni N. Ultrahigh Performance Liquid Chromatography-Tandem Mass Spectrometry Method for Fast and Robust Quantification of Anionic and Aromatic Metabolites. *Anal Chem* 2010; 82: 4403-12.
- Bunn HF, May MH, Kocholaty WF, Shields CE. Hemoglobin function in stored blood. *J Clin Invest* 1969;48(2):311-21.

- Buscher, J.M. et al. Cross-Platform Comparison of Methods for Quantitative Metabolomics of Primary Metabolism. *Anal. Chem.* 2009; 81, 2135–2143.
- Calvo KR, Liotta LA, Petricoin EF. Clinical proteomics: from biomarker discovery and cell signaling profiles to individualized personal therapy. *Biosci Rep* 2005;25(1–2):107–25.
- Card RT. Red cell membrane changes during storage. *Transfus Med Rev* 1988;2:40–7.
- Carless PA, Henry DA, Moxey AJ, O'connell DL, Brown T, Fergusson DA. Cell salvage for minimising perioperative allogeneic blood transfusion. *Cochrane Database Syst Rev* 2006;(4):CD001888.
- Chou J, Choudhary PK, Goodman SR. Protein profiling of sickle cell versus control RBC core membrane skeletons by ICAT technology and tandem mass spectrometry. *Cell Mol Biol Lett* 2006;11(3):326–37.
- Christians U, Klawitter J, Hornberger A, Klawitter J. How unbiased is non-targeted metabolomics and is targeted pathway screening the solution? *Curr Pharm Biotechnol* 2011; 12(7): 1053-66.
- Civenni G, Test ST, Brodbeck U, Butikofer P. In vitro incorporation of GPI-anchored proteins into human erythrocytes and their fate in the membrane. *Blood* 1998;91:1784-92.
- Clark MR, Shohet SB. Red cell senescence. *Clin Haematol* 1985;14:223-57.
- Clasquin MF, Melamud E, Rabinowitz JD. LC-MS Data Processing with MAVEN: A Metabolomic Analysis and Visualization Engine. 2012. *Current Protocols in Bioinformatics*. 37:14.11.1-14.11.23.
- Clasquin MF, Melamud E, Rabinowitz JD. LC-MS data processing with MAVEN: a metabolomic analysis and visualization engine. *Curr Protoc Bioinformatics*. 2012;Chapter 14:Unit14.11.
- Cluitmans JC, Hardeman MR, Dinkla S, Brock R, Bosman GJ. Red blood cell deformability during storage: towards functional proteomics and metabolomics in the Blood Bank. *Blood Transfus.* 2012 May;10 Suppl 2:s12-8. doi:10.2450/2012.004S.
- Cluitmans JC, Hardeman MR, Dinkla S, Brock R, Bosman GJ. Red blood cell deformability during storage: towards functional proteomics and metabolomics in the Blood Bank. *Blood Transfus.* 2012;10 Suppl 2:s12-8.
- Council of Europe. Guide to the preparation, use and quality assurance of blood components. Recommendation no R (95) 15 on the preparation, use and quality assurance of blood components. 14th ed. Strasbourg: Council of Europe Press; 2008.
- Cristea IM, Gaskell SJ, Whetton AD. Proteomics techniques and their application to hematology. *Blood* 2004;103:3624–34.
- D'Amici GM, Rinalducci S, Zolla L. Proteomic analysis of RBC membrane protein degradation during blood storage. *J Proteome Res* 2007;6:3242–55.
- D'Alessandro A and Zolla L. Pharmacoproteomics: a chess game on a protein field. *Drug Discov Today*. 2010; 15(23-24), 1015-1023.
- D'Alessandro A, D'Amici GM, Vaglio S, Zolla L. Time-course investigation of SAGM-stored erythrocyte concentrates: from metabolism to proteomics. *Hematologica* 2012;97(1): 107–15.
- D'Alessandro A, D'Amici GM, Vaglio S, Zolla L. Time-course investigation of SAGM-stored leukocytefiltered red blood cell concentrates: from metabolism to proteomics. *Haematologica* 2012; 97(1): 107-15.

- D'Alessandro A, Federica G, Palini S, et al. A mass spectrometry-based targeted metabolomics strategy of human blastocoele fluid: a promising tool in fertility research. *Mol Biosyst* 2012; 8(4): 953-8.
- D'Alessandro A, Gevi F, Zolla L. A robust high resolution reversed-phase HPLC strategy to investigate various metabolic species in different biological models. *Mol Biosyst*. 2011;7(4):1024-32.
- D'Alessandro A, Gevi F, Zolla L. Targeted mass spectrometry-based metabolomic profiling through Multiple Reaction Monitoring of Liver and other biological matrices. In *Liver Proteomics*. In: Josic D, Hixson DC (editors): *Methods and Protocols Series: Methods in Molecular Biology*, vol. 909. New York, NY, USA: Springer Protocols, Humana Press: 2012.
- D'Alessandro A, Liumbruno G, Grazzini G, Zolla L. Red blood cell storage: the story so far. *Blood Transfus*. 2010;8(2):82-8.
- D'Alessandro A, Righetti PG, Zolla L. The red blood cell proteome and interactome: an update. *J Proteome Res* 2010; 9(1): 144-63.
- D'Alessandro A, Zolla L. Metabolomics and cancer drug discovery: let the cells do the talking. *Drug Discov Today* 2012; 17(1-2): 3-9.
- D'Alessandro A, Zolla L. Pharmacoproteomics: a chess game on a protein field. *Drug Discov Today* 2010; 15(23-24): 1015-23.
- D'Alessandro A, Zolla L. The SODyssey: superoxide dismutases from biochemistry, through proteomics, to oxidative stress, aging and nutraceuticals. *Expert Rev Proteomics*. 2011;8(3):405-21.
- D'Alessandro A. et al. A robust high resolution reversed-phase HPLC strategy to investigate various metabolic species in different biological models. *Mol Biosyst*. 2011; 7(4), 1024-1032.
- D'Amici GM, Rinalducci S, Zolla L. Proteomic analysis of RBC membrane protein degradation during blood storage. *J Prot Res* 2007; 6: 3242-55.
- De Benedetti E. Michele Tsvet, the discoverer of chromatography. *Minerva Med* 1956; 47(25): 536-8.
- de Hoog CL, Mann M. Proteomics. *Annu Rev Genomics Hum Genet* 2004;5:267-93.
- De Rosa MC, Carelli Alinovi C, Galtieri A, Scatena R, Giardina B. The plasma membrane of erythrocytes plays a fundamental role in the transport of oxygen, carbon dioxide and nitric oxide and in the maintenance of the reduced state of the heme iron. *Gene* 2007;398(1-2):162-71.
- Dinkla S, Wessels K, Verdurmen WP, Tomelleri C, Cluitmans JC, Franssen J, Fuchs B, Schiller J, Joosten I, Brock R, Bosman GJ. Functional consequences of sphingomyelinase-induced changes in erythrocyte membrane structure. *Cell Death Dis*. 2012;3:e410.
- Dodge JT, Phillips GB. Composition of phospholipids and of phospholipid fatty acids and aldehydes in human red cells. *J Lipid Res* 1967;8(6):667-75.
- Dougherty RM, Galli C, Ferro-Luzzi A, Iacono JM. Lipid and phospholipid fatty acid composition of plasma, red blood cells, and platelets and how they are affected by dietary lipids: a study of normal subjects from Italy, Finland, and the USA. *Am J Clin Nutr* 1987;45(2):443-55.
- Dumaswala UJ, Zhuo L, Jacobsen DW, et al. Protein and lipid oxidation of banked human erythrocytes: role of glutathione. *Free Radic Biol Med* 1999; 27: 1041-9.

- Dumont LJ, Yoshida T, AuBuchon JP. Anaerobic storage of red blood cells in a novel additive solution improves in vivo recovery. *Transfusion* 2009; 49: 458-64.
- Dunn WB and Ellis DI. Metabolomics: current analytical platforms and methodologies. *Trends Anal. Chem.* 2005; 24, 285–294.
- Dwyre DM, Holland PV. Transfusion-associated graft-versus-host disease. *Vox Sang* 2008;95(2):85-93.
- Ebaugh FG Jr, Ross JF. The radioactive sodium chromate method for erythrocyte survival. *Vox Sang* 1985;49:304–307.
- Echan LA, Tang HY, Ali-Khan N, Lee KB, Speicher DW. Depletion of multiple high-abundance proteins improves the protein profiling capacities of human serum and plasma. *Proteomics* 2005;5: 3292–303.
- Edna TH, Bjerkeset T. Association between transfusion of stored blood and infective bacterial complications after resection for colorectal cancer. *Eur J Surg* 1998; 164: 449-56.
- Ekins S, Nikolsky Y, Bugrim A, et al. Pathway mapping tools for analysis of high content data. *Methods Mol Biol* 2007; 356: 319-50.
- Evans WE, Relling MV. Moving towards individualized medicine with pharmacogenomics. *Nature* 2004;429:464–8.
- Fahy E, Subramaniam S, Brown HA et al. A comprehensive classification system for lipids. *J Lipid Res* 2005;46(5):839-61.
- Farquhar JW, Ahrens EH Jr. Effects of dietary fats on human erythrocyte fatty acid patterns. *J Clin Invest.* 1963;42:675-85.
- Fergusson DA. The Age of Red Blood Cells in Premature Infants (ARIP) - International Standard Randomized Controlled Trial Number Register (ISRCTN) 2010. Available from: <http://www.controlledtrials.com/isrctn/pf/65939658>. Last access on 16/05/2012.
- Fernandes CJ Jr, Akamine N, De Marco FV, et al. Red blood cell transfusion does not increase oxygen consumption in critically ill septic patients. *Crit Care* 2001; 5: 362-7.
- Flegel WA. Fresh blood for transfusion: how old is too old for red blood cell units? *Blood Transfus.* 2012;10(3):247-51.
- Florens L, Liu X, Wang Y, Yang S, Schwartz O, Peglar M, et al. Proteomics approach reveals novel proteins on the surface of malaria-infected erythrocytes. *Mol Biochem Parasitol* 2004;135:1–11.
- Fransen E, Maessen J, Dentener M, Senden N, Buurman W. Impact of blood transfusions on inflammatory mediator release in patients undergoing cardiac surgery. *Chest* 1999;116:1233–9.
- Gajic O, Rana R, Winters JL, et al. Transfusion-related acute lung injury in the critically ill: prospective nested case-control study. *Am J Respir Crit Care Med* 2007; 176: 886-91.
- Gevi F, D'Alessandro A, Rinalducci S, Zolla L. Alterations of red blood cell metabolome during cold liquid storage of erythrocyte concentrates in CPD-SAGM. *J Proteomics.* 2012;76 Spec No.:168-80.
- Gibson JG, Rees SB, McManus TJ, Scheitlin WA II. A citrate phosphate dextrose solution for the preservation of human blood. *Am J Clin Pathol* 1957;28:569–78.

- Giovane A, Balestrieri A, Napoli C. New insights into cardiovascular and lipid metabolomics. *J Cell Biochem* 2008; 105(3): 648-54.
- Goodman SR, Kurdia A, Ammann L, Kakhniashvili D, Daescu O. The human red blood cell proteome and interactome. *Exp Biol Med* (Maywood) 2007;232:1391-408.
- Gowda GA, Zhang S, Gu H, et al. Metabolomics-based methods for early disease diagnostics. *Expert Rev Mol Diagn* 2008; 8(5): 617-33.
- Granger J, Siddiqui J, Copeland S, Remick D. Albumin depletion of human plasma also removes low abundance proteins including the cytokines. *Proteomics* 2005;5(18):4713-8.
- Grazzini G, Vaglio S. Red blood cell storage lesion and adverse clinical outcomes: post hoc ergo propter hoc? *Blood Transfus.* 2012;10 (2):s4-6.
- Greenaway F. The early development of analytical chemistry. *Endeavour* 1962; 21: 91.
- Greenwalt TJ, McGuinness CG, Dumaswala UJ. Studies in red cell preservation: 4. Plasma vesicle hemoglobin exceeds free hemoglobin. *Vox Sang* 1991;61:14-7.
- Greenwalt TJ, Rugg N, Dumaswala UJ. The effect of hypotonicity, glutamine, and glycine on red cell preservation. *Transfusion* 1997;37(3):269-76.
- Greinacher A, Warkentin TE. Transfusion medicine in the era of genomics and proteomics. *Transfus Med Rev* 2005;19:288-94.
- Griffin JL. The Cinderella story of metabolic profiling: does metabolomics get to go to the functional genomics ball? *Philos. Trans. R Soc. Lond. B Biol. Sci.* 2006; 361(1465), 147-161.
- Griffiths, W.J. et al. Targeted metabolomics for biomarker discovery. *Angew Chem. Int. Ed. Engl.* 2010; 49, 5426-5445.
- Hamasaki N, Okubo K. Band 3 protein: physiology, function and structure. *Cell Mol Biol* 1996;42(7):1025-39.
- Han X, Gross RW. Electrospray ionization mass spectroscopic analysis of human erythrocyte plasma membrane phospholipids. *Proc Natl Acad Sci U S A* 1994;91(22):10635-9.
- Hanahan DJ, Watts RM, Papajohn D. Some chemical characteristics of the lipids of human and bovine erythrocytes and plasma. *J Lipid Res.* 1960;1:421-32.
- Harmening DM. Modern blood banking and transfusion practices. Philadelphia, PA, F.A. Davis Company 1999; 9 – 11.
- Harrigan GG and Goodacre R. *Metabolic Profiling: Its Role in Biomarker Discovery and Gene Function Analysis*, Kluwer Academic Publishers eds (2003)
- Head DJ, Lee ZE, Poole J, Avent ND. Expression of phosphatidylserine (PS) on wild-type and Gerbich variant erythrocytes following glycophorin-C (GPC) ligation. *Br J Haematol* 2004;129:130-7.
- Head DJ, Lee ZE, Swallah MM, Avent ND. Ligation of CD47 mediates phosphatidylserine expression on erythrocytes and a concomitant loss of viability in vitro. *Br J Haematol* 2005;130:788-90.
- Heaton WAL, Holme S, Smith K, Brecher ME, Pineda A, AuBuchon JP, et al. Effects of 3-5 log₁₀ pre-storage leucocyte depletion on red cell storage and metabolism. *Br J Haematol* 1994; 87:363-8.

- Hébert PC, Chin-Yee I, Fergusson D, et al. A pilot trial evaluating the clinical effects of prolonged storage of red cells. *Anesth Analg* 2005; 100: 1433-8.
- Heddle NM. Febrile nonhemolytic transfusion reactions to platelets. *Curr Opin Hematol* 1995;2(6):478-83.
- Heller M, Michel PE, Morier P, et al. Two-stage off-gel isoelectric focusing: protein followed by peptide fractionation and application to proteome analysis of human plasma. *Electrophoresis* 2005;26(6):1174-88.
- Hess JR, Greenwalt TJ. Storage of red blood cells: new approaches. *Transfus Med Rev* 2002; 16: 283-95.
- Hess JR, Hill HR, Oliver CK, Lippert LE, Greenwalt TJ. Alkaline CPD and the preservation of red blood cell 2,3-DPG. *Transfusion* 2002;42:747-52.
- Hess JR, Hill HR, Oliver CK, Lippert LE, Rugg N, Joines AD, et al. 12-week red blood cell storage. *Transfusion* 2003; 43:867-72.
- Hess JR, Rugg N, Joines AD, Gormas JF, Pratt PG, Silberstein EG, et al. Buffering and dilution in red blood cell storage. *Transfusion* 2005;45:50-4.
- Hess JR, Rugg N, Knapp AD, Gormas JF, Hill HR, Oliver CK, Lippert LE, et al. The role of electrolytes and pH in RBC additive solutions. *Transfusion* 2001; 41:1045-51.
- Hess JR, Rugg N, Knapp AD, Gormas JF, Hill HR, Oliver CK, Lippert LE, et al. The role of electrolytes and pH in RBC additive solutions. *Transfusion* 2001; 41:1045-51.
- Hess JR, Sparrow RL, van der Meer PF, et al. Red blood cell hemolysis during blood bank storage: using national quality management data to answer basic scientific questions. *Transfusion* 2009; 49: 2599-603.
- Hess JR. An update on solutions for red cell storage. *Vox Sang* 2006; 91: 13-9.
- Hess JR. Red blood cell storage: when is better not good enough? *Blood Transfus* 2009; 7: 172-3.
- Hess JR. Red cell freezing and its impact on the supply chain. *Transfus Med* 2004;14:1-8.
- Hess JR. Storage of red cells under anaerobic conditions. *Vox Sang* 2007;93:183.
- Hill HR, Oliver CK, Lippert LE, Greenwalt TJ, Hess JR. The effects of polyvinyl chloride and polyolefin bags on red blood cells stored in a new additive solution. *Vox Sang* 2001;81:161-6.
- Himmelsbach M. 10 years of MS instrumental developments--impact on LC-MS/MS in clinical chemistry. *J Chromatogr B Analyt Technol Biomed Life Sci* 2012; 883-884: 3-17.
- Ho J, Sibbald WJ, Chin-Yee IH. Effects of storage on efficacy of red cell transfusion: when is it not safe? *Crit Care Med* 2003;31(12):687-97.
- Hogman CF, de Verdier CH, Ericson A, Hedlund K, Sandhagen B. Effects of oxygen on red cells during liquid storage at +4 degrees C. *Vox Sang* 1986; 51:27-34.
- Hogman CF, Hedlund K, Zetterstrom H. Clinical usefulness of red cells preserved in protein-poor media. *N Engl J Med* 1978;299:1377-82.
- Hogman CF, Knutson F, Loof H, Payrat JM. Improved maintenance of 2,3 DPG and ATP in RBC stored in a modified additive solution. *Transfusion* 2002; 42:824-9.
- Hogman CF, Meryman HT. Red blood cells intended for transfusion: quality criteria revisited. *Transfusion* 2006;46(1):137-42.

- Hogman CF, Meryman HT. Storage parameters affecting red blood cell survival and function after transfusion. *Transfus Med Rev* 1999;13:275 – 96.
- Hogman CF. Liquid-stored red blood cells for transfusion: A status report. *Vox Sang* 1999;76:67–77.
- Högman CF. Preparation and preservation of red blood cells. *Vox Sang* 1998;74:177 – 87.
- Holme S. Current issues related to the quality of stored RBCs. *Transfus Apher Sci* 2005; 33: 55-61.
- Holmes E, Li JV, Athanasiou T, et al. Understanding the role of gut microbiome-host metabolic signal disruption in health and disease. *Trends Microbiol* 2011; 19(7): 349-59.
- Holmes E, Nicholson JK. Human metabolic phenotyping and metabolome wide association studies. *Ernst Schering Found Symp Proc* 2007; (4): 227-49.
- Isbell TS, Sun CW, Wu LC, et al. SNO-hemoglobin is not essential for red blood cell-dependent hypoxic vasodilation. *Nat Med* 2008; 14: 773–7.
- Ivanova PT, Milne SB, Brown HA. Identification of atypical ether-linked glycerophospholipid species in macrophages by mass spectrometry. *J. Lipid Res.* 2010; 51:1581-1590.
- Jamshidi N, Edwards JS, Fahland T, et al. Dynamic simulation of the human red blood cell metabolic network. *Bioinformatics* 2001; 17(3): 286-7.
- Jamshidi N, Palsson BØ. Systems biology of the human red blood cell. *Blood Cells Mol Dis* 2006; 36(2): 239-47.
- Jamshidi N, Palsson BØ. Top-down analysis of temporal hierarchy in biochemical reaction networks. *PLoS Comput Biol* 2008; 4(9): e1000177.
- Jarvis HG, Gore DM, Briggs C, Chetty MC, Stewart GW: Cold storage of ‘cryohydrocytosis’ red cells: the osmotic susceptibility of the cold-stored erythrocyte. *Br J Haematol* 2003; 122:859–68.
- Jay DG. Role of band 3 in homeostasis and cell shape. *Cell* 1996;86(6):853-4.
- Jiang M, Jia L, Jiang W, Hu X, Zhou H, Gao X, et al. Protein dysregulation in red blood cell membranes of type 2 diabetic patients. *Biochem Biophys Res Commun* 2003;309:196–200.
- Kabagambe EK, Tsai MY, Hopkins PN et al. Erythrocyte Fatty Acid Composition and the Metabolic Syndrome: A National Heart, Lung, and Blood Institute GOLDN Study. *Clin Chem* 2008;54(1):154-62.
- Kaddurah-Daouk R, Kristal BS, Weinshilboum RM. Metabolomics: a global biochemical approach to drug response and disease. *Annu Rev Pharmacol Toxicol* 2008; 48: 653-83.
- Kakhniashvili DG, Bulla Jr LA, Goodman SR. The human erythrocyte proteome: analysis by ion trap mass spectrometry. *Mol Cell Proteomics* 2004;3:501–9.
- Kakhniashvili DG, Griko NB, Bulla Jr LA, Goodman SR. The proteomics of sickle cell disease: profiling of erythrocyte membrane proteins by 2D-DIGE and tandem mass spectrometry. *Exp Biol Med* 2005;230:787–92.
- Kamp D, Sieberg T, Haest CW. Inhibition and stimulation of phospholipid scrambling activity. Consequences for lipid asymmetry, echinocytosis, and microvesiculation of erythrocytes. *Biochemistry* 2001; 40:9438–46.
- Kanehisa, M. et al. From genomics to chemical genomics: new developments in KEGG. *Nucleic Acids Res.* 2006; 34, D354–D357
- Karon BS, Hoyer JD, Stubbs JR, Thomas DD. Changes in band 3 oligomeric state precede cell membrane phospholipid loss during blood bank storage of red blood cells. *Transfusion* 2009; 49: 1435-42.

- Kay M. Immunoregulation of cellular life span. *Ann N Y Acad Sci* 2005;1057:85-111.
- Kay MM. Generation of senescent cell antigen on old cells initiates IgG binding to a neoantigen. *Cell Mol Biol* 1993;39(2):131-53.
- Keele KD. The impact of science on clinical methods: the basic sciences enter clinical medicine. In: *The Evolution of Clinical Methods in Medicine, Part III*. London: Pitman Medical; 1961. p. 50-74
- Kell DB. Systems biology, metabolic modelling and metabolomics in drug discovery and development. *Drug Discov. Today*. 2006; 11(23-24), 1085-1092.
- Keller ME, Jean R, LaMorte WW, et al. Effects of age of transfused blood on length of stay in trauma patients: a preliminary report. *J Trauma* 2002; 53: 1023-5.
- Kendall SJ, Weir J, Aspinall R, Henderson D, Rosson J. Erythrocyte transfusion causes immunosuppression after total hip replacement. *Clin Orthop Relat Res* 2000;(381):145-55.
- Kitano H. Introductions to systems biology. *Tanpakushitsu Kakusan Koso* 2003;48(7):789-93.
- Klein HG, Spahn DR, Carson JL. Red blood cell transfusion in clinical practice. *Lancet* 2007; 370: 415-26.
- Koch C. The Red Cell Storage Duration and Outcomes in Cardiac Surgery study. 2009. Available from: <http://clinicaltrials.gov/>. Last access on 16/05/2012.
- Koch CG, Li L, Sessler DI, et al. Duration of red-cell storage and complications after cardiac surgery. *N Engl J Med* 2008; 358: 1229-39.
- Kooyman DL, Byrne GW, McClellan S, Nielsen D, Tone M, Waldmann H, et al. In vivo transfer of GPI-linked complement restriction factors from erythrocytes to the endothelium. *Science* 1995;269(5220):89-92.
- Körbel S, Büchse T, Prietzsch H, Sasse T, Schümann M, Krause E, et al. Phosphoprotein profiling of erythropoietin receptor-dependent pathways using different proteomic strategies. *Proteomics* 2005;5(1):91-100.
- Kortz L, Helmschrodt C, Ceglarek U. Fast liquid chromatography combined with mass spectrometry for the analysis of metabolites and proteins in human body fluids. *Anal Bioanal Chem* 2011; 399(8): 2635-44.
- Koshkaryev A, Zelig O, Manny N, et al. Rejuvenation treatment of stored red blood cells reverses storage-induced adhesion to vascular endothelial cells. *Transfusion* 2009; 49: 2136-43.
- Koulman A, Lane GA, Harrison SJ, Volmer DA. From differentiating metabolites to biomarkers. *Anal Bioanal Chem* 2009; 394(3): 663-70.
- Koury MJ, Sawyer ST, Brandt SJ. New insights into erythropoiesis. *Curr Opin Hematol* 2002;9(2):93-100.
- Kriebardis AG, Antonelou MH, Stamoulis KE, Economou-Petersen E, Margaritis LH, Papassideri IS. Membrane protein carbonylation in non-leukodepleted CPDA-preserved red blood cells. *Blood Cells Mol Dis* 2006;36:279-82.
- Kriebardis AG, Antonelou MH, Stamoulis KE, Economou-Petersen E, Margaritis LH, Papassideri IS. Progressive oxidation of cytoskeletal proteins and accumulation of denatured hemoglobin in stored red cells. *J Cell Mol Med* 2007;11:148-55.
- Kriebardis AG, Antonelou MH, Stamoulis KE, Economou-Petersen E, Margaritis LH, Papassideri IS. Storage-dependent remodeling of the red blood cell membrane is associated with increased immunoglobulin G binding, lipid raft rearrangement, and caspase activation. *Transfusion* 2007;47:1212-20.

- Krisp C, Randall SA, McKay MJ, Molloy MP. Towards clinical applications of selected reaction monitoring for plasma protein biomarker studies. *Proteomics Clin Appl* 2012; 6(1-2): 42-59.
- Kurata M, Suzuki M, Agar NS. Antioxidant systems and erythrocyte life-span in mammals. *Comp Biochem Physiol B* 1993;106(3):477-87.
- Kurup PA, Arun P, Gayathri NS, Dhanya CR, Indu AR. Modified formulation of CPDA for storage of whole blood, and of SAGM for storage of red blood cells, to maintain the concentration of 2,3-diphosphoglycerate. *Vox Sang* 2003; 85:253–61.
- Kuypers FA, Yuan J, Snyder LM, Kiefer CR, Bunyaratvej A, Fucharoen S, et al. Membrane phospholipid asymmetry in human thalassemia. *Blood* 1998;91:3044-51.
- Lacroix J. The Age of Blood Evaluation (ABLE) Study - International Standard Randomized Controlled Trial Number Register (ISRCTN) 2008. Available from: <http://www.controlledtrials.com/isrctn/pf/44878718>. Last access on 16/05/2012.
- Lane AN, Fan TW, Higashi RM, et al. Prospects for clinical cancer metabolomics using stable isotope tracers. *Exp Mol Pathol* 2009; 86(3): 165-73.
- Lang F, Gulbins E, Lerche H, Huber SM, Kempe DS, Foller M. Eryptosis, a window to systemic disease. *Cell Physiol Biochem* 2008;22(5-6):373-80.
- Lang F, Lang KS, Lang PA, et al. Mechanisms and significance of eryptosis. Antioxidants and redox signaling 2006; 8: 1183-92.
- Leal-Noval SR, Jara-Lopez I, Garcia-Garmendia JL, et al. Influence of erythrocyte concentrate storage time on postsurgical morbidity in cardiac surgery patients. *Anesthesiology* 2003; 98: 815-22.
- Leal-Noval SR, Munoz-Gomez M, Arellano-Orden V, et al. Impact of age of transfused blood on cerebral oxygenation in male patients with severe traumatic brain injury. *Crit Care Med* 2008; 36: 1290-6.
- Lelubre C, Piagnarelli M, Vincent JL. Association between duration of storage of transfused red blood cells and morbidity and mortality in adult patients: myth or reality? *Transfusion* 2009; 49: 1384-94.
- Lindon JC, Holmes E, Nicholson JK. Metabonomics: systems biology in pharmaceutical research and development. *Curr Opin Mol Ther* 2004; 6(3): 265-72.
- Lindon JC, Holmes E, Nicholson JK. So what's the deal with metabonomics? *Anal Chem* 2003; 75(17): 384A-391A.
- Lines JG. A chronicle of the development of clinical chemistry. *IFFC Newsletter* 1977; 18: 3-9.
- Liumbruno G, D'Amici GM, Grazzini G, Zolla L. Transfusion medicine in the era of proteomics. *J Proteomics* 2008;71(1):34–45.
- Liumbruno GM, Calteri D, Petropulacos K, et al. The Chikungunya epidemic in Italy and its repercussion on the blood system. *Blood Transfus* 2008; 6: 199-210.
- Liumbruno GM. Proteomics: applications in transfusion medicine. *Blood Transfus* 2008;6(2):70–85.
- Lo B, Fijnheer R, Nierich AP, Bruins P, Kalkman CJ. C-reactive protein is a risk indicator for atrial fibrillation after myocardial revascularization. *Ann Thorac Surg* 2005;79:1530 –5.
- Loutit JF, Mollison PL. Advantages of a disodium-citrate-glucose mixture as a blood preservative. *Br Med J* 1943; 2:744–5.

- Lovric VA. Modified packed red cells and the development of the circle pack. *Vox Sang* 1986;51(4):337-8.
- Low PS, Kannan R. Effect of hemoglobin denaturation on membrane structure and IgG binding: role in red cell aging. *Prog Clin Biol Res* 1989;319:525-52.
- Low PS, Rathinavelu P, Harrison ML. Regulation of glycolysis via reversible enzyme binding to the membrane protein, band-3. *J Biol Chem* 1993;268:14627-31.
- Low TY, Seow TK, Chung MC. Separation of human erythrocyte membrane associated proteins with one-dimensional and two-dimensional gel electrophoresis followed by identification with matrix-assisted laser desorption/ionization-time of flight mass spectrometry. *Proteomics* 2002;2:1229-39.
- Lutz HU. Innate immune and non-immune mediators of erythrocyte clearance. *Cell Mol Biol* 2004;50:107-16.
- Lux SE. Dissecting the red cell membrane skeleton. *Nature* 1979;281:426-9.
- Mandal D, Moitra PK, Saha S, Basu J. Caspase 3 regulates phosphatidylserine externalization and phagocytosis of oxidatively stressed erythrocytes. *FEBS Lett* 2002;513:184-8.
- Mansouri A, Lurie AA. Concise review: methemoglobinemia. *Am J Hematol.* 1993;42(1):7-12.
- Marchesi VT. The red cell membrane skeleton: recent progress. *Blood* 1983;61:1-10.
- Marik PE, Sibbald WJ. Effect of stored-blood transfusion on oxygen delivery in patients with sepsis. *JAMA* 1993; 269: 3024-9.
- Marko-Varga G, Fehniger TE. Proteomics and disease: the challenges for technology and discovery. *J Proteome Res* 2004;3:167-78.
- Matarrese P, Straface E, Pietraforte D, Gambardella L, Vona R, Maccaglia A, et al. Peroxynitrite induces senescence and apoptosis of red blood cells through the activation of aspartyl and cysteinyl proteases. *FASEB J* 2005;19:416-8.
- Matsuyama H, Niklasson F, de Verdier CH, Högman CF. Phosphoenolpyruvate in the rejuvenation of stored red cells in SAGM medium: optimal conditions and the indirect effect of methemoglobin formation. *Transfusion* 1989;29(7):614-9.
- Mayr M. Metabolomics: ready for the prime time? *Circ Cardiovasc Genet* 2008; 1(1): 58-65.
- McFaul SJ, Corley JB, Mester CW, Nath J. Packed blood cells stored in AS-5 become proinflammatory during storage. *Transfusion* 2009; 49:1451-60.
- McNiven EM, German JB, Slupsky CM. Analytical metabolomics: nutritional opportunities for personalized health. *J Nutr Biochem* 2011, 22(11): 995-1002.
- McRedmond JP, Park SD, Reilly DF, Coppinger JA, Maguire PB, Shields DC, et al. Integration of proteomics and genomics in platelets: a profile of platelet proteins and platelet-specific genes. *Mol Cell Proteomics* 2004;3:133-44.
- Meldon JH, Abboud OK. DPG - a link between blood acid-base status and respiratory function. *Adv Exp Med Biol* 1983;159:519-24.
- Mendes, P. et al. Why and when channeling can decrease pool size at constant net flux in a simple dynamic channel. *Biochim. Biophys. Acta* 1996; 1289, 175-186

- Moore GL, Ledford ME, Peck CC. The in vitro evaluation of modifications in CPD-adenine preserved blood at various hematocrits. *Transfusion* 1980; 20:419–26.
- Moroff G, Sohmer PR, Button LN. Proposed standardization of methods for determining the 24-hour survival of stored red cells. *Transfusion* 1984; 24 :109-14.
- Morris M Watkins SM. Focused metabolomic profiling in the drug development process: advances from lipid profiling. *Curr Opin Chem Biol*. 2005; 9(4), 407-412.
- Muñoz M, García-Vallejo JJ, Ruiz MD, Romero R, Olalla E, Sebastián C. Transfusion of post-operative shed blood: laboratory characteristics and clinical utility. *Eur Spine J* 2004;13(1):107-13.
- Murrell Z, Haukoos JS, Putnam B, Klein SR. The effect of older blood on mortality, need for ICU care, and the length of ICU stay after major trauma. *Am Surg* 2005; 71:781–5.
- Mynster T, Nielsen HJ. The impact of storage time of transfused blood on postoperative infectious complications in rectal cancer surgery. Danish RANX05 Colorectal Cancer Study Group. *Scand J Gastroenterol* 2000; 35: 212-7.
- Nebert DW, Zhang G, Vesell ES. From human genetics and genomics to pharmacogenetics and pharmacogenomics: past lessons, future directions. *Drug Metab Rev* 2008;40:187–224.
- Nel-Themaat L, Nagy ZP. A review of the promises and pitfalls of oocyte and embryo metabolomics. *Placenta* 2011; 32 (Suppl 3): S257-63.
- Nicholson JK, Lindon JC. Systems biology: Metabonomics. *Nature* 2008; 455 (7216): 1054-6.
- Nicholson JK, Wilson ID, Lindon JC. Pharmacometabonomics as an effector for personalized medicine. *Pharmacogenomics* 2011; 12(1): 103-11.
- Nicholson, J.K., et al. 'Metabonomics': understanding the metabolic responses of living systems to pathophysiological stimuli via multivariate statistical analysis of biological NMR spectroscopic data. *Xenobiotica*. 1999; 29(11), 1181-1189.
- Novgorodtseva TP, Karaman YK, Zhukova NV, Lobanova EG, Antonyuk MV, Kantur TA. Composition of fatty acids in plasma and erythrocytes and eicosanoids level in patients with metabolic syndrome. *Lipids Health Dis*. 2011;10:82.
- Offner PJ, Moore EE, Biffl WL, et al. Increased rate of infection associated with transfusion of old blood after severe injury. *Arch Surg* 2002; 137: 711-6.
- Olukoga AO, Bolodeoku J, Donaldson D. Laboratory instrumentation in clinical biochemistry: an historical perspective. *J R Soc Med* 1997; 90(10): 570-7.
- Olukoga AO, Bolodeoku J, Donaldson D. Origins of cerebrospinal fluid analysis in clinical diagnosis. *J Clin Pathol* 1997; 50: 187-92
- Orlina AR, Josephson AM. Comparative viability of RBC stored in ACD and CPD. *Transfusion* 1969;9:62–9.
- Owen JS, Bruckdorfer KR, Day RC, McIntyre N. Decreased erythrocyte membrane fluidity and altered lipid composition in human liver disease. *J Lipid Res* 1982;23(1):124-32.
- Page MJ, Griffiths TAM, Bleackley MR, MacGillivray RTA. Proteomics: applications relevant to transfusion medicine. *Transfus Med Rev* 2006;20:63–74.
- Palis J. Ontogeny of erythropoiesis. *Curr Opin Hematol* 2008; 15: 155-61.

- Pallotta V, D'Amici GM, D'Alessandro A, et al. Red blood cell processing for cryopreservation: from fresh blood to deglycerolization. *Blood Cells Mol Dis* 2012; DOI: 10.1016/j.bcnd.2012.02.004
- Pasini EM, Kirkegaard M, Mortensen P, et al. In-depth analysis of the membrane and cytosolic proteome of red blood cells. *Blood* 2006; 108: 791-801.
- Pauling L, Robinson AB, Teranishi R, Cary P. Quantitative analysis of urine vapor and breath by gas-liquid partition chromatography. *Proc Natl Acad Sci USA* 1971; 68: 2374-6.
- Percy AK, Schmell E, Earles BJ, Lennarz WJ. Phospholipid biosynthesis in the membranes of immature and mature red blood cells. *Biochemistry* 1973;12(13):2456-61.
- Pert JH, Moore R, Schork PK. Low-temperature preservation of human erythrocytes. *Bibliotheca Haematologica* 1965; 23:674-82.
- Peters AM, Osman S, Reavy HJ, Chambers B, Deenmamode M, Lewis SM. Erythrocyte radiolabelling: in vitro comparison of chromium, technetium, and indium in undamaged and heat damaged cells. *J Clin Pathol.* 1986;39(7):717-21.
- Peters C. Granulocyte transfusions in neutropenic patients: beneficial effects proven? *Vox Sang* 2009;96(4):275-83.
- Petersen WS, Schmidt RE. Hospital laboratories. *Surg Gynecol Obstet* 1920; 31: 539-48
- Petricoin EF, Belluco C, Araujo RP, Liotta LA. The blood peptidome: a higher dimension of information content for cancer biomarker discovery. *Nat Rev Cancer* 2006;6(12):961-7.
- Philips GB, Roome NS. Phospholipids of human red blood cells. *Proc Soc Exp Biol Med.* 1959 Mar;100(3):489-92.
- Pichini S, Altieri I, Zuccaro P, Pacifici R. Drug monitoring in nonconventional biological fluids and matrices. *Clin Pharmacokinet* 1996; 30(3): 211-28.
- Pieper R, Gatlin CL, Makusky AJ, et al. The human serum proteome: display of nearly 3700 chromatographically separated protein spots on two dimensional electrophoresis gels and identification of 325 distinct proteins. *Proteomics* 2003;3:1345-64.
- Prabakaran S, Wengenroth M, Lockstone HE, Lilley K, Leweke FM, Bahn S. 2-D DIGE analysis of liver and red blood cells provides further evidence for oxidative stress in schizophrenia. *J Proteome Res* 2007;6(1):141-9.
- Price ND, Reed JL, Papin JA, et al. Network-based analysis of metabolic regulation in the human red blood cell. *J Theor Biol* 2003; 225(2): 185-94.
- Purdy FR, Tweeddale MG, Merrick PM. Association of mortality with age of blood transfused in septic ICU patients. *Can J Anaesth* 1997; 44: 1256-61.
- Queloz PA, Thadikkaran L, Crettaz D, Rossier JS, Barelli S, Tissot JD. Proteomics and transfusion medicine: future perspectives. *Proteomics* 2006;6:5605-14.
- Racek J, Herynkova R, Holecek V, et al. Influence of antioxidants on the quality of stored blood. *Vox Sang* 1997; 72: 16-9.
- Raine DN. The development of clinical chemistry up to 1900. *Proc Assoc Clin Biochem* 1966; 4: 89-92.
- Rao SV, Jollis JG, Harrington RA, Granger CB, Newby LK, Armstrong PW, et al. Relationship of blood transfusion and clinical outcomes in patients with acute coronary syndromes. *JAMA* 2004;292(13):1555-62.

- Rao SV, Jollis JG, Harrington RA, Granger CB, Newby LK, Armstrong PW, et al. Relationship of blood transfusion and clinical outcomes in patients with acute coronary syndromes. *JAMA* 2004;292(13):1555-62.
- Rawn J. The silent risks of blood transfusion. *Curr Opin Anaesthesiol* 2008;21(5):664-8.
- Reddy KS, Perrotta PL. Proteomics in transfusion medicine. *Transfusion* 2004;44:601-4.
- Rensing H. Storage dependent effects on the oxygen transport capacity of erythrocyte concentrates. *Anaesthesist* 2001;50(1):9-15.
- Reynolds JD, Ahearn GS, Angelo M, et al. Nitrosohemoglobin deficiency: a mechanism for loss of physiological activity in banked blood. *Proc Nat Acad Sci USA* 2007; 104: 17058-62.
- Rhee EP, Gerszten RE. Metabolomics and cardiovascular biomarker discovery. *Clin Chem* 2012; 58(1): 139-47.
- Righetti PG, Castagna A, Herbert B, Candiano G. How to bring the “unseen” proteome to the limelight via electrophoretic pre-fractionation techniques. *Biosci Rep* 2005;25(1-2): 3-17.
- Rise P, Eligini S, Ghezzi S et al. Fatty acid composition of plasma, blood cells and whole blood: relevance for the assessment of the fatty acid status in humans. *Prostaglandins Leukot Essent Fatty Acids* 2007 June;76(6):363-9.
- Robertson DG, Watkins PB, Reilly MD. Metabolomics in toxicology: preclinical and clinical applications. *Toxicol Sci* 2011; 120 (Suppl 1): S146-70.
- Rocks BF, Riley C. Automatic analysers in clinical biochemistry. *Clin Phys Physiol Meas* 1986; 7(1): 1-29.
- Rosenblum BB, Hanash SM, Yew N, Neel JV. Two-dimensional electrophoretic analysis of erythrocyte membranes. *Clin Chem* 1982;28(4:2):925-31.
- Ross JF, Finch CA, Peacock WC, Sammons ME. The in vitro preservation and post-transfusion survival of stored blood. *J Clin Invest* 1947;26(4):687-703.
- Rouault C. Red cell oxygen delivery. Effect of 2,3-diphosphoglycerate. *Postgrad Med* 1973;53(3):201-3.
- Rous P, Turner JW. The preservation of living red blood cells in vitro. *J Exp Med* 1916; 23:219-237.
- Roux A, Lison D, Junot C, Heilier JF. Applications of liquid chromatography coupled to mass spectrometry based metabolomics in clinical chemistry and toxicology: A review. *Clin Biochem* 2011; 44(1): 119-35.
- Sakr Y, Chierago M, Piagnerelli M, et al. The microvascular response to red blood cell transfusion in patients with severe sepsis. *Crit Care Med* 2007; 35:1639-44.
- Salhany JM, Mathers DH, Eliot RS. Molecular basis for oxygen transport. Hemoglobin function and controlling factors. *Adv Cardiol* 1973;9:53-67.
- Salzer U, Hinterdorfer P, Hunger U, Borcken C, Prohaska R. Ca⁺⁺-dependent vesicle release from erythrocytes involves stomatin-specific lipid rafts, synexin (annexin VII), and sorcin. *Blood* 2002;99:2569-77.
- Sana TR, Waddell K, Fischer SM. A sample extraction and chromatographic strategy for increasing LC/MS detection coverage of the erythrocyte metabolome. *J Chromatogr B Analyt Technol Biomed Life Sci* 2008; 871: 314-1.
- Schifferli JA, Taylor RP. Physiological and pathological aspects of circulating immune complexes. *Kidney Int* 1989;35:993-1003.
- Ramsey G. Frozen red blood cells: cold comfort in a disaster? *Transfusion* 2008;48(10):2053-5.

- Schmaier AH, Petruzzelli LM. Red blood cell Biochemistry and physiology. In "Hematology for the medical student". Lippincott Williams & Wilkins 2003;3:22-3;
- Scott KL, Lecak J, Acker JP. Biopreservation of red blood cells: past, present, and future. *Transfus Med Rev* 2005;19(2):127-42.
- Scott KL, Lecak J, Acker JP. Biopreservation of red blood cells: past, present, and future. *Transfus Med Rev* 2005;19(2):127-42.
- Sennels L, Salek M, Lomas L, Boschetti E, Righetti PG, Rappsilber J. Proteomic analysis of human blood serum using peptide library beads. *J Proteome Res*. 2007;6(10):4055-62.
- Serkova NJ, Standiford TJ, Stringer KA. The emerging field of quantitative blood metabolomics for biomarker discovery in critical illnesses. *Am J Respir Crit Care Med* 2011; 184(6): 647-55.
- Shah RR. Pharmacogenetics in drug regulation: promise, potential and pitfalls. *Philos Trans R Soc Lond B Biol Sci* 2005;360(1460):1617-38.
- Shapiro MJ. To filter blood or universal leukoreduction: what is the answer? *Crit Care* 2004;8 (2):S27-30.
- Sharifi S, Dzik WH, Sadrzadeh SM. Human plasma and tirilazad mesylate protect stored human erythrocytes against the oxidative damage of g-irradiation. *Transfus Med* 2000; 10: 125-30.
- Sheehan, D. Detection of redox-based modification in twodimensional electrophoresis proteomic separations. *Biochem Biophys Res Commun* 2006;349:455-62.
- Shichishima T, Terasawa T, Hashimoto C, Ohto H, Takahashi M, Shibata A, et al. Discordant and heterogeneous expression of GPI-anchored membrane proteins on leukemic cells in a patient with paroxysmal nocturnal hemoglobinuria. *Blood* 1993;81(7):1855-62.
- Shields CE. Effect of adenine on stored erythrocytes evaluated by autologous and homologous transfusions. *Transfusion* 1969;9:115-9.
- Shields CE. Effect of adenine on stored erythrocytes evaluated by autologous and homologous transfusions. *Transfusion* 1969;9:115-9.
- Shinozuka T. Changes in human red blood cells during aging in vivo. *Keio J Med* 1994;43(3):155-63.
- Shushan B. A review of clinical diagnostic applications of liquid chromatography-tandem mass spectrometry. *Mass Spectrom Rev* 2010; 29(6): 930-44.
- Siems WG, Sommerburg O, Grune T. Erythrocyte free radical and energy metabolism. *Clin Nephrol* 2000;53(1):9-17.
- Silliman CC, Ambruso DR, Boshkov LK. Transfusion-related acute lung injury. *Blood* 2005; 105: 2266-73.
- Simó C, Bachi A, Cattaneo A, Guerrier L, Fortis F, Boschetti E, et al. Performance of combinatorial peptide libraries in capturing the low-abundance proteome of red blood cells. 1. Behavior of mono- to hexapeptides. *Anal Chem* 2008;80 (10):3547-65.
- Simon ER, Chapman RG, Finch CA. Adenine in red cell preservation. *J Clin Invest* 1962;41:351-9.
- Singh R, Sinclair KD. Metabolomics: approaches to assessing oocyte and embryo quality. *Theriogenology* 2007; 68 (Suppl 1): S56-62.

- Skeaff CM, Hodson L, McKenzie JE. Dietary-induced changes in fatty acid composition of human plasma, platelet, and erythrocyte lipids follow a similar time course. *J Nutr* 2006;136(3):565-9.
- Skeggs LU Jr. An automatic method for colorimetric analysis. *Am J Clin Pathol* 1957; 28: 311
- Smith AU. Prevention of hemolysis during freezing and thawing of red blood cells. *Lancet* 1950;2:910-1.
- Smith, C.A. et al. METLIN: a metabolite mass spectral database. *Ther. Drug. Monit.* 2005; 27, 747-751.
- Sparrow RL. Time to revisit red blood cell additive solutions and storage conditions: a role for "omics" analyses. *Blood Transfus.* 2012 May;10 Suppl 2:s7-11.
- Sparrow RL. Time to revisit red blood cell additive solutions and storage conditions: a role for "omics" analyses. *Blood Transfus.* 2012 May;10 Suppl 2:s7-11.
- Spieß B. Red cell transfusion and guidelines: a work in progress. *Heme Clin NA* 2007; 21: 185-200.
- Stein LD. Human genome: end of the beginning. *Nature* 2004;431(7011):915–6.
- Steiner ME, Stowell C. Does red blood cell storage affect clinical outcome? When in doubt, do the experiment. *Transfusion* 2009; 49: 1286-90.
- Sud M, Fahy E, Cotter D, Brown A, Dennis EA, Glass CK, Merrill AH Jr, Murphy RC, Raetz CR, Russell DW, Subramaniam S. LMSD: LIPID MAPS structure database. *Nucleic Acids Res.* 2007 Jan;35(Database issue):D527-32.
- Sweeney J, Kouttab N, Kurtis J. Stored red blood cell supernatant facilitates thrombin generation. *Transfusion* 2009; doi: 10.1111/j.1537-2995.2009.02196.x
- Tanemoto K, Kuinose M, Kanaoka Y. Predonation of autologous blood for up to 6 weeks in MAP solution prior to elective cardiac surgery *Nippon Kyobu Geka Gakkai Zasshi* 1994;42(2):212-6.
- Tannert C, Schmidt G, Klatt D, Rapoport SM. Mechanism of senescence of red blood cells. *Acta Biol Med Ger* 1977;36(5-6):831-6.
- Tautenhahn R, Patti GJ, Rinehart D, Siuzdak G. XCMS Online: a web-based platform to process untargeted metabolomic data. *Anal Chem.* 2012;84(11):5035-9.
- Taylor RW, O'Brien J, Trottier SJ, et al. Red blood cell transfusions and nosocomial infections in critically ill patients. *Crit Care Med* 2006; 34: 2302-8.
- Thadikaran L, Siegenthaler MA, Crettaz D, Queloz PA, Schneider P, Tissot JD, et al. Recent advances in blood-related proteomics. *Proteomics* 2005;5:3019–34.
- Thiele T, Steil L, Völker U, Greinacher A. Proteomics of blood-based therapeutics. *BioDrugs* 2007;21:179–93.
- Tinmouth A, Chin-Yee I. The clinical consequences of the red cell storage lesion. *Transfus Med Rev* 2001;15: 91-107.
- Tiselius A. A new apparatus for electrophoretic analysis of colloidal mixtures. *A Tiselius - Trans Faraday Soc* 1937; 33: 524-31.
- Tiselius A. Electrophoresis of serum globulin. I. *Biochem J* 1937;31(2):313–7.
- Tsai AG, Cabrales P, Intaglietta M. Microvascular perfusion upon exchange transfusion with stored red blood cells in normovolemic anemic conditions. *Transfusion* 2004;44:1626-34.

- Turrini F, Arese P, Yuan J, Low PS. Clustering of integral membrane proteins of the human erythrocyte membrane stimulates autologous IgG binding, complement deposition and phagocytosis. *J Biol Chem* 1991;236:23611–7.
- Tyan YC, Jong SB, Liao JD, Liao PC, Yang MH, Liu CY, et al. Proteomic profiling of erythrocyte proteins by proteolytic digestion chip and identification using two-dimensional electrospray ionization tandem mass spectrometry. *J Proteome Res* 2005;4:748–57.
- Untucht-Grau R, Schirmer RH, Schirmer I, Krauth-Siegel RL. Glutathione reductase from human erythrocytes: amino-acid sequence of the structurally known FAD-binding domain. *Eur J Biochem* 1981;120(2):407-19.
- Unwin KS, Morgan GJ, Davies FE. Proteomics and the haematologist. *Clin Lab Haem* 2004;26:77–86.
- Unwin RD, Whetton AD. How will haematologists use proteomics? *Blood Rev* 2007;21(6):315–26.
- Urbanczyk-Wochniak, E. et al. Parallel analysis of transcript and metabolic profiles: a new approach in systems biology. *EMBO Rep.* 2003; 4, 989–993.
- US Public Health Service: Department of Health & Human Services. July 11, 2008. Available at: <http://www.hhs.gov/ohps/bloodsafety/recommendations/resmay08.pdf> Last accessed on the 13th of July, 2009.
- Valeri CR, Collins FB. Physiologic effects of 2,3-DPG-depleted red cells with high affinity for oxygen. *J Appl Physiol* 1971;31:823-7.
- Valeri CR, Pivacek LE, Cassidy GP, Ragno G. The survival, function and hemolysis of human RBCs stored at 4°C in additive solution (AS-1, AS-3 or AS-5) for 42 days and then biochemically modified, frozen, thawed, washed and stored at 4°C in sodium chloride and glucose solution for 24 hours. *Transfusion* 2000;40:1341-5.
- Valeri CR, Ragno G, Pivacek LE, Cassidy GP, Srey R, Hansson-Wicher M, et al. An experiment with glycerol-frozen red blood cells stored at -80 degrees C for up to 37 years. *Vox Sang* 2000;79:168–74.
- Valeri CR, Ragno G, Pivacek LE, Srey R, Hess JR, Lippert LE, et al. A multicenter study of in vitro and in vivo values in human RBCs frozen with 40-percent (wt/vol) glycerol and stored after deglycerolization for 15 days at 4 degrees C in AS-3: assessment of RBC processing in the ACP 215. *Transfusion* 2001;41:933–9.
- Valtis DJ, Kennedy AC. Defective gas-transport function of stored red blood cells. *Lancet* 1954;1:119–24.
- Vamvakas EC, Blajchman MA. Transfusion-related immunomodulation (TRIM): an update. *Blood Rev* 2007; 21: 327-48.
- Vamvakas EC, Blajchman MS. Universal WBC reduction: the case for and against. *Transfusion* 2001; 41: 691-712.
- Vamvakas EC, Carven JH. Length of storage of transfused red cells and postoperative morbidity in patients undergoing coronary artery bypass graft surgery. *Transfusion* 2000; 40: 101-9.
- Vamvakas EC, Carven JH. Transfusion and postoperative pneumonia in coronary artery bypass graft surgery: effect of the length of storage of transfused red cells. *Transfusion* 1999; 39: 701-10.
- van deWatering L, Lorinser J, Versteegh M, et al. Effects of storage time of red blood cell transfusions on the prognosis of coronary artery bypass graft patients. *Transfusion* 2006; 46: 1712-8.
- van Wijk R, van Solinge WW. The energy-less red blood cell is lost: erythrocyte enzyme abnormalities of glycolysis. *Blood* 2005;106(13):4034-42.
- Vinayavekhin N, Homan EA, Saghatelian A. Exploring disease through metabolomics. *ACS Chem Biol* 2010; 5(1): 91-103.

- Walker WH, Netz M, Ganshirt KH. 49 day storage of erythrocyte concentrates in blood bags with the PAGGS mannitol. *Beitr Infusions Ther* 1990;26:55-9.
- Walsh A. The application of atomic absorption spectra to chemical analysis. *Spectrochim Acta* 1955; 7: 108.
- Walsh TS, McArdle F, McLellan SA, et al. Does the storage time of transfused red blood cells influence regional or global indexes of tissue oxygenation in anemic critically ill patients? *Crit Care Med* 2004; 32:364-71.
- Wasinger VC, Cordwell SJ, Cerpa-Poljak A, Yan JX, Gooley AA, Wilkins MR, et al. Progress with gene-product mapping of the Mollicutes: *Mycoplasma genitalium*. *Electrophoresis* 1995;16:1090-4.
- Wasser MN, Houbiers JG, D'Amaro J, et al. The effect of fresh versus stored blood on post-operative bleeding after coronary bypass surgery: a prospective randomized study. *Br J Haematol* 1989; 72: 81-4.
- Ways P, Hanahan DJ. Characterization and quantification of red cell lipids in normal man. *J Lipid Res.* 1964;5(3):318-28.
- Weber RE, Voelter W, Fago A, et al. Modulation of red cell glycolysis: interactions between vertebrate hemoglobins and cytoplasmic domains of band 3 red cell membrane proteins. *Am J Physiol Regul Integr Comp Physiol* 2004; 287: 454-64.
- Wei R. Metabolomics and its practical value in pharmaceutical industry. *Curr Drug Metab* 2011; 12(4): 345-58.
- Weinberg JA, McGwin G Jr, Griffin RL, et al. Age of transfused blood: an independent predictor of mortality despite universal leukoreduction. *J Trauma* 2008; 65: 279-82.
- Wiback SJ, Palsson BO. Extreme pathway analysis of human red blood cell metabolism. *Biophys J* 2002;83(2):808-18.
- Willekens FL, Werre JM, Groenen-Dopp YA, et al. Erythrocyte vesiculation: a self-protective mechanism? *Br J Haematol* 2008; 141: 549-56.
- Williams RJ et al. *Biochemical Institute Studies IV. Individual metabolic patterns and human disease: An exploratory study utilizing predominantly paper chromatographic methods.* U. Texas Publication No. 5109 Univ. of Texas, Austin, 1951,204 pp.
- Wiltgen M, Tilz GP. DNA microarray analysis: principles and clinical impact. *Hematology* 2007;12(4):271-87.
- Winsten S. The skeptical chemist. *Clin Chem* 1969; 15: 737-44.
- Winterbourn CC: Oxidative denaturation in congenital hemolytic anemias: The unstable anemias. *Semin Hematol* 1990;27:41-50.
- Wishart DS. Applications of metabolomics in drug discovery and development. *Drugs R. D.* 2008; 9(5), 307-322.
- Wishart DS. Computational approaches to metabolomics. *Methods Mol Biol* 2010; 593: 283-313.
- Wolfe L, Byrne A, Chiu D. The storage lesion of liquid preserved erythrocytes is blocked in vivo by treatment with carbon monoxide. *Blood* 1987;70:335-7.
- Wolfe LC, Byrne AM, Lux SE. Molecular defect in the membrane cytoskeleton of blood bank-stored red cells. Abnormal spectrin-protein 4.1-actin complex formation. *J Clin Invest* 1986;78:1681-6.
- Wolfe LC. Oxidative injuries to the red cell membrane during conventional blood preservation. *Semin Hematol* 1989; 26: 307-12.

- Yap CH, Lau L, Krishnaswamy M, et al. Age of transfused red cells and early outcomes after cardiac surgery. *Ann Thorac Surg* 2008; 86: 554-9.
- Yocum AK, Yu K, Oe T, Blair IA. Effect of immunoaffinity depletion of human serum during proteomic investigations. *J Proteome Res* 2005;4(5):1722–31.
- Yoshida T, AuBuchon JP, Dumont LJ, et al. The effects of additive solution pH and metabolic rejuvenation on anaerobic storage of red cells. *Transfusion* 2008; 48: 2096-105.
- Yoshida T, AuBuchon JP, Tryzelaar L, et al. Extended storage of red blood cells under anaerobic conditions. *Vox Sang* 2007; 92: 22-31.
- Zallen G, Offner PJ, Moore EE, et al. Age of transfused blood is an independent risk factor for postinjury multiple organ failure. *Am J Surg* 1999; 178: 570-2.
- Zhang D, Kiyatkin A, Bolin JT, Low PA. Crystallographic structure and functional interpretation of the cytoplasmic domain of erythrocyte membrane band 3. *Blood* 2000;96:2925-33.
- Zhou M, Lucas DA, Chan KC, et al. An investigation into the human serum interactome. *Electrophoresis* 2004;25:1289–98.
- Zimrin AB, Hess JR. Current issues relating to the transfusion of stored red blood cells. *Vox Sang* 2009; 96: 93-103.
- Zolla L, D'Alessandro A. Proteomic Investigations on Stored Red Blood Cells. In *Chemistry and Biochemistry of Oxygen Therapeutics: From Transfusion to Artificial Blood*. 2010; Mozzarelli A. Editor; John Wiley and Sons Ltd The Atrium, Southern Gate Chichester, West Sussex, PO19 8SQ
- Zolla L, Liunbruno G, D'Amici GM, Grazzini G. Adverse effects related to storage lesions: proteomic profiles of red blood cells during storage. *Blood Transfus* 2009; s22-3.
- Zolla L. Proteomics studies reveal important information on small molecule therapeutics: a case study on plasma proteins. *Drug Discov Today*. 2008; 13(23-24), 1042-1051.
- Zolla L. Proteomics studies reveal important information on small molecule therapeutics: a case study on plasma proteins. *Drug Discov Today* 2008;13(23-24):1042–51.
- Zuck TF, Bensinger TA, Peck CC, Chillar RK, Beutler E, Button LN, et al. The in vivo survival of red blood cells stored in modified CPD with adenine: report of a multi-institutional cooperative effort. *Transfusion* 1977;17:374–82.

Chapter 2: *In silico* analyses and protein-protein interactions

Contents

2.1 The red blood cell proteome and interactome: an update

2.2 Native protein complexes in the cytoplasm of Red Blood Cells

The contents of this chapter report the contents of the the following publications by the candidate:

1. D'Alessandro A, Righetti PG, Zolla L.
The red blood cell proteome and interactome: an update.
J Proteome Res. 2010;9(1):144-63.
 13. Pallotta V, D'Alessandro A, Rinalducci S, Zolla L.
Native protein complexes in the cytoplasm of Red Blood Cells
J Proteomics 2013; *under review*
-

TAKE HOME MESSAGE

In this chapter, we focus on *in silico* analyses and protein-protein interaction determination of erythrocyte cytosolic proteins through preliminary fractionation and native gel-based approaches. The results reported in this chapter will pave the way for the results described in the upcoming chapters, whereby we will describe the application of Integrated Omics approaches to red blood cell biology and transfusion medicine issues, especially in relation to the quality assessment of erythrocyte concentrates.

The “selfish –omics” or the clash of the “omics”

More than a decade has passed since the beginning of the genomic era (Boguski et al. 1996). However, 20-25,000 sequenced genes later (Stein, 2004), no definitive advances have been made in the biological quest for the infinite small, as Pascal would say. At the end of the beginning biological systems still stood fierce (Stein, 2004), shrouded in as much mystery as when the race began. It soon became evident that, when the genetic horizons had been reached, deeper and detailed information about its actual expression was still lacking. Proteomics (Wasinger et al., 1995) (and transcriptomics – Scheel et al., 2002) has become popular in this very phase, for bridging the gap towards the new horizon of the protein complement to the genome. As we approach to this horizon as well, multiple directions are unveiled, yet unexplored and just as much stimulating: metabolomics, lipidomics (Griffiths et al., 2009), PTMomics (Liu et al., 2008) and, last but not least, interactomics (Kandpal et al., 2009).

The next goal is to determine interactions among the whole expressed gene products in each cell/tissue so as to retrieve biologically relevant information from the mapped relations. The “omics-centered” view of scientific evolution recalls the gene-centric view of evolution from Dawkins’s masterpiece “The selfish gene” (Dawkins, 1976), as it holds that, whether we will ever have at disposal the final tool to delve into biological complexity, it will be a holistic, system complexity-oriented one.

This article is intended to give an updated view of the red blood cell (RBC) proteome and interactome (Goodman et al., 2007). RBCs play a pivotal role in gas transport (i.e. oxygen and carbon dioxide) and a minor, but not less important, role in a range of other functions, such as transfer of GPI-linked proteins (Shichishima et al., 1993; Kooyman et al., 1995) and transport of iC3b/C3b-carrying immune complexes (Civenni et al., 1998).

In humans, the circulating mature RBC is the end stage of a developmental process which starts in the bone marrow, as hematopoietic stem cells differentiate to enucleated reticulocytes (Schifferli and Taylor, 1989). Being enucleated, erythrocytes display a meager amount of mRNA, as a limited heritage from their reticulocyte ancestors. After extrusion of nuclei and degradation of internal organelles and endoplasmic reticulum, reticulocytes emerge in the circulation, where they rapidly develop into mature RBCs (Pasini et al., 2006; Palis, 2008). Until the end of its life span of 120 ± 4 days, with 120 miles of travel and $1.7 \cdot 10^5$ circulatory cycles, the human RBC has successfully coped with a number of dangers, such as passages across narrow capillaries and splenic slits, periodic high turbulences and high shear stresses, along with extremely hypertonic conditions. Owing to its constant cytoskeleton rearrangement, RBCs are able to traverse passage ways as narrow as $1 \mu\text{m}$ in diameter, by changing their shape from a biconcave disc of $8 \mu\text{m}$ diameter to a cigar shape.¹⁶ In this perfectly-balanced cellular carrier, hemoglobin accounts for more than 90% of the cellular dry weight and approximately 98% of the overall cytoplasmic protein content. This biological/technical shortcoming has hitherto hampered a comprehensive analysis of the RBC proteome by altering the outcomes with minor, albeit inevitable, losses of information about a whole “hidden proteome”. Therefore, although RBCs have always been eligible targets for proteomics investigations, only in the last few years new technical advancements tackling the dynamic range issue, such as pre-fractionation methods adopting hexapeptide combinatorial ligand libraries have allowed a substantial improvement in this field (Boschetti and Righetti, 2009).

Hereby we briefly resume a few milestones in the erythrocyte proteomics research and present an updated interactomics analysis of these newly available data.

Proteomics of RBCs: a brief update

The story of RBC proteomics is full of gradual constant progresses over the last decade, as it has been recently reviewed (**Table 1 – Chapter 1**) (Liumbruno et al., 2009). Nonetheless, early proteomics investigations on the RBC membrane proteome date back to 1982, when Rosenblum and co-workers firstly outlined the 2-DE profiles of normal adults, neonates and patients with erythrocyte membrane disorders (Roseblum et al., 1982). However, more in-depth proteomic studies on RBC membranes had to wait the advent of mass spectrometry. In 2002 Low and colleagues individuated overall 102 proteins (59 distinct polypeptides, 43 isoforms, mostly membranaceous) by means of 2-DE and MALDI-TOF analysis (Low et al., 2002).

In 2004, Kakhniashvili investigated the RBC proteome by means of an IT-MS/MS coupled on-line with a RP-LC, which yielded identification of 182 proteins, equally distributed between the cytosolic and the membrane fractions (Kakhniashvili et al., 2004).

In a recent study, Tyan and colleagues (2005) adopted a special proteolytic chip, consisting of 11-mercaptoundecanoic acid bonded on self-assembled monolayers of alkanethiols onto gold surfaces. Subsequent 2D-nano-HPLC and MS/MS analyses enabled the identification of 272 proteins from erythrocyte samples.

In 2005, Bruschi and co-workers individuated 500 spots with soft Immobiline gels, among which noteworthy was the presence of high levels of filamentous proteins (e.g. alpha-spectrin and ankyrins), or integral membrane proteins (e.g. band 3, band 4.1 and 4.2). Both classes of proteins are not usually displayed or barely present in maps exploiting immobilized pH gradients in the first dimension, while they were revealed through this alternative approach. Indeed, several drawbacks limit the use of 2-DE for proteomics research. Although 2-DE has many benefits, the technique does not lend itself to large-scale, high-throughput proteomic analyses due to a series of major shortcomings. For example, not all types of proteins are well resolved in this system, while proteins bearing extremes of size, hydrophobicity, or charge fail to enter the gel and are poorly represented (Page et al., 2006). Soft Immobiline gels replacing IPG strips in the first dimension of 2-DE allowed to partially overcome these obstacles, especially as far as it regarded high molecular mass proteins.

One of the most recent and complete studies on the RBC proteome dates back to 2006, when Pasini et al. carried out a thorough analysis consisting of 1-DE (SDS-PAGE) followed by in-gel digestion and LC-ESI-MS/MS (either Q-TOF and FTICR). The overall analyses helped the Authors compiling a final list of 340 membrane and 252 soluble proteins.

Recently-debated clinical retrospective (Koch et al., 2008) studies have prompted the transfusion medicine establishment to wonder about the safety and efficiency of long-stored blood components and, in particular, of erythrocyte concentrates. In this scenario, proteomics has revealed an innovative instrument to re-establish quality criteria anew, first of all addressing the molecular changes at the protein level which accompany RBCs as they age. Zolla's (D'Amici et al., 2007) and Bosman's (2008) group papers, though fundamentally addressing the storage

Table 1 – RBC interactome: Top 15 Pathways (out of 850)

Category	Function	Function Annotation	P-value	Molecules	# Molecules
1. Molecular Transport	transport	transport of protein	1,39E-22	AP1B1, AP1G1, AP1M1, AP2A1, AP2A2, AP2M1, AP3S1, AP4S1, ARCNI, ARFI, ARF6, ARFGAP1, ARFIP1, ASPSCR1, CALR, CFL1, CHMP5, DCTN1, DNAJA2, DNAJA4, EIF5A, ERP29, GDI2, HTT, IPO7, IPO9, IPO11, KPNA4, KPNA6, KPNB1, LGTN, MYH9, NAPA, NDE1, NEDD4, NPM1 (includes EG:4869), NRBP1, NUTF2, PDIA3, PEX5, PTPN11, RAB10, RAB13, RAB1A, RAB2A, RAB3GAP2, RAB4A, RAB7A, RAN, RANGAP1, RFFL, RHOB, SCAMP2, SCFD1, SEC22B, SEC23IP, SNX1, SNX9 (includes EG:51429), STX7, TMED10, TMX1, TRAPPC3, USE1, USO1, VAPA, VCP, VPS45, XPO1, XPO5, XPO7, YKT6, YWHAH, ZW10	73
2. Protein Synthesis	metabolism	metabolism of protein	2,67E-17	ABCF1, ACHE, ACO1, ADRM1, ANAPC5, ANPEP, APP, ARIH1, ARIH2, ATG7, ATG4A, ATG4B, BAG1, BAG2, BCL10, BLMH, CALR, CAPN1, CAPN2, CAPNS1, CASP3, CASP8, CAST, CKAP5, COPSS, CTSB, CUL2, CUL3, DPP3, EEF2, EEF1A1, EEF1A2, EGLN2, EIF5, EIF2B1, EIF2B2, EIF2B3, EIF2B4, EIF2S1, EIF2S3, EIF3F, EIF3G, EIF3I (includes EG:8668), EIF3J, EIF4A1, EIF4A3 (includes EG:9775), EIF4B, EIF4E, EIF4G1, EIF5A, ELANE, FAF1, FBXO7, FLNA, FN1, GLMN, GSPT1, HBS1L, HDAC6, HGS, HNRNP, HSPB1, HTT, IDE, IL18, IMPACT, INPP5D, KIAA0368, LNPEP, MAP2K3, MAPK1, METAP1, MTOR, MYH9, NACA, NCSTN, NEDD4, NFX1, PAIP1, PDIA2, PEPD, PIK3R1, PREP, PSMB3, PSMB5, PSMC2, PSMC4, PSMD14, PTBP1, RAD23A, RBM3, RNPEP, RPL8, RPL11, RPL22, RPL26, RPL30, RPL31, RPS2, RPS3, RPS5, RPS6, RPS9, RPS10, RPS11, RPS19, RPS12 (includes EG:6206), RPS17 (includes EG:6218), RPS3A, RPS4X, RPS6KA1, RPS6KB1, SERPINB1, SSB, STAT5B, THBS1, THOP1, TPP2, TSG101, UBA3, UBE2A, UBE2H (includes EG:7328), UBE2I, UBE2K, UBE2L3, UBE2N, UBE4B, UBR1, UFD1L, USE1, USP11, USP9X, VCP, XPNPEP1, XPO1	135
3. Cellular Assembly and Organization	transport	transport of vesicles	2,83E-16	ACTR1A, AP1B1, AP1G1, AP1M1, AP1S1, AP2A1, AP2A2, AP2M1, AP3S1, AP4S1, APOA1, APOE, ARF1, ARF6, CHMP1A, CLINT1, COPZ1, CPNE1, CPNE3, CYTH1, DENND1A, EPN1, EPS15, GSN, HDAC6, HTT, ITSN1, M6PRBP1, MAP2K1, NAPA, NAPG, NDE1, PAFAH1B1, PICALM, RAB13, RAB1A, SCAMP2, SCFD1, SEC22B, SEC23B, SNAP23, SNCA, SOD1, SPTBN4, STX4, STX6, STX7, STX16, SYNJ1, USO1, VPS33B, VPS4A	52
4. Post-Translational Modification and Protein folding	folding	folding of protein	3,94E-14	AARS, BAG2, BAG5, CALR, CCT3, CCT7, CCT6A, DNAJA2, DNAJA4, DNAJB6, DNAJB2 (includes EG:3300), ERAF, ERP29, FKBP4, FKBP5, HSP90AA1, HSP90AB1, HSPA5, HSPA8, HSPBP1, PDIA2, PFDN2, PFDN4, PIN4, PPIA (includes EG:5478), RP2, RUVBL2, SH3GLB1, ST13, TBCA, TCPI1, TXN, UGCGLI1	33
5. Cellular Assembly and Organization	fusion	fusion of cellular membrane	1,43E-12	ANXA1, ANXA7, ATG7, CTBP1, GCA, NAPA, NAPG, NPLOC4, NSFL1C, RABEP1, RABIF, SNAP23, SNAP29, USO1, VAMP3, VAPA, VPS4B, VTI1A	18
6. Immunological Disease	acute allergic pulmonary eosinophilia	acute allergic pulmonary eosinophilia	1,22E-10	ACTB, ALB, ALDOA, ARG1, ENO1, HNRNPAB, HSPA5, MYH9, P4HB, PDIA3, PRDX1, PRDX6, SELENBP1, STAT6, TKT, TPI1, TUBB	17
7. Cellular Function and Maintenance	endocytosis	endocytosis	1,02E-09	ACTN4, AP1S1, AP2A2, APP, ARF6, ARRB2, ATP5B, ATP6V1H, CAPI, CD44, CD2AP, CDC42, CTTN, DENND1A, DNM2, EHD1, EPN1, EPS15, HGS, HTT, ITSN1, KRAS, NAE1, NECAP1, NEDD4, PICALM, RAB15, RAB22A, RAB7A, RABEP1, RAC1, REPS1, RHOA, RHOB, SCAMP2, SNX1, SNX2, SNX3, SYNJ1	39
8. Protein Degradation	catabolism	catabolism of protein	1,27E-09	ANAPC5, ARIH1, ARIH2, ATG7, ATG4B, CAST, CUL2, CUL3, EGLN2, FAF1, FBXO7, FLNA, HDAC6, HGS, KIAA0368, LNPEP, MTOR, NCSTN, NEDD4, PSMB3, PSMC2, PSMD14, SERPINB1, UBE2A, UBE2H (includes EG:7328), UBE2I, UBE2K, UBE2L3, UBE2N, UBE4B, UBR1, UFD1L, USE1, USP11, VCP, XPO1	36
9. Protein Synthesis	synthesis	synthesis of protein	2,24E-09	ABCF1, ACO1, APP, BCL10, CALR, CASP3, CKAP5, COPSS, DCTN2, EEF2, EEF1A1, EEF1A2, EIF5, EIF2B1, EIF2B2, EIF2B3, EIF2B4, EIF2S1, EIF2S3, EIF3F, EIF3G, EIF3I (includes EG:8668), EIF3J, EIF4A1, EIF4A3 (includes EG:9775), EIF4B, EIF4E, EIF4G1, EIF5A, ELANE, FN1, GLMN, GSN, GSPT1, HBS1L, HNRNP, HSPB1, IL18, IMPACT, INPP5D, MAP2K3, MAPK1, METAP1, METAP2 (includes EG:10988), MTOR, NACA, NFX1, NPM1 (includes EG:4869), PAIP1, PIK3R1, PTBP1, PTPN11, RBM3, RPL8, RPL11, RPL22, RPL26, RPL30, RPL31, RPS2, RPS3, RPS5, RPS6, RPS9, RPS10, RPS11, RPS19, RPS12 (includes EG:6206), RPS17 (includes EG:6218), RPS3A, RPS4X, RPS6KA1, RPS6KB1, SSB, STAT5B, THBS1	76
10. Cellular Assembly and Organization	development	development of cytoskeleton	4,00E-09	ACTB, ADD1, AP1G1, APOE, ARF6, ARHGAP4, ARHGD1B, ARPC5, CALR, CAP1, CDC42, CFL1, CNP, CORO1C, CRK, CSRP1, EPB49, FLG (includes EG:2312), FLNA, FLNB, FSCN1, GABARAP, KRAS, LSP1, MAEA, MAP1S, MYH10, PACSIN2, PAFAH1B1, PLEK2, RAC1, RAN, RHOA, ROCK1, ROCK2, SHC1, SHROOM3, TLN1, TPM1, TUBG1, VASP	41

11	Cellular Assembly and Organization	formation	formation of vesicles	5,56E-09	ANXA5, AP2A2, ARF1, ARFGAP1, ARFGF2, ATG9A, C3, CAST, CLTC, EPS15, HGS, HTT, MTOR, NSF, PITPNA, PRKACA, ROCK1, ROCK2, YKT6	19
12	Cellular Assembly and Organization	biogenesis	biogenesis of cytoskeleton	5,96E-09	ADD1, APIG1, APOE, ARF6, ARHGAP4, ARHGDIB, ARPC5, CALR, CAP1, CDC42, CFL1, CNP, CORO1C, CRK, CSRP1, EPB49, FLG (includes EG:2312), FLNA, FLNB, FSCN1, GABARAP, KRAS, LSP1, MAEA, MAP1S, MYH10, PACSIN2, PAFAH1B1, PLEK2, RAC1, RAN, RHOA, ROCK1, ROCK2, SHC1, SHROOM3, TLN1, TPM1, TUBG1, VASP	40
13	Cell Death	cell death	cell death of cell lines	7,99E-09	ABCC1, ABCC4, ABCE1, ABCG2, ACHE, ACTB, ADRM1, AHS1, AKT1S1, ALDH3A1, AP2A2, APOE, APP, ARHGAP4, ARRB2, ATG7, ATP2B1, ATXN3, BAD, BAG1, BAT3, BCL10, BCL2L1, BID, BTK, CALR, CAPNS1, CARD8, CASP3, CASP8, CAST, CAT, CCDC6, CCT2, CCT3, CCT5, CCT7, CCT8, CCT6A, CD44, CD47, CD55, CD59, CD99 (includes EG:4267), CDC42, CDKN2C, CHMP5, CIAPIN1, CIB1, CLU, COPS5, CRK, CSNK1A1, CSNK2A1, CSNK2A2, CSTA, CTBP1, CTTN, CYB5R3, DCTN2, DDX3X, DFFA, DNAJB1, DNML, EEF1A1, EEF1A2, EIF4E, ENO1, FADD, FAF1, FASN, FKBP5, FN1, FNTA, FREQ, FTH1, FUBP1, G6PD, GAB1, GAPDH (includes EG:2597), GLO1, GLRX, GMFB, GNAS, GNB1, GNB2, GPI, GPX4, GSN, GSR, GSTP1, HCLS1, HNRNP1A, HNRNPC, HSP90A1, HSPA5, HSPA8, HSPB1, HTATIP2, HTT, HUWE1, IGHM, IL18, INPP5D, ITSN1, JUP, KRAS, LCMT1, LDHA, LGALS3, LGALS9, LSP1, MAP2K1, MAP2K4, MAPK1, MAPKAP1, MCT5, MIB1, MSN, MTOR, NAMPT, NAPA, NFKBIB, NME1, NMNAT3 (includes EG:349565), NPM1 (includes EG:4869), NRAS, NUDCD3, P4HB, PA2G4, PAK2, PARK7, PCBP2, PDCC6IP, PDIA3, PEA15, PEBP1, PIK3R1, PIN1, PLSCR1, PML, PPIA (includes EG:5478), PPM1A, PPP2CA, PPP2R1A, PPP2R1B, PPP2R2A, PPP5C, PRDX1, PRDX2, PRKAA1, PRKACA, PRKAR1A, PRKAR2B, PTPN6, PTPN11, PURA, RABGGTA, RABGGTB, RAC1, RAD23B, RDX, RGS10, RHOA, RHOB, RNF7, RPLP0 (includes EG:6175), RPS6KA1, RPS6KB1, S100A4, S100A6, S100A8, S100A9, S100A11, SERPINB3, SERPINB5, SFN, SH3GLB1, SHC1, SIRT2, SLC2A1, SLK, SMAD2, SNCA, SOD1, SRPK1, STAT6, STAT5B, SYK, TAOK3, TCP1, TGM2, THBS1, TMX1, TPM1, TPP2, TRADD, TRAP1, TSG101, TUBA1A, TXN, TXNDC17, TXNRD1, UBA1, UBQLN1, USE1, VCP, VPS28, XRCC5, YARS, YWHAB, YWHAH, YWHAQ (includes EG:10971), ZMYND11	214
14	Post-Translational Modification	modification	modification of protein	1,29E-08	AADACL1, AARS, ACP1, ALDH1A1, ALDH3A1, APOA1, APOE, APP, ARAF, ARD1A, ARRB2, ATG3, ATG7, BAG2, BAG5, BCL10, BCL2L1, BSG, BTK, CALR, CAND1, CAPN1, CARM1, CAST, CAT, CCT3, CCT7, CCT6A, CD44, CD47, CD55, CDK2, CRK, CSNK2A1, CUL1, CUL2, CUL5, DNAJA2, DNAJA4, DNAJB6, DNAJB2 (includes EG:3300), ERAF, ERP29, FKBP4, FKBP5, FN1, FTH1, FTL, GSPT1, GYPC, HDAC6, HSP90A1, HSP90A1, HSPA5, HSPA8, HSPB1, HUWE1, IGHM, IMPACT, KEL, LCMT1, MAP2K4, MAPK1, METAP2 (includes EG:10988), MLST8, MOBKL1A, MTOR, NAE1, NCSTN, NEDD4, NME1, P4HB, PAK2, PARK7, PCMT1, PCNP, PDIA2, PDIA3, PFDN2, PFDN4, PIN4, PML, PPAP2A, PPIA (includes EG:5478), PPM1A, PPM1B, PPM1F, PPM1E, PPP1CB, PPP2CA, PPP2R1A, PPP2R2A, PPP5C, PPP6C, PRDX1, PRDX6, PRKACA, PRKDC, PTPN6, PTPN7, PTPN11, RABGGTA, RFFL, RP2, RUVBL2, SET, SH3GLB1, SIRT2, SIRT5, SNCA, SPTBN1, ST13, STK38, STK38L (includes EG:23012), SYK, TAOK3, TBCA, TCEB1, TCEB2, TCP1, THBS1, TPP2, TSG101, TSTA3, TTN, TXN, UBA1, UBA3, UBE2H (includes EG:7328), UBE2I, UBE2L3, UBE2M, UBE2N, UBE3C, UBE4B, UBL4A, UGCG1, USP7, WNK1	139
15	Cell Death	cell death	cell death	4,08E-08	AARS, ABCC1, ABCC4, ABCE1, ABCG2, ACHE, ACIN1, ACSL4, ACTB, ACTN4, ADRM1, AHS1, AKT1S1, ALB, ALDH1A1, ALDH3A1, ALDOA, ALDOC, ANP32A, ANPEP, ANXA1, ANXA7, AP2A2, APEX1, APOA1, APOE, APP, APRT, ARF6, ARG1, ARHGAP4, ARRB2, ATG7, ATP1A1, ATP1A2, ATP2B1, ATP2B4, ATXN3, BAD, BAG1, BAG5, BAT3, BCL10, BCL2L1, BID, BLVRA, BRCC3, BRE, BSG, BTK, C3, CALR, CAPN1, CAPNS1, CARD8, CASP3, CASP8, CAST, CAT, CCDC6, CCT2, CCT3, CCT5, CCT7, CCT8, CCT6A, CD44, CD47, CD55, CD59, CD2AP, CD99 (includes EG:4267), CDC37, CDC42, CDK2, CDKN2C, CHMP5, CIAPIN1, CIB1, CLU, CNP, COPS5, CR1, CRADD, CRK, CSDA, CSE1L, CSNK1A1, CSNK2A1, CSNK2A2, CSTA, CTBP1, CTSG, CTTN, CUL1, CUL2, CUL3, CUL5, CUL4A, CYB5R3, DCTN2, DDX3X, DFFA, DNAJB1, DNAJB6, DNAJB2 (includes EG:3300), DNAJC5, DNML2, DNML, EEF1A1, EEF1A2, EEF1D, EEF1E1, EIF2S1, EIF4E, EIF5A, ELANE, ENO1, ERAF, EZR, FADD, FAF1, FASN, FIS1, FKBP5, FLNA, FN1, FNTA, FREQ, FTH1, FUBP1, G6PD, GAB1, GAPDH (includes EG:2597), GCLC, GCLM, GLO1, GLRX, GMFB, GNA13, GNAQ, GNAS, GNB1, GNB2, GPI, GPX4, GSN, GSPT1, GSR, GSTP1, HCLS1, HDGF, HIST1H1C, HMGB1 (includes EG:3146), HNRNP1A, HNRNPC, HPR1, HSP90A1, HSP90A1, HSPA2, HSPA5, HSPA8, HSPB1, HTATIP2, HTT, HUWE1, IGHG1, IGHM, IL18, INPP5D, IQGAP2, IRF3, ITSN1, JMD6, JUP, KRAS, LCMT1, LDHA, LGALS3, LGALS9, LSP1, LYZ, MAEA, MAP1S, MAP2K1, MAP2K2, MAP2K3, MAP2K4, MAPK1, MAPKAP1, MCT5, MDH1, MIB1, MSN, MTOR, NAE1, NAMPT, NAPA, NFKBIB, NME1, NMNAT3 (includes EG:349565), NP, NPM1 (includes EG:4869), NQO2, NRAS, NSF, NUDCD3, OPTN, P4HB, PA2G4, PAFAH1B1, PAFAH1B2, PAFAH1B3, PAK2, PARK7, PCBP2, PDCC5, PDCC6, PDCC6IP, PDIA2, PDIA3, PEA15, PEBP1, PIK3CB, PIK3R1, PIN1, PITPNA, PLSCR1, PML, PPIA (includes EG:5478), PPM1A, PPM1F, PPP2CA, PPP2R1A, PPP2R1B, PPP2R2A, PPP2R5A, PPP5C, PRDX1, PRDX2, PRDX5, PRDX6, PRG2 (includes EG:5553), PRKAA1, PRKACA, PRKAR1A, PRKAR2B, PRKDC, PSMB1, PSMG2, PTPN6, PTPN11, PURA, RABGGTA, RABGGTB, RAC1, RAD50, RAD23B, RDX, RGS10, RHOA, RHOB, RNF7, ROCK1, RPLP0 (includes EG:6175), RPS3, RPS6, RPS6A, RPS6KA1, RPS6KB1, S100A4, S100A6, S100A8, S100A9, S100A11, SEMA7A, SERPINB3, SERPINB5, SET, SFN, SH3BGL3, SH3GLB1, SHC1, SIRT2, SLC2A1, SLC2A3, SLK, SMAD2, SNCA, SOD1, SRPK1, STAM, STAMBIP, STAT6, STAT5B, STIP1, STK24, SWAP70, SYK, TAOK3, TCP1, TGM2, THBS1, THG1L, TMX1, TPM1, TPM3, TPP2, TRADD, TRAP1, TSG101, TUBA1A, TXN, TXNDC17, TXNL1, TXNRD1, UBA1, UBA3, UBE2K, UBE2M, UBE4B, UBQLN1, UBR4, USE1, USP7, VAMP3, VAPA, VAPB, VCL, VCP, VPS28,	337

					XRCC5, YARS, YWHAB, YWHAE, YWHAQ (includes EG:10971), ZMYND11	
--	--	--	--	--	---	--

issue, have nonetheless provided a detailed portrait of the membrane and secreted micro- and nano-vesicle proteomes as well (257 proteins).

A substantial stride in the field of RBC proteomics has been favored by the introduction of the “Proteominer Technology”, which is a method enabling the capture of all species present in a proteome, but at much reduced protein concentration differences. It consists on a combinatorial library of hexapeptide ligands coupled to spherical porous beads of polymethacrylate. When these beads are contacted with proteomes of widely differing protein composition and relative abundances, they are able to “normalize” the protein population, by sharply reducing the level of the most abundant components while simultaneously enhancing the concentration of the most dilute species. In the joint study by Bachi et al. (2008) and Simò et al. (2008) individual amino acids or peptides of different length (from 2 to 6 amino acids) were packed as stationary phases of chromatographic affinity columns, and used as baits for capturing the low-abundance cytoplasmic proteome of RBCs. Aminoacids were named “petit catchers” and “grand catchers” after their capacity to interact and retain proteins. This protocol allowed the identification of approximately 800 proteins upon 2-DE (SDS-IEF) and by nanoLC-ESI-MS/MS (Bachi et al., 2008; Simò et al., 2008). Being repeatedly eluted from each one of the 16 affinity columns, a group of 72 proteins represented the “maximum common denominator”. It is worthwhile to underline that better outcomes were obtained with hydrophobic aminoacids, as polarity seemed to be a negative influencing-factor for interactions with the stationary phase. Simultaneously and independently, Roux-Dalvai et al. (Righetti and Boschetti, 2008), through the refinement of the ProteoMiner Technology (Roux-Dalvai et al., 2008), and the adoption of the fast and high-throughput ORBITRAP MS analysis, have utterly lead to the astonishing identification of 1,578 cytosolic proteins.³⁰ The striking conclusion was that, in an RBC lysate where haemoglobin alone constitutes 98% of the total proteins, the remaining 2% proteome is constituted by an incredible array of unique gene products. However, the debate is still open about their role as actually bioactive molecules or simple remnants of degraded/under degradation proteins inherited from reticulocyte ancestors.

From proteomics to interactomics: fostering complexity

Although a preliminary attempt to dive into the mare magnum of the RBC interactome has been recently made (Goodman et al., 2007), new advancements in the field of RBC proteomics claim for an update of the map of the erythrocyte complexity (Roux-Dalvai et al., 2008). In 2007, Goodman and colleagues elaborated an *in silico* analysis of the interactome of RBCs based on a summary of overall 751 proteins from previously published studies. However, out of those 751 gene products from the original dataset only 279 could be represented as nodes interacting among each others, while the remaining were omitted. In particular, a series of biologically relevant information could be retrieved from this analysis. Strikingly, the “interactome” scheme orbited around a central fulcrum of expressed proteins. This central core of expression encompassed a series of proteins involved in physiological responses to oxidative stress and unfolding (e.g. peroxiredoxins, catalases, chaperonines, heat shock proteins and proteasomal subunits). Thus, the authors named it the Repair or Destroy (ROD) box after the biological

role of these classes of proteins. These findings highlighted the molecular behavior of RBCs, which are enucleated and base their survival on the maintenance and repair of the existing proteome instead of on the synthesis of new proteins (Goodman et al., 2007).

During the last 2 years, new software platforms have become available as the interactomics discipline has started attracting a growing deal of interest. We exploited what is perhaps the most promising one for performing the present network and pathway analysis.

A list of 2,086 proteins reporting gene IDs was created merging the data from a series of proteomics paper available from literature.^{15, 26, 29-32} This dataset was submitted for elaboration of pathway and network analyses to the Ingenuity Pathway Analysis software (Ingenuity® Systems, www.ingenuity.com).

Each gene identifier from the submitted list was mapped to its corresponding gene object in the Ingenuity Pathways Knowledge Base. Redundant proteins were excluded, while isoforms of the same proteins were maintained to reach a total of 1,989 distinct gene products (**Supplementary material 1** of D'Alessandro et al., 2010). A total of 1,574 proteins had a match in the database and were eligible for network analysis (79,18%), while only 1,374 (69,08%) for pathway analysis. The significance of the association between the data set and the canonical and disease/toxicity pathways was measured in 2 ways: 1) A ratio of the number of proteins from the data set that map to the pathway divided by the total number of proteins that map to the canonical pathway is displayed. 2) Fischer's exact test was used to calculate a p-value determining the probability that the association between the proteins in the dataset and the canonical pathway is explained by chance alone. Highest scores are proportional to a lower probability of casual association. In the end, the software determines and graphs unbiased networks, in which gene products are represented as nodes, and the biological relationship between two nodes is represented as an edge (line). All edges are supported by at least 1 reference from the literature, from a textbook, or from canonical information stored in the Ingenuity Pathways Knowledge Base. Nodes are displayed using various shapes that represent the functional class of the gene product. Grey nodes represent the proteins from the submitted dataset which have a match in the canonical pathway from the database, while white nodes represent gene products that the software attributed to the same networks, although they were not present in the elaborated dataset. Continuous lines (edges) represent direct interactions, while indirect ones are represented by interrupted lines. Circular lines around one node describe a feedback loop of activity of that node on itself (e.g. by self-modulating its activity or expression). Grey edges represent interactions within a single network, while orange edges cross-link nodes from multiple interacting networks. The program could either graph single networks alone or merged together to stress their interactions.

The Ingenuity Pathway Analysis software allowed us to perform an unbiased elaboration of the available data, in order to focus subsequent analyses and discussions on the pivotal pathways and networks which are revealed upon the elaboration phase.

Pathway analysis

Software elaboration of the submitted dataset identified 69 main canonical pathways which could be further divided into 850 different subpathways, ranging from a minimum probability of 1.39 E-22 (highest score) to a maximum of 9.76 E-03 (lowest score). A list of the pathways is fully reported in the **supplementary material 2** of D'Alessandro

et al., 2010, while **Table 1** reports the top 15 canonical pathways, pointing out their functions, relative scores and protein entries. On the other hand **Figure 1** reports the top 10 disease/toxicity pathways, which enlist a series of proteins accounting for specific stresses/pathologies.

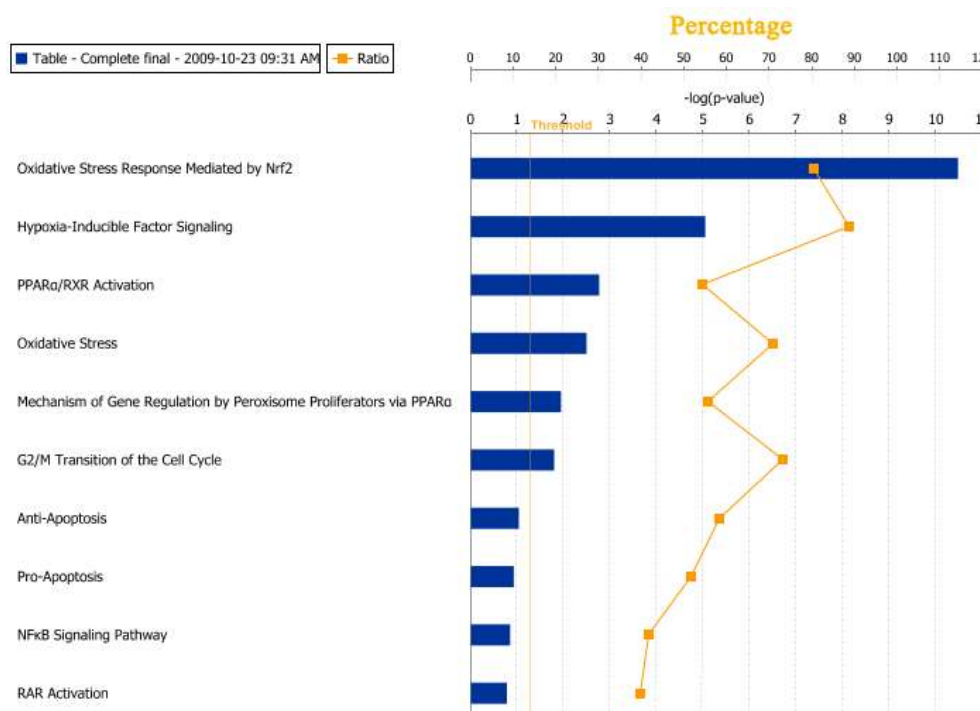


FIGURE 1 Top ten toxicity pathways. As it emerges from this analysis, oxidative stress likely plays a crucial role in the toxicity towards RBCs. This “*quasi-truism*” is useful to correlate the oxidative stress (3 out of 4 top pathways) with the regulation of apoptotic and anti-apoptotic signaling.

From these analyses it clearly emerges a role of oxygen in the toxicity towards RBCs, as it is intuitive. Being the main RBC function, oxygen transport exposes the RBC to a dramatic dose of continuous oxidative stress. Three out of four top toxicity pathways are clearly related to oxidative stress, as expected. However, it is notably that these pathways are likely related with regulation of apoptosis and anti-apoptotic signaling, as the three “apoptosis”, “anti-apoptosis” and “Nf κ B signaling” pathways explicitly suggest. This is in agreement with the mainstream theory about erythrocyte ageing in vivo and in vitro being closely related to apoptosis, as Lang’s group has resumed the well-known RBC-related senescence phenomena under the name of eryptosis (Lang et al., 2006). Similar considerations could be made when analyzing the list of top canonical pathways. Indeed, being constantly exposed to oxidative stresses while being enucleated and thus incapable of synthesizing new proteins, RBCs seem to be primarily devoted to protect their accumulated protein machinery from oxidative stresses, as Goodman and colleagues had suggested (Goodman et al., 2007). Most of the top canonical pathway functions involve protein (synthesis, folding, post-translational modifications, protein transport, and metabolism/degradation) or cell death, almost meaning that RBC philosophy could be resumed with a simple “save or sacrifice”, whether they fail to counteract oxidative stresses.

Cellular assembly and organization also play a fundamental role, as 6 out of 15 top canonical pathways include proteins involved in vesiculation (transport of vesicles, fusion of cellular membrane, endocytosis) or cytoskeleton formation and maintenance. Once again, this recalls either the need for structural elasticity in order to exert their biological function even in peripheral districts or the senescence-induced vesiculation events. The latter end up determining the spherocytotic phenotype and account for the gradual elimination of not yet viable, terminally denatured proteins through membrane blebbing of micro- and nano-vesicles as a sort of self-protecting mechanism (Willekens et al., 2008).

Strikingly, although being enucleated and devoted of protein synthesis, RBCs still display an actual arsenal of proteins involved in translational activities, such as a series of elongation factors and other proteins listed in table 2 in the protein synthesis canonical pathway. These proteins could be vestigial remnants of the very last translational activity of the yet enucleated reticulocyte, which still inherits meager amounts of mRNA from its nucleated ancestors (Palis, 2008). However, it should be highlighted that most of these proteins are actually fragmented, degraded or under-degradation, sometimes represent actual remnants of cellular organelles (although RBCs loose organelles during maturation), while their functionality is controversial.

Table 2 – RBC interactome: Top 50 Networks

ID	Molecules in Network	Score	Focus	
			Molecules	Top Functions
1	ACAP2, ANXA5, ARF6, C6ORF211, CIAPIN1, DDX17, EIF6, EPPK1, FIBP, GANAB, GLRX3, ILF3, IQSEC1, NCAPD2, NCAPG (includes EG:64151), NCAPH, NPEPPS, NPM1 (includes EG:4869), PFDN2, PGLS, PLS1, PLSCR1, PLSCR4, PTBP1, RAB3GAP2, RPS29, SAR1B, SBDS, SEC13, SEPT2, SHC1, SMC2, SMC4, TARS, TFG	43	35	DNA Replication, Recombination, and Repair, Cell Cycle, Cellular Assembly and Organization
2	ARL3, ASPSCR1, ATXN3, CUL3, FAF1, GLMN, GOLGA3, GOLGA7, Mapk, NFIA, NGLY1, NPLOC4, NSFL1C, PAAF1, PLAA, PSMC1, PSMD1, PSMD7, RAD23A, RAD23B, RASA2, RP2, RPL22, TP53I3, TSN, TSNAX, UBA3, UBE4B, UBR1, UBR4, UBXN1, UBXN6, UFD1L, VCP, VCIPI1	41	34	Protein Degradation, Protein Synthesis, Cellular Assembly and Organization
3	Ap1, BLVRA, CCT2, CCT3, CCT5, CCT7, CCT8, CCT6A, CD58, CSNK2A2, HMBS, IGBP1, NACA, PACS1, PAFAH1B2, PBK, PPI/PP2A, PPP1CB, PPP1R7, PPP1R11, PPP2CA, PPP2R4, PPP2R1A, PPP2R1B, PPP2R2A, PPP2R5A, PPP2R5B, PPP2R5D, PPP4C, PPP4R1, PPP6C, SSSCA1, TCP1, TIPRL, TOM1	38	33	Cancer, Cell Death, Reproductive System Disease
4	ACAT2, ADD3, AKR1A1, AKR1B1, AKR7A2, Aldehyde reductase, ATG3, ATG7, ATG4A, ATG4B, FN3K, GABARAP, GABARAPL2 (includes EG:11345), GBAS, GOT1, HBB (includes EG:3043) , HBD , HBE1 , HBG1 , HBQ1 (includes EG:3049) , HBZ , HEBP1, IRGQ, LRSAM1, MDH1, NANS, NFE2, PDGF BB, PDLIM1, SLC29A1, SNX2, VAPA, VAPB, VPS35, YARS	38	33	Cell Morphology, Cellular Compromise, Small Molecule Biochemistry
5	APRT, ARFIP1, ARL6IP5, C6ORF108, COMMD9, COMMD10, EHBP1L1, FREQ, LIN7C, MIR1, MTM1, MTMR12, PAICS, PGM2, PGRMC2, PHGDH, Rab11, RAB14, RAB11B, RAB2B, RABGAP1L, RNH1, RPS10, RPS11, SARS, SLC2A4, SYNGR2, TKT, TMX1, TRAPPC3, TRAPPC2L, TRAPPC6B, TWF1, UGCG1L1, WDR44	38	33	Genetic Disorder, Skeletal and Muscular Disorders, Carbohydrate Metabolism
6	ACTBL2, Alpha catenin, ANXA2, ARD1A, ARRB2, Cadherin, CCS, CLTA, CLTB, CPNE1, DDX27, EIF5A, FLNA, FLNC, HNRNPk, JUP, LGALS9, NAT13, PDIA2, PIK3R1, RPL30, RPS2, RPS5, RPS13, RPS19, RPS20, RPS23, RPS17 (includes EG:6218), RPS3A, Sapk, SNX8, SORBS1, TTN, TUBA1B, VPS13A	36	32	Protein Synthesis, Hematological System Development and Function, Hematopoiesis
7	ABCC1, ACIN1, ATP5B, ATP6V0A1, ATP6V0C, ATP6V1A, ATP6V1B2, ATP6V1D, ATP6V1F, ATP6V1G1, ATP6V1H, ATPase, BAT1, DDX19B, DHX15, H+-transporting two-sector ATPase, IDE, NSF, PSMB5, Psmb5-Psmb6-Psmb8-Psmb9, PSMC2, PSMC3, PSMC4, PSMC6, PSMD6, RAB6C, RP11-529H10.4, RPS15A, RUVBL1, RUVBL2, SKIV2L, SPAST, TRAP1, TXNL1, UBE3C	36	32	Molecular Transport, Cellular Compromise, Infectious Disease
8	ABCG2, ADK, APP, ATP7A, CAPI, CLIC1, EIF4E, FERMT3, FLNB, FLOT1, FLOT2, Flotillin, GBE1, GLRX, GLUL, GRHPR, GSR, ILF2 (includes EG:3608), LSM1, LSM2, LSM3, LSM4, LSM5, LSM6, LSM7, LSM8, NAGK, NARS, PGD, PLEKHF2 (includes EG:79666), PPME1, RTN3,	36	34	RNA Post-Transcriptional Modification, Carbohydrate Metabolism, Small Molecule Biochemistry

	TALDO1, UBE2K, ZNF259			
9	C4, C3-Cfb, C4B, CALCOCO1, CAND1, CD55, COPS2, COPS3, COPS4, COPS5, COPS6, COPS8, COPS7A, COPS7B, CR1, CUL1, CUL2, CUL4A, CUL4B, CYB5R3, DDB1, GPS1 (includes EG:2873), HDGF, IQWD1, LSP1, NFKB (complex), OPTN, RBX1 (includes EG:9978), RNF7, STK10, TBC1D17, TRAFD1, UBXN7, WDR23, WDR26	34	32	Cell-To-Cell Signaling and Interaction, Hematological System Development and Function, Hematopoiesis
10	AGFG1 (includes EG:3267), ATP1A2, BSG, C10ORF97, Catalase, CSTA, DENR (includes EG:8562), DUSP23, EIF4A3 (includes EG:9775), EPS15L1, IFI35, IPO11, LPIN2, LPIN3, MAGOH, MAPK1, MCTS1, METAP2 (includes EG:10988), Na-k-ATPase, NT5C3, PA2G4, Phosphatidate phosphatase, Pki, PPAP2A, RANBP3, RBM8A, RNF123 (includes EG:63891), RPL8, RPL27, RPL12 (includes EG:6136), RSU1, SLC16A1, SLC43A1, UBAC1, ZMYND11	34	31	Molecular Transport, Small Molecule Biochemistry, RNA Damage and Repair
11	BAG2, EEA1, GAPVD1, GDI1, GDI2, GNL1, M6PRBP1, NAE1, NAPA, NAPB, NAPG, P38 MAPK, RAB4, Rab5, RAB1A, RAB22A, RAB4A, RAB4B, RAB5B, RAB5C, RAB7A, RABEP1, RABGEF1, RABGGTA, RABGGTB, RILP, Snare, STX6, STX7, STX16, TXNDC17, VAMP3, VPS45, VTH1A, YKT6	34	31	Cellular Assembly and Organization, Molecular Transport, Protein Trafficking
12	ACO1, AGTRAP, ANXA11, BANF1, CDC2L5, CPNE3, FTH1, FTL, GABARAPL1, GAPDH (includes EG:2597), GSS, HCCA2, HIST1H1C, HNF4α dimer, HNRNPH3, HPCAL1, Jnk, MOBKL1A, PDXK, PON1, POSTN, PRPS1, PRPS1L1, PRPSAP2, Ribose-phosphate diphosphokinase, RPS4X, S100A6, SERPINB3, SHMT1, STK24, STK38, STK38L (includes EG:23012), SYNCRIP, TAOK3, Transferase	34	31	Cancer, Cellular Growth and Proliferation, Hematological Disease
13	BAT3, CD99 (includes EG:4267), CSDA, FCN1, FKBP2, FKBP3, FKBP4, FKBP5, FKBP15, Peptidylprolyl isomerase, peroxidase (miscellaneous), PIN1, PIN4, Pka, PPIA (includes EG:5478), PPIB, PPL1, PPL4, PRDX1, PRDX2, PRDX5, PRDX6, RALA, Rap, RAPIA, RAPIB, RAP2A, RAP2B, RIC8A, RPL13A, SEMG1 (includes EG:6406), UBL7, UBQLN1, UBQLN4, UROS	34	31	Molecular Transport, Small Molecule Biochemistry, Drug Metabolism
14	ADRM1, APOL3 (includes EG:80833), HDDC3, IL-2R, Immunoproteasome Pa28/20s, Interferon alpha, ISG20, MAPRE2, NIF3L1, NMI, NRBP1, PSMA, PSMA1, PSMA2, PSMA3, PSMA5, PSMA6, PSMA7, PSMB1, PSMB3, PSMB8, PSMB10, PSMD2, PSMD3, PSMD14, PSME1, PSME2, RPIA, STAT5B, TRIM21, TROVE2, TSC22D4, UBLCP1, VTA1, WARS	32	31	Protein Degradation, Dermatological Diseases and Conditions, Infectious Disease
15	CCDC6, CD2AP, CHMP5, CHMP7, CHMP1A, CHMP1B, CHMP2A, CHMP4A, CHMP4B, Clathrin, Endophilin, ERK, F11R, HGS, PDCD6, PDCD6IP, PEF1, PTPN23, ROCK1, SH3GLB2 (includes EG:56904), SNF8, STAM, STAMBP, TSG101, Tsg101-Vps28-Vps37, UBA5, VPS25, VPS28, VPS36, Vps22-Vps25-Vps36, VPS37A, VPS37B, VPS37C, VPS4A, VPS4B	32	30	Infection Mechanism, Molecular Transport, Protein Trafficking
16	Adaptor protein 1, AP1B1, AP1G1, AP1M1, AP1S1, AP1S2, AP2A1, AP2A2, AP2B1, AP2S1, ARF1, CLINT1, COP 1, E3 HECT, ENaC, EPN1, EPS15, GGA3, LASP1, NECAP1, NECAP2, NEDD4, NEDD4L, OXSR1, PI3K, PICALM, SLC12A6, SLC12A7, SNAP91, SRP14, SWAP70, UBE3B, UBQLN2, WBP2, WNK1	32	30	Cellular Assembly and Organization, Cellular Function and Maintenance, Molecular Transport
17	Ap2a2-Cltc-Hd, BZW2, CUL5, DNAJ, DNAJA2, DNAJB1, DNAJC13, Hd-perinuclear inclusions, HSP90AB1, HSPA14, HSPA1L, HTT, HYPK, LANCL1, Ldh, LDHA, LDHB, Mre11, MRE11A, NPTN, OSTF1, PPA2, PTGES3 (includes EG:10728), RAD50, SEC22B, SRM, ST13, STIP1, TAGLN3, TERF2IP, TESC, USE1, XRCC5, ZFYVE19, ZW10	32	30	Drug Metabolism, Endocrine System Development and Function, Lipid Metabolism
18	AHSA1, ARIH2, C11ORF59, CARS, DARS, EEF2, EEF1A1, EEF1A2, EEF1B2, EEF1D, EEF1E1, EEF1G, EPRS, ERK1/2, FUBP1, KARS, LARS, MVD, PDCD5, POMP, Proteasome PA700/20s, Protein-synthesizing GTPase, PSMA4, PSMB4, PSMB6, PSMB7, PSMB8, PSMD, PSMD11, RARS, SCAMP2, UGP2, VARS, WDR91, XPO5	30	30	Protein Synthesis, Molecular Transport, Nucleic Acid Metabolism
19	14-3-3 (β, ε, ζ), 14-3-3 (β, γ, θ, η, ζ), 14-3-3 (η, θ, ζ), ABCB6, CLNS1A, CTPS, DHRS12, ERAF, G6PD, Histone h3, Histone h4, JMJD6, KIF5B, KLC3, KLC4, LARP1, MARK3, OLA1, PARP10, PARP12, PCBD2, Poly ADP-ribose polymerase, PRMT5, RBBP7, RPS9, SAAL1, SEC31A, WDR1, WDR77, YWHAB, YWHAH, YWHAQ (includes EG:10971), YWHAZ	30	29	Protein Trafficking, Nucleic Acid Metabolism, Small Molecule Biochemistry
20	ABCE1, APEX1, BAG5, CIAO1, DNAJA4, DNAJB, DNAJB4, DNAJB6, DNAJB2 (includes EG:3300), DPP3, FAM96A, G3BP2, GTF3C5, Hdac, HELLS, Hsp27, Hsp70, HSPA2, HSPA5, HSPA6, HSPA8, HSPB1, HSPBP1, LRRC47, MAP3K7IP1, MAP3K7IP3, MMS19, NFKBIB, Nos, NUBP1, NUBP2, PSMD4, PSMD13, SNCA, Ubiquitin	30	29	Post-Translational Modification, Protein Folding, Cellular Function and Maintenance
21	Alcohol group acceptor phosphotransferase, BCL10, BTF3, C8, CAD, CARD8, CASP8, Caspase, CD8, CK1/2, CRADD, CSNK1A1, CSNK2A1, ETF1, FADD, GLO1, GSPT1, HNRNPA1, HNRNPC, IFN TYPE 1, IPO7, NAMPT, NAP1L1, NF-kappaB (family), PAK2, PEA15, PEBP1, PKN1, PKP1, PRKAA1, RNF14, RPS3, RPS25, TARDBP, TRADD	28	28	Cancer, Cell Death, Embryonic Development
22	ANK3, ARIH1, C18ORF25, CARM1, Cbp/p300, Ctpb, DCUN1D1, ENG, EPB42, Ligase, MAPK1IP1L, PARK7, PEX19, Pias, PML, PURA, PURB, RANGAP1, RPL11, SENP8, Smad, SMAD2, Smad2/3, SPTAN1, SPTBN4, TES, Tgf beta, TGM2, TMCC2, TOLLIP, TOMIL2, TSSC4, UBA1, UBE2I, UBE2L3	28	28	Cellular Assembly and Organization, Gene Expression, Drug Metabolism

23	ABCC4, ACOT7, Aldehyde dehydrogenase (NAD), ALDH, ALDH16A1, ALDH1A1, ALDH9A1, ATL3, BLVRB, Cdc2, DHDH, DIS3L2, E2f, EGLN2, ENDOD1, FAH, FCHO2, G3BP1, GAS2L1, GOLTB1B, KRAS, MIR124, NARG1, NASP, NAT5, OSBP2, Oxidoreductase, PPL, Rb, RP3-402G11.5, SYPL1, TMBIM1, TMEM109, USP7, VIM	28	28	Small Molecule Biochemistry, Drug Metabolism, Molecular Transport
24	ARHGDI2, ARHGDI3, CNBP, eIF, Eif2, EIF1AY, eIF2B, EIF2B1, EIF2B2, EIF2B3, EIF2B4, EIF2C2, EIF2S1, EIF2S2, EIF2S3, Glucose Transporter, Gsk3, HNRNPA3, HNRNPAB, IL1, IMPACT, IPO4, IPO9, LYZ, PP1-C, PSMF1, RAB1B (includes EG:81876), RBMX, RNF126, RPL26, RPL31, RPL35A, RPS7, RPS16, SLC2A3	27	28	Protein Synthesis, Gene Expression, Genetic Disorder
25	ACTR3, ANAPC5, AQP1, CDC34 (includes EG:997), Cyclin B, DNA-directed RNA polymerase, E3 RING, FBXO4, FBXO7, GTF2A2, HEXIM1, HTATIP2, MLL2, PGK1, PKLR, PKP3, POLR2D, POLR2G, POLR2H, PRUNE, RNA polymerase II, Secretase gamma, SFN, SHROOM3, SKP1, SND1, STAT6, SUGT1, TAF15, TCEA1, TCEB1, TCEB2, Vegf, VHL-Cul2-Elongin-RBX1, WDR68	27	28	Carbohydrate Metabolism, Cellular Assembly and Organization, Gene Expression
26	Akt, AKT1S1, EIF3, EIF5, EIF3F, EIF3G, EIF3I (includes EG:8668), EIF3J, EIF3K, EIF4A, EIF4A1, EIF4B, EIF4F, Eif4g, EIF4G1, GPI, HNRNPD, HNRNPH1, KHSRP, MAPKAP1, MLST8, MTOR, MTORC1, mTORC2, NCBP2, NCBP1 (includes EG:4686), p70 S6k, PABPC1, PAIP1, PCBP2, PCBP1 (includes EG:5093), RPTOR, SEC14L2, TNPO2, TPP2	26	27	Protein Synthesis, RNA Post-Transcriptional Modification, Gene Expression
27	26s Proteasome, AKAP7, ANPEP, ARFGF2, CARHSP1, CYFIP1, FH, FHOD1, Glycogen synthase, Ikb, Insulin, KIAA0368, LNPEP, MDH2, Membrane alanyl aminopeptidase, PKAr, PRKAC, PRKACA, PRKACB, PRKAG1, PRKAR1A, PRKAR2A, PRKAR2B, PSMB2, PSMC5, PSMD5, PSMD8, PSMD9, PSMD10, PSMD12, Rar, RNPEP, RPS6, RPS6KA1, VASP	26	27	Carbohydrate Metabolism, Lipid Metabolism, Small Molecule Biochemistry
28	ACLY, ALDOC, C12ORF30, CaMKII, CDK2, CKAP5, COMT, EEFSEC, HNRNPA2B1, HUWE1, Ikk (family), MTHFD1, Ndkp, NME1, PKM2, PP1, Pp2c, PPM1A, PPM1B, PPM1F, Proteasome, Pyruvate kinase, RAB35, S100A8, SELENBP1, SET, TAGLN2, TBCA, UBA6, UBE2, UBE2A, UBE2H (includes EG:7328), UBE2M, UBE2N, UBE2R2 (includes EG:54926)	26	27	Post-Translational Modification, Nervous System Development and Function, Cell Signaling
29	ABCF1, ACTA1, ATP1A1, ATP8A1 (includes EG:10396), BID, BLMH, C1q, CALR, CNDP2, Collagen(s), Cpla2, CTSG, ELANE, GMPS, GYG1, GYS1, HPRT1, LAP3, LTA4H, LTF, NCSTN, NUDT5, NUTF2, PEPP, peptidase, PLP2, PREP, PRKAB1, S100A4, SERPINB1, SSB, SSR4, THBS1, THOP1, UFM1	26	31	Protein Synthesis, Protein Degradation, Cell-To-Cell Signaling and Interaction
30	ANP32A, Apoptosome, AVEN, CASP3, Caspase 8/10, CSE1L, CYTH1, DFF, DFFA, FNTA, FNTB, Importin alpha, Importin alpha/beta, Importin beta, IPO5, KPNA1, KPNA3, KPNA4, KPNA6, KPNB1, Lamin b, LMNA, LOC389842, MIB1, NAP1L5, NUP50, NUPL1, RAN, RFFL, SCFD1, SLK, SRP19, Tap, TNPO1, USO1	25	27	Molecular Transport, Protein Trafficking, Amino Acid Metabolism
31	Alpha Actinin, ANKRD28, Calpain, CAPN1, CAPN2, CAPN5, CAPNS1, CAST, CIRBP, DPYSL2, FAK, FCGR1A/2A/3A, Filamin, FN1, Integrin alpha 3 beta 1, Integrin&beta.;, LXN, Myosin Light Chain Kinase, PANK2, RBM3, RPS21, RPSA, SAPS1, SAPS2, SAPS3, SEC23B, SNAP23, STOM, Talin, TLN1, TLN2, TNS1, TSTA3, VAT1, VCL	25	26	Cell-To-Cell Signaling and Interaction, Cellular Assembly and Organization, Cellular Function and Maintenance
32	ACTR2, ACTR3B, ADD1, ADD2, AHCY, Alpha actin, ANK1, ANXA7, Arp2/3, ARPC2, ARPC5, ARPC5L (includes EG:81873), CORO1B, DSTN, F Actin, Fascin, FSCN1, G-Actin, GCA, GSN, LCPI, Myosin, PFN, PITPNA, PITPNB, Pkc(s), SPTA1, SPTB, SPTBN1, SRI, TMOD1, TPM1, TPM3, TPM4, Tropomyosin	24	26	Cell Morphology, Cellular Assembly and Organization, Cellular Movement
33	Adaptor protein 2, Ap2 alpha, AP2M1, Arf, ASAP1, BCCIP, Beta Arrestin, CAPZA1, CAPZA2, CAPZB, Caveolin, CLTC, DBNL, DN2M, DNML1, DNPEP, DRG2, Dynammin, EHD1, Epsin, FIS1, FLJ11506, GABAR-A, KRT31, PACSIN2, PDAP1, Pdgf, PFN1, RPL23, RWDD1 (includes EG:51389), SH3GL1, SH3GLB1, SNX9 (includes EG:51429), SYNJ1, TWF2	24	26	Cell Morphology, Cellular Assembly and Organization, Cell Cycle
34	ACTB, ACTR10, ACTR1A, ACTR1B (includes EG:10120), AKR1C1, ALDOA, BCL2L1, Caspase 3/7, CCNDBP1, CDKN2C, Creatine Kinase, Cyclin D, DCTN1, DCTN2, DCTN3, DCTN4, DCTN6, DR1, DRAP1, ENO1, Enolase, FGA, Fibrin, MAPRE1, Nuclear factor 1, RPLP1, RPLP2, RPLP0 (includes EG:6175), RPS12 (includes EG:6206), RPS24 (includes EG:6229), Sef, SRPK1, Stat3-Stat3, T3-TR-RXR, VDACC3	24	26	Cellular Assembly and Organization, Hematological Disease, Immunological Disease
35	14-3-3, ATP2B1, ATP2B4, C20ORF27, Calcineurin A, CALML5, Calmodulin, Ck2, CNP, Dynein, Girk, GPHN, HDAC6, Hexokinase, HMGB1 (includes EG:3146), KCNN4, LYPLA2, NDE1, NUDCD3, PAFAH1B1, PFK, PFKL, PFKM, PHKB, Pmca, RAB8B, RGS10, SIRT2, TUBA1A, TUBA1C, TUBB, TUBB1, TUBB2C, TUBG1, Tubulin	21	25	Cancer, Reproductive System Disease, Cardiovascular Disease
36	ARCNI, ARFGAP1, ARHGAP1, ARHGAP4, ARHGAP17, ARHGEF6/7, CD47, CDC42, COPA, COPG, COPZ1, Dgk, DGKA, Ephb, Ephb dimer, Integrin alpha V beta 3, IQGAP, IQGAP1, IQGAP2, ITSN1, NWASP, Phosphatidylinositol4,5 kinase, Rac, RAC1, RHAG, RHCE, RHD, RhoGap, SACM1L, SLC4A1, SNX5, TMED7, TMED9, TMED10, WASP	21	24	Genetic Disorder, Hematological Disease, Cellular Assembly and Organization
37	AADACL1, APEH, APOBEC3B, APOE, BAG1, CPPED1, CPT1A, FASN, GC-GCR dimer, GCLC, GCLM, HDHD1A, HDL, Hydrolase, IDH1, IRF3, JINK1/2, KIAA0174, LDL, N-cor, NCOR-LXR-Oxysterol-RXR-9 cis RA, Nr1h, PTMS, PTPN7, REXO2, RPS14, Rxr, SAA@, SNX1, SNX6, SNX15, TAF9, THPA, Thyroid hormone receptor, VPS29	20	24	Drug Metabolism, Amino Acid Metabolism, Small Molecule Biochemistry

38	Actin, CD44, CFL1, Cofilin, DAAM1, EPB41, Erm, EZR, GNA13, GYPC, HSPH1, Mlc, Mlcp, MPP1, MrIc, MSN, MYH9, MYH10, MYL3, MYL4, MYL6, MYL12B, Myosin phosphatase, Pak, PDE6D, PDXP (includes EG:57026), RAB13, RAB18, Ras homolog, RDX, RHOA, Rock, ROCK2, RPS6KA3, S100A11	19	25	Cellular Assembly and Organization, Cellular Compromise, Cell Morphology
39	ATG9A, BPGM, C7ORF64, CCDC90B, CDC42EP3, CYP7A1, DERA, DLST, FDPS, FNTB, FTSJ1, GIPC2, HNF4A, NP, NRB2F, NUDT2, OTUD6B, PAAF1, PHPT1, PPARGC1B, PSMC4, PSMD1, PSMD7, PSMD8, PSMD10, PYGL, RIF1, RPL18A, RPRD1B, RRM1 (includes EG:6240), RTCD1, SEMA7A, SETDB1, SREBF2, UMPS	18	22	Gene Expression, Genetic Disorder, Metabolic Disease
40	ALB, AMPK, APOA1, ARG1, BTK, C3, CA2, CA3, CA8, CA1 (includes EG:759), Calcineurin protein(s), Carbonic anhydrase, Cytochrome c, FSH, GIPC1, GYPA, IGHG1, IGHM, Igm, ITPR, KCMF1, NFAT (complex), Nfat (family), NMDA Receptor, PCMT1, PGM2L1, PI4K2A, PTP4A1, QDPR, RAB33B, SAFB2, SLC2A1, SNAP29, SOD1, STX4	18	25	Cardiovascular Disease, Metabolic Disease, Genetic Disorder
41	Androgen-ARA55-AR-ARA70-HSP40-HSP70-HSP90, AR-HSP40-HSP70-HSP90, ATIC, CAT, CHORDC1, CLU, DNAJC, DNAJC5, DNAJC9, DNAJC17, FKBPL, G protein beta gamma, Glutathione peroxidase, Glutathione transferase, GMFB, GOT, GPX4, GST, GSTO1, GSTP1, GSTT1, HSP, Hsp22/Hsp40/Hsp90, HSP40-HSP70-HSP90, HSP90AA1, HSPA4, IL12 (complex), PEX5, RAB10, RAB15, RAB8A, RABIF, SERPINB5, SGTA, Sod	17	22	Drug Metabolism, Endocrine System Disorders, Small Molecule Biochemistry
42	APRT, ARHGAP18, BMP6, CER1, CISD2, DDT, DNAJB6, DNAJC8, EIF2S3, EIF3M, FAM49B, GH1, GLOD4, IKBKE, ISYNA1, LPHN2, LTA4H, MIR298 (includes EG:723832), MTAP (includes EG:4507), NCDN, NFYB, NUDT5, PDHB, PFDN5, PIP4K2C, PRKCSH, RAB21, SESN1, SLC43A2, SLC8A2, SLITRK2, SORD, TKT, TLL12, TXNDC12	17	21	Cardiovascular System Development and Function, Cellular Function and Maintenance, Embryonic Development
43	ACHE, AChR, AMPD3, AP1B1, ATP2B1, C8ORF55, CFTR, CLTCL1, COLQ, DAZAP1, FAT1, IFIT5, KCNJ1, L-carnitine, LGTN, MAPKAP1, MAT2A, MAT2B, Methionine adenosyltransferase, MUC2, NOS1, PDDC1, protoporphyrin IX, PRSS23, PSME2, RASD1, S100A7, SH3BGR12, SLC9A3, SP2, TMEM222, TNF, TPD52L2, VAC14, ZNF330	14	19	Small Molecule Biochemistry, Amino Acid Metabolism, Nucleic Acid Metabolism
44	AGPAT6, C12ORF34, CSE1L, DCD, DSG1, EFHD2, GF11B, GRIN1, GRIN3A, HLCS, INPP5K, KALRN, KLHL18, MATR3, MIR20A (includes EG:406982), MIR210 (includes EG:406992), MYH14, NELF, OTUB1, PCCA, PCCB, PPP2R2B, R3HCC1, RAD51L3, RAN, RANBP10, RANGRF, RTN1, STT3B, SYNGR1, ULK3, XPO5, XPO7, XPOT	12	17	Molecular Transport, RNA Trafficking, Genetic Disorder
45	ALDH3A1, ARAF, ATYPICAL PROTEIN KINASE C, BAD, BCAM, Complement component 1, Creb, Cyclin A, Cyclin E, Fcer1, hCG, ICAM4 (includes EG:3386), Ige, IgG, Integrin, IVL, KLC1, Laminin, LGALS3, MAP2K1, MAP2K2, MAP2K3, MAP2K4, MAP2K1/2, MAP3K, Mek, MVP, Pkg, PLEK2, PP2A, PPA1, RAB2A, Rap1, SPAG9, TSHR	12	18	Cardiac Hypertrophy, Cardiovascular Disease, Cellular Development
46	7-dehydrocholesterol, amino acids, ASNA1, BMPR2, Ck2, CTBP1, FLAD1 (includes EG:80308), GMFB, GMFG, LANCL2, LCMT1, MAP2K5, MAP3K1, MAP3K6, MAP4K2, MERTK, MIR193A, MOS, MYLK2, MYO1D, NAP1L4, NOP2, PHKG2, phosphatase, PI4KA, PIP4K2A, PMM2, RABGGTA, RPL10A (includes EG:4736), SIRT5, SRPK1, TRIM23, TWF1, UBAP1, ZNF516	12	17	Amino Acid Metabolism, Post-Translational Modification, Small Molecule Biochemistry
47	BAT2, BAT3, BMI1, C11ORF67, C11ORF73, C14ORF133, C9ORF64, CHCHD3, CHCHD6, CRYZL1, FN3KRP, GSTK1, HBS1L, HNF4A, IMMT, INTS4, KIF22, MRPL44, PNPO, RAP2C, RNF113A, SAMM50, SEC23A, SEC23IP, SLC7A6OS, SREBF1, TXNDC9, VPS33B	11	15	Cell Morphology, Cellular Assembly and Organization, Cellular Function and Maintenance
48	ALP, BMP2K (includes EG:55589), CK1, CMPK1, COASY, CTTN, DDX3X, Fgf, Fibrinogen, Growth hormone, HCLS1, HS1BP3, Ifn, IFN Beta, Ifn gamma, Igf, IL18, IL12 (family), IRAK, IRAK4, MHC Class II, Mmp, Na ⁺ , K ⁺ -ATPase, NGF, PLC gamma, PRG2 (includes EG:5553), RPS6KB1, SF3B4, STAT, STAT5a/b, Tlr, TXN, TXNRD1, WBP4, XPO1	11	16	Cell Morphology, Cell-mediated Immune Response, Cellular Growth and Proliferation
49	ANP32E, BMF, C20ORF3, CD70, DBI, DYNCH11, DYNLL2, ERRF11, FKBP5, GLCC11, HECTD3, HOXB7, HSD17B12, MAEA, MIR195, MIR26A1, MIR26A2, NfκB-RelA, NFKBIA, NKIRAS2, NOD2, NR3C1, OSBP19, PDCL3, PIR, PPCDC, PSMG2, RAB28, SLC1A6, SLC1A7, TNFAIP8, TNFSF14, TRAF3IP2, WIBG, ZNF346	11	16	Amino Acid Metabolism, Small Molecule Biochemistry, Cell-To-Cell Signaling and Interaction
50	ADPRHL2, ASCC2, ATP5G3, ATP6V0A4, ATP6V0D1, ATP6V1C1, ATP6V1C2, ATP6V1E1, ATP6V1E2, ATP6V1G2, ATP6V1G3, C8ORF30A, CORO1C, ERK, ETNK2, FAM63B, GBP6, GUK1, H ⁺ -exporting ATPase, IFNB1, IgG, MAP3K3, Mg ²⁺ , NDUFB2, PFDN4, PFDN5, POLA2, RNF114, RPU5D1, TBCB, UBC, UBL4A, URM1, VBP1, XPNPEP1	11	16	Molecular Transport, Antigen Presentation, Cell-To-Cell Signaling and Interaction

Pathway analysis and CDA II

The introductory observations of the statistical pathway analyses allowed us to assess that this kind of approach could be useful for a general description of the system under analysis. We now wanted to evaluate pathway analyses when adopted to gain insights of more a targeted issue.

The greatest portion of the entries included in our dataset derived from the paper by Roux-Dalvai et al. (2008). This huge dataset had recently been exploited to perform a proteomics and genomics integrated approach to glean insight of the molecular candidates which could be likely responsible of the congenital dyserythropoietic anemia type II (CDA II) (Bianchi et al., 2009). Basing on the list of 1,578 proteins and a linkage analysis, the Authors were able to determine a list of 17 candidates whose gene products were encoded on the incriminated region on chromosome 20: SNX5, SEC23B, DTD1, NAT5, GINS1, BCL2L1, MAPRE1, CHMP4B, EIF2S2, AHCY, ACSS2, GSS, EIF6, CPNE1, EPB41L1, RPRD1B(C20orf77), and TGM2. From thereon, a progressive exclusion was performed by the Authors on the basis of a series of acute observations, as to restrain the list to 4 candidates only: SNX5, MAPRE1, CPNE1, and SEC23B. Among these four proteins, SEC23B was individuated as the eligible candidate, since it encodes for a protein possibly involved in ER-to-Golgi vesicle-mediated transport and in vesicle budding from the ER, in line with the recent evidence of a defect affecting cis- to trans-Golgi processing in CDAII erythroblasts.³⁸

We expected to find that, whether our pathway analysis reflected the biological complexity of the sample under analysis, we could have individuated SEC23B in one of the top score pathways and with a p-value lower (higher probability) than each one of the other 16 candidates. Therefore, we performed a protein-by-protein search in our pathway analysis datasheet. Among the 850 canonical pathways, SEC23B mapped only in the “Cellular assembly and organization – transport of vesicle” pathway, which was the third top score pathway in the whole list (in red in **Table 1**).

It is worthwhile to underline that each one of the other eligible candidates had a far lower score than SEC23B, while an exception could be made for CPNE1, which mapped in the same pathway as SEC23B. Notably, CPNE1 was one of the 4 candidates of the restrained list proposed by the Authors, and it was not excluded until the very last phase, basing on the genetic observation of the logarithm of the odds (LOD) score in CDAII changing from 20q to 20p11 (Denecke and Marquardt, 2008).

It is therefore possible to conclude that pathway analyses could be exploited for targeted evaluation of proteomics data and allows unbiased results which guarantee as much credibility as the acute and subtle reasoning by expert Authors.

Network analysis

Network analysis is perhaps the most intuitive and well-known aspect of interactomics. It allows mapping a series of molecules depending on their connections among each other. Our analysis has been focused on the top 50 networks which could be individuated by the software (**Table 2**). This limitation permitted us to consider only 1,336 nodes out of the 1,574 proteins eligible for network analysis instead of focusing on the whole list of 1,989 distinct gene products from the original dataset. For 238 proteins, the program did not attribute a score which allowed them to enter the top 50 network list and thus they were apparently lost in the process. This is true to some extent, since

when performing complementary analyses on these specific proteins, further 36 networks were individuated. However, half of these networks had an extremely low score (1 on average), while the first half presented high scores which were on the other hand biased by this separated analyses (supplementary material 3). Therefore, we decided not to include them in the main body of the article.

At a rapid glance, network analysis agrees with the observations from canonical and toxicity pathway analyses. Top networks include proteins mainly devoted to gas transport (such as the series of hemoglobins in the “small molecule biochemistry – Network 3” – bold green), oxidative stress response (catalase in “Network 10”, peroxiredoxins in “Network 13”), protein control (folding, metabolism, degradation, protein trafficking, post-translational modification; Network 2, 6, 11, 14, 15, 19, 20, 24, 26, 28-30, 46), cellular assembly and organization (cytoskeleton formation and cell morphology, molecular transport, vesiculation and vesicular trafficking; Networks 1, 2, 7, 11, 16, 20, 22, 25, 31, 32, 33, 34, 36, 38, 47, 48, 50) and cell death/apoptosis/anti-apoptotic signaling (Networks 1, 3, 21, 36, 42).

Meta-analysis

A more in-depth observation of the networks pointed out two main ultra-networks, cross-linking a series of networks sharing similar functions and at least one node (**Figure 2**). The first one includes networks 6, 14-16, 20, 24, 26, 29, 34, 35, 42, 43, 46, 50 and regroups those networks which play physiological functions related to protein control (as previously mentioned) (**Figure 3A**). The second one includes networks 2, 7, 13, 18, 27, 30, 39, 44, 47, 49 and regroups proteins involved in molecular transport activities (**Figure 3B**). These ultra-networks, although containing hundreds of nodes, display a well-ordered structure which focuses around the activity of a reduced number of key nodes. Some of these key nodes represent pivotal points in the interaction network, although some of them were absent from the submitted dataset and thus graphed as white nodes. For example, in the second network HNF4A, absent from the dataset, interacts with a series of proteins which have been individuated during the primitive experimental phase (grey nodes) (**Figure 4**). Indeed HNF4A is abundantly expressed by fetal liver hepatocytes and plays a crucial role in the regulation of early erythropoiesis (Makita et al., 2001). Therefore it is plausible that, although absent, its interacting/induced partners in the RBC are both present in the dataset and graphed in the same network. Vice versa, this could account for the quality of the elaborated networks, as it suggested proteins that should be there (or are somehow related), but have not been actually identified.

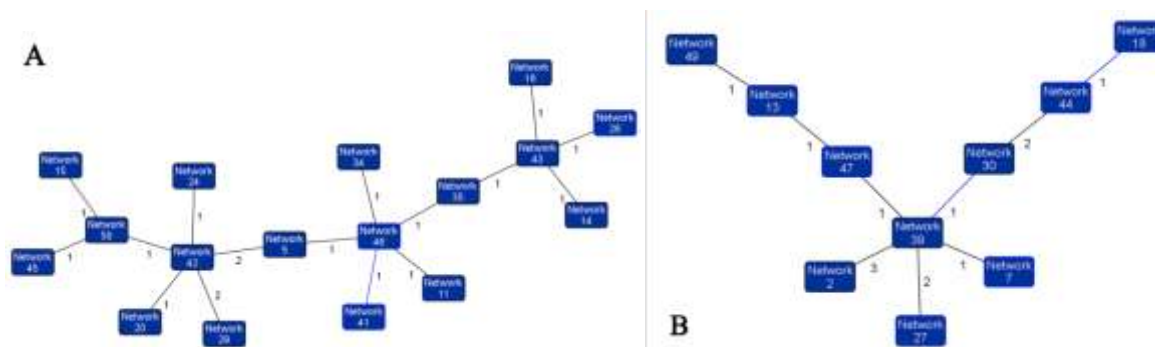


FIGURE 2 Representation of the individuated “ultra-networks”. They were created by calculating networks with function affinity which shared at least one node.

The first one includes networks 6, 14-16, 20, 24, 26, 29, 34, 35, 42, 43, 46, 50 and regroups those networks which play physiological functions related to protein control (protein synthesis, folding, post-translational modifications, degradation, trafficking, molecular transport, cell function and maintenance, cellular assembly and organization – Fig 2.A). The second one includes networks 2, 7, 13, 18, 27, 30, 39, 44, 47, 49 and regroups proteins involved in molecular transport and metabolic activities (cellular assembly and organization, molecular transport, small molecule biochemistry, carbohydrate, amino acid and lipid metabolism, cell morphology – Fig 2.B).

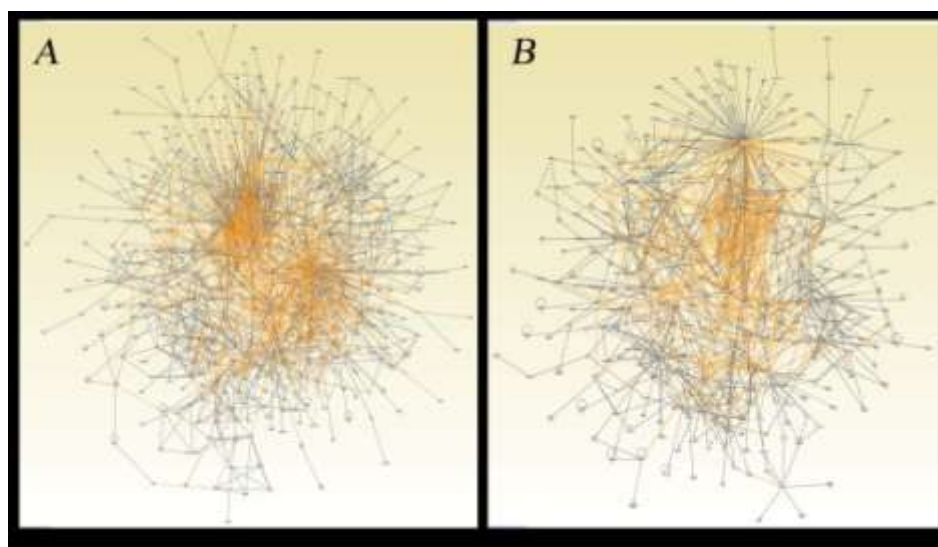


FIGURE 3 Graphic representations of the individuated “ultra-networks”. **Fig. 3.A** shows ultra-network 1 (including networks 6, 14-16, 20, 24, 26, 29, 34, 35, 42, 43, 46, 50), while **Fig. 3.B** shows ultra-network 2 (including networks 2, 7, 13, 18, 27, 30, 39, 44, 47, 49). They were created by calculating networks with function affinity which shared at least one node. Ultra-networks representations were

obtained by merging sub-networks in each case. It is not relevant that nodes ID could not be read in this compressed version of the graph. What is notable is that, although containing hundreds of nodes, these ultra-networks display a quite ordered disposition, especially the ones in **B**.

As far as the shapes of the networks are concerned, we noted that the “order” of the networks increases (less cross-interactions, individuation of crucial nodes) proportionally to the increase of the “grey nodes/white nodes” ratio (the number of the gene entries from the original dataset which have a match with the database). A simple analysis supports this statement. We elaborated data from all the aforementioned studies, (Pasini et al., 2006; D’Amici et al., 2007; Bachi et al., 2008; Simò et al., 2008; Haudek et al., 2009) and excluded from the broadest list available (Roux-Dalvai et al., 2008). A final dataset of 508 non-redundant entries was determined out of which 466, having a

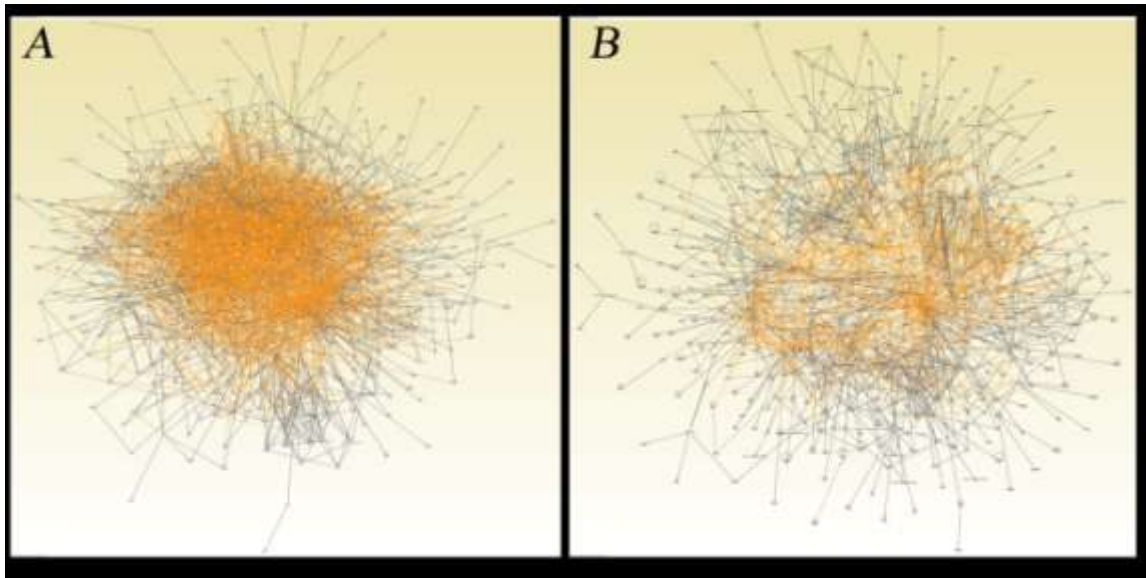


FIGURE 5 Merging the first 500 nodes from top network analysis of the whole dataset when excluding (A) or not (B) Roux-Dalvai et al. from the original list. The networks merged in B display a more ordered shape: pivotal nodes are more evident and a centre of the map could be located. On the other hand, the lower number of original data accounts for an increased “disorder” in the map in A, which still provides information about specific nodes while being impossible to read as a whole. From comparison of Fig. 5.A and 5.B it clearly emerges the role of the newly gained insights in red blood cell proteomics, which justify this updated overview of the red blood cell interactome.

Analogously, the analysis of a maximum of 500 nodes restrained our chances to obtain a comprehensive map of the whole interactome. Thus we decided to perform a progressive analysis, including 14 networks at a time. In particular, network 1 to 14 included 490 nodes; network 15 to 28 included 490 nodes as well; network 29 to 42 included 487 nodes, while network 43 to 50 only 271 nodes. When excluding the latter, due to an extremely lower number of networks and corresponding nodes, we could underline a particular trend in the complexity of those networks, since the map became difficult to read as we progressively merged lower score networks (**Figure 6**).

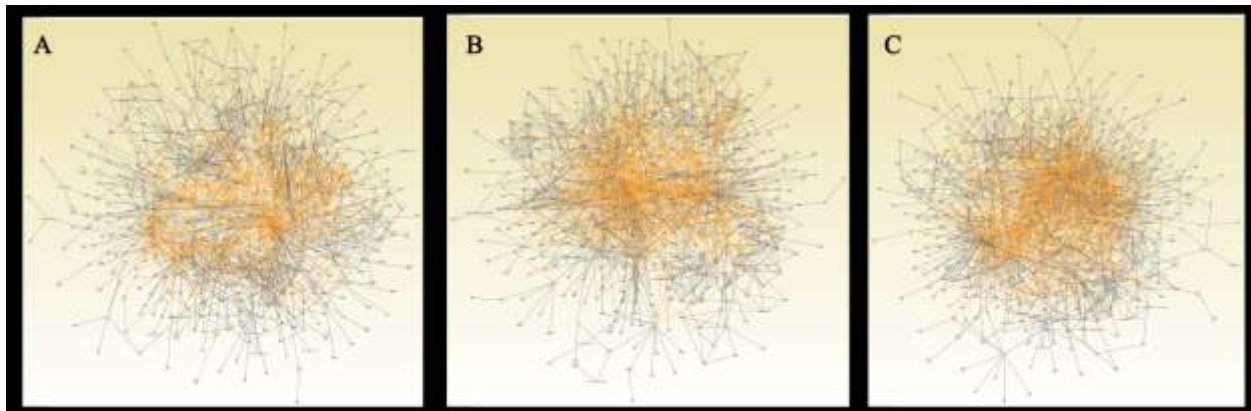


FIGURE 6 Schematic view of the maps obtained by progressively merging groups of 14 networks based on their scores. Networks 1-14 (A) maps 490 nodes, as well as Networks 15-28 (B), while networks 29-42 (C) harbors 487 nodes. It is worthwhile to underline that, even if the number of the nodes is almost identical in each case, the shape of each network group differs consistently with the diminution of the networks scores. Lower score networks include a series of proteins which are absent from the original dataset and are introduced by the software to fill up the determined network, even if this reduces the “interaction noise” thus making the map more difficult to read

This could be explained as an effort of the program to bias for those networks which appear to be incomplete. A number of proteins are absent in the original dataset, but the program includes them since it calculates that they should take part in the individualized network. As a result, the program includes a series of “white nodes” which end up completing the network on the one hand, although at the expenses of the “noise” (improper connections) on the other. A technical caveat could be represented by the adoption of a higher cutoff for choosing molecules eligible for the analyses. This is particularly meaningful when performing comparative/quantitative analyses among several datasets (this is not the case), in which the cut off represents the fold-change value for the same proteins among replicates (a 3 cut-off value is more stringent than 2, since it implies a 3 fold-change variation among samples). This is often the case of analyses performed on microarray data (Wognum et al., 2009). This strategy allows decreasing the total number of genes to be analyzed and thus the likelihood of possible false-positives (Timperio et al., 2009).

Repair or destroy box: Goodman revisited

In the previous section we focused on the meta-analysis of the elaborated protein networks. One of the ultra-networks individualized harbored a series of proteins involved in protein folding and degradation control, as well as in response to oxidative stress.

Notably, it is becoming increasingly accepted that oxidative stress is the main cause of the reduced viability of long-stored RBC concentrates (Yoshida et al., 2007 and 2008; Dumont et al., 2009). In parallel, accumulating evidence has recently suggested for a peripheral component to schizophrenia, mainly due to an increased susceptibility to oxidative injuries (Prabakaran et al., 2007).

Interestingly, in their proteomics and interactomics review, Goodman et al. (2007) had already located a core of interacting proteins, which they named the Repair or destroy box (ROD) after the biological activity of many of its nodes. The ROD box contained proteins that utilize the energy of ATP hydrolysis to fold nascent proteins or refold damaged proteins (heat shock proteins and chaperonins). As mature RBCs are thought not to synthesize nascent proteins only the latter function was considered to be relevant. The ROD box also contained proteins involved in the proteasomal degradation of ubiquitinated proteins (ex proteasomal subunits).

We wanted to investigate and graph an updated version of the ROD. To this end, we merged networks 7, 10, 13, 17, 20, 28, 38, 41 and analyzed the obtained map (**Figure 7**). Although displaying few peripheral sub-graphs, this merged network presented a central core of a few pivotal nodes. These nodes were evidenced (light blue) as to highlight their edges. A counterclockwise list includes: huntingtin (HTT), heat shock protein 70kDa (HSP70), heat shock protein 90kDa alpha class A member 1 (HSP90AA1), heat shock 70kDa protein 8 (HSPA8), nuclear factor of kappa light polypeptide gene enhancer in B-cells inhibitor beta (NFKBIB), heat shock protein 90kDa alpha class B member 1 (HSP90AB1).

These proteins are involved in cell protection to denaturing stress and folding control (HSPs)⁴⁷, vesiculation (HTT)⁴⁸ and apoptotic signaling cascades (NFKBIB)⁴⁹. As postulated by Capra (1996), a series of proteins/enzymes playing partially-overlapped biological functions could potentially act as catalytic ring. A catalytic ring is a closed number of interactors which induce the activity of the subsequent node in the row, up until the last one interacts with the first so as to close a hypothetical ring. Within this ring, the activity of each gene is reinforced in

every cycle. The catalytic ring hereby individuated could exploit the basis of this principle to counteract oxidative stress (PRDX1 intermediate) and protein damage (HSPs) or, when this no longer possible, activate vesiculation events (HTT) in order to remove damaged proteins, or trigger apoptosis (NFKB1B). Such an oversimplified view of the biological complexity of these merged networks conveys the idea that, although it is relevant to determine and classify protein actors through proteomics, it is still fundamental to determine if and how these proteins finally interact in order to comprehensively understand their relevance.

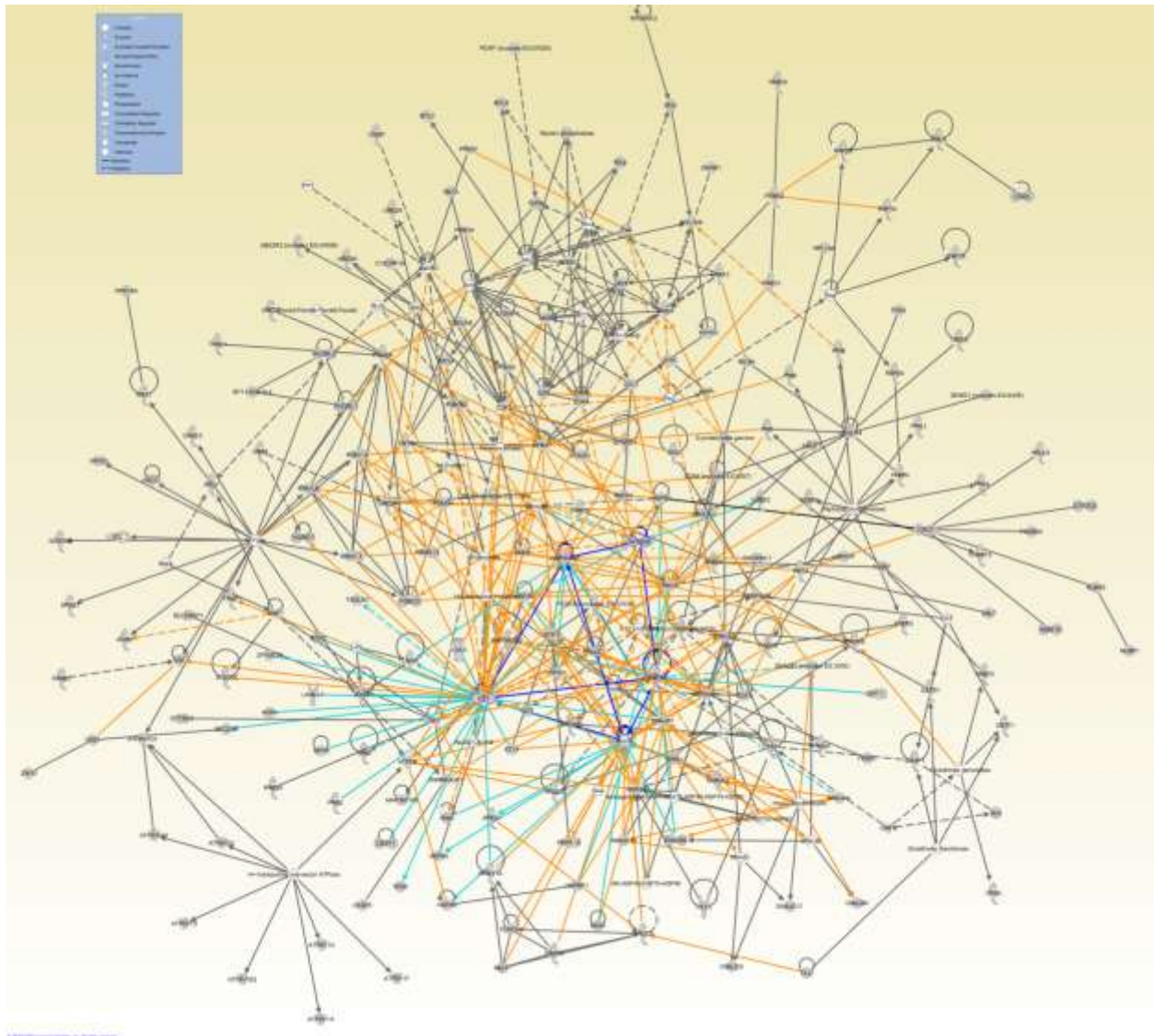


FIGURE 7 An updated representation of the Repair or Destroy box (ROD) from the paper by Goodman et al.⁷ Merged networks 7, 10, 13, 17, 20, 28, 38, 41 are graphed together. Notably, the central core is represented by a series of proteins which are known to counteract protein unfolding (HSPs), oxidative stress (PRDX1), apoptotic signaling (NFKB1B) form a sort of catalytic ring, which could guarantee a strengthened response to denaturing stresses. Grey nodes: proteins from the dataset having a match in the database; White nodes: proteins from the database which were not identified (if present) upon the experimental phase; Grey edges: interactions within a network; Orange edges: interactions between networks; Light blue edges: interactions involving HTT, HSP70, HSP90AA1, HSPA8, NFKB1B, HSP90AB1.

Conclusion

Recent technical advancements in the field of proteomics and interactomics have provided us with the basilar tools for this updated overview. A list of 1,989 non redundant proteins has been compiled based on data available from literature (Pasini et al., 2006; D'Amici et al., 2007; Bachi et al., 2008; Simò et al., 2008; Roux-Dalvai et al., 2008; Haudek et al., 2009).

Although it has always been intuitive that RBCs suffer from an increased oxidative stress, pathway analyses of the canonical and toxicity pathways produced an unbiased score-based evaluation (**Figure 1**).

Network analysis provided a list of 50 networks among which top score networks were mainly devoted to protein protection to folding damage (**Table 2**). In particular, an organized web of interactions involving a handful of proteins has been individuated and could likely constitute a catalytic ring to enhance the Repair or Destroy box activity (**Figure 7**) which Goodman and colleagues proposed in 2007. Network analyses also pinpoint at a series of proteins which appear to be the likely trigger of central molecular cascades, even of some proteins which have not yet been individuated experimentally, thus suggesting further research directions, or indicating crucial molecules that induce signaling events in the sample tissue/cell, albeit being produced elsewhere (HNF4A).

Although conveying valuable new insights on the biology of RBC response to oxidative stress, our analysis supports recent proteomics and genomics integrated studies on the likely relation of SEC23B with CDA II, in a faster and unbiased way which does not necessarily rely on the acuteness of the Authors (Bianchi et al., 2009).

Interactomics certainly holds a future ahead, which will be disclosed as newly spreading software platforms will allow progressively more in-depth analyses on a broader dataset, without numerical or graphical limitations (for example: 50 networks threshold and the maximum limit of 500 nodes to be represented at the same time).

We are still in that early phase in which a dictionary is being written, when a biological meaning is attributed to a specific interactomic profile (networks shape complexity, sub-graph localization, catalytic ring, “interactomics noise”, crucial interactors). When this phase will be over, we will be confidently relying on the study of the whole proteome profile (genome, transcriptome, PTMome and other “-omes” as well), instead of focusing on specific molecules or specific pathways alone.

2.2 Native protein complexes in the cytoplasm of Red Blood Cells

Overview of this section

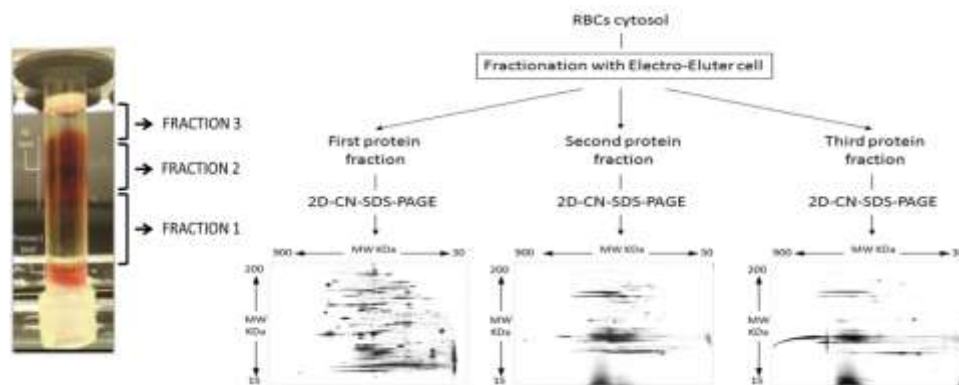
Despite decades of advancements, the red blood cell (RBC) cytosolic proteome still represents a treasure trove of biological information. The unbalanced abundance of cytosolic RBC proteins, with hemoglobin alone accounting for approximately the 98% of the soluble proteome fraction, has hitherto hampered any extensive investigation of non-hemoglobin native multi-protein complexes.

Recently, we optimized a preparative hemoglobin-depletion strategy that preserves native protein conformation and allows recovery of three distinct fractions. We hereby further investigated these three fractions with 2D-clear native(CN)-SDS-PAGE separation, followed by mass spectrometry-based identification.

Overall, we could observe and describe 55 complexes from the RBC native cytosolic proteome, among which ultra-tetrameric hemoglobin. Protein complexes were characterized by proteins mainly involved in oxygen transport, anti-oxidant responses, metabolism and protein degradation cascades, in agreement with recent *in silico* models. Metabolic enzyme oligomers also interacted with complexes of proteins involved in oxidative stress-responses, in a sort of a cross-talk between metabolic modulation and anti-oxidant defenses.

Future investigations should expand the existing knowledge and determine whether and how these complexes might influence RBC ageing *in vivo* and *in vitro*, other than the insurgence of specific pathologies.

Keywords: red blood cell, proteome, native protein complexes, cytosol, hemoglobin depletion.



Introduction

Recent strides in the understanding of red blood cell (RBC) biology have been achieved through proteomics approaches (Liumbruno et al., 2010). Indeed, RBCs represent a key cellular model for proteomics investigations, owing to the extrusion of nuclei and degradation of internal organelles and endoplasmic reticulum during the maturation process, which hampers any *de novo* protein synthesis capacity and thus decreases the biological complexity of RBCs in comparison to other cell types.

Nevertheless, proteomics analyses of RBCs still represent a challenging task, in the light of the overwhelming abundance of hemoglobin (Hb), which make up for the 90 % and 98% of the whole and cytoplasmic RBC proteome, respectively. Despite this significant technical issue, remarkable advancements have been made in the definition and expansion of the RBC proteome during the last three decades (Rosenblum et al., 1982; Low et al., 2002; Pasini et al., 2006; Roux-Dalvai et al., 2008).

Early attempts to delve into the RBC proteome complexity were put forward by Rosenblum and colleagues in 1982, who exploited two-dimensional electrophoresis (isoelectrofocusing-SDS-PAGE) to individuate approximately 600 spots from RBC membrane. However, it was not before the introduction of mass spectrometry-based identification of proteins that those spots were further characterized by Low's group, resulting in the determination of 102 RBC membrane proteins (Low et al. 2002). Four years later, Pasini and co-workers (2006) published one of the most comprehensive studies ever in the field, where they focused both on the membrane and cytosolic RBC proteome and reported the identification of 340 membrane and 252 soluble proteins, respectively.

In 2008, Roux-Dalvai et al. claimed the identification of 1578 distinct gene products from that 2% protein fraction of the non-Hb RBC cytosolic proteome pre-fractionation via combinatorial peptide ligand libraries and Orbitrap MS analysis.

Proteomics successes in the field of RBC biology also paved the way for a wide series of translational applications, including those concerning RBC responses to storage under blood bank conditions (Bosman et al., 2008; D'Alessandro et al., 2012). Taken together, these results helped compiling a non-redundant list of 1989 RBC proteins and to propose *in silico* models of their actual interactions (D'Alessandro et al., 2010 – **first part of Chapter 2**). However, it must be noted that protein-protein interaction models for the RBC cytoskeleton and membranes had already been proposed and consolidated prior to the widespread diffusion of proteomics datasets, especially as far as it concerns the role of band 3 protein as a competitive docking site for deoxy-Hb and glycolytic enzymes, other than for structural proteins (Low, 1986; Galtieri et al., 2002; Bruce et al., 2003). Nonetheless, native proteomics analyses, such as blue native (BN) and clear native (CN) (Schagger and von Jagow, 1991; Wittig et al., 2007) might contribute further advancements in the understanding of RBC physiology, to the extent it is modulated by multi-protein complexes (MPCs) and their interactions. In this view, van Gestel and colleagues (van Gestel et al., 2010) recently published a quantitative erythrocyte membrane proteome analysis with BN/SDS-PAGE.

While native proteomics approaches have been already applied to the investigation of RBC membranes, cytoplasmic RBC complexes still remain unresolved. This is mainly due to the Hb concentration issue, which compromises detection of any other multi-protein aggregate other than Hbs and their most abundant interactors. In order to cope with this technical/biological inconvenience, several strategies have been proposed over the years, including (i)

preparative cation exchange chromatography (Bhattacharya et al., 2007); (ii) a double depletion strategy to remove Hb by exploiting its affinity for Ni(II), and carbonic anhydrase-1 (CA1) through ion exchange chromatography (Ringrose et al., 2008); (iii) combinatorial hexapeptide (HAP) ligand libraries which exploit the affinity of each HAP for distinct proteins and thus the overloading of the separation column (in which the HAPs represent the stationary phase) results in a flow through elution of most abundant proteins (rapidly saturating their HAP baits), while low abundant proteins are retained by different HAPs and thus enriched (Boschetti et al., 2008); (iv) antibody-based approaches to selectively deplete Hb (Walpurgis et al., 2012); (v) electrolyte-based depletion strategies that selectively target and deplete Hb (Alvarez-Llamas et al., 2009); (vi) four-dimensional electrophoresis approaches (based upon non-denaturing IEF/native electrophoresis/denaturing IEF/SDS-PAGE in a row) yielding poor complex recovery (6 cytosolic complexes) owing to alkaline cleavage during earlier separation steps (Wang et al., 2010). However, it has been recently noted that each of the above-listed depletion strategies holds advantages and disadvantages (D'Amici et al., 2011a and 2011b). Indeed, most of these affinity-strategies efficiently work under denaturing conditions, which would discourage any effort to further analyse MPCs in Hb-depleted RBC samples. Also, the removal of Hb and other most abundant proteins, such as CA1 (Ringrose et al., 2008), might be advantageous only to some extent, since low-abundance proteins might be removed as well in the process, owing to the so-called “sponge effect”. Within this framework, we recently envisaged a preparative method that could synthesize the main advantages of each distinct Hb-depletion strategies: (i) ease, rapidity and reproducibility of the workflow; (ii) possibility to load high amounts of samples (up to 150 µg of proteins, in order to recover higher quantities of low-abundance species); (iii) possibility to separate Hb from the other protein fractions without losing “biological information” (Hb-binding proteins should be still present in the Hb containing sub-fractions of the cytosolic proteome); (iv) the conservation of the native conformation of MPCs (i.e. denaturation steps-free protocol) (D'Amici et al., 2011a and 2011b). The depletion method we suggested involves performing native gel electrophoresis in a polyacrylamide gel tube using a modified electro elution cell. The electrophoretic run is interrupted intermittently to allow the recovery of at least three different liquid fractions, that can be further assayed through either denaturing or native methods. While in the preliminary studies we limited to describe the feasibility of the method and assessed the possibility to separate up to 800 protein spots through denaturing 2D-IEF-SDS-PAGE (D'Amici et al., 2011a), we are hereby reporting an in-depth and systematic mass spectrometry-based identification of the native protein complexes of the RBC cytosolic proteome by analyzing the spots detected from 2D-CN-SDS-PAGE of three fractions (fraction 1, 2 and 3 – F1, F2, F3, respectively). Besides, we provide a list of the main RBC cytosolic protein complexes, by suggesting multimeric conformation on the basis of the apparent molecular weight of CN-PAGE first dimension complexes and second dimension SDS-PAGE of thereby present distinct proteins. To the best of the authors' knowledge, this is the first report providing compelling evidence that at least 55 multimeric protein-complexes coexist with Hb in RBCs, as they are likely to play a critical role in the maintenance of RBC functionality and survival *in vivo*.

Materials and methods

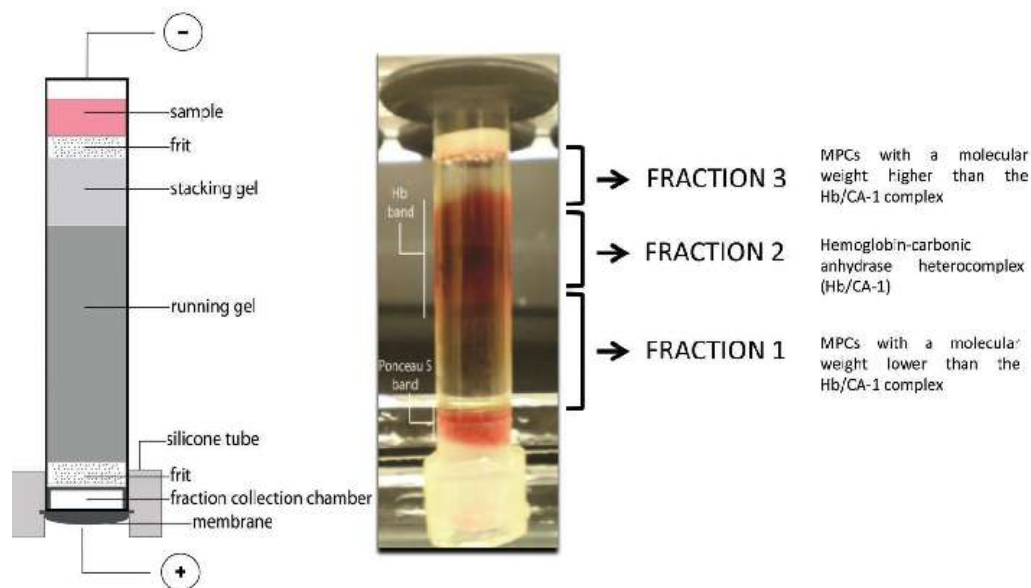
Sample collection

Red blood cell units were drawn from healthy donor volunteers according to the policy of the Italian National Blood Centre (“Blood Transfusion Service for donated blood”) and upon informed consent in accordance with the declaration of Helsinki. We studied RBC samples obtained from 6 healthy male donor volunteers [age 32.2 ± 4.5 (mean \pm S.D.)] upon centrifugation of whole blood and leukofiltration, as in (D’Alessandro et al., 2012).

Lysis of RBCs and protein extraction were performed based on the method proposed by Olivieri et al. (2001).

Fraction separations via Electro-Eluter cell

RBC cytosolic protein fractions were separated through a preparative native-gel electrophoresis performed in a modified Electro-Eluter cell (model 422; BioRad), as previously reported and summarized in **Supplementary Figure 1** (D’Amici et al., 2011a and 2011b). Six vertical glass tubes (length: 60 mm; internal diameter: 10 mm) were filled with a polyacrylamide gel at two different concentrations. The stacking gel had an acrylamide concentration of 4% w/v and was 8 mm long. The acrylamide concentration of the cylindrical separation gel was 6.5 % w/v and the gel was about 40mm long. The negative electrode is at the top, while positive electrode is located at the bottom of the tube, where a membrane cap was located. The cap was endowed with a dialysis membrane (with a MW limit of 3500 Da). One hundred and fifty microgram of total proteins in 1 mL of PBS 5mM, pH 8.0, were mixed with 100 μ L of sample buffer (0.1M Bis-Tris HCl, pH 7, 0.5M 6-aminocaproic acid, 30% w/v sucrose and 0.001% w/v Ponceau red), while only 1 mL was loaded onto the stacking gel. The run was carried out at 4°C (in a cold chamber with controlled temperature) and at increasing voltages starting from 60 to 150 V for a total of 4 h.



Supplementary Figure 1 A brief overview of the preparative workflow allowing the separation of three main fraction, with hemoglobin and carbonic anhydrase mainly recovered in fraction 2, thus enabling detection of low abundance multi-protein complexes from the other fractions (1 and 3). The method is the same as the one detailed in our previous technical reports (D’Amici et al., 2011).

Fractions started to be collected from the gel in the membrane cap after the Ponceau red front reached the lower end of the gel. Three fractions of about 200 μ L each were collected and were separately dialyzed in PBS 5 mM pH 8.0 for 10 h.

1D and 2D Native analyses

For each fraction, protein concentrations were estimated by the 2D-Quant Kit (GE Healthcare). Proteins from each fraction were then run either on 1-D CN-PAGE or 2-D CN-SDS-PAGE.

1-D CN-PAGE was performed according to Schagger and von Jagow (1991) using 0.75-mm-thick 8-12% (for fraction 1) or 5–12.5% (for fraction 2 and 3) w/v acrylamide gradient gels (Protean II xi cell, BioRad) loading 130 (fraction 1) or 150 μ g (fraction 2 and 3) of total proteins. HMW native protein mixture (66-669kDa) (GE Healthcare, Uppsala, Sweden) was taken as molecular weight marker. Runs were carried out at 4°C in a cold chamber under controlled temperature condition, while voltage was increased from 50 to 250 V.

Lanes from the 1D native electrophoresis were cut and equilibrated for 30 min through two subsequent incubation steps of 15 min each, including (i) incubation under gentle agitation in presence of 50 mM TrisHCl pH 8.8, 4% SDS, 30% glycerol and 6 M urea upon incubation with 3% DTT followed by (ii) a second incubation in 12% iodacetamide (reducing conditions). For the second dimension, lanes were loaded on a 11% (fraction 1) or 12.5% (fraction 2 and 3) acrylamide SDS gel and covered with cathode buffer with 0.5% agarose. The molecular weight of the proteins was determined by the Wide Range SigmaMarker™ protein standard (Sigma Aldrich, St. Louis, MO, USA).

Mass spectrometry identification of protein spots

Spots excised from the second dimension gels and subjected to in gel trypsin digestion according to Shevchenko et al. (1996), with minor modifications. The gel pieces were swollen in a digestion buffer containing 50 mM NH_4HCO_3 and 12.5 ng/mL trypsin (modified porcine trypsin, sequencing grade, Promega, Madison, WI) in an ice bath. After 30 min, the supernatant was removed and discarded; then 20 μ L of 50 mM NH_4HCO_3 was added to the gel pieces, and digestion was allowed to proceed overnight at 37 °C. The supernatant containing tryptic peptides was dried by vacuum centrifugation prior to MALDI-TOF/TOF (Suckau et al., 2003) and nano-LC-ESI-IT MS/MS identification (Baldwin et al., 2004).

MALDI-based identifications were performed through an Autoflex II MALDI-TOF/TOF mass spectrometer with the LIFT module (Bruker Daltonics) was used for mass analysis of peptide mixtures. Twenty microliters of the tryptic protein digests was loaded onto activated (0.1% TFA in acetonitrile) ZipTip columns and washed three times with 10 μ L of 0.1% TFA in DD- H_2O . The peptides were eluted with 1 μ L of matrix solution (0.7 mg/mL α -cyano-4-hydroxy-trans-cinnamic acid (Fluka, Germany) in 85% acetonitrile, 0.1% TFA and 1 mM $\text{NH}_4\text{H}_2\text{PO}_4$) and spotted directly on the MALDI-TOF target plate for automatic identifications (PAC384 pre-spotted anchor chip) Proteins were identified by PMF using the database search program MASCOT (<http://www.matrixscience.com/>) upon removal of background ion peaks. Accuracy was set within 50 ppm, while the enzyme chosen was trypsin and only 1 missed cleavage was allowed; fixed carbamidomethyl Cys and variable Met-oxidation, was used as optional search criterion. PMF-based protein identification was confirmed by MS/MS analyses of precursor ions and repeated

MASCOT-based database searches. Runs were performed automatically through FlexControl setting and Biotoools processing of MS data (PMF) and validation of identifications through MS/MS (LIFT analysis) on the three most intense ion peaks. A peptide mixture (Peptide calibration standard I, Bruker Daltonics) was used for external calibration.

Nano-LC-ESI-IT MS/MS identifications were obtained through a split-free nano-flow chromatography separation system (EASY-nLC II, Proxeon, Odense, Denmark) coupled to a 3D-ion trap (model AmaZon ETD, Bruker Daltonik, Germany) equipped with an online ESI nano-sprayer (the spray capillary was a fused silica capillary, 0.090 mm o.d., 0.020 mm i.d.). For all experiments, a sample volume of 15 μ L was loaded by the autosampler onto a homemade 2 cm fused silica precolumn (100 μ m I.D.; 375 μ m O.D.; Reprosil C18-AQ, 5 μ m, Dr. Maisch GmbH, Ammerbuch-Entringen, Germany). Sequential elution of peptides was accomplished using a flow rate of 300 nL/min and a linear gradient from Solution A (2% acetonitrile; 0.1% formic acid) to 50% of Solution B (98% acetonitrile; 0.1% formic acid) in 40 min over the precolumn in-line with a homemade 15 cm resolving column (75 μ m I.D.; 375 μ m O.D.; Reprosil C18-AQ, 3 μ m, Dr. Maisch GmbH, Ammerbuch-Entringen, Germany). The acquisition parameters for the instrument were as follows: dry gas temperature, 220 $^{\circ}$ C; dry gas, 4.0 L/min; nebulizer gas, 10 psi; electrospray voltage, 4000 V; high-voltage end-plate offset, -200 V; capillary exit, 140 V; trap drive: 63.2; funnel 1 in, 100 V out 35 V and funnel 2 in, 12 V out 10 V; ICC target, 200 000; maximum accumulation time, 50 ms. The sample was measured with the “Enhanced Resolution Mode” at 8100 m/z per second (which allows mono isotopic resolution up to four charge stages) polarity positive, scan range from m/z 300 to 1500, 5 spectra averaged, and rolling average of 1. The “Smart Decomposition” was set to “auto”.

Acquired spectra were processed in DataAnalysis 4.0, and deconvoluted spectra were further analyzed with BioTools 3.2 software and submitted to Mascot search program (in-house version 2.2, Matrix Science, London, UK). The following parameters were adopted for database searches: NCBI nr database (release date 22/10/2011; 15 670 865 sequences; 5 387 755 057 residues); taxonomy = *Homo sapiens*; peptide and fragment mass tolerance of \pm 0.3 Da; enzyme specificity (trypsin) with 2 missed cleavages considered; fixed modifications: carbamidomethyl (C); variable modifications: oxidation (M).

Results

Three fractions were collected upon preparative CN-PAGE through Electro Eluter cells (**Supplementary Figure 1**): (i) F1, containing MPCs with a MW lower than the Hb/CA1 complex (< approximately 500kDa); (ii) F2, containing Hb (α and β chains), CA1 and other complexes with MW similar to the Hb/CA1 heterocomplex (\approx 500kDa); (iii) F3, containing MPCs with a MW higher than the Hb/CA-1 complex (\geq 500kDa). Each fraction then underwent CN-PAGE first dimension separation of protein complexes and subsequent second dimension separation of the proteins from each complex through SDS-PAGE, as schematized in the workflow in **Figure 1**.

First dimension CN-PAGE yielded the separation of 55 unique bands accounting for distinct protein complexes, out of which 31 belonged to F1, 18 to F2, while 6 were exclusively found in the third fraction (**Figure 2**). Hb and CA1 were mainly present in F2 (Silverman et al., 1979) although also F3 contained traces of Hb contamination (**Figure**

2). Of note, most of the protein bands below 100kDa in 1D-CN-PAGE of F1 account for non-complexed RBC proteins (**Figure 3**).

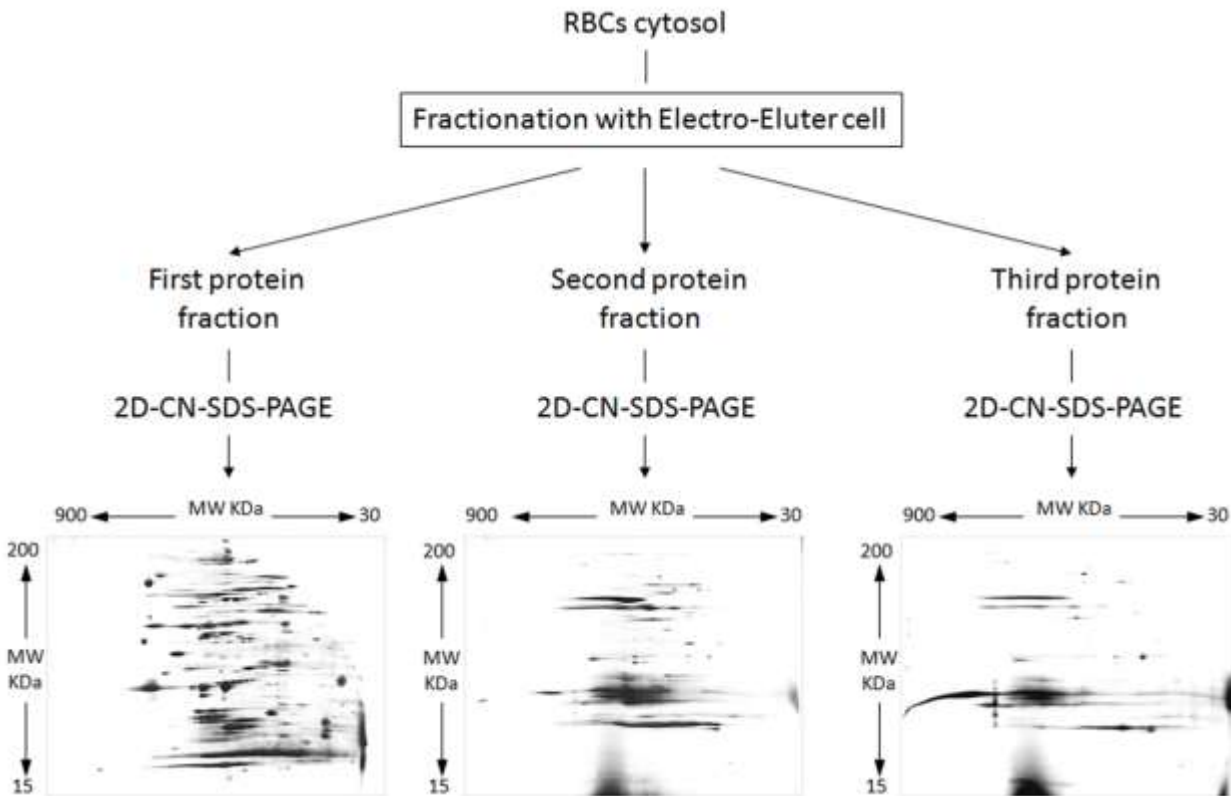


FIGURE 1 A brief overview of the analytical workflow. Red blood cell cytosolic protein extract underwent separation through electro-eluter cell fractionation, which allowed separation and recovery of three fractions on the basis of their molecular weight and electrophoretic mobility of native complexes. Each fraction then was further analysed with 1D-clear native PAGE (separating the cytosolic native complexes), followed by a second SDS-PAGE electrophoretic separation (orthogonally separating the proteins within each distinct complex).

Fractions 1–3 were further analyzed by 2-D CN-SDS-PAGE (**Figure 3-5**). Overall, a total of 238 distinct protein spots were detected, out of which 144 were unique to F1, 60 to F2 and 34 to F3.

Protein spots were excised from the gels, trypsin digested and analyzed through mass spectrometry to pursue the identification of the separated spots. Results are reported in **Table 1**, along with the spot number (referred to those attributed in **Figures 3-5**), the extended protein name and indications about the theoretical molecular weight and isoelectric point of each entry, gene identifiers, and identification details (number of peptides and MASCOT scores). It is worthwhile to underline that these proteins represent distinct interactors from the 55 different complexes separated through the preparative electro elution and the first CN-PAGE separation dimension (allineated on top of each second dimensions, from **Figures 3-5**) (Rosenblum et al., 1982; Low et al., 2002; Pasini et al., 2006; Roux-Dalvai et al., 2008; Bosman et al., 2008). Since this study focuses on protein complexes alone, it does not represent an explorative study of the RBC proteome. Hence, any direct comparison against existing literature on the overall number of the distinct entries individuated should be avoided. On the other hand, it deserves to be stressed that, of

the 55 observed cytosolic MPCs, we could suggest homo- and hetero-complexes by supposing the approximated stoichiometry of protein subunits in the multimers on the basis of the experimental molecular weight of the identified proteins, protein-protein interaction prediction tools (**Supplementary Figures 3-5**) and information available from the literature, as detailed in **Table 2**. MPCs included: (i) proteins involved in oxygen transport and transport metabolon (Hb-CA1); (ii) oxidative stress responses and molecular chaperones; (iii) enzymatic complexes; (iv) mixed metabolism/anti-oxidant/chaperone complexes; (v) protein degradation systems (ubiquitin and 20S core proteasome components).

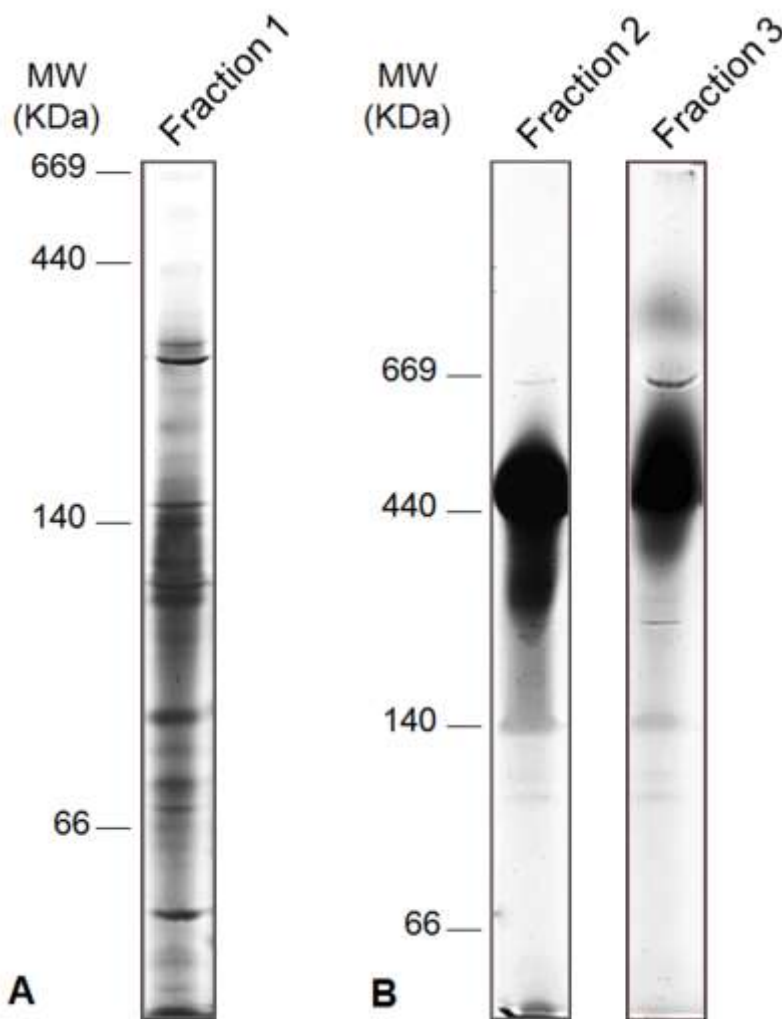


FIGURE 2 A detail of first dimension clear native (CN)-PAGE of fractions 1 to 3. The most abundant complex was the one containing hemoglobin and carbonic anhydrase in fraction 2 (and, in part, also contaminating fraction 3) at approximately 500kDa.

Some proteins took part in several MPCs, though displaying the same apparent molecular weight upon second dimension SDS-PAGE separation (a particular of this phenomenon in F1 2D gels **Supplementary Figure 2**). In classic 2D-isoelectrofocusing-SDS-PAGE electrophoresis, protein spots showing the same molecular weight albeit different *pI*s are likely to be differentially phosphorylated (Seo and Lee, 2004). Although in the present study the first isoelectrofocusing dimension has

been replaced with CN separation of MPCs, questions arise as to which biological process might end up influencing protein-protein interaction partners of a given protein without substantially altering the molecular weight. Our first guess was to test a subset of post translational modifications, namely phosphorylations of serine/threonine or tyrosine residues (altering MW by only 80Da). Indeed, phosphorylations are long known to modulate interactions in MPCs, especially in RBCs, whereas the thoroughly investigated model of the cytosolic domain of band 3 has revealed phosphorylation specific patterns of structural components interaction with the anion exchanger 1 protein at

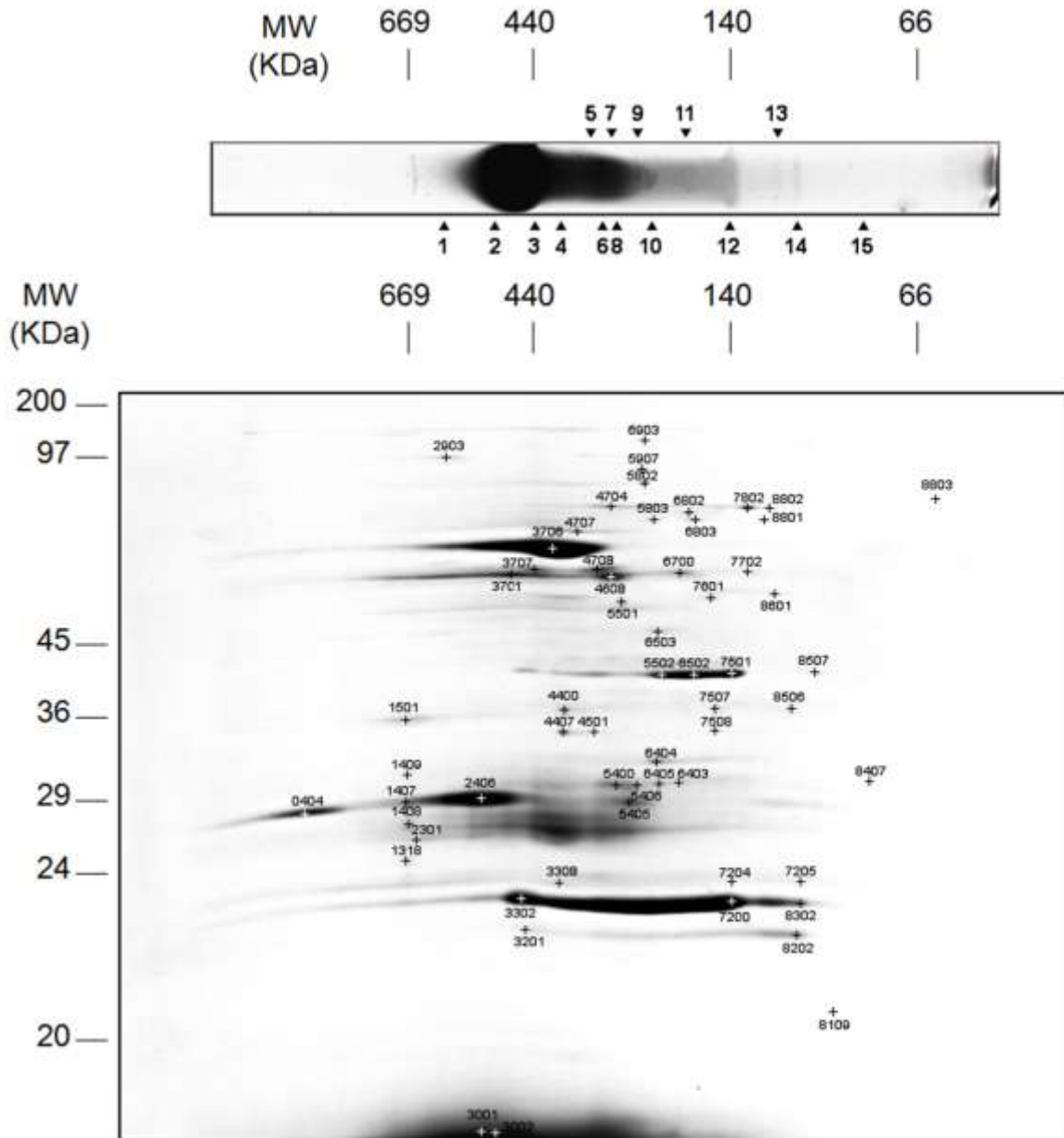


FIGURE 4 The resulting gel upon 2D-clear native (CN)-SDS-PAGE separation of proteins from fraction 2. Protein spots were identified with mass spectrometry and results are reported in Table 1 (fraction 2 section). The first CN-PAGE dimension is allineated on top, in order to highlight the separated bands each one consisting of at least a multi-protein complex, as detailed in Table 2 (fraction 2).

Discussion

Despite decades of strides in the definition of the RBC proteome, the comprehensive assessment of the multi-protein organization of erythrocytes is still a virgin area of investigation. While *in silico* predictions have been purported with encouraging results (Goodman et al., 2007; D'Alessandro et al., 2010), it still remains undisclosed as to whether and to which extent bioinformatic models would live up to actual experimental observation. Indeed, persisting gaps in this research endeavor exist, since less than a handful of research articles have addressed the RBC

membrane (van Gestel et al., 2010) and cytosol (Wang et al., 2010) native proteome, the latter mainly from a mere technical rather than a biological standpoint (only 6 complexes were individuated in the RBC cytosol, two of which accounting for Hbs). The present investigation has been designed as to bridge this gap, a goal that could be achieved through the auxilium of a sample preparation strategy that endows fractionation of the RBC cytosolic proteome and, in particular, of the vastly abundant Hb sub-fraction, while conserving native conformation of less abundant MPCs (D'Amici et al. 2011a and 2011b) without chemical cross-linking (Rappsilber et al., 2000). *In silico* models of the RBC interactome agreed about the presence of a so called Repair or Destroy box (Goodman et al., 2007), also referred to as the Save or Sacrifice (D'Alessandro et al., 2010) sub-network, accounting for highly connected proteins (mainly Heat shock proteins – HSPs – and anti-oxidant enzymes) which are involved in the regulation of the redox poise. Indeed, RBC ageing *in vivo* and *in vitro* (blood bank conditions) is accompanied by the progressive accumulation of oxidative stress-triggered lesions utterly leading to RBC removal from the bloodstream (Bosman et al., 2010; D'Alessandro et al., 2012). It is thus small wonder that 20 out 55 individuate cytosolic MPCs in RBCs were characterized by proteins/enzymes involved in self-defensive mechanisms against oxidative stress (**Table 2**). This is further evidenced by protein-protein interaction elaborations of proteins identified in each different fraction, as graphed in **Supplementary figure 3-5**. These results are consistent with existing interactomics elaborations by Goodman's (2007) and our group (2010), which pinpointed at a likely cross-talk between anti-oxidant defenses and metabolic enzymes, through the probable direct interaction of specific proteins (especially HSP70 and HSP90, but also catalase, superoxide dismutases and peroxiredoxins) with metabolic enzymes (such as lactate dehydrogenase – LDH, glyceraldehyde 3-phosphate dehydrogenase - GAPDH – **Supplementary Figures 3, 4 and 5**). In the present investigation, we could confirm and expand these models by providing direct evidence of the co-participation of several metabolic enzymes with anti-oxidant/chaperone molecules in numerous MPCs (see for example the complex CAT-LDHB - **Table 2, Supplementary Figure 5**), as detailed below.

Hb-CA1 complex and Hb smear

The most abundant complex is a diffused band at approximately 500kDa in F2 and 3 (**Figure 2** and band 2 from **Figure 4**). This band corresponded to two main protein spots from F2 (2406 and 3001 – **Table 2** and **Figure 4**), accounting for CA1 and beta Hb, respectively. Interaction between those two proteins has long been postulated (Silverman et al., 1979) and confirmed (D'Amici et al, 2011a and 2011b), though the current approach does not allow us to determine the exact stoichiometry of the proteins in the complex. However, it is not to be excluded that native gel bands at 440kDa might account for independent multimers of CA1 and Hbs. Indeed, multimerization of CA1 in \approx 440kDa complexes (band 3 F3–**Figure 5**) had already been reported (Wang et al., 2010). However, hereby we produce the first evidence about further dimerization of this high molecular weight complex at approximately \approx 800kDa (band 1 from F3 – **Figure 5** and **Table 2**).

First dimension CN-PAGE of the most abundant fraction (the one where Hb could be found – band 2 to 8 in F2 – **Figure 2, Table 2**) also shows a smear from 440kDa down to \approx 280kDa. In this molecular weight span, Hb is always present (**Figure 4**), while the smeared nature of the band does not allow to rule out any reliable contribution of Hbs to RBC cytosol MPCs. As a mere suggestion, it is interesting to note that certain marine (among which

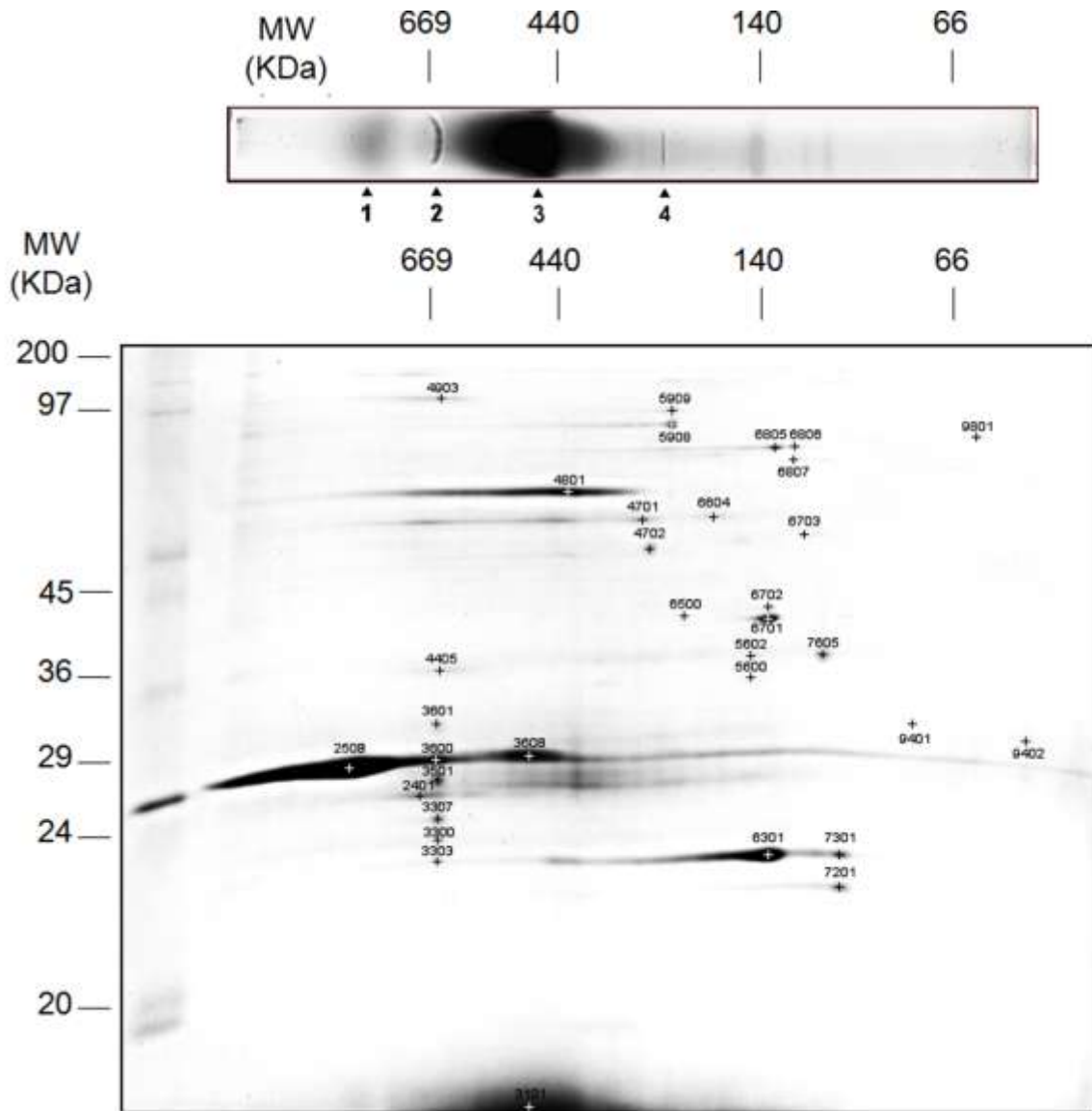
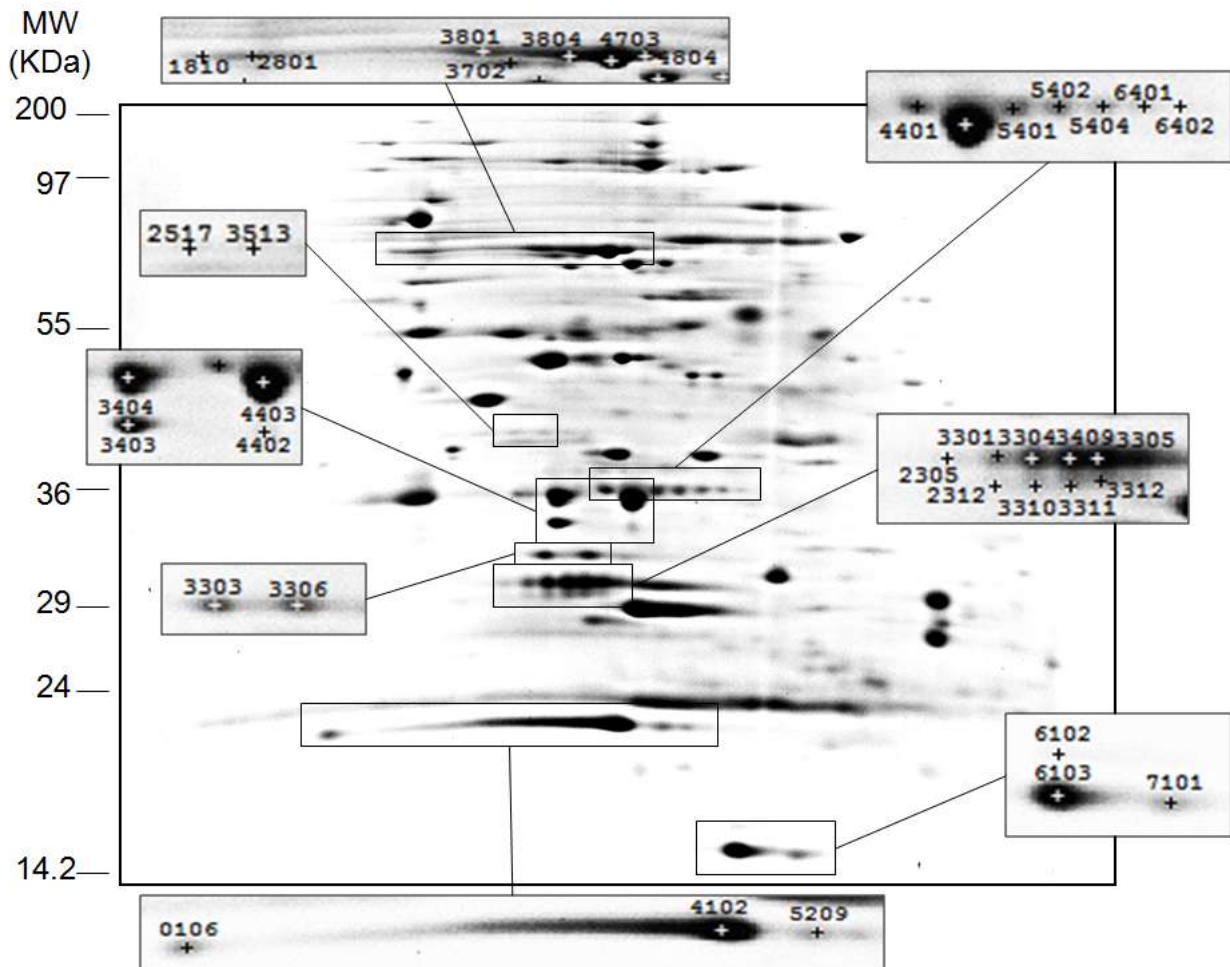


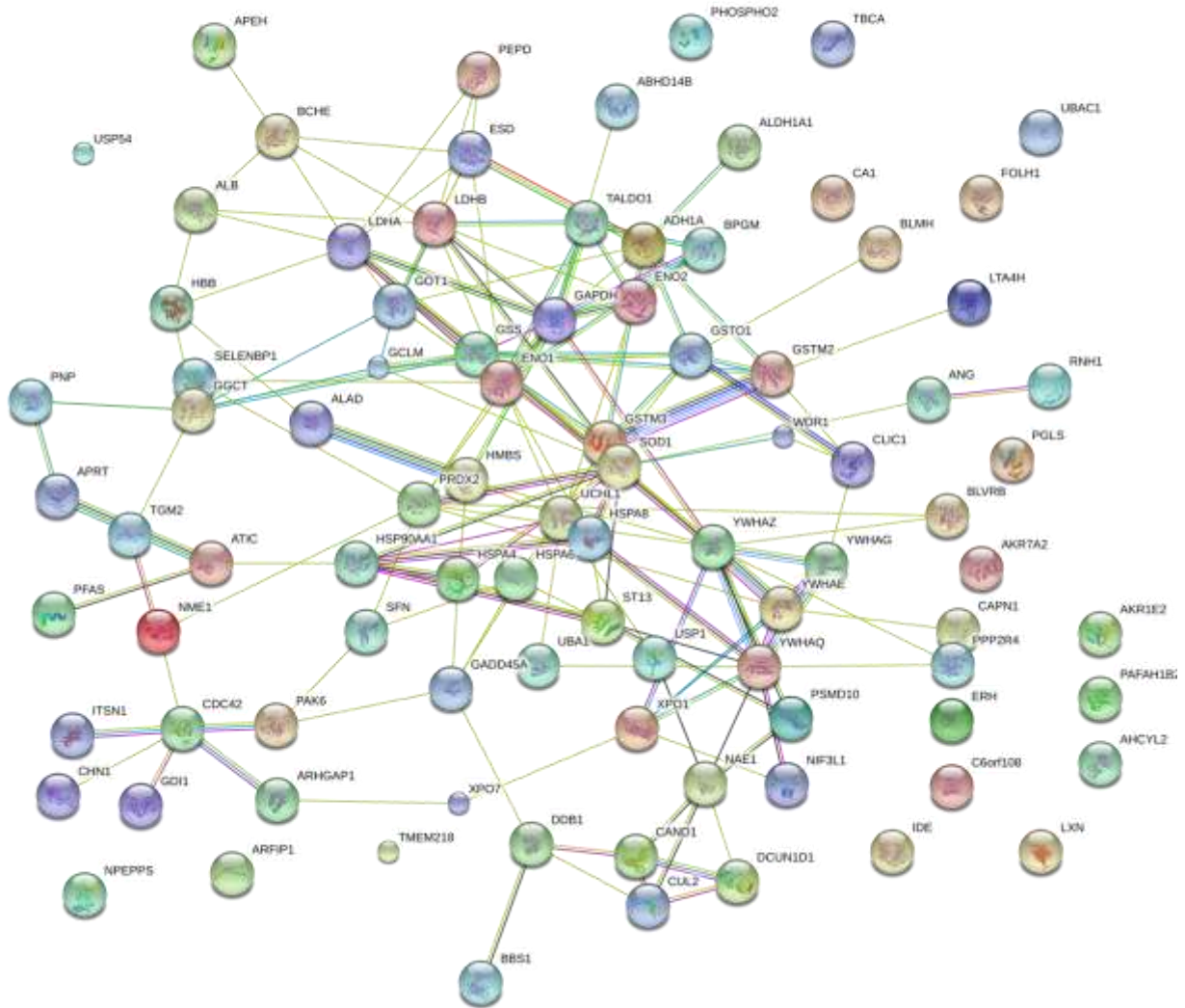
FIGURE 5 The resulting gel upon 2D-clear native (CN)-SDS-PAGE separation of proteins from fraction 3. Protein spots were identified with mass spectrometry and results are reported in Table 1 (fraction 3 section). The first CN-PAGE dimension is allineated on top, in order to highlight the separated bands each one consisting of at least a multi-protein complex, as detailed in Table 2 (fraction 3).

Oligobranchia mashikoi) and terrestrial (such as *Lumbricus terrestris*) invertebrates do not host Hb within erythrocytes, while they rely for oxygen transport on giant respiratory extracellular proteins made up of globin chains of 3-3.6kDa, which are complexed in 350-440kDa multimers (Nagakawa et al., 2005). However, while normal HbA molecules (tetramers of $\alpha\beta_2$ globin chains) should weigh up to 64kDa, multimerization of human Hb is a phenomenon occurring in the frame of sickle cell anemia, whereas Hb S polymerizes in aqueous solution owing to the S alpha 2A beta 2(6)Glu \rightarrow Val mutation (Rhoda et al., 1984). Since no anemic patient was enrolled in this study, the observed smear in the first native gel dimension of F2 alone (**Figure 2**) might be rather attributable to technical artifacts resulting from the overwhelming abundance of Hb in F2. Nevertheless, it is worthwhile

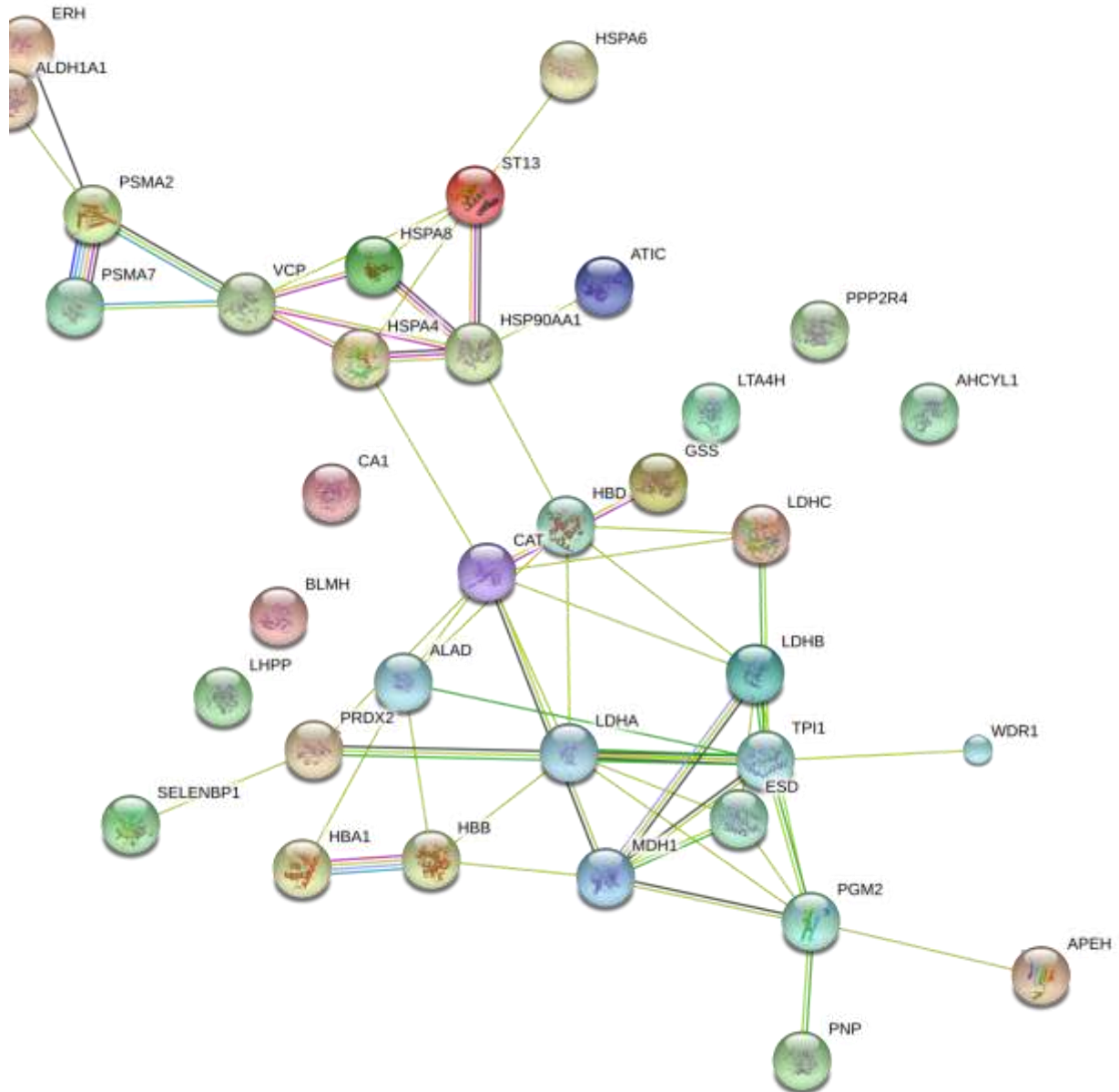
mentioning that Hb heterocomplexes (Hb $\alpha\beta_2$ and $\alpha_2\delta_2$) had already been reported by Wang et al. at 180 or 237kDa the former and 352kDa the latter and suggested as an actual biological evidence of Hb tetramer multimerization (Wang et al., 2010). Since our approach relied on a Hb-depletion strategy (D'Amici et al., 2011a and 2011b), and Hb was largely collected in F2 in order to unravel the otherwise hidden low abundance complexes in the other fractions, we could not discriminate as many Hb chain isoforms with different PTMs as in Wang et al. (2010).



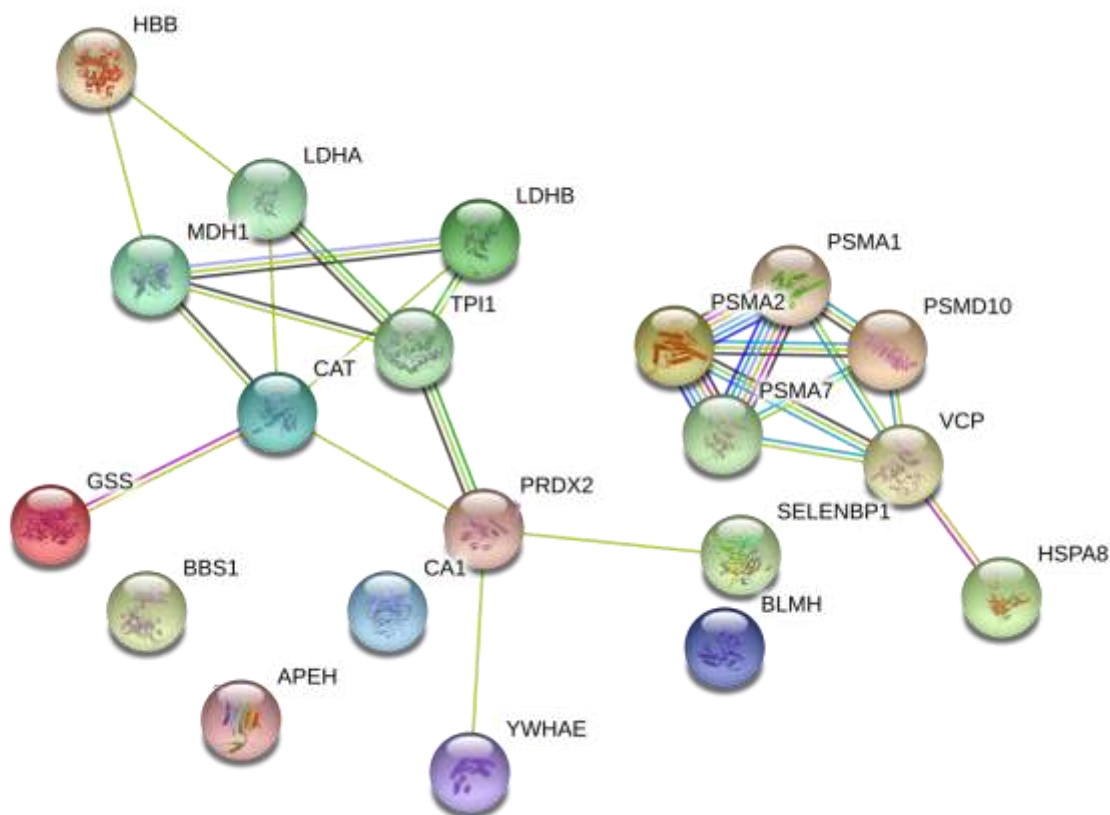
Supplementary FIGURE 2 A detail of the second CN-SDS-PAGE dimension of fraction 1. A series of spots (eventually identified as the same protein – please, refer to **Table 1**, fraction 1) are highlighted that show the same apparent molecular weight though belong to different protein complexes. The mechanisms that influence differential interaction/oligomerization of cytosolic proteins in red blood cells seem to mainly involve mechanisms that do not substantially alter the apparent molecular weight, such as specific post translational modifications (e.g. phosphorylations). However, no definitive clue underpinning this assumption could be obtained from the present study.



Supplementary FIGURE 3 Protein-protein interaction *in silico* predictions of proteins identified in Fraction 1. Images have been obtained through String (<http://string-db.org/>) on the basis of experimental evidences on the *Homo sapiens* protein-protein interaction database (confidence score was set to high confidence = 0.7).



Supplementary FIGURE 4 Protein-protein interaction *in silico* predictions of proteins identified in Fraction 2. Images have been obtained through String (<http://string-db.org/>) on the basis of experimental evidences on the *Homo sapiens* protein-protein interaction database (confidence score was set to high confidence = 0.7).



Supplementary FIGURE 5 Protein-protein interaction *in silico* predictions of proteins identified in Fraction 3. Images have been obtained through String (<http://string-db.org/>) on the basis of experimental evidences on the *Homo sapiens* protein-protein interaction database (confidence score was set to high confidence = 0.7).

Anti-oxidant enzymes and chaperones

Peroxiredoxin 2 (Prdx2) is the third most abundant cytosolic RBC protein, after Hb and CA1 (Low et al., 2008). Eight homo- and heterocomplexes of Prdx2 have been identified in the present study (band 1, 14 and 17 from F1; 3, 8, 12a and 12b and 14 from F2 – **Table 2**). Multimeric conformation of Prdx2 has been reported to result from the oxidative stress-dependent oligomerization of dimers (Li et al., 2005) in decamers (Rinalducci et al., 2011) (further dimerized in band 1 in F1 – **Table 2, Figure 3**). Analogously, the ≈ 140 kDa (bands 12a and 12b in F2 – **Table 2**) Prdx2 complex has been suggested to result from an eptameric organization (Rinalducci et al., 2011). A ≈ 440 kDa complex of decameric Prdx2 with tetrameric catalase (CAT) has been reported as well within the framework of RBC storage under blood bank conditions (Rinalducci et al., 2011) (band 3 in F2 – **Table 2, Figure 4**).

Interestingly, Prdx2 was found to be complexed with flavin reductase NADPH and alcohol dehydrogenase NADP⁺, both the enzymes catalyzing the reduction to NADPH (band 14 and 17, F1 – **Table 2, Figure 3**). Indeed, the oxidized Prdx2 is regenerated by thioredoxin reductase, with reducing equivalents derived from NADPH (Low et al., 2008).

Interaction between Prdx2 and selenium binding protein (SELENBP1 – band 8, F2 – **Table 2**) had been predicted, yet not assessed, through *in silico* models (Goodman et al., 2007; D'Alessandro et al., 2010) (**Supplementary Figure 4 and 5**). Analogous considerations can be made for Prdx2 and Prdx6 (tetramer of homodimers, band 14, F2).

However, the anti-oxidant enzymatic system in RBCs is not only limited to Prdxs and catalase, since also Cu/Zn superoxide dismutase (SOD1) play a critical role in RBC physiology (D'Alessandro and Zolla, 2011).

While aberrant oligomerization of SOD1 dimers underlies the insurgence of familial amyotrophic lateral sclerosis (Svensson et al., 2010), we hereby describe the previously unreported association of SOD1 dimers with the monomer of the ribonuclease inhibitor protein (band 21, F1 – **Figure 3, Table 2**). On the other hand, the interaction of homo- or heterocomplexes of 14-3-3 protein isoforms (epsilon, gamma, theta - band 22, F1) had already been reported in other cell types, including human epidermal keratinocytes (Liang et al., 2009) (**Supplementary Figure 3**).

Human glutathione synthetase (GSS) has a dimeric structure (Slavens et al., 2011), that we hereby confirm (band 13, F2 – **Table 2, Figure 4**). On the other hand, we also provide the first evidence of the interaction between HSPA8 and GSS in RBCs (band 15, F1).

The central role of HSPs in the interactome of RBCs had been previously hypothesized *in silico* [8,30] and hereby confirmed with the presence of multiple heterocomplexes of HSPs with antioxidant and metabolic enzymes (bands 4,6,6a,10,12,13,15 in F1; band 9 in F2 - **Table 2, Supplementary Figure 3**).

Acylamino acid-releasing enzyme/oxidized protein hydrolase is a homotetramer (hereby confirmed in band 5 from F1) displaying endopeptidase activity against oxidized and glycated proteins (Scaloni et al., 1992), both recurring phenomena in RBCs (e.g. Hb glycation).

Metabolic enzymes and cross-talks with antioxidant defenses

Since RBCs are devoid of any organelle, mitochondria included, they mainly rely on glycolysis to produce ATP and sustain their energy requirements. Lactate dehydrogenase catalyzes the interconversion of pyruvate and lactate with concomitant interconversion of NADH and NAD⁺. Functional lactate dehydrogenase are homo or hetero tetramers composed of M and H protein subunits encoded by the LDHA and LDHB genes respectively (Holmes and Goldberg, 2009), hereby observed in band 11 of F1 and band 11 of F2 (**Table 2, Supplementary Figure 3-5**). Aldehyde dehydrogenase 1 is organized in homotetramers (Agarwal et al., 1989) and requires NAD⁺ for its correct functioning. It is thus interesting to note its oligomerization with LDH tetramers (band 5, F2 – **Table 2**).

Human biphosphoglycerate mutase (BPGM) is dimeric, in contrast to yeast BPGM that displays a tetrameric structure (Fothergill-Gilmore, 1989). However, we could observe that BPGM-positive band (no.16) at approximately ≈120kDa in F1 (spot no. 5301 - **Figure 3**), that might account for tetramers made up of two BPGM

dimers. Dimeric structure of phosphoglucomutase 2 has been already reported in rabbit muscles and human RBCs (Lin et al., 1986) (band 6, F2).

In addition to the aforementioned oligomers, a wide series of metabolic enzyme complexes were observed for the first time in the RBC cytosol, especially in the Hb-depleted F1, though confirming consolidated *in vitro* evidences as it emerged from a rapid search in the UniProt database. Results included: hexamers of bleomycin hydrolase, homo-octamers of delta-aminolevulinic acid dehydratase, dimers of gamma enolase, homotetramers of adenosylhomocysteinase isoform 2, hexamers (2 homotrimers) of purine nucleoside phosphorylase, trimers of nucleoside diphosphate kinase A, dimers of human prolidase, dimers of intracellular chloride ion channel, homohexamers of transitional endoplasmic reticulum ATPase, homodimers of esterase D and of cytoplasmic aspartate aminotransferase (**Table 2**).

It is also worthwhile to stress that these oligomers also further interacted to give rise to actual MPCs, and these interactions were not only limited to metabolic enzyme oligomers but also involved anti-oxidant enzymes, in a sort of a cross-talk between metabolic modulation and anti-oxidant defenses (see for example ALAD-HSPA8, SOD-TALDO and CAT-LDHB, and complexes in bands 4 and 19b of F1, band 4 of F2, respectively – **Table 2, Supplementary Figures 3-5**).

RBC proteasome

Recent evidences indicated the presence of functional 20S proteasome in leukocyte-depleted reticulocyte-depleted RBCs (Neelam et al., 2011). A presence that might result in untoward burdens to those recipients transfused with longer stored packed RBC units, in the light of the progressive accumulation of 20S proteasomes in the supernatants of *in vitro* ageing RBCs (Geng et al., 2009). Native assessment of RBC cytosol have previously evidenced the presence of a functional 20S proteasome complex weighing approximately 669kDa (Bosu and Kipreos, 2008). Our results agree with this observation, since 20S proteasome core particles represent the main contributors to oligomers found in F3 (band 2 in **Figure 5** and **Table 2**). The core particles interact to form a hollow cylindrical structure composed of 28 subunits arranged in four stacked rings ($\alpha 7\beta 7\beta 7\alpha 7$). Notably, we could discriminate at least four different α and β subunits (spots no. 3301,3302,3501,3601 in F3 – **Table 1**).

Since the proteasome-dependent protein degradation process implies the cooperation with the ubiquitin system, it is of note the identification of ubiquitin-carboxyl terminal hydrolase 14 (USP14-spot no. 5704 from F1 – **Table 1**). USP14 is a proteasome-associated deubiquitinase which releases ubiquitin from the proteasome targeted ubiquitinated proteins. We could hereby assess for the first time in RBCs the presence of a complex characterized by the interaction of USP14a and NEDD8 (band 18, F1 – **Table 2**). We expected that this complex should have included also cullin (Bosu and Kipreos, 2008), that was indeed identified (spots no.1809-**Table 1**) although it interacted with cullin-associated NEDD8-dissociated protein 1 (band 2 from F1-**Table 2, Supplementary Figure 3**), whose role is to prevent NEDD8 association to cullin and thus justified our observations.

Conclusions

The RBC cytosolic proteome still represents a treasure trove of biological information. In the present investigation, we could detect and describe 55 native complexes, mainly involved in oxygen transport, metabolism, anti-oxidant responses and protein degradation cascades. Future investigations should pursue the expansion of the current knowledge and the integration with the understanding of how these complexes end up influencing RBC ageing *in vivo* and *in vitro* and whether/to which extent alterations to the oligomeric configuration of cytosolic complexes is associated with specific pathologies.

Table 1 – Protein identification in each fraction upon 2D-CN-SDS-PAGE in freshly drawn RBCs
Fraction 1

N° spot	Mr, Da	pI	N° of peptides identified	Mascot Score	NCBI Accession Number	Protein ID [Homo sapiens]
0106	21795	5.44	5	73	gi 9955007	Chain A, Thioredoxin Peroxidase B From Red Blood Cells
1403	36301	6.16	12	107	gi 248839	Delta-aminolevulinatase dehydratase
1603	52242	6.00	11	81	gi 7245509	Chain A, Human Bleomycin Hydrolase
1604	54800	6.30	11	86	gi 2183299	Aldehyde dehydrogenase 1
1702	64425	6.39	9	100	gi 1263196	AICAR formyltransferase/IMP cyclohydrolase Bifunctional enzyme
1703	82170	5.29	13	559	gi 7144648	Oxidized protein hydrolase
1704	68521	7.70	2	116	gi 181630	DNF1552 protein
1805	125186	5.91	3	105	gi 21315062	Exportin 7
1809	87554	6.45	7	219	gi 19482174	Cullin-2 isoform c
	82529	5.49	5	175	gi 189054948	Calpain-1 catalytic subunit
	82210	5.29	2	85	gi 556514	Acylamino acid-releasing enzyme
1810	71082	5.37	6	229	gi 5729877	Heat shock cognate 71 kDa protein isoform 1
	70755	5.76	3	136	gi 188492	Heat shock induced protein
	71440	5.81	3	137	gi 34419635	Heat shock 70 kDa protein 6
1813	81173	5.29	14	108	gi 23510451	Acylamino-acid-releasing enzyme
1901						NOT IDENTIFIED
1905	137999	5.52	9	304	gi 21361794	Cullin-associated NEDD8-dissociated protein 1 (CAND1)
2305						NOT IDENTIFIED
2312						NOT IDENTIFIED
2403	36900	5.71	5	118	gi 4557032	L-lactate dehydrogenase B chain
	36950	8.44	4	112	gi 5031857	L-lactate dehydrogenase A chain isoform 1
2503						NOT IDENTIFIED
2506	44630	6.02	14	105	gi 239937451	Adenosylhomocysteinase isoform 2
2517	46219	6.52	5	64	gi 4504067	Aspartate aminotransferase, cytoplasmic
2518	39265	5.91	3	142	gi 10197632	MDS015
2601	45538	4.82	8	323	gi 55770884	Ubiquitin-associated domain-containing protein 1
2602	52358	5.93	11	86	gi 16306550	Selenium-binding protein 1
2801	70855	5.28	7	82	gi 62897129	Heat shock 70kDa protein 8 isoform 1 variant
2804	68329	5.11	11	116	gi 83318444	HSP90AA1 protein
2805	95096	5.18	5	175	gi 4579909	Apg-2 (Heat shock 70kDa protein 4)
2901						NOT IDENTIFIED
2902						NOT IDENTIFIED

2906	137999	5.52	11	299	gi 38678112	Cullin-associated NEDD8-dissociated protein 1
3102	19641	5.42	4	77	gi 38045913	Nucleoside diphosphate kinase A isoform a
3301	32097	6.45	16	573	gi 157168362	Purine nucleoside phosphorylase
3303	34181	8.35	8	338	gi 1882265	Esterase D
	31956	6.54	7	302	gi 33413400	S-formylglutathione hydrolase
3304	32325	6.45	23	735	gi 157168362	Purine nucleoside phosphorylase
	28909	6.59	2	95	gi 4502517	Carbonic anhydrase 1
3305	32097	6.45	18	111	gi 157168362	Purine nucleoside phosphorylase
3306	34181	8.35	10	485	gi 182265	Esterase D
	32077	6.12	6	207	gi 10092677	Pyridoxal phosphate phosphatase
3310	32382	7.09	7	261	gi 387033	Purine nucleoside phosphorylase
	28909	6.59	3	117	gi 4502517	Carbonic anhydrase 1
3311	32382	7.09	7	267	gi 387033	Purine nucleoside phosphorylase
3312	32325	6.45	22	639	gi 157168362	Purine nucleoside phosphorylase
3403	36666	7.63	7	86	gi 62897717	Lactate dehydrogenase A variant
3404	36900	5.71	25	830	gi 4557032	L-lactate dehydrogenase B chain
	36950	8.44	10	343	gi 5031857	L-lactate dehydrogenase A chain
	36758	6.16	4	178	gi 248839	Delta aminolevulinatase
	37688	6.36	6	161	gi 5803187	Transaldolase
3409	32097	6.45	12	103	gi 157168362	Purine nucleoside phosphorylase
3513	46447	6.52	8	296	gi 4504067	Aspartate aminotransferase, cytoplasmatic
3602	53161	5.71	10	365	gi 15620780	Glutamate carboxypeptidase
	52928	5.93	6	277	gi 16306550	Selenium-binding protein 1
3603	41477	5.18	12	421	gi 19923193	Hsc 70-interacting protein
3606	52358	5.93	7	95	gi 16306550	Selenium-binding protein 1
3702	69995	5.48	6	79	gi 4529893	HSP70 1
3705	66138	6.17	9	94	gi 12652891	WD repeat domain 1
3801	70855	5.28	10	113	gi 62897129	Heat shock 70kDa protein 8 isoform 1 variant
3804	70854	5.37	7	103	gi 5729877	Heat shock cognate 71 kDa protein isoform
3901	124447	5.71	9	333	gi 4507943	Exportin-1
	118858	5.49	2	113	gi 23510338	Ubiquitin like modifier activating enzyme 1
	118745	6.30	2	73	gi 184556	Insulin-degrading enzyme
4102	21795	5.44	12	136	gi 9955007	Chain A, Thioredoxin Peroxidase B From Red Blood Cells
4105	19766	5.78	4	142	gi 4502171	Adenine phosphoribosyltransferase isoform a
	22048	5.66	6	139	gi 440308	Enhancer protein
4204	22105	7.13	5	72	gi 4502419	Flavin reductase (NADPH)
4301						NOT IDENTIFIED
4401	37688	6.36	15	463	gi 5803187	Transaldolase
	37024	6.23	6	233	gi 2736256	Aflatoxin aldehyde reductase AFAR
	36758	6.16	4	177	gi 248839	Delta aminolevulinatase
4402	36900	5.71	20	679	gi 4557032	L-lactate dehydrogenase B chain
4403	36615	5.71	12	135	gi 4557032	L-lactate dehydrogenase B chain
4506	36892	6.32	8	250	gi 5174391	Alcool dehydrogenase NADP+
	36900	5.71	4	162	gi 4557032	L-lactate dehydrogenase B chain
	35481	7.14	2	87	gi 12804019	AKR1CL2 protein
4507	39506	6.50	2	116	gi 224510663	Chain A, the crystal structure of human Porphobilinogen deaminase
	52523	5.67	2	87	gi 4504169	Glutathione synthetase
4603	52352	5.67	7	89	gi 4504169	Gutathione synthetase
4605						NOT IDENTIFIED
4703	70855	5.28	8	100	gi 62897129	Heat shock 70kDa protein 8 isoform 1 variant
4705	69109	5.87	16	130	gi 29726225	Chain A, Structure Of Leukotriene A4 Hydrolase D375n Mutant
4706						NOT IDENTIFIED
4803						NOT IDENTIFIED
4804	70855	5.28	5	73	gi 62897129	Heat shock 70kDa protein 8 isoform 1 variant

5103	19766	5.78	3	70	gi 4502171	Adenine phosphoribosyltransferase isoform a
5209	18315	5.19	4	67	gi 1617118	TSA
5301	29987	6.10	12	133	gi 4502445	Bisphosphoglycerate mutase
5302	27548	6.23	2	79	gi 4758484	Glutathione S-transferase omega-1 isoform 1
5401	37688	6.36	15	504	gi 5803187	Transaldolase
	37024	6.23	12	488	gi 2736256	Aflatoxin aldehyde reductase AFAR
	36900	5.71	10	256	gi 4557032	L-lactate dehydrogenase B-chain
5402	37385	6.35	9	84	gi 48257056	TALDO1 protein
5404	37688	6.36	4	170	gi 5803187	Transaldolase
5503	39533	6.68	2	59	gi 35309	Porphobilinogen deaminase
5504	37037	5.89	8	255	gi 29725611	Serine/threonine-protein phosphatase 2A activator isoform b
5601	51635	4.71	2	76	gi 3892027	Chain A ribonuclease inhibitor-angiogenin complex
5602	47055	4.99	10	343	gi 33186798	DNA-damage inducible protein 2
	52523	5.67	2	81	gi 4504169	Glutathione synthetase
5603	54560	5.64	7	89	gi 112491419	Chain A, Crystal Structure Of Human Prolidase
5604	51766	4.71	10	365	gi 21361547	Ribonuclease inhibitor
	47421	7.01	7	264	gi 693933	2-phosphopyruvate-hydratase alpha-enolase
5605	47421	7.01	5	248	gi 693933	2-phosphopyruvate-hydratase alpha-enolase
5701	56489	5.20	11	301	gi 4827050	Ubiquitin carboxyl-terminal hydrolase 14 isoform a
5702						NOT IDENTIFIED
5704	56489	5.20	11	357	gi 4827050	Ubiquitin carboxyl-terminal hydrolase 14 isoform a
	60655	5.25	3	104	gi 4502169	NEDD8-activating enzyme E1 regulatory subunit isoform a
5705						NOT IDENTIFIED
5706						NOT IDENTIFIED
5810	72719	5.74	8	78	gi 4557625	Glutamate-cystein ligase catalytic subunit isoform a
5811	96596	4.90	11	315	gi 1122278	De-ubiquitinase
5821	96596	4.90	3	102	gi 1122278	De-ubiquitinase
5901	117715	5.57	2	54	gi 35830	Ubiquitin activating enzyme E1
5902	117774	5.49	10	74	gi 23510338	Ubiquitin-like modifier-activating enzyme 1
5903	144573	5.50	10	79	gi 148922280	Phosphoribosylformylglycinamide synthase
5904	99695	5.04	6	70	gi 119594343	Damage-specific DNA binding protein 1, 127kDa, isoform CRA_e
6003						NOT IDENTIFIED
6102	15749	5.04	2	52	gi 305677635	Chain A, monomeric human Cu/Zn superoxide dismutase without Cu ligands
6103	16096	5.86	2	66	gi 1237406	Cu/Zn-superoxide dismutase
6124	20035	5.50	6	215	gi 374977519	Chain A, Structure Of Designed Orthogonal Interaction Between Cdc42 And Nucleotide Exchange Domains Of Intersectin
	21674	6.15	5	187	gi 126031529	Chain A, The Crystal Structure Of Human Cdc42 In Complex With The Crib Domain Of Human P21-Activated Kinase 6
	21601	6.73	2	132	gi 119613210	hCG393694 isoform CRA_a
6204						NOT IDENTIFIED
6205	25729	6.02	4	184	gi 494186	Chain A, crystal structure of human class Mu Glutathione transferase Gstm2-2
6212	22105	7.13	6	67	gi 4502419	Flavin reductase (NADPH)
6304	25931	5.47	2	94	gi 119599089	Latexin isoform CRA_a
6401	37688	6.36	14	439	gi 5803187	Transaldolase
6402						NOT IDENTIFIED
6501	37037	5.89	9	273	gi 29725611	Serine/threonine-protein phosphatase 2A activator isoform b
6601	47581	4.91	13	515	gi 5803011	Gamma enolase
	47421	7.01	11	363	gi 693933	2-phosphopyruvate-hydratase alpha-enolase

6602	51635	4.71	2	106	gi 3892017	Chain A ribonuclease inhibitor-angiogenin complex
6603	37922	6.90	2	72	gi 292385	Hydroxymethylbilane synthase
6605	52928	5.93	2	55	gi 16306550	Selenium binding protein 1
6606	51766	4.71	2	72	gi 21361547	Ribonuclease inhibitor
6801	98441	5.23	16	199	gi 4210726	Puromycin sensitive aminopeptidase
6804	78420	5.11	8	821	gi 39777597	Protein-glutamine gamma-glutamyltransferase 2 isoform a
7002	12904	5.25	5	137	gi 4759212	Tubulin-specific chaperone A
7101	16096	5.86	2	58	gi 1237406	Cu/Zn-superoxide dismutase
7202						NOT IDENTIFIED
7203	30333	5.18	3	157	gi 36030883	DCN1-like protein 1
7204	25837	6.33	8	201	gi 4505587	Platelet-activating factor acetylhydrolase IB subunit Gammaplatelet-activating factor acetylhydrolase IB subunit gamma Glutathione transferase M3
	27127	5.37	2	60	gi 306820	
7205	38632	6.10	2	55	gi 7657210	Arfaptin 1 isoform 2
7306						NOT IDENTIFIED
7604						NOT IDENTIFIED
7606	50461	5.85	7	180	gi 4757766	RhoGTPase-activating protein 1
7703	68484	5.73	14	432	gi 332356380	Albumin
7705	68484	5.73	8	102	gi 332356380	Albumin
7804	82538	5.02	9	110	gi 18491024	Dpeptidyl peptidase 3
8104	19211	4.97	7	362	gi 5454002	Deoxyribonucleoside 5'-monophosphate N-glycosidase isoform 1 Gamma-glutamylcyclotransferase isoform 1
	21222	5.07	8	255	gi 13129018	
8201	22219	7.13	4	186	gi 4502419	Flavin reductase (NADPH) Rho GDP-dissociation inhibitor 2
	23031	5.10	5	145	gi 56676393	
8203	7952	8.16	2	78	gi 4262000	14-3-3 protein/cytosolic phospholipase A2
8204	24697	5.71	5	108	gi 4506217	26S proteasome non-ATPase regulatory subunit 10 isoform 1 Glyceraldehyde-3-phosphate dehydrogenase
	36202	8.26	2	89	gi 31645	
8205	22446	5.94	4	141	gi 14249382	Abhydrolase domain-containing protein 14B Flavin reductase (NADPH)
	22219	7.13	2	99	gi 4502419	
8206	24697	5.71	2	67	gi 4506217	26S proteasome non-ATPase regulatory subunit 10 isoform 1 Flavin reductase (NADPH)
	22219	7.13	2	54	gi 4502419	
8208	21966	4.71	3	98	gi 21361547	Biliverdin-IX beta reductase isozyme I Abhydrolase domain-containing protein 14B
	22446	5.94	2	68	gi 14249382	
8304	29155	4.63	2	67	gi 5803225	14-3-3 protein epsilon
8305	28032	4.68	7	245	gi 5803227	14-3-3 protein theta 14-3-3 protein gamma Tyrosine 3-monooxygenase/tryptophan 5-Monooxygenase activation protein, theta polypeptide 6-phosphogluconolactonase 14-3-3 protein sigma 14-3-3 protein epsilon
	28528	4.66	8	237	gi 5726310	
	28031	4.72	6	209	gi 54696890	
	27815	5.70	5	179	gi 6912586	
	27871	4.68	4	113	gi 5454052	
	29326	4.63	2	83	gi 5803225	
8306	27177	5.09	8	271	gi 4588526	Chloride ion channel intracellular
8307						NOT IDENTIFIED
8308						NOT IDENTIFIED
8311						NOT IDENTIFIED
8403						NOT IDENTIFIED

8504	41653	4.84	15	486	gi 4506013	Protein phosphatase 1 regulatory subunit 7
8505	41653	4.84	2	84	gi 4506013	Protein phosphatase 1 regulatory subunit 7
8506	41653	4.84	6	171	gi 4506013	Protein phosphatase 1 regulatory subunit 7
8602						NOT IDENTIFIED
8603						NOT IDENTIFIED
8607						NOT IDENTIFIED
8703						NOT IDENTIFIED
8705	51177	5.00	7	238	gi 4503971	Rab GDP dissociation inhibitor alpha
9202	26337	4.84	27	343	gi 5174741	Ubiquitin carboxyl-terminal hydrolase isozyme
Fraction 2						
N° spot	Mr, Da	pI	N° of peptides identified	Mascot Score	NCBI Accession Number	Protein ID [Homo sapiens]
0404	28797	6.88	6	462	gi 14719797	Chain A, Solution Structure Of The Cai Michigan 1 Variant, Carbonic anhydrase
1318	25996	6.92	2	220	gi 4506181	Proteasome subunit alpha type-2
1407	28909	6.59	5	369	gi 4502517	Carbonic anhydrase 1
1408	28238	8.54	3	149	gi 12314029	Proteasome subunit, alpha type, 7
1409						NOT IDENTIFIED
1501	36631	6.91	8	340	gi 5174539	Malate dehydrogenase, cytoplasmic isoform 2
2301	26938	6.45	16	570	gi 4507645	Triosephosphate isomerase isoform 1
2406	28797	6.88	31	908	gi 14719797	Chain A, Solution Structure Of The Cai Michigan 1 Variant
	28408	6.90	31	888	gi 158428858	Chain A, X Ray Structure Of The Complex Between Carbonic Anhydrase I And The Phosphonate Antiviral Drug Foscarnet
2903	89950	5.14	3	641	gi 6005942	Transitional endoplasmic reticulum ATPase
3001	16101	7.86	55	1442	gi 71727231	Beta globin
	16163	7.05	20	570	gi 73762521	Delta-globin Troodos variant
3002	15257	8.72	6	426	gi 57013850	Hemoglobin subunit alpha
3201	22048	5.66	3	149	gi 440308	Enhancer protein
3302	21909	5.44	23	595	gi 9955007	Chain A, Thioredoxin Peroxidase B From Red Blood Cells
3308	24903	6.02	4	223	gi 31657160	Peroxiredoxin-6
3701	52928	5.93	5	749	gi 16306550	Selenium-binding protein 1
3706	59947	6.90	55	2025	gi 4557014	Catalase
3707	55454	6.30	14	520	gi 21361176	Retinal dehydrogenase 1
	52928	5.93	6	279	gi 16306550	Selenium-binding protein 1
4400	36900	5.71	14	464	gi 4557032	L-lactate dehydrogenase B chain
	36758	6.16	6	233	gi 248839	Delta-aminolevulinatase
	36950	8.44	7	219	gi 5031857	L-lactate dehydrogenase A chain isoform 1
	36630	7.08	5	204	gi 4504973	L-lactate dehydrogenase C chain
4407	36950	8.44	2	224	gi 5031857	L-lactate dehydrogenase A chain isoform 1
4501	36950	8.44	2	396	gi 5031857	L-lactate dehydrogenase A chain isoform 1
4608	52928	5.93	25	901	gi 16306550	Selenium-binding protein 1
4704	71082	5.37	10	361	gi 5729877	Heat shock cognate 71 kDa protein isoform 1
	68812	6.17	11	315	gi 14603253	Phosphoglucomutase 2
	71440	5.81	3	126	gi 34419635	Heat shock 70 kDa protein 6
4707	65089	6.27	4	649	gi 20127454	Bifunctional purine biosynthesis protein PURH
4708	55427	6.30	2	791	gi 2183299	Aldehyde dehydrogenase 1
	52928	5.93	2	248	gi 16306550	Selenium-binding protein 1
5400	28909	6.59	3	239	gi 4502517	Carbonic anhydrase 1
	32382	7.09	3	210	gi 387033	Purine nucleoside phosphorylase
5405	28909	6.59	3	387	gi 4502517	Carbonic anhydrase 1
5406	28909	6.59	6	185	gi 4502517	Carbonic anhydrase 1
	32382	7.09	2	157	gi 387033	Purine nucleoside phosphorylase
5501	52928	5.93	2	77	gi 16306550	Selenium-binding protein 1
	53155	5.87	2	54	gi 4557367	Bleomycin hydrolase

5502	22049	5.66	8	729	gi 32189392	Peroxioredoxin-2 isoform a
5802	82170	5.29	6	715	gi 7144648	Oxidized protein hydrolase
5803	66822	6.17	2	201	gi 12652891	WD repeat domain 1
5907	98652 83584	5.07 4.97	11 9	398 341	gi 83699649 gi 306891	Heat shock 90kDa protein 1, alpha 90kDa heat shock protein
6404	31956 23123	6.54 6.74	10 3	306 137	gi 33413400 gi 55960000	S-formylglutathione hydrolase Phospholysine phosphohistidine inorganic pyrophosphate phosphatase
6405	32382	7.09	3	405	gi 387033	Purine nucleoside phosphorylase
6403	32382	7.09	2	153	gi 387033	Purine nucleoside phosphorylase
6502	22049	5.66	2	529	gi 32189392	Peroxioredoxin-2 isoform a
6503	48254	6.03	10	317	gi 178277	S-adenosylhomocysteine hydrolase
6700	52928	5.93	9	480	gi 16306550	Selenium-binding protein 1
6802	7011 70792 71440	5.42 5.76 5.81	6 5 4	231 184 132	gi 386785 gi 3461866 gi 34419635	Heat shock protein Heat shock protein 70 testis variant Heat shock 70 kDa protein 6
6803	66822	6.17	7	314	gi 12652891	WD repeat domain
6903	95127	5.11	2	225	gi 38327039	Heat shock 70 kDa protein 4
7200	21909	5.44	12	119	gi 9955007	Chain A, Thioredoxin Peroxidase B From Red Blood Cells
7204	24903	6.02	3	224	gi 31657160	Peroxioredoxin-6
7205	24903	6.02	4	256	gi 31657160	Peroxioredoxin-6
7501	21909	5.44	8	120	gi 9955007	Chain A, Thioredoxin Peroxidase B From Red Blood Cells
7507	36900 36950 36758	5.71 8.44 6.16	11 6 2	314 154 137	gi 4557032 gi 5031857 gi 248839	L-lactate dehydrogenase B chain L-lactate dehydrogenase A chain isoform 1 Delta-aminolevulinate dehydratase
7508	36950	8.44	13	350	gi 5031857	L-lactate dehydrogenase A chain isoform 1
7601	41477	5.18	3	205	gi 19923193	Hsc70-interacting protein
7702	52928	5.93	7	272	gi 16306550	Selenium binding protein 1
7802	71082	5.37	7	981	gi 5729877	Heat shock cognate 71 kDa protein isoform 1
8109						NOT IDENTIFIED
8202	21909	5.44	13	374	gi 9955007	Chain A, Thioredoxin Peroxidase B From Red Blood Cells
8302	21909	5.44	2	530	gi 9955007	Chain A, Thioredoxin Peroxidase B From Red Blood Cells
8407	25848	5.54	2	68	gi 194473714	Latexin
8506	36900 36758	5.71 6.16	3 2	410 128	gi 4557032 gi 248839	L-lactate dehydrogenase B chain Delta-aminolevulinate dehydratase
8507	37037	5.89	4	338	gi 29725611	Serine/threonine-protein phosphatase 2A activator isoform b
8601	52523	5.67	2	527	gi 4504169	Glutathione synthetase
8801	69868	5.80	15	493	gi 4505029	Leukotriene A-4 hydrolase isoform 1
8802	71082 70237 71440	5.37 5.56 5.81	5 2 2	299 104 94	gi 5729877 gi 4204880 gi 34419635	Heat shock cognate 71 kDa protein isoform 1 Heat shock protein Heat shock 70 kDa protein 6
8803						NOT IDENTIFIED
Fraction 3						
N° spot	Mr, Da	pI	N° of peptides identified	Mascot Score	NCBI Accession Number	Protein ID [Homo sapiens]
2401	26894	7.10	8	570	gi 136066	Triosephosphate isomerase
2508	28408	6.90	13	578	gi 158428858	Chain A, X Ray Structure Of The Complex Between Carbonic Anhydrase I And The Phosphonate Antiviral Drug Foscarnet
3101	16102	6.75	16	741	gi 4504349	Hemoglobin subunit beta
3300	23053	8.66	2	145	gi 558526	Proteasome subunit X
3303						NOT IDENTIFIED

3307	25996	6.92	2	166	gi 4506181	Proteasome subunit alpha-type 2
3501	20238	8.54	2	193	gi 12314029	Proteasome subunit alpha-type 7
3601	29822	6.15	3	216	gi 4506179	Proteasome subunit alpha type-1 isoform 2
3600						NOT IDENTIFIED
3608	28797	6.88	6	534	gi 14719797	Chain A, Solution Structure Of The Cai Michigan 1 Variant; carbonic anhydrase
4405	36631	6.91	2	158	gi 5174539	Malate dehydrogenase, cytoplasmic isoform 2
4701	52928	5.93	3	482	gi 16306550	Selenium binding protein 1
4702	53155	5.87	2	91	gi 4557367	Bleomycin hydrolase
4801	59947	6.90	6	765	gi 4557014	Catalase
4903	89950	5.14	4	454	gi 6005942	Transitional endoplasmic reticulum ATPase
5600						NOT IDENTIFIED
5602	36709	6.73	2	147	gi 229620	Dehydrogenase H4,lactate
5908	82210	5.29	6	559	gi 556514	Acylamino acid-releasing enzyme
5909						NOT IDENTIFIED
6301	21909	5.44	4	609	gi 9955007	Chain A, Thioredoxin Peroxidase B From Red Blood Cells
6500						NOT IDENTIFIED
6604	52928	5.93	2	135	gi 16306550	Selenium binding protein 1
6701	21909	5.44	3	434	gi 9955007	Chain A, Thioredoxin Peroxidase B From Red Blood Cells
6702	21909	5.44	2	61	gi 9955007	Chain A, Thioredoxin Peroxidase B From Red Blood Cells
6703	52523	5.67	2	81	gi 4504169	Glutathione synthetase
6805	71082	5.37	3	979	gi 5729877	Heat shock cognate 71 kDa protein isoform 1
6806						NOT IDENTIFIED
6807						NOT IDENTIFIED
7201	21909	5.44	3	367	gi 9955007	Chain A, Thioredoxin Peroxidase B From Red Blood Cells
7301	21909	5.44	3	245	gi 9955007	Chain A, Thioredoxin Peroxidase B From Red Blood Cells
7605	36900	5.71	3	367	gi 4557032	L-lactate dehydrogenase B chain
9401						NOT IDENTIFIED
9402	29326	4.63	2	335	gi 5803225	14-3-3 protein epsilon
9801	79600	4.96	4	267	gi 375331941	Dipeptidyl peptidase 3 isoform 2

Table 2– Multiprotein complexes identified in each Fraction
Fraction 1

Multiprotein complex	Protein subunit		Spot number	MW (KDa)	Subunit structure	
	Band number	MW (KDa)				
Prdx2 homocomplex	1	~ 440	Peroxiredoxin-2	0106	21.8	Dimer of decamers
CUL-CAND1 heterocomplex	2	313	Cullin	1809	87.5	Dimer
			Cullin-associated NEDD8-dissociated protein 1	1905	138	
ALAD homocomplex	3	290	Delta-aminolevulinate dehydratase	1403	36.3	Octamer (4 dimers)
ALAD-HSPA8 heterocomplex	4	287	Delta-aminolevulinate dehydratase	1403	36.3	Homohexamer (3 dimers)
			Heat shock 70 KDa protein 8	1810	70	
APEH homo complex	5	324	Acylamino-acid-releasing enzyme	1813	81	Tetramer
ALDH1-HSPA8 heterocomplex	6	289	Aldehyde dehydrogenase 1	1604	54.8	Homotetramer
			Heat shock 70 KDa protein 8	2801	70	Monomer
HSP90AA1-HSPA8	6a	289	Heat shock 70 KDa protein 8	2801	70.8	Homodimer
			Heat shock 70kDa protein 8 isoform 1 variant	2804	68.3	Homodimer
AHCY homocomplex	7	178	HSP90AA1 protein	2506	44.6	Tetramer

NDPKA-PNP heterocomplex	8	155	Adenosylhomocysteinas e isoform 2	3102	19.6	Homotrimer
			Nucleoside diphosphate kinase A isoform a	3301	32.3	Homotrimer
ESD-GOT1 heterocomplex	9a	160	Purine nucleoside phosphorylase	3303	34	Heterotetramer of homodimers
				3513	46.4	
HIP homocomplex	9b	160	Esterase D Aspartate aminotransferase. cytoplasmic	3603	41.4	Homotetramer
				3702	70	
PNP-HSPA8 heterocomplex	10	166	Hsc 70-interacting protein	3304	32.3	Homotrimer
			HSP70 1	3801	70	Monomer
LDHB homocomplex	11	147	Purine nucleoside phosphorylase	3404	36.9	Tetramer
LDHB-TALDO heterocomplex	11b	147	Heat shock 70 KDa protein 8	3404	36.9	Homodimer
				3404	37.7	Homodimer
ESD-HSPA8 heterocomplex	12	138	Lactate dehydrogenase B chain	3306	34	Homodimer
			Lactate dehydrogenase B Transaldolase	3804	70	Monomer
PNP-HSPA8 heterocomplex	13	134	Esterase D Heat shock 70 KDa protein 8	3305	32.3	Homodimer
				3804	70	Monomer
Prdx2-ALDR1 heterocomplex	14	139	Purine nucleoside phosphorylase	4102	21.8	Homotrimer
			Heat shock 70 KDa	4506	36.8	Homodimer

			protein 8			
	15	122		4603	52.3	
GSS-HSPA8 heterocomplex			Peroxiredoxin-2	4804	70	Monomer
			Alcohol dehydrogenase NADP+			Monomer
	16	119		5301	29.9	
BPGM homocomplex			Glutathione synthetase			Tetramer
			Heat shock 70 KDa			(2 dimers)
	17	110	protein 8	4204	22	
FLR-Prxd2 heterocomplex				5209	21.8	Monomer
			Bisphosphoglycerate mutase			Homotetramer
	17b	110		5302	27.5	
GSS-GSTO heterocomplex			Flavin reductase			Homodimer
			NADPH			Monomer
	18	112	Peroxiredoxin-2	5704	56.4	
USP14-NEDD8 heterocomplex						Heterodimer
			Glutathione S-transferase omega-1 isoform 1	5704	60.6	
			Glutathione synthetase			
	19	109	Ubiquitin-carboxyl terminal hydrolase 14	5603	54.5	
PEPD homocomplex			isoform a	6102/6103	16	Dimer
			NEDD8-activating enzyme E1 regulatory	6402	37.6	Homodimer
			subunit isoform a			Homodimer
SOD1-TALDO1 heterocomplex	19c	≈110		5504	37	
			Human prolidase			Trimer
PP2A homocomplex	19d	≈110	Cu/Zn SOD Transaldolase	6603	37.9	
						Trimer
	19e	≈110	Serine/threonine-protein phosphatase 2A activator	5401	36.9	
HMBS homocomplex			isoform b	5602	52.5	Homodimer
						Monomer

LDHB-GSS heterocomplex	20a	95	Hydroxymethylbilane synthase	6601	47.5	Homodimer
	21	83		6102/6103	16	
ENO2 homocomplex			L-lactate dehydrogenase B	6606	51.7	Homodimer
	22	58		8203	29	Monomer
SOD1-RNH1 heterocomplex			Glutathione synthetase	8304	29	Homodimer
				8305		Heterodimer
14-3-3 protein homocomplex/heterocomplex	23	54	Gamma enolase			
			Cu/Zn SOD	8306	27	
			Ribonuclease inhibitor			Dimer
CLIC homocomplex			14-3-3 protein epsilon			
			14-3-3 protein epsilon			
			14-3-3 protein gamma/sigma/theta			
			Chloride ion channel intracellular			

References

- Agarwal DP, Cohn P, Goedde HW, Hempel J. Aldehyde dehydrogenase from human erythrocytes: structural relationship to the liver cytosolic isozyme. *Enzyme*. 1989;42(1):47-52.
- Alvarez-Llamas G, de la Cuesta F, Barderas MG, et al. A novel methodology for the analysis of membrane and cytosolic sub-proteomes of erythrocytes by 2-DE. *Electrophoresis*. 2009;30(23):4095-4108.
- Bachi A, Simó C, Restuccia U, Guerrier L, Fortis F, Boschetti E, Masseroli M, Righetti PG. Performance of combinatorial peptide libraries in capturing the low-abundance proteome of red blood cells. 2. Behavior of resins containing individual amino acids. *Anal Chem*. 2008 May 15;80(10):3557-65.
- Baldwin MA. Protein identification by mass spectrometry: issues to be considered. *Mol Cell Proteomics*. 2004;3(1):1-9.
- Bhattacharya D, Mukhopadhyay D, Chakrabarti A. Hemoglobin depletion from red blood cell cytosol reveals new proteins in 2-D gel-based proteomics study. *Proteomics Clin Appl*. 2007;1(6):561-564.
- Bianchi P, Fermo E, Vercellati C, Boschetti C, Barcellini W, Iurlo A, Marcello AP, Righetti PG, Zanella A. Congenital dyserythropoietic anemia type II (CDAII) is caused by mutations in the SEC23B gene. *Hum Mutat*. 2009;30(9):1292-8.
- Boguski M, Chakravarti A, Gibbs R, Green E, Myers RM. The end of the beginning: the race to begin human genome sequencing. *Genome Res*. 1996;6(9):771-2.
- Boschetti E, Righetti PG. The art of observing rare protein species in proteomes with peptide ligand libraries. *Proteomics*. 2009; 9:1492-510.
- Boschetti E, Righetti PG. The ProteoMiner in the proteomic arena: a non-depleting tool for discovering low-abundance species. *J Proteomics*. 2008;71(3):255-264.
- Bosman GJ, Lasonder E, Groenen-Döpp YA, et al. Comparative proteomics of erythrocyte aging in vivo and in vitro. *J Proteomics*. 2010;73(3):396-402.
- Bosman GJ, Lasonder E, Luten M, et al. The proteome of red cell membranes and vesicles during storage in blood bank conditions. *Transfusion* 2008;48(5):827-835.
- Bosman GJ, Lasonder E, Luten M, Roerdinkholder-Stoelwinder B, Novotný VM, Bos H, De Grip WJ. The proteome of red cell membranes and vesicles during storage in blood bank conditions. *Transfusion* 2008; 48: 827-835.
- Bosu DR, Kipreos ET. Cullin-RING ubiquitin ligases: global regulation and activation cycles. *Cell Div*. 2008;3:7.
- Bruce LJ, Beckmann R, Ribeiro ML, et al. A band 3-based macrocomplex of integral and peripheral proteins in the RBC membrane. *Blood*. 2003;101(10):4180-4188.
- Bruschi M, Seppi C, Arena S, Musante L, Santucci L, Balduini C, Scaloni A, Lanciotti M, Righetti PG, Candiano G. Proteomic analysis of erythrocyte membranes by soft Immobiline gels combined with differential protein extraction. *J Proteome Res*. 2005; 4:1304-1309.
- Capra F. *The web of life: A New Scientific Understanding of Living Systems*. Anchor Books, Doubleday, New York, 1996.

- Civenni G, Test ST, Brodbeck U, Butikofer P. In vitro incorporation of GPI-anchored proteins into human erythrocytes and their fate in the membrane. *Blood* 1998; 91: 1784-1792.
- D'Alessandro A, D'Amici GM, Vaglio S, Zolla L. Time-course Investigation of SAGM-Stored Erythrocyte Concentrates: from Metabolism to Proteomics. *Hematologica* 2012; 97(1):107-115.
- D'Amici GM, Rinalducci S, Zolla L. Proteomic analysis of RBC membrane protein degradation during blood storage. *J Proteome Res.* 2007; 6: 3242–3255.
- D'Alessandro A, Blasi B, D'amici GM, Marrocco C, Zolla L. Red blood cell subpopulations in freshly drawn blood: application of proteomics and metabolomics to a decades-long biological issue. *Blood Transfus.* 2012; doi:10.2450/2012.0164-11.
- D'Alessandro A, Righetti PG, Zolla L. The red blood cell proteome and interactome: an update. *J Proteome Res.* 2010;9(1):144-163.
- D'Alessandro A, Zolla L. The SODyssey: superoxide dismutases from biochemistry, through proteomics, to oxidative stress, aging and nutraceuticals. *Expert Rev Proteomics.* 2011;8(3):405-421.
- D'Amici GM, Rinalducci S, Zolla L. An easy preparative gel electrophoretic method for targeted depletion of hemoglobin in erythrocyte cytosolic samples. *Electrophoresis.* 2011;32(11):1319-1322.
- D'Amici GM, Rinalducci S, Zolla L. Depletion of hemoglobin and carbonic anhydrase from erythrocyte cytosolic samples by preparative clear native electrophoresis. *Nat Protoc.* 2011;7(1):36-44.
- Dawkins R. The Selfish Gene.* Oxford: Oxford University Press, 1976.
- Denecke J, Kranz C, Nimtz M, Conradt HS, Brune T, Heimpel H, Marquardt T. Characterization of the N-glycosylation phenotype of erythrocyte membrane proteins in congenital dyserythropoietic anemia type II (CDA II/HEMPAS). *Glycoconj J.* 2008; 25: 375–382.
- Denecke J, Marquardt T. Congenital dyserythropoietic anemia type II (CDAII/ HEMPAS): Where are we now? *Biochim Biophys Acta.* 2008 [<http://dx.doi.org/10.1016/j.bbadis.2008.12.005>]
- Dumont LJ, Yoshida T, AuBuchon JP. Anaerobic storage of red blood cells in a novel additive solution improves in vivo recovery. *Transfusion* 2009; 49:458-464.
- Fothergill-Gilmore LA, Watson HC. The phosphoglycerate mutases. *Adv Enzymol Relat Areas Mol Biol.* 1989;62:227-313.
- Galtieri A, Tellone E, Romano L, et al. Band-3 protein function in human erythrocytes: effect of oxygenation-deoxygenation. *Biochim Biophys Acta.* 2002;1564(1):214-218.
- Geng Q, Romero J, Saini V, Patel MB, Majetschak M. Extracellular 20S proteasomes accumulate in packed red blood cell units. *Vox Sang.* 2009;97(3):273-274.
- Goodman SR, Kurdia A, Ammann L, Kakhniashvili D, Daescu O. The human red blood cell proteome and interactome. *Exp Biol Med (Maywood).* 2007;232(11):1391-1408.
- Goodman SR, Kurdia A, Ammann L, Kakhniashvili D, Daescu O. The human red blood cell proteome and interactome. *Exp Biol Med (Maywood)* 2007; 232:1391–408.
- Griffiths WJ, Wang Y. Mass spectrometry: from proteomics to metabolomics and lipidomics. *Chem Soc Rev.* 2009; 38: 1882-1896.

- Haudek VJ, Slany A, Gundacker NC, Wimmer H, Drach J, Gerner, C. Proteome maps of the main human peripheral blood constituents. *J Proteome Res.* 2009; 8:3834-3843.
- Holmes RS, Goldberg E. Computational analyses of mammalian lactate dehydrogenases: human, mouse, opossum and platypus LDHs. *Comput Biol Chem.* 2009;33(5):379-385.
- Ingenuity Pathway Analysis (Ingenuity® Systems, www.ingenuity.com).
- Kakhniashvili DG, Bulla Jr LA, Goodman S.R. The human erythrocyte proteome: analysis by ion trap mass spectrometry. *Mol Cell Proteomics* 2004; 3:501–509.
- Kandpal R, Saviola B, Felton J. The era of 'omics unlimited. *Biotechniques.* 2009; 46: 351-355.
- Koch CG, Li L, Sessler DI, Figueroa P, Hoeltge GA, Mihaljevic T, Blackstone EH. Duration of red-cell storage and complications after cardiac surgery. *N Engl J Med.* 2008; 358: 1229-1239.
- Kooyman DL, Byrne GW, McClellan S, Nielsen D, Tone M, Waldmann H, Coffman TM, McCurry KR, Platt JL, Logan JS. In vivo transfer of GPI-linked complement restriction factors from erythrocytes to the endothelium. *Science* 1995; 269: 89-92.
- Koury MJ, Sawyer ST, Brandt SJ. New insights into erythropoiesis. *Curr Opin Hematol.* 2002; 9: 93-100.
- Lang F, Lang KS, Lang PA, Huber SM, Wieder T. Mechanisms and significance of eryptosis. *Antioxidants and Redox Signaling* 2006; 8: 1183-1192.
- Lanneau D, de Thonel A, Maurel S, Didelot C, Garrido C. Apoptosis versus cell differentiation: role of heat shock proteins HSP90, HSP70 and HSP27. *Prion.* 2007; 1: 53-60.
- Li S, Peterson NA, Kim MY, et al. Crystal Structure of AhpE from *Mycobacterium tuberculosis*, a 1-Cys peroxiredoxin. *J Mol Biol.* 2005;346(4):1035-1046.
- Liang S, Yu Y, Yang P, et al. Analysis of the protein complex associated with 14-3-3 epsilon by a deuterated-leucine labeling quantitative proteomics strategy. *J Chromatogr B Analyt Technol Biomed Life Sci.* 2009;877(7):627-634.
- Lin Z, Konno M, Abad-Zapatero C, et al. The structure of rabbit muscle phosphoglucomutase at intermediate resolution. *J Biol Chem.* 1986;261(1):264-274.
- Liu N, Chao S, Tsay Y. Human Plasma Protein PTMome Project and Biomarker Discovery. *J Proteom Bioinf.* 2008; 2: 195.
- Liumbruno G, D'Alessandro A, Grazzini G, Zolla L. Blood-related proteomics. *J Proteomics.* 2010;73(3):483-507.
- Liumbruno G, D'Alessandro A, Grazzini G, Zolla L. Blood-related proteomics. *J Proteomics.* 2009; [doi:10.1016/j.jprot.2009.06.010](https://doi.org/10.1016/j.jprot.2009.06.010)
- Low FM, Hampton MB, Winterbourn CC. Peroxiredoxin 2 and peroxide metabolism in the erythrocyte, *Antioxid. Redox Signal.* 2008; 10:1621e1629.
- Low PS. Structure and function of the cytoplasmic domain of band 3: center of erythrocyte membrane-peripheral protein interactions. *Biochim Biophys Acta.* 1986;864(2):145-167.
- Low TY, Seow TK, Chung MC. Separation of human erythrocyte membrane associated proteins with one-dimensional and two-dimensional gel electrophoresis followed by identification with matrix-assisted laser desorption/ionization-time of flight mass spectrometry. *Proteomics* 2002;2:1229–1239.

- Low TY, Seow TK, Chung MC. Separation of human erythrocyte membrane associated proteins with one-dimensional and two-dimensional gel electrophoresis followed by identification with matrix-assisted laser desorption/ionization-time of flight mass spectrometry. *Proteomics* 2002; 2: 1229–1239.
- Makita T, Hernandez-Hoyos G, Chen TH, Wu H, Rothenberg EV, Sucov HM. A developmental transition in definitive erythropoiesis: erythropoietin expression is sequentially regulated by retinoic acid receptors and HNF4. *Genes Dev.* 2001; 15: 889-901.
- Nakagawa T, Onoda S, Kanemori M, Sasayama Y, Fukumori Y. Purification, characterization and sequence analyses of the extracellular giant hemoglobin from *Oligobranchia mashikoi*. *Zoolog Sci.* 2005;22(3):283-291.
- Neelam S, Kakhniashvili DG, Wilkens S, Levene SD, Goodman SR. Functional 20S proteasomes in mature human red blood cells. *Exp Biol Med (Maywood).* 2011;236(5):580-591.
- Olivieri E, Herbert B, Righetti PG. The effect of protease inhibitors on the two-dimensional electrophoresis pattern of red blood cell membranes. *Electrophoresis* 2001;22(3):560-5.
- Page MJ, Griffiths TAM, Bleackley MR, MacGillivray RTA. Proteomics: applications relevant to transfusion medicine. *Transfus Med Rev.* 2006; 20: 63–74.
- Palis J. Ontogeny of erythropoiesis. *Curr Opin Hematol.* 2008; 15: 155-161.
- Pasini EM, Kirkegaard M, Mortensen P, et al. In-depth analysis of the membrane and cytosolic proteome of red blood cells. *Blood.* 2006;108(3):791-801.
- Pasini EM, Kirkegaard M, Mortensen P, Lutz HU, Thomas AW, Mann M. In-depth analysis of the membrane and cytosolic proteome of red blood cells. *Blood* 2006; 108: 791–801.
- Prabakaran S, Wengenroth M, Lockstone HE, Lilley K, Leweke FM, Bahn S. 2-D DIGE analysis of liver and red blood cells provides further evidence for oxidative stress in schizophrenia. *J Proteome Res.* 2007; 6: 141-149.
- Rappsilber J, Siniosoglou S, Hurt EC, Mann M. A generic strategy to analyze the spatial organization of MPCs by cross-linking and mass spectrometry. *Anal Chem.* 2000;72(2):267-275.
- Rhoda MD, Blouquit Y, Caburi-Martin J, et al. Effects of the alpha 20 mutation on the polymerization of Hb S. *Biochim Biophys Acta.* 1984;786(1-2):62-66.
- Righetti PG, Boschetti E. The ProteoMiner and the FortyNiners: searching for gold nuggets in the proteomic arena. *Mass Spectrom Rev.* 2008; 27: 596-608.
- Rinalducci S, D'Amici GM, Blasi B, Zolla L. Oxidative stress-dependent oligomeric status of erythrocyte peroxiredoxin II (PrxII) during storage under standard blood banking conditions. *Biochimie.* 2011;93(5):845-853.
- Ringrose JH, van Solinge WW, Mohammed S, et al. Highly efficient depletion strategy for the two most abundant erythrocyte soluble proteins improves proteome coverage dramatically. *J Proteome Res.* 2008;7(7):3060-3063.
- Rosenblum BB, Hanash SM, Yew N, Neel JV. Two-dimensional electrophoretic analysis of erythrocyte membranes. *Clin Chem.* 1982; 28: 925-931.
- Rosenblum BB, Hanash SM, Yew N, Neel JV. Two dimensional electrophoretic analysis of erythrocyte membranes. *Clin Chem.* 1982; 28:925–931.

- Roux-Dalvai F, Gonzalez de Peredo A, Simó C, et al. Extensive analysis of the cytoplasmic proteome of human erythrocytes using the peptide ligand library technology and advanced mass spectrometry. *Mol Cell Proteomics*. 2008;7(11):2254-2269.
- Roux-Dalvai F, Gonzalez de Peredo A, Simó C, Guerrier L, Bouyssié D, Zanella A, Citterio A, Bulet-Schiltz O, Boschetti E, Righetti PG, Monsarrat B. Extensive analysis of the cytoplasmic proteome of human erythrocytes using the peptide ligand library technology and advanced mass spectrometry. *Mol Cell Proteomics* 2008; 7: 2254-2269.
- Scaloni A, Jones WM, Barra D, Pospischil M, Sassa S, et al. Acylpeptide hydrolase: inhibitors and some active site residues of the human enzyme. *J Biol Chem*. 1992;267:3811–3818.
- Schägger H, von Jagow G. Blue native electrophoresis for isolation of membrane protein complexes in enzymatically active form. *Anal Biochem*. 1991;199(2):223-231.
- Scheel J, Von Brevern MC, Hörlein A, Fischer A, Schneider A, Bachi A. Yellow pages to the transcriptome. *Pharmacogenomics*. 2002; 3: 791-807.
- Schifferli JA, Taylor RP. Physiological and pathological aspects of circulating immune complexes. *Kidney Int*. 1989; 35: 993-1003.
- Seo J, Lee KJ. Post-translational modifications and their biological functions: proteomic analysis and systematic approaches. *J Biochem Mol Biol*. 2004;37(1):35-44.
- Shevchenko A, Wilm M, Vorm O, Mann M. Mass spectrometric sequencing of proteins from silver-stained polyacrylamide gels. *Anal Chem*. 1996;68:850–858.
- Shichishima T, Terasawa T, Hashimoto C, Ohto H, Takahashi M, Shibata A, Maruyama Y. Discordant and heterogeneous expression of GPI-anchored membrane proteins on leukemic cells in a patient with paroxysmal nocturnal hemoglobinuria. *Blood* 1993; 81: 1855-1862.
- Siciliano A, Turrini F, Bertoldi M, et al. Deoxygenation affects tyrosine phosphoproteome of red cell membrane from patients with sickle cell disease. *Blood Cells Mol Dis*. 2010;44(4):233-242.
- Silverman DN, Backman L, Tu C. Role of hemoglobin in proton transfer to the active site of carbonic anhydrase. *J Biol Chem*. 1979;254(8):2588-2591.
- Simó C, Bachi A, Cattaneo A, Guerrier L, Fortis F, Boschetti E, Podtelejnikov A, Righetti PG. Performance of combinatorial peptide libraries in capturing the low-abundance proteome of red blood cells. 1. Behavior of mono- to hexapeptides. *Anal Chem*. 2008 May 15;80(10):3547-56.
- Simó C, Bachi A, Cattaneo A, Guerrier L, Fortis F, Boschetti E, Podtelejnikov A, Righetti PG. Performance of combinatorial peptide libraries in capturing the low-abundance proteome of red blood cells. 1. Behavior of mono- to hexapeptides. *Anal Chem*. 2008; 80: 3547-3565.
- Slavens KD, Brown TR, Barakat KA, Cundari TR, Anderson ME. Valine 44 and valine 45 of human glutathione synthetase are key for subunit stability and negative cooperativity. *Biochem Biophys Res Commun*. 2011;410(3):597-601.
- Stein LD. Human genome: end of the beginning. *Nature* 2004; 431: 915-916.

- Suckau D, Resemann A, Schuerenberg M, et al. A novel MALDI LIFT-TOF/TOF mass spectrometer for proteomics. *Anal Bioanal Chem.* 2003;376: 952–965.
- Svensson AK, Bilsel O, Kayatekin C, et al. Metal-free ALS variants of dimeric human Cu,Zn-superoxide dismutase have enhanced populations of monomeric species. *PLoS One.* 2010;5(4):e10064.
- Timperio AM, D'Alessandro A, Pariset L, D'Amici GM, Valentini A, Zolla, L. Comparative proteomics and transcriptomics analyses of livers from two different *Bos taurus* breeds: "Chianina and Holstein Friesian". *J Proteomics* 2009 [doi:10.1016/j.jprot.2009.09.015](https://doi.org/10.1016/j.jprot.2009.09.015)
- Truant R, Atwal R, Burtnik A. Hypothesis: Huntingtin may function in membrane association and vesicular trafficking. *Biochem Cell Biol.* 2006; 84: 912-917.
- Tyan, Y.C.; Jong, S.B.; Liao, J.D.; Liao, P.C.; Yang, M.H.; Liu, C.Y.; Klauser, R.; Himmelhaus, M.; Grunze, M. Proteomic profiling of erythrocyte proteins by proteolytic digestion chip and identification using two-dimensional electrospray ionization tandem mass spectrometry. *J Proteome Res.* 2005, 4, 748–757.
- van Gestel RA, van Solinge WW, van der Toorn HW, et al. Quantitative erythrocyte membrane proteome analysis with Blue-native/SDS PAGE. *J Proteomics.* 2010;73(3):456-465.
- Walpurgis K, Kohler M, Thomas A, et al. Validated hemoglobin-depletion approach for red blood cell lysate proteome analysis by means of 2D PAGE and Orbitrap MS. *Electrophoresis.* 2012; 33(16):2537-2545.
- Wang X, Chen G, Liu H, Zhao Z, Li Z. Four-dimensional orthogonal electrophoresis system for screening protein complexes and protein-protein interactions combined with mass spectrometry. *J Proteome Res.* 2010;9(10):5325-34.
- Wasinger VC, Cordwell SJ, Cerpa-Poljak A, Yan JX, Gooley AA, Wilkins MR, Duncan MW, Harris R, Williams, KL, Humphery-Smith I. Progress with gene-product mapping of the Mollicutes: *Mycoplasma genitalium*. *Electrophoresis* 1995; 16: 1090–1094.
- Willekens FLA, Were JM, Groenen-Dopp YAM, Roerdinkholder-Stoelwinder B, De Pauw B, Bosman GJCGM. Erythrocyte vesiculation: A selfprotective mechanism? *Brit J Haematol.* 2008; 141: 549-556.
- Wittig I, Karas M, Schägger H. High resolution clear native electrophoresis for in-gel functional assays and fluorescence studies of membrane protein complexes. *Mol Cell Proteomics.* 2007;6(7):1215-1225.
- Wognum S, Lagoa CE, Nagatomi J, Sacks MS, Vodovotz Y. An exploratory pathways analysis of temporal changes induced by spinal cord injury in the rat bladder wall: insights on remodeling and inflammation. *PLoS One.* 2009; 4: e5852.
- Yoshida T, AuBuchon JP, Dumont LJ, Gorham JD, Gifford SC, Foster KY, Bitensky MW. The effects of additive solution pH and metabolic rejuvenation on anaerobic storage of red cells. *Transfusion* 2008; 48: 2096-2105.
- Yoshida T, AuBuchon JP, Tryzelaar L, Foster KY, Bitensky MW. Extended storage of red blood cells under anaerobic conditions. *Vox Sang.* 2007; 92: 22-31.
- Zhuang WJ, Fong CC, Cao J, Ao L, Leung CH, Cheung HY, Xiao PG, Fong WF, Yang MS. Involvement of NF-kappaB and c-myc signaling pathways in the apoptosis of HL-60 cells induced by alkaloids of *Tripterygium hypoglaucom* (levl.) Hutch. *Phytomedicine.* 2004; 11: 295-302.

Chapter 3: Set up of the metabolomics methods

Contents

-
- 3.1 A robust high resolution reversed-phase HPLC strategy to investigate various metabolic species in different biological models.
 - 3.2 Targeted mass spectrometry-based metabolomic profiling through Multiple Reaction Monitoring of Liver and other biological matrices.
-

The contents of this chapter report the contents of the the following publications by the candidate:

1. D'Alessandro A, Gevi F, Zolla L.
A robust high resolution reversed-phase HPLC strategy to investigate various metabolic species in different biological models.
Mol Biosyst. 2011; 7(4):1024-32.
 2. D'Alessandro A, Gevi F, Zolla L.
Targeted mass spectrometry-based metabolomic profiling through Multiple Reaction Monitoring of Liver and other biological matrices.
Methods Mol Biol. 2012; In *Liver Proteomics. In Methods and Protocols Series: Methods in Molecular Biology.* 2012; vol. 909. Josic, Djuro; Hixson, Douglas C. (Eds.)
-

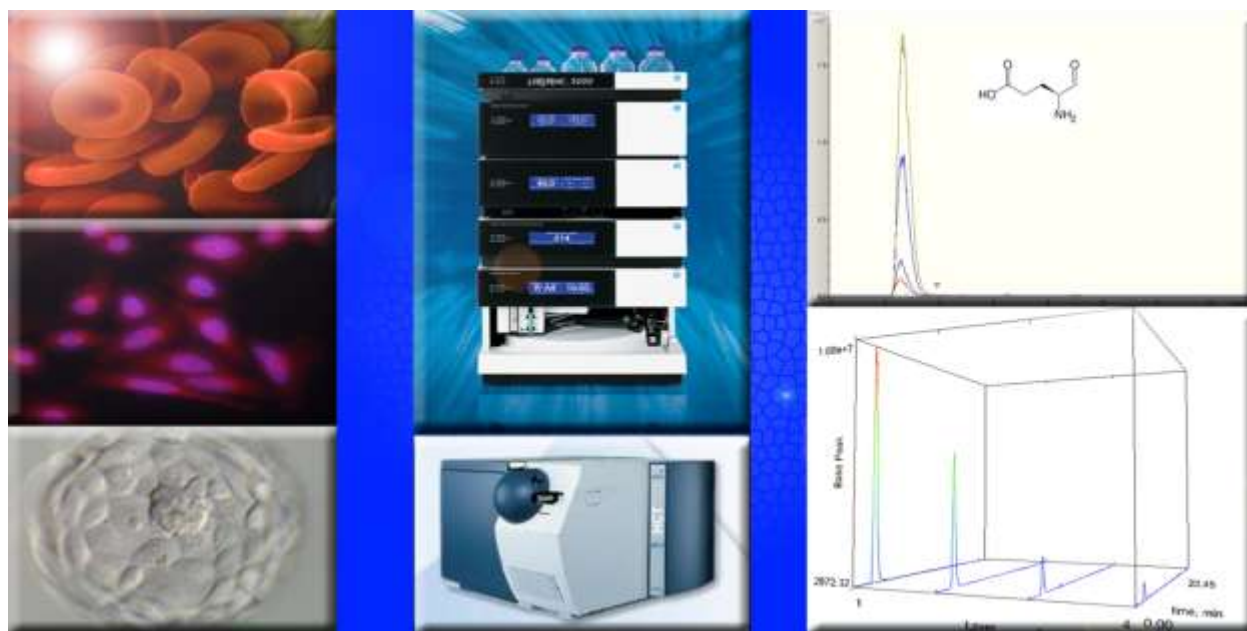
In order to achieve a metabolomics-wide overview of red blood cell ageing *in vivo* and *in vitro*, we firstly set up the analytical strategy by targeting a subset of metabolites of specific pathways (such as glycolysis) through multiple reaction monitoring (MRM) and optimizing technical reproducibility (intra-day and inter-day) and determining linearity range, limits of detection and quantification.

3.1 A robust high resolution reversed-phase HPLC strategy to investigate various metabolic species in different biological models

Overview of this section

Recent advancements in the field of omics sciences have paved the way for further expansion of metabolomics. Originally tied to NMR spectroscopy, metabolomic disciplines are constantly and growingly involving HPLC and mass spectrometry (MS)-based analytical strategies and, in this context, we hereby propose a robust and efficient extraction protocol for metabolites from four different biological sources which are subsequently analysed, identified and quantified through high resolution reversed-phase fast HPLC and mass spectrometry. To this end, we demonstrate the elevated intra- and inter-day technical reproducibility, ease of an MRM-based MS method, allowing simultaneous detection of up to 10 distinct features, and robustness of multiple metabolite detection and quantification in four different biological samples. This strategy might become routinely applicable to various samples/biological matrices, especially for low-availability ones. In parallel, we compare the present strategy for targeted detection of a representative metabolite, L-glutamic acid, with our previously-proposed chemical-derivatization through dansyl chloride. A direct comparison of the present method against spectrophotometric assays is proposed as well. An application of the proposed method is also introduced, using the SAOS-2 cell line, either induced or non-induced to express the TAp63 isoform of the p63 gene, as a model for determination of variations of glutamate concentrations.

Keywords: metabolomics; mass spectrometry; multiple reaction monitoring; red blood cells.



Introduction

In the complex scenario of the “omics” sciences -genomics, proteomics and interactomics- metabolomics plays a fundamental and complementary role in that it aims at delivering qualitative and quantitative profiles of small molecules of biological relevance in the low molecular weight range (molecular weight less than 1500 Daltons) (Griffiths et al., 2010). While nuclear magnetic resonance (NMR) spectroscopy has represented the eligible tool to delve into metabolite complexity in the earliest phases of the metabolomic era, dating back to the 1960s (Griffiths et al., 2010), mass spectrometry (MS)-based techniques are growingly but constantly gaining momentum. Several reasons lie at the basis of this exploit, among which are the higher sensitivity, improved metabolite discrimination, coverage of the metabolome space, and modularity to perform compound-class-specific analyses (Griffiths et al., 2010).

MS-based metabolomics could be either non-targeted, for comprehensive exploratory analyses of all the metabolites in a given sample, or targeted, when predefined metabolite-specific signals m/z of metabolites of interest are isolated and monitored with selected reaction monitoring (SRM; or multiple reaction monitoring -MRM). In the latter case, it is implicit that only limited number of known and expected endogenous metabolites could be investigated, although it is possible to precisely and accurately determine their relative abundances and concentrations. In the last few years, the greatest efforts have been put forward to constantly enlarge the list of metabolite entries for targeted MS purposes. However, most of the proposed methods pursued the quantitation of a broader number of species and the simplicity of the method (Buescher et al., 2010), while only a few prompted considerations on the robustness of the metabolite extraction and MS strategies (Zelena et al., 2009), that is to say, their applicability in most various biological systems without any significant adjustment of the instrumental settings and analytical conditions.

To overcome these hurdles, most laboratories have so far addressed only specific metabolites (Timperio et al., 2007) or metabolite classes (Wamelink et al., 2005). This is mainly due to the fact that certain metabolites have been long tied to relevant biological functions and have thus attracted the most of attention, as in the case of glutamate in neural cells (Timperio et al., 2007). In this very case, the sample processing procedure included liquid-liquid extraction, derivatization with dansyl chloride and a final cation-exchange extraction to generate spectrophotometric absorbance in the UV/visible-range and clean extracts for LC/MS/MS analysis (Timperio et al., 2007). While enhancing the MS signal, thus allowing direct quantification of glutamate, this procedure has some detrimental pitfalls in the reliability of the absolute quantification, in that the extraction procedure is followed by another step of

purification upon derivatization with dansyl-chloride, which add two further variables to the extraction efficiency (Timperio et al., 2007).

Basing on these considerations, we hereby present a robust, rapid and simple targeted metabolomic method, which exploits High Resolution reversed-phase fast (RR-RP-HPLC)/ESI-MS, for MRM-based quantitation of glutamate, without any need for chemically-enhanced derivatization steps. Besides, we optimize a straightforward extraction protocol and test this RR-RP-HPLC/ESI-MS analytical strategy to determine and quantify a list of pivotal compounds from the main metabolic pathways (glycolysis, Krebs's cycle, pentose phosphate pathway). To test the validity of the extraction and quantitation methods, we performed multiple analyses on four different biological samples. Considerations on the reproducibility, linearity and robustness of the analyses are discussed as well.

Materials and Methods

Acetonitrile, formic acid, and HPLC-grade water, purchased from Sigma Aldrich (Milano, Italy).

Standards (equal or greater than 98% chemical purity) ATP, L-lactic acid, phosphogluconic acid, NADH, D-fructose 1,6 biphosphate, D-fructose 6-phosphate, glyceraldehyde phosphate, phosphoenolpyruvic acid, L-malic acid, L-glutamic acid, oxidized glutathione, α -ketoglutarate were purchased from Sigma Aldrich (Milan).

Standards were stored either at -25°C , 4°C or room temperature, *following manufacturer's instructions*.

Each standard compound was weighted and dissolved in nanopure water. Starting at a concentration of 1 mg/ml of the original standard solution, a dilution series of steps (in 18 M Ω , 5% formic acid) was performed for each of the standards in order to reach the limit of detection (LOD) and limit of quantification (LOQ).

Sample preparation

Red blood cells

RBC units were drawn from healthy human volunteers according to the policy of the Italian Blood Transfusion Service for donated blood and all the volunteers provided their informed consent in accordance with the declaration of Helsinki. . We studied RBC units collected from 4 donors [male=2, female=2, age 48 ± 11.5 (mean \pm S.D.)] in the middle region of Italy. RBC units were stored for 42 days under standard conditions (CDP-SAGM, 4°) and samples were removed aseptically for the analysis at day 1 of storage. For each sample, 0.5mL from the pooled erythrocyte stock was transferred into a microcentrifuge tube and processed for metabolite extraction. Erythrocyte samples were then centrifuged at 1000g for 2 minutes at 4°C . Tubes were then placed on ice while supernatants were carefully

aspirated, paying attention not to remove any erythrocyte at the interface. Samples were further processed for metabolite extraction.

Saos cell lines

Transformed Saos-2 cells, both induced and non-induced to express TAp63 α , were kindly provided by Prof. Melino Gerry (University of "Tor Vergata", Rome - Italy) and prepared as previously reported (Melino et al., 2003).

Human osteosarcoma cell line Saos-2 (p53, p63 and pRb null) was purchased from ATCC (Rockville, MD). Cells were grown in monolayer cultures in Dulbecco-MEM media supplemented with 10% heat-inactivated FBS, L-glutamine (2 mM), penicillin (100 IU/ml), and streptomycin (100 mg/ml) at 37°C in a humidified atmosphere of 5% CO₂ and 95% air. The cells were split every 3 days using 0.25% (v/v) trypsin (Gibco BRL, Gaithersburg, MD) in versene buffer. Cells were routinely checked to be mycoplasma free.

Saos-2 cells with doxycycline (Dox)-inducible expression of HA-TAp63 α were generated as described previously.¹⁶ For the experiments 8 x 10⁵ cells were plated and allowed to attach on plastic dishes (100 x 20 mm) prior to treatment. Proliferation was determined by a count of cells in a Neubauer cytometer chamber. Viability was assessed by 0.4% (w/v) trypan blue dye (Gibco BRL) exclusion. 10⁶ cells (either non-induced controls or induced with 2.5 μ g/ml doxycycline at 24h from induction) were further processed for metabolite extraction and glutamate level assessment through mass spectrometry, as described below.

Retina diffusion media

The diffusion media for the incubation of WT (C57BL/6) cells from retinas were furnished by Professor Giovanni Casini (Università della Tuscia, Viterbo, Italy) (Timperio et al., 2007). Retina diffusion media samples were only tested for glutamate concentrations (*further details below*), as a direct comparison with the previously-proposed chemical-derivatization HPLC-MS method (Timperio et al., 2007).

Blastocoele fluid

The method for blastocyst micropuncturing and aspiration of blastocoele fluid was adapted from Brison et al. (1993). In brief, expanded day 8 blastocysts were removed from culture and transferred to a 10 nl droplet of pre-warmed Hepes-SOFaaBSA under a mineral oil underlay. The blastocysts were immobilized by a holding pipette connected to an air-filled syringe and mounted on a micromanipulator. The medium surrounding the embryo was gently removed to ensure that the site of micropuncture was not contaminated by external culture medium. A finely pulled,

oil-filled pipette was introduced through the mural trophectoderm to avoid damaging the ICM cells, and blastocoel fluid was aspirated gently until the blastocyst had fully collapsed around the pipette. The retrieved fluids were expelled into a dish under oil and frozen at -80°C alongside 0.5 nl control droplets of SOFaaBSA. Blastocoel fluid samples were then thawed and directly processed for metabolic extraction.

Sample extraction and determination of extraction efficiency

Samples were extracted following the protocol by Sana et al. (2008), with minor modifications. A schematized version of the protocol is described in **Table 1**. Cell-free samples (blastocoel fluid) were treated following the same protocol, exception made for step 1 and 13, in which no cell lysates were present and thus no cells were visible at the interface.

Finally, the dried samples were re-suspended in 1 mL of water, 5% formic acid and transferred to glass autosampler vials for LC/MS analysis.

The efficiency of the extraction protocol was determined using L-malic acid as an internal standard (at incremental concentrations) in Krebs' cycle-devoid red blood cell extracts (though malate can still be detected in RBCs) at step 4 at different concentrations (0; 1; 5; 10 mg). Detected L-malic acid concentrations were calculated upon independent determination of the L-malic acid standard curve. In brief L-malic acid five-points (three technical replicates each) standard curve was calculated by plotting integrated peak areas versus concentrations. Extracted samples with L-malic acid as internal standard at different concentrations (0; 1; 5; 10 mg) were tested and L-malic acid detected peak areas were used to determine concentrations through standard curves. Detected concentrations were thus divided by the expected concentrations, as to determine a percentage value indicating extraction efficiency. In order to verify the linearity and reproducibility of the extraction method 4 technical replicates were performed for each extraction. Extraction efficiency for all the detected/expected concentrations are reported in **Table 2** as a unique value indicating the mean \pm SD.

High Resolution Reversed-Phase HPLC

An Ultimate 3000 High Resolution fast HPLC system (LC Packings, DIONEX, Sunnyvale, USA) was used to perform metabolite separation. The system featured a binary pump and vacuum degasser, well-plate autosampler with a six-port micro-switching valve, a thermostated column compartment. A Dionex Acclaim RSLC 120 C18 column 2.1mm \times 150mm, 2.2 μm was used to separate the extracted metabolites.

LC parameters: injection volume, 20 μ L; column temperature, 30°C; and flowrate of 0.2 mL/min. The LC solvent gradient and timetable were identical during the whole period of the analyses. A 0–95% linear gradient of solvent A (0.1% formic acid in water) to B (0.1% formic acid in acetonitrile) was employed over 15 min followed by a solvent B hold of 2 min, returning to 100% A in 2 minutes and a 6-min post-time solvent A hold.

ESI Mass Spectrometry

Metabolites were directly eluted into a High Capacity ion Trap HCTplus (Bruker-Daltonik, Bremen, Germany). Mass spectra for metabolite extracted samples were acquired in positive ion mode. ESI capillary voltage was set at 3000V (+) ion mode. The liquid nebulizer was set to 30 psi and the nitrogen drying gas was set to a flow rate of 9 L/min. Dry gas temperature was maintained at 300°C. Data was stored in centroid mode. Internal reference ions were used to continuously maintain mass accuracy. Data were acquired at a rate of 5 spectra/s with a stored mass range of m/z 50–1500. Data were collected using Bruker Esquire Control (v. 5.3 – build 11) data acquisition software. In MRM analysis, m/z of interest were isolated, fragmented and monitored (either the parental and fragment ions) throughout the whole RT range. Validation of HPLC on-line MS-eluted metabolites was performed by comparing transitions fingerprint, upon fragmentation and matching against the standards metabolites through direct infusion with a syringe pump syringe pump (infusion rate 4 μ l/min). Standard curve calibration were performed either on precursor and fragment ion signals. Only the former were adopted for quantitation, as precursor ion signals guaranteed higher intensity and thus improved LOQ and LOD. Transitions were monitored to validate each detected metabolite.

Data elaboration and statistical analysis

LC/MS data files were processed by Bruker DataAnalysis 4.0 (build 234) software. Files from each run were either analyzed as .d files or exported as mzXML files, to be further elaborated for spectra alignment, peak picking and quantitation with InSilicos Viewer 1.5.4 (Insilicos LLC; Seattle, USA).

For Total Ion Current (TIC) analyses, all compounds and compound-related components (i.e. features) in a spectrum were considered for quantitation. In positive-ion mode this included adducts (H⁺, Na⁺ and K⁺), isotopes and dimers. These related ions were treated as a single compound or feature for preliminary quali-quantitative analysis of metabolites of interest.

Quantitative analyses of standard compounds were performed on MRM data. Each standard metabolite was run in triplicate, at incremental dilution until LOD and LOQ were reached. The limit of detection for each compound was calculated as the minimum amount injected which gave a detector response higher than three times the signal-to-noise ratio (S/N).

To evaluate the potential of the method for quantitative analysis of selected metabolites, intra- and inter-day repeatability of retention times, and linearity of the RR-RP-HPLC-ESI-MS method were tested. Intra-day repeatability was measured by injecting the same standard solution (1 µg/ml) three times in a single day. Inter-day repeatability was measured by analysing the same standard solution over 5 different days. Five-point standard curves were established by plotting integrated peak areas versus concentration. Each point on the calibration curve is the mean value of three independent measurements using the RR-RP-HPLC-ESI-MS method.

Linearity of the observed quantities, slope, intercept and linear correlation values were all calculated via Microsoft Excel (Microsoft, Redmond, WA, USA).

To test the robustness of the method, three biological samples were assayed to quantify four representative metabolites, including NADH, ATP, oxidized glutathione and glyceraldehyde-3-phosphate.

Glutamate levels were also tested in the same biological samples (RBCs, blastocoel fluid and non-induced control SAOS-2 cells) and in retina diffusion media, the same biological model as in our previous investigation on glutamate through chemical-derivatization/HPLC-MS.

Differential glutamate levels were assayed in SAOS-2 cell lines, prior to or at 24h from doxycycline induced expression of TAp63 α in five independent runs each and quantified according to calibration curves obtained as reported above. Student's *t*-test was performed on the two groups of data, as to determine statistical significance (*p*-value < 0.05).

Data were further refined and plotted with GraphPad Prism 5.0 (GraphPad Software Inc.)

Table 1 – Extraction of metabolites: workflow

1	Resuspend the erythrocytes by adding 0.15 mL of ice cold ultra-pure water (18 MΩ) to lyse cells.
2	Plunge the tubes into dry ice or a circulating bath at -25°C for 0.5 min.
3	Plunge the tubes into a water bath at 37°C for 0.5 min.
4	Add 0.6 mL of -20°C methanol containing internal standards (malic acid at different concentrations 0; 1; 5; 10 mg) *
5	Vortex the tubes to ensure complete mixing
6	Transfer the tubes to room temperature
7	Add 0.45 mL chloroform to each tube
8	Vortex the tube to briefly every 5 min for 30 minutes returning the tubes to the cold to the cold bath between vortexing
9	Transfer the tubes to room temperature
10	Add 0.15 mL of ice cold pH adjusted ultra-pure water (18 MΩ) to the tubes
11	Centrifuge the tube at 1000 x g for 1 min at 4 °C
12	Transfer the tube to -20°C freezer for 2-8 h
13	Transfer the top and the bottom phases together, while removing the lysed cells at the interface
14	Add an equivalent volume of acetonitrile to precipitate any proteins and transfer to refrigerator (4°C) for 20 min
15	Centrifuge at 10000 x g for 10 min at 4 °C
16	Recover the supernatant in a 2 ml tube
17	Dry the tube under vacuum
18	Resuspend the content of each tube by adding 1 ml water (18 MΩ), 5% formic acid

* L-malic acid was used as internal standard in red blood cell extracts at incremental exogenous additions
(See also Materials and Methods)

Table 2- Malic acid internal standard during RBC extraction: extraction efficiency.

* Below LOD and LOQ – minimum counts detected

Linearity	$Y = 326299.1 X + 6713.113$
r	0.999952
Extraction efficiency (±SD)	99.662% ± 2.978

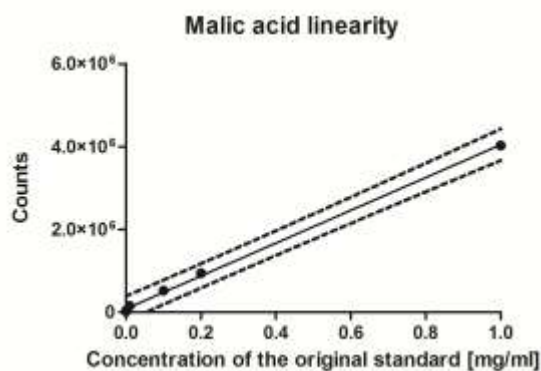


FIGURE 1 Standard curve for calibration of malic acid. based on MRM analysis of 135 *m/z*. Plotting was performed through GraphPad Prism 5.0 (GraphPad Software Inc.). Continuous line: standard curve. Gaped line: 99% confidence interval.

Results and Discussion

Extraction efficiency and technical reproducibility of MS runs (intra-day and inter-day repeatability)

An efficient and effective metabolomic analytical strategy should primarily take into account a series of crucial parameters, including extraction efficiency and technical reproducibility of the extraction protocol.

In order to assess the efficiency of the extraction protocol and thus provide a reliable quantification of the monitored metabolites, we introduced L-malic acid at different concentrations (0; 1; 5; 10 mg), as internal standard in red blood cell (RBC) extracts at step 4 of the extraction protocol (**Table 1**). Four technical replicates were performed in order to assess the reproducibility of the extraction process. Because of the lack of nuclei and mitochondria, mature RBCs are incapable of generating energy via the (oxidative) Krebs cycle. Therefore erythrocytes mainly rely on 4 main metabolic pathways: the Embden-Meyerhof pathway (glycolysis), in which most of the RBC adenosine triphosphate (ATP) is generated through the anaerobic breakdown of glucose; the hexose monophosphate shunt (HMS), which produces NADPH to protect RBCs from oxidative injury; the Rapoport-Lubering shunt and the methemoglobin (met-Hb) reduction pathway (Gressner et al., 2005; Wiback and Palsson, 2002). RBCs do maintain a number of proteins which have been demonstrated to be potentially enzymatically active, such as malate dehydrogenase, although they represent but a functionless remainder after the de-differentiation of reticulocytes into the mature RBCs (Schmaier and Petruzzelli, 2003). The exogenously introduced malic acid (incremental exogenous addition method) has been thus used as an internal standard to test the efficiency of the extraction protocol and thus calculate a coefficient to derivitize the absolute concentration of the monitored metabolite in the original sample.

MS-detected L-malic acid counts were used to calculate its concentration, basing on an independently calculated standard curve ($r = 0.999952$ – **Figure 1**; see the *Experimental section for further details*). As a result, we confirmed the efficiency of the extraction method ($99.662\% \pm 2.978$ – mean \pm SD) in all the replicates at each tested concentration of the internal standard. Details of the analysis are reported in **Table 2**.

Technical reproducibility of HPLC and MS runs was also tested for all the compounds included in this investigation (**Table 3**). The linearity of the RR-RP-HPLC-ESI-MS response was measured for each compound by recording the responses at different concentrations. Intra-day and inter-day repeatability of retention times gave relative standard deviations (RSD) of less than 2%. Intra- and inter-day variability were tested with positive results (reproducibility >98%) also for MS analyses. A panoramic view of the inter-day reproducibility of a representative standard

(injected concentration 1 $\mu\text{g/ml}$) has been graphed in **Figure 2.A** through the auxilium of the InsilicosViewer software.

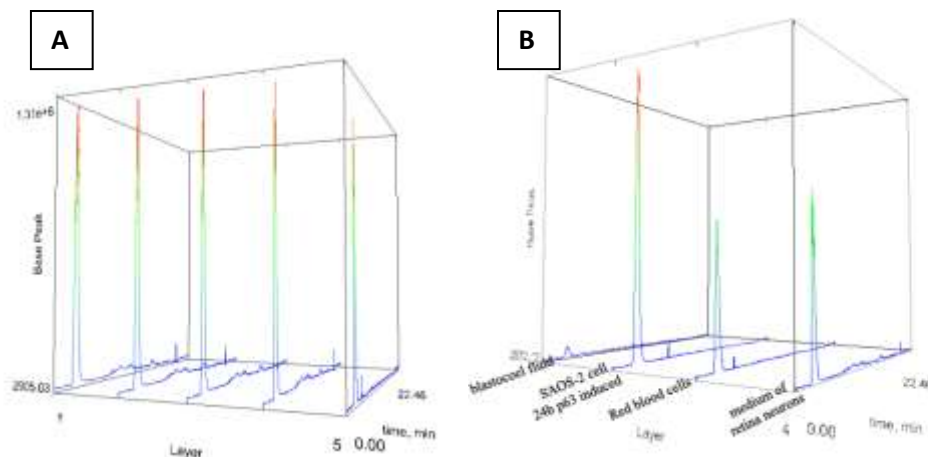


FIGURE 2 Multiple MRM runs for one representative metabolite, L-glutamic acid (1 $\mu\text{g/ml}$) plotted with InsilicosViewer. representing inter-day reproducibility (A) and robustness of the analyses in four different biological samples (B).

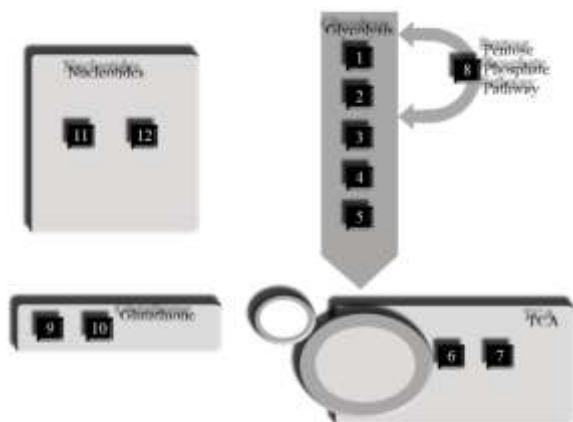


FIGURE 3 A schematic visualization of the main metabolic pathways including metabolites investigated in this study. Numbers refer to metabolites listed in **Table 3**.

Testing of multiple metabolites from the main metabolic pathways through a single strategy on different biological samples

Targeted multiple reaction monitoring (MRM) was performed to quantify a series of metabolites involved in glycolysis, Krebs' cycle, pentose phosphate pathway, redox homeostasis and nucleotide metabolism, as reported in **Figure 3**. Retention times, linear regression coefficients and standard curves are also reported in **Table 3**.

Up to 10 metabolites were simultaneously monitored through MRM in samples from SAOS-2 cell lines, RBCs, diffusion medium of retina neural cells and blastocoel fluid. Reproducibility of retention times and peak elution was very high (>98%) in each tested sample (a detail for glutamic acid is proposed in **Figure 2.B**). The elevated

sensitivity of the method and the possibility to perform multiple metabolite qualitative and quantitative identification (**Figure 4**), allowed overcoming the hurdles deriving from low sample availability, as in the case of the blastocoele fluid (only 1 μ l of sample available for the analysis).

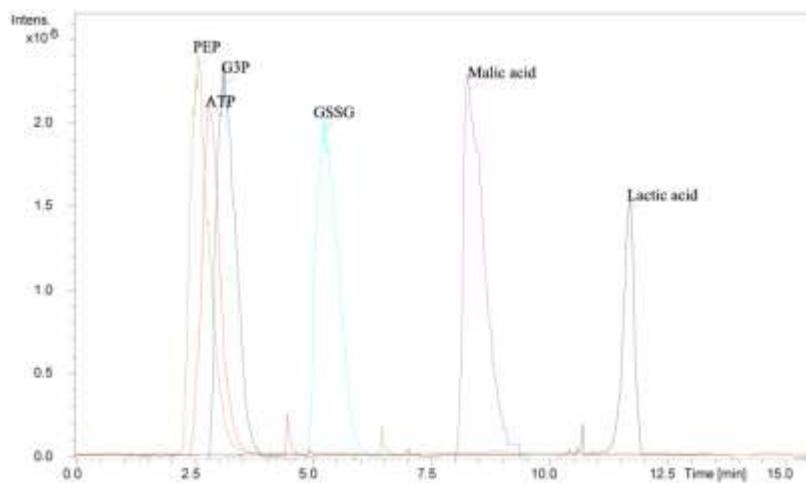


FIGURE 4 Multiple MRM analysis of six different (standard) metabolites, including phosphoenolpyruvate (PEP), adenosine triphosphate (ATP), glyceraldehyde-3-phosphate (G3P), oxidized glutathione (GSSG), malic and lactic acids.

This is particularly evident in MRM analyses of single metabolites on three biological samples (RBCs, SAOS induced to express TAp63 and blastocoele fluid) – details of the analyses of four metabolites (NADH, ATP, oxidized glutathione and glyceraldehyde-3-phosphate) are provided in **Figure 5 (A-D)**. From these analyses it emerged that, despite the scarce starting biological material, it was possible to detect and quantify metabolites in blastocoele fluids, as well as in the other biological samples. Retention times of MS-peaks were highly reproducible, independently from the nature of the biological sample (**Figure 5**). The targeted MRM approach allowed to detect and quantify also those metabolites displaying very close retention times (either base-peak separated or overlapping), without any further need for optimization of the HPLC settings (i.e. phases, gradient), which could have ended up slowing the analysis or rather focus on the discrimination of hydrophilic metabolites (early eluted) at the expenses of later eluted compounds.

Glutamic acid and the advantages over chemical derivatization

Glutamic acid is a small molecule with neither fluorescent nor strong absorbance in the UV–vis region. Quantification of glutamic acid was performed monitoring the $m/z = 148$ ion in positive ion mode (**Table 2**), as to determine LOQ, which was calculated as ≈ 67.578 nM (minimum injected quantifiable quantity = 1.35 pmol), with elevated linearity over 5 orders of magnitude in the range from 1 mg/ml to 10 ng/ml ($r = 0,999327$ - **Figure 6.A** and

B) and reproducibility (**Figure 3**). In comparison to chemical derivatization (Timperio et al., 2007), the SRM method allows dramatically expanding of the dynamic range of linear concentrations (20-300 ng/ml for dansyl-

Table 3 – Metabolites identified through RR-RP-HPLC – MRM-ESI/MS								
	Metabolite	PubChem ID	Monoisotopic mass	MS/MS	Retention time (min)	Standard curves	Linear correlation coefficient	Number in Figure 3
Glycolysis	Fructose 6 Phosphate (F6P)	69507	260.0297	99	2.6	$Y = 437467.7 X + 3383.886$	0.993721	1
	Fructose 1.6 biphosphate (FBP)	10267	339.9960	99	2.8	$Y = 139519.1 X + 6106.018$	0.999991	2
	Glyceraldehyde 3 phosphate (G3PD)	729	169.9980	99	3	$Y = 168431.94 X + 6446.423$	0.996182	3
	Phosphoenolpyruvate (PEP)	1005	167.9824	151	2.8	$Y = 1667498 X + 4095.535$	0.999987	4
	Lactic acid	612	90.0317	63	11.8	$Y = 563010.1X + 1423.73$	0.998704	5
Krebs	α -ketoglutaric acid	164533	144.0822	55	3	$Y = 441223.6X + 4870.91$	0.995342	6
	Malic acid	525	134.0215	73	8.7	$Y = 326299.1 X + 6713.113$	0.999952	7
Pentose phosphate pathway	6-phosphogluconic acid	91493	276.0246	259	3.1	$Y = 792357X + 5951.28$	0.994114	8
Redox defenses	Glutamic acid	611	147.0532	128	2.5	$Y = 26772.17X + 1450.912$	0.999327	9
	Glutathione (oxidized)	65359	612.1520	355	5.4	$Y = 44122.36 X + 4870.91$	0.996585	10
Nucleotides	ATP	5957	506.9957	410	2.9	$Y = 93015.19 X + 6734.24$	0.997755	11
	NADH	928	665.1248	524	3.8	$Y = 43921X + 1306.532$	0.997223	12

chloride derivatized glutamic acid) detected and a sensible reduction of the LOQ. Moreover, the proposed extraction protocol excludes the derivatization steps, which ended up to represent a further burden on the extraction efficiency.⁴ Indeed, the derivatization is a critical part of the previously adopted methodology, which is influenced by many conditions, such as temperature, reaction time, pH of medium and concentration of dansyl (Timperio et al., 2007).

Applicability of the method on real samples: quantification of glutamic acid levels in SAOS cells through MRM.

Over the last decades, developments in cancer research have growingly highlighted the strong commitment of metabolic dysfunctions (including glutamic acid metabolism) in cancer cell proliferation and differentiation (Leskovac et al., 1975; Warburg, 1956).

Classical work in tumor cell metabolism focused on bioenergetics, particularly enhanced glycolysis and suppressed oxidative phosphorylation (the 'Warburg effect'). In cells, glutamate can be further converted into α -ketoglutarate, which is an important substrate for the citric acid cycle (TCA) to produce ATP in mitochondria. Furthermore, glutamate is a precursor of reduced GSH, one of the most important antioxidant molecules and a scavenger for ROS (Brison et al., 1993). Alterations in glutamate levels have been observed in tumour cells upon induced expression of p53 and subsequent activation of the glutamine synthase 2 gene, an enzyme which catalyzes the hydrolysis of glutamine to glutamate (Warburg, 1956; Suzuki et al., 2010).

The increase glutaminase 2 level upon p53-induction in tumour cells has been related either to improvement of anti-oxidant stress responses and activation of pro-apoptotic cascades, hinting at a likely association of glutamate levels with impaired proliferation and survival capacities in tumour cells.

p63 and p73 give rise to proteins that have p53-agonistic as well as p53-antagonistic functions and new functions (Deberardinis et al., 2008). p53 and p63 share a conserved transactivation domain (TA), which promotes the transcription triggering activity of these proteins and hints at a likely overlap between the downstream targets of p53 and p63 (Hu et al., 2010). Glutaminase 2 is supposed to be one of these shared downstream targets, although supporting evidence for p63 has not been hitherto provided. Glutamate levels were thus assayed in p53 and p63-null SAOS-2 cell lines transformed to express the TAp63 α isoform under doxycycline induction, as an indirect marker of glutaminase 2 expression levels. Metabolite extraction was performed at day 0 and at 24h upon induction with doxycycline, resulting in a significant increase (1.5 fold change; Student's *t*-test $p < 0.05$) in glutamate concentrations in the latter case (**Figure 7**). This result indirectly hints at a likely increase in glutaminase 2 levels, which is consistent with the hypothesis of a positive transcriptional activity of the TAp63 α on this enzyme. This holds relevant considerations, including the demonstration of at least a partial overlap between this p63 isoform and p53 downstream targets, although further experimentations targeting mRNAs and proteins through microarray and proteomics approaches are mandatory and currently underway. Whether these preliminary metabolomic results will

be confirmed and complemented, relevant pitfalls might include the induction of p63 isoforms in tumour districts as a counter-measure against tumour progression through turning on glutaminase 2 expression as a switch in the metabolic poise.

Under a mere technical standpoint, glutamate concentrations in tumour cells have been so far assessed only through commercial kits (glutamine/glutamate determination kit – Sigma Aldrich – Saint Louis, USA), which exploit spectrophotometric detection upon enzymatic reaction in a linear range between 0.1 – 2 mM (Suzuki et al., 2010). Our method allows far more sensitive analyses, which both imply an increase in sensitivity (≈ 4 orders of magnitude) and a reduction in quantities of the starting biological material (number of cells).

These partial results are only representative of the likely applicability of the technique in this biological issue and, theoretically, for glutamate level determination in most various samples (**Figure 2.B**).

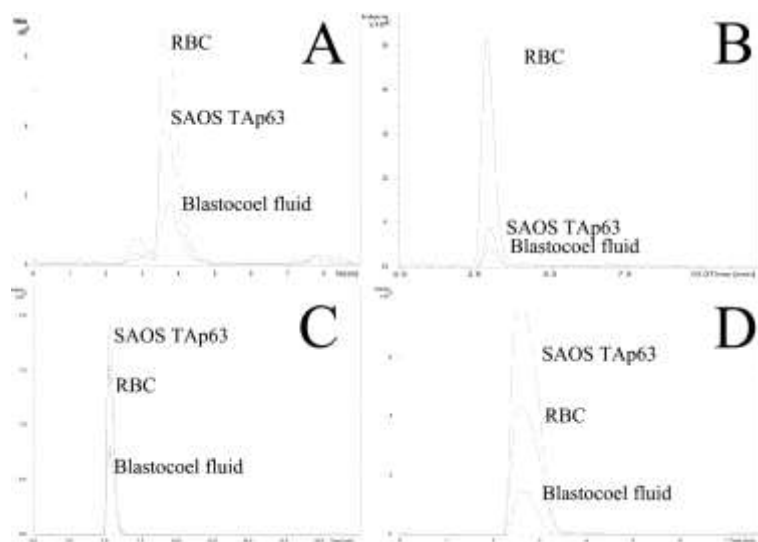


FIGURE 5 MRM spectra of four representative metabolites (NADH (A); ATP (B); GSSG (C) and glyceraldehydes-3-phosphate (D)) in three different biological samples (Red blood cells – RBC; SAOS induced to express TAp63 at 24h from induction with doxycyclin; blastocoels fluid).

Conclusions

We hereby presented a rapid, efficient and robust metabolite extraction strategy in four different biological samples. In parallel, we optimized RR-RP-HPLC/MS parameters in order to qualitatively and quantitatively identify several metabolite classes in MRM mode, simultaneously.

Finally, we evidenced the advantages of the present method over two previously-proposed strategies, either involving chemical derivatization and mass spectrometry or spectrophotometric assays for one representative metabolite (Timperio et al., 2007), glutamic acid, which holds relevant biological implications in most various

physiological activities, including nervous system functioning and cancer cell proliferation and apoptosis. These advantages include a reduced sample handling during sample preparation through the elimination of the chemical derivatization steps, increased sample extraction efficiency, sensitivity and linearity over an increased dynamic range of concentrations. These advantages are pivotal when it comes to low available samples, such as in the case of blastocoel fluid. The possibility to perform extensive targeted metabolite screening on such low available blastocoel fluid samples might hold relevant biomedical pitfalls in the field of fertility research, as specific metabolite pattern might represent a marker of embryo viability (ability to implant and develop in healthy offspring) in like fashion to the preliminary studies proposed on embryo culture media (Botros et al., 2008), though in a direct and more targeted way.

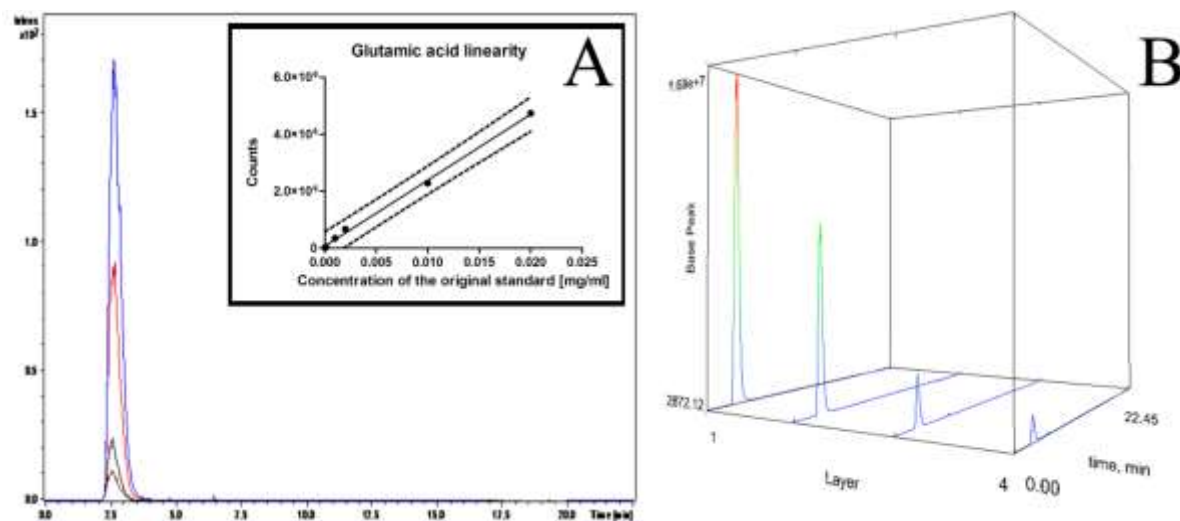


FIGURE 6 MRM spectra and standard curve calibration for glutamic acid (only a reduced interval is plotted in A). Linearity and reproducibility of spectra peaks is stressed by InsilicosViewer plotting of the same MS runs (B).

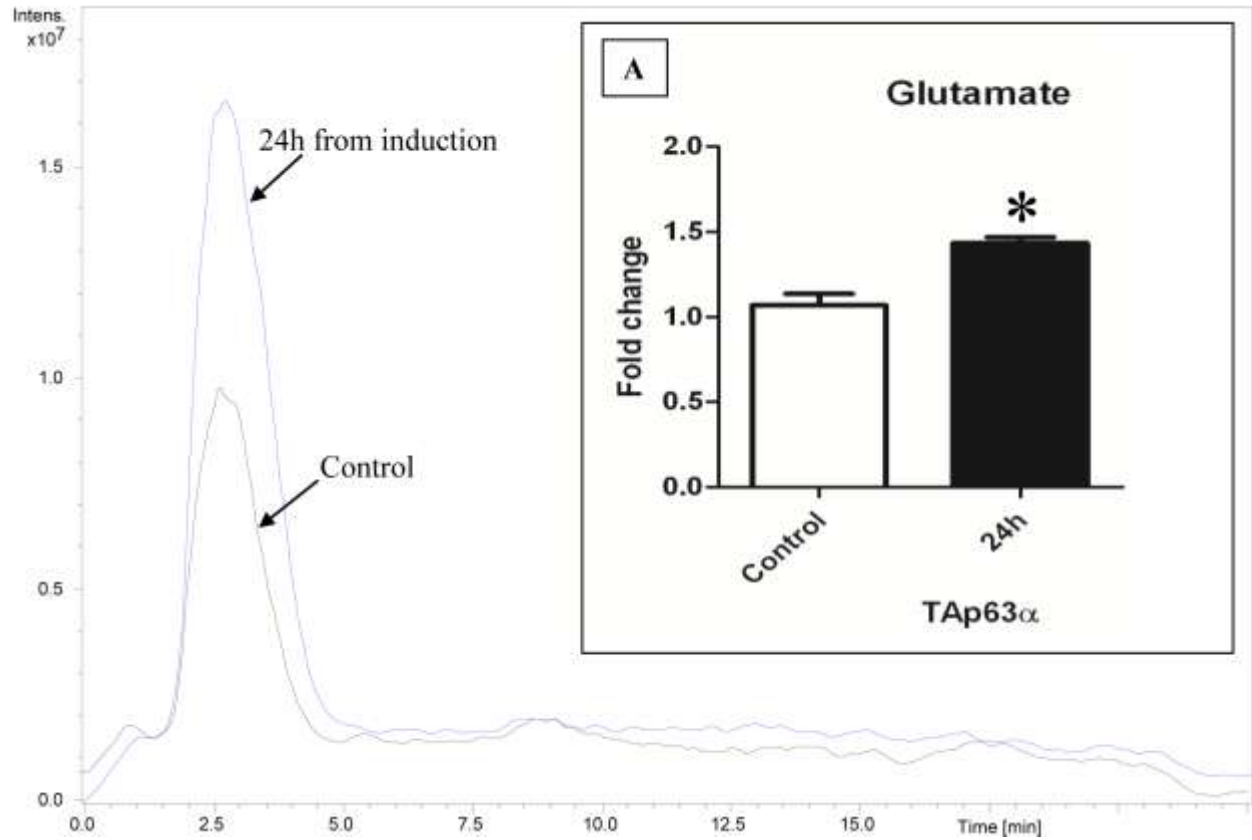


FIGURE 7 Glutamic acid quantitation in SAOS-2 cell lines. prior to (control) or upon 24h from induction. Two MRM spectra are reported, along with a detail of the relative quantitation after five independent runs (A). * = significant increase (p -value < 0.05 Student's t -test)

Chapter 3: Set up of the metabolomics methods

3.2 Targeted mass spectrometry-based metabolomic profiling through Multiple Reaction Monitoring of Liver and other biological matrices.

Overview of this section

In a systemic viewpoint, relevant biological information on living systems can be grasped from the study of small, albeit pivotal molecules which constitute the fundamental bricks of metabolic pathways. This holds true for liver which plays, among its unique functions, a key role in metabolism. The non-biased analysis of all this small-molecule complement in its entirety is known as metabolomics. However, no practical approach currently exists to investigate all metabolic species simultaneously without including a technical bias towards acidic or basic compounds, especially when performing mass spectrometry-based investigations. Technical aspects of rapid resolution reversed phase HPLC online with mass spectrometry are hereby described. Such an approach allows to discriminate and quantify a wide array of metabolites with extreme specificity and sensitivity, thus enabling to perform complex investigations even on extremely low quantities of biological material. The advantages also include the possibility to perform targeted investigations on a single (or a handful of) metabolite(s) simultaneously through single (multiple) reaction monitoring, which further improves the dynamic range of concentrations to be monitored.

Such an approach has already proven to represent a valid tool in the direct (on the liver) or indirect (on human red blood cell metabolism which is hereby presented as a representative model, but also on blood plasma or other biological fluids) assessment of metabolic poise modulation and pharmacokinetics for drug development.

Keywords: metabolomics; mass spectrometry; multiple reaction monitoring; red blood cells.

Introduction

Liver is a vital organ playing a wide range of functions, including protein synthesis, and production of biochemicals necessary for digestion. Liver also plays a key role in metabolism and detoxification, which makes it a critical target for those studies aiming at the determination of pathological conditions or at the assessment of metabolization/adverse effects upon drug assumption. Indeed, hepato- and nephrotoxicity are major attrition factors in preclinical drug development and thus investigative studies on the alterations of the small-molecule complement in the liver represent the basis of a recently expanding discipline which goes under the name of predictive toxicology (Suter et al., 2010). The liver is the major site of synthesis of endogenous metabolites, and the alterations in the profiles of endogenous metabolites ("the metabolome") may precede development of clinically overt drug-induced liver injury (O'Connell and Watkins, 2010). This could be either assessed directly on liver, as in the case of animal trials on drugs (Harris et al., 2010), or indirectly on other biological fluids, like blood plasma or urine. The latter option is more practical and informative, especially in human clinical trials on drugs, such as in the recent cases of acetaminophen (APAP) and ximelagatran (O'Connell and Watkins, 2010).

On the other hand, direct on liver analyses in mice models have already proven useful to improve comprehension of the physiological alterations taking place in obese individuals, paving the way for characterization of optimal diets for those patients seeking health improvements through scientifically validated dietary regimens (Kim et al., 2010; Pilvi et al., 2008). In all the cases mentioned above, metabolomics has been proposed as a precious tool to produce fundamental data to shed light into these hot biological questions.

From clinical biochemistry to "omic" sciences and metabolomics

However, the root of this discipline shares consistent traits with clinical biochemistry, which has historically pursued determination of standard and anomalous parameters (i.e. absolute concentration, relative abundance, etc.) of small molecular compounds in blood and its components (plasma/serum and cellular fractions). Recent advancements in the field of clinical biochemistry, especially in transfusion medicine and immunohaematology closely-related fields (D'Alessandro and Zolla, 2010a and 2010b), are mainly tied to the big technical strides in "omic" disciplines, including transcriptomics, proteomics and metabolomics. During the last decades, "omic"-oriented strategies have constantly gained momentum, which delve into biological complexity as a whole (e.g. proteins in proteomics, mRNAs in transcriptomics) rather than dissecting biological samples through targeted analysis of single molecules (Vinayavekhin et al., 2010).

Metabolomics is "the nonbiased quantification and identification of all metabolites present in a biological system", although the term metabolomics is routinely used in a broader acceptance as to include global identification of as many small molecule (MW lower than 1500 Da) metabolites as possible or of a subset of them (acidic compounds; basic compounds; sugar phosphates; just to mention few). While the dawn of metabolomics dates back to 1960's, it was only in 1971 that Pauling, Robinson et al. conceived the core idea that information-rich data reflecting the functional status of a complex biological system resides in the quantitative and qualitative pattern of metabolites in body fluids (Pauling et al., 1971).

Part of the ambiguity in the use of the term metabolomics is a result of the fact that truly nonbiased quantification and identification of all metabolites present in biological systems is currently not obtainable, due to technical limitations (Evans et al., 2009). The main technical obstacles hindering the way to an omni-comprehensive metabolome portrait stem both from the optimization of sample extraction efficiency of a series of metabolites as broad as possible and from the approach used to perform metabolic analyses, either nuclear magnetic resonance (NMR) or mass spectrometry (MS). In this respect, literature has recently flourished around these topics (Sana et al., 2008; Michopoulos et al., 2009; Bruce et al., 2009; Parab et al., 2009; Buescher et al., 2010; Lee et al., 2010).

1.2 Technical evolution of metabolomics: from NMR to MS

Earliest approaches to metabolomic investigations mainly relied on NMR which was favoured by machine accessibility, established data handling, and the nondestructive nature of the analysis (Parab et al., 2009). Nonetheless, MS has gradually replaced NMR due to the higher sensitivity, improved metabolite discrimination, coverage of the metabolome space, and modularity to perform compound-class-specific analyses, other than to a dramatically reduced demand for starting material necessary to perform an extensive analysis (Griffiths et al., 2010). MS also offers the advantage to perform targeted analyses, thus to follow one (or a handful) of metabolites through isolation and fragmentation of precursor ion and subsequent isolation of the product ions or features of interest, through selected/multiple reaction monitoring (SRM or MRM) (D'Alessandro et al., 2011 – **first part of Chapter 3**). Such an approach holds the advantage to monitor metabolites through a wide spread range of linear concentrations (from mM to nM, down to picomole quantities, depending on the characteristics of the MS instruments), while allowing to directly test the levels of metabolites of interest even in samples as low as 0.5 μ l (as in the case of blastocoele fluid) (D'Alessandro et al., 2011).

On the other hand, MS could be also exploited to perform a non-targeted strategy which potentially enables de novo target discovery since the exploration of the chemical space is only limited by the sample preparation and the characteristics of the analytical technique (sensitivity and coverage). However, it is often difficult to process huge amounts of raw data to unequivocally elucidate the chemical identity of the potential targets, mainly due to platform-dependant software limitations or by the elevated noise of the recorded m/z signals, especially when performing analyses on very low amounts of samples or on extremely low-abundance metabolites. Another level of complexity is added by the necessity to include all the possible adducts of the species of interest depending on the ion mode in which the experiments are performed (e.g. H^+ , K^+ and Na^+ adducts in positive ion mode), which requires time-consuming manual data handling or post hoc bioinformatic elaboration of raw data.

Targeted strategies offer the potential to lower both limits of detection (LOD) and limits of quantification (LOQ), which eases quantification of low-abundance metabolic species also in scarcely available samples. Nevertheless, absolute quantification, which is the ultimate goal in biomarker individuation and testing, can be only performed through monitoring metabolite concentrations against signals of calibration standards, either internal (added to the sample before extraction) or external standards (added to the sample after extraction). In so doing, individual variance between the preparation of the samples and, more importantly, matrix effects and other inferences in the sample are minimized (Burnum et al., 2009).

The role of sample extraction efficiency

A successful analytical strategy for untargeted metabolomics workflows ideally should be rapid, robust and follow an extraction and separation protocol that gives adequate consideration to variables such as the nature of extraction solvent, quenching of metabolic turnover and inclusion of internal standards that helps gauge the success of the extraction procedure (Sana et al., 2008).

On the other hand, sample-handling steps should be kept to a minimum as they introduce uncontrolled analyte loss, and by their very nature are selective and thus discriminating in a global analysis. Such a bias can be purposely introduced when performing targeted analyses, as to enrich specific classes of compounds (for example water or hydrophilic solvents represent the eligible choice for extraction of sugar-phosphates and other hydrophilic species) (Parab et al., 2009).

There are also a series of additional parameters which should be considered during sample preparation for MS-based metabolomic analyses, viz sample storage temperature, protein precipitation methods and processing-time considerations. The extraction solvent pH is but a minor parameter to be adjusted in order to bring analytes to a state where they can be extracted from one of the matrices, maximizing selectivity at a particular pH with minimal loss of recovery (Hendriks et al., 2007).

Recent investigations have compared a wide series of solvents for the optimization of metabolite extraction in model biological matrices, such as red blood cells (Zhang et al., 2009; D'Alessandro et al., 2011). Projection to latent structure of the GC/MS and LC/MS data suggested that the most efficient solution for the extraction of metabolites from wet erythrocytes (50 mg) could be a methanol-chloroform-water mixture (950 μ l, 700:200:50, v/v/v) (Zhang et al., 2009). Independent investigators came to the same conclusion, although they pointed out that the time sequence in which the solvents are used is essential to the optimal outcome of the extraction (Sana et al., 2008). A methanol-chloroform-water extraction protocol is but an evolution of the Bligh/Dyer protocol for lipid extraction (Bligh and Dyer, 1959). In 1959, when studying lipid deterioration in frozen seafood, Bligh and Dyer optimized a chloroform-methanol-water phase diagram, based on the hypothesis that 'optimum lipid extraction should result when the tissue is homogenized with a mixture of chloroform and methanol which, when mixed with the water in the tissue, would have yielded a monophasic solution' (Bligh and Dyer, 1959). The resulting homogenate could then be diluted with water and/or chloroform to produce a biphasic system, the chloroform layer of which should contain the lipids and the methanol—water layer the non-lipids (Bligh and Dyer, 1959). These conclusions are still widely accepted by the scientific community and corroborated by further experimentation on optimum extraction protocol setting up (Sana et al., 2008).

HPLC settings: recent advancements in liquid chromatography columns and chemistry

Three main pre-MS analytical approaches have been proposed over the years, namely gas chromatography (GC), liquid chromatography (LC) and capillary electrophoresis (CE). GC is dampened by the poor discrimination against

large intermediates such as nucleotides, flavines, and coenzyme A derivatives. On the other hand, LC holds several advantages including widespread coverage, sensitivity, ease-of-use, robustness to matrix, and robustness in routine operation. CE is equivalent to LC in terms of separation and sensitivity, although it lacks in robustness, which is pivotal for routine analysis of biological extracts (Buescher et al., 2009).

However, LC suffers from some drawbacks as well, especially concerning the analysis of very polar compounds, such as a wide array of anionic metabolites of primary metabolism. Several solutions have been proposed to overcome this hurdle, including i) the use of ion exchange chromatography; ii) the addition of post-column sodium-proton exchanger; iii) hydrophilic interaction chromatography (HILIC) with an aminopropyl stationary phase or ion pairing-reversed phase chromatography in the analysis of phosphorylated compounds, carboxylic acids, nucleotides, and coenzyme A esters; iv) normal-phase chromatography on silica hydride (Coulier et al., 2006; Cai et al., 2009; Taymaz-Nikerel et al., 2009).

Nonetheless, all of these methods have some detrimental pitfalls as well, including reduction of peak width and sensitivity, over-exposure of the MS to ion-pairing coupling agents (Buescher et al., 2010).

Most of the recent HPLC-MS-based studies mainly relied on the use of RP-HPLC with C18 columns (Sana et al., 2008; Buescher et al., 2010). As elegantly described by Buescher et al. (12), the interaction with the end-capped C18 phase depends on inherent and ion pairing mediated hydrophobic properties, both influencing separation of isomers and coverage of many different compounds. It is thus possible to perform compound class specific analyses as they tend to have similar retention time, in a chronological order which also depends on the mobile phases (water for phase A, methanol or, more often, acetonitrile for phase B) and the gradient (either linear or multi-step, reducing the initial slope to obtain an improved discrimination of early-eluting polar compounds). A frequent RP-HPLC gradient on C18 columns tends to elute i) sugars and aliphatic compounds with a positive net charge earlier; then ii) purines and pyrimidines; iii) acetic and aromatic amino acids; iv) sugar phosphates and monocarboxylic acids; v) dicarboxylic acids and nucleotide monophosphates; v) nucleotide diphosphates and redox cofactors and sugar diphosphates; and vi) nucleotide triphosphates and aromatics and coenzyme A esters (Buescher et al., 2010). Hydrophobic characteristics or selective interaction with the end-capping groups allow further separating even identically charged compounds (i.e., dicarboxylic acids and sugar phosphates, respectively) (Buescher et al., 2010). Charged groups could attract ion pairing molecules thus to render molecules more hydrophobic, which results in delayed retention times (Vinayavekhin et al., 2010).

Recent advancements in the field of HPLC not only involve an in-depth understanding of the chemistry behind small-molecule interaction with novel sub-2 μm or fused silica stationary phases, but also the introduction of technical innovation, such as rapid resolution (RR) and ultra HPLC (UHPLC). In RR and UHPLC short columns are used which are packed with 2.7 μm fused-core silica particles that are made by fusing a 0.5 μm layer of porous silica onto a solid silica particle (Hsieh et al., 2007). These unique particles enable very rapid chromatographic separation at the expense of very high backpressures, which can be easily handled with UHPLC and RR-RP-HPLC, with the advantage to obtain very sharp separation profiles in 10-25 minutes runs (Sana et al., 2008; Evans et al., 2009; Buescher et al., 2010; D'Alessandro et al., 2011).

MS settings and physicochemical properties of metabolic species

Ion pairing agents (formic acid, trifluoroacetic acid) are introduced in HPLC phases and do influence retention times of analysed molecules. Nonetheless, their main function is to enhance ionization of the analytes in order to improve MS detection and quantitation. Theoretically, anionic compounds at physiological pH such as several acids of the Krebs cycle and sugar phosphates can be better monitored in negative ion mode, as they naturally tend to lose protons in solution. This is the main reason why most of the common MS-based metabolomics studies have been performed in negative ion mode or, at least, switching between negative and positive modes (Sana et al., 2008; Evans et al., 2009; Buescher et al., 2010). Indeed, ionization in positive mode is in principle possible with excellent results in sensitivity, which allows improving the dynamic range of linear concentrations and thus to reduce the requirements for the quantities of biological materials needed to perform the analysis (D'Alessandro et al., 2011). Unfortunately, routine operation in positive mode drastically increases maintenance and cleaning on the initial stages of the mass spectrometer to remove the sediments of ion pairing agent (Buescher et al., 2010).

Ion traps, Fourier transform mass spectroscopy (FT-ICR-MS), Orbitrap instruments and triple quadrupole MS instruments are routinely used in MS-based metabolomics. In the case of the analysis of tissue metabolomes, extraction is a necessary prerequisite, except in cases where analysis is to be performed directly on the tissue, as is the case with matrix-assisted laser desorption/ionization (MALDI) imaging or desorption electrospray ionization (DESI) (Griffiths et al., 2010).

The advantages of one mass analyzer over the other have been resumed by Griffiths et al. (2010), which described in detail how the analyzers can be arranged in series in space, such as on hybrid instruments (for example, tandem quadrupole, Q-TOF instruments), or in time, such as with ion traps. Ion traps are particularly suited to record MS^3 and further MS^n spectra. Triple quadrupole instruments offer other advantages such as SRM “scans”, where MS_1 is “parked” on an m/z value of interest and MS_2 on the m/z value(s) of a known fragment ion (SRM) or multiple fragment ions (MRM) (Griffiths et al., 2010).

Data analysis: on-line databases and in silico elaboration

One of the main issues to deal with when performing untargeted metabolomics analyses is data filtering and interpretation, as signals over the whole retention time range are often noisy and difficult (or time-consuming) to interpret manually. A joint effort is currently underway to put into place a public database of tandem MS spectra. This is not an easy task as results obtained through different instruments (or from the same instruments from different vendors) tend to differ in fragmentation spectra (Evans et al., 2009). Despite these issues, it is now possible to rely on freely accessible databases such as HMDB (Wishart et al., 2007), MassBank, Metlin (Smith et al., 2005), LipidMaps, ChemACX, and ChemSpider which have been built as to contain millions of m/z profiles and chemical

structures. However, they only represent just a preliminary tool to ease the data interpretation steps, since they are far from containing all relevant structures and. For example, small molecules in biological systems are subject to phase I and II metabolism (glucuronidation, reduction, oxidation, sulfation, amino acid conjugation, etc.), and many of these modified small molecules are not covered in current databases (Evans et al., 2010). Independent laboratories have thus sought to build up their personal databases for high-throughput untargeted purposes, although at the expenses of lengthy and expensive investments on instruments, in-house software and trained personnel (Evans et al., 2010).

On the other hand, targeted metabolomics analyses through SRM or MRM also suffer from minor bioinformatic issues, which include partial drift of HPLC peaks over different HPLC-MS runs, standardization of peak picking criteria for optimal quantitation of MRM spectra and normalization of S/N ration against technical variables (intra- and inter-day reproducibility).

In order to overcome these obstacles, a series of open source valid programs for peak alignment, normalization and peak picking have been realized and freely distributed. These software packages ease standardization of data handling in proteomics (but also metabolomics), such as ToppView OpenMS, InsilicosViewers and other tools for *in silico* elaboration of mass spectra, 3D visualization of MS outputs (retention times, m/z and MS-detected counts on each axis) (Nasso et al., 2010; Bertsch et al., 2011).

Materials

HPLC and metabolite extraction

1. Acetonitrile;
2. Formic acid;
3. HPLC-grade water;
4. Metanol;
5. Chloroform.

An Ultimate 3000 Rapid Resolution HPLC system (LC Packings DIONEX (Sunnyvale, CA, USA)) was used to perform metabolite separation. The system featured a binary pump and vacuum degasser, well-plate autosampler with a six-port micro-switching valve, a thermostated column compartment. A Dionex Acclaim RSLC 120 C18 column 2.1mm×150mm, 2.2 μm was used to separate the extracted metabolites.

Mass spectrometry

Metabolites were directly eluted into a High Capacity ion Trap HCTplus (Bruker-Daltonik (Bremen, Germany)).

Metabolite standards

Standards (equal or greater than 98% chemical purity) were purchased from Sigma Aldrich (Milan, Italy):

1. ATP,
2. L-lactic acid,
3. phosphogluconic acid,
4. NADH,
5. D-fructose 1,6 biphosphate,
6. D-fructose 6-phosphate, glyceraldehyde phosphate,
7. Phosphoenolpyruvic acid,
8. L-malic acid,
9. L-glutamic acid,
10. Oxidized glutathione,
11. α -ketoglutarate.

Alternative internal standards were purchased from Sigma Aldrich (St. Louis, MO, USA) and Acros organics (Morris Plains, NJ, USA), respectively:

1. 1-naphthylamine and
2. 2-(methylthio)benzothiazole.

Standard storage and preparation

Standards were stored either at -25°C , 4°C or room temperature, *following manufacturer's instructions*. Each standard compound was weighted and dissolved in nanopure water. Starting at a concentration of 1 mg/ml of the original standard solution, a dilution series of steps (in 18 M Ω , 5% formic acid) was performed for each of the standards in order to reach the limit of detection (LOD) and limit of quantification (LOQ).

Methods

Red blood cells

RBC units were drawn from healthy human volunteers according to the policy of the Italian Blood Transfusion Service for donated blood and all the volunteers provided their informed consent in accordance with the declaration of Helsinki. RBC units were collected from 3 donors [male=2, female=1, age 44 ± 6.5 (mean \pm S.D.)] in Latium (Italy). Saline adenine glucose-mannitol (SAGM) erythrocyte concentrates were removed aseptically for the analysis within the first day of storage. For each sample, 0.5ml from the pooled erythrocyte stock was transferred into a microcentrifuge tube and processed for metabolite extraction, as described below. Erythrocyte samples were then

centrifuged at 1000g for 2 minutes at 4°C as to remove SAGM and any further contaminant. Tubes were then placed on ice while supernatants were carefully aspirated, paying attention not to remove any erythrocyte at the interface. Samples were further processed for metabolite extraction.

Sample extraction

Samples were extracted following the protocol proposed by Sana et al. (2009), with minor modifications (D'Alessandro et al., 2011) (*see Note 1*).

1. The sample was resuspended by adding 0.15 ml of ice cold ultra-pure water (18 MΩ - *see Note 2*) to lyse cells;
2. The tubes (2 ml original eppendorf - (*see Note 3*)) were plunged into dry ice or a circulating bath at -25°C for 0.5 min and then into a water bath at 37°C for 0.5 min (*see Note 4*);
3. To each tube was added first 0.6 ml of -20°C methanol containing L-malic acid for red blood cells or 1-naphthylamine and 2-(methylthio)benzothiazole as internal standards(*see Note 5*);
4. 0.45 ml of -20 °C chloroform were added (*see Note 6, 7*);
5. The tubes were mixed every 5 min for 30 minutes;
6. 0.15 ml of ice cold pH adjusted ultra-pure water (18 MΩ) was added to each tube;
7. The tubes were centrifuged at 1000 x g for 1 min at 4 °C (*see Note 8*);
8. The tubes were transferred to -20° C for 2-8 h (*see Note 9*). An equivalent volume of acetonitrile was added to precipitate any proteins and then the tubes were transferred to refrigerator (4°C) for 20 min;
9. Each tube was centrifuged at 10000 x g for 10 min at 4 °C and the supernatant was recovered into a 2 ml tube;
10. Collected supernatants were dried as to obtain visible pellets (*see Note 10, 11*);
11. Finally, the dried samples were re-suspended in 1 ml of 5% formic acid in water and transferred to glass autosampler vials for LC/MS analysis (*see Note 12*).

Determination of extraction efficiency: the red blood cell as a model

Internal standards were added in order to assess extraction efficiency. L-malic acid was used as internal standard in red blood cell extracts, through exogenous addition at step 3 of the extraction protocol at different concentrations (0; 1; 5; 10 mg/ml – **Figure 1**). This allowed testing the linearity and reproducibility (4 technical replicates for each extraction) of the extraction method. Since mature red blood cells are devoid of nuclei and mitochondria,

erythrocytes are incapable of generating energy via the (oxidative) Krebs cycle. Therefore erythrocytes mainly rely on 4 main metabolic pathways:

1. the Embden-Meyerhof pathway (glycolysis), in which most of the red blood cell adenosine triphosphate (ATP) is generated through the anaerobic breakdown of glucose;
2. the hexose monophosphate shunt (HMS), which produces NADPH to protect red blood cells from oxidative injury;
3. the Rapoport-Lubering shunt, responsible for the production of 2,3-diphosphoglycerate (DPG) for the control of Hb oxygen affinity;
4. finally, the methemoglobin (met-Hb) reduction pathway, which reduces ferric heme iron to the ferrous form to prevent Hb denaturation (Leskovac et al., 1975; Schmaier et al., 2003). Red blood cells do maintain a number of proteins which have been demonstrated to be potentially enzymatically active, such as malate dehydrogenase, although they represent but a functionless remainder after the dedifferentiation of reticulocytes into the mature red blood cells. The exogenously introduced L-malic acid at increasing concentration (method of exogenous incremental additions) could be thus useful to test the efficiency of the extraction protocol and thus calculate a coefficient to derivitize the absolute concentration of the monitored metabolite in the original sample.

Rapid Resolution Reverse-Phase HPLC settings

LC parameters: injection volume, 20 μ l; column temperature, 25°C; and flow-rate of 0.2 ml/min. The LC solvent gradient and timetable were identical during the whole period of the analyses. A 0–95% linear gradient of solvent A (0.1% (v/v) formic acid in water) to B (0.1% (v/v) formic acid in acetonitrile) was employed over 15 min followed by a solvent B hold of 2 min, returning to 100% A in 2 minutes and a 6-min post-time solvent A hold (see *Note 12-15*).

ESI Mass Spectrometry settings

Mass spectra for metabolite extracted samples were acquired in positive ion mode. ESI capillary voltage was set at 3000V (+) ion mode. The liquid nebulizer was set to 30 psig and the nitrogen drying gas was set to a flow rate of 9 L/min. Dry gas temperature was maintained at 300°C. Data was stored in centroid mode. Internal reference ions were used to continuously maintain mass accuracy. Data was acquired at a rate of 5 spectra/s with a

stored mass range of m/z 50–1500. Data was collected using Bruker Esquire Control (v. 5.3 – build 11) data acquisition software. In MRM analysis, m/z of interest were isolated and monitored throughout the whole RT range. Validation of HPLC on-line MS-eluted metabolites was performed by comparing transitions fingerprint, upon fragmentation and matching against the standards metabolites through direct infusion with a syringe pump (infusion rate 4 $\mu\text{l}/\text{min}$).

Data elaboration and statistical analysis

LC/MS data files were processed by Bruker DataAnalysis 4.0 (build 234) software. Files from each run were either analyzed as .d files or exported as mzXML files, to be further elaborated for spectra alignment, peak picking and quantitation with InSilicos Viewer 1.5.4 (Insilicos LLC (Seattle, WA, USA)). For Total Ion Current (TIC) analyses, all compounds and compound-related components (i.e. features) in a spectrum were considered for quantitation. In positive-ion mode this included adducts (H^+ , Na^+ and K^+), isotopes and dimers. These related ions were treated as a single compound or feature for preliminary quali-quantitative analysis of metabolites of interest (untargeted analysis). Absolute quantitative analyses of standard compounds were performed on MRM data (targeted analyses). Each standard metabolite was run in triplicate, at incremental dilution until LOD and LOQ were reached. Precursor ions, fragmentation energies and transition features to be isolated and monitored were determined through direct infusion through a syringe pump (4 $\mu\text{l}/\text{min}$). The limit of detection for each compound was calculated as the minimum amount injected which gave a detector response higher than three times the signal-to-noise ratio (S/N). Basic compounds were tested in positive ion mode, while acidic compounds, including sugar phosphates were preferentially monitored in negative ion mode. However, positive ion mode was preferred to negative ion mode also for the latter group, especially when performing analyses on samples displaying a high dynamic range of metabolite concentrations, since positive ion mode guaranteed a broader range of linearity for MS signals. For scarce samples, negative ion mode represented the method of choice, due to improved signal-to-noise (S/N) ratio.

To evaluate the potential of the method for quantitative analysis of selected metabolites, intra- and inter-day repeatability of retention times, and linearity of the RR-RP-HPLC-ESI-MS method were tested. Intra-day repeatability was measured by injecting the same standard solution (standard metabolite at a concentration of 1 $\mu\text{g}/\text{ml}$) three times in a single day. Inter-day repeatability was measured by analysing the same standard solution over 6

different days. Intra-day and inter-day repeatability of retention times using our method gave relative standard deviations (RSD) of less than 2%. The linearity of the RR-RP-HPLC-ESI-MS response (LOQ) was measured for each compound by recording the responses at different concentrations (**Figure 2**), over the range of at least 1 mg/ml to 1 µg/ml (down to 10 ng/ml for glutamic acid, from 6.8 mM to \approx 68 nM, corresponding to a minimum of 1.35 pmol). Five-point standard curves were established by plotting integrated peak areas versus concentrations. Each point on the calibration curve is the mean value of three independent measurements using the RR-RP-HPLC-ESI-MS method (**Figure 2**). Linearity of the observed quantities, slope, intercept and linear correlation values were all calculated via Microsoft Excel (Redmond, WA, USA). Data were further refined and plotted with GraphPad Prism 5.0 (GraphPad Software Inc. (San Diego, CA, USA)).

For absolute quantification in all tested biological matrices (**Figure 3**), detected m/z signals were used to calculate quantities against calibration curves and normalized against internal standard signals, as to include any influence of the sample extraction protocol efficiency.

Notes

1. This method is robust as it can be applied to a wide array of biological matrices. Consistency in sample handling is very important. When collecting, it is important to minimize operational variation (*e.g.* collection technique, time of sampling, time to freezer, *etc.*). Materials collected for other experimental work and stored at -80°C can be used for metabolomic studies as long as all of the samples were treated in a consistent way during the collection process. When performing analyses on tissues (liver samples), 20 (liver) to 100 mg (other) of tissue samples are the routine requirement for metabolomics preparations; for cell samples (hepatocarcinoma cell lines, red blood cells), quantities should range from 1×10^7 viable cells (optimal) to 0.5×10^5 - 1×10^6 cells (average) for good quality MS results.
2. Ultra-pure 18 M Ω water is fundamental during the extraction and the HPLC-phases preparation. In the latter case, non-ultra pure water might end up covering MS signals or contributing to Na^+ or K^+ adducts of metabolite species of interest.
3. Only original eppendorf tubes should be used, since other tubes might release polymers altering MS signals.
4. Check water bath temperature carefully as the thermal shock directly influences the outcome of the cell lysis step.
5. For tissue samples, such as liver samples (20-100 mg of tissue), a homogenization step should be introduced with a common laboratory homogenizer, such as Micro Dismembrator S (Sartorius, Goettingen, Germany) by using glass beads (0.5-0.75 mm) and 3000 rpm for 3 min.
6. Methanol and chloroform are toxic. Be cautious. Prepare methanol and chloroform stock aliquots and store them at -20°C . Low temperatures positively affect the metabolite extraction efficiency and protein precipitation steps.

7. Low temperatures are important as to prevent any metabolite degradation. In general, all sample preparation and processing steps should be as fast as possible and performed at low temperature, in order to exclude any metabolite degradation due to residual enzymatic contamination of the samples.
8. After this step, a three phase system can be observed, with liquid upper and lower phases and an intermediate cellular phase. This is particularly evident for extractions of erythrocytes, where the intermediate band is completely red. When extracting metabolites from biological fluids (such as urine or plasma), only two main bands will be visible.
9. This step can be prolonged overnight, if necessary.
10. Sample drying could be effectively performed with a common rotavapor (Rotray evaporator) at 50°C for at least 3 hours.
11. After this step, a pellet should be visible at the bottom of the eppendorf tube. The absence of this pellet might be a symptom of an inefficient extraction.
12. Although HPLC separation could be also performed with classic HPLC, fast (rapid resolution) HPLC holds the advantage to perform faster separation while maintaining high resolution of metabolites over the whole retention time range. This is particularly time-saving when performing targeted analyses on multiple biological samples and elevated numbers of technical replicates, as it ends up cutting analytical times at least by a factor 2 to 4. For example, the chromatographic flow-rate can be increased up to 0.6 ml/min when working with RR-RP-HPLC and specific columns (such as in the present case), which can sustain far higher backpressures (up until 800 bars), thus reducing by a factor 3 the length of the run. However, this can be done only when working on-line with ion trap MS, which can receive such a consistent volume per minute, while other MS need the flux to be splitted prior to direct injections into the source of the spectrometer.
13. Remember to activate and condition columns with mobile phases by performing at least two blank runs prior to the first analysis. This helps regularizing pressures over the whole retention time range.
14. Column temperature could be raised to improve chromatographic peak separation and reduce backpressure. Depending on the column used, temperature should not be raised above 50°C as it may results in shortening column half-lives.
15. Formic acid (FA) is the optimal coupling agent, as it works best in enhancing MS signals. However, overexposure to FA might result in increased need for maintenance of the MS instrument. The operator might think of switching to negative ion mode for the analysis of anionic compounds, especially when handling abundant starting biological material.

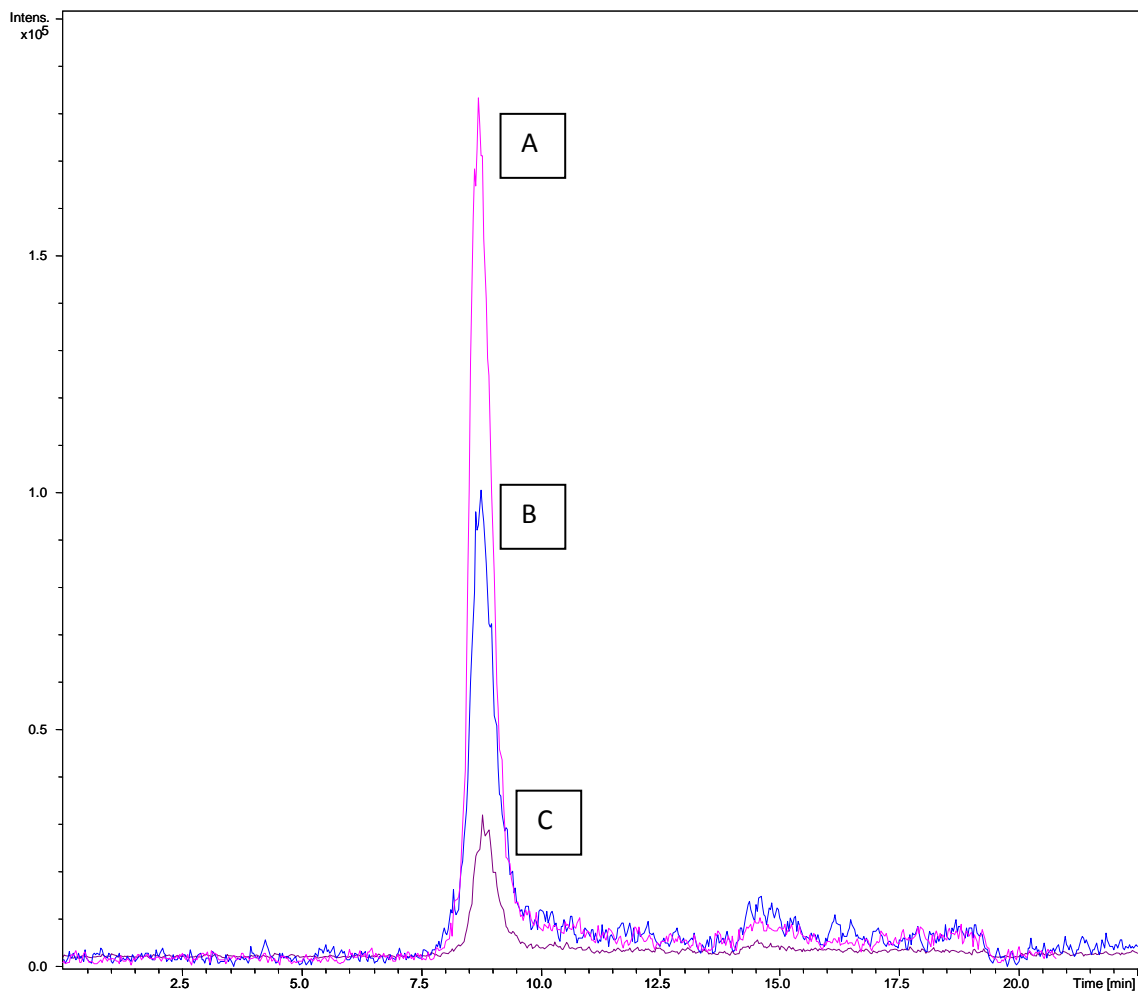


FIGURE 1 MRM spectra for exogenously added L-malic acid, as internal standard to test sample extraction efficiency in three independent extractions from red blood cells at different concentrations of the standard metabolite: 1 mg (A), 5 mg (B) and 10 mg (C).

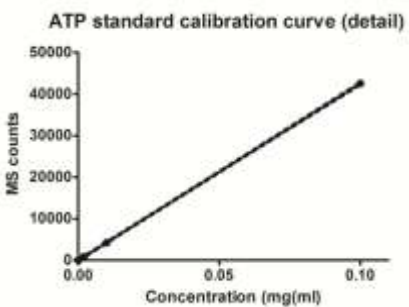


FIGURE 2 A detail of the ATP standard calibration curve in the low concentration range (from 0,1 mg/ml to 0,1 μ g/ml). Higher concentration points are not graphed in this curve due to space limitations. The gaped lines indicate the 99% confidence interval for linear regression calculated for the independent points in this graph. X-axis indicates concentrations while y-axis graphs MS-counts

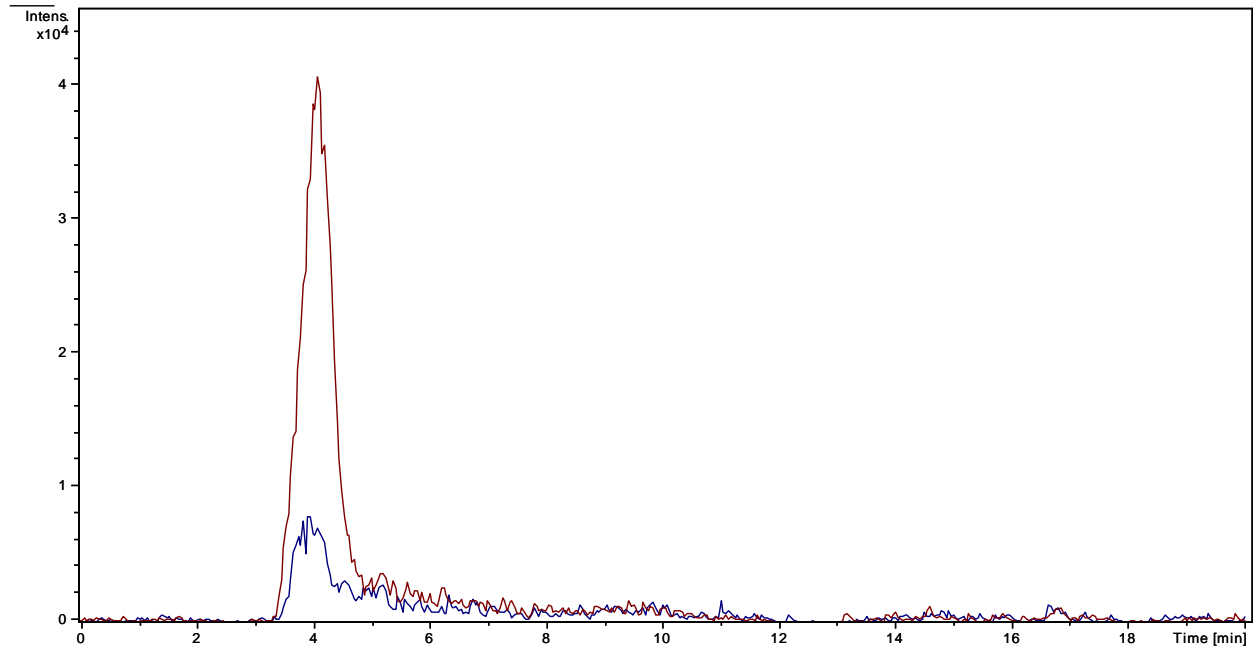


FIGURE 3 Differential levels of ATP as detected from measurements on TAp73 $\alpha^{+/−}$ (A) versus TAp73 $\alpha^{-/-}$ (B) MEF cells through MRM (positive ion mode, 508 m/z \rightarrow 410 m/z).

References

- Bertsch A, Gröpl C, Reinert K, Kohlbacher O. OpenMS and TOPP: open source software for LC-MS data analysis. *Methods Mol Biol* 2011; 696: 353-367
- Bligh EG, Dyer WJ. A rapid method of total lipid extraction and purification. *Can J Biochem Physiol* 1959; 37: 911-917
- Boguski M, Chakravarti A, Gibbs R, Green E, Myers RM. The end of the beginning: the race to begin human genome sequencing. *Genome Res.* 1996;6(9):771-2.
- Botros L, Sakkas D, Seli E. Metabolomics and its application for non-invasive embryo assessment in IVF. *Mol Hum Reprod.* 2008;14(12):679-90.
- Brison DR, Hewitson LC, Leese HJ. Glucose, pyruvate, and lactate concentrations in the blastocoel cavity of rat and mouse embryos. *Mol Reprod Dev.* 1993;35(3):227-32.
- Bruce SJ, Tavazzi I, Parisod V et al (2009) Investigation of human blood plasma sample preparation for performing metabolomics using ultrahigh performance liquid chromatography/mass spectrometry. *Anal Chem* 81: 3285-3296.
- Buescher JM, Moco S, Sauer U, Zamboni N. Ultrahigh performance liquid chromatography-tandem mass spectrometry method for fast and robust quantification of anionic and aromatic metabolites. *Anal Chem.* 2010;82(11):4403-12.
- Burnum KE, Cornett DS, Puolitaival SM et al. Spatial and temporal alterations of phospholipids determined by mass spectrometry during mouse embryo implantation. *J Lipid Res* 2009; 50: 2290-2298
- Buscher JM, Czernik D, Ewald JC. Cross-Platform Comparison of Methods for Quantitative Metabolomics of Primary Metabolism. *Anal Chem* 2009; 81: 2135–2143
- Cai X, Zou L, Dong J et al. Analysis of highly polar metabolites in human plasma by ultra-performance hydrophilic interaction liquid chromatography coupled with quadrupole-time of flight mass spectrometry. *Anal Chim Acta* 2009; 650: 10-15
- Coulier L, Bas R, Jespersen S et al. Simultaneous quantitative analysis of metabolites using ion-pair liquid chromatography-electrospray ionization mass spectrometry. *Anal Chem* 2006; 78: 6573–6658
- D'Alessandro A, Gevi F, Zolla L. A robust high resolution reversed-phase HPLC strategy to investigate various metabolic species in different biological models. *Mol Biosyst* 2011; doi:10.1039/C0MB00274G.

- D'Alessandro A, Zolla L. Pharmacoproteomics: a chess game on a protein field. *Drug Discov Today* 2010a; 15:1015-1023
- D'Alessandro A, Zolla L. Proteomics for quality-control processes in transfusion medicine. *Anal Bioanal Chem* 2010b; 398:111-124
- Deberardinis RJ, Sayed N, Ditsworth D, Thompson CB. Brick by brick: metabolism and tumor cell growth. *Curr Opin Genet Dev.* 2008;18(1):54-61
- Evans AM, DeHaven CD, Barrett T et al (2009) Integrated, non targeted ultrahigh performance liquid chromatography/electrospray ionization tandem mass spectrometry platform for the identification and relative quantification of the small-molecule complement of biological systems. *Anal Chem* 81:6656-6667
- Gressner O, Schilling T, Lorenz K, Schulze Schleithoff E, Koch A, Schulze-Bergkamen H, Lena AM, Candi E, Terrinoni A, Catani MV, Oren M, Melino G, Krammer PH, Stremmel W, Müller M. TAp63 α induces apoptosis by activating signaling via death receptors and mitochondria. *EMBO J.* 2005 Jul 6;24(13):2458-71.
- Griffiths WJ, Koal T, Wang Y et al. Targeted metabolomics for biomarker discovery. *Angew Chem Int Ed Engl* 2010; 49: 5426-5445.
- Harris SR, Zhang GF, Sadhukhan S et al. Metabolism of levulinate in perfused rat livers and live rats: conversion to the drug of abuse 4-hydroxypentanoate. *J Biol Chem* 2010; doi/10.1074/jbc.M110.196808
- Hendriks G, Uges DRA, Franke JP. Reconsideration of sample pH adjustment in bioanalytical liquid-liquid extraction of ionisable compounds. *J Chromatogr B* 2007; 853: 234–241
- Hsieh Y, Duncan CJ, Brisson JM. Fused-core silica column high-performance liquid chromatography/tandem mass spectrometric determination of rimonabant in mouse plasma. *Anal Chem* 2007; 79: 5668-5673
- Hu W, Zhang C, Wu R, Sun Y, Levine A, Feng Z. Glutaminase 2, a novel p53target gene regulating energy metabolism and antioxidant function. *Proc Natl Acad Sci U S A.* 2010;107(16):7455-60.
- Kim HJ, Kim JH, Noh S et al. Metabolomic Analysis of Livers and Serum from High-Fat Diet Induced Obese Mice. *J Proteome Res* 2010; 10:722-31.
- Lee do Y, Bowen BP, Northen TR. Mass spectrometry-based metabolomics, analysis of metabolite-protein interactions, and imaging. *Biotechniques* 2010; 49: 557-565

- Leskovac V, Jerance D, Burany E. Comparative enzymology of malate dehydrogenases-VIII. Cytoplasmic characteristics of pig erythrocyte malate dehydrogenase.** *Int. J. Biochem.* 1975; 6(8): 563-568.
- Melino G, Lu X, Gasco M, Crook T, Knight RA. Functional regulation of p73 and p63: development and cancer. *Trends Biochem Sci.* 2003;28(12):663-70.
- Michopoulos F, Lai L, Gika H et al. UPLC-MS-based analysis of human plasma for metabonomics using solvent precipitation or solid phase extraction. *J Proteome Res* 2009; 8: 2114-2121
- Nasso S, Silvestri F, Tisiot F, et al. An optimized data structure for high-throughput 3D proteomics data: mzRTree. *J Proteomics* 2010; 73: 1176-1182
- O'Connell TM, Watkins PB. The application of metabonomics to predict drug-induced liver injury. *Clin Pharmacol Ther* 2010; 88:394-399
- Parab GS, Rao R, Lakshminarayanan S et al. Data-driven optimization of metabolomics methods using rat liver samples. *Anal Chem* 2009; 81: 1315-1323.
- Pauling L, Robinson AB, Teranishi R, Cary P. Quantitative analysis of urine vapor and breath by gas-liquid partition chromatography. *Proc Natl Acad Sci USA* 1971; 68:2374 – 2376
- Pilvi TK, Seppanen-Laakso T, Simolin H et al. Metabolomic changes in fatty liver can be modified by dietary protein and calcium during energy restriction. *World J Gastroenterol* 2008; 14:4462-4472.
- Sana TR, Waddell K, Fischer SM. A sample extraction and chromatographic strategy for increasing LC/MS detection coverage of the erythrocyte metabolome. *J Chromatogr B Analyt Technol Biomed Life Sci.* 2008;871(2):314-21.
- Schmaier AH and Petruzzelli LM, In “Hematology for the medical student”. Lippincott Williams & Wilkins 2003, 3, 22-23;
- Smith CA, O'Maille G, Want EJ et al. METLIN: a metabolite mass spectral database. *Ther Drug Monit* 2005; 27: 747-751
- Suter L, Schroeder S, Meyer K et al. EU Framework 6 Project: Predictive Toxicology (PredTox)-overview and outcome. *Toxicol Appl Pharmacol* 2010; doi:10.1016/j.taap.2010.10.008
- Suzuki S, Tanaka T, Poyurovsky MV, Nagano H, Mayama T, Ohkubo S, Lokshin M, Hosokawa H, Nakayama T, Suzuki Y, Sugano S, Sato E, Nagao T, Yokote K, Tatsuno I, Prives C.

- Phosphate-activated glutaminase (GLS2), a p53-inducible regulator of glutamine metabolism and reactive oxygen species. *Proc Natl Acad Sci U S A*. 2010;107(16):7461-6.
- Taymaz-Nikerel H, Mey M, Ras C et al. Development and application of a differential method for reliable metabolome analysis in *Escherichia coli*. *Anal Biochem* 2009; 386: 9–19
- Timperio AM, Fagioni M, Grandinetti F, Zolla L. Chemically enhanced liquid chromatography/tandem mass spectrometry determination of glutamic acid in the diffusion medium of retinal cells. *Biomed Chromatogr*. 2007;21(10):1069-76.
- Vinayavekhin N, Homan EA, Saghatelian A. Exploring disease through metabolomics. *ACS Chem Biol* 2010; 15:91-103
- Wamelink MM, Struys EA, Huck JH, Roos B, van der Knaap MS, Jakobs C, Verhoeven NM. Quantification of sugar phosphate intermediates of the pentose phosphate pathway by LC-MS/MS: application to two new inherited defects of metabolism. *J Chromatogr B Analyt Technol Biomed Life Sci*. 2005;823(1):18-25.
- Warburg O. On the origin of cancer cells. *Science* 1956; **123**: 309–314.
- Wiback SJ, Palsson BO. Extreme pathway analysis of human red blood cell metabolism. *Biophys J*. 2002;83(2):808-18.
- Wishart DS, Tzur D, Knox C et al. HMDB: the Human Metabolome Database. *Nucleic Acids Res* 2007; 35: 521-526
- Zelena E, Dunn WB, Broadhurst D, Francis-McIntyre S, Carroll KM, Begley P, O'Hagan S, Knowles JD, Halsall A; HUSERMET Consortium, Wilson ID, Kell DB. Development of a robust and repeatable UPLC-MS method for the long-term metabolomic study of human serum. *Anal Chem*. 2009 Feb 15;81(4):1357-64.
- Zhang Y, Wang G, Huang Q et al. Organic solvent extraction and metabolomic profiling of the metabolites in erythrocytes. *J Chromatogr B Analyt Technol Biomed Life Sci* 2009; 877: 1751-1757.

Chapter 4: *In vivo* ageing of red blood cells

Contents

4.1 Red blood cell populations in freshly drawn blood: application of proteomics and metabolomics to a decades-long biological issue

The contents of this chapter report the contents of the the following publications by the candidate:

1. D'Alessandro A, Blasi B, D'Amici GM, Marrocco C, Zolla L.
Red blood cell populations in freshly drawn blood: application of proteomics and metabolomics to a decades-long biological issue
Blood Transfusion; 2012; doi:10.2450/2012.0164-11.
-

In silico predictions and cytosolic protein-protein interaction analyses helped us configuring the intertwinement of energy and anti-oxidant metabolic enzymes. In this view, we set up a targeted metabolic strategy to delve into red blood cell metabolism, in order to understand age-related changes to the “Omes” (namely proteome and metabolome) of senescent erythrocytes. In the present chapter, we describe how the application of proteomics and targeted metabolomics to density gradient-separated erythrocytes allowed us to conclude that *in vivo* ageing corresponds to a progressive loss of metabolic modulation, as far as it concerns both energy and redox metabolism.

4.1 Red blood cell populations in freshly drawn blood: application of proteomics and metabolomics to a decades-long biological issue

Overview of this section

Red blood cells are long known to be characterized by subsets of populations, which can be separated through Percoll density gradients.

In this study, we performed integrated flow-cytometry, proteomics and metabolomics analyses on five distinct red blood cell sub-populations, as obtained upon Percoll density gradient separation of freshly drawn leukocyte-depleted erythrocyte concentrates. The relation of density gradient fractions to cell age was confirmed through band 4.1a/4.1b assays.

We could observe a decrease in size and increase in cell rugosity in older (denser) populations. Metabolomics analysis of fraction 5 (the oldest population) evidenced a decrease of glycolytic metabolism and of the anti-oxidant defense-related mechanism, resulting in a decreased activation of the pentose phosphate pathway and lower accumulation of NADPH and reduced glutathione and increased levels of oxidized glutathione. These observations strengthen conclusions about the role of oxidative stress in the erythrocyte ageing in vivo, in analogy with recent in vitro studies.

On the other hand, no substantial proteomics changes were observed among fractions. This result was partly explained by intrinsic technical limitations of the 2DE approach and the likely clearance from the bloodstream of erythrocytes displaying membrane protein alterations. Conversely, this mechanism is absent in vitro (blood bank conditions), where proteomics has been reported to evidence substantial lesions targeting the membrane.

Finally, from this analysis it emerges that the three main red blood cell populations, accounting for over 92% of the total, are rather homogeneous soon after withdrawal. Major ageing-related alterations in vivo are likely to affect enzyme activities through post-translational mechanisms rather than the overall proteomics profile of red blood cells.

Keywords: red blood cell; population; density gradient; proteomics; metabolomics.

Introduction

Human red blood cells (RBCs) survive in peripheral circulation for approximately 120 days, while shelf life of erythrocyte concentrates stored under refrigeration is currently limited to 42 days (D'Alessandro et al., 2010).

Clearance of RBCs *in vivo* is the result of a series of progressive events which affect cell viability and lead to an “aberrant” senescent phenotype, resulting in rapid removal from the bloodstream via phagocytosis (for a detailed review about the hypothesized models of erythrocyte clearance through phagocytosis the interested reader is referred to Bratosin et al.)². Briefly, phagocytosis is mainly triggered and mediated by the membrane exposure of phosphatidylserine (PS), or rather by formation of hemichrome-induced band 3 clusters that are recognized by naturally occurring antibodies (Schroit et al., 1985; Lutz et al., 1988; Bratosin et al., 1998).

RBC senescence has been so far addressed through the isolation of RBC populations of different mean cell age. Most of the investigations have been performed with erythrocytes separated on the basis of differences in cell density or volume/size (Bosch et al., 1992; Connor et al., 1994). Among the most exploited techniques, only a handful has found an extensive application in basic science studies: plain centrifugation, angle-head centrifugation, and the use of several discontinuous gradients, including albumin and stractan, which resulted in a more or less efficient separation (Bosch et al., 1992). The use of Percoll has proven to be an easy preparative and efficient separation technique (Connor et al., 1992; Bosch et al., 1994). Nevertheless, it has been suggested that density is not a good criterion of RBC age and it has been proposed that separation exploiting differences in RBC volumes through counterflow centrifugation might yield better results. However, a direct comparative study has concluded that each separation approach holds specific advantages over the other and both are characterized by one major drawback, that is the poor yield (low RBC number) in every fractions. This issue has so far hampered untargeted strategies, which on the other hand have now enabled by the increased sensitivity and specificity of mass spectrometry analytical approaches for proteomics and metabolomics analyses (D'Alessandro and Zolla, 2010; D'Alessandro et al., 2011).

Studies have been reported over the years addressing the peculiar characteristics of RBC sub-populations, from younger to older fractions. RBC ageing has been reported to correlate with decreased cell volume, size and mean corpuscular volume (MCV) (Nash et al., 1980; Linderkamp et al., 1982; van Oss et al., 1982; Bosch et al., 1992), increased mean corpuscular hemoglobin concentration (MCHC – Bosch et al., 1992) and hemoglobin glycation (Hb1Ac) (Bunn et al., 1976), reduced 2,3-DiPhosphoGlycerate/hemoglobin ratios (Samaja et al., 1990) and cell deformability (Clark et al., 1983; Gifford et al., 2006), increased osmotic fragility (Rifkind et al., 1983) in consequence to the loss of electrolytes and microvesiculation (Dumaswala et al., 1984; Greenwal and Dumaswala, 1988). Other than PS membrane exposure (Bratosin et al., 1998) and increased Hb1Ac levels (Bunn et al., 1976), older RBCs also display higher creatine levels (Syllm-Rapoport et al., 1981).

Membrane-related alterations include PS exposure and decreased surface charge density (Bratosin et al., 1998), alteration of the membrane lipid content due to loss of sialic acid residues (Bartosz et al., 1984), susceptibility to phospholipase A2 (Shukla and Hanahan, 1982) and microvesiculation (Bartosz, 1990). Age-dependent change in lipid asymmetry correlates with the cells propensity to be cleared from the peripheral circulation and bind to autologous mononuclear cells *in vitro*. Indeed, it has been observed that membrane alterations result in increased

adhesiveness to endothelial and reticuloendothelial cells (Dhermy et al., 1987), changes in membrane cation transport (Hentschel et al., 1986) and decreased enzymatic activities (Jain, 1988), along with the accumulation of lipid peroxidation products (Jain, 1988). Most of these phenomena closely resemble apoptosis and have led to the formulation of the concept of eryptosis, an erythrocyte specific apoptotic phenomenon (Lang et al., 2008).

While alterations of RBC populations in membrane shape and lipid parameters have been widely investigated, other biologically relevant molecules, such as proteins and metabolites, are still poorly investigated in the frame of RBC ageing. This prompts considerations about the need to understand whether RBC ageing *in vivo* and *in vitro* (blood bank conditions) could be actually compared in order to grasp biologically relevant considerations through translation of results that have been obtained from application of omics strategies to transfusion medicine issues (D'Alessandro et al., 2012). Proteomics and metabolomics are two increasingly widespread “omics” strategies which exploit recent advancements in the fields of two-dimensional gel-electrophoresis (2DE), High Performance Liquid Chromatography (HPLC), mass spectrometry and bioinformatics, in order to assay qualitatively and quantitatively all the protein and metabolite complement to the genome in a given cell type in the very exact moment in which the analysis is performed.

It would be relevant to determine whether a correlation exists between the proteomics and metabolomics changes which have been observed in total RBC populations during aging (*in vitro*) (D'Alessandro et al., 2012) and the distribution of these alterations throughout the subsets of age-related erythrocyte fractions.

In this view, we performed integrated flow-cytometry, proteomics and metabolomics analyses on five distinct RBC sub-populations, as obtained upon Percoll density gradient separation of freshly drawn leukocyte-depleted erythrocyte concentrates. As a result, we could observe a decrease in size and increase in cell rugosity in older (denser) populations, which was not accompanied by substantial proteomics changes. Metabolomics analysis of fraction 5 (the oldest population) evidenced a decreased efficiency of the anti-oxidant defense-related mechanism, through a reduced activation of the pentose phosphate pathway (PPP) and lower accumulation of NADPH and reduced glutathione.

Finally, from this analysis it emerges that the great majority of RBC populations are rather homogeneous soon after withdrawal. This allows to conclude that there is no evident necessity to perform storage lesion-assessing studies on separated fractions, since a consistent percentage of the RBCs in the total populations belong to homogenous fractions as far as the proteome and metabolism are concerned.

Materials and Methods

Blood sampling

Whole blood (450 mL \pm 10%) was collected from healthy volunteer donors into CPD anticoagulant (63 mL). After separation of plasma and buffy coat by centrifugation, leukocyte-filtered RBCs were suspended in 100 mL of SAGM solution. Samples were collected from four RBC units withdrawn from four different donors (two male, two female, mean \pm SD age 48 \pm 11.5 years).

Percoll gradient

Density-fractionated RBCs were prepared using Percoll (Sigma-Aldrich, St. Louis, MO, USA) discontinuous gradients, as previously described (Vettore et al., 1980; Bosch et al., 1992). Briefly, the gradient was built up in five layers of 2 ml containing 80% (1.096 g/mL), 71% (1.087 g/mL), 67% (1.083 g/mL), 64% (1.080 g/mL) and 40% (1.060g/mL) Percoll, respectively, buffered with buffer A [26.3 g/L bovine serum albumin, 132 mmol/L NaCl, 4.6 mmol/L KCl, and 10 mmol/L HEPES pH 7.1]. RBCs were washed with buffer B [9 mmol/L Na₂HPO₄, 1.3 mmol/L NaH₂PO₄, 140 mmol/L NaCl, 5.5 mmol/L glucose, and 0.8 g/L bovine serum albumin] and diluted with 1 vol of buffer A. One-half milliliter of this suspension was layered on the Percoll gradient and separation was achieved after 15 minutes of centrifugation at 3000 rpm at room temperature. Fractions were collected by careful pipetting and extensively rinsed with buffer B to remove residual Percoll.

Flow cytometry assay

The five different erythrocytes populations were washed twice in 5 mmol/L phosphate buffer, pH 8.0, containing 0.9% (w/v) NaCl to remove Percoll and isolated by centrifuging twice at 1000 X g for 10 minutes at 4°C. Subsequently they were analyzed by flow cytometry with a sample of whole erythrocytes as control. The cells were monitored for their morphology with a FACScalibur (Becton-Dickinson, USA). Analysis was done using the Cellquest program on 10,000 events acquired without gating. Events were analysed by the following parameters: side scatter (SSC), forward scatter (FSC).

RBC membrane preparation

Extraction of human RBC membrane proteins was performed based on the conventional method as described by Olivieri and colleagues (2001) with some modifications. The five RBCs populations were washed twice in 5 mmol/L phosphate buffer, pH 8.0, containing 0.9% (w/v) NaCl to remove Percoll and isolated by centrifuging twice at 1000 X g for 10 minutes at 4°C. Lysis of RBCs were performed with 9 vol of cold 5 mmol/L phosphate buffer, pH 8.0, containing 1 mmol/L EDTA, 1 mmol/L phenylmethanesulfonyl fluoride. Membranes were collected by centrifugation at 17,000 X g for 20 minutes at 4°C and further washed until free of Hb. To remove nonspecifically membrane-bound cytosolic proteins, RBC membranes were further washed three times with 0.9% NaCl and collected by centrifugation at 17,000 X g for 20 minutes at 4°C. Protein content was estimated by the bicinchoninic acid method (Smith et al., 1985). Resulting membrane protein extracts were used for the subsequent analytical steps.

Determination of the band 4.1a/4.1b ratio

Membrane proteins run on SDS PAGE, as previously described (Alaia et al., 2009). Using Coomassie blue staining, bands 4.1a and 4.1b were quantified with a GS-800 calibrated densitometer (Bio-Rad Laboratories, Hercules, CA, USA), and the ratio 4.1a/4.1b was calculated.

2D IEF SDS-PAGE

To remove lipids, proteins were precipitated from a desired volume (containing 400 µg of proteins) of each sample with cold (4 °C) acetone (80% v/v) over-night, then centrifuged at 18000 g for 20 min. The supernatant was removed and the pellet was air-dried and then solubilized in the focusing solution 8 M urea, 2% (w/v) ASB-14, 0.5% (w/v) pH 3-10 carrier ampholyte (Bio-lyte; Bio-Rad, Hercules, CA, USA) and 40 mM Tris base with continuous stirring. Proteins were subsequently reduced (10 mM tributylphosphine, 1 h) and alkylated (40 mM IAA, 1h). To prevent over-alkylation, iodoacetamide (IAA) excess was destroyed by adding 10 mM DTE. IEF was performed using Biorad Multiphore II and Dry Strip Kit (Bio-Rad-Protean-IEF-Cell-System). Seventeen centimeter IPG strips (Bio-Rad, Hercules, CA, USA) pH 3-10 were rehydrated overnight with 345 µL of rehydration solution containing 8 M urea, 2% (w/v) ASB, 0.5% (w/v) pH 3-10 carrier ampholyte (Bio-lyte; Bio-Rad, Hercules, CA, USA), 10 mM DTE and 100µL of sample was loaded using the cup - loading method. The total product time × voltage applied was 80 000 V h for each strip at 20 °C. For the second dimension, IPG strips were incubated in the equilibration solution [6 M urea, 50 mM Tris-HCl (pH 6.8), 30% (v/v) glycerol, 3% (w/v) SDS, 0.002% (w/v) bromophenol blue] for 30 min with gentle agitation. Equilibrated strips were then placed on SDS-polyacrylamide gels, 16 cm × 20 cm, 11% acrylamide, and sealed with 0.5% (w/v) agarose. SDS-PAGE was performed using the Protean II xi Cell, large gel format (Bio-Rad) at constant current (35 mA per gel) at 7 °C until the bromophenol blue tracking dye was approximately 2-3 mm from the bottom of the gel. Protein spots were stained by Coomassie Brilliant Blue G-250 stain (Candiano et al., 2004).

Image analysis

Twenty stained gels (1 technical replicates x 4 biological replicates x 5 RBC fractions) were digitalized using an ImageScanner and LabScan software 3.01 (Bio-Rad Hercules, CA). It was not possible to perform more than 1 replicate per fraction per individual, as cell recovery and membrane extraction steps reduced the biological material available for 2DE analyses. The 2-DE image analysis was carried out and spots were detected and quantified using the Progenesis SameSpots software v.2.0.2733.19819 software package (Nonlinear Dynamics, New Castle UK). Each gel was analyzed for spot detection and background subtraction. Among-fractions comparisons were determined by ANOVA (Analysis of Variance) procedure in order to classify sets of proteins that showed a statistically significant difference with a confidence level of 0.05. All statistical analyses were performed with the Progenesis SameSpots software v.2.0.2733.19819 software package. After the background subtraction, spot detection and match, one standard gel was obtained for each group (RBC fractions) through normalization of the biological replicates. These standard gels were then matched to yield information about the spots of differentially modulated proteins. Differentially modulated protein spots were considered significant at p-value < 0.05 and the change in the photodensity of protein spots among fractions had to be more than 2 fold. Owing to the impossibility to perform technical replicates for each fraction due to scarce amounts of membrane protein material, we further performed a Bonferroni post-test to exclude false positive results.

Metabolomics

Samples containing 5×10^5 cells from each separated fraction were extracted following the protocol by D'Alessandro et al. (2011). Briefly, For each sample, 0.5mL from the pooled erythrocyte stock was transferred into a microcentrifuge tube (Eppendorf ® Germany). Erythrocyte samples were then centrifuged at 1000g for 2 minutes at 4°C. Tubes were then placed on ice while supernatants were carefully aspirated, paying attention not to remove any erythrocyte at the interface. Samples were extracted following the protocol by D' Alessandro et al.³⁴. The erythrocytes were resuspended in 0.15 mL of ice cold ultra-pure water (18 MΩ) to lyse cell, then the tubes were plunged into a water bath at 37°C for 0.5 min. Samples were mixed with 0.6 mL of -20°C methanol and then with 0.45 mL chloroform. Subsequently, 0.15ml of ice cold ultra-pure water were added to each tube and they were transferred to -20°C freezer for 2-8 h. An equivalent volume of acetonitrile was added to the tube and transferred to refrigerator (4°C) for 20 min. Samples with precipitated proteins were thus centrifuged for 10000 x g for 10 min at 4 °C .

Finally, samples were dried in a rotational vacuum concentrator (RVC 2-18 - Christ GmbH; Osterode am Harz, Germany) and re-suspended in 200 µl of water, 5% formic acid and transferred to glass auto-sampler vials for LC/MS analysis.

Rapid Resolution Reversed-Phase HPLC

An Ultimate 3000 Rapid Resolution HPLC system (LC Packings, DIONEX, Sunnyvale, USA) was used to perform metabolite separation. The system featured a binary pump and vacuum degasser, well-plate autosampler with a six-port micro-switching valve, a thermostated column compartment. A Dionex Acclaim RSLC 120 C18 column 2.1mm×150mm, 2.2 µm was used to separate the extracted metabolites. Acetonitrile, formic acid, and HPLC-grade water, purchased from Sigma Aldrich (Milano, Italy). LC parameters: injection volume, 20 µL; column temperature, 30°C; and flowrate of 0.2 mL/min. The LC solvent gradient and timetable were identical during the whole period of the analyses. A 0–95% linear gradient of solvent A (0.1% formic acid in water) to B (0.1% formic acid in acetonitrile) was employed over 15 min followed by a solvent B hold of 2 min, returning to 100% A in 2 minutes and a 6-min post-time solvent A hold.

ESI Mass Spectrometry

Metabolites were directly eluted into a High Capacity ion Trap HCTplus (Bruker-Daltonik, Bremen, Germany). Mass spectra for metabolite extracted samples were acquired in positive and negative ion mode, as previously described.³⁴ ESI capillary voltage was set at 3000V in (+) ion mode. The liquid nebulizer was set to 30 psig and the nitrogen drying gas was set to a flow rate of 9 L/min. Dry gas temperature was maintained at 300°C. Internal reference ions were used to continuously maintain mass accuracy. Data were acquired at a rate of 5 spectra/s with a stored mass range of m/z 50–1500. Data were collected using Bruker Esquire Control (v. 5.3 – build 11) data acquisition software. In MRM analysis, m/z of interest were isolated, fragmented and monitored (either the parental and fragment ions) throughout the whole RT range. Validation of HPLC on-line MS-eluted metabolites was performed by comparing transition fingerprints, upon fragmentation and matching against the standard metabolites

through direct infusion with a syringe pump (infusion rate 4 $\mu\text{l}/\text{min}$). Standard curve calibrations were performed either on precursor and fragment ion signals. Only the former were adopted for quantitation, as precursor ion signals guaranteed higher intensity and thus improved limit of detection (LOD) and quantitation of metabolites of interest.³⁴ However, transitions were monitored in independent runs to validate each detected metabolite.

Metabolite analysis and data elaboration

Quantitative analyses of standard compounds were performed on MRM data against comparison to standard metabolite runs. Each standard compound was weighted and dissolved in nanopure water (18 m Ω). Calibration curves were calculated as previously reported (D'Alessandro et al., 2011). In brief, each standard metabolite was run in triplicate, at incremental dilution until limit of detection LOD was reached. The LOD for each compound was calculated as the minimum amount injected which gave a detector signal response higher than three times the noise ($S/N > 3$).

Standards (equal or greater than 98% chemical purity) D-fructose and D-glucose 6-phosphate (G6P/F6P), D-fructose 1,6 biphosphate (FDP), glyceraldehyde phosphate (G3P), 1,3 and 2,3 diphosphoglycerate (DPG), phosphoenolpyruvic acid (PEP), L-lactic acid (LA), NADPH, 6-phosphogluconic acid (6PG), ATP, NADH, glutathione (GSH), oxidized glutathione (GSSG), glutamine (GLTM) and glutamate (GLUT) were purchased from Sigma Aldrich (Milan).

Standards were stored either at -25°C , 4°C or room temperature, following manufacturer's instructions.

LC/MS data files were processed by Bruker DataAnalysis 4.0 (build 234) software.

Results were plotted with GraphPad Prism 5.0 (GraphPad Software Inc.) as fold-change variations values upon normalization of the results obtained among the five fractions for each independent metabolite, as in D'Alessandro et al. (2012) and Nishino et al. (2009).

Results and Discussion

RBC ageing *in vivo* is a highly investigated topics in biological research, as erythrocytes are largely available and substantially less complex than most other cellular biological matrices (Shinozuka et al., 1994). Researchers have at first addressed the main alterations influencing RBCs as they age in blood vessels, including altered membrane sialiation, appearance of band-3 dimer neopitopes at the membrane, shape alterations (decreased size and surface/volume ratios), as it has been extensively reviewed (the interested reader is referred to Shinozuka for further details) (Shinozuka et al., 1994). Biochemical studies have been performed over the last decades in order to shed light on the observed increase in MCHC and MCH in older cells, as well as slightly increased oxygen affinity and altered enzymatic activities (Shinozuka et al., 1994). However, most of the information collected so far were related to alterations to single parameters, while to the best of the Authors' knowledge no untargeted "omics" study has been reported so far.

In the present study, we performed flow-cytometry, proteomics and metabolomics investigations on Percoll density gradient fractionated RBCs.

Percoll density gradients allowed us to separate five distinct populations (**Figure 1**) from freshly withdrawn blood from healthy donor volunteers, upon separation of erythrocytes from whole blood through centrifugation and leukofiltration. It has already been reported that, depending on the density gradient ladder, it is possible to obtain from four to nine distinct populations (Salvo et al., 1982; Mosca et al., 1991; Connor et al., 1992; Bosch et al., 1994).

It is long known that denser populations correspond to older RBCs (Bosch et al., 1994). The causes of the altered hydrodynamic density of older RBCs have been only postulated to depend on membrane lipid scrambling resulting in shape alterations (Clark et al., 1983; Gifford et al., 2006) and/or altered hemoglobin/water ratios due to unbalanced loss of the latter during life of erythrocytes (Vaughn et al., 1992). Fraction density relation to age was further confirmed through monitoring the band 4.1a/4.1b ratio via 1D-SDS-PAGE (**Figure 1**). The ratio between the amounts of the proteins band 4.1 and 4.1b is known to increase proportionally to age (Inaba et al., 1988). This phenomenon has been reported to occur in several mammals and has been related deamidation of Asn 478 and 502 of the band 4.1b protein which results in altered electrophoretic mobility and thus different apparent molecular weight in SDS-PAGE runs (Inaba et al., 1992).

Upon Percoll gradient separation, distribution of RBC populations was largely biased towards the youngest population (less dense, fraction 1 in **Figure 1**), the abundance of which was significantly higher than the other ones (cell recovery for this fraction was $63.29 \pm 14.31\%$ of the total – **Figure 1**). Taken together, the three upper (least dense) bands accounted for > 92% of the total RBC populations, while the denser/older populations represented only a minoritarian percentage, especially as far as the densest/oldest and barely visible fraction 5 was concerned (approximately 2% of the total).

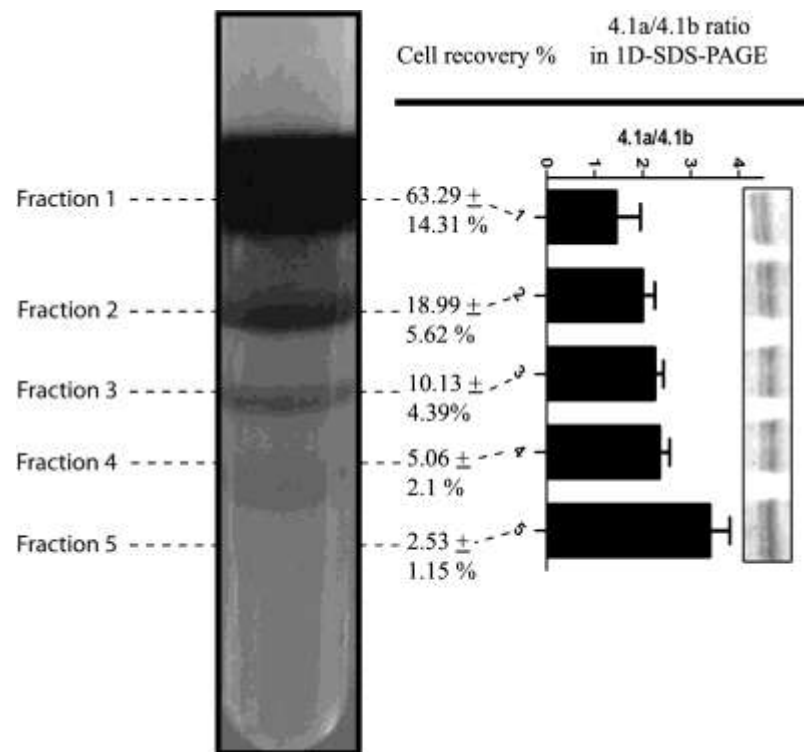


FIGURE 1 Percoll density gradient of freshly drawn, leukocyte-filtered, red blood cell concentrates. Five distinct populations are visible, which are numbered from top to bottom. The gradient was prepared as to stack layers of different densities, in agreement with Bosch et al. (2006) : 1.096 g/mL, 1.087 g/mL, 1.083 g/mL, 1.080 g/mL and 1.060g/mL. Cell recovery percentages are reported for each fractions as means \pm SD (total = 100%). In the right panel, the graph reports densitometric analysis for the band 4.1a/4.1b ratio from the 1D-SDS-PAGE runs for each distinct population.

While it has been reported in the literature that Percoll separation might hold some limitations and thus does not necessarily yield RBCs which are also separated in size (Bosch et al., 1994), in the present study we could confirm through flow cytometry that differences existed in volumes (forward scattering - FS) and membrane rugosity (side scattering - SS) among the five different fractions (**Figure 2**). In particular, older cell fractions displayed higher rugosity (SS distributions moved upwards from fraction 1 to 5 – **Figure 2**) and lower cell volume (FS distributions moved leftwards to the vertical axis from fraction 1 to 5 – **Figure 2**), as we should have expected (Nash et al., 1980; Linderkamp and Meiselman, 1982; van Oss, 1982; Clark et al., 1983; Gifford et al., 2006). A decrease in cell size and increase in cell rugosity has been so far related to progressive dehydration (Waugh et al., 1992), alterations to the membrane shape deriving from membrane shedding through vesiculation (Dumaswala et al., 1984; Greenwalt and Dumaswala, 1984; Bartosz, 1981), membrane lipid scrambling (Clark et al., 1983; Schroit et al., 1985; Gifford et al., 2006) and sub-sequent increase in osmotic fragility in consequence to a decreased surface/volume ratio¹⁶ upon acquisition of a spherocytocyte/spherocyte shape (Vettore et al., 1980; Shinozuka et al., 1988).

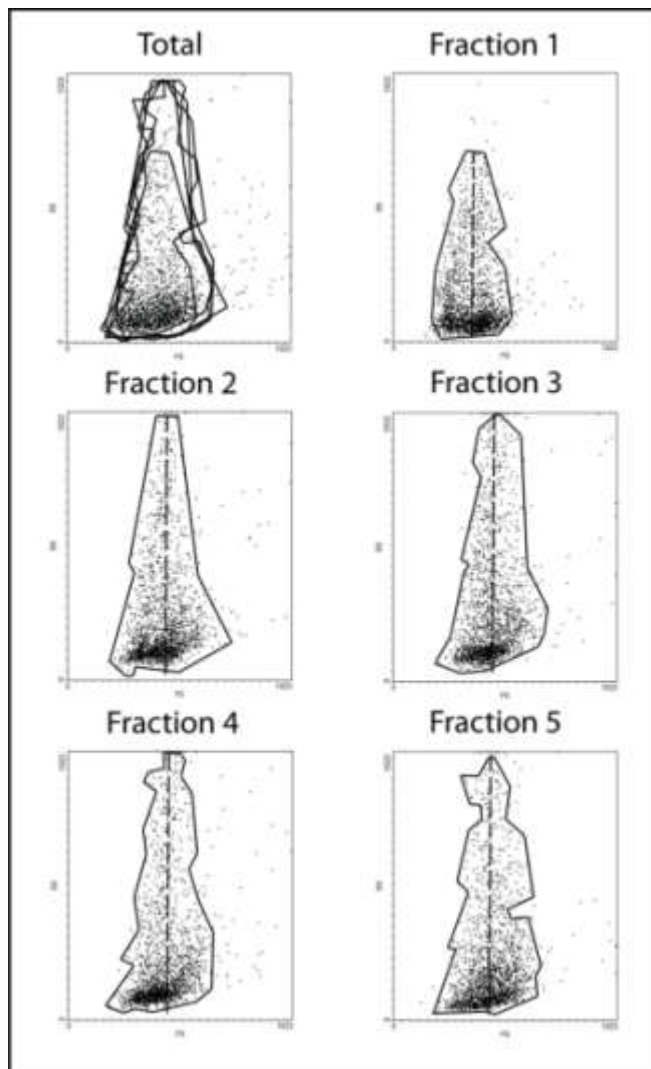


FIGURE 2 Flow cytometry analysis displaying forward scattering (FS) and side scattering (SS) on the x and y axis, respectively, for the total red blood cell population (upper left frame) and for each one of the five fractions, as labeled. Each population has been delimited into a shape enclosing >95% of the countered events, and then overlapped in the frame labeled as Total (upper left corner). As it emerges from this analysis, fractions from 2 to 5 display higher SS in comparison to fraction 1. The core of events is countered with a homogeneous distribution for fraction 1 as far as FS is concerned. For the other fractions, FS events are mainly shifted leftwards from the main axis (dotted line).

The trends for FS decrease and SS increase from **Figure 2** are particularly evident despite the limited number of events (10,000) recorded through flow cytometry. Indeed, this minor technical limitation, which did not hamper us to draw conclusions in line with literature, was mainly due to the poor recovery rate of cells from Percoll fractions. Since flow cytometry assays were planned only to confirm the quality of our separation in agreement with published literature, we decided to limit the extent of this part of the experimental workflow while looking for a compromise which might have guaranteed us the most meaningful information. On the other hand the main goal of the present study was to exploit the exact same samples in order to carry on multiple “omics” investigations, such as proteomics and metabolomics, the former being extremely demanding in terms of samples needed to perform the analyses.

No proteome targeting study has been reported so far in the frame of RBC aging *in vivo*, except for 1D-SDS-PAGE-based investigations (Suzuki et al., 1989; Keegan et al., 1992; Minetti et al., 2001), while recent literature delivered a consistent body of evidences cataloguing the protein-targeting storage lesions in *in vitro* (blood-bank conditions) refrigerated models (Bosman et al., 2008; Lion et al., 2010; Antonelou et al., 2010; D’Alessandro et al., 2012). The question is whether it is possible to assimilate the 120 days of life-span *in vivo* with the 42 days shelf-life *in vitro*, as it has already been reviewed in recent years (Bosman et al., 2010).

In the present study, we could not observe any significant ($p < 0.05$ ANOVA; fold-change variation > 2) difference among spots (number of spots and spot intensities) from 2-DE electrophoresis of membrane proteins of RBCs from the five fractions (**Figure 3**). However the overall number of spots detected through Coomassie staining in the total population (136 ± 16 spots) was always higher than in each subfraction (fraction 1= $118 + 10$; fraction 2= $109 + 26$; fraction 3= $116 + 12$; fraction 4= $111 + 14$; fraction 5= $125 + 14$). Nevertheless, due to the scarce technical reproducibility and the intrinsic limitations of the 2DE approach, we were not able to individuate spots whose apparent amounts were modulated in a statistically significant fashion. While it was to be expected that only few proteins (band 4.1a/4.1b; glycated hemoglobin) should significantly vary in the frame of RBC subpopulations, as it emerged from previous 1D-SDS-PAGE approaches (Suzuki et al., 1989; Keegan et al., 1992; Minetti et al., 2001), it hereby appears technically difficult to unravel these finely tuned alterations in RBC proteins through 2DE approaches. One main technical limitation is characterized by the poor membrane protein recovery, which is also a function of cell fraction recovery, and results hampering the possibility to perform further technical replicates, thus affecting statistical analyses and forcing us to run stringent post-test analyses in order to exclude false positive results. Therefore, since our impossibility to individuate statistically significant results might be attributed either to biological or technical variability, affecting statistical outcomes, further studies are mandatory to better understand whether differences are actually minimal or they are only difficult to be highlighted. Taken together, these considerations further stress the recent conclusion about 1D-SDS-PAGE still representing a reliable analytical approach despite the introduction of a wide number of gel-based techniques over the last forty years (Cottingham, 2010).

On the other hand, RBC membrane alterations have been reported to be irreversible in long-term SAGM-stored erythrocytes under blood bank conditions (D’Alessandro et al., 2012). It is rather likely that these RBC membrane protein lesions also arise in older RBC populations *in vivo*, although at this very stage RBCs might be promptly cleared from the bloodstream and be no longer present, or be present in traces, in freshly withdrawn blood. In other

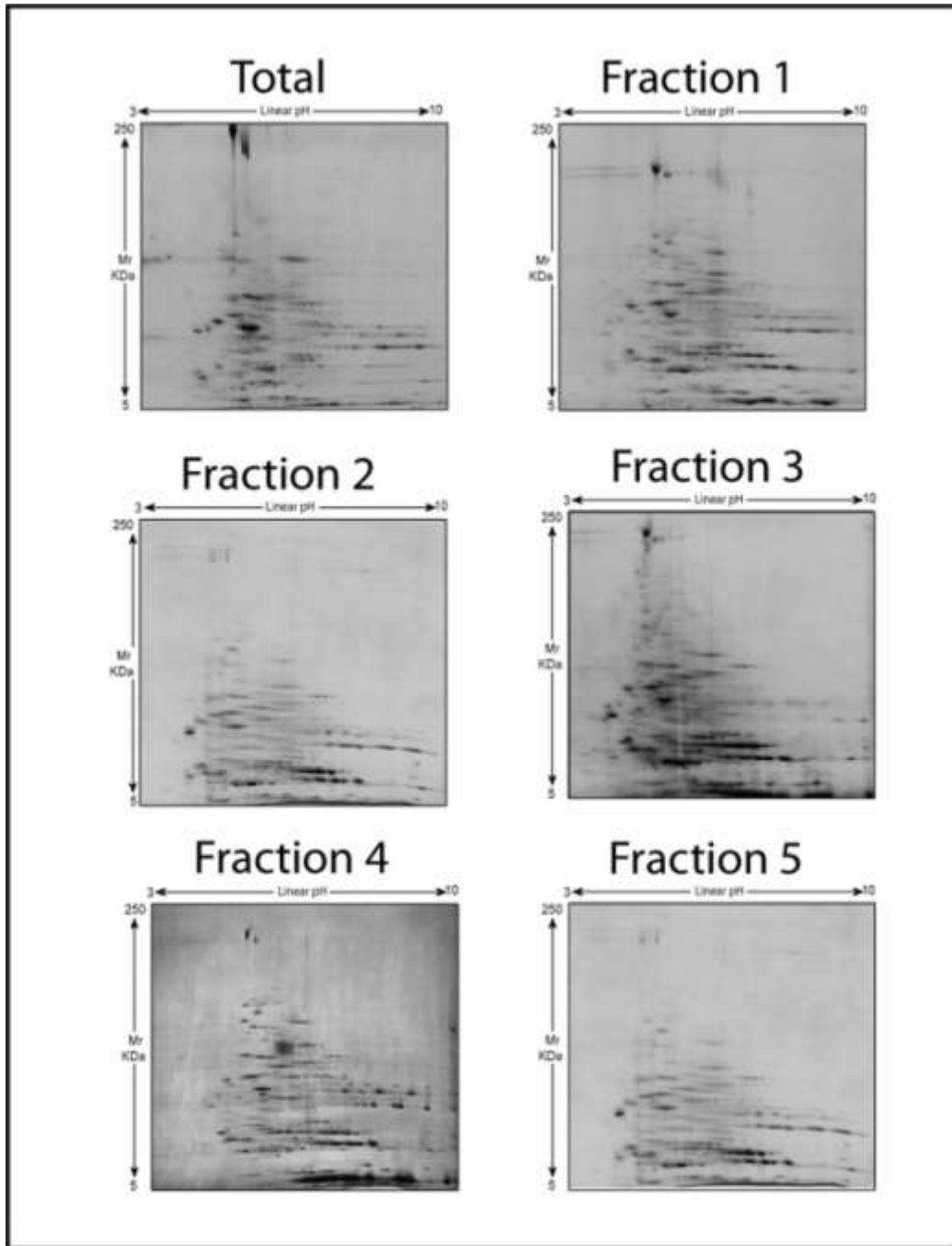


FIGURE 3 Two-dimensional gel electrophoresis of freshly withdrawn red blood cells upon separation into five distinct populations through Percoll density gradient. First dimension IEF *pI* values linearly span between 3 and 10, while MW are indicated in the left.

terms, a closed system like a stored RBC unit allows to push the model to its limits, while *in vivo* ageing in healthy subjects results in a continuous turn-over hampering the observation of extreme phenotypes at the proteome level.

While RBC membrane proteome-targeting lesions are known to occur on average from day 21 onwards *in vitro* (blood banking conditions) (D'Alessandro et al., 2012), RBCs stored under refrigeration are known to suffer from early age-related symptoms of reduced cell integrity which affect RBC metabolism (Nishino et al., 2009; Bennet-Guerrero et al., 2009; D'Alessandro et al., 2012).

The rationale behind our simultaneous investigation on the RBC membrane proteome and metabolism stems from previous observations about the strong intertwinement between glycolytic rate and the oxygen-dependent binding of glycolytic enzymes to the cytosolic domain of band 3, the most abundant integral membrane protein in RBCs (Campanella et al., 2005; Castagnokla et al., 2010). While we could not observe significant proteomics differences among subpopulations at the membrane level, a limited, albeit biologically meaningful, number of changes are known to occur in senescent erythrocytes (Suzuki et al., 1989).

In the frame of *in vivo* ageing, RBC metabolism has been studied only by addressing enzyme activities, phosphate intermediates (ATP, 2,3-DPG) or creatine (Nakao et al., 1962; Rennie et al., 1979; Vettore et al., 1980; Strange et al., 1982; Jansen et al., 1985; Suzuki and Dale, 1988; Dale et al., 1989; Mosca et al., 1991; Romero and Romero, 2004; Brajovich et al., 2009; Conversely to proteome-targeting studies, few - albeit relevant - information is available in the context of RBC metabolic fluxes as cell age in *in vivo* conditions. It has indeed been reported that the activities of the main rate-limiting enzymes of glycolysis, among which hexokinase, glucose 6-phosphate dehydrogenase and pyruvate kinase, decrease in Percoll density gradient-separated older RBC populations (Bennet-Rennie et al., 1979; Guerrero et al., 2009). This is consistent with the increased alkalosis (in older RBCs pH is higher by 0.2 units on average) and decreased organic phosphate compounds contents, both positively influencing hemoglobin affinity for oxygen and thus resulting in a theoretically reduced capacity of older RBCs to oxygenate peripheral tissues (Romero and Romero, 2004). For ATP and 2,3-DPG it has been reported that older cells do contain approximately 76 to 79% of the amounts detected in younger populations (Nakao et al., 1962; Vettore et al., 1980). In the present investigation, we could confirm the same trends for ATP, as levels detected in fraction 5 corresponded to 0.781 of the normalized group (values for ATP and other metabolites are reported as means \pm SD of fold-change variations against inter-fractions normalizations for each tested individual - **Figure 4**). Interestingly enough, through direct assay of a handful of glycolytic metabolic intermediates such as G6P/F6P, FBP, G3P, PEP and LH, we could evidence a general trend leading to gradual decrease of the contents of these metabolites in older populations (especially from fractions 4 and 5) in comparison to fraction 1 and to fractions 2 to 3 (**Figure 4** – upper panel). The most significant of these alterations influenced G6P/F6P levels, which were cut by half in fraction 5 in comparison to fraction 1, in agreement with the reports about a decreased hexokinase activity in older populations (Jansen et al., 1985).

The age-related decline in enzymatic activities has been also shown to involve a series of enzymes including GSH-transferase (Jansen et al., 1985), glucose 6-phosphate dehydrogenase and 6-phosphogluconate dehydrogenase (Strange et al., 1982), which are related to anti-oxidant stress responses, through the activation of the PPP, production of reducing intermediates such as NADPH, regeneration of GSH levels from GSSG and reduction of

oxidized anti-oxidant defense proteins, such as superoxide dismutases (SODs) (D'Alessandro et al., 2011). On the other hand, only GSH levels have been assayed in younger and older populations so far (Sass et al., 1965), which resulting in evidencing a trend toward decrease proportional to RBC age.

In the present study, we could confirm this trend (**Figure 4** – lower panel), through a substantial decrease in GSH levels from fraction 1 to fraction 2 and from fraction 2 to the other fractions. Besides, we could evidence a substantial increase in oxidized glutathione (GSSG) levels in fraction 3 and 4, in comparison to the first 3 fractions. As far as the PPP is concerned, fraction 1 displayed significantly higher ($p < 0.01$ ANOVA) fold change variation in G6P levels, while 6PG was rather homogeneous in all the tested populations (though still approximately 10% higher in fraction 1) (**Figure 4** – central panel). NADPH is a reduced intermediate of the oxidative phase of the PPP which is required for reduction of GSSG to GSH and for restoring of the activity of several anti-oxidant enzymes, including glutathione peroxidase. From our analyses it emerged a net decrease of NADPH from fraction 1 to fraction 2 and, consistently, in all the other fractions (**Figure 4** – central panel). Finally, since GSH is tripeptide of glutamate (GLUT), glycine and cysteine, reduced levels of GSH might be affected by the observed decrease in GLUT levels from fraction 1 to fraction 4 and 5, other than by the already mentioned enzymatic issues (Strange et al., 1982).

It is worthwhile to stress that analogous results have been obtained from the analysis of *in vitro* ageing of RBCs under blood bank condition (refrigerated storage in CPD-SAGM-containing plastic bags at 4°C), where early accumulating storage lesions affect metabolic fluxes of RBCs through a decrease in glycolytic rates and increase of the PPP from day 14 onwards, while reaching unsustainable levels of oxidation from day 28 onwards (D'Alessandro et al., 2012). Furthermore, it is notable enough that measurable alterations of the normal metabolic fluxes occur prior to any evident alteration of the proteome machinery either *in vitro* (D'Alessandro et al., 2012) or *in vivo* (present study).

Through the present metabolomics analyses we could provide confirmatory evidence of the theory relating RBC ageing, either *in vitro* (D'Alessandro et al., 2012) or *in vivo* (present study), to an exacerbation of the oxidative stress and a decreased capacity of RBCs to cope with it (D'Alessandro et al., 2010; Kaniyas and Acker, 2010; Antonelou et al., 2010; D'Alessandro et al., 2012). Anti-oxidant defenses represent the central core of protein activities in RBCs as proteins involved in these phenomena are direct or indirect interactors of the great majority of the residual proteome (D'Alessandro et al., 2010).

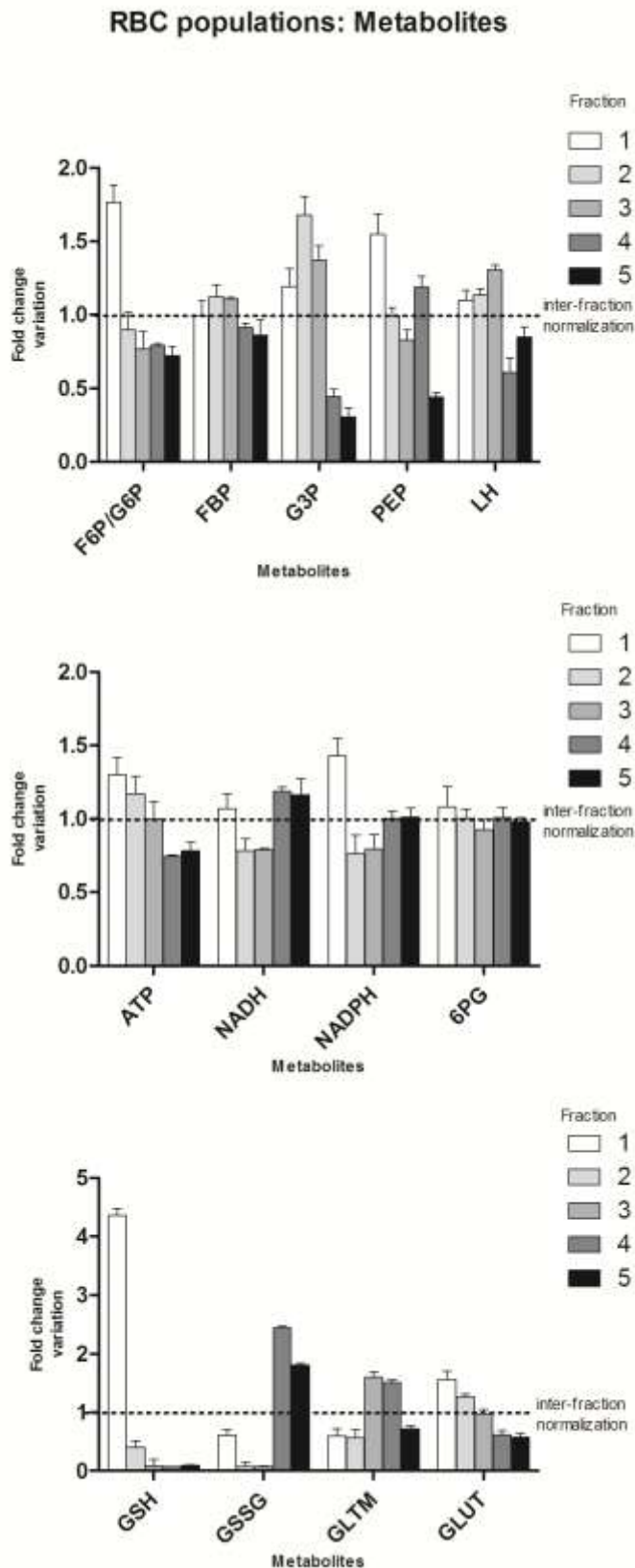


FIGURE 4 Time course metabolomic analyses of leukocyte-filtered red blood cell concentrates, upon separation through Percoll density gradient. Internal normalization has been performed against the average value for each metabolite among the five distinct populations for all the tested individuals (results are plotted as means \pm SD).

Abbreviations: F6P/G6P = fructose/glucose 6-phosphate; FBP = fructose 1,6 biphosphate; G3P = glyceraldehyde 3-phosphate; PEP = phosphoenolpyruvate; LH = lactate; ATP = adenosine triphosphate; NADH = reduced nicotinamide adenine dinucleotide; NADPH = nicotinamide adenine dinucleotide phosphate; PG = 6-phosphogluconate; GSH = reduced glutathione; GSSG = oxidized glutathione; GLTM = glutamine; GLUT = glutamate.

Conclusion

In the present study, we performed an integrated flow cytometry, proteomics and metabolomics study to investigate the differences among RBC populations from leukocyte-filtered erythrocyte concentrates as obtained from freshly drawn blood and Percoll density gradient separation.

We could confirm the efficiency of the separation process through flow cytometry, which evidenced a decrease in cell size and increase in rugosity, probably due to the accumulation of membrane shape alterations, as previously reported.^{6,9-11,14,15}

Proteomics analyses did not allow us to evidence any substantial difference among RBC fractions. This might be mainly due to i) the likely clearance from the bloodstream of those RBCs displaying altered membrane protein profiles and/or ii) to the difference between the models of RBCs ageing *in vivo* when compared against *in vitro* (blood banking conditions) models,²⁸ where stresses to RBCs tend to accumulate, since oxidative stress and reactive oxygen radical species are catalytic processes, thus allowing the investigations of extreme conditions as well.

We could compare alterations of the RBC metabolic fluxes in different fractions to the metabolic storage lesions arising yet at the early stages of RBC storage under blood banking conditions,²⁸ and thus conclude that oxidative stress seems to represent the leading cause of RBC senescent phenotype also *in vivo*.^{28,48,65,66}

On the other hand, the observations that the two main diverging RBC fractions accounted for less than 8% of the total original populations, prompted us to conclude that the great majority of RBCs from freshly withdrawn blood undergoing treatment for blood banking in transfusion settings is to be considered as homogeneous. This consideration underpins the statement that, when planning studies to assess RBC storage lesions for transfusion purposes, it appears that fractionation of RBCs into distinct populations should not be a mandatory step, as more than 92% of the total population displays homogeneous properties. Indeed, previous studies have already reported that only RBCs from the oldest (gerocytes) and youngest (neocytes) subpopulations are differentially affected by storage conditions.^{43,44} This prompts two main considerations: (i) alternative mechanisms (cationic dysregulation, for example⁴³) affect RBC survival *in vitro* which are not necessarily the same as *in vivo* ageing; (ii) changes affecting youngest RBC subpopulations are also the ones targeting a substantial percentage (from 65 to 92 %) of the whole unfractionated RBC population, which makes it statistically likely that most of the observations so far reported on unfractionated RBCs mainly reflect molecular lesions to the most abundant fractions.

In the near future, it would be worth exploring the changes to these very same parameters (flow cytometry, proteomics, metabolomics on Percoll density gradient separated fractions) in those scenarios where RBCs are partially compromised by genetic defects (e.g. glucose 6-phosphate dehydrogenase deficiency, beta thalassemia) or diseases (for example, malaria), other than further delving into the storage issue.

References

- Alaia V, Frey BM, Siderow A, Stammli P, Kradolfer M, Lutz HU. A pair of naturally occurring antibodies may dampen complement-dependent phagocytosis of red cells with a positive antiglobulin test in healthy blood donors. *Vox Sang*. 2009; 97(4):338-47.
- Antonelou MH, Kriebardis AG, Stamoulis KE, Economou-Petersen E, Margaritis LH, Papassideri IS. Red blood cell aging markers during storage in citrate-phosphate-dextrose-saline-adenine-glucose-mannitol. *Transfusion*. 2010; 50(2):376-89.
- Bartosz G, Grzelinska E, Bartkowiak A. Aging of the erythrocyte. XIX. Decrease in surface charge density of bovine erythrocytes. *Mech Ageing Dev*. 1984; 24(1):1-7.
- Bartosz G. Aging of the erythrocyte. IV. Spin-label studies of membrane lipids, proteins and permeability. *Biochim Biophys Acta*. 1981 Jun 9;644(1):69-73.
- Bartosz, G. (1990) *Blood Cell Biochemistry: Erythroid Cells* (Harris, J. R., ed) Vol. 1, pp. 45-79, Plenum Press, New York
- Bennett-Guerrero E, Stafford-Smith M, Waweru PM, Bredehoeft SJ, Campbell ML, Haley NR, et al. A prospective, double-blind, randomized clinical feasibility trial of controlling the storage age of red blood cells for transfusion in cardiac surgical patients. *Transfusion*. 2009; 49(7):1375-83.
- Bosch FH, Werre JM, Roerdinkholder-Stoelwinder B, Huls TH, Willekens FL, Halie MR. Characteristics of red blood cell populations fractionated with a combination of counterflow centrifugation and Percoll separation. *Blood*. 1992; 79(1):254-60.
- Bosman GJ, Lasonder E, Groenen-Döpp YA, Willekens FL, Werre JM, Novotný VM. Comparative proteomics of erythrocyte aging in vivo and in vitro. *J Proteomics*. 2010; 73(3):396-402.
- Bosman GJ, Lasonder E, Luten M, Roerdinkholder-Stoelwinder B, Novotný VM, Bos H, De Grip WJ. The proteome of red cell membranes and vesicles during storage in blood bank conditions. *Transfusion*. 2008; 48(5):827-35.
- Brajovich ML, Rucci A, Acosta IL, Cotruello C, García Borrás S, Racca L, Biondi C, Racca A. Effects of aging on antioxidant response and phagocytosis in senescent erythrocytes. *Immunol Invest*. 2009; 38(6):551-9.
- Bratosin D, Mazurier J, Tissier JP, Estaquier J, Huart JJ, Ameisen JC, Aminoff D, Montreuil J. Cellular and molecular mechanisms of senescent erythrocyte phagocytosis by macrophages. A review. *Biochimie*. 1998;80(2):173-95.
- Bunn HF, Haney DN, Kamin S, Gabbay KH, Gallop PM. The biosynthesis of human hemoglobin Alc. Slow glycosylation of hemoglobin in vivo. *J Clin Invest* 1976; 57:1652-9.
- Campanella E, Chu H, Low PS. Assembly and regulation of a glycolytic enzyme complex on the human erythrocyte membrane. *PNAS* 2005; 102(7):2402-7.
- Candiano G, Bruschi M, Musante L, et al. Blue silver: a very sensitive colloidal Coomassie G-250 staining for proteome analysis. *Electrophoresis* 2004; 25: 1327-33.
- Castagnola M, Messana I, Sanna MT, Giardina B. Oxygen-linked modulation of erythrocyte metabolism: state of the art. *Blood Transfus* 2010;8(3): 53-8.
- Clark MR, Mohandas N, Shohet SB. Osmotic gradient ektacytometry: comprehensive characterization of red cell volume and surface maintenance. *Blood*. 1983; 61(5):899-910.
- Connor J, Pak CC, Schroit AJ. Exposure of phosphatidylserine in the outer leaflet of human red blood cells. Relationship to cell density, cell age, and clearance by mononuclear cells. *J Biol Chem*. 1994; 269(4):2399-404.
- Cottingham K. IDE proves its worth... again. *J Proteome Res*. 2010;9(4):1636.
- Dale GL, Norenberg SL, Suzuki T, Forman L. Altered adenine nucleotide metabolism in senescent erythrocytes from the rabbit. *Prog Clin Biol Res* 1989;319:259-69.
- D'Alessandro A, D'Amici GM, Vaglio S, Zolla L. Time-course investigation of SAGM-stored leukocyte-filtered erythrocyte concentrates: from metabolism to proteomics. *Haematologica*. 2012; 97(1):107-15.
- D'Alessandro A, Gevi F, Zolla L. A robust high resolution reversed-phase HPLC strategy to investigate various metabolic species in different biological models. *Mol Biosyst*. 2011; 7(4):1024-32.
- D'Alessandro A, Gevi F, Zolla L. A robust high resolution reversed-phase HPLC strategy to investigate various metabolic species in different biological models. *Mol Biosyst*. 2011; 7(4):1024-32.
- D'Alessandro A, Liumbruno G, Grazzini G, Zolla L. Red blood cell storage: the story so far. *Blood Transfus*. 2010;8(2):82-8.
- D'Alessandro A, Righetti PG, Zolla L. The red blood cell proteome and interactome: an update. *J Proteome Res*. 2010; 9(1):144-63.

- D'Alessandro A, Zolla L. Proteomics for quality-control processes in transfusion medicine. *Anal Bioanal Chem.* 2010; 398(1):111-24.
- D'Alessandro A, Zolla L. The SODyssey: superoxide dismutases from biochemistry, through proteomics, to oxidative stress, aging and nutraceuticals. *Expert Rev Proteomics.* 2011; 8(3):405-21.
- Dhermy D, Simeon J, Wautier MP, Boivin P, Wautier JL. Role of membrane sialic acid content in the adhesiveness of aged erythrocytes to human cultured endothelial cells. *Biochim Biophys Acta.* 1987; 904(2):201-6.
- Dumaswala UJ, Greenwalt TJ. Human erythrocytes shed exocytic vesicles *in vivo*. *Transfusion.* 1984; 24(6):490-2.
- Gifford SC, Derganc J, Shevkopyas SS, Yoshida T, Bitensky MW. A detailed study of time-dependent changes in human red blood cells: from reticulocyte maturation to erythrocyte senescence. *Br J Haematol.* 2006; 135(3):395-404.
- Greenwalt TJ, Dumaswala UJ. Effect of red cell age on vesiculation *in vitro*. *Br J Haematol.* 1988; 68(4):465-7.
- Hentschel WM, Wu LL, Tobin GO, Anstall HB, Smith JB, Williams RR, Ash KO. Erythrocyte cation transport activities as a function of cell age. *Clin Chim Acta.* 1986; 157(1):33-43.
- Inaba M, Gupta KC, Kuwabara M, Takahashi T, Benz EJ Jr, Maede Y. Deamidation of human erythrocyte protein 4.1: possible role in aging. *Blood.* 1992;79(12):3355-61.
- Inaba M, Maede Y. Correlation between protein 4.1a/4.1b ratio and erythrocyte life span. *Biochim Biophys Acta.* 1988;944(2):256-64
- Jain SK. Evidence for membrane lipid peroxidation during the *in vivo* aging of human erythrocytes. *Biochim Biophys Acta.* 1988; 937(2):205-10.
- Jansen G, Koenderman L, Rijkse G, Cats BP, Staal GE. Characteristics of hexokinase, pyruvate kinase, and glucose-6-phosphate dehydrogenase during adult and neonatal reticulocyte maturation. *Am J Hematol.* 1985; 20(3):203-15.
- Kanias T, Acker JP. Biopreservation of red blood cells--the struggle with hemoglobin oxidation. *FEBS J.* 2010; 277(2):343-56.
- Keegan TE, Heaton A, Holme S, Owens M, Nelson EJ. Improved post-transfusion quality of density separated AS-3 red cells after extended storage. *Br J Haematol.* 1992;82(1):114-21.
- Lang F, Gulbins E, Lerche H, Huber SM, Kempe DS, Foller M. Eryptosis, a window to systemic disease. *Cell Physiol Biochem* 2008; 22(5-6):373-80.
- Linderkamp O, Meiselman HJ. Geometric, osmotic, and membrane mechanical properties of density-separated human red cells. *Blood.* 1982; 59(6):1121-7.
- Lion N, Crettaz D, Rubin O, Tissot JD. Stored red blood cells: a changing universe waiting for its map(s). *J Proteomics.* 2010; 73(3):374-85.
- Lutz HU, Fasler S, Stammler P, Bussolino F, Aresè P. Naturally occurring anti-band 3 antibodies and complement in phagocytosis of oxidatively-stressed and in clearance of senescent red cells. *Blood Cells.* 1988; 14(1):175-203.
- Minetti G, Ciana A, Profumo A, Zappa M, Vercellati C, Zanella A, Arduini A, Brovelli A. Cell age-related monovalent cations content and density changes in stored human erythrocytes. *Biochim Biophys Acta.* 2001; 1527(3):149-55.
- Mosca A, Paleari R, Modenese A, Rossini S, Parma R, Rocco C, Russo V, Caramenti G, Paderi ML, Galanello R. Clinical utility of fractionating erythrocytes into "Percoll" density gradients. *Adv Exp Med Biol.* 1991; 307:227-38.
- Mosca A, Paleari R, Modenese A, Rossini S, Parma R, Rocco C, Russo V, Caramenti G, Paderi ML, Galanello R. Clinical utility of fractionating erythrocytes into "Percoll" density gradients. *Adv Exp Med Biol.* 1991; 307:227-38.
- Nakao K, Wada T, Kamiyama T, Nakao M, Nagano K. A direct relationship between adenosine triphosphate-level and *in vivo* viability of erythrocytes. *Nature* 1962; 194:877-87852.
- Nash GB, Wyard SJ. Changes in surface area and volume measured by micropipette aspiration for erythrocytes ageing *in vivo*. *Biorheology.* 1980;17(5-6):479-84.
- Nishino T, Yachie-Kinoshita A, Hirayama A, Soga T, Suematsu M, Tomita M. *In silico* modeling and metabolome analysis of long-stored erythrocytes to improve blood storage methods. *J Biotechnol.* 2009; 144(3):212-23.
- Olivieri E, Herbert B, Righetti PG. The effect of protease inhibitors on the two-dimensional electrophoresis pattern of red blood cell membranes. *Electrophoresis* 2001; 22:560-5.
- Rennie CM, Thompson S, Parker AC, Maddy A. Human erythrocyte fraction in "Percoll" density gradients. *Clin Chim Acta.* 1979; 98(1-2):119-25.
- Rifkind JM, Araki K, Hadley EC. The relationship between the osmotic fragility of human erythrocytes and cell age. *Arch Biochem Biophys.* 1983;222: 582-9.

- Romero PJ, Romero EA. Determinant factors for an apparent increase in oxygen affinity of senescent human erythrocytes. *Acta Cient Venez.* 2004; 55(1):83-5.
- Salvo G, Caprari P, Samoggia P, Mariani G, Salvati AM. Human erythrocyte separation according to age on a discontinuous "Percoll" density gradient. *Clin Chim Acta.* 1982; 122(2):293-300.
- Samaja M, Rovida E, Motterlini R, Tarantola M, Rubinacci A, diPrampere PE. Human red cell age, oxygen affinity and oxygen transport. *Respir Physiol.* 1990; 79(1):69-79.
- Sass MD, Caruso CJ, O'Connell DJ: Decreased glutathione in aging red cells. *Clin Chim Acta* 1965; 11: 334
- Schroit AJ, Madsen JW, Tanaka Y. *In vivo* recognition and clearance of red blood cells containing phosphatidylserine in their plasma membranes. *J Biol Chem.* 1985; 260(8):5131-8.
- Shinozuka T, Takei S, Yanagida J, Watanabe H, Ohkuma S. Binding of lectins to "young" and "old" human erythrocytes. *Blut* 1988; 57:117-123.
- Shinozuka T. Changes in human red blood cells during aging *in vivo*. *Keio J Med.* 1994; 43(3):155-63.
- Shukla SD, Hanahan DJ. Membrane alterations in cellular aging: susceptibility of phospholipids in density (age)-separated human erythrocytes to phospholipase A2. *Arch Biochem Biophys.* 1982; 214(1):335-41.
- Smith PK, Krohn RI, Hermanson GT, Mallia AK, Gartner FH, Provenzano MD, Fujimoto EK, Goeke NM, Olson BJ, Klenk DC. Measurement of protein using bicinchoninic acid. *Anal Biochem* 1985;150:76-85.
- Strange RC, Johnson PH, Lawton A, Moulton JA, Tector MJ, Tyminski RJ, Cotton W. Studies on the variability of glutathione S-transferase from human erythrocytes. *Clin Chim Acta.* 1982; 120(2):251-60.
- Suzuki T, Dale GL. Membrane proteins in senescent erythrocytes. *Biochem J.* 1989;257(1):37-41.
- Suzuki T, Dale GL. Senescent erythrocytes: isolation of *in vivo* aged cells and their biochemical characteristics. *Proc Natl Acad Sci U S A* 1988;85(5):1647-51.
- Syllm-Rapoport I, Daniel A, Starck H, Hartwig A, Gross J. Creatine in density-fractionated red cells, a useful indicator of erythropoietic dynamics and of hypoxia past and present. *Acta Haematol.* 1981; 66(2):86-95.
- van Oss CJ. Shape of ageing erythrocytes. *Biorheology.* 1982;19(6):725.
- Vettore L, Concetta de matteis M, Zampini P: A new density gradient system for the separation of human red blood cells. *Am J Hematol* 1980; 8:291.
- Waugh RE, Narla M, Jackson CW, Mueller TJ, Suzuki T, Dale GL. Rheologic properties of senescent erythrocytes: loss of surface area and volume with red blood cell age. *Blood.* 1992;79(5):1351-8.

Chapter 5: *In vitro* ageing of red blood cells: storage under blood bank conditions

Contents

- 5.1 Time-course Investigation of SAGM-Stored Erythrocyte Concentrates: from Metabolism to Proteomics.
 - 5.2 Alterations of Red Blood Cell metabolome during cold liquid storage of erythrocyte concentrates in CPD-SAGM.
 - 5.3 Red blood cell storage and cell morphology
 - 5.4 Red blood cell storage in SAGM and AS3: a comparison through the membrane two-dimensional electrophoresis proteome
 - 5.5 Hemoglobin alpha glycation (Hb1Ac) increases during red blood cell storage: a MALDI-TOF mass spectrometry-based investigation.
 - 5.6 Red Blood Cell Lipidomics analysis through HPLC-ESI-qTOF: application to red blood cell storage.
-

The contents of this chapter report the contents of the the following publications by the candidate:

1. Blasi B, D'Alessandro A, Nicola Ramundo, Zolla L.
Red blood cell storage and cell morphology
Transfusion Medicine 2012; 22(2):90-6.
 2. Gevi F*, D'Alessandro A*, Rinalducci S, Zolla L. (* = shared first authorship)
Alterations of Red Blood Cell metabolome during cold liquid storage of erythrocyte concentrates in CPD-SAGM.
Journal of Proteomics. 2012; doi.org/10.1016/j.jprot.2012.03.012.
 3. D'Alessandro A, D'Amici GM, Vaglio S, Zolla L.
Time-course Investigation of SAGM-Stored Erythrocyte Concentrates: from Metabolism to Proteomics.
Hematologica 2012 ;97(1):107-15.
 4. D'Amici GM, Mirasole C, D'Alessandro A, Yoshida T, Dumont LJ, Zolla L.
Red blood cell storage in SAGM and AS3: a comparison through the membrane two-dimensional electrophoresis proteome
Blood Transfusion 2012; 10 Suppl 2:s46-54.
 5. D'Alessandro A, Mirasole C, Zolla L.
Hemoglobin alpha glycation (Hb1Ac) increases during red blood cell storage: a MALDI-TOF mass spectrometry-based investigation.
Vox Sanguinis 2012; DOI: 10.1111/vox.12029
 6. Timperio AM, Mirasole C, D'Alessandro A, Zolla L.
Red Blood Cell Lipidomics analysis through HPLC-ESI-qTOF: application to red blood cell storage
J Integrated Omics 2013;waiting for final decision after minor revisions
-

In vitro ageing of red blood cells, or in other terms, ageing under blood bank storage conditions, shares some common features with *in vivo* ageing. However, most of senescence-related phenomena are likely exacerbated under hypothermic storage in the blood bank. In this chapter, we report the results of extensive Integrated Omics investigations on CPD-SAGM cold-stored erythrocyte concentrates. The obtained results will pave the way for the formulation of alternative storage strategies which could likely improve the field of transfusion medicine, as it will be discussed in the following chapters.

5.1 Time-course Investigation of SAGM-Stored Erythrocyte Concentrates: from Metabolism to Proteomics.

Overview of this section

Results from recent highly-debated retrospective studies raised concerns and prompted considerations about further testing the quality of long stored red blood cells under a biochemical standpoint.

We hereby performed an integrated mass spectrometry-based metabolomics and proteomics time-course investigation on SAGM-stored RBCs. In parallel, structural changes over storage duration were monitored through scanning electron microscopy.

We could detect increased levels of glycolytic metabolites over the first two weeks of storage.

From day14 onwards, we could observe a significant consumption of all metabolic species, and diversion towards the oxidative phase of the pentose phosphate pathway. These phenomena coincided with the accumulation of reactive oxygen species and oxidation markers (protein carbonylation and malondialdehyde accumulation) up to day28.

Proteomics evidenced changes at the membrane protein level from day14 onwards. Changes included membrane structural protein fragmentation (spectrin, band3, band4.1), membrane accumulation of hemoglobin, anti-oxidant enzymes (peroxiredoxin-2) and chaperones.

While at day14 the integrity of red blood cells did not show major deviations, at day21 Scanning Electron Microscope images revealed that 50% of the erythrocytes displayed severely altered shape profiles.

We could thus correlate SEM observations to the onset of the vesiculation phenomenon, through a proteomics snapshot of the differential membrane proteome at day0 versus day35. We could detect proteins involved in vesicle formation and docking to the membrane, such as SNAP alpha.

Biochemical and structural parameter did not display significant alterations within the first two weeks of storage, while they constantly declined from day14 onwards.

Besides, we highlight several parallelisms between long-stored erythrocytes and hereditary spherocytosis.

Keywords: red blood cell; storage; mass spectrometry, proteomics; metabolomics.

Introduction

Red blood cell (RBC) concentrates may be stored for up to 42 days under controlled conditions before transfusion. However, concerns still arise and persist on the suitability of older blood units for transfusion purposes. This is especially true for certain categories of recipients, such as traumatized, post-operative and critically ill patients (Lelubre et al., 2009). Despite accumulating retrospective evidence of reduced blood viability after the first two weeks of storage (Koch et al., 2008), definitive results from randomized double-blind clinical prospective trials are still missing (Bennet-Guerrero et al., 2009; Steiner et al., 2010) or inconclusive. These difficulties are mainly due to the intrinsic statistical limitations of the experimental model (Bennet-Guerrero et al., 2009) or to the lack of common methods and shared standards between laboratories (Hess, 2011). A frequent conclusion to the debate has underscored radical questions about the balance of risks and benefits of RBC transfusion (Adamson, 2008). Nevertheless, the attempts to produce prospective clinical evidences have lead to the quasi-philosophical statement that “available data do not support an adequate suspicion that long-stored RBCs may be associated with common adverse morbidity and/or mortality outcomes, so as to justify exposing experimental subjects to the other known or probable, albeit rare, risks of old RBCs” (Vamvakas, 2010).

It is beyond the scope of this article to provide a proper clinical answer to the critical question on the quality of long-stored RBCs. We are hereby performing a multi-faceted investigation of RBC storage trying to support and expand existing knowledge from a mere biochemical perspective. Biochemical approaches have already provided convincing evidence that refrigerated storage causes alterations to RBCs, which are only reversible to some extent, an array of phenomena which collectively goes by the name of “storage lesions” (Zimrin and Hess, 2009; Lion et al., 2010; Antonelou et al., 2010).

Numerous changes occur in RBCs during storage that may irreversibly alter their biological function, including delivery of oxygen to cells (Bennet-Guerrero et al., 2007). In stored RBCs, increases in O₂ affinity are well documented (Bennet-Guerrero et al., 2007; Valeri and Hirsch, 1969), which reflect progressive decreases in 2,3-diphosphoglycerate (2,3-DPG) levels over the weeks of storage (Valeri and Hirsch, 1969). However, O₂ delivery-capacity by transfused RBCs upon storage is deficient even early after processing and before significant decline in 2,3-DPG (Hess, 2010). Further lesions indeed occur in stored RBCs, which have been shown to lose potassium, deplete ATP stores, and alter lipids and membranes. These lesions result in more rigid cell structure and reduced oxygen off-loading (Zimrin and Hess, 2009; Lion et al., 2010; Antonelou et al., 2010). The suspending fluid becomes enriched with free haemoglobin and biologically active lipids, along with great quantities of negatively charged microvesicles (Hess, 2010; Bosman et al., 2008). Membrane protein fragmentation (D’Amici et al., 2007) and accumulation of membrane biomarkers (Kriebardis et al., 2007; Rinalducci et al., 2011) have been also reported to correlate with storage duration.

In the present study we report an integrated overview of the biochemical processes taking place in RBCs over storage duration. New tests such as metabolomics (D’Alessandro et al., 2011) have been performed for the first time on SAGM-stored RBCs. Recent literature only covers mannitol-adenine-phosphate (MAP)-stored RBC concentrates²⁰. We observed that the RBC metabolism plays a central role over the first two weeks of storage. Then reactive oxygen species (ROS) rapidly accumulate up to day 21, when they reach a plateau. In parallel, oxidations

(carbonylations) to protein and lipids (malondialdehyde – MDA) increase as well. Proteomics evidenced two major phenomena: i) fragmentation of structural proteins at the membrane level and ii) translocation of cytosolic proteins, mainly enzymes involved in anti-oxidant responses and vesiculation-associated proteins. These observations are consistent with the changes at the structural level, as reported through SEM analyses.

We conclude with a parallelism between RBC storage and hereditary spherocytosis.

Materials and Methods

Extensive details for this section are provided in the **supplementary material 1** file (Materials and Methods extended). The present study has been approved by Italian National Blood Centre.

Sample collection Whole blood (450 mL \pm 10%) was collected from healthy volunteer donors into CPD anticoagulant (63 mL) and leukodepleted. After separation of plasma by centrifugation, RBCs were suspended in 100 mL of SAG-M (Saline, Adenine, Glucose, Mannitol) additive solution. We studied RBC units collected from 8 donors [male = 4, female = 4, age 45 \pm 11.5 (mean \pm S.D.)]. RBC units were stored under standard blood bank conditions (1-6 °C) and samples were removed aseptically for the analysis every week from day 0 up to day 42 of storage.

Determination of intracellular pH.

Red cell pellets obtained by centrifuging 600 μ l of suspension in a nylon tube at 30,000 \times g for 10 min, were frozen, thawed during 5 min and then refrozen. To prevent an acid shift observed when samples are kept unfrozen, triplicate measurements of pH were made immediately after a second thawing of each lysate with a Radiometer pH glass capillary electrode maintained at 20°C and linked to a Radiometer PHM acid-base analyzer.

Metabolomics

Samples from the eight units were extracted and treated as extensively reported in the **Chapter 3** (D'Alessandro et al., 2011).

Rapid Resolution Reversed-Phase High Performance Liquid Chromatography (HPLC)

An Ultimate 3000 Rapid Resolution HPLC system (LC Packings, DIONEX, Sunnyvale, USA) was used to perform metabolite separation. A Dionex Acclaim RSLC 120 C18 column 2.1mm \times 150mm, 2.2 μ m was used to separate the extracted metabolites. Acetonitrile, formic acid, and HPLC-grade water, purchased from Sigma Aldrich (Milano, Italy). Details about the HPLC settings and gradient are reported in **Chapter 3**

ESI Mass Spectrometry

Metabolites were directly eluted into a High Capacity ion Trap HCTplus (Bruker-Daltonik, Bremen, Germany). In Multiple Reaction Monitoring (MRM) analysis, m/z of interest were isolated, fragmented and monitored (either the parental and fragment ions) throughout the whole RT range.

Metabolite analysis and data elaboration

Quantitative analyses of standard compounds were performed on MRM data against comparison to standard metabolite runs.

Standards (equal or greater than 98% chemical purity) D-fructose and D-glucose 6-phosphate (G6P/F6P), D-fructose 1,6 biphosphate (FDP), glyceraldehyde phosphate (G3P), 1,3 and 2,3 diphosphoglycerate (DPG), phosphoenolpyruvic acid (PEP), L-lactic acid (LA), NADPH, phosphogluconolactic acid (PGL), ATP, NADH, glutathione (GSH), oxidized glutathione (GSSG), were purchased from Sigma Aldrich (Milan).

LC/MS data files were processed by Bruker DataAnalysis 4.0 (build 234) software. Data were further refined (normalization of treated/controls) and plotted with GraphPad Prism 5.0 (GraphPad Software Inc.). Results were plotted as fold-change variations values upon normalization to day 0 controls, as in Nishino et al. (2009).

Oxidative stress

Reactive Oxygen Species - ROS

N,N-diethyl-para-phenylendiamine was dissolved in 0.1M sodium acetate buffer (pH 4.8) to obtain a final concentration of 100 g/ml (R1 solution as a chromogen). Ferrous sulfate was dissolved in 0.1M sodium acetate buffer (pH 4.8) to obtain a final concentration of 4.37 M (R2 solution as a transition-metal ion). The hydrogen peroxide solution, at increasing dilutions, was used as standard solution for generating a calibration curve. To process the reaction, 96-well microtiter plates (Nalge Nunc International, USA) were used. The Spectra Max Plus (Molecular Device Corp., USA) was used as a spectrophotometric plate reader. A volume of 5 µl of either hydrogen peroxide standard solution (for generating a calibration curve) or red blood cells lysate was added to 140 µl of 0.1M sodium acetate buffer (pH 4.8) in 1 well of a 96-well microtiter plate, which reached a temperature of 37 °C after 5 min. A volume of 100 µl of the mixed solution, which was prepared from R1 and R2 at a ratio of 1:25 before use, was added to each well as a starter. Then, after pre-incubation at 37 °C for 1 min using a spectrophotometric plate reader, absorbance at 505 nm was measured for a fixed time (between 60 and 180 s) at 15 s intervals. A calibration curve was automatically constructed from the slopes, which were calculated based on varying (Δ) absorbance at 505 nm each time (min) corresponding to the concentration of hydrogen peroxide. ROS levels in RBCs were calculated by the analyzer (spectrophotometric plate reader) from the calibration curve, and expressed as equivalent to levels of hydrogen peroxide (1 unit = 1.0 mg H₂O₂/l).

Carbonyl content

Levine et al. (1994). Proteins were precipitated from RBCs lysates by addition of 10% trichloroacetic acid (TCA) and resuspended in 1.0 ml of 2 M HCl for blank and 2 M HCl containing 2% 2,4- dinitrophenyl hydrazine. After incubation for 1 h at 37°C, protein samples were washed with alcohol and ethyl acetate, and re-precipitated by addition of 10% TCA. The precipitated protein was dissolved in 6 M guanidine hydrochloride solution and measured at 370 nm. Calculations were made using the molar extinction coefficient of $22 \times 10^3 \text{ M}^{-1} \text{ cm}^{-1}$ and expressed as nmol carbonyls formed per mg protein. Total protein in RBC pellet was assayed according to the method of Lowry et al. 16 using bovine serum albumin as standard.

RBC membrane lipoperoxidation

Malondialdehyde (MDA) levels were estimated in RBCs following the Stocks and Dormandy's method with some modifications¹¹. Briefly, 0.2 mL of packed RBCs was suspended in 3.0 mL of Krebs's Ringer phosphate buffer (KRBP) solution (pH 7.4) and 1 mL of the cell suspension was treated with 1 mL of 10% trichloroacetic acid and centrifuged at $1,000 \times g$ for 5 min. 1 mL of supernatant was then mixed with 1 mL of 0.67% thiobarbituric acid and heated over a water bath for 20 min at 85–90 °C. The solution was cooled and read against a complementary blank at 532 nm (OD1) and 600 nm (OD2). A blank was prepared separately without packed RBCs. The net optical density (OD) was calculated after subtracting absorbance at OD2 from that at OD1. The MDA level was determined from the standard plot and expressed as nmol/mL of packed RBCs.

Proteomics

RBC protein extraction Extraction of human erythrocyte membrane and cytosol proteins was performed at day 0, day 14 and day 35 based as previously reported (D'Amici et al., 2007), with minor modifications, including either the presence or absence of N-ethylmaleimide (NEM) in the extraction protocol to prevent artifactual oxidation of thiol groups (Low et al., 2007).

Two-Dimensional Electrophoresis (2-DE) Protein precipitates were prepared as previously reported (D'Amici et al., 2007), either in presence or absence of NEM. A total of 250 μ L of the resulting protein solution was then used to perform a two-dimensional electrophoresis (13 cm long IPG 3-10 NL (Amersham Biosciences) for the first dimension and a 5-16% T gradient SDS-PAGE gel). Further experimental details are provided in the supplementary material (materials and methods extended). Proteins were visualized by Coomassie Brilliant Blue G-250 stain.

Image statistical analysis

Ninety-six stained gels (3 technical replicates \times 8 biological replicates \times 2 groups \times 2 periods – day 0 and 35 – with or without NEM) were digitalized and elaborated for among-group comparisons (ANOVA) as previously reported¹⁶ and extensively described in the supplementary material file. Differential protein expression was considered significant at $P < 0.05$ and the change in the photodensity of protein spots between day 0, day 14 and 35 samples (with or without NEM, independently) had to be more than 2 fold. Moreover, as protein fragments were the main changes to be expected (D'Amici et al., 2007), we took into account only protein spots below approximately 60 kDa apparent MW.

In-Gel Digestion and Protein identification by MS/MS Protein spots were carefully excised from stained gels and subjected to in-gel trypsin digestion, as previously reported (D'Amici et al., 2007). Peptide mixtures were separated using a nanoflow-HPLC system (Ultimate; Switchos; Famos; LC Packings, Amsterdam, The Netherlands). Mass spectrometry settings and bioinformatic identification details are provided in the **supplementary material 1** (materials and methods extended).

Structural analyses

Scanning electron microscopy Scanning electron microscopic studies of RBC were performed by means of a JEOL JSM 5200 electron microscope. Samples were prepared as extensively described in the supplementary material

(materials and methods extended). The different cell shapes were identified using Bessis' classification (1972). The percentages of discocytes, echinocytes, spherocytocytes, stomatocytes, spherostomatocytes, and spherocytes were evaluated by counting 1000 to 1500 cells in randomly chosen fields. Although there is still an open debate about reversible and irreversible shape classification, shape changes were classified as in Berezina et al. (2002). According to this classification, RBC manifesting echinocyte and stomatocyte shapes are capable of returning to the discocyte shape under certain conditions. Thus, these RBC shape changes are considered potentially reversible transformations. In contrast, RBC assuming spherocytocyte, spherostomatocyte, spherocyte, ovalocyte, and degenerated shapes are irreversibly changed cells.

Results

Metabolomics, proteomics and SEM analyses were performed simultaneously on 8 leukodepleted RBC units (residual WBC < 1×10^6 /unit*) (Council of Europe, 2011). At the end of the storage (42 days), haemolysis was <0.8% for all the tested products.

It is worth mentioning that the possibility to perform multi-faceted investigations covering both proteomics and metabolomics aspects stems from the sensitivity (down to the fmol level) and specificity of the HPLC and MS techniques. Although these approaches are not routinely performed in the clinical setting, they are becoming widespread diffused in research laboratories given their versatility and robustness. For example, the integrated metabolomics analysis hereby allowed to perform relative quantification analyses of 12 different metabolites through HPLC-mediated elution of 20 μ l of the original sample into the MS.

Time-course metabolomics

Fold-change variation values upon normalization to day 0 controls are graphed in **Figure 1**.

Glycolytic phosphate precursors apparently slightly accumulated over the first two weeks of storage, as observed for G6P/F6P, DPG and G3P (**Figure 1**). On the other hand FDP significantly accumulated at day 7. From day 14 onwards the trend was inverted and metabolites were rapidly consumed and, at the end of the storage, they were below (75.6 ± 3.4 % for G6P/F6P) or far below (51.4 ± 2.1 % for FDP and 29.2 ± 1.4 % for G3P) the initial concentration levels.

DPG levels followed trends already reported in literature (Bennet-Guerrero et al., 2007; Nishino et al., 2009), with early moderate accumulation up to day 7 and constant diminution up to day 21 onwards, at which point it reached concentrations as low as 0.05 ± 0.01 % as the original day 0 values.

On the other hand, PEP followed an anomalous trend, with a constant decrease up to day 28, in which we could detect in almost all the tested units a 1.6 ± 0.1 fold-change increase, which was reverted into lower than day 0 control values at day 42 (0.65 ± 0.04 %).

Lactate (LA), which is a frequent parameter in metabolic analyses of RBCs (Bennet-Guerrero et al., 2007; Nishino et al., 2009), constantly accumulated as storage progressed as to reach a final value of 20.39 ± 0.9 fold-change increase in comparison to day 0 controls.

In parallel, we observed a moderate, albeit constant accumulation of pentose phosphate pathway (PPP) intermediates: i) 6-phosphogluconic acid reached a plateau at day 28, and ii) NADPH. At day 42 both metabolites had doubled their levels in comparison to day 0 controls.

ATP appeared to be increased up to day 7, while it was rapidly consumed soon after the first week, as to reach initial values and below. However, ATP consumption-rate decreased from day 14 to day 21, and from day 21 onwards.

NAD⁺ accumulated until day 7, then it decreased constantly until the end of the storage, when we recorded 59.99 ± 0.2 % levels in comparison to day 0 controls.

Finally, GSH and GSSG levels followed opposing trends. The former decreasing constantly over storage duration halving its levels by day 42, while the latter increasing constantly by day 14 onwards (1.56 ± 0.02 fold-change increase at the end of the storage).

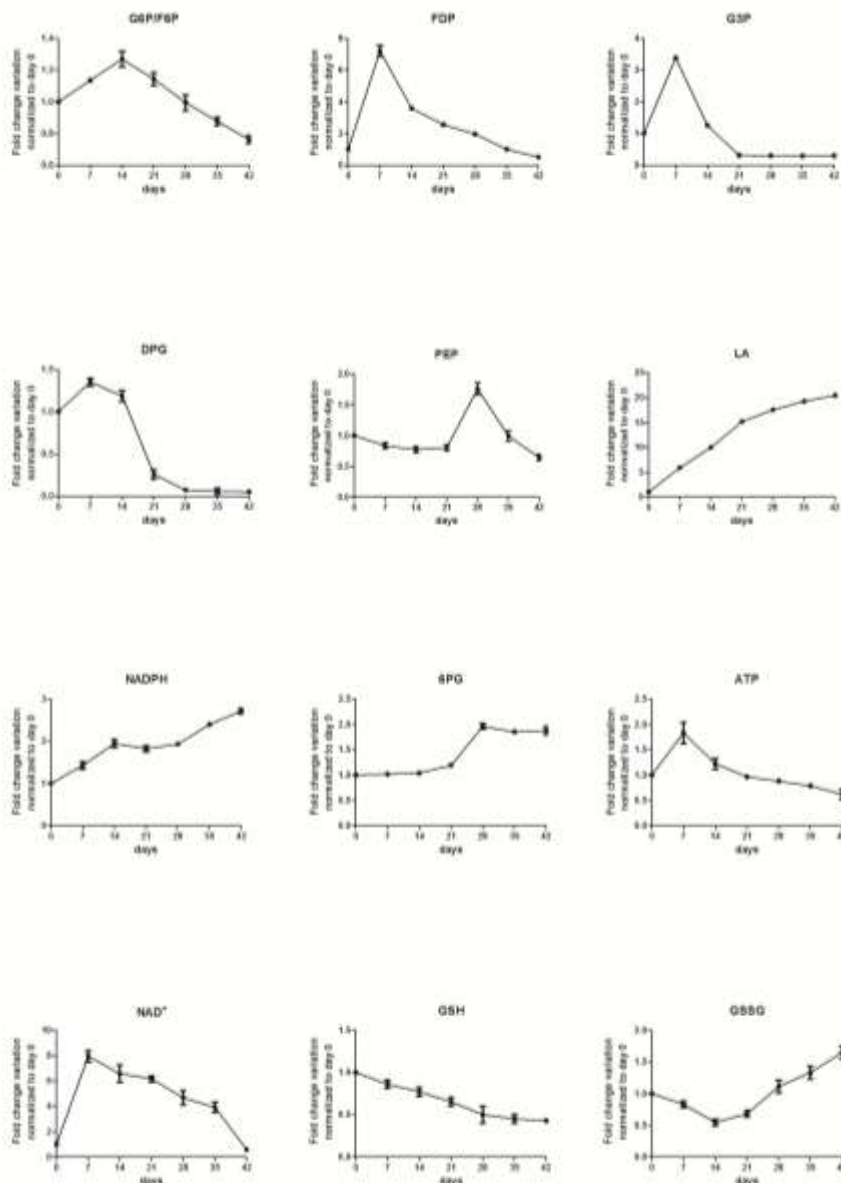


FIGURE 1 Time course metabolomic analyses of SAGM-stored RBCs, upon normalization against day 0 controls, as in MS-based metabolomics analysis on MAP-stored RBCs²⁰.

Abbreviations: G6P/F6P = glucose/fructose 6-phosphate; FDP = fructose 1,6 biphosphate; G3P = glyceraldehyde 3-phosphate; DPG = biphosphoglycerate; PEP = phosphoenolpyruvate; LA = lactate; NADPH = nicotinamide adenine dinucleotide phosphate; 6PG = 6-phosphogluconate; ATP = adenosine triphosphate; NAD⁺ = nicotinamide adenine dinucleotide; GSH = reduced glutathione; GSSG = oxidized glutathione.

Oxidative stress

ROS

ROS accumulated over the first three weeks of storage, to reach a plateau at 21 days (252.4 ± 12.5 units) (**Figure 2.A**).

Protein carbonylation

Protein carbonylation increased constantly and uniformly in all the tested samples from day 0 (41.3 ± 2.4 mmol/ml) until the fourth week of storage (62.1 ± 2.5 mmol/ml). From the 28th day onwards carbonylation trends seemed to be reversed. Detected protein carbonyls were reduced in almost all of the tested subjects at the end of the storage (48.2 mmol/ml), while in others it reached a plateau with only slight decreases (59 mmol/ml), in agreement with Papassideri's group previous observations (Kriebardis et al., 2007) (**Figure 2.B**).

Malondialdehyde (MDA)

MDA assay resulted in progressive and constant accumulation of oxidized lipid markers from 3.4 ± 0.3 mmol/ml at day 0 up to 7.1 ± 0.6 mmol/ml at day 42 (**Figure 2.C**).

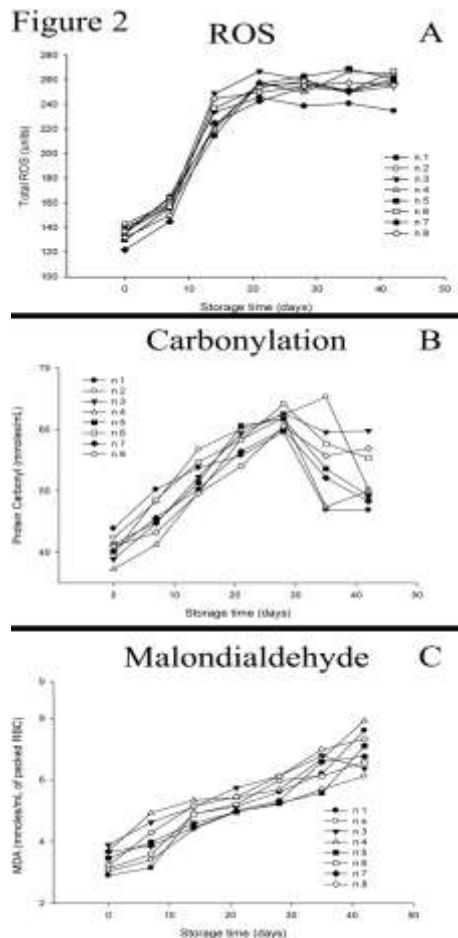


FIGURE 2 Reactive oxygen species (ROS) levels (1 unit = 1.0 mg $\text{H}_2\text{O}_2/\text{l}$) over the whole duration of the storage for each tested unit (**A**). Protein carbonylation measurements (mmol/mL) over the whole duration of the storage for each tested unit (**B**). Malondialdehyde (MDA) measurements (mmol/mL) over the whole duration of the storage for each tested unit (**C**).

Proteomics

In our previous study on RBC fragmentation over storage we observed an increase of fragments in the time window between the second and the fifth week. However, that study had some major limitations since the analyses had been performed on non-buffy coat-depleted nor leukofiltered RBC units (D'Amici et al, 2007). Therefore, early fragments might have been provoked by white blood cells in the unit. On the other hand, when testing leukocyte-filtered erythrocyte concentrates, protein fragments accumulated in the period between the third and the fifth week, as we could eventually assess. Indeed, in the present study, 2-DE differential analyses between day 0 and day 14 samples highlighted the presence of a limited number of statistically significant differential spots (spot number 320, 327 and 342, all

identified as protein band 4.1; and spots 389, 402 and 417 as peroxiredoxin 2 – **Figure 3A2** and **Table 1A**). Conversely, significant levels of fragments were observed at day 35 in all the tested units. Thus, we hereby performed a targeted 2-DE analysis of samples from the 8 leukocyte-filtered RBC units at day 0 and day 35 mainly aimed at determining significant variations ($p < 0.05$ ANOVA, $|\text{fold-change}| > 2.0$) in the low molecular weight region, below 60 kDa. Since protein fragments have been supposed to be masked or triggered by artifactual oxidation during sample preparation (Low et al., 2007), we decided to perform the 2-DE analysis both in presence and absence of the alkylating agent NEM.

Results for both arms of the study are reported in **Figure 3A** and **B**, respectively.

Results obtained without NEM included the individuation of 15 different highly statistically significant protein spots, which were further identified as eight distinct proteins (**Table 1A**).

In presence of NEM, the overall number of spots (yet at day 0 in comparison to samples without NEM) visibly increased. Although it is beyond the scope of this article to understand the reasons behind this biochemical phenomenon, it is not to be excluded that NEM-modified proteins could have been hydrolysed to the corresponding N-ethylsuccinimide cysteine residue. This may provide additional protease cleavage sites and thus promote enzyme mediated protein-fragmentation (Gehring et al., 1980). However, the effect is the same both in day 0, day 14 and day 35 samples and thus it does not compromise differential analyses. Besides, fragments evidenced at day 35 were the same both in presence and absence of NEM, while NEM addition only allowed for resolving further non-fragmented proteins, as it could be grasped by the relation between the theoretical and the observed molecular weight (**Figure 3**, and **Table 1**). On the other hand, no significant fragmentation was observed in day 14 samples with NEM in comparison to day 0 controls treated with NEM (data not shown).

As for the present study, we could determine the significant increase at day 35 against day 0 control gels of 27 differential spots which enabled identification of 33 distinct protein entries (**Table 1B**). Notably, all of the protein entries individuated without NEM could be still individuated upon addition of the alkylating agent, prompting us to confirm that observations performed so far on protein fragments (D'Amici et al., 2007) were not artifactual results from oxidation of thiol groups during preparation steps.

Addition of NEM favoured the separation and identification of an increased number of protein spots, which accumulated in the membrane fraction at day 35 in comparison to day 0 controls.

Indeed, a comparison of proteins found with NEM against the same analyses without NEM revealed a series of new protein entries. These mainly included proteins which were characterized by thiol groups in their functional/catalytic domain (thioredoxin-like fold (IPR012336) in TXNL1, CLIC1, GSTO1, GPX1, for example).

These proteins were destined to artifactual over-oxidation during the extraction and their fluctuations ended up to be under-estimated in the absence of the alkylating agent NEM, in agreement with previous observations (Low et al., 2007; Ito et al, 2011).

Since RBCs are devoid of any new protein synthesis capacity, the increased number (and increased photodensity) of protein spots in the low MW range of the membrane fraction could be due either to the increase in fragmentation events involving higher MW proteins or the migration to the membrane fraction of cytosolic proteins (soluble fraction (GO:0005625)).

Fragmentation of high MW protein implies the experimental individuation through 2DE of protein spots, the MW of which might not be lower than expected theoretically through online available databases. A series of proteins, could be included in this group (**Table 1A** and **B**):

- i) oxidative stress-related enzymes with oxidoreductase activity (GO:0016491) (glutamate—cysteine ligase catalytic subunit isoform a, stress-induced-phosphoprotein 1);
- ii) structural proteins (spectrin alpha and beta chains, band 3 and protein 4.1 isoform 6 - structural constituent of cytoskeleton (GO:0005200)) and
- iii) apoptosis-related proteins (ALG-2 interacting protein 1),

Another group of proteins of cytosolic origin became increasingly represented at the membrane fraction of day 35 samples, which included:

- i) structural proteins (stomatin and flotilin-2);
- ii) vesicle-related proteins (alpha-soluble NSF attachment protein, alpha SNAP, 55 KDa erythrocyte membrane protein isoform 1 – belonging to the BioCarta pathway “Synaptic Proteins at the Synaptic Junction (h_PDZsPathway)”);
- iii) oxidative stress-related enzymes (glutathione S-transferase omega-1 isoform 1, glutathione peroxidase, thioredoxin-like protein 1 - Glutathione metabolism (hsa00480); 6-phosphogluconolactonase, nicotinate phosphoribosyltransferase-like protein, biliverdin-IX beta reductase isozyme I – KEGG pathway: pentose phosphate pathway (hsa00030) and gene ontology: cofactor metabolic process (GO:0051186));
- iv) chaperones (stress-induced-phosphoprotein 1, DNA-damage inducible protein 2, KIAA0002, T-complex protein 1 subunit beta isoform 1, peptidyl-prolyl cis-trans isomerase FKBP4, HSPC263, Hsc70-interacting protein);
- v) ion channels (nuclear chloride channel).

Structural analyses: Scanning Electron Microscope (SEM)

SEM images were collected and analysed following Bessis classification²² and discrimination between reversible and irreversible membrane shape alterations over storage duration (from day 7 to day 42), in agreement with Berezina et al. (2002). Results are reported in **Table 2**, as mean \pm S.D. of discocytes, cells with reversibly and irreversibly-altered membrane, as percentages of the overall number of cells taken into account in randomly chosen fields (ranging from 1000 to 1500 per subject). While at day 7 the percentage of discocyte RBCs was high (75.3 ± 4.1) and the fraction of RBCs displaying irreversible modification of the membrane averaged below the 10 % (9.2 ± 3.5), SEM images at day 42 showed a substantial percentage of reversibly (45.3 ± 3.8) and irreversibly (31.0 ± 2.9) membrane-altered RBCs (**Table 2**). **Figure 4** shows a detail and an overview of a 42 day-stored RBC sample (**Figure 4.A** and **4.C**) in comparison to a 28 day-stored RBC sample (**Figure 4.B**).

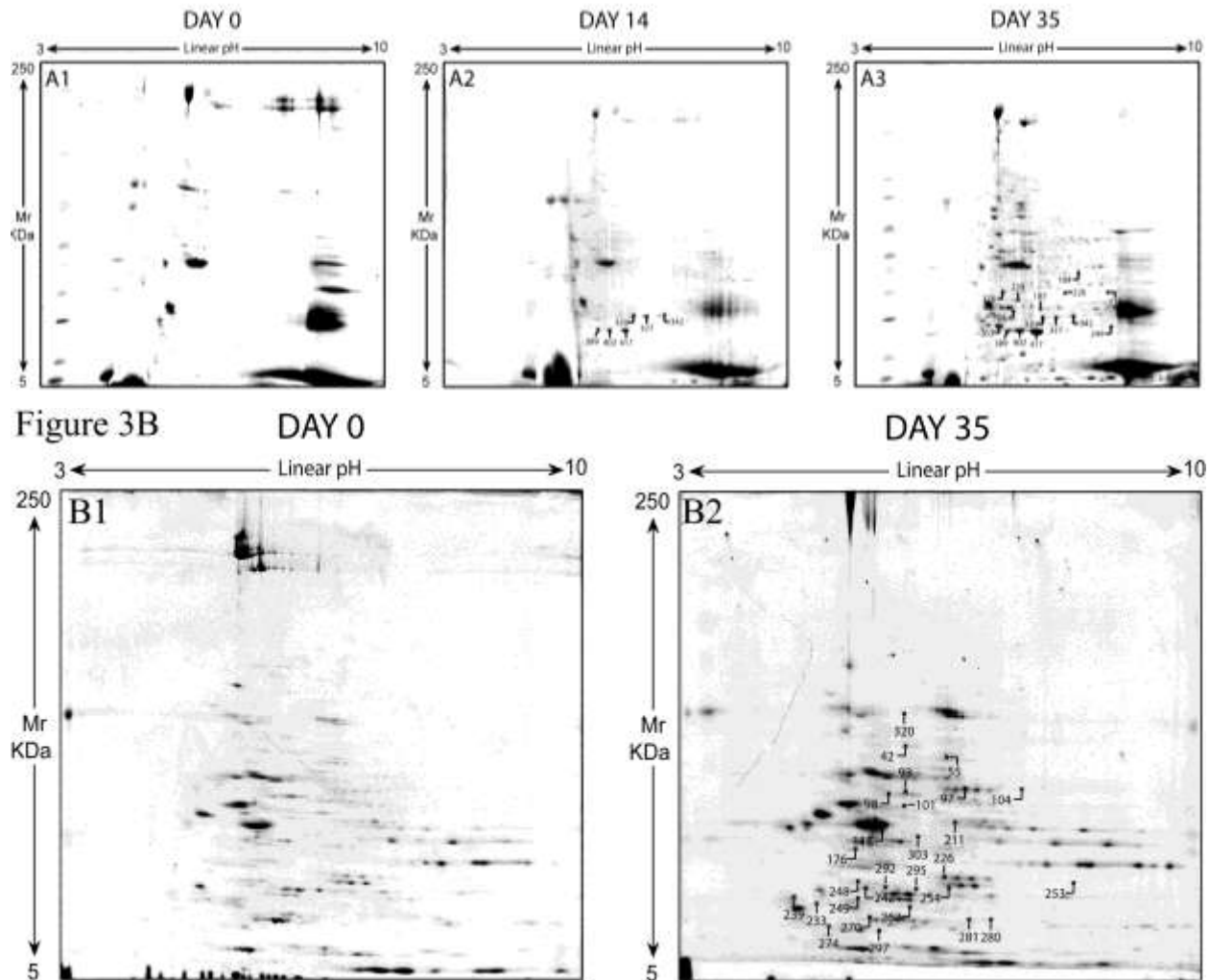


FIGURE 3 In A Two-dimensional gel electrophoresis (extraction protocol without the incubation with the alkylating agent N-ethyl maleimide - NEM) of day 0 (**A1**) versus day 14 (**A2**) and 35 (**A3**) RBCs. First dimension IEF pI values linearly span between 3 and 10, while MW are indicated in the left. Spots characterized by different photodensities in the low MW region have been individuated and further identified through mass spectrometry (**Table 1A**).

In **B** Two-dimensional gel electrophoresis (extraction protocol including incubation with the alkylating agent N-ethyl maleimide – NEM) of day 0 (**B1**) versus day 35 (**B2**) RBCs. First dimension IEF pI values linearly span between 3 and 10, while MW are indicated in the left. Spots displaying different photodensities in the low MW region have been individuated and further identified through mass spectrometry (**Table 1B**).

Discussions

Metabolic parameters rapidly change over the first two weeks of storage

We hereby simultaneously tested RBCs for metabolism, oxidative stress and protein parameters and monitored them throughout the whole shelf-life (42 days) of eight SAGM RBC units under refrigeration.

Sugar-phosphates and their glycolytic metabolites seemed to accumulate during the first week and then began to decrease as storage progressed, so as to reach low or extremely low levels at the end of the third week (**Figure 1**). DPG followed a similar trend, in agreement with previous observations for SAGM⁴ and MAP-stored RBC units (Nishino et al., 2009). Consumption of both 1,3 and 2,3 DPG (we could not discriminate between the isomers through MS/MS) had already been reported and had been related to the impaired oxygen delivery capacity of RBC upon transfusion (Ito et al., 2011). Indeed DPG, in association with pH and HCO₃⁻/CO₂ modulates position and shape of the oxygen dissociation curve (Rouault, 1973).

Glycolysis rate decreases as pH falls, which is known to occur over storage progression (Hess, 2010). Another limiting factor should be represented by complete NAD⁺ reduction to NADH. This is confirmed to some extent by our observations, which both include constant decrease of pH (data not shown) and NAD⁺ diminution as storage progressed (although we could also notice a significant increase of NAD⁺ levels upon the first week) (**Figure 1**). Lactate accumulation over the whole period of storage might suggest that glycolysis did not stop, or at least was diverted towards the PPP, since NADPH and 6PG accumulated.

On the other hand, ATP depletion was constant over the whole 42 day period, which testified an inefficient ATP production-rate. This is relevant in the light of the role of ATP in the maintenance of electrolyte balance by powering sodium-potassium cationic pumps. However, Na⁺/K⁺ pumps are known to be turned off at 4°C (Wallas et al., 1979).

In the present study ATP depletion has been associated with impairment of parameters of cell shape, in agreement with literature (Haradin et al., 1969).

Overall, we could conclude that, if metabolism plays a role in RBC storage, it is to sustain RBC energy production during the first two weeks and then it is switched to produce metabolites involved in anti-oxidant responses from day 14 onwards.

Oxidative stress: from metabolism to ROS accumulation

Several Authors have proposed that oxidative stress might underpin *ex vivo* ageing of RBCs (Lion et al., 2010; Antonelou et al, 2010). In this study, we report both the accumulation of ROS, reaching a plateau at day 21 (**Figure 2.A**). Protein carbonyls and MDA (**Figure 2.B and C**) accumulated as well, in parallel to a decrease in GSH and increase in GSSG levels (**Figure 1**).

Conversely, we could observe an increase of PPP oxidative phase metabolic intermediates NADPH and 6PG as storage progressed. 2DE analyses of NEM-extracted samples indicated relocation to the membrane of the 6PG-limiting enzyme (6-phosphogluconolactonase – **Table 1B**) and nicotinate phosphoribosyltransferase-like protein, which catalyzes the conversion of nicotinic acid (NA) to NA mononucleotide and is essential for NA to increase cellular NAD⁺ levels and prevent oxidative stress of the cells (Hara et al., 2007). As we could detect higher levels of the product metabolites of these enzymes, it is likely that they relocate at the membrane level, where they are needed the most.

Additionally, GSH-homeostasis-related enzymes were relocated to the membrane as well, such as glutathione S-transferase, glutathione peroxidase and thioredoxin-like protein 1 (hsa00480 – KEGG pathway annotation).

Since G3P levels did not increase again upon 6PG and NADPH accumulation, we could assume that the non-oxidative phase of the PPP is somehow inhibited, while the oxidative phase alone is over-activated. This assumption is coherent with the observation by Giardina's group (Messana et al., 2000) that the ratio of G3P which is produced through glycolysis and PPP does not show major fluctuation over storage duration, though their interesting conclusions were grasped from NMR-based data about (^{13}C -2 and ^{13}C -3 derived from ^{13}C -glucose) G3P levels alone instead of a whole subset of metabolites.

In conclusion, oxidative stress appeared to severely increase from day 14 to day 21, when it reaches the maximum levels.

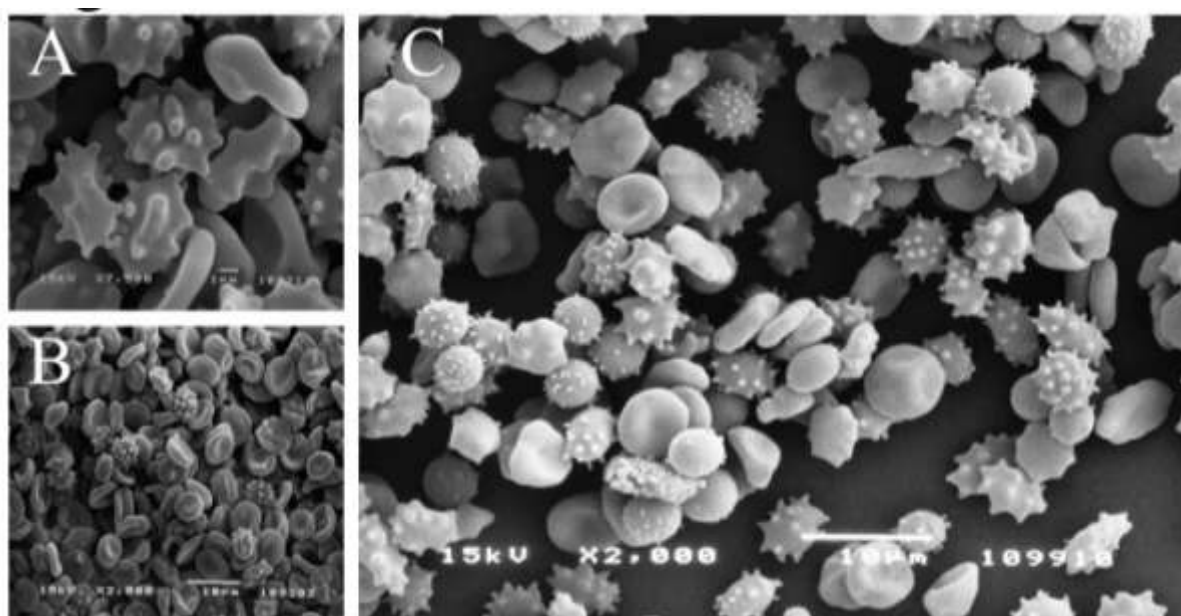


FIGURE 4 Scanning electron images (JEOL JSM 5200 scanning electron microscope) of long-stored RBCs. A detail of a 42 day echinocyte (7,500x; scale bar = 1 μm) (A). A panoramic view of a 28 day RBC sample (2,000x; scale bar = 10 μm) (B). A 2,000x field of 42 day RBCs (scale bar = 10 μm) (C).

Alteration of RBC membrane shape and vesiculation: a timely snapshot through proteomics

Through proteomics we could also determine an increase of oxidative stress-related enzymes in RBC membranes. We could detect proteins involved in the GSH-homeostasis, which relocated at the membrane level yet at day 14 (peroxiredoxin 2 – **Figure 3A2** and **Table 1A**) or later on, at 35 days (**Figure 3A and B; Table 1A and B**). Most of these oxidative stress-related proteins, as well as most of the chaperones individuated have been indicated as key regulatory nodes in the protein-protein interaction analysis of the RBC proteome and interactome in the 2010 study by our group³², as they mapped at the very heart of the “Save or Sacrifice - SOS” sub-network. The “SOS” sub-

network represented the top-score result of a bioinformatic elaboration cataloguing all the RBC protein discovered so far based on the relevance of their role in sustaining RBC survival and functionality.

We could not conclude whether this enrichment of oxidative stress-related proteins might be due to an increased necessity to face oxidative stress in the membrane region or rather these no-longer functional proteins are relocated to the membrane through the docking of vesicles prior to their extrusion from the cell. However, the former hypothesis seems reliable enough, in the light of recent observations from our laboratory which clearly indicate that membrane peroxiredoxin-2 in long-stored RBCs is still functional (Rinalducci et al., 2011).

The likely effect of oxidative stress at the membrane protein level appeared not only to be limited to an increase in carbonyl levels (**Figure 2.B**), but also to the increase in fragmentation events involving structural proteins (spectrin alpha and beta chains, band 3 and protein 4.1 isoform 6 - structural constituent of cytoskeleton (GO:0005200)). Fragments of band 4.1 were evidenced at the membrane level yet at day 14 (**Figure 3A2**). This is in agreement with SEM analyses, which highlighted that significant membrane alterations accumulated yet at day 14 (approximately 45% of RBCs showed membrane alterations), and accumulated as storage progressed (by day 35 over 65% of the examined RBCs displayed relevant alterations of the membrane shape).

In the presence of alkylating agent NEM during the extraction we could detect, through 2DE, differential photodensity for those protein spots containing oxidation-sensitive thiol groups, which are otherwise artifactually oxidized during the extraction protocol (Gehring et al., 1980; Low et al., 2007; Ito et al., 2011). Notably enough, a series of proteins involved in vesiculation were detected, such as alpha SNAP and 55 kDa erythrocyte membrane protein isoform 1 (h_PDZsPathway - Biocarta annotation). The former, in particular, is known to play a pivotal role in the exocytosis process, as it mediates vesicle docking to the membrane also, but not uniquely, in a calcium dependent way (Barnard et al., 1996). Since internal Ca^{2+} is subjected to metabolic control via an ATP-dependent extrusion mechanism (Ca^{2+} pump) (Barnard et al., 1996; Romero and Romero, 1999), decreased ATP content attained during red cell ageing should lead to a raised cellular Ca^{2+} . This has been reported in the literature through the use of the fluorescent probe Fura-2 in cells separated on Percoll density gradients, which revealed that *in vivo* aged RBCs (senescent) contained a higher free Ca^{2+} content (almost four times) than the younger cells (Schatzmann et al., 1966). The consistency of the role of Ca^{2+} in the frame of RBC storage is strengthened by the consideration about the role of this ion in modulating the Ca-dependent K channel (K(Ca) channel) (Barnard et al., 1996) and the influence on RBC membrane shape (LaCelle et al., 1972; Palek et al., 1974).

Most of the proteins detected through our 2DE approach, both in presence and absence of NEM, had already been reported to accumulate in RBC-leaked micro- and nano-vesicles, such as stomatin, ankyrin, biliverdin reductase, 14-3-3 zeta/delta (**Table 1A** in comparison to Bosman et al. (2008)), just to mention few.

The list included fragments of structural proteins, out of which the cytosolic domain of band 3 deserves a special mention, since it is known to represent an actual “respiratory metabolon” docking site at the RBC membrane (Low et al., 1993), which is also found in RBC vesicles (Bosman et al., 2008).

Red blood cell storage: parallelism with hereditary spherocytosis

Among the observed membrane anomalies that we could relate to storage progression, we evidenced an increased osmotic fragility of long-stored RBCs (data not shown). It is long known that an elevated osmotic fragility is correlated to hereditary spherocytosis (Korones et al., 1989).

Hereditary spherocytosis is an hemolytic anemia characterized by the production of sphere-shaped rather than bi-concave disk shaped RBCs, with an increased tendency to hemolyse. This is due to a decreased surface/volume ratio, which results in a reduced capacity to face increased osmotic stresses.

Our SEM results, in agreement with literature (Berezina et al., 2002), support the characterization of progressive membrane-targeting storage lesions, which end up severely altering RBC shape (**Table 1**).

Moreover, a recent proteomic investigation on RBCs from patients suffering from hereditary spherocytosis concluded that these cells were characterized by altered redox-regulation, nucleotide metabolism, protein aggregation and/or degradation, cytoskeletal disorganization and severe oxidative stress (Saha et al., 2011). In particular, Rocha et al. (2008) have reported that peroxiredoxin 2 located at the membrane level in RBCs from hereditary spherocytosis patients, in coincidence to an increase in oxidative stress. As we had previously observed (Rinalducci et al., 2011) through western blot, and hereby confirmed with 2-DE (**Figure 3A, Table 1A**), peroxiredoxin-2 relocated progressively at the membrane level from the third week to the end of the storage.

Hemoglobin chains have been shown to bind to the RBC membrane in hereditary spherocytosis patients (Gallagher et al., 1998), but also in long-stored RBCs in literature (Antonelou et al., 2010) and in the present study (**Table 1A and B**).

Protein degradation at the membrane level has been previously reported to begin at day 14 and reach a climax at day 33 (D'Amici et al., 2007). We hereby observed a significant accumulation of protein fragments for a series of structural proteins at day 35 (spectrin alpha and beta chains, band 3 and protein 4.1 isoform 6 - structural constituent of cytoskeleton – **Table 1 A and B**), as a further parallelism between prolonged storage and hereditary spherocytosis in which mutations/fragmentations events targeting these very same proteins have been reported (Gallagher et al., 1998; Perrotta et al., 2008).

Finally, oxidative stress seems to represent another common pattern between hereditary spherocytosis, as we could notice both an increase of ROS and protein carbonylation (**Figure 2.A and B**), climating at day 21 and 28, respectively. Also lipid oxidation was observed, through the accumulation of MDA (**Figure 2.C**).

Conclusion

Storage lesions stem from a domino of events leading to the utter accumulation of irreversible alterations in long-stored RBCs. While clinical concerns about safety and effectiveness are still under evaluation, biochemical information are largely available, although not conclusive.

In this frame, we hereby performed an integrated metabolomics and proteomics study to further delve into the dynamics of the phenomena underlying RBC storage. Storage progression corresponded to a phenomenon which could be roughly described as a progressive modulation of the erythrocyte metabolism, which was in part coherent with previous *in silico* models and in part expanded NMR-based observations about the ratio of G3P generation rate through glycolysis and PPP, available in the literature (Messana et al., 1999 and 2000). Taken together, our results

indicated that the oxidative steps of the PPP might be over-activated while, whether a blockade exists (Messana et al., 2000), it is at the non-oxidative steps.

If on the one hand RBC metabolism resulted to be active within the first 14 days of storage at the utmost, the rapid accumulation of ROS resulted in a significant increase in oxidized proteins and lipids. Oxidative stress appeared to represent the triggering factor of changes at the protein level especially in the membrane fraction, to a lesser extent by day 14, while these changes accumulated significantly by day 35. These changes included i) fragmentation of structural proteins, ii) relocation of anti-oxidant enzymes from the cytosol to the membrane, iii) promotion of vesiculation through proteins associated to vesicle formation and docking to the membrane.

Vesiculation results in membrane loss and thus in the final acquisition of the spherocytic phenotype, as confirmed via SEM.

From the present study it finally emerges that, under a mere biochemical and molecular standpoint, the parameters defining the integrity of SAGM-stored leukodepleted RBCs might be still acceptable within the first 14 days of storage and then begin to slowly decline at day 21 and onwards.

All the tested parameters appeared to be modified over storage as they are in RBCs from hereditary spherocytosis patients. Indeed, membrane structural protein fragmentation, accumulation in the membrane district of anti-oxidant enzymes and chaperones, as well as the increase in protein carbonylation and MDA accumulation are representative of a significant and prolonged exposure to oxidative stress in *ex vivo* RBCs.

Table 1 – Protein spots showing statistically-significant differential photodensity between day 0 and day 35 RBC membrane samples

Table 1A - Extraction performed in absence of NEM (day 0, 14 and 35)				
SPOT	Mr, kDa theor.	Seq Cov (%)	NCBI Accession Number	Protein ID [Homo sapiens]
104	247026	9%	gi 338441	Beta-spectrin
176	282024	4%	gi 338438	Erythroid alpha spectrin
211	282024	4%	gi 338438	Erythroid alpha spectrin
226	11537	17%	gi 66473265	Beta globin chain
239	281039	15%	gi 115298659	Spectrin alpha chain, erythrocyte
249	6595	38%	gi 13492060	Truncated beta-globin
303	42623	21%	gi 14277739	Chain P, crystal structure of the cytoplasmic domain of human erythrocyte band-3 protein
320	66756	3%	gi 4758274	Protein 4.1 isoform 6
327	92774	4%	gi 62088878	Protein 4.1 variant
342	92774	4%	gi 62088878	Protein 4.1 variant
402	22049	40%	gi 32189392	Peroxiredoxin 2 isoform a
417	22049	40%	gi 32189392	Peroxiredoxin 2 isoform a
389	22049	40%	gi 32189392	Peroxiredoxin 2 isoform a
187	28876	36%	gi 5453990	Proteasome activator subunit 1 isoform 1

Table 1 B - Extraction performed in presence of NEM (day 0 and 35)

SPOT	Mr, kDa theor.	Seq Cov (%)	NCBI Accession Number	Protein ID [Homo sapiens]
42	73518	24%	gi 4557625	Glutamate—cysteine ligase catalytic subunit isoform a
55	63227	15%	gi 5803181	Stress-induced-phosphoprotein 1
93	52928	34%	gi 16306550	Selenium-binding protein 1
97	57794	48%	gi 5453603	T-complex protein 1 subunit beta isoform 1
98	52492	4%	gi 4505237	55 kDa erythrocyte membrane protein isoform 1 (ankyrin 1)
	52928	25%	gi 16306550	Selenium-binding protein 1
101	59035	21%	gi 1136741	KIAA0002
	60981	17%	gi 37787305	Nicotinate phosphoribosyltransferase-like protein
104	52057	16%	gi 4503729	Peptidyl-prolyl cis-trans isomerase FKBP4
	247026	9%	gi 338441	Beta-spectrin
118	42938	26%	gi 13277550	FLOT2 protein
176	282024	4%	gi 338438	Erythroid alpha spectrin
211	47055	32%	gi 33186798	DNA-damage inducible protein 2
	41477	25%	gi 19923193	Hsc70-interacting protein

226	35325	24%	gi 4506127	Ribose-phosphate pyrophosphokinase 1
	11537	17%	gi 66473265	Beta globin chain
233	31951	23%	gi 6841176	HSPC263
	32630	5%	gi 4759274	Thioredoxin-like protein 1
239	281039	15%	gi 115298659	Spectrin alpha chain, erythrocyte
242	33681	45%	gi 3929617	Alpha SNAP
248	27249	59%	gi 4588526	Nuclear chloride channel
	31050	10%	gi 504011	Glutamate—cysteine ligase regulatory subunit
249	31956	68%	gi 33413400	S-formylglutathione hydrolase
	6595	38%	gi 13492060	Truncated beta-globin
253	31860	46%	gi 181184	Stomatin peptide
254	29243	61%	gi 24119203	Tropomyosin alpha-3 chain isoform 2
263	27815	58%	gi 6912586	6-Phosphogluconolactonase
	27833	48%	gi 4758484	Glutathione S-transferase omega-1 isoform 1
270	33667	32%	gi 47933379	Alpha-soluble NSF attachment protein
274	26337	50%	gi 5174741	Ubiquitin carboxyl-terminal hydrolase isozyme L3
	27899	21%	gi 4507953	14-3-3 Protein zeta/delta
280	21960	52%	gi 544759	Biliverdin-IX beta reductase isozyme I
281	21960	35%	gi 544759	Biliverdin-IX beta reductase isozyme I
292	27833	48%	gi 4758484	Glutathione S-transferase omega-1 isoform 1
	27704	47%	gi 312597295	Chain A, crystal structure of human glutathione transferase omega 1, delta 155
295	27815	48%	gi 6912586	6-Phosphogluconolactonase
297	22178	46%	gi 577777	Glutathione peroxidase
	21699	37%	gi 119623103	Proteasome 26S subunit, non ATPase, 10, isoform
303	42623	21%	gi 14277739	Chain P, crystal structure of the cytoplasmic domain of human erythrocyte band-3 protein
320	96646	26%	gi 6424942	ALG-2 interacting protein 1
	66756	3%	gi 4758274	Protein 4.1 isoform 6

Table 2 – SEM erythrocyte shape classification			
Day	Discocyte (%)	Reversibly* changed RBC (%) (echinocyte and stomatocyte shape)	Irreversibly* changed RBC (%) (spherochinocyte, spherostomatocyte, spherocyte, ovalocyte, and degenerated shapes)
7	75.3 ± 4.1	15.5 ± 1.9	9.2 ± 3.5
14	55.8 ± 2.7	29.1 ± 2.4	15.1 ± 0.9
21	51.0 ± 4.0	32.6 ± 2.6	16.4 ± 1.4
28	45.6 ± 3.3	35.6 ± 1.7	18.8 ± 1.6
35	35.2 ± 1.9	42.3 ± 2.2	22.5 ± 3.1
42	23.7 ± 2.5	45.3 ± 3.8	31.0 ± 2.9
* Reversible and irreversible changes were classified based on classification by Berezina et al. (2002). However, Bessis' shape classification details are provided as well (bold)			

5.2 Alterations of Red Blood Cell metabolome during cold liquid storage of erythrocyte concentrates in CPD-SAGM

Overview of this section

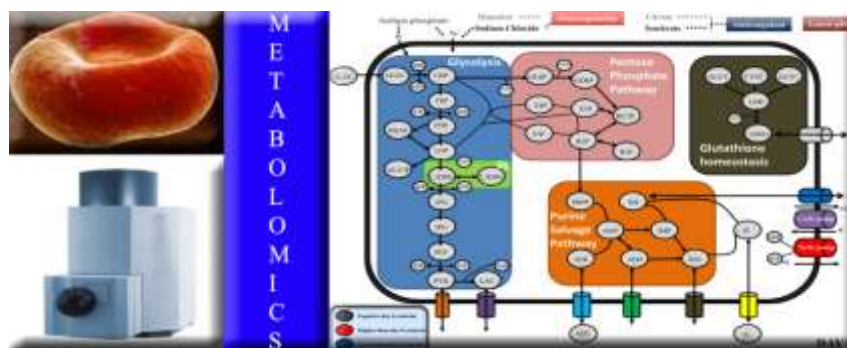
Erythrocyte concentrates for transfusion purposes represent a life-saving therapeutics of primary relevance in the clinical setting. However, efforts have been continuously proposed to improve safety and efficacy of long-term stored red blood cells.

By means of liquid chromatography coupled with high sensitive Q-TOF mass spectrometry, we were able to perform an untargeted metabolomics analysis in order to highlight metabolic species (i.e. low molecular biochemicals including sugars, lipids, nucleotides, aminoacids, etc.), both in red blood cells and supernatants, which showed fluctuations against day 0 controls over storage duration on a weekly basis.

We could confirm and expand existing literature about the rapid fall of glycolytic rate and accumulation of glycolysis end products. A shift was observed towards the oxidative phase of pentose phosphate pathway, in response to an exacerbation of oxidative stress (altered glutathione homeostasis and accumulation of peroxidation/inflammatory products in the supernatant).

The present study provides the first evidence that over storage duration metabolic fluxes in red blood cells proceed from pentose phosphate pathway towards purine salvage pathway, instead of massively re-entering glycolysis via the nonoxidative phase.

Keywords: red blood cell; storage; mass spectrometry; metabolomics.



Introduction

Red blood cells (RBCs) are the most commonly transfused blood component, with 20-70 units of RBCs per thousand individuals transfused in countries with High Human Development Index each year (Hess, 2010). However, despite the strict International guidelines for collection and preservation of blood-derived therapeutics (Council of Europe, 2011), there is still no definitive solution to the controversial issue about the need to pursue a better, rather than a longer storage or, in other terms, to privilege safety and effectiveness over availability (Liumbruno et al., 2010). Indeed, while current guidelines allow storing RBC concentrates for as long as 42 days under cold (1-6°C) liquid blood-bank conditions, there is still no definitive solution to the controversial issue about the need for improved quality of RBC concentrates (Koch et al., 2008). While this hot topic has been largely reviewed (Lelubre et al., 2009), no definitive evidence has been hitherto gathered upon screening of data from early prospective clinical trials (Steiner et al., 2010). On the other hand, *in vitro* studies seemed to underpin the “no longer than 14 days” hypothesis through the observation that RBCs undergo dramatic and statistically significant morphologic, metabolic and proteomics modifications from the second week of storage onwards (D’Alessandro et al., 2012). While oxidative stress has been reported as the triggering factor behind the accumulation of the so-called storage lesions (D’Alessandro et al., 2012), it should be noted that RBCs are naturally equipped to strive against intense oxidative stress. Indeed, it is worthwhile to underline that the 2% of non-hemoglobin cytosolic proteins in RBCs are made up of 1578 distinct gene products (Roux-Dalvai et al., 2008) which, along with membrane proteins, characterize a huge proteome of approximately 1989 unique proteins that are mostly involved in anti-oxidative stress responses (D’Alessandro et al., 2010). Therefore, one major point should be stressed: RBC storage exacerbates the effects of oxidative stress through triggering physiologic unbalance. While in our previous study we could only postulate this consideration, due to the limited coverage of the metabolome (only 12 metabolic species were investigated), in the present study we decided to perform an extensive metabolomics investigation to address the physiologic issue. Metabolomics can be roughly defined as the next stage of clinical biochemistry, where a biological matrix is investigated to unravel quali-quantitative trends for all metabolites (i.e. chemical species below the 1.5 kDa molecular weight threshold – including sugars and sugar-phosphates, lipids, nucleotides, aminoacids, etc.) (D’Alessandro and Zolla, 2012). While early attempts tried to retrieve biologically-relevant information through spectroscopic assay-based monitoring of a handful of metabolites (including 2,3-diphosphoglycerate – DPG, adenosine triphosphate – ATP or lactate) (Valeri and Hirsch, 1969; Burger et al., 2010), alternative approaches to the RBC metabolome have been proposed over the last decade, which either rely on Nuclear Magnetic Resonance (NMR) (Messana et al., 1999; Messana et al., 2000) or Mass Spectrometry (MS) (Nishino et al., 2009; Darghouth et al., 2010, 2011a and 2011b). Since these approaches yield massive amounts of data, which need statistical filtering upon bioinformatics elaboration, specific software has been developed for data handling and *in silico* simulation of metabolic trends (Nakayama et al., 2005).

The role of metabolism in buffering the extent of RBC-targeting storage lesions has been long demonstrated, through the correlation of few key metabolic parameters such as pH, K⁺, saline, ATP, DPG, hexose phosphates and lactate to the occurrence of haemolytic phenomena, reduced oxygen off-loading capacity and *in vivo* survival at 24 hours upon transfusion (Hogman and Meryman, 1999; Hess et al., 2000). Based upon these observations, it was

proposed that metabolic modulation through the introduction of additive solutions alternative to the acidic SAGM would have helped counteracting metabolic dysregulation and delaying the insurgence of RBC lesions, while enabling to prolong the shelf-life of the erythrocyte concentrate therapeutic up to twelve weeks (Hess et al., 2002; Hess et al., 2003; Hogman et al., 2006; Hess et al., 2006). Despite the efforts produced over decades of research, additive solutions have been mostly patented only when in compliance with two mainstream criteria, haemolysis (below 0.8%) and *in vivo* survival at 24 h upon transfusion (above 75%). It is thus interesting to note that metabolic criteria were marginally adopted, and often on the basis of the chemical sensibility of the proposing researcher rather than actual requirements by the issuing institution. While it is largely accepted since Valtis and Kennedy's report that DPG levels correlate with oxygen off-loading capacity (Valtis and Kennedy, 1954), or that ATP modulates cation homeostasis and thus RBC morphology through regulation of osmotic stress (Bennet-Guerrero et al., 2007), other metabolic parameters have been almost totally ignored, often due to technical limitations and scarce biological understanding of their role in the frame of RBC storage.

In the study by D'Alessandro et al. (2012) twelve metabolites were *a priori* selected on the basis of the expected mass/charge ratio and fragmentation pattern upon comparison to an external standard for the same molecule, a workflow known as Multiple Reaction Monitoring or MRM. In other terms, in MRM metabolites could be screened only after testing a standard for that molecule, one metabolite at a time. Conversely, one of the main advantages of untargeted approaches stems from the possibility to theoretically investigate all MS-detectable species simultaneously, expanding the boundaries of the analysis up to the instrument limits. In this view, we hereby assayed all chemical species below the 1.5 kDa threshold without any *a priori* restriction. Detected metabolites were monitored over storage duration and highlighted when modulated (fold-change variation against day 0 controls) in a statistically significant fashion ($p < 0.01$ ANOVA). Relative quantitative variations have been then graphed and discussed for those metabolites emerging from the main catabolic pathways in RBCs. The present study could provide a biochemical basis to further assess the advantages of newly proposed additive solutions or rather set up a background knowledge in order to comparatively test the effectiveness of alternative storage strategies, such as anaerobic storage.

Design and Method

Sample collection

Red blood cells units were drawn from healthy human volunteers according to the policy of the Italian National Blood Centre guidelines (Blood Transfusion Service for donated blood) and all the volunteers provided their informed consent in accordance with the declaration of Helsinki. We studied RBC units collected from 10 healthy donor volunteers [male=5, female=5, age 42.3 ± 10.5 (mean \pm S.D.)]. In details, whole blood (450 mL + 10%) was collected from healthy volunteer donors into CPD anticoagulant (63 mL) and leukodepleted (i.e. 4-log WBC depletion). After separation of plasma by centrifugation, RBCs were suspended in 100 mL of SAG-M (Saline, Adenine, Glucose, Mannitol) additive solution. RBC units were stored for up to 42 days under standard conditions ($1-6^\circ$), while samples were removed aseptically for the analysis on a weekly basis (at 0, 7, 14, 21, 28, 35 and 42 days of storage).

Cation measurements and haemolysis

Supernatant potassium, internal and external pH and calcium levels and haemolysis were measured as previously reported (Bennet-Guerrero et al., 2007; Hogman et al, 2006; Burger et al., 2010).

Untargeted Metabolomics Analyses

Metabolite extraction

For each sample, 0.5mL from the pooled erythrocyte stock was transferred into a microcentrifuge tube (Eppendorf® Germany). Erythrocyte samples were then centrifuged at 1000g for 2 minutes at 4°C. Tubes were then placed on ice while supernatants were carefully aspirated, paying attention not to remove any erythrocyte at the interface. Samples were extracted following the protocol by D'Alessandro et al. (2011). The erythrocytes were resuspended in 0.15 mL of ice cold ultra-pure water (18 MΩ) to lyse cell, then the tubes were plunged into a water bath at 37°C for 0.5 min. Samples were mixed with 0.6 mL of -20°C methanol and then with 0.45 mL chloroform. Subsequently, 0.15ml of ice cold ultra-pure water were added to each tube and they were transferred to -20°C freezer for 2-8 h. An equivalent volume of acetonitrile was added to the tube and transferred to refrigerator (4°C) for 20 min. Samples with precipitated proteins were thus centrifuged for 10000 x g for 10 min at 4 °C .

Finally, samples were dried in a rotational vacuum concentrator (RVC 2-18 - Christ GmbH; Osterode am Harz, Germany) and re-suspended in 200 µl of water, 5% formic acid and transferred to glass auto-sampler vials for LC/MS analysis.

Rapid Resolution Reversed-Phase HPLC

An Ultimate 3000 Rapid Resolution HPLC system (LC Packings, DIONEX, Sunnyvale, USA) was used to perform metabolite separation. The system featured a binary pump and vacuum degasser, well-plate autosampler with a six-port micro-switching valve, a thermostated column compartment. Samples were loaded onto a Reprosil C18 column (2.0mm×150mm, 2.5 µm - Dr Maisch, Germany) for metabolite separation.

Chromatographic separations were achieved at a column temperature of 30°C; and flow rate of 0.2 mL/min. For downstream negative ion mode (-) MS analyses, A 0–100% linear gradient of solvent A (10mM tributylamine aqueous solution adjusted with 15mM acetic acid, pH 4.95) to B (methanol mixed with 10 mM TBA and with 15 mM acetic acid, pH 4.95) was employed over 30 min, returning to 100% A in 2 minutes and a 6-min post-time solvent A hold. For downstream positive ion mode (+) MS analyses, a 0–100% linear gradient of solvent A (ddH₂O, 0.1% formic acid) to B (acetonitrile, 0.1% formic acid) was employed over 30 min, returning to 100% A in 2 minutes and a 6-min post-time solvent A hold.

Mass Spectrometry: Q-TOF settings

Due to the use of linear ion counting for direct comparisons against naturally expected isotopic ratios, time-of-flight instruments are most often the best choice for molecular formula determination. Thus, mass spectrometry analysis was carried out on an electrospray hybrid quadrupole time-of flight mass spectrometer MicroTOF-Q (Bruker-Daltonik, Bremen, Germany) equipped with an ESI-ion source. Mass spectra for metabolite extracted samples were

acquired both in positive and in negative ion mode. ESI capillary voltage was set at 4500V (+) (-) ion mode. The liquid nebulizer was set to 27 psi and the nitrogen drying gas was set to a flow rate of 6 L/min. Dry gas temperature was maintained at 200°C. Data were stored in centroid mode. Data were acquired with a stored mass range of m/z 50–1200. Automatic isolation and fragmentation (AutoMSⁿ mode) was performed on the 4 most intense ions simultaneously throughout the whole scanning period (30 min per run).

Calibration of the mass analyzer is essential in order to maintain a high level of mass accuracy. Instrument calibration was performed externally every day with a sodium formate solution consisting of 10 mM sodium hydroxide in 50% isopropanol: water, 0.1 % formic acid. Automated internal mass scale calibration was performed through direct automated injection of the calibration solution at the beginning and at the end of each run by a 6-port divert-valve.

Data elaboration and statistical analysis

In order to reduce the number of possible hits in molecular formula generation, we exploited the SmartFormula3D™ software (Bruker Daltonics, Bremen, Germany), which directly calculates molecular formulae based upon the MS spectrum (isotopic patterns) and transition fingerprints (fragmentation patterns). This software generates a confidence-based list of chemical formulae on the basis of the precursor ions and all fragment ions, and the significance of their deviations to the predicted intact mass and fragmentation pattern (within a predefined window range of 5 ppm). Triplicate runs for each one of the 10 biological replicate over storage duration were exported as mzXML files and processed through XCMS data analysis software (Scripps Centre for Metabolomics) (Tautenhahn et al., 2011). Mass spectrometry chromatograms were elaborated for peak alignment, matching and comparison of parent and fragment ions, and tentative metabolite identification (within a 20 ppm mass-deviation range between observed and expected results against the internal database – METLIN (Smith et al., 2005)). XCMS is an open-source software and is freely available from the website (<http://metlin.scripps.edu/download/>). Quantitative variations were determined against day 0 controls and only statistically significant results were considered (ANOVA p -values < 0.01). Data were further refined and plotted with GraphPad Prism 5.0 (GraphPad Software Inc.)

Results and Discussions

HPLC-MS runs were performed in triplicate on samples extracted at 0, 7, 14, 21, 28, 35, 42 days of storage. Due to the massive amount of output data, only significant results displaying absolute values for fold-change variations higher than 10 (7, 14, 21, 28, 35 or 42 day against day 0) were summarized as in **Supplementary Tables 1-6**, along with feature number, feature name, p -value, mass to charge ratio (m/z), chromatographic retention times, day specific intensities and tentative identification (with isotope description, molecular weight deviation in ppm from database top hit reports, name, presence of K⁺, Na⁺, NH₄⁺ adducts and METLIN identifier), as identified by XCMS. In order to report the main results in a more readable layout, metabolites accounting for the most relevant catabolic pathways in RBCs were grouped and plotted as follows: relevant biochemical parameters or metabolites from the (i) supernatant (**Figure 1**) or involved in (ii) glycolysis (**Figure 2**); (iii) pentose phosphate pathway (PPP – **Figure 3**); (iv) glutathione homeostasis (**Figure 4**); and (v) purine salvage pathway (PSP – **Figure 5**).

Nutrients in the supernatant were slowly depleted and cation homeostasis dysregulated

Alterations to RBC pH over storage duration have been long reported (Bennet-Guerrero et al., 2007), although few studies show discriminations between cytoplasmic and supernatant pH (**Figure 1**) (Hogman et al., 2006). Our results are in agreement with Högman et al. (2006) and Burger et al. (2010) for CPD-SAGM-stored controls, with slightly higher external pH at the beginning of the storage period, while internal pH dropping to 6.4 to 6.5 values at day 42. From day 0 to day 42, hemolysis values for each tested unit were below the 0.8 % maximum threshold allowed by the European Council Guidelines (2011). (**Figure 1**). Analogous considerations can be made for potassium (K^+), accumulating in the supernatant (Bennet-Guerrero et al., 2007; Burger et al., 2010). Electrolyte balance is maintained by sodium-potassium cationic pumps in an ATP and temperature dependent fashion, as they are inhibited at 4°C (Wallas et al., 1979).

Cationic pump activity is pivotal to preserve the cytoplasmic ionic milieu thus preventing colloidal osmotic lysis. Calcium cytosolic accumulation (**Figure 1**) was significant as well, with a net increase within the first seven days of storage prior to reaching a plateau in between 1.5 – 2 fold change levels in comparison to day 0 controls. Similar trends have been reported in literature *in vitro* (Wiley et al., 1982) or *in vivo* (LaCelle et al., 1972). Since internal Ca^{2+} is subjected to metabolic control via an ATP-dependent extrusion mechanism (Ca^{2+} pump) (Schatzmann, 1966), decreased ATP content attained during red cell ageing should lead to a raised cellular Ca^{2+} . Multiple evidences underpin this statement: through the use of the fluorescent probe Fura-2 in cells separated on Percoll density gradients, LaCelle et al. revealed that *in vivo* aged RBCs (senescent) contained a higher free Ca^{2+} content (almost four times) than the younger cells (LaCelle et al., 1972). The consistency of the role of Ca^{2+} in the frame of RBC storage is strengthened by the consideration about the role of this ion in modulating the Ca-dependent K channel (K/Ca channel) (Romero, 1976) and the influence on RBC membrane shape.

Glucose consumption from the supernatant was gradual albeit constant throughout the whole storage duration (approximately cut by half by day 42 in comparison to day 0 controls - **Figure 1**), in agreement with Burger et al. (2010) who reported a 0.6 fold change decrease by day 35. This result suggests both that glucose internalization is not apparently inhibited over storage and initial glucose levels are higher than actual cellular requirement.

On the other hand, adenine appeared to be almost fully depleted in the supernatant in the storage window range between 14 and 21 days (**Figure 1**). Kreuger and Åkerblom (1980) found that about 20 percent of extracellular adenine in CPD-adenine whole blood containing 0.125 mmol per unit had disappeared after 1 week and 70 percent after 2 weeks. On the other hand, the addition of adenine-containing SAGM to CPDA should in theory increase the levels of adenine and thus delay its full consumption in the supernatant. Therefore, in the present study, the complete depletion of adenine from the supernatant might be either biased by technical issues (concentrations outside the linearity detection range of the MS instrument which can result in underestimation of this metabolite through mass spectrometry) or might in part be due to actual chemical modifications (such as deamination to inosine, which is known to partially occur over storage duration (Hess et al., 2010)). Nevertheless, the overall trend towards adenine decrease in the supernatant is consistent with literature and further supports the rationale behind supplementation of rejuvenation solutions to replenish adenine levels (other than pyruvate, inosine, phosphate) in the storage medium, to the end of extending the shelf life of erythrocyte concentrates up to 120 days (Meyer et al., 2011).

Likewise, mannitol levels decreased significantly over storage duration (**Figure 1**), which is relevant in the light of the role of mannitol as free radical scavenger in additive solutions (Beutler and Kuhl, 1988). It is worthwhile to underline that sample testing at the end of the storage period allowed us to exclude microbial contaminations of the RBC units. Indeed, while human RBCs do not metabolize mannitol to a significant extent, though they have been long suggested to metabolize the oxidized product by hydroxyl radicals – mannose (Beutler and Teeple, 1969)). Scavenging of hydroxyl groups by mannitol could have resulted in the alteration of the molecular mass and thus of the mass to charge ratio to be monitored through mass spectrometry in order to quantitatively assess the levels of this metabolite.

On the other hand, we were not able to outline a precise trend for citrate, a nondiffusible anticoagulant that chelates Ca^{2+} (Hogman and Meryman, 2006), in the storage medium. In fact, we found discontinuous alterations of citrate levels in the supernatant, probably due to formation of unscreened adducts (e.g. with Ca^{2+}) or multimers, masking MS outputs and tentative identification.

Glycolytic intermediates were rapidly depleted over the first two weeks, while end-products accumulated

Rapid pH drop over storage duration is long known to relate to active glycolysis and lactate accumulation, other than cation homeostasis dysregulation. In our previous targeted investigation we could only monitor six distinct glycolytic metabolites, including hexoses 6-phosphate (either glucose or fructose 6-phosphate, as it is not possible to discriminate these molecules from MS analysis of intact mass or fragmentation patterns), fructose 1,6-biphosphate, glyceraldehyde 3-phosphate, DPG, phosphoenolpyruvate and lactate (D'Alessandro et al., 2012).

Through shifting from a targeted (MRM) to an untargeted (MicroTOFQ-based) platform, we were hereby able to confirm trends for the aforementioned glycolytic metabolites and complete the list with dihydroxyacetone phosphate, phosphoglycerate and pyruvate (**Figure 2**). While technical advantages of actual metabolome-wide rather than targeted approaches have been already reported in the frame of RBCs (i.e. hereditary stomatocytosis and sickle cell disease) (Nishino et al., 2009; Darghouth et al., 2010, 2011a and 2011b), no actual metabolomics study has so far addressed the storage issue.

In biological terms, we could confirm (Nishino et al., 2009; D'Alessandro et al., 2012) increases of early glycolytic intermediates (hexose 6-phosphate, fructose 1,6-biphosphate, glyceraldehyde 3-phosphate and dihydroxyacetone phosphate) within the first week of storage, while a rapid decrease of all glycolytic metabolites was observed soon afterwards. On the other hand, late glycolytic intermediates, such as phosphoenolpyruvate, pyruvate and lactate followed different trends, with pyruvate and lactate slowly increasing throughout the whole storage period (**Figure 2**), partly confirming and partly expanding available data from literature for SAGM-stored erythrocyte concentrates (Hess et al., 2006; Burger et al., 2010; D'Alessandro et al., 2012).

Glycerol 3-phosphate was observed to increase within the first two weeks of storage and thus rapidly decrease. The trend for this metabolite is interesting since glycerol 3-phosphate, a precursor to glycerol which is synthesized from glyceraldehyde 3-phosphate, in human cells is exploited in lipidogenesis for biosynthesis of triglycerids. However, phospholipid synthesis is known to be active in reticulocytes and suppressed in mature RBCs (Percy et al., 1973). Alteration of membrane lipid homeostasis has been widely documented in the frame of RBC storage, due to lipid

peroxidation leading to membrane-targeting shape alterations, which are characterized by progressive loss of lipids (and membrane-associated proteins) through vesiculation (Bosman et al., 2008; D'Alessandro et al., 2012).

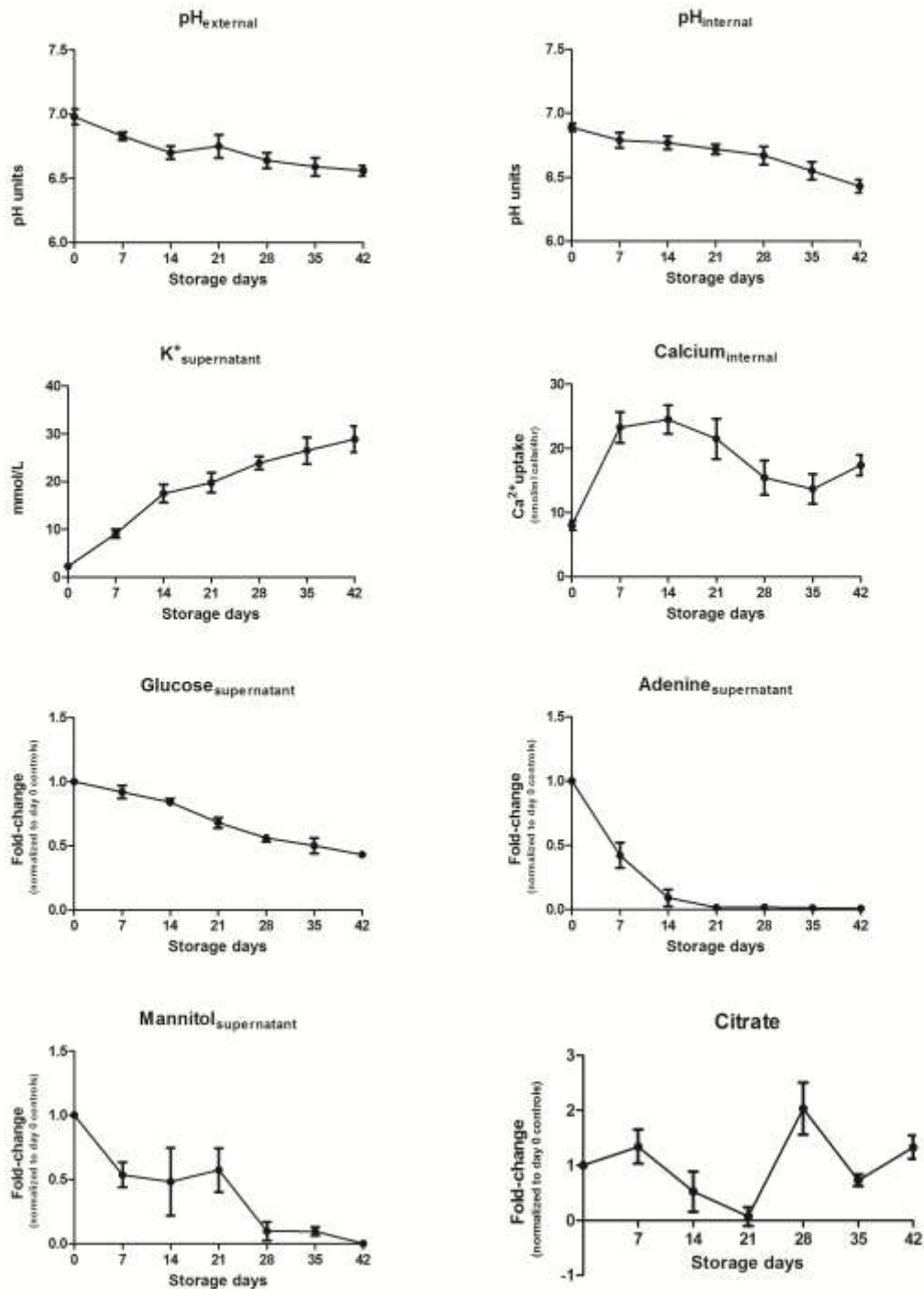


FIGURE 1 Biochemical analyses of RBC supernatants over storage duration. Weekly repeated measurements are reported for external and internal pH, supernatant potassium and intracellular calcium. Fold-change variations against day 0 controls are reported for glucose, adenine, mannitol and citrate. Averages and standard deviations were calculated on 10 biological replicates, each one run in triplicate.

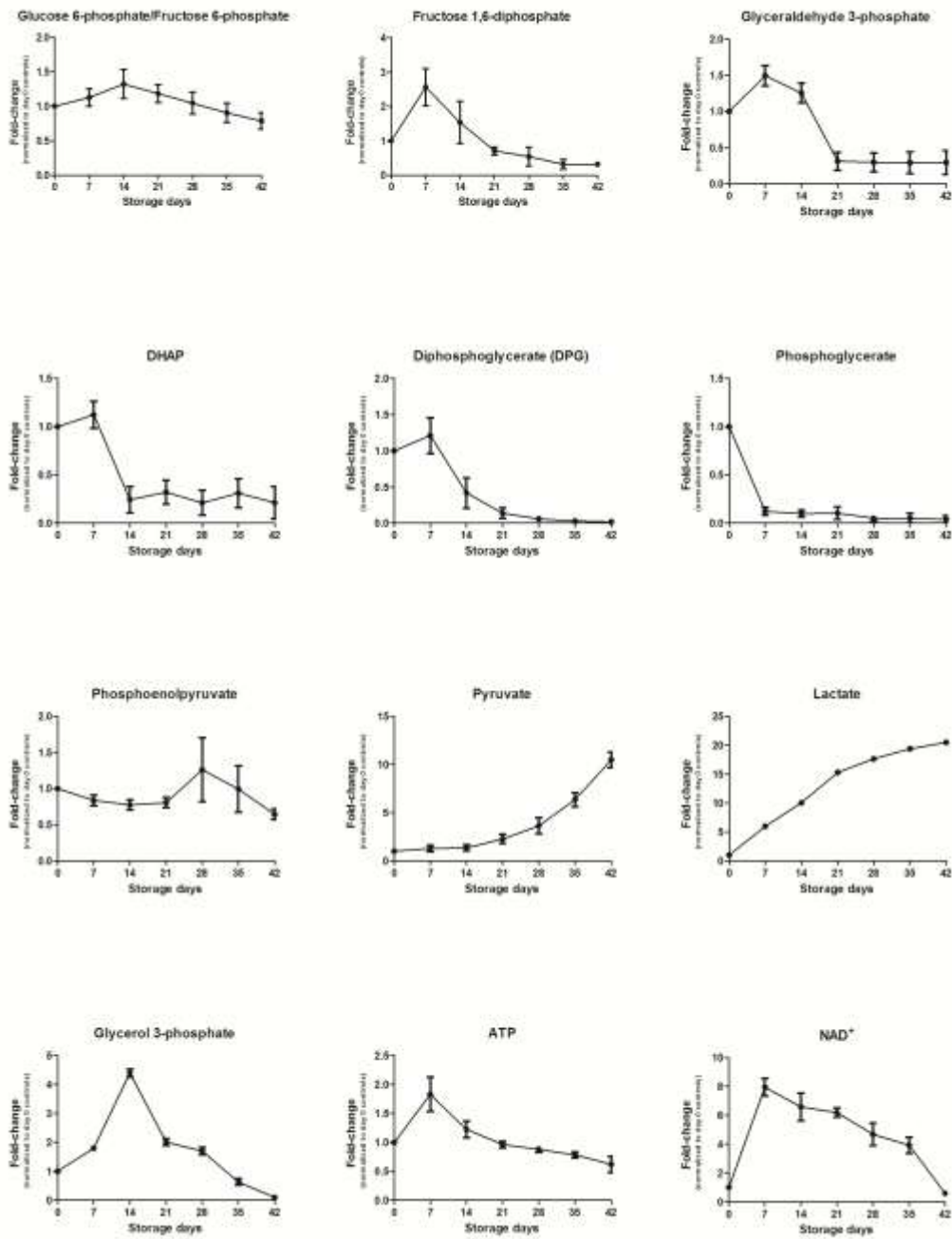


FIGURE 2 Time course metabolomic analyses of SAGM-stored RBCs, upon normalization against day 0 controls, through plotting of fold-change variations in agreement with analogous studies of untargeted metabolomics applied to RBC investigations (Nishino et al., 2009; Darghouth et al., 2010, 2011a and 2011b; D'Alessandro et al., 2012). An overview of trends for glycolytic metabolites. Averages and standard deviations were calculated on 10 biological replicates, each one run in triplicate.

ATP and DPG drops were consistent with published literature relying on classic spectrophotometric assays (Valeri et al., 1969, Bennet-Guerrero et al., 2007; Burger et al., 2010). DPG, in association with pH and $\text{HCO}_3^-/\text{CO}_2$ The progressive drop of glycerol 3-phosphate levels from day 14 onwards might reflect the extent of vesiculation phenomena. In parallel with this statement, a significant increase within the first two weeks of storage and a subsequent rapid decrease was hereby observed for a wide series of fatty acids and lipids over storage duration (**Supplementary Tables 1-5 in Gevi et al., 2012**). A handful of lipids showed rapid accumulation at day 7 (TG(20:5(5Z,8Z,11Z,14Z,17Z)/22:3(10Z,13Z,16Z)/22:5 (7Z,10Z,13Z,16Z,19Z))[iso6]; TG(17:0/18:2(9Z,12Z)/20:0)[iso6]; DG(17:1(9Z)/17:1(9Z)/0:0; Anandamide (20:1, n-9) – **Supplementary Table 1 in Gevi et al., 2012**) in comparison to day 0 controls. On the other hand, a long series of lipids decreased significantly from day 21 onwards (C-8 Ceramide – **Supplementary Table 3 in Gevi et al., 2012**; Sphingosine; PC(O-1:0/O-18:0) - **Supplementary Table 4 in Gevi et al., 2012**; C-8 Ceramide; PI(13:0/0:0); Ceramide (d18:1/12:0); 5,13-docosadienoic acid – **Supplementary Table 5 in Gevi et al., 2012**; C-2 Ceramide; PC(10:0/18:0) – **Supplementary Table 6 in Gevi et al., 2012**).

modulates position and shape of the oxygen dissociation curve (Rouault, 1973). In RBCs, CO_2 is rapidly hydrated to H_2CO_3 inside RBCs by carbonic anhydrase, and the H_2CO_3 promptly dissociates into H^+ and HCO_3^- . Band 3 protein, the major integral membrane protein of RBCs, exchanges the cellular HCO_3^- with Cl^- in plasma, a process that is conventionally known as the “chloride shift”. As the result of the anion exchange, the weak acid H_2CO_3 is converted to the strong acid HCl, and consequently the intracellular pH of RBCs is rendered acidic. This acidification is the trigger for the dissociation of O_2 from oxyhemoglobin (HbO_2) and, *in vivo*, the dissociated O_2 is supplied to tissues that metabolically produce CO_2 . Protons formed in RBCs are accepted by the groups of deoxyhemoglobin (HbH^+) participating in the “Bohr Effect”, and the pH within the RBCs is restored in order to prevent further dissociation of oxygen from HbO_2 . Deoxyhemoglobin has been shown to bind to the cytosolic domain of band 3, thus triggering dissociation of a group of glycolytic enzymes (including glyceraldehyde 3-phosphate dehydrogenase, phosphofructokinase and aldolase which directly bind to N-ter of band 3; pyruvate kinase and lactate dehydrogenase, which bind in close proximity to it) through direct competition for docking sites (Low et al., 1993; Lewis et al., 2009). Displacement of glycolytic enzymes from membrane to cytosol corresponds to an increase in glycolytic enzyme activities, utterly resulting in promoting glycolytic fluxes and cytosol pH lowering. In parallel, pH lowering has a negative feedback on enzyme activities (Burr, 1972). One factor altering this strictly modulated mechanism in the frame of cold liquid storage is at the protein level, since band 3 has been shown to undergo fragmentation at the cytosolic domain level over storage duration (D’Alessandro et al., 2012). As far as fragmentation is concerned, for senescent RBCs *in vivo* it has been postulated a role for calcium homeostasis dysregulation in triggering apoptosis-like phenomena through proteolytic cascades involving calpains (Pompeo et al., 2010). In RBC ageing *in vitro* (liquid cold storage), fragmentation is further exacerbated by oxidative stress (D’Alessandro et al., 2012).

Metabolix fluxes towards the Pentose Phosphate Pathway were altered

An indirect parameter to assess an increase in oxidative stress in RBCs is the ratio of glycolysis/pentose phosphate pathway (PPP) fluxes. Under normal steady-state conditions, 92% of glucose is metabolized along glycolysis (Embden Meyerhoff) and 8% along PPP. Under oxidant conditions up to 90% of glucose can be metabolized along PPP (Messana et al., 1999 and 2000; Kuchel and Philip, 2008).

The main purpose of the PPP is to regenerate NADPH from NADP⁺ through an oxidation/ reduction reaction. This reaction is coupled to the formation of ribose 5-phosphate from glucose 6-phosphate. In RBCs, the major role of NADPH is to reduce the disulfide form of glutathione to the sulfhydryl form. The reduced glutathione is pertinent for maintaining the normal structure of RBCs and for keeping hemoglobin in the ferrous state [Fe(II)].

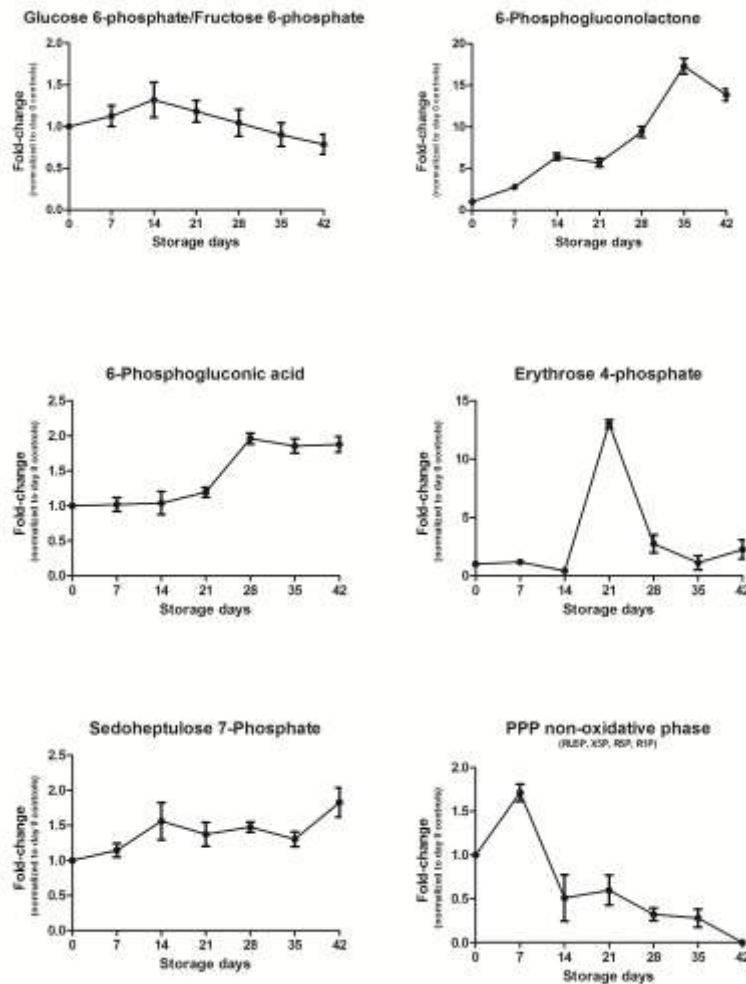


FIGURE 3 Time course metabolomic analyses of SAGM-stored RBCs, upon normalization against day 0 controls, through plotting of fold-change variations in agreement with analogous studies of untargeted metabolomics applied to RBC investigations (Nishino et al., 2009; Darghouth et al., 2010, 2011a and 2011b; D'Alessandro et al., 2012). An overview of trends for Pentose Phosphate Pathway metabolites. Averages and standard deviations were calculated on 10 biological replicates, each one run in triplicate.

The nonoxidative portion of the pathway creates carbon chain molecules ranging from 3 to 7 carbons. These compounds are intermediates in glycolysis and gluconeogenesis or other biosynthetic processes. The oxidative phase of PPP primarily produces NADPH and ribose 5-phosphate, while the nonoxidative phase yields fructose 6-phosphate, and glyceraldehyde 3-phosphate, and glyceraldehyde 3-phosphate.

In our previous investigation, we concluded that PPP appeared to be over-activated at the oxidative phase level. However, we could only postulate that some blockade might have existed at the nonoxidative phase, since it had been reported by NMR that no glyceraldehyde 3-phosphate was produced via PPP in long stored RBCs (Messana et al., 1999 and 2000).

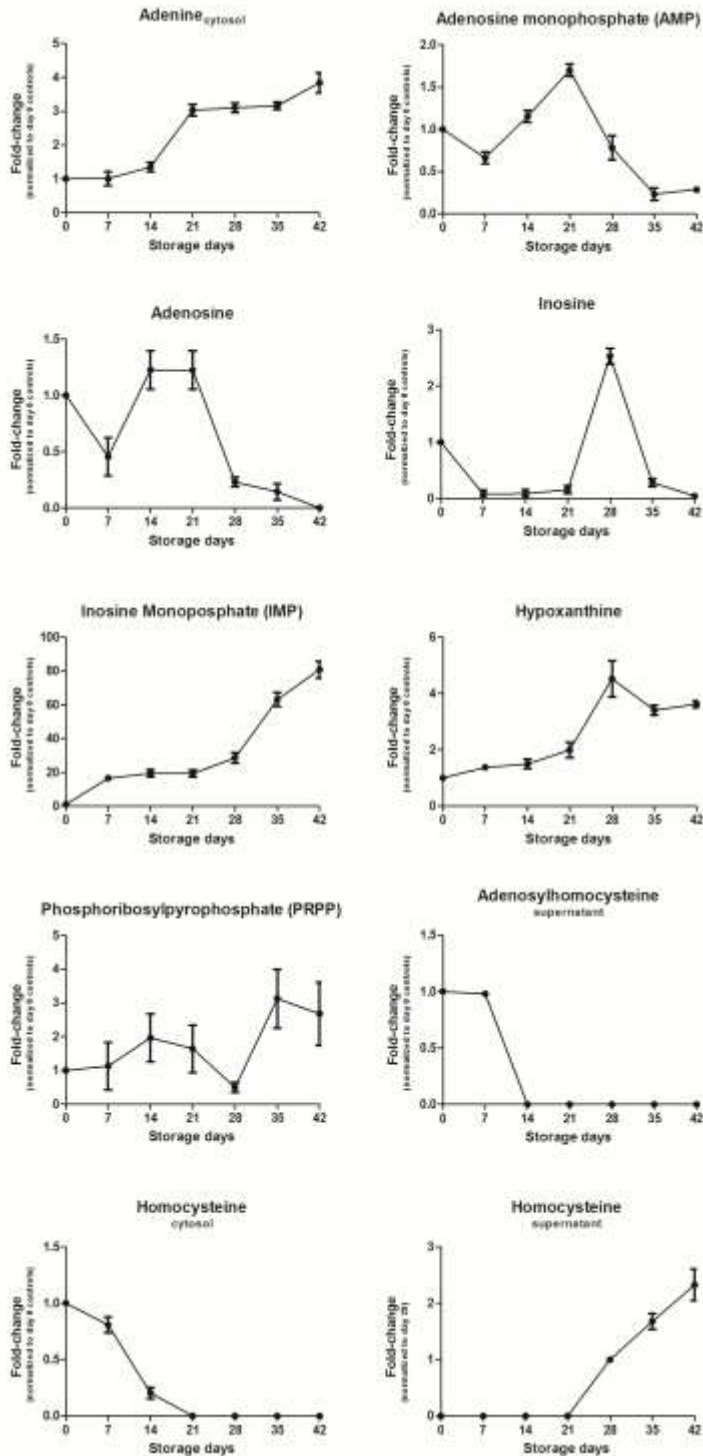


FIGURE 4 Time course metabolomic analyses of SAGM-stored RBCs, upon normalization against day 0 controls, through plotting of fold-change variations in agreement with analogous studies of untargeted metabolomics applied to RBC investigations (Nishino et al., 2009; Darghouth et al., 2010, 2011a and 2011b; D'Alessandro et al., 2012). An overview of trends for Purine Salvage Pathway metabolites. Averages and standard deviations were calculated on 10 biological replicates, each one run in triplicate.

Hereby, we could confirm and expand previous observation about the increase of metabolic intermediates and byproducts of the oxidative phase of PPP (6-phosphogluconolactone, 6-phosphogluconic acid, NADPH) (**Figure 3**). Additionally, we could further delve into our previous hypothesis about a blockade at the nonoxidative phase level, through monitoring trends for sedoheptulose 7-phosphate (increasing its levels over storage duration) and other metabolic intermediates of the nonoxidative phase (erythrose 4-phosphate, ribose 5-phosphate, ribose 1-phosphate, xilulose 5-phosphate), which decreased progressively over storage duration (**Figure 3**).

A net increase was observed from PPP towards the Purine Salvage Pathway rather than re-entering glycolysis

Since glyceraldehyde 3-phosphate was confirmed not to increase over storage duration, in agreement with literature (Messana et al., 1999 and 2000; Burger et al., 2010; D'Alessandro et al., 2012), the increase of oxidative phase intermediates might be explained through diversion to Purine Salvage Pathway (PSP). Purine nucleotides may be synthesized in cells *de novo* or reconstructed from already existing free purine bases through the salvage reactions (reutilization) (Schuster and Kevanov, 2005). Mature erythrocytes cannot synthesize 5-phosphoribosylamine and that is why the synthesis of nucleotides *de novo* is not possible in these cells (Schuster and Kevanov, 2005). However, RBCs rely on alternate routes by which nucleosides or bases can be recycled to give nucleotide triphosphates, hence the name of salvage pathway (Schuster and Kevanov, 2005). Adenine nucleotides are 70-80% of all free erythrocyte nucleotides, and their precursors in RBCs are adenine and adenosine, the transport of which through the erythrocyte membranes takes place through the facilitated diffusion (Schuster and Kevanov, 2005). Over RBC storage duration, we observed a decrease of phosphorylated forms of adenine (ATP – **Figure 2**; ADP, AMP and adenosine – **Figure 4**), while adenine itself increased throughout storage duration (**Figure 4**), probably due to penetration of adenine from the supernatant, which indeed progressively decreased (**Figure 1**). Hypoxanthine, phosphorybosylpyrophosphate and inosine monophosphate, which are major substrates for salvage reactions (Schuster and Kevanov, 2005), increased constantly as storage progressed (**Figure 4**). Increases in inosine monophosphate levels in particular might result from deamination of AMP, which is known to occur as storage progresses (Kreuger and Akerblom, 1980). Adenosinehomocysteine, which serves as a substrate to produce adenosine and homocysteine, was rapidly depleted from the supernatant along with both adenosine and homocysteine, the latter accumulating in the supernatant (**Figure 4**). Anomalies to homocysteine fine-tuning are known to be related to oxidative stress and glutathione homeostasis in RBCs as indices for middle-aged untreated essential hypertension patients (Muda et al., 2003).

Oxidative stress parameters reflected alterations to PPP and PSP pathways, resulting in the accumulation of oxidation byproducts in the supernatant

Oxidative stress and RBC storage have been strictly correlated in the last few years (Dumont et al., 2009; D'Alessandro et al., 2012). We recently documented dysregulation of glutathione homeostasis through simple monitoring of GSH and GSSG trends in long-stored RBCs (D'Alessandro et al., 2012). In the present study, we

could further expand the study of glutathione homeostasis through monitoring of additional metabolites involved in these cycles, including NADPH, glutamine and cysteine (**Supplementary Figure 1**). As a result, we could confirm progressive lowering of GSH/GSSG (reduced/oxidized glutathione) ratios (**Supplementary Figure 1**), through a rapid drop in GSH and constant increase in GSSG. GSH is the main protector of thiol groups, scavenger of oxides, peroxides, oxidant radicals and detoxificant of foreign compounds. Glutathione cycling from GSSG to the reduced form (GSH) is dependent upon NADPH generation, during the first two reactions of PPP, by via G6PD and 6-phosphogluconate dehydrogenase. NADPH is the substrate for GSH-reductase to regenerate glutathione after oxidant insults and protect catalases and peroxiredoxins from inactivation (Untucht-Grau et al., 1981).



The metabolic shift towards PPP yielding NADPH accumulation does not appear to be sufficient to protect cell from oxidative stress, while *de novo* synthesis of GSH, which is ATP dependent, is depressed in the long term (day 21 onwards), when we could detect accumulation of glutamate and cysteine (two of the three aminoacids which constitute the building blocks for GSH, along with glycine) (**Supplementary Figure 1**).

ROS accumulation and lipid peroxidation has been reported in the frame of RBC storage and correlated to lipid peroxidation (malondialdehyde accumulation), protein oxidation (accumulation of carbonylations) irreversible RBC shape alteration (acquisition of spherocytic phenotype), vesiculation phenomena (D'Alessandro et al., 2012). Hereby we report accumulation of 8-isoprostane and PGF_{2α} 1-15 lactone, two markers of lipid oxidation which belong to the PGF_{2α} family (**Figure 5**). An unexpected finding included accumulation of ferrous gluconate in the supernatant. Ferrous gluconate is a dimer of gluconic acid co-ordinated by a Fe(II) atom, which might result from accumulation in the supernatant of iron from heme groups of hemolysed RBCs and oxidation of glucose in the storage medium.

Trends for carnitine, a fatty acid transporter which is involved in fatty acid transport and membrane turn-over (Darghouth et al., 2011), were similar to the ones observed for glycerol 3-phosphate and lipids (see previous paragraphs), as we could observe a net increase in the supernatant until storage day 21 and a subsequent rapid drop (**Figure 5**).

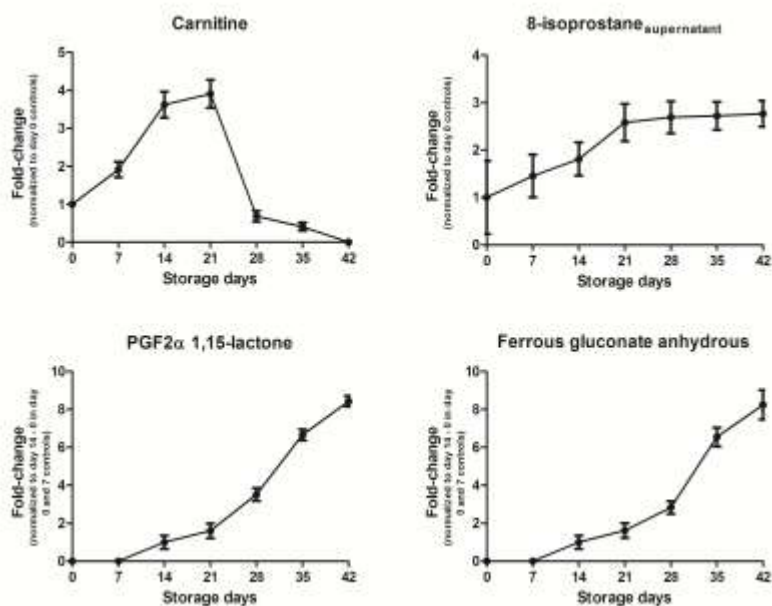


FIGURE 5 Time course metabolomic analyses of SAGM-stored RBCs, upon normalization against day 0 controls, through plotting of fold-change variations in agreement with analogous studies of untargeted metabolomics applied to RBC investigations (Nishino et al., 2009; Darghouth et al., 2010, 2011a and 2011b; D'Alessandro et al., 2012). An overview of trends for a handful of biologically-relevant oxidation products in the supernatant. Averages and standard deviations were calculated on 10 biological replicates, each one run in triplicate.

Finding the unexpected

Owing to the sensitivity of the method, we could highlight statistically significant ($p < 0.01$) fold-change variations (>10) for a wide series of unexpected chemicals which mainly highlighted biological variability of the samples collected from different healthy donor volunteers rather than actual physiological issues related to storage duration. As reported in **Supplementary Tables 1-6** in Gevi et al, 2012, untargeted MS-analyses highlighted the presence of anomalous substances in RBC extracts, such as insecticides (e.g. dichlorvos), drugs (e.g. gentamicin; ampicilloid acid), doping agents (e.g. nandrolone), food additives/food-derived contaminants (e.g. campesterol; canthaxanthin; phytosphingosine; glucosan), water contaminants (e.g. halazone; arsenate adducts - ribose-1-arsenate). Low molecular weight deviations (below 10 ppm in most cases) from expected results based on the METLIN database (Smith et al., 2005), isotopic and fragmentation patterns, allow us to exclude spurious identification of chemical compounds. However, it is beyond the scope of the present article to further delve into the biological variability issue through the determination of lower abundance contaminants, which should be purposed via targeted approaches (i.e. MRM) for definitive confirmation prior to formulating any hypothesis on the biological relevance of these findings.

Conclusion

In the present study, we performed a thorough statistically-robust metabolome-wide analysis via MS on RBC samples over storage duration under cold liquid blood bank conditions. Results are summarized in **Figure 6A**, which has been designed as to plot metabolic variations in the main RBC-relevant pathways, through highlighting of increased (red) or decreased (blue) fold-change variations over storage duration on a weekly basis (day 7, 14, 21, 28, 35 and 42, upon normalization to day 0 controls – from **Figure 6B-G**, respectively). As a result, we could confirm and expand existing literature about the rapid fall of glycolytic rate and accumulation of glycolysis end products. A shift was observed towards the oxidative phase of PPP, in response to an exacerbation of oxidative stress (altered glutathione homeostasis and accumulation of peroxidation/inflammatory products in the supernatant). However, metabolic fluxes proceeded from PPP towards PSP, instead of massively re-entering glycolysis via the nonoxidative phase, thus providing supporting evidence to previous hypotheses (D'Alessandro et al., 2012).

The present study will pave the way for future investigations aiming to assess the validity of newly proposed additive solutions or alternative storage strategies through monitoring of metabolism via a broader array of metabolic parameters.

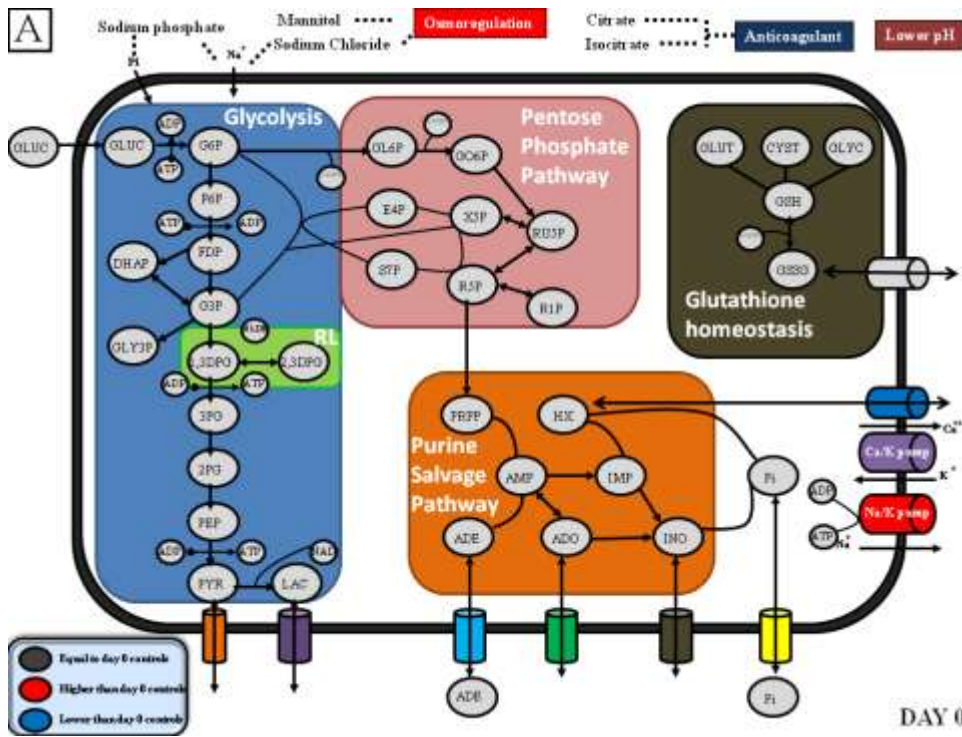
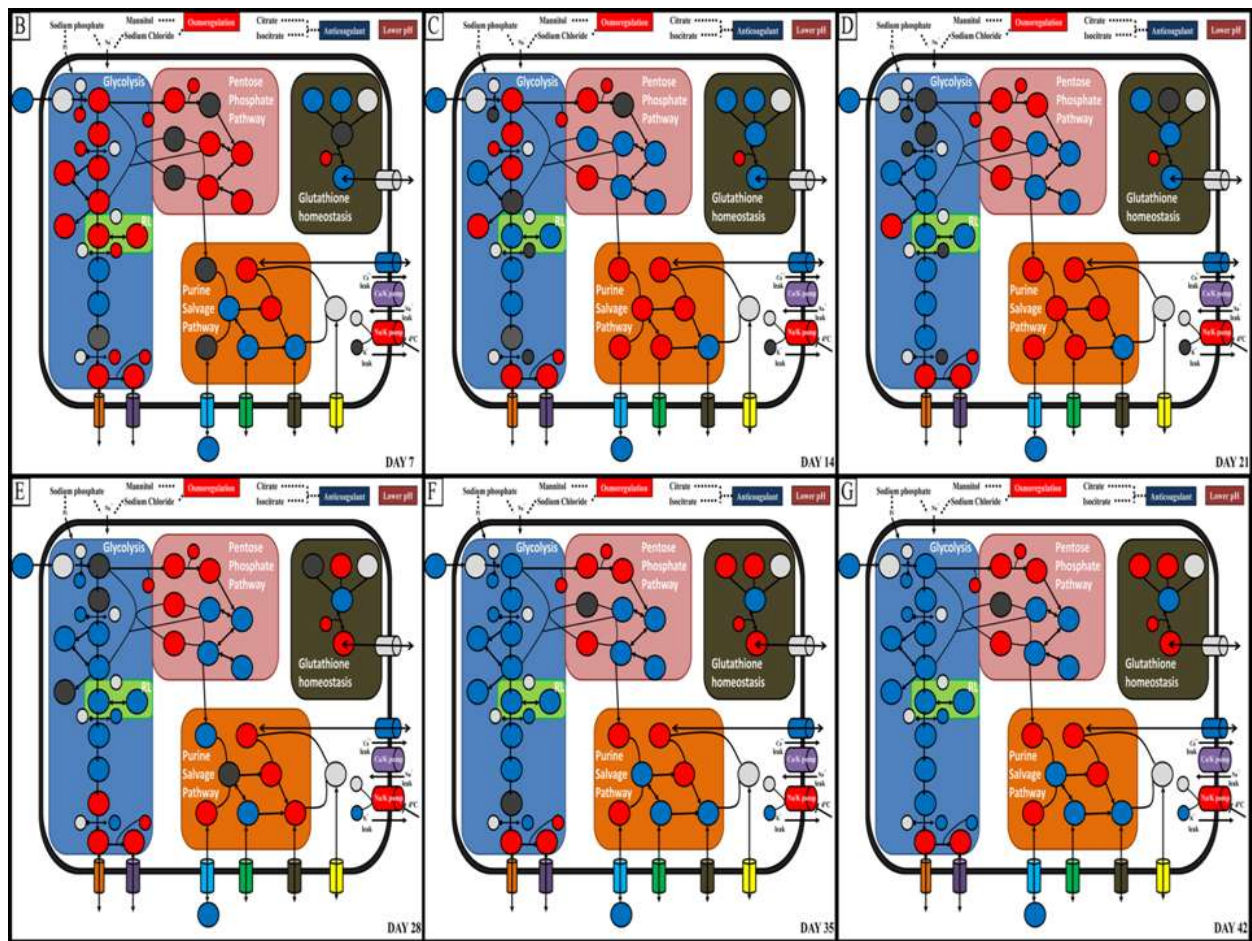
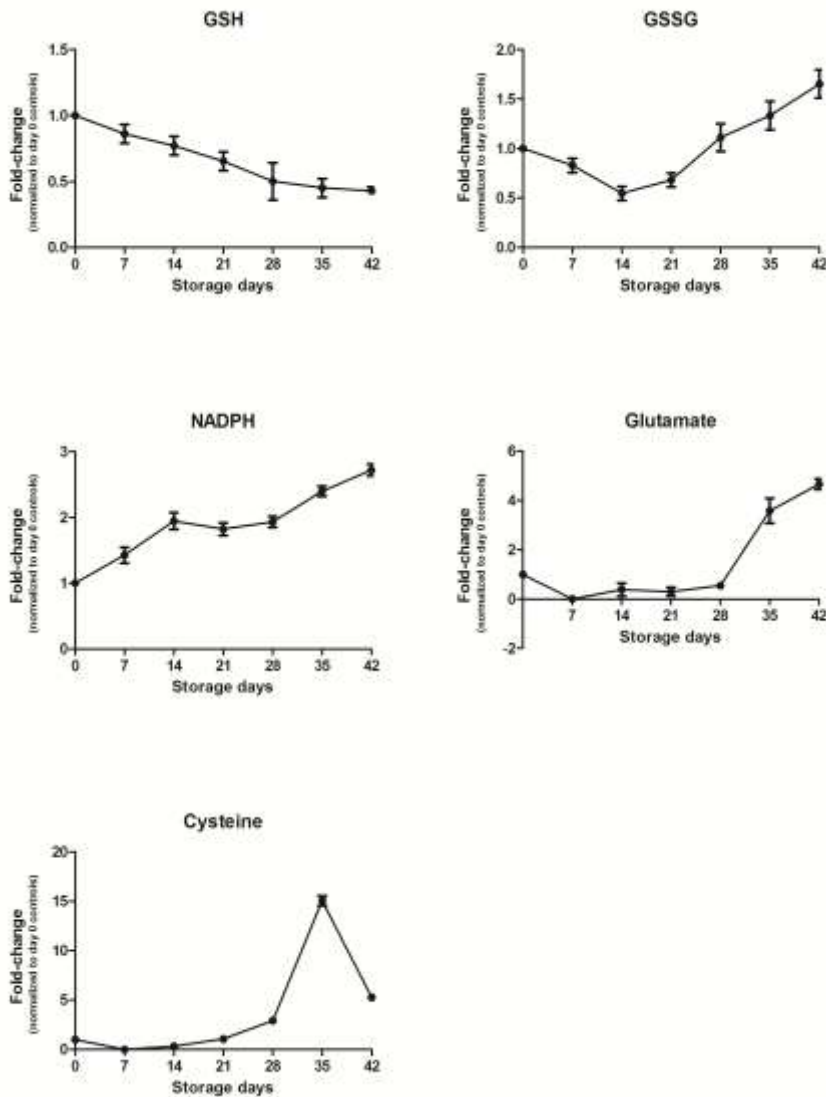


FIGURE 6 An overview of the main red blood cell metabolic pathways, including glycolysis (Embden Meyerhoff pathway), pentose phosphate pathway, purine salvage pathway, glutathione homeostasis, along with cation homeostasis. Metabolites are highlighted in circles along with canonical Kegg pathway abbreviations. Colours indicate:

- Blue: decreased against day 0 controls;
- Red: increased against day 0 controls;
- Dark grey: not significantly different from day 0 controls.



**Supplementary FIGURE 1**

Time course metabolomic analyses of SAGM-stored RBCs, upon normalization against day 0 controls, through plotting of fold-change variations in agreement with analogous studies of untargeted metabolomics applied to RBC investigations (Nishino et al., 2009; Darghouth et al., 2010, 2011a and 2011b; D'Alessandro et al., 2012). An overview of trends for metabolites involved in glutathione homeostasis. Averages and standard deviations were calculated on 10 biological replicates, each one run in triplicate.

5.3 Red blood cell storage and cell morphology

Overview of this section

Liquid storage of red blood cells (RBCs) delivers a blood-derived therapeutic which is safe, available, effective, and affordable for most patients who need transfusion therapy in developed countries. However, a growing body of accumulating controversial evidences, either from biochemical or retrospective clinical studies, prompted safety concerns about longer stored RBCs.

In the present study, we performed weekly assessment of morphology-related parameters through monitoring of CPD-SAGM leuko-filtered erythrocyte concentrates from blood withdrawal until the 42nd day of storage.

Statistical image analysis through scanning electron microscope was coupled to osmotic fragility and erythrocyte sedimentation rate.

We could observe that by day 21 more than 50% of RBCs displayed non-discocyte phenotypes. This observation was related to an increase in osmotic fragility, which was totally overlapped in day 0 controls and day 7 RBCs while only slightly augmented in day 14 samples. Cation dysregulation (pH internal/external alteration and potassium) might both reflect and trigger a negative feedback loop with metabolic fluxes and membrane cation pumps.

Morphology parameters suggest that significant alterations to RBC morphology over storage duration occur soon after the 14th day of storage, as to become significant enough within the 21st day.

Keywords: red blood cell; storage; osmotic stress curve; scanning electron microscopy.

Introduction

Liquid storage of red blood cells (RBCs) delivers a blood-derived therapeutic which is safe, available, effective, and affordable for most patients who need transfusion therapy in developed countries (Hess *et al.*, 2010). Over the last decade, most of the efforts of transfusionists have sought to promote storage strategies which would allow longer liquid storage, in order to increase availability of RBCs in isolated locations and make autologous RBC transfusion more effective (Hess *et al.*, 2003).

The introduction of plastic bags, the diffusion of new collection and additive solutions other than the introduction of leukocyte filtering strategies have dramatically improved our approach to RBC processing for transfusion purposes (Hess 2006; D'Alessandro *et al.*, 2010).

Despite these notable advancements, current European Council guidelines suggest that RBC concentrates may be stored for up to 42 days under controlled conditions before transfusion (Council of Europe 2011). The main obstacle hindering the way to a prolonged shelf-life of erythrocyte concentrates is characterized by the growing body of accumulating controversial evidences, either from biochemical (Valeri *et al.*, 1969; Bennet-Guerrero *et al.*, 2007; D'Amici *et al.*, 2007; Bosman *et al.*, 2008; Karon *et al.*, 2009; Antonelou *et al.*, 2010 a,b; Lion *et al.*, 2010; Rubin *et al.*, 2010; Chaudhary *et al.*, 2011; D'Alessandro *et al.*, 2011; Rinalducci *et al.*, 2011) or retrospective clinical studies (Koch *et al.*, 2008; Lelubre *et al.*, 2009). These studies brought about concerns over the safety-related risks when administering longer stored RBC concentrate units, especially when dealing with certain categories of recipients, such as traumatized, post-operative and critically ill patients. While randomized double-blind clinical prospective trials are still missing or inconclusive (Bennet-Guerrero *et al.*, 2009; Steiner *et al.*, 2010), it is now widely accepted that storage affects a wide array of biochemical and biological properties of RBCs to a significant extent, a phenomenon which goes by the name of storage lesions.

Storage lesions include i) alterations to RBC morphology (shape changes leading from a discoid to a spherocytic phenotype); or ii) RBC functionality (metabolism and oxygen delivery capacity, through an increase in oxygen affinity mediated by a rapid fall in 2,3-diphosphoglycerate concentrations) (Valeri *et al.*, 1969; Bennet-Guerrero *et al.*, 2007; D'Amici *et al.*, 2007; Bosman *et al.*, 2008; Karon *et al.*, 2009; Antonelou *et al.*, 2010 a,b; Lion *et al.*, 2010; Rubin *et al.*, 2010; Chaudhary *et al.*, 2011; D'Alessandro *et al.*, 2011; Rinalducci *et al.*, 2011).

A more detailed list of storage lesions to RBCs, which are only reversible to some extent, also include (Valeri *et al.*, 1969; Bennet-Guerrero *et al.*, 2007; D'Amici *et al.*, 2007; Bosman *et al.*, 2008; Karon *et al.*, 2009; Antonelou *et al.*, 2010 a,b; Lion *et al.*, 2010; Rubin *et al.*, 2010; Chaudhary *et al.*, 2011; D'Alessandro *et al.*, 2011; Rinalducci *et al.*, 2011):

- potassium leakage to the supernatant;
- depletion of ATP stores;
- alteration of lipids (phospholipid loss, phosphatidylserine exposure to the outer membrane leaflet);
- alteration of membrane proteins (membrane protein fragmentation and migration to the membrane and/or vesiculation of subsets of structural or cytosolic anti-oxidant proteins);
- oligomerization of band 3;

- accumulation of protein biomarkers at the membrane level (CD47, Apo-J/Clusterin, peroxiredoxin 2);
- more rigid cell structures;
- increased vesiculation rate;
- reduced oxygen off-loading capacity;
- decreased S-nitrosothiohemoglobin;
- increased lipid oxidation (storage duration-dependent accumulation of malondialdehyde and 8-isoprostane);
- increased protein oxidation (storage duration-dependent accumulation of carbonylated proteins).

In other terms, biochemical studies explicitly suggested that transfusionists should be also concerned about further improving storage quality (Liumbruno *et al.*, 2010).

In the present study, we provide supporting evidence about the relation between RBC storage duration, alterations to RBC morphology and osmotic fragility. In agreement with previous studies from our and other groups (Karon *et al.*, 2009; Chaudhary *et al.*, 2011; D'Alessandro *et al.*, 2011), we define a time window within which RBCs do not seem to suffer from major deviations as far as the main morphology-related parameters are concerned. Although clinical prospective evidences will outline a more definitive scenario, we conclude that RBCs do not seem to suffer from major membrane alterations within the first fourteen days of storage, while most meaningful deviations from freshly drawn RBC-controls were observed from day 21 onwards.

Materials and Methods

Sample collection Whole blood (450 mL \pm 10%) was collected from healthy volunteer donors into CPD anticoagulant (63 mL). After separation of plasma and buffy coat by centrifugation, RBCs were suspended in 100 mL of SAG-M (Saline, Adenine, Glucose, Mannitol) additive solution. We studied RBC units collected from 8 donors [male = 4, female = 4, age 45 ± 11.5 (mean \pm S.D.)] in Rome (Italy), upon signing of informed consent according to the declaration of Helsinki. RBC units were stored under standard blood bank conditions (4 ± 2 °C) and samples were removed aseptically for the analysis every week from day 0 up until day 42 of storage.

Determination of intracellular pH.

Red cell pellets obtained by centrifuging 600 μ l of suspension in a nylon tube at $30,000 \times g$ for 10 min, were frozen, thawed during 5 min and then refrozen. To prevent an acid shift observed when samples are kept unfrozen, triplicate measurements of pH were made immediately after a second thawing of each lysate with a Radiometer pH glass capillary electrode maintained at 20°C and linked to a Radiometer PHM acid-base analyzer.

Determination of potassium in the supernatants

Potassium levels in packed RBC supernatants were determined using the ion-selective electrode methodology (AVL 983-S, Graz, Austria)

Structural analyses

Hemolysis and osmotic fragility

Hemolysis was calculated following the method by Harboe (1959). Samples were diluted in distilled water and incubated at room temperature for 30 min to lyse red blood cells. Samples from lysed RBCs were diluted 1/300 while supernatants were diluted 1 / 10 in distilled water. After stabilizing during 30 min and vortex mixing (Titramax 100, Heidolph Elektro, Kelheim, Germany), the absorbance of the hemoglobin was measured at 380, 415 and 450 nm (PowerWave 200 Spectrophotometer, Bio-Tek Instruments, Winooski, Vermont, USA). The mean blank was subtracted and the corrected OD (OD*) was calculated as follows: $2 \times OD_{415} - OD_{380} - OD_{450}$.

Erythrocyte hemolysis curve was determined by osmotic fragility behavior using different NaCl solutions. A 25 μ L of blood samples were added to a series of 2.5 ml saline solutions (0.0 to 0.9 % of NaCl). After gentle mixing and resting for 15 min at room temperature the erythrocytes suspensions were centrifuged at 1500 rpm for 5 min. The absorbance of released hemoglobin into the supernatant was measured at 540 nm according to Kraus et al. (1997).

Measurement of the erythrocyte sedimentation rate (ESR) The ESR was measured by the Westergren method (ICSH 1993). Two milliliters of packed RBCs were collected into a tube containing 0.5 mL of sodium citrate. RBCs were stored no longer than 2 hours at room temperature. RBCs were drawn into a Westergren-Katz tube to the 200 mm mark. The tube was placed in a rack in a strictly vertical position for 1 hour at room temperature, at which time the distance from the lowest point of the surface meniscus to the upper limit of the red cell sediment was measured. ESR was calculated as the distance of fall of erythrocytes, expressed as millimeters in 1 hour.

Scanning electron microscopy Scanning electron microscopic studies of RBC were performed by means of an JEOL JSM 5200 electron microscope. Blood samples were fixed in phosphate-buffered (pH 7.2–7.4) 2.5% glutaraldehyde for 1 h, washed two times in 0.1 M phosphate buffer (pH 7.2–7.4), and mounted on poly-Llysine-coated glass slides. The glass slides were kept in a moist atmosphere for 1 h, washed in phosphate buffer, postfixed in 1% osmium tetroxide for 1 h, rinsed in distilled water, and dehydrated in graded ethanol (50–70–90–100%). After critical-point drying with liquid CO₂ in a vacuum apparatus and covering with a gold-palladium layer, the samples underwent scanning electron microscopic analysis. The different cell shapes were identified using Bessis' classification (Bessis 1972). The percentages of discocytes, echinocytes, spherocytocytes, stomatocytes, spherostomatocytes, and spherocytes were evaluated by counting 600 cells in randomly chosen fields. Reversible and irreversible shapes were determined according to Berezina *et al.* (2002). RBC manifesting echinocyte and stomatocyte shapes are capable of returning to the discocyte shape under certain conditions. Thus, these RBC shape changes are considered potentially reversible transformations. In contrast, RBC assuming spherocytocyte, spherostomatocyte, spherocyte, ovalocyte, and degenerated shapes are irreversibly changed cells.

Results

Biochemical analyses

Ph

Storage of RBCs resulted in a constant supernatant and internal RBC pH drop from initial 7.0 ± 0.06 and 6.9 ± 0.05 , respectively, down to 6.55 ± 0.05 and 6.45 ± 0.05 , respectively (**Figure 1.A**). At the beginning and at the end of the storage supernatant pH was higher than internal RBC pH, although the trend was slightly inverted from day 14 to 28, when internal RBC pH was slightly, albeit not significantly, higher (**Figure 1.B**).

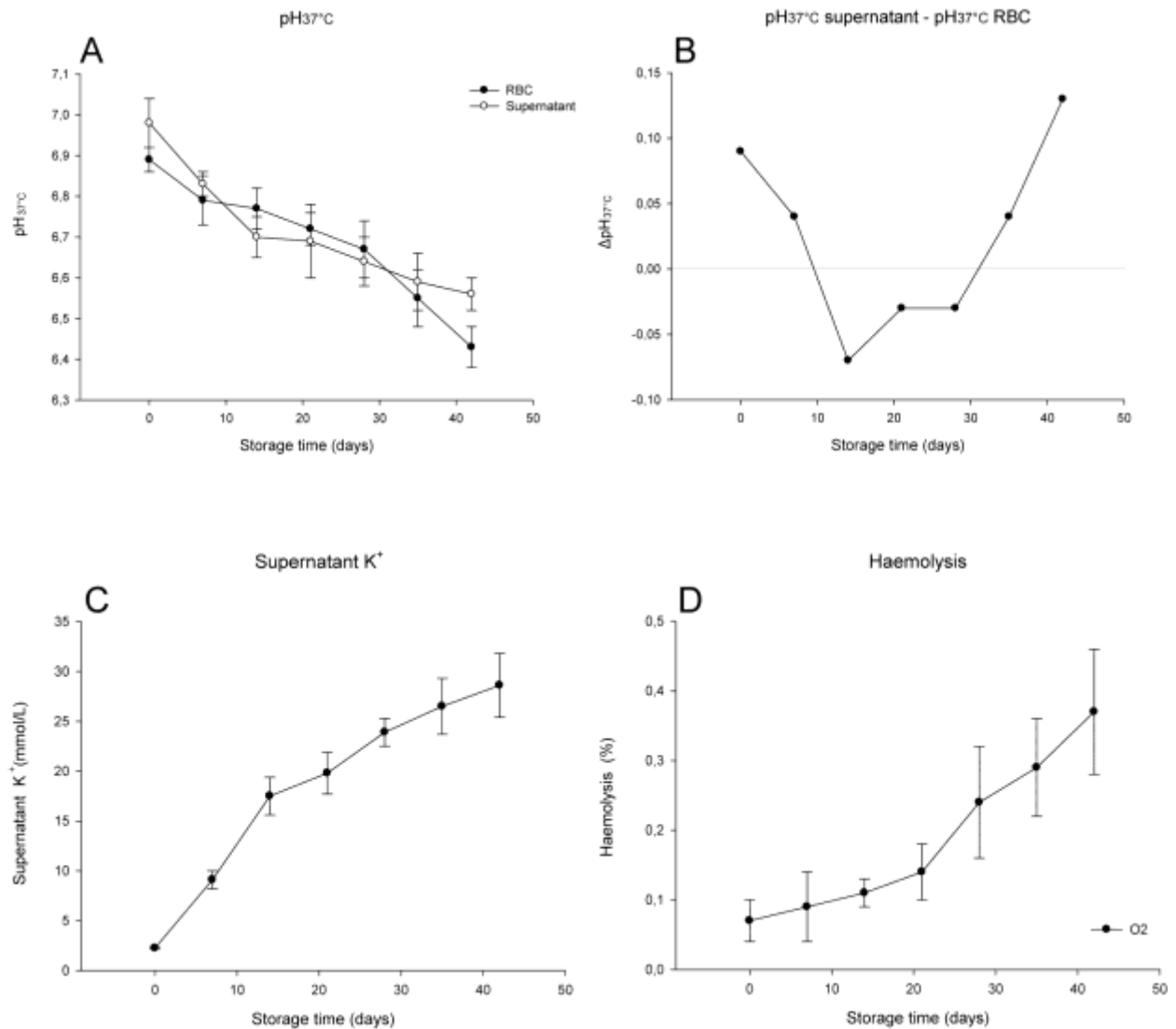


FIGURE 1 Time course measurements of RBC internal and supernatant pH (A) and Δ pH (supernatant – internal pH) (B). Time course measurements of supernatant potassium concentrations in mmol/L (C). Time course haemolysis percentage measurements (D).

Supernatant potassium

Potassium in the supernatant accumulated constantly from approximately 2.5 ± 0.5 mmol/L up until 27.5 ± 2.5 mmol/L. The slope of the potassium leakage trend was higher up until day 14, when K^+ accumulation in the supernatant continued though at a lower rate (**Figure 1.C**).

Haemolysis

Free haemoglobin accumulation rate in the supernatant was slower up until day 21, while it increased significantly from day 28 onwards. However, at the end of the storage (42 days), haemolysis was lower than the 0.8% threshold for all the tested subjects (0.34 ± 0.1 (**Figure 1.D**)).

Structural analyses

Osmotic fragility

Osmotic fragility was performed as to measure RBC resistance to hemolysis when exposed to a series of increasingly dilute saline solutions.

Osmotic fragility test showed that prolonged storage caused linear increases in haemolysis curve percentages proportionally to osmotic stress increase (at increasingly dilute NaCl solutions. Highest values of osmotic fragility (increase likelihood of hemolysis at lower osmotic stress or, in other terms, even at higher NaCl concentrations) were obtained for day 42 samples, in comparison with day 0 controls, which showed the lowest osmotic fragility (**Figure 2**). While haemolysis curves for i) day 0 to day 7; ii) day 7 to day 14 samples did not show any significant deviation (curves were almost overlapped), differences significant from iii) day 14 to day 21; iv) day 28 to day 35 and from v) day 35 to day 42.

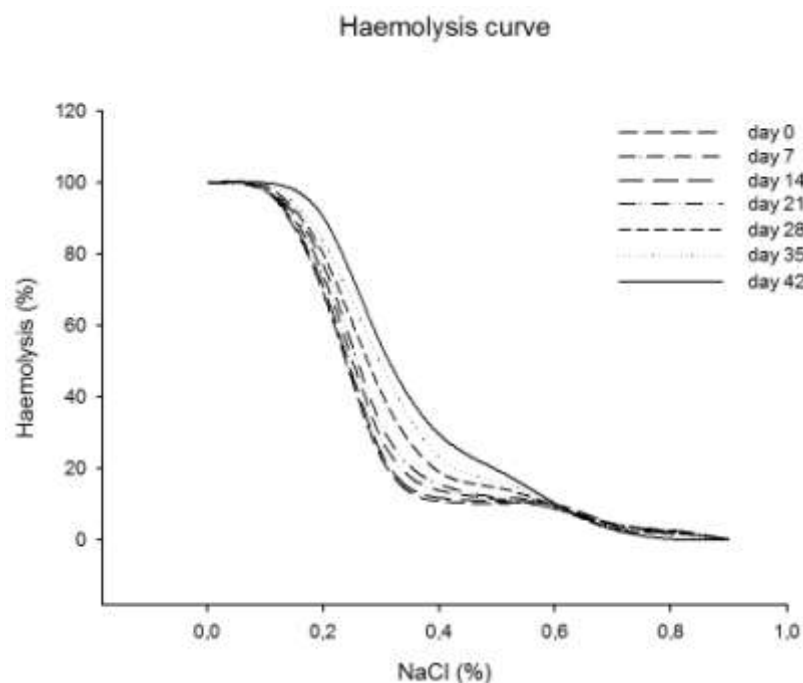


FIGURE 2 Measurements of osmotic fragility for RBCs exposed at increasingly dilute NaCl concentrations (from 1.0 % to 0 %). Continuous or gaped lines indicate different storage periods, as explained in the legend. Controls and RBCs stored within the first two weeks display higher osmotic resistance (curves are shifted leftwards as RBCs endure higher osmotic stresses prior to hemolyse), while longer stored RBCs hemolyse earlier, even when exposed to higher

concentrations of NaCl (curves are shifted rightwards).

ESR

The erythrocyte sedimentation rate (ESR), also called sedimentation rate or Biernacki Reaction, is the rate at which RBCs sediment in a period of 1 hour. There are three major factors that influence erythrocyte aggregation: the surface-free energy of the cells, the charge of the cells, and the dielectric constant (Jurado 2001). In particular, morphological abnormalities of the RBCs can interfere with RBC pellet formation and thus alter the ESR (Jurado 2001).

Despite the high hematocrit of SAGM-stored packed RBCs (60% on average), we decided to calculate the ESR to indirectly monitor membrane shape alterations paralleling storage duration. The ESR value resulted to increase in all the tested subjects (**Figure 3.A**) from day 0 to day 42 (**Figure 3.B**). RBCs seemed to behave as if they aggregated as storage progressed.

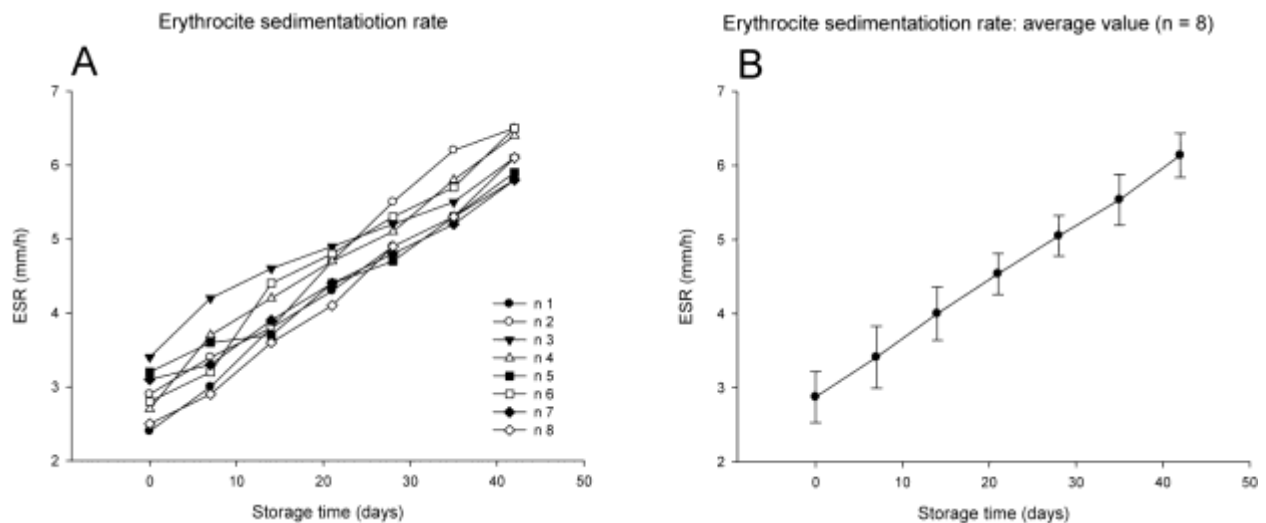


FIGURE 3 Erythrocyte sedimentation rate (ESR) in mm/h over storage duration. The graph in **A** indicates results from each of the 8 tested units, while in **B** averages are displayed.

Scanning Electron Microscope (SEM)

SEM images were collected and analysed following Bessis classification (Bessis 1972) and discrimination between reversible and irreversible membrane shape alterations over storage duration (from day 7 to day 42), in agreement with Berezina *et al.* (2002). Results are reported as mean \pm S.D. of discocytes, cells with reversibly and irreversibly-altered membrane, as percentages of the overall number of cells taken into account in randomly chosen fields (600

per period), as in our previous study (D'Alessandro 2011). Up until day 21 the percentage of discocytes and RBCs showing reversibly altered shapes (echinocyte and stomatocyte shape) was on average above a 75% threshold (75.9 ± 4.7). However, at day 21 it was already possible to count more than 15% of RBCs displaying irreversible modification of the membrane (16.4 ± 4.4) (**Table 1**). SEM images at day 42 showed a substantial percentage of RBCs showed no or reversible shape modifications ($60.5 + 3.8$), while irreversibly modified RBCs characterized the remaining $39.5 + 6.1$ of the cells (**Figure 4.A**). In RBCs stored for 42 days, discocyte phenotypes (**Figure 4.B** from day 0 controls) were very rare to observe. Spheroechnocytes and spherocytes were rather abundant in 42 days samples (**Figure 4.C**), indicating that membrane loss in a significant percentage of long-stored RBCs had reached extreme levels.

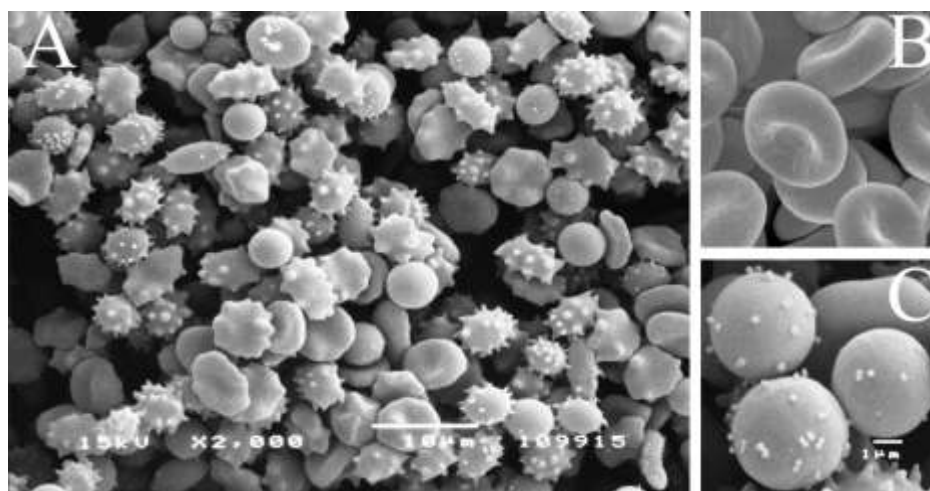


FIGURE 4 Scanning electron images of long-stored RBCs. A panoramic view of a 42 RBC sample (2,000x; scale bar = 10 μ m) (**A**). A detail of a 42 day spherocyte (scale bar = 1 μ m) (**B**). A detail of day 0 control RBCs (scale bar = 1 μ m) (**C**).

Table 1 – SEM erythrocyte shape classification

Day	Discocytes	RBCs showing non-discocyte phenotypes	Discocytes and Reversibly* changed RBC (%) (echinocyte and stomatocyte shape)	Irreversibly* changed RBC (%) (spherocochinocyte, spherostomatocyte, spherocyte, ovalocyte, and degenerated shapes)
7	76.2 \pm 3.8	23.8 \pm 5.2	91.2 \pm 5.7	8.8 \pm 4.3
14	54.2 \pm 2.4	45.8 \pm 6.6	85.3 \pm 5.3	14.7 \pm 4.7
21	49.8 \pm 3.1	50.2 \pm 5.9	83.6 \pm 5.6	16.4 \pm 4.4
28	44.3 \pm 4.1	55.7 \pm 5.7	75.9 \pm 4.7	24.1 \pm 5.3
35	33.6 \pm 2.7	66.4 \pm 5.1	73.3 \pm 3.2	26.7 \pm 4.6
42	22.9 \pm 3.1	77.1 \pm 6.8	60.5 \pm 3.8	39.5 \pm 6.1

* Reversible and irreversible changes were classified based on classification by Berezina et al.²⁷, based upon Bessis²⁸ shape classification (**bold**)

Discussions

We hereby simultaneously tested eight CPD-SAGM RBC units for morphology-related parameters and monitored them throughout the whole shelf-life (42 days) under liquid storage.

While haemolysis levels constantly increased, although remaining below the acceptable threshold for all the tested units, early changing parameters included biochemical modulation of the internal and external pH and continuous

accumulation of potassium in the supernatant (**Figure 1.A-C**), in agreement with previous reports from literature (Hogman *et al.*, 2006; Bennet-Guerrero *et al.*, 2007).

Potassium accumulation in the supernatant is mainly due to adenosine triphosphate (ATP) depletion, since potassium homeostasis depends on ATP-dependent maintenance of proper functioning of sodium-potassium cationic pumps, and by low temperature, negatively affecting pump kinetics (Wallas 1979). ATP levels decrease over storage duration (Hogman *et al.*, 2006; Bennet-Guerrero *et al.*, 2007; D'Alessandro *et al.*, 2011), mainly due to glycolysis rate stopping as pH falls.

Differences between internal and external pH actually reflect changes to cation homeostasis, which should end up influencing enzyme kinetics. Indeed, current data could be better interpreted by referring to a recent metabolomics analysis on CPD-SAGM RBCs over storage duration, in which glycolytic activity was shown to be high over the first week of storage and rapidly declined within the second week of storage duration, when a shift towards the oxidative phase of the pentose phosphate pathway was observed (D'Alessandro *et al.*, 2011). We hereby report a delta variation between the supernatant and internal pH which is positive within the first seven days of storage and shifts towards negative values until day 28 (**Figure 1.B**).

Internal/external pH variations also affect membrane potential, resulting in shape alterations (Wallas 1979). Indeed, pH internal/pH external and supernatant potassium changes accumulating over the first two weeks of storage were closely followed by alteration of the RBC structure. In line with this consideration, we observed that RBCs resulted to be progressively suffering from osmotic fragility as storage progressed, especially from day 21 onwards, as they failed to withstand higher osmotic stresses as they aged *ex vivo* (**Figure 2**). It has been shown that the osmotic fragility of spherocytic RBCs is higher than that of normal shaped RBCs (Wallas 1979; Hogman *et al.*, 2006). In other terms, sphere shaped RBCs display a surface/volume ratio which reaches its minimum threshold, after which hemolysis rapidly occur following even slight osmotic stresses (Ionescu-Zanetti *et al.*, 2005; Hogman *et al.*, 2006). Since we classified spherocytocytes and spherocytes as RBCs showing irreversibly modified membrane shape phenotypes, in agreement with Berezina *et al.* (2002), we could conclude that yet at day 21 a significant percentage of RBCs showed substantial alterations to the membrane (**Table 1**) and were thus responsible for the observed increase in osmotic fragility. The acquisition of spherocytic phenotypes is the distinctive trait of hereditary spherocytosis (Ionescu-Zanetti *et al.*, 2005; Hogman *et al.*, 2006), an auto-hemolytic anemia characterized by the production of sphere-shaped rather than bi-concave disk shaped RBCs, with an increased tendency to hemolyse (Kumar 2002; Pribush *et al.*, 2003). In line with recent literature (Berezina *et al.*, 2002; D'Alessandro *et al.*, 2011), we could observe progressive membrane shape alterations (**Figure 4.A-C**) through progressive membrane shedding of microvesicles, a phenomenon reaching a significant extent from day 21 onwards. Indeed, by day 21 only 50% of RBCs still showed a discocyte phenotype, while the remaining half already showed both reversible and irreversible shape changes (**Table 1**). It is worthwhile to stress that, in the frame of RBC storage, the parallelism between long stored RBCs and RBCs from patients suffering from hereditary spherocytosis is further supported by redox balance dysregulation, cytoskeletal disorganization, migration of anti-oxidant enzymes to the membrane and altered metabolism (Rocha *et al.*, 2008; D'Alessandro *et al.*, 2011).

The observed variations about a constant increase in the erythrocyte sedimentation rate (ESR) over storage duration deserve an independent consideration. ESR is a simple and inexpensive laboratory test for assessing the inflammatory or acute response, though it is often meaningful in the frame of whole blood in the clinical setting (Sadeeh 2011). ESR is slightly influenced by cell age and morphology, but also by the presence of inflammatory cytokines. While erythrocyte concentrates in the present study have been leukofiltered (residual WBC < 1×10^6 /unit*) (Council of Europe 2011), progressive elevations in multiple pro-inflammatory mediators (e.g. cytokines, immunologically active phospholipids, CD-40 ligand) from diverse cellular origin have already been reported and reviewed for these RBC preparations despite white blood cell thorough removal prior to storage beginning (Kor *et al.*, 2009). Moreover, based upon recent bioinformatic analyses providing an overview of the red blood cell whole protein complement, the proteome, and the subsequent protein-protein interactions through *in silico* modeling, the interactome (D'Alessandro *et al.*, 2010), it has been argued whether RBCs might play a direct role in mediating immune-modulatory responses (Morera *et al.*, 2011).

An increase in ESR over storage duration might thus reflect both shape-phenotype alterations and accumulation in the supernatant of low doses of these cytokines, though further studies are mandatory.

Conclusion

In the present study, we performed structural analyses on RBCs over liquid storage under refrigeration. As a result, we could confirm the accumulation of membrane targeting storage lesions which ended up to increase osmotic fragility and subsequent hemolysis. These changes might be triggered both by cation homeostasis dysregulation (pH internal/pH external decrease, potassium accumulation in the supernatant) and, like other studies suggest (Chaudhary *et al.*, 2011; D'Alessandro *et al.*, 2011), metabolic alteration and oxidative stress (formation of reactive oxygen species through hemoglobin iron-triggered Fenton reactions (Carrel *et al.*, 1975)). In addition to previous studies, we could determine that the events of accumulation of morphology alterations became significant from day 21 onwards. This conclusion is in line with previous laboratory studies on other parameters (metabolomics and proteomics analyses, band 3 oligomerization state, accumulation of reactive oxygen species and byproducts and protein and lipid oxidation, methemoglobin production) (Karon *et al.*, 2009; Chaudhary *et al.*, 2011; D'Alessandro *et al.*, 2011), and retrospective clinical observations about a likely decreased safety of RBCs stored for more than two weeks (Koch *et al.*, 2008).

5.4 Red blood cell storage in SAGM and AS3: a comparison through the membrane two-dimensional electrophoresis proteome

Overview of this section

SAGM is currently the standard additive solution used in Europe, while AS-3 is the third additive solution that has been licensed in the USA, and is also the one used exclusively in Canada. Although AS-3 is based on a saline-adenine-glucose solution, it also contains citrate and phosphate.

Storage of red blood cell concentrates in CPD-SAGM is known to lead to the accumulation of a wide series of storage lesions, including membrane protein fragmentation and vesiculation, as we could previously determine through 2-dimensional gel electrophoresis.

Through 2D-SDS-IEF-polyacrilamide gel electrophoresis we performed a time course analysis (day 0, 21 and 42 of storage) of red blood cell membranes from leukocyte-filtered concentrates either stored in CPD-SAGM or CP2D-AS-3. From the present study it emerges that the membrane protein profile of red blood cells stored in presence of AS-3 appears to be slightly different from (better than) previous reports on SAGM-stored counterparts. However, the increase of total membrane spot number due to the presence of fragments at day 21 and the significant decrease at day 42 are suggestive of a universal phenomenon which is not efficiently tackled by none of the two additive solutions investigated in the present study.

To further delve into the storage lesion issue for RBCs stored in AS-3, it would be interesting in the future to assay metabolic changes over storage progression as well.

Keywords: red blood cell; storage; SAGM; AS-3; proteomics.

Introduction

In a recent and comprehensive review (Hess, 2006), Hess shed light on the history of red blood cell (RBC) storage solutions, whose early days date back to the 1900 (Hess, 2006), when Rous and Turner developed the first citrate and glucose mixture for storing rabbit RBCs (Rous and Turner, 1916) and Robertson used it in the first blood bank in France during World War I (Robertson, 1918).

The inclusion of phosphate in 1950s and adedine in 1970s paved the way for the design and diffusion of additive solutions (1980s), which allowed further extending the shelf life and improving the quality of the RBC storage (Hess, 2006). Of note, most of the additive solutions which are routinely exploited everyday worldwide have been known for decades (Moore, 1987).

Compositional changes over the years were mainly based on the need to improve storage safety and effectiveness. Indeed, at first mixtures of sodium citrate and dextrose caramelized when the solutions were heated, whereas solutions of sodium citrate alone could be autoclaved (Hess, 2006). On the other hand, pH lowering to 5.8 allowed sterilization of citrate and glucose (acid citrate dextrose – ACD) solutions as well, enabling storage of RBCs for up to 21 days (Loutit and Mollison, 1943).

The subsequent development in the field of additive solutions was characterized by the addition of sodium phosphate to ACD (citrate phosphate dextrose – CPD), which reduced phosphate leakage from stored RBCs by reducing the gradient in phosphate concentration between the cytosol and the supernatant. In clinical terms, storage of whole blood in CPD resulted in improved *in vivo* recovery at 24h from transfusion, although it did not produce any substantial improvement to the shelf life of the transfusion product (Ebaugh and Ross, 1985).

The introduction of plastic bags (Artz et al., 1954) and adenine (CPDA-1 – Shields, 1969) to the blood processing workflow resulted in further improvements (storage up to five weeks), the latter being related to the restoration of cell shape, ATP concentration and viability. Indeed, RBCs lose adenine and adenosine through deamination reactions over storage durations, which leads to impaired RBC recovery and osmotic fragility (Simon et al., 1962).

Additive solutions came soon afterwards, as they were added to packed RBCs to provide additional volume and nutrients for longer storage and better flow (Moore, 1987). The first additive solution was SAG, named after its constituents, saline, adenine and glucose, decreasing storage haematocrit and viscosity to approximately 55% and 10 cps, respectively (Hogman et al., 1978). However, high biological variability of haemolysis still hampered the extension of the shelf life of RBC concentrates over 5 weeks, at least until the introduction of mannitol (a free radical scavenger and membrane stabilizer) by Hogman et al. (1978). This solution, SAGM, gained widespread distribution and is now the standard additive solution used in Europe, while AS-1 and AS-5 (widely used in the USA) are two SAGM variants which differ only modestly in their concentrations of salt, sugar and mannitol.¹ AS-3 is the third additive solution that has been licensed in the USA, and is also the one used exclusively in Canada (Hess, 2006). Again, it is based on SAG but also contains citrate and phosphate (the compositional differences between AS-3 and SAGM are highlighted in **Table 1**). Citrate and mannitol both serve the same membrane-protective function in AS-3 and SAGM, respectively, although the former also functions as an impermeable ion that balances the osmotic pressure of small ion-permeable RBCs (Jarvis et al., 2003). Another main difference is that AS-3 additive solution depends on a higher dextrose version of the primary CPD anticoagulant, called CP2D (**Table 1**).

It is reported in the literature that none of these additive solutions appears to have significant advantages over the others. Indeed, AS-3 and SAGM are both associated with 78–84% recovery and 0.4% haemolysis after 6 weeks of storage (Moore, 1987; Hess, 2006). However, although liquid storage of RBCs delivers a blood-derived therapeutic which is safe and effective, concerns still arise and persist about the quality issue of units stored longer than 14 days, as it emerged from clinical retrospective studies,^{14,15} and laboratory evidences (about morphology (Berezina et al., 2002; Blasi et al., 2012), metabolism (Bennet-Guerrero et al., 2007; Gevi et al., 2012), membrane protein profiles (D'Amici et al., 2007; Bosman et al., 2008; D'Alessandro et al., 2012), and protein biomarkers (Antonleou et al., 2010; Rinalducci et al., 2011)). Although clinical prospective studies are either not yet conclusive or still in progress (Bennet-Guerrero et al., 2009; Steiner et al., 2010; Lacroix et al., 2011), questions arise and persist as to whether the actual guidelines for RBC collection and processing in the frame of storage for transfusion purposes might already be good, albeit not good enough (Hess, 2009).

Laboratory studies have already provided clear hints about the necessity to pursue a better, rather than a longer storage (Liumbruno and Aubuchon, 2010). Indeed, in recent years the application of proteomics technologies to the field of transfusion medicine (Liumbruno et al., 2010a and 2010b) has allowed revealing major changes in the RBC membrane proteome as storage progresses, either in leukofiltered (D'Alessandro et al., 2012) and non leukofiltered (D'Amici et al., 2007) RBC concentrates stored in CPD-SAGM.

Through two-dimensional gel-electrophoresis (2DE), an approach which allows separating proteins on the basis of their isoelectric point and molecular weight (MW), we previously reported that, as storage progresses, the membrane proteome undergo some major alterations including the increase from the second to the third week of storage of the overall number of protein spots and the subsequent progressive decrease until the end of storage (D'Amici et al., 2007; D'Alessandro et al., 2012). While late decrease of overall spot number is consistent with an increased rate of vesiculation (Bosman et al., 2008), transitional increase of the protein spot number might be attributed to (i) migration of intact proteins to the membrane; (ii) fragmentation of higher MW proteins; (iii) protein aggregation; all these phenomena being triggered by metabolic alterations (Gevi et al., 2012; D'Alessandro et al., 2012) and oxidative stress (D'Amici et al., 2007; D'Alessandro et al., 2012).

In the present study, we wanted to assess through a gel-based approach (2DE) whether the membrane protein profiles of RBCs stored in CP2D-AS-3 followed a trend that could be compared to the one we have already reported for CPD-SAGM counterparts.

Materials and Methods

Sample collection

SAGM

RBC samples to be stored in SAGM were collected as previously reported (D'Amici et al., 2007; D'Alessandro et al., 2012). Whole blood (450 mL \pm 10%) was collected from healthy volunteer donors into CPD anticoagulant (63 mL) and leukodepleted. After separation of plasma by centrifugation, RBCs were suspended in 100 mL of SAG-M (Saline, Adenine, Glucose, Mannitol) additive solution. We studied RBC units collected from 4 male donors [age 38 \pm 12.5 (mean \pm S.D.)], upon signing of informed consent according to the declaration of Helsinki.

AS-3

RBC samples to be stored in AS-3 were collected as previously reported (Yoshida et al., 2007).

Four units of whole blood (450 mL \pm 10%) from four different donors were collected in CP2D (Pall Medical, Covina, CA) and held for 1–2 h at room temperature before a soft spin and manual separation and leukoreduction. Two 50-mL aliquots were transferred to 150 mL polyvinyl chloride (PVC; PL146) bags (Baxter Healthcare, Round Lake, IL). AS-3 additive solution (Pall Medical) was added to each of the two aliquots at the ratio of 200 mL per unit (33 mL per aliquot) and stored at 4 °C.

RBC units were stored under standard blood bank conditions (1–6 °C) and samples were removed aseptically for the analysis at day 0, 21 and 42 of storage for subsequent membrane protein extraction and 2DE analysis.

RBC protein extraction Extraction of human erythrocyte membrane proteins was performed at day 0, 21 and day 42, based on the conventional method as described by Olivieri et al. (2001). The erythrocytes were isolated by centrifuging twice at 1000 \times g for 10 min. Packed cells were washed three times in 5 mM phosphate buffer pH 8.0, containing 0.9% w/v NaCl; then, they were centrifuged at 300 \times g for 10 min, at 4 °C. Erythrocytes were then processed as in D'Amici et al. (2007). After 15 min of incubation at room temperature, cells were pelleted and then lysed with 9 vol of cold 5 mM phosphate buffer pH 8.0 containing 1 mM EDTA, 1 mM phenylmethanesulfonyl fluoride (PMSF) and, in one of the two groups of samples, also 100 mM NEM. Cytosol was collected after centrifugation at 17,000 \times g for 20 min at 4 °C and its protein content was estimated by the DC protein assay method (Bio-Rad, Hercules, CA, USA). Membranes were washed with the same buffer until free of hemoglobin and then, in order to remove non-specifically membrane-bound cytosolic proteins, were washed three times with 0.9% w/v NaCl and collected at 17,000 \times g, for 20 min at 4 °C. Protein content was estimated by the bicinchoninic acid method (Smith et al., 1985) and ghosts prepared in this way were used for the following steps.

Two-Dimensional Electrophoresis To remove lipids, proteins were precipitated from a desired volume of each sample with a cold mix of tri-n-butyl phosphate/acetone/methanol (1:12:1). After incubation at 4 °C for 90 min, the precipitate was pelleted by centrifugation at 2800g, for 20 min at 4 °C. After washing with the same solution, the pellet was air-dried and then solubilized in the focusing solution containing 7 M urea, 2 M thiourea, 2% (w/v) ASB 14, 0.8% (w/v) pH 3-10 carrier ampholyte, 40 mM Tris, 5 mM TBP, 10 mM acrylamide, 0.1 mM EDTA (pH 8.5), 2% (v/v) protease inhibitor cocktail (Sigma-Aldrich), and 2 mM PMSF. Before focusing, the sample was incubated in this solution for 3 h at room temperature, under strong agitation. To prevent over-alkylation, acrylamide was destroyed by adding an equimolar amount of DTE. A total of 250 μ L of the resulting protein solution was then used to rehydrate 13 cm long IPG 3-10 NL (Amersham Biosciences) for 8 h. IEF was carried out on a Multiphor II (Amersham Biosciences) with a maximum current setting of 50 μ A/strip at 20 °C. The total product time voltage applied was 40 000 Vh for each strip. For the second dimension, the IPG strips were equilibrated for 30 min in a solution containing 6 M urea, 2% (w/v) SDS, 20% (v/v) glycerol, and 375 mM Tris-HCl (pH 8.8), with gentle agitation. The IPG strips were then laid on a 5-16% T gradient SDS-PAGE gel with 0.5% (w/v) agarose in the cathode buffer (192 mM glycine, 0.1% w/v SDS and Tris to pH 8.3). The anode buffer was 375 mM Tris-HCl, pH

8.8. The electrophoretic run was performed at a constant current (10 mA for 60 min, followed by 40 mA until the run was completed). During the whole run, the temperature was set at 13 °C. Proteins were visualized by Coomassie Brilliant Blue G-250 stain (Candiano et al., 2004).

Image statistical analysis

Twenty-four stained gels (4 biological replicates × 3 periods – day 0, 21 and 42 – × 2 groups – SAGM and AS-3) were digitalized using an ImageScanner and LabScan software 3.01 (Bio-Rad Hercules, CA).

Overall spot number has been calculated through *ad hoc* statistical software PDQuest 8.0 (Bio-Rad). Normalization and background subtraction have been automatically performed and a Master Map has been created for day 0, 21 and 42 gels for both groups (SAGM and AS-3). In Master Maps, spots have been included only if present in at least 3 out of 4 replicates. Total spot numbers have been thus calculated for each Master Map.

In-Gel Digestion and Protein identification by MALDI-TOF TOF

In the light of our previous investigations in the field of RBC storage through membrane proteomics via gel-based approaches, we expected an increase in protein fragmentation proportional to the storage duration and inversely proportional to the extent of vesiculation events (Rous et al., 1916; Loutit et al., 1943). Since newly appearing spots in the low MW range (below 25 kDa) could not derive from *de novo* protein synthesis, since RBCs are enucleated and thus devoid of any new protein synthesis capacity, differential protein expression (changes in the photodensity of protein spots) in the low apparent MW region of the 2DE gels was taken into account and considered significant at *p*-values < 0.05. Protein spots were carefully excised from stained gels and subjected to in-gel trypsin digestion according to Shevchenko et al. (1996).

Twenty microliters of the tryptic protein digests was loaded onto activated (0.1% TFA in acetonitrile) ZipTip columns and washed three times with 10 µL of 0.1% TFA in DD-H₂O. The peptides were eluted with 1 µL of matrix solution (0.7 mg/mL α -cyano-4-hydroxy-trans-cinnamic acid (Fluka, Germany) in 85% acetonitrile, 0.1% TFA and 1 mM NH₄H₂PO₄) and spotted directly on the MALDI-TOF target plate for automatic identifications (PAC384 pre-spotted anchor chip). Proteins were identified, as previously reported (Suckau et al., 2003) and per manufacturer's specifications, through an Autoflex II MALDI-TOF/TOF mass spectrometer with the LIFT module (Bruker Daltonics) was used for mass analysis of peptide mixtures. A peptide mixture (Peptide calibration standard I, Bruker Daltonics) was used for external calibration, while thinternal calibration was performed using the trypsin autolysis products. Proteins were identified by PMF using the database search program MASCOT (<http://www.matrixscience.com/>) upon removal of background ion peaks. Accuracy was set within 50 ppm, while the enzyme chosen was trypsin and only 1 missed cleavage was allowed; fixed carbamidomethylCys and variable Met-oxidation, was used as optional search criterion. PMF-based protein identification was confirmed by MS/MS analyses of precursor ions and repeated MASCOT based database searches. Runs were performed automatically through FlexControl setting and Biotools processing of MS data (PMF) and validation of identifications through MS/MS (LIFT analysis) on the three most intense ion peaks.

Table 1 – Composition of SAGM and AS-3 additive solution	
CP2D + AS-3	CPD + SAGM
<p style="text-align: center;">CP2D</p> <p style="text-align: center;">Each 100 mL contains:</p> <p style="text-align: center;">Citric Acid (Monohydrate), 0.327 g Sodium Citrate (Dihydrate), 2.630 g Monobasic Sodium Phosphate (Monohydrate), 0.222 g <u>Dextrose (Anhydrous), 4.640 g</u></p>	<p style="text-align: center;">CPD</p> <p style="text-align: center;">Each 100 mL contains:</p> <p style="text-align: center;">Citric Acid (monohydrate), 0.327 g Sodium Citrate (dehydrate), 2.630 g Sodium Dihydrogen Phosphate (dihydrate), 0.251 g <u>Dextrose (monohydrate), 2.55 g</u></p>
<p style="text-align: center;">AS-3</p> <p style="text-align: center;">Each 100 mL contains:</p> <p style="text-align: center;">Dextrose (Anhydrous), 1.000 g Sodium Chloride, 0.410 g Adenine, 0.030 g <u>Citric Acid (Monohydrate), 0.042 g</u> <u>Sodium Citrate (Dihydrate), 0.588 g</u> <u>containing 15 mEq of Sodium.</u> <u>Monobasic Sodium Phosphate (Monohydrate), 0.276 g</u></p>	<p style="text-align: center;">SAGM</p> <p style="text-align: center;">Each 100 mL contains:</p> <p style="text-align: center;">Dextrose (monohydrate), 0.900 g Sodium Chloride, 0.877 g Adenine, 0.0169g <u>Mannitol, 0.525 g</u></p>

Results and Discussions

Twenty-four 2DE gels were performed to monitor changes of the RBC membrane proteome over storage under blood bank conditions in presence of AS-3 or SAGM. **Figure 1** summarizes the overall number of biological replicates for each arm of the study (four each for AS-3 and SAGM) and the master maps for each storage period (day 0, 21 or 42 of storage). Below each figure, the overall number of protein spots from Coomassie staining is indicated.

Although the results are not directly comparable to our previous paper on 2DE analyses of RBC membrane proteome in CPD-SAGM²¹, since in that case RBCs had not been leukoreduced, it is still possible to observe that after three weeks of storage (two in D'Amici et al., 2007) the overall number of spots almost doubles both in the previous (from 161 ± 4.85 to 232.80 ± 7.66) and in the current investigation (from 263 ± 13 to 417 ± 32). It is also worthwhile to stress that, in the report by D'Amici et al. (2007), spot number increased in the Silver Stained gels as well (from 392 ± 15 to 487 ± 24 spots in day 0 and 14, respectively), although inconsistencies in the SAGM initial spot number might be either due to bioinformatic improvements in the PDQuest software, different staining protocol and the non-leukodepleted nature of the RBC concentrates tested in 2007, rather than to actual technical advances in 2DE runs over the last two years.

Nevertheless, it is also worthwhile to stress that the overall spot number decreased again after the third week of storage, as to remain only slightly higher than day 0 SAGM controls by day 42 (**Figure 1**). This was evident both in the present study (263 ± 13 vs 345 ± 26 at day 0 and 42, respectively) and in the previous one (D'Amici et al., 2007) (392 ± 15 vs 447 ± 21 at day 0 and 42 in Silver staining stained gels), which we previously interpreted as fragmentation events occurring in the early weeks of storage (second to the third – D'Amici et al., 2007) and vesiculation taking place soon afterwards. In a more recent investigation (D'Alessandro et al., 2012), we could further confirm the latter hypothesis and delve into membrane protein profiles through 2DE analyses of RBCs extracted in presence of N-ethylmaleimide. We could indeed individuate the progressive accumulation at the

membrane level at storage day 35 of vesicle-related proteins, such as alpha-soluble NSF attachment protein, alpha SNAP, 55 KDa erythrocyte membrane protein isoform 1, stomatin, ankyrin and biliverdin reductase, and 14-3-3 zeta/delta (D'Alessandro et al., 2012).

Figure 1 also indicates for the first time that a similar trend could be observed as well for RBCs stored in presence of AS-3. While the overall number of protein spots at day 0 was almost comparable for SAGM and AS3 membrane protein profiles (263 ± 13 vs 279 ± 13 , respectively), a slight increase could be observed after three weeks of storage (312 ± 28 total spots) and a significant decrease by day 42 (216 ± 24 , 69% of the total spot number after 21 day of storage).

Qualitative differences among Master Maps (at day 0, 21 and 42 of RBC storage in AS3) are further highlighted in **Figure 2**. The overall decrease in spot number from Master Maps at day 42 in comparison to day 0 controls are particularly evident in the areas delimited by the red ellipse (high MW region, previously reported in SAGM-stored RBCs to host structural proteins undergoing fragmentation) and the yellow trapezoid. Of note, the high MW region (red ellipse in **Figure 2**) appears to be depleted in protein spots yet at day 21, when new protein spots appear, especially at low MW (yellow trapezoid).

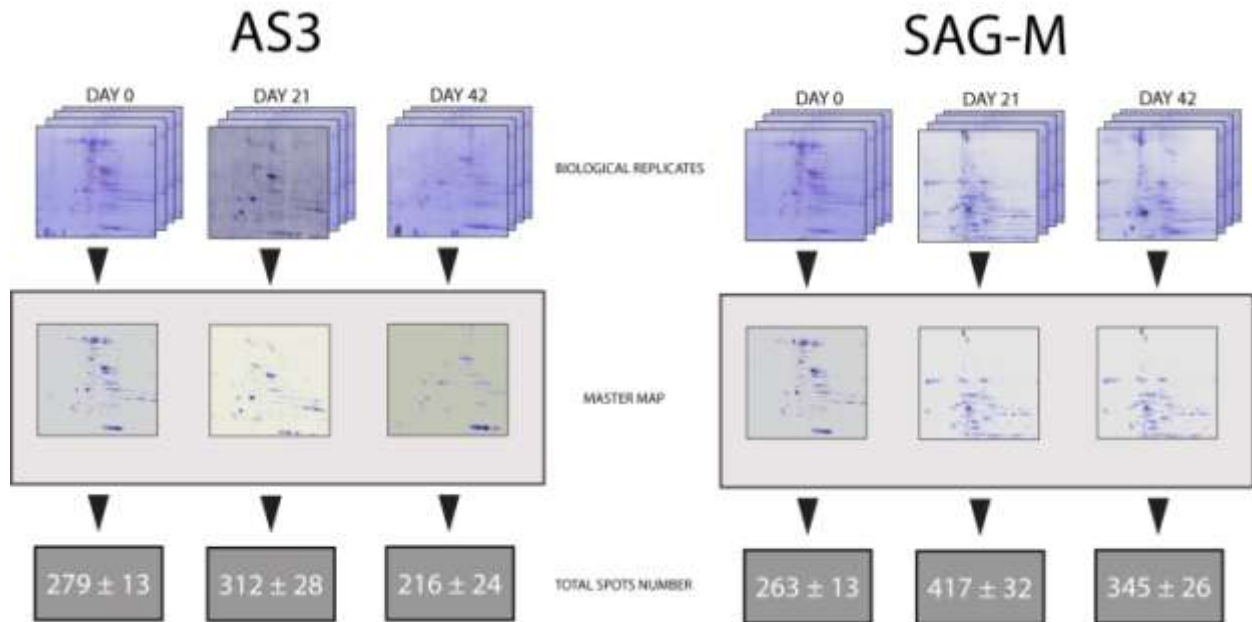


FIGURE 1 Total spot number at day 0, 21 and 42 of storage from 2DE analyses of RBC membranes obtained from cells stored in AS-3 (left side) or SAGM (right side). Total spot numbers were calculated on master maps obtained from 4 distinct biological replicates for each group by means of the PDQuest 8.0 software. Results are reported as means \pm S.D..

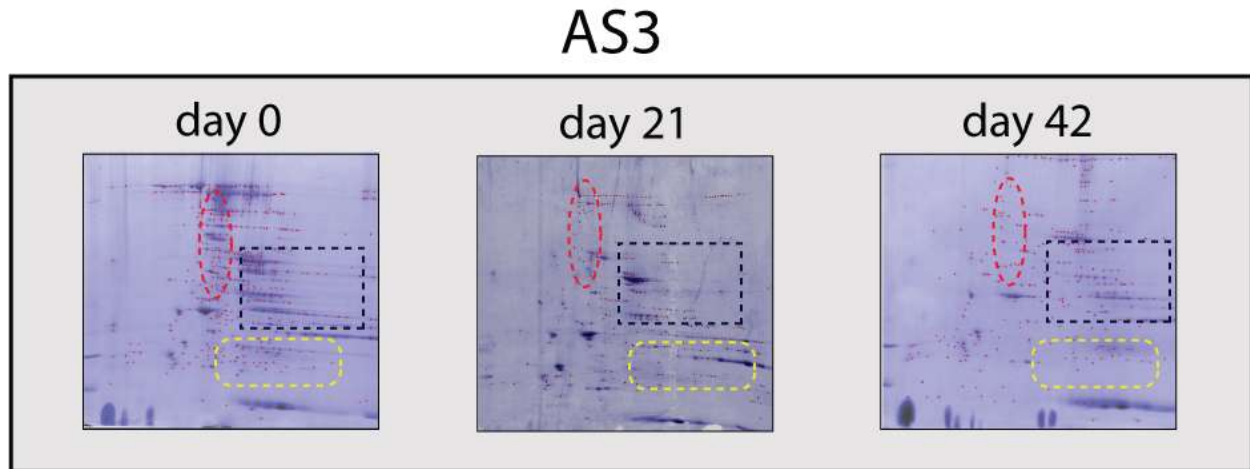


FIGURE 2 A detail of 2DE maps for AS-3-stored RBC membranes at day 0, 21 and 42 (from left to right). The red ellipse, blue rectangle and yellow trapezoid indicate a high MW region, average MW region with medium to high pI and a low MW region, respectively. As storage progresses, fragmentation of proteins from the red ellipsoid region increases the number of spots at low MW. A right-shift (increase in apparent pI) can be observed for most of the spots by storage day 42.

Prolonged storage (42 days) resulted in a right-shift of the pIs (spots display higher apparent pIs). This is particularly evident in the blue rectangle in **Figure 2**.

Although the less drastic increase in the total spot number at day 21 in comparison to day 0 controls suggested that the fragmentation phenomenon was less intense in AS-3 than in SAGM-stored RBCs, protein fragments still accumulated at the membrane level in AS-3-stored RBCs, as we could highlight through the selection of newly appearing protein spots by day 21 in the low MW range (below 25 kDa apparent MW - **Figure 3**). Indeed, we could find at least eight newly appearing protein spots ($p\text{-value} < 0.05$) from 2DE analyses of RBC membrane obtained from cells stored in AS3 for 21 days (**Figure 3**). Spot excision and tryptic digestion allowed MALDI-TOF/TOF-based identification of each spot as follows (**Table 2**): (i) protein fragments of higher MW structural proteins (spots no. 121 – spectrin beta; 148 – ankyrin 2.2; 153 – heat shock cognate 71 kDa protein isoform 1; 234 – protein 4.1 isoform 4; 247 – ankyrin isoform 2; 282 - heat shock 70kDa protein 8 isoform 1; 315 – protein 4.1 isoform 4); (ii) intact proteins migrating to the membrane (spots no. 111 - alpha globin).

Notably, two distinct fragments of protein 4.1 could be detected (spots no. 234 and 315), which in the 2DE map showed highly divergent apparent pIs and MWs. However, through mass spectrometry we could only distinguish them on the basis of the presence of two additional peptides in spot no. 234 in comparison to spot no. 315 (highlighted in bold red and yellow in the peptide list and protein sequence, respectively, in **Figure 4**), which indicate a higher sequence coverage of the former, at least justifying the higher apparent MW (sequence coverage 15% and 13% for spot no. 234 and 315, respectively).

Fragmentation of structural proteins in the frame of RBC storage has long been reported (Messana et al., 2000; Bosman et al., 2008; D'Alessandro et al., 2012) and might stem from the exacerbation of oxidative stress under cold liquid storage conditions (D'Alessandro et al., 2012). This in turn results from the alteration of the metabolic poise (Messana et al., 2000; Bennet-Guerrero et al., 2007), which leads to the impaired capability of RBCs to face

oxidative stress as storage progresses (D'Alessandro et al., 2012). Although the present study is only based upon 2DE proteomics observations, it appears that RBCs stored either in CPD-SAGM or AS-3 are affected by the same

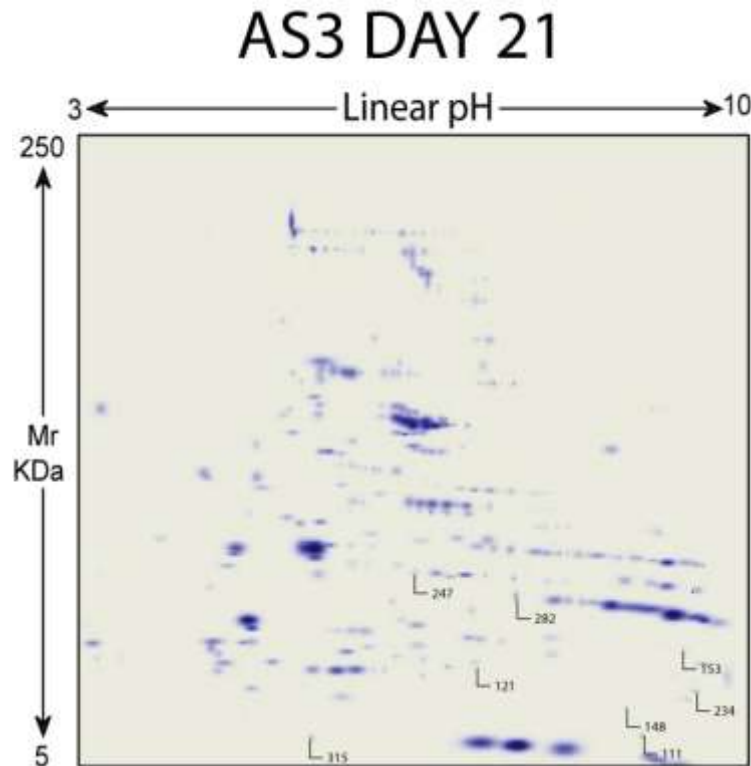


FIGURE 3 Eight newly appearing protein spots in day 21 2DE gels of RBC membranes, in comparison to day 0 controls.

Table 2 – Protein spots identified through mass spectrometry as protein fragments

N° spot	Mr, Da	pI	N° of peptides identified	Mascot Score	NCBI Accession Number	Protein ID [Homo sapiens]
111	13574	7.98	1 (MS/MS)	126	gi 28549	alpha globin
121	173310	4.93	10 (MS)	103	gi 119601287	spectrin, beta, erythrocytic (includes spherocytosis, clinical type I), isoform CRA_g
148	188894	6.15	28 (MS)	180	gi 747710	alt. ankyrin (variant 2.2)
153	70854	5.37	1 (MS/MS)	131	gi 5729877	heat shock cognate 71 kDa protein isoform 1
234	71911	6.19	10 (MS)	131	gi 42716291	protein 4.1 isoform 4
247	188882	6.15	8 (MS)	69	gi 70780355	ankyrin-1 isoform 2
282	70855	5.28	11 (MS)	87	gi 62897129	heat shock 70kDa protein 8 isoform 1 variant
315	71911	6.19	8 (MS)	114	gi 42716291	protein 4.1 isoform 4

fragmentation/vesiculation phenomena, though to a different extent, underlying a universal mechanism for RBC ageing *in vitro* (Bosman et al., 2010; Lion et al., 2010) that none of the hereby tested additive solutions appears to attenuate.

Start-End	Observed	Mr(expt)	Mr(calc)	Delta	Miss	Sequence
79-93	1762.7983	1761.7911	1761.8374	-0.0663	0	K.FYPPDPAQLTEDNTRY
94-101	1128.5710	1127.5638	1127.5797	-0.0160	0	K.YYLCIQLERQ Carbamidoethyl (C)
120-217	1057.5764	1056.5691	1056.5869	-0.0178	1	R.IKRFVWPKV
242-257	1881.8617	1880.8343	1880.9268	-0.0724	0	K.IKPGEEQYVESTIGFKL
270-279	1331.6053	1330.5980	1330.6241	-0.0261	0	K.VCVEHHTFFRL Carbamidoethyl (C)
310-324	1707.8283	1706.8210	1706.8852	-0.0643	0	R.QASALIDRPAPHFERT
429-439	1377.6783	1376.6710	1376.7048	-0.0338	1	R.EKLDGENIYIR.H
451-439	1092.5473	1091.5400	1091.5611	-0.0211	0	R.LKLDGENIYIR.H
485-492	944.4831	943.4758	943.4878	-0.0118	0	R.LKSTHSPPFLT
586-595	1089.5640	1088.5568	1088.5826	-0.0238	1	K.KGISETRIEK.R

Matched peptides shown in **Bold Red**

1	MICKVSLLD	TYVECVVEKH	ARGQQLNRY	CEHMLLEED	YFGIAIWDIA
51	TSKTNLDEAK	EIKKQVGRVF	WFTFNVVFF	FPDPAQLTED	IKRYVLCGLI
101	WQDIVAGRLP	CSFATLALLG	SYTIQSELGD	YDFELNGVOY	VSDFFLAFHQ
151	TEELEERVME	LKHSYRMTF	AQADLEFLN	AFRLSMGVD	LHFAKDLGV
201	DIILGVCSGF	LLVYKDLF	IKRFVWPKV	ISYKRSFFI	KIKPGEEQY
251	ESTIQFLRF	YFAAKELNEV	GVKHTFFRL	TSDTIPSK	FLALGSKFRY
301	SGRTQAGTRQ	ASALIDRPAP	HFERTASRR	SRSLDGAAY	DSADRSPRT
351	SAPAITGGQV	ARGGVLDASA	KRTVYVFAK	ETVKAEVKEE	DEPPEQAEPE
401	PTKANKVKT	HIEVTVPTSH	GDQTKKREK	LDGENIYIR	SHMLKDLDM
451	SGEIKKHHA	SISELKNFM	ESVPEKPEE	NDKRLSTHS	PKLNLINGGI
501	PTGEGFPLK	TQTTISDHA	NAVFSEIPE	QVDIVNTET	TITVEAAQTD
551	DHSGDLDFV	LLTAQITSE	TFSSTTTQI	TRTVGGISE	TRIEKRVIT
601	GDADIDRDQV	LWQAIKAKE	QKFDNAVTV	VVHQETIAD	E

FIGURE 4 A detail of the output from Mascot search algorithm for trypsin digested spot no. 234 and 315, both identified as protein band 4.1 isoform 4. Although from 2DE gels they show opposite pI and slightly different MWs, mass spectrometry-based identification could only shed light on the latter through the individuation of two peptides only in spot no. 234 (higher apparent MW). These two peptides unique for spot no. 234 are indicated in red, to distinguish them from the rest of the peptides identified in both spots. The protein sequence is reported as well, along with the peptides (bold red) which have been hereby identified through mass spectrometry. Unique peptides from spot no. 234 are further highlighted in yellow.

Conclusion

From the present study it emerges that the membrane protein profile of RBCs stored in presence of AS-3 appears to be slightly different from previous reports on SAGM-stored RBC counterparts. However, the increase of total membrane spot number due to the presence of fragments at day 21 and the significant decrease at day 42 are suggestive of a universal phenomenon which is not efficiently tackled by none of the two additive solutions investigated in the present study. To further delve into the storage lesion issue for RBCs stored in AS-3, it would be interesting in the future to assay metabolic changes over storage progression as well, in like fashion to the recently proposed study for RBCs stored in CPD-SAGM (Bennet-Guerrero et al., 2007).

Since oxidative stress is now universally recognized as one of the main underlying phenomena triggering alterations of the RBC proteome and a whole series of storage lesions (Karon et al., 2009; Kanas et al., 2010; Chaudhary et al., 2011; D'Alessandro et al., 2012;), it is mandatory to pursue alternative storage strategies which tackle oxidative stress at its roots, either implying the use of additive solutions with substantial compositional modifications (for example, alkaline pH (Hogman and Meryman, 2006)) or the introduction of novel strategies for RBC storage which envisage elimination of oxygen (Yoshida et al., 2007, 2008 and 2010; Dumont et al., 2009).

5.5 Hemoglobin alpha glycation (Hb1Ac) increases during red blood cell storage: a MALDI-TOF mass spectrometry-based investigation.

Overview of this section

Hemoglobin A1c (HbA1c) represents a key biomarker in diabetes diagnosis and management, as it is indicative of recent blood glucose concentrations. Glycation of hemoglobin is a nonenzymatic irreversible process that is promoted by the prolonged exposure of erythrocytes to high glucose concentrations, a condition that is known to occur under blood banking conditions. However, controversial data indicate no clear hint as to whether and to which extent HbA1c accumulates during red blood cell storage. Hereby we propose the application of a validated MALDI-TOF-mass spectrometry-based method to this issue and report the observation about HbA1c levels apparently increasing over storage progression.

Keywords: red blood cell; hemoglobin; glycation; MALDI TOF/TOF.

Introduction

Hemoglobin A_{1c} (HbA_{1c}) represents a key biomarker in diabetes diagnosis and management, since it allows clinicians to estimate mean blood glucose concentration in the recent period preceding withdrawal (Stevens et al., 1977). Indeed, glycation of hemoglobin is a non-enzymatic irreversible process that is promoted by the prolonged exposure of erythrocytes to high glucose concentrations (Stevens et al., 1977), a condition that is known to occur under blood banking conditions, where additive solutions (such as SAGM) expose red blood cells (RBCs) to higher than normal glyceemic levels (Szelényi et al., 1983). However, controversial data indicate no clear hint as to whether and to which extent HbA_{1c} accumulates during red blood cell storage (Szelényi et al., 1983; Weinblatt et al., 1986; Spencer et al., 2011). Indeed, data from the older literature support the hypothesis that high glucose concentrations in RBC storage medium end up promoting glycation of Hb, thus resulting in the accumulation of HbA_{1c} over time (Szelényi et al., 1983; Weinblatt et al., 1986). These results would underpin the prediction about HbA_{1c} increasing in transfused recipients, though no statistically significant correlation between these two events has been observed by Spencer and colleagues, who thus concluded that “glycation of hemoglobin in stored RBC units is negligible despite the high glucose concentrations in stored RBC units” (Spencer et al., 2011).

Hereby we propose the application of a validated (Bursell et al., 2000; Biroccio et al., 2005; Zurbriggen et al., 2005) MALDI-TOF mass spectrometry-based method to this issue and report the observation about HbA_{1c} levels apparently increasing over storage progression.

Materials and Methods

In brief, leukodepleted RBC units were collected from 10 healthy volunteers upon informed consent. MALDI-TOF MS analysis of HbA_{1c} was performed according to the method by Biroccio et al. (2005). All MALDI analyses were performed with an AutoflexIII MALDI-TOF mass spectrometer (Bruker Daltonics-Bremen, Germany). Relative concentrations of HbA_{1c} were calculated as a percentage of the glycated forms (15.289 and 16.030 m/z) with respect to the total of the free form of alpha and beta globin chains (Hb= 15.127 +15.868 m/z), within the linearity range of the instrument (Biroccio et al., 2005), according to the following equation:

$$\text{HbA}_{1c} \% = \frac{\text{HbA}_{1c} \times 100}{(\text{Hb} + \text{HbA}_{1c})}$$

Results and Discussions

The analytical approach exploited in the present study holds several advantages over routine methods for HbA_{1c}, including the rapidity and robustness of the approach, along with the higher sensitivity of MALDI TOF-TOF last generation instruments in comparison to triple quadrupoles mass spectrometers. Triple-quadrupoles are more diffused in the clinical setting (Gevi et al., 2012), despite their low tolerance for salts and sample impurities, instrumentation costs, length of the analysis and laborious sample handling/preparation (Gevi et al., 2012).

In **Figure 1** we report a sample MALDI-TOF spectrum. In **Figure 2**, where spectra from the analysis of RBCs at 0, 14, 28 and 42 days of storage are graphed, storage progression corresponded to a visible increase of the glycated forms of Hb chains. Results reported in **Table 1** are representative of the quantification of the relative percentages of

HbA_{1c}, according to the formula indicated in **Table 1**. As it emerges from these results, relative quantities of glycosylated Hb form A_{1c} in relation to free Hb alpha chain increase over storage progression, as to become statistically significant (p -value<0.05 ANOVA) after the 14th day of storage, at 28 days. Therefore, our results are consistent with older direct measurements of HbA_{1c} in stored RBC units (Szelényi et al., 1983; Weinblatt et al., 1986).

Though these results are in apparent contradiction with the report by Spencer and colleagues (2011), it should be noted that indirect measurements of HbA_{1c} in the recipients upon transfusion are both affected by pre-transfusion HbA_{1c} levels and dilution of the HbA_{1c} levels of long-stored transfused unit (in a healthy patient this ratio is approximately 1:10 for a single RBC unit in a 5L adult male healthy individual). Also, the final HbA_{1c} upon long-term storage might indeed increase over initial values (of the donor), but still be lower than the one that could be observed in the pre-transfusion recipient's blood.

Accumulation of HbA_{1c} might be dependent on the additive solution. Indeed, absolute and relative quantifications of glucose levels in CPD-SAGM-stored erythrocyte concentrates indicate that, despite ongoing glycolysis (Gevi et al., 2012; D'Alessandro et al., 2012), at the end of the storage glucose levels in the supernatants are approximately of 12±1mmol/L, which is still higher than circulating glucose in diabetic patients (subjects with a consistent glycaemia above 7 mmol/l are generally held to have diabetes) (Burger et al., 2010). If we consider that HbA_{1c} formation is a non-enzymatic phenomenon that is both dependent on glucose concentrations and oxidative stress, one leading cause triggering RBC storage lesions during prolonged storage (Gevi et al., 2012; D'Alessandro et al., 2012), it is realistic enough to conclude that CPD-SAGM-stored RBCs should be more susceptible to the formation of HbA_{1c} than RBCs storage in presence of other, less "glucose loaded", additive solutions. In this view, it is worthwhile to stress that oxidative stress in CPD-SAGM-stored RBC units becomes significant upon two weeks of storage (Gevi et al., 2012; D'Alessandro et al., 2012), in line with the hereby reported observations(**Table 1**).

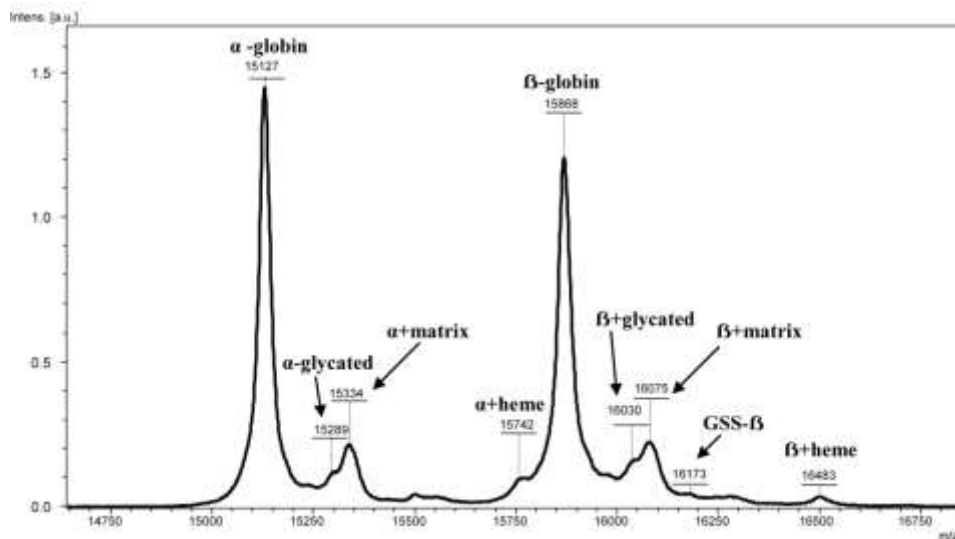


FIGURE 1 – MALDI TOF intact mass spectrum of alpha and beta globin chains.

Spectrum interpretation and peak attribution has been performed on the basis of Biroccio et al. (2005) and Zurbriggen et al. (2005). A sample RBC intact mass

spectrum is reported in the range between 14.500 and 17.000 m/z. We could identify the main alpha (15.127 m/z) and beta globin (15.868 m/z) chains, their main glycosylated variants showing a +162Da adduct (at 15.289 and 16.030 m/z, respectively), and the respective heme adducts (+165Da, at 15.742 and 16.483 m/z, respectively) (Biroccio et al., 2005; Zurbriggen et al., 2005). Also, +207Da adducts with the SA matrix were visible as well, in agreement with Biroccio et al. (2005).

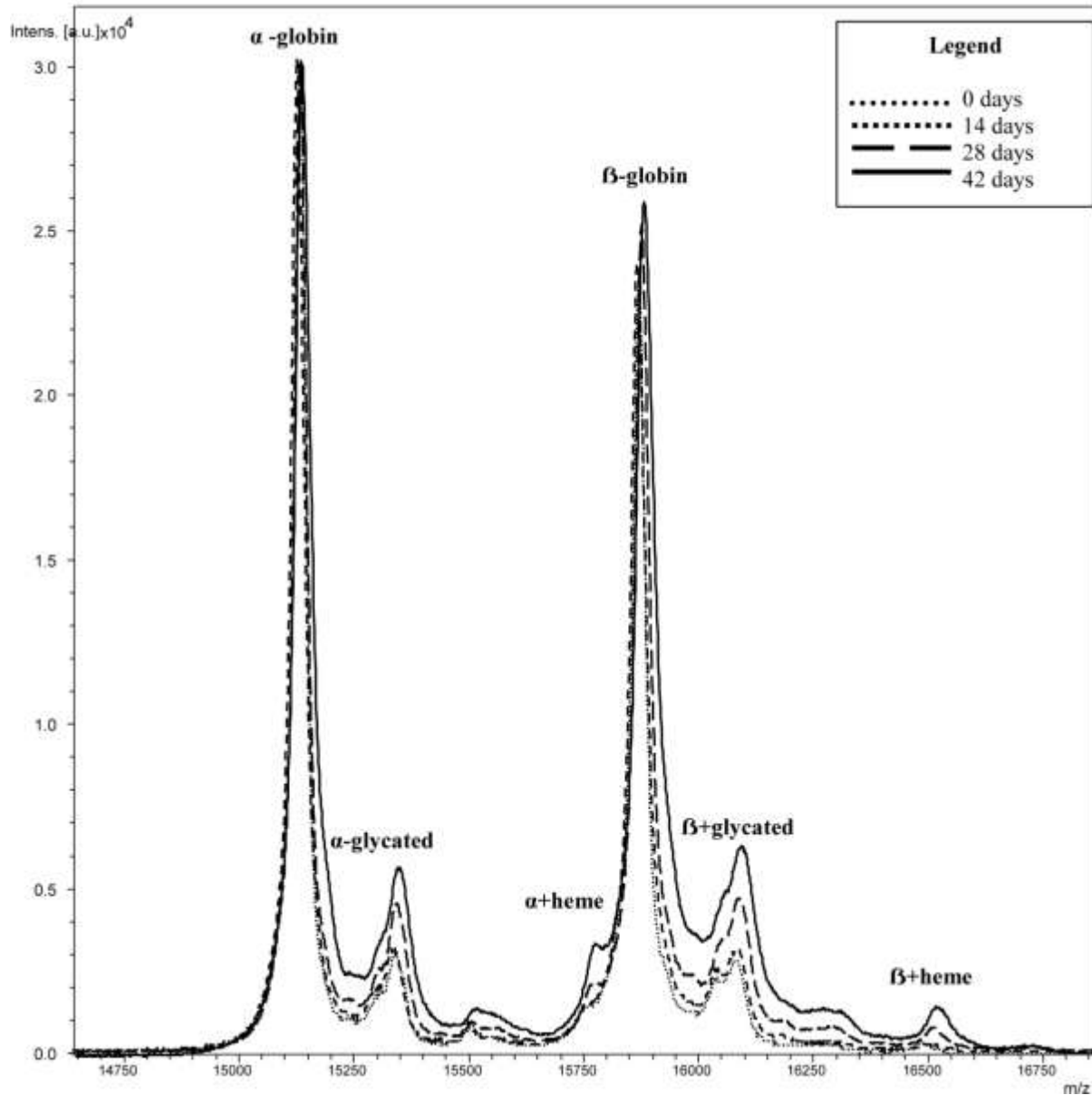


FIGURE 2 - Time course analysis of RBC extracts over storage duration under blood bank conditions. Samples were assayed fortnightly at 0, 14, 28 and 42 days of storage. HbA_{1c} glycated form of alpha globin evidently increased in proportion to storage duration. A small peak was also visible (especially in long stored RBC samples) at 16.173 m/z, corresponding to the +305Da glutathionylated adduct of the Hb beta chain, in agreement with (Bursell et al., 2000).

Table 1 – Time course analysis of HbA_{1c} during red blood cell storage	
Sample	Mean Value $\text{HbA}_{1c}\% = \frac{\text{HbA}_{1c} \times 100}{(\text{Hb} + \text{HbA}_{1c})}$
0-day	4,13 + 0.25
14-day	5,36 + 0.18
28-day	7,59 + 0.21*
42-day	10,90 + 0.25*

Hb: ion counts at 15127 m/z + 15868; **HbA_{1c}:** ion counts at 15289 + 16030 m/z
* = statistically significant at $p < 0.05$ ANOVA

Conclusion

Although recent evidences suggest that storage duration ends up influencing HbA_{1c} measurements in transfused recipients only to a negligible extent (Spencer et al., 2011), we hereby confirm old literature data (Szelényi et al., 1977; Weinblatt et al., 1986) through alternative, yet validated, MALDI-TOF mass-spectrometry-based approaches, that the relative quantities of glycated HbA_{1c} increase over storage duration.

5.6 Red Blood Cell Lipidomics analysis through HPLC-ESI-qTOF: application to red blood cell storage

Overview of this section

Recent developments in mass spectrometry (MS) have enabled fast and sensitive detection of lipid species in different biological matrices.

In the present study we performed an on-line HPLC-microTOF-Q MS approach to the red blood cell (RBC) lipidome. We thus exploited bioinformatic tools for the interrogation of novel databases, such as LIPID MAPS. By means of ad hoc software suites for mass spectrometry-based metabolomics analyses, we could address the key biological issue of the RBC lipidome, within the framework of RBC storage for transfusion purposes. Samples were collected from subjects living in the province of Viterbo, where olive oil consumption represents a central aspect of the diet. On this ground, we could postulate a diet specific effect on the accumulation of lipid-specific storage lesions.

The analyses yielded the tentative identification of a huge number of lipid molecules on the basis of accurate intact mass values and retention times, and MS/MS validation. This analytical workflow was exploited to consolidate existing knowledge on the RBC lipid composition and individuate statistically significant fluctuations of lipids throughout storage duration of RBC concentrates under blood bank conditions. Our analysis indicated ceramides, glycerophospholipids and sterols as key targets of RBC storage lesions to the lipidome, that will deserve further targeted investigations in the future. It also emerged how compositional analyses of the RBC lipidome might end up yielding different results on the basis of the background of the blood donor (i.e. diet), which might translate into region-specific lipidomic alterations over storage progression of RBC concentrates.

Keywords: Red Blood Cells; Mass Spectrometry; Blood Storage; Lipidomics.

Introduction

Lipidomics is the systematic identification of the lipid molecular species of a biological matrix (either a cell, organelle, globule, or whole organism) with emphasis on the relative quantitation of composition changes in response to a perturbation, such as ageing or drug treatments (Alex Brown, 2012). While the term “lipidomics” dates back to a decade ago, investigations of the lipid content of specific biological matrices was an already consolidated field of research over the last fifty years (Philips and Roome, 1959). In particular, this holds true for those matrices that are largely available and display limited biological complexity, such as anucleated cells and, in particular red blood cells (RBCs) (Philips and ROome, 1959; Hanahan et al., 1960; Farquahar et al., 1963; Ways and Hanahan, 1964; Dodge and Philips, 1967; Owen et al., 1982; Dougherty et al., 1987; Han and Gross, 1994; Beerman et al., 2005; Skeaff et al., 2006; Rise et al., 2007; Kabagambe et al., 2008; Novgorodtseva et al., 2011).

Indeed, RBCs are also devoid of organelles and of any *de novo* lipid synthesis capacity, which makes their lipidome rather stable in comparison to other cell types. Indeed, phospholipid synthesis is known to be active in reticulocytes and suppressed in mature RBCs (Percy et al., 1973). Nonetheless, alteration of lipid homeostasis is strictly tied to membrane reorganization during RBC ageing *in vivo* and *in vitro* (RBC storage), mainly owing to lipid peroxidation phenomena which promote membrane shape alterations through the progressive loss of lipids (and membrane-associated proteins) via vesiculation (D'Alessandro et al., 2012; Gevi et al., 2012; Dinkla et al., 2012). Therefore, it is small wonder that the RBC lipidome has long attracted a great deal of interest over the last five decades.

Yet in 1959, Phillips and Roome provided a preliminary portrait of the human RBC phospholipidome. However, it was only in 1960 that Hanahan and colleagues described a more complex scenario, also by including species-specific differences between human and bovine RBCs. Four years later, Ways and Hanahan (1964) reported a detailed lipid class composition of normal human RBCs, indicating the following percentages: cholesterol 25%, choline glycerophosphatides 30%, sphingomyelin 24%, ethanolamine glycerophosphatides 26%, and serine glycerophosphatides 15%. Meanwhile, Farquahar and Ahrens (1963) had showed that 67% of the PE, 8% of the PS, and 10% of the lecithin of human RBCs are in the plasmalogen form, with a vinyl ether linkage at the sn-1 and an ester linkage at the sn-2 position. In 1967, Dodge and Philips described a silicic acid thin-layer chromatography strategy to investigate the phospholipid and phospholipid fatty acids and aldehydes in human RBCs (Dodge and Philips, 1967). Thirty-three fatty acids and five aldehydes were separated and tentatively classified into lipid classes, including phosphatidyl ethanolamine (PE), phosphatidyl serine (PS), lecithin, and sphingomyelin (SM) 24:0 and 24:1, while fatty acid moieties were tentatively attributed. Of note, the values reported by Dodge and Philips (1967) were consistent with those by Ways and Hanahan (1964). Interesting results were obtained also as far as it concerned the composition in fatty acid moieties of the different lipid classes. About 37% of the total fatty acid in PS was 18:0, while only about 3% was 16:0; in PE and lecithin, 16:0 was the major saturated fatty acid, with the level in lecithin being over twice that in PE. The relative amount of 18:1 was also much lower in PS than in PE and lecithin. The fatty acid distribution of sphingomyelin differed markedly from that of the glycerophospholipids (GP), in particular in the greater degree of saturation (Dodge and Philips, 1967). Only about 33% of the fatty acids were unsaturated; in addition, less than 6% of the fatty acids appeared to have more than one double bond and less than

3% more than two double bonds. The 16:0, 24:0, and 24:1 made up almost 7% of the total fatty acids. Essentially all of the 24:0 and most of the 24:1 of the human RBC phospholipids appeared to reside in sphingomyelin.

Different instrumentations and techniques have been tested for the improvement of lipid analysis. During the last two decades, big technological strides have prompted the dissemination of chromatography separation and mass spectrometry-based lipidomics studies of RBCs (Han and Gross, 1994; Beerman et al., 2005; Skeaff et al., 2006; Rise et al., 2007; Kabagambe et al., 2008; Novgorodtseva et al., 2011). At the dawn of the mass spectrometry-based lipidomics era the complexity of the lipidome did not enable comprehensive studies like the ones performed with thin layer chromatography (TLC) or gas chromatography (GC) described in the previous paragraphs (Philips and ROome, 1959; Hanahan et al., 1960; Farquahar et al., 1963; Ways and Hanahan, 1964; Dodge and Philips, 1967; Owen et al., 1982; Dougherty et al., 1987; Han and Gross, 1994; Beerman et al., 2005; Skeaff et al., 2006; Rise et al., 2007; Kabagambe et al., 2008; Novgorodtseva et al., 2011). The expensive instrumentation and the lack of bioinformatic tools to handle the high-throughput amount of data collected via the mass spectrometry-based workflow hampered at first its diffusion in the field (Alex Brown, 2012). More recently, the introduction of highly accurate and less expensive instruments (in comparison to the ones available decades ago) was also paralleled by consistent improvements in the field of bioinformatic elaboration of the raw mass spectra (Alex Brown, 2012). The acquired expertise have helped laboratories worldwide to cope with the intrinsic difficulties related to lipid mass attribution and fueled new efforts to bring about the systematic classification of lipid species and structures (Fahy et al., 2005; Sud et al., 2007). The current burgeoning of OMICS disciplines has thus given new verve to the field of lipidomics research, while enabling further steps forward.

Regarding RBC lipid homeostasis, as premised by Farquahar and Ahrens (1963), lipid composition of human RBCs is largely influenced by the diet. In this view, Dougherty and colleagues performed an extensive investigation to relate region specific diets to the lipid content of plasma, platelets and RBCs (Dougherty et al., 1987). By comparing RBCs of individuals from rural areas in Finland, Italy (province of Viterbo) and the United States, the Authors demonstrated how diets largely relying on fish and olive oil consumption (in Finland and Italy, respectively), resulted in a significant decrease (in comparison to the US counterparts) in the levels of polyunsaturated fatty acids (PUFA), which they relate to the potential production of unhealthy prostaglandins (thromboxane and prostacyclins) byproducts (Dougherty et al., 1987). Finally, the Authors also noted that in all plasma and RBC glycerolphospholipids, the monounsaturated fatty acids (especially oleic acid 16:1 and palmitic acid, 16:0) were highest in the Italian and the saturated fatty acids were highest in the Finnish samples. In this frame, we exploit novel databases such as LIPID MAPS and *ad hoc* software suites for mass spectrometry-based metabolomics analyses (such as MAVEN (Clasquin et al., 2012)) to address the key biological issue of the RBC lipidome. Our investigation shares some features with the study by Dougherty and colleagues (1987), for it was performed on RBCs collected from subjects living in the province of Viterbo, where olive oil consumption represents a central aspect of the diet. We further address the RBC storage issue (from a lipidomic standpoint) as to conclude that wider transfusion medicine-relevant studies should be carried out to investigate whether inter-regional donor differences might lie upon peculiar RBC lipidomic profiles, which in turn are likely to reflect the heterogeneity of local alimentation regimes across Italy.

Materials and Method

Sample collection

Red blood cell units were drawn from healthy donor volunteers according to the policy of the Italian National Blood Centre guidelines (Blood Transfusion Service for donated blood) and upon informed consent in accordance with the declaration of Helsinki. We studied RBC units collected from 10 healthy donor volunteers [male=5, female=5, age 39.4 ± 7.5 (mean \pm S.D.)]. RBC units were stored for up to 42 days under standard conditions (CDP-SAGM, 4°C), while samples were removed aseptically for the analysis on a weekly basis (at 0, 7, 14, 21, 28, 35 and 42 days of storage).

Untargeted Metabolomics Analyses

Metabolite extraction

For each sample, 0.5mL from the pooled erythrocyte stock was transferred into a microcentrifuge tube (Eppendorf® Germany). Erythrocyte samples were then centrifuged at 1000g for 2 minutes at 4°C. Tubes were then placed on ice while supernatants were carefully aspirated, paying attention not to remove any erythrocyte at the interface. Samples were extracted following the protocol by D'Alessandro et al. (2011). The erythrocytes were resuspended in 0.15 mL of ice cold ultra-pure water (18 MΩ) to lyse cell, then the tubes were plunged into a water bath at 37°C for 0.5 min. Samples were mixed with 0.6 mL of -20°C methanol and then with 0.45 mL chloroform. Subsequently, 0.15ml of ice cold ultra-pure water were added to each tube and they were transferred to -20°C freezer for 2-8 h. An equivalent volume of acetonitrile was added to the tube and transferred to refrigerator (4°C) for 20 min. Samples with precipitated proteins were thus centrifuged for 10000 x g for 10 min at 4 °C .

Finally, samples were dried in a rotational vacuum concentrator (RVC 2-18 - Christ GmbH; Osterode am Harz, Germany) and re-suspended in 200 µl of water, 5% formic acid and transferred to glass auto-sampler vials for LC/MS analysis.

Rapid Resolution Reversed-Phase HPLC

An Ultimate 3000 Rapid Resolution HPLC system (LC Packings, DIONEX, Sunnyvale, USA) was used to perform metabolite separation. The system featured a binary pump and vacuum degasser, well-plate autosampler with a six-port micro-switching valve, a thermostated column compartment. Samples were loaded onto a Reprosil C18 column (2.0mm×150mm, 2.5 µm - Dr Maisch, Germany) for metabolite separation.

For lipids multi-step gradient program was used. It started with 8% solvent A (ddH₂O, 20 mmol L⁻¹ ammonium formiate; pH 5) to 6% solvent A for 3 min than to 2% solvent A for 35 min and finally to 100% solvent B (methanol) in 30 minutes. At the end of gradient, the column was reconditioned with 8% solvent A for 10 min. The overall run time was 68 min. Column oven was set to 50°C and the flow rate was 0.2 mL/min.

Mass spectrometry analysis through microTOF-Q

Due to the use of linear ion counting for direct comparisons against naturally expected isotopic ratios, time-of-flight instruments are most often the best choice for molecular formula determination. Thus, mass spectrometry analysis was carried out on an electrospray hybrid quadrupole time-of flight mass spectrometer MicroTOF-Q (Bruker-Daltonik, Bremen, Germany) equipped with an ESI-ion source.

MS analysis was carried out in negative ion mode capillary voltage 2800V, nebulizer 45 psi and dry gas of 9 l/min, scan mode 100-1500 m/z. For sample injection, solutions were evaporated to dryness and reconstituted in an adequate volume of methanol:ethanol 1:1. Lipids extracts were prepared by dilution to a concentration of 5 pmol · L⁻¹ (where total phospholipids concentration was 2.5 pmol · L⁻¹). Tandem mass spectrometry (MS/MS) is used for glycerophospholipid species structural characterization. Unambiguous species identification is done by analysis of the retention time and fragmentation pattern and through direct comparison against the same parameters, as acquired from chemically defined standards (Avant Polar Lipids, Inc., Alabaster, Al.), in agreement with Ivanova et al. (2010).

Automatic isolation and fragmentation (AutoMSⁿ mode) was performed on the 4 most intense ions simultaneously throughout the whole scanning period (30 min per run). Calibration of the mass analyzer is essential in order to maintain an high level of mass accuracy. Instrument calibration was performed externally every day with a sodium formate solution consisting of 10 mM sodium hydroxide in 50% isopropanol: water, 0.1 % formic acid. Automated internal mass scale calibration was performed through direct automated injection of the calibration solution at the beginning and at the end of each run by a 6-port divert-valve.

Data elaboration and statistical analysis

In order to reduce the number of possible hits in molecular formula generation, we exploited the in house SmartFormula application of MAVEN (Clasquin et al., 2012), which directly calculates molecular formulae based upon the MS spectrum (isotopic patterns) and transition fingerprints (fragmentation patterns). This software generates a confidence-based list of chemical formulae on the basis of the precursor ions and all fragment ions, and the significance of their deviations to the predicted intact mass and fragmentation pattern (within a predefined window range of 5 ppm). Triplicate runs for each one of the 10 biological replicate at day 0 and over storage duration were exported as mzXML files and processed through METLIN/XCMS data analysis software (Scripps Centre for Metabolomics) (Tautenhahn et al., 2012; Belosludtsev et al., 2010) and MAVEN (Clasquin et al., 2012). Mass spectrometry chromatograms were elaborated for peak alignment (mzwidth = 0.025, minfrac = 0.5, bw = 5), matching and comparison of parent and fragment ions, and tentative metabolite identification (within a 20 ppm mass-deviation range between observed and expected results against the imported LIPID MAPS database (Sud et al., 2007) – annotations included adduct ions in positive ion mode). XCMS and MAVEN are open-source software that could be freely used or downloaded from their websites (<http://metlin.scripps.edu/download/> and <http://genomics-pubs.princeton.edu/mzroll/index.php?show=download>). Quantitative variations were determined against day 0 controls and only statistically significant results were considered (fold change > 2.5 and ANOVA *p-values* < 0.01). Data were further refined and plotted with GraphPad Prism 5.0 (GraphPad Software Inc.)

Results and Discussion

HPLC-MS analysis of the RBC lipidome yielded the tentative identification of a huge number of lipid molecules on the basis of accurate intact mass values and retention times (RT) (**Supplementary Tables 1-5** of Timperio et al., 2013). Results were further validated against MS/MS feature transitions (fragmentation patterns) for RBC storage time course analyses, where we reported statistically significant variations ($p < 0.01$ ANOVA) of specific lipid molecules over storage duration on a weekly basis in comparison to day 0 controls (**Table 1**). This helped coping with the difficulties related to the attribution of fatty acid moieties in detected lipids, a problem that hampered major translational applications of early MS-based approaches to the RBC lipidome (Han and Gross, 1994; Beerman et al., 2005).

A 2D map overview of the lipid features identified in a single run is provided in **Figure 1**, where compound class specific separations are indicated according to the established nomenclature (fatty acids – FA; glycerolipids – GL; glycerophospholipids – GP; sphingolipids – SP; sterols – ST; prenols – PR and polyketides – PK). While FA, GL, GP and SP eluted rather early (within the first six minutes of RT), ST first and PR or PK displayed higher RTs, consistently with their more hydrophobic nature.

In the following paragraphs, we will detail the major findings of the currently proposed investigation through the description of the main distinct lipid classes. Results will be discussed in the light of existing literature in the field.

Fatty acids

Fatty acid distribution indicated that palmitic acid (FA C16:0 – **Figure 2**) was the most abundant free fatty acid (extended results are reported in **Supplementary Table 1** – Timperio et al., 2013). This is also consistent with oldest reports on the RBC fatty acid composition available from the literature (Ways and Hanahan, 1964), despite the extreme differences between the TLC and the HPLC-MS analytical approaches. Palmitic acid might be tied to the modulation of calcium signaling in RBCs by mediating Ca^{2+} fluxes via specific membrane pores (Tautenhahn et al., 2012), thereby modulating RBC survival.

Among the most abundant individual fatty acids we could detect 16:0 (palmitic), 18:0 (stearic), 18:1 (oleic), and 22:6 n-3 (docosahexaenoic acid), in agreement with previous studies on fatty acids of erythrocytes obtained from healthy Italian subjects (Pala et al., 2001). Furthermore, octadecadienoic acid (18:2 n-1,5) had already been reported among the most abundant ten fatty acids of RBCs (Ways and Hanahan, 1964). The abundance of oleic acid in particular was an expected result, since olive oil holds a key role in the frame of the Mediterranean diet and, in particular, in the province of Viterbo (Italy) where blood samples were collected from healthy donor volunteers. The intertwinement between oleic acid relative concentrations and high olive oil consumption rates had already been postulated and demonstrated through TLC approaches (Dougherty et al., 1987), and hereby confirmed through MS.

On the other hand, no previous investigation indicated myristic acid (14:0) as one of the most abundant fatty acid in RBCs, except for those studies suggesting a role for myristic acid supplementation as a substitute of oleic acid in the diet, which results in the relative increase of α -linolenic and docosahexaenoic acid levels (Rioux et al., 2008) and alterations of RBC membrane fluidity (Dabadie et al., 2006). Analogously, heptadecanoic acid (17:0) has been proposed as a controversial biomarker for the assessment of energy and macronutrient composition in response to specific diets (Poppit et al., 2005).

Eicosanoids and octadecanoids and their peroxidation products (relative abundances are reported in **Figure 1**) are thought to play a role in mediating RBC maturation from reticulocytes by promoting the degradation of mitochondrial membranes and thus elimination of these organelles (Grulich et al., 2001). Also, eicosanoids serve as substrates for cyclooxygenase, lipoxygenase and epoxygenase activities, which result in the production of pro-inflammatory factors that are associated with increased cardiovascular risk and cancer (Smith and Murphy, 2002).

Glycerolipids and glycerophospholipids

Relative abundances of RBCs glycerolipids (GL) and glycerophospholipids (GP) are reported in **Figure 3** and **4** (extended results are reported in **Supplementary Table 2** and **3** – Timperio et al., 2013), respectively, whereas the latter class has been further sub-divided into phosphatidic acid (PA), phosphatidylcholines (PC), phosphatidylethanolamines (PE) and phosphatidylserine (PS), in the light of the observed elevated concentrations in RBCs. Fatty acid incorporation stages into RBC membrane GLs and GPs has been long investigated (Oliveira et al., 1964; Donabedian et al., 1967; Mulder et al., 1962), indicating higher rates for reticulocytes in comparison to adult RBCs (Van Gastel et al., 1965; Shohet et al., 1968). Indeed, RBC GL and GP metabolism is a key aspect in RBC survival (Mulder et al., 1965), since during their 120 days approximate lifespan in the circulatory system RBCs shed approximately 1 microvesicle/h, thus continuously remodeling their membrane and its lipid composition. Also, early approaches to GP composition of RBCs have been purported via TLC (Skipski et al., 1964) indicated a relation of GP composition with RBC membrane anomalies, such as in the case of spherocytosis (Kates et al., 1961). These considerations are relevant in the light of the incomplete long chain fatty acid synthesizing system which characterizes RBCs (Pittman et al., 1966). The introduction of high-resolution capillary gas chromatography approaches recently shed new light on this delicate issue (Jakobik et al., 2009), further evidencing compositional anomalies of GL and GP in cancer patients (Mikirova et al., 2004).

Our results provide further supporting evidence about increased levels of elevated levels of C16:0 and C18:0 fatty acids in lyso-PCs from adult RBCs (**Figure 4**), as previously reported with different approaches (Dougherty et al., 1987; Leidl et al., 2008; Jakobik et al., 2009). Analogous considerations can be made for PE 38:4, PE 40:6 and lyso-PE 18:0, as well as for PS 38:4 (**Figure 4**), in agreement with the literature (Dougherty et al., 1987; Leidl et al., 2008). In particular, PS 38:4 had been recently indicated as the most abundant RBC-specific PS, in comparison to other blood cell types (Leidl et al., 2008). Distribution of saturated and unsaturated fatty acids in GL and GP was also consistent with the literature (Ways and Hanahan, 1964; Dougherty et al., 1987; Leidl et al., 2008).

As expected, compositional differences were observed as well, which are probably attributable to the different diets of the subjects enrolled in the present study in comparison to data available from the literature.

Sphingolipids, sterols and prenol lipids

Sphingolipids (SP), among which ceramides (Cer), have been recently associated with *in vivo* and *in vitro* ageing of RBCs (Dinkla et al., 2012). Though the mechanisms have not yet been fully elucidated, sphingosines and ceramides seem to affect RBC survival by serving as signaling molecules upon acid sphingomyelinase hydrolysis of sphingomyelin into ceramide (Smith et al., 2008) or rather they directly affect RBC membrane stability by forming specific pores and thus altering membrane permeability and potential (Siskind et al., 2005). Ceramide-enriched

membrane domains have been indeed associated with hot-cold hemolysis (Montes et al., 2008). Besides, SP metabolites, including ceramides, sphingosine and sphingosine 1-phosphate have recently emerged as a new class of lipid biomodulators also in the extracellular space (Tani et al., 2007).

In **Figures 5 and 6** we report the relative abundances of the top SP, with a focus on ceramides, respectively. Of note, C16 sphingosine (**Figure 5**) has been recently reported to be the most abundant RBC-specific SP (Leidl et al., 2008). On the other hand, while we expected elevated levels of Cer 24:1 and 24:0, in agreement with Leidl et al. (2008), we could instead observe elevated levels of Cer 18:0 and 18:1 in all the ceramide subclass (**Figure 6**), which might reflect the relative composition of free fatty acid, as mentioned the previous paragraphs.

Recent studies have also demonstrated that sphingolipids dynamically cluster with sterols to form lipid microdomains or rafts, which function as platforms for effective signal transduction and protein sorting (Simons and Ikonen, 1997). Sterol profiling of RBCs is also a powerful diagnostic tool to investigate the effects of total parental nutrition diet supplementation to the newborn, a lifesaving therapy in children with intestinal failure (Pianese et al., 2008).

An overview of the most abundant sterol lipids is provided in **Figure 7**, where sterol lipids are reported with their relative name from the Lipid Maps database (Sud et al., 2007), owing to the impossibility to adapt graphic limitations to the lengthy extended names of each sterol lipid. However, full details are provided in the **Supplementary Table 4** – Timperio et al., 2013.

Prenol lipids are an often under-investigated class of lipids, which are synthesized from five carbon isoprene units. Recent lipidomics studies focused on plasma levels of dolichols (a group of α -saturated polyprenols characterized by 14 to 24 isoprene subunits) and ubiquinones (a group of 1,4-benzoquinones modified with 9-10 repeated isoprene units) (Quehenberger et al., 2010). However, to the best of the Authors' knowledge, little is known about the composition of prenyl lipids in adult RBCs.

While in **Figure 8** we graphed the relative abundances of prenyl lipids on the basis of their relative molecular formula, in **Supplementary Table 5** – Timperio et al., 2013 we also provided extended details about their common name and abbreviations, according to the Lipid Maps database nomenclature (Sud et al., 2007). However, further dedicated studies are mandatory to shed further lights on the relative concentrations and biological functions of these molecules within the framework of RBC biology.

Red blood cell Lipidomics: application to the storage of erythrocyte concentrates

RBC concentrates for transfusion purposes are routinely stored at 2-6°C for up to 42 days, according to international standard guidelines (Council of Europe, 2011).

Despite decades of substantial improvements in the field of RBC storage (D'Alessandro et al., 2010), concerns still arise and persist about the quality of longer stored RBCs, since it is clearly emerging –at least from a biochemical standpoint– that storage progression corresponds to the accumulation of a wide series of RBCs storage lesions (D'Alessandro et al., 2010), as, among others, we could recently document at the morphologic, metabolomics and proteomics level (Blasi et al., 2012; D'Amici et al., 2012). On the other hand, lipidomic aspects of RBC storage in the blood bank still lie undisclosed. Recently, Bosman's group (Dinkla et al., 2012) demonstrated that specific

treatment with exogenous sphingomyelinases resulted in the accumulation of ceramides RBC morphological lesions, thereby mimicking the effects of long-stored RBCs. Indeed, accumulation of ceramides and their metabolites (sphingosine and sphingosine 1-phosphate – S1P) might promote intrinsic stimuli leading to the exacerbation of ageing phenomena in RBCs (Dinkla et al., 2012), by altering membrane conformation (Montes et al., 2008) or mediating specific intra- or extra-cellular signaling cascades (Smith et al., 2008). In this view, it is worthwhile noting that plasma S1P mainly originates from erythrocytes, since RBCs display alkaline (but not acid or neutral) ceramidase activity on D-e-C(18:1)-ceramide (Neidlinger et al., 2006). First of all, we wish to stress that the most abundant ceramides we could detect in control adult RBCs could be catalogued as C18:0 or 18:1 (**Figure 6**). Moreover, in the present study prolonged storage of RBC was apparently associated with statistically significant decrease ($p < 0.01$ ANOVA) of ceramides (C-8, Ceramide d18:1/12:0 and ceramide C-2 – **Table 1**) after three weeks of storage, which is a critical timespan threshold for the accumulation of storage lesions at the biochemical level, as we could previously report at the proteomics and metabolomics level (D'Amici et al., 2012; Blasi et al., 2012). These results are suggestive of a likely ceramidase-mediated digestion of ceramides, or rather of an alteration of the lipid composition of long-stored RBCs probably reflecting the membrane remodeling occurring over RBC storage duration (D'Alessandro et al., 2010). However, we could also observe a decrease in the levels of several sphingosines (N,N,N-trimethyl sphingosine, sphingosine, phytosphingosine and D-erythro-Sphingosine C-15 – **Table 1**), which did not help us ruling out any definitive scenario to explain the observed phenomena.

After an initial increase (attributable to phospholipase activities (Chaudhary et al., 2012)), prolonged storage of RBC concentrates hereby resulted in the progressive statistically significant ($p < 0.01$ ANOVA) decrease of a wide series of fatty acids, prostaglandins (such as PGF 2α and prostaglandin E 2) and fatty acid oxidation products ((1R,2R)-3-oxo-2-pentyl-cyclopentanehexanoic acid) (**Table 1**). This is consistent with the reported progressive accumulation of lipid oxidation byproducts in the supernatants of long-stored erythrocyte concentrate units (D'Alessandro et al., 2012; Chaudhary et al., 2012).

The initial increase in the levels of diacyl-glycerols (DG) and triacyl-glycerols (TG) (**Table 1**) is difficult to interpret, if not in the light of the need for RBCs to cope with the initial free fatty acid accumulation through their sequestering and accumulation in the form of DGs and TGs. This is consistent with the hypothesis that, whether a Save or Sacrifice mechanism is innate in RBCs, as suggested by *in silico* elaborations (Goodman et al., 2007; D'Alessandro et al., 2010), this mechanism is active within the first two weeks of storage (D'Alessandro et al., 2012).

Recently, Bicalho et al. (2013) investigated the alterations to the RBCs phospholipidome by performing a direct comparison of fresh RBC phospholipids against the phospholipid composition of RBC-shed microvesicles. As a result, the Authors could point out the alterations of PS 38:4 and PS 38:1 composition in fresh controls and RBC-derived microvesicles (Bicalho et al., 2013). In the present study, while we could confirm previous evidences about PS 38:4 being preponderant in RBCs (**Figure 4**), also in agreement with Leidl et al. (2008), we could not detect any statistically significant variation as far as PS are concerned. On the other hand, we could detect significant decrease in the levels of two PCs (O-1:0/O-18:0 and 10:0/18:0 – **Table 1**), PEs (lyso-PE(0:0/22:2(13Z,16Z))) and lyso-

PE(0:0/22:2(13Z,16Z)) – **Table 1**), while PIs followed a controversial trend, especially within the first two weeks of storage.

Finally, sterols, prenols, saccharolipids and polyketides were hereby investigated for the first time within the framework of RBC storage. Intriguingly, all these classes of lipids statistically significant decreases throughout storage duration (**Table 1**). Most of the observed decreases account for sterols (e.g. desmosterol, gorgosterol), and in particular for vitamin D3-related metabolites (**Table 1**). This is relevant in the light of the well-established role for Vitamin D in modulating RBC survival (Alexander, 1977), also by influencing anti-oxidant potential and Ca²⁺ permeability (Holmes et al., 1983), a phenomenon which is strictly tied to erythrocyte-specific apoptosis, also known as eryptosis (Pompeo et al., 2010).

On the other hand, earliest studies on the likely long term effect of RBC storage on the lipidome suggested that cholesterol loss is limited in comparison to the loss of phospholipids and phosphoinositides (Greenwalt et al., 1990). Finally, our results about a generalized decrease in lipid contents of the major lipid classes in long stored RBCs also confirm and expand/complement recent evidences by Acker's group (Bicalho et al., 2013; Almizraq et al., 2013).

Conclusion

Despite decades of investigations, the field of lipidomics recently drained new lymph from the introduction of recent technical innovations. From TLC to gas chromatography and MS, consolidated lipidomics expertise in the field of RBC biology has paved the way for a deeper understanding of the functioning of this pivotal cell and, in parallel, to the accumulation of a wealth of knowledge that will be soon transferred to the clinical setting. Indeed, owing to their relative abundances and widespread biological activities, lipids are well suited to play the role of biological markers and will soon serve this purpose.

In this study, we presented an HPLC-microTOF-Q approach to investigate the RBC lipidome. We could exploit this analytical workflow to consolidate existing knowledge on the RBC lipid composition and individuate statistically significant fluctuations of lipids throughout storage duration of RBC concentrates under blood bank conditions. While this field of research still warrants future investigations, we could indicate ceramides, glycerophospholipids and sterols as key targets of RBC storage lesions to the lipidome, that will deserve further targeted investigations in the future.

Finally, in the light of minor differences with other reports available from the literature, we posited how compositional analyses of the RBC lipidome might end up yielding different results on the basis of the background of the blood donor (above all, the diet), which might translate into region-specific lipidomic alterations over storage progression of RBC concentrates. This is relevant in the light of the constant efforts pursued by transfusion services to improve the quality of blood-derived therapeutics (D'Alessandro et al., 2010 – **Chapter 1**), by shifting the focus of attention from the end-product (RBC concentrates) to their providers (the donors).

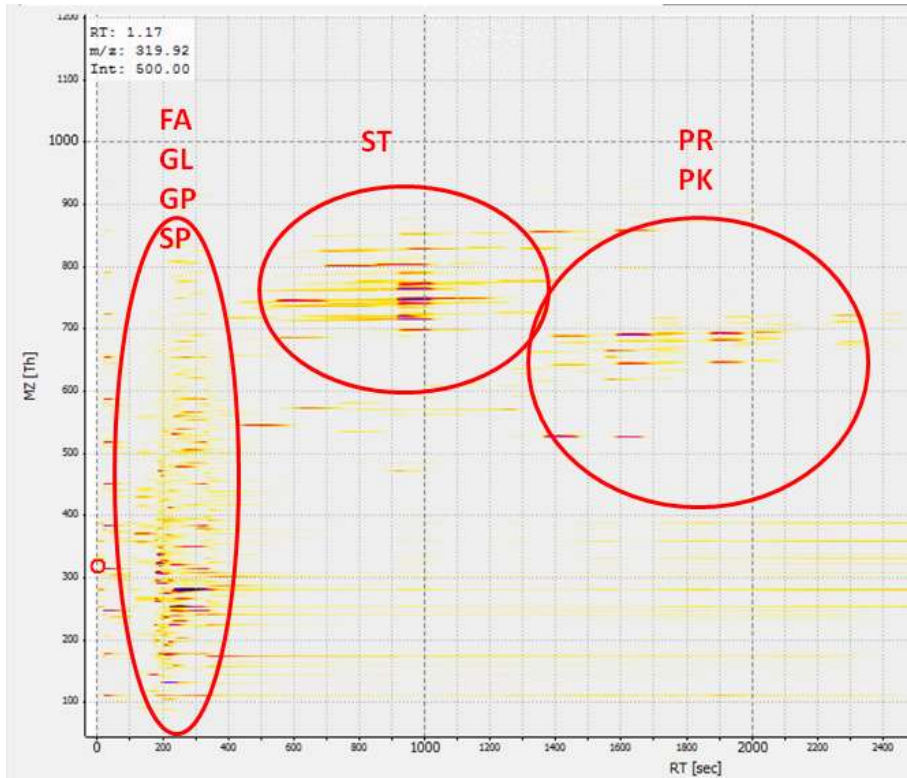


FIGURE 1 2D map overview of the lipid features identified in a single run compound. Class specific separations are indicated according to the established nomenclature (fatty acids – FA; glycerolipids – GL; glycerophospholipids – GP; sphingolipids – SP; sterols – ST; prenols – PR and polyketides – PK).

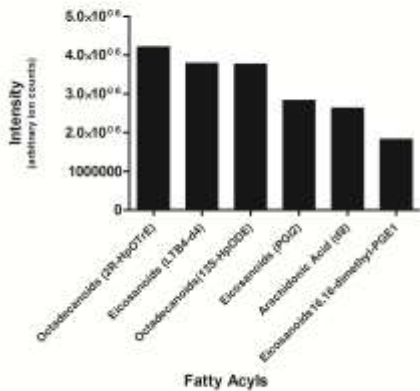
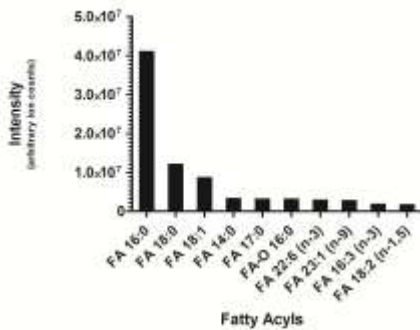


FIGURE 2 Fatty acid distribution obtained by exporting data from microQtof as mzXML files and processed through MAVEN by interrogating LIPID MAPS database (Sud et al., 2007).

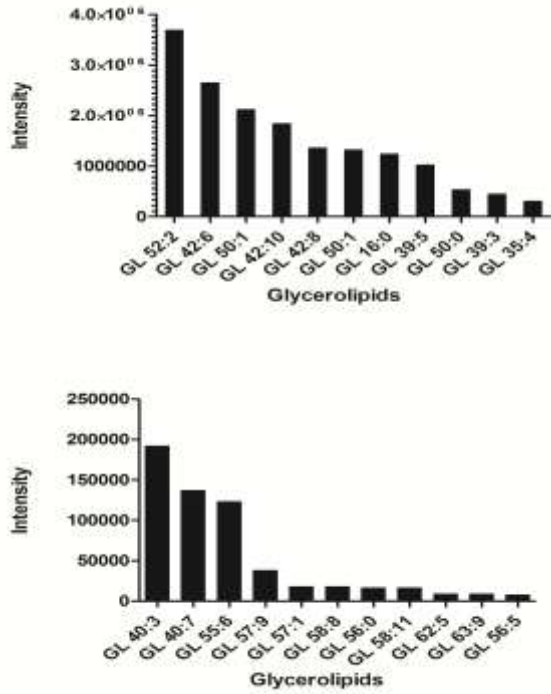


FIGURE 3 Glycerolipids distribution obtained by exporting data from microQtof as mzXML files and processed through MAVEN by interrogating LIPID MAPS database (Sud et al., 2007).

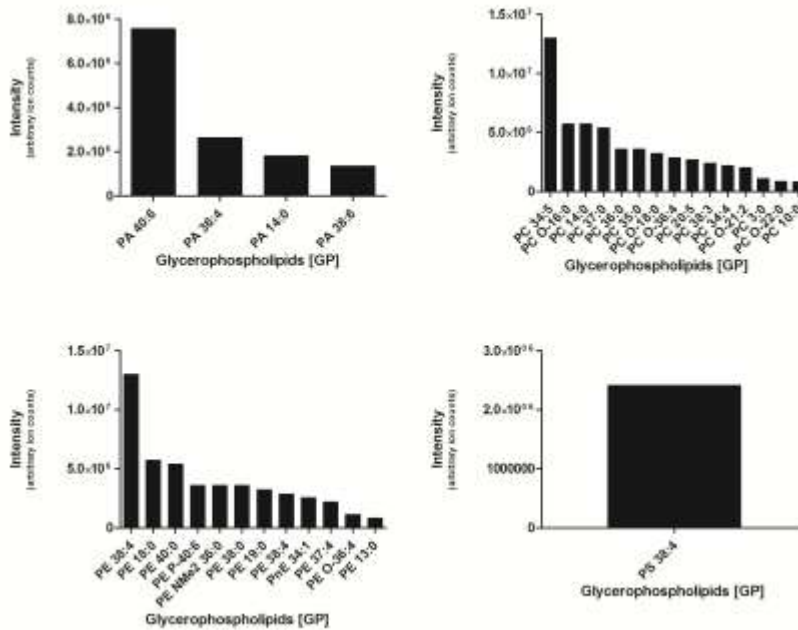


FIGURE 4 Glycerophospholipids distribution obtained by exporting data from microQtof as mzXML files and processed through MAVEN by interrogating LIPID MAPS database (Sud et al., 2007).

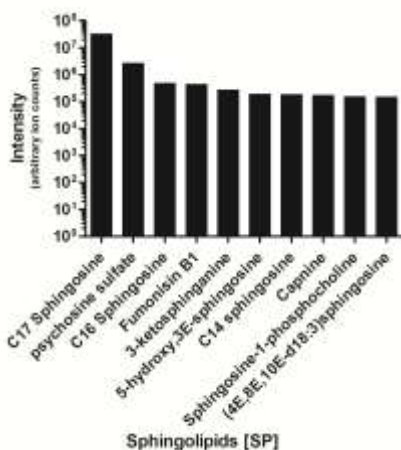


FIGURE 5 Sphingolipids distribution obtained by exporting data from microQtof as mzXML files and processed through MAVEN by interrogating LIPID MAPS database (Sud et al., 2007).

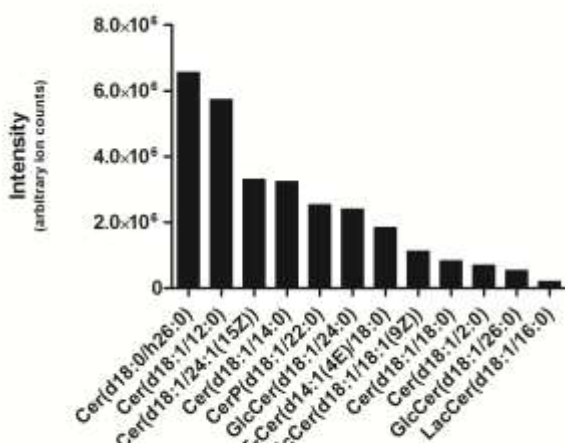


FIGURE 6 Ceramides distribution obtained by exporting data from microQtof as mzXML files and processed through MAVEN by interrogating LIPID MAPS database (Sud et al., 2007).

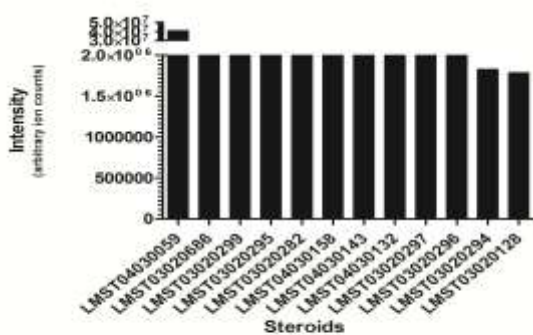
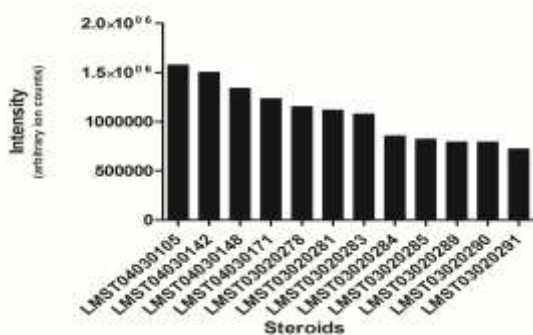


FIGURE 7 Steroids distribution obtained by exporting data from microQtof as mzXML files and processed through MAVEN by interrogating LIPID MAPS database (Sud et al., 2007).



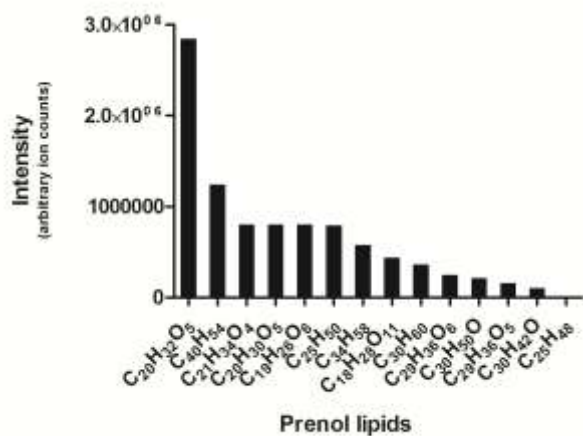


FIGURE 8 Prenols distribution obtained by exporting data from microQtof as mzXML files and processed through MAVEN by interrogating LIPID MAPS database (Sud et al., 2007).

References

- Adamson JW. New blood, old blood, or no blood? *N Engl J Med*. 2008;358(12):1295-6.
- Alex Brown H. Lipidomics: when apocrypha becomes canonical. *Curr Opin Chem Biol*. 2012;16(1-2):221-6.
- Alexander M. Contribution of the study of anemia in vitamin D deficiency rickets. I. Study of red blood cell survival. *Biomedicine*. 1977 Apr;27(3):108-10.
- Almizraq R, Tchir JD, Holovati JL, Acker JP. Storage of red blood cells affects membrane composition, microvesiculation, and *in vitro* quality. *Transfusion*. 2013. doi: 10.1111/trf.12080.
- Antonelou MH, Kriebardis AG, Stamoulis KE, Economou-Petersen E, Margaritis LH, Papassideri IS. Red blood cell aging markers during storage in citrate-phosphate-dextrose-saline-adenine-glucose-mannitol. *Transfusion*. 2010;50(2):376-89.
- Antonelou, M., Kriebardis, A., Stamoulis, K., Trougakos, I.P., Papassideri, I.S. (2010b) Secretory apolipoprotein J/Clusterin is an integral component of human erythrocytes and a novel biomarker of vesiculation and senescence *in vivo* and in stored red cells. XXXIst International Congress of the International Society of Blood Transfusion (ISBT), Berlin, Germany. *Vox Sanguinis*, 99, (s1):213.
- Artz CP, Howard JM, Davis JH, Scott R Jr: Plastic bags for intravenous infusions: observations in Korea with saline, dextran and blood; in Howard JM (eds): *Battle Casualties in Korea: Studies of the Surgical Research Team*, vol 2. Army Medical Service Graduate School, Washington, DC, 1954:219–224.
- Barnard RJ, Morgan A, Burgoyne RD. Domains of alpha-SNAP required for the stimulation of exocytosis and for N-ethylmaleimide-sensitive fusion protein (NSF) binding and activation. *Mol Biol Cell*. 1996;7(5):693-701.
- Beermann C, Mobius M, Winterling N et al. sn-position determination of phospholipid-linked fatty acids derived from erythrocytes by liquid chromatography electrospray ionization ion-trap mass spectrometry. *Lipids* 2005 February;40(2):211-8.
- Belosludtsev KN, Trudovishnikov AS, Belosludtseva NV, Agafonov AV, Mironova GD. Palmitic acid induces the opening of a Ca²⁺-dependent pore in the plasma membrane of red blood cells: the possible role of the pore in erythrocyte lysis. *J Membr Biol*. 2010 Sep;237(1):13-9.
- Bennett-Guerrero E, Stafford-Smith M, Waweru PM, Bredehoeft SJ, Campbell ML, Haley NR, et al. A prospective, double-blind, randomized clinical feasibility trial of controlling the storage age of red blood cells for transfusion in cardiac surgical patients. *Transfusion*. 2009;49(7):1375-83.
- Bennett-Guerrero E, Veldman TH, Doctor A, Telen MJ, Ortel TL, Reid TS, et al. Evolution of adverse changes in stored RBCs. *Proc Natl Acad Sci U S A*. 2007;104(43):17063-8.
- Berezina TL, Zaets SB, Morgan C, Spillert CR, Kamiyama M, Spolarics Z, et al. Influence of storage on red blood cell rheological properties. *J Surg Res*. 2002;102(1):6-12.
- Bessis M. Red cell shapes. An illustrated classification and its rationale. *Nouv Rev Fr Hematol*. 1972;12(6):721-45.
- Beutler E, Teeple L. Mannose metabolism in the human erythrocyte. *J Clin Invest*. 1969;48(3):461-6.
- Bicalho B, Holovati JL, Acker JP. Phospholipidomics reveals differences in glycerophosphoserine profiles of hypothermically stored red blood cells and microvesicles. *Biochim Biophys Acta*. 2013 Feb;1828(2):317-26.

- Biroccio A, Urbani A, Massoud R, et al.: A quantitative method for the analysis of glycated and glutathionylated hemoglobin by matrix-assisted laser desorption ionization-time of flight mass spectrometry. *Anal Biochem* 2005;336(2):279-288.
- Blasi B, D'Alessandro A, Ramundo N, et al.: Red blood cell storage and cell morphology. *Transfus Med* 2012;22(2):90-96.
- Bosman GJ, Lasonder E, Groenen-Döpp YA, Willekens FL, Werre JM, Novotný VM. Comparative proteomics of erythrocyte aging in vivo and in vitro. *J Proteomics*. 2010;73(3):396-402.
- Bosman GJ, Lasonder E, Luten M, Roerdinkholder-Stoelwinder B, Novotný VM, Bos H, De Grip WJ. The proteome of red cell membranes and vesicles during storage in blood bank conditions. *Transfusion*. 2008 May;48(5):827-35.
- Burger P, Korsten H, De Korte D, Rombout E, Van Bruggen R, Verhoeven AJ. An improved red blood cell additive solution maintains 2,3-diphosphoglycerate and adenosine triphosphate levels by an enhancing effect on phosphofructokinase activity during cold storage. *Transfusion*. 2010;50(11):2386-92.
- Burr MJ. The relationship between pH and aerobic glycolysis in human and canine erythrocytes. *Comp Biochem Physiol B*. 1972;41(4):687-94.
- Bursell SE, King GL: The potential use of glutathionyl hemoglobin as a clinical marker of oxidative stress. *Clin Chem* 2000; 46:145–146.
- Candiano G, Bruschi M, Musante L, Santucci L, Ghiggeri GM, Carnemolla B, Orecchia P, Zardi L, Righetti PG. Blue silver: a very sensitive colloidal Coomassie G-250 staining for proteome analysis. *Electrophoresis*. 2004;25(9):1327-33.
- Carrell RW, Winterbourn CC, Rachmilewitz EA. Activated oxygen and hemolysis. *Br J Haematol* 1975; 30: 259-264.
- Chaudhary R, Katharia R. Oxidative injury as contributory factor for red cells storage lesion during twenty eight days of storage. *Blood Transfus*. 2012 Jan;10(1):59-62.
- Clasquin MF, Melamud E, Rabinowitz JD. LC-MS Data Processing with MAVEN: A Metabolomic Analysis and Visualization Engine. 2012. *Current Protocols in Bioinformatics*. 37:14.11.1-14.11.23.
- Council of Europe 2011. European Directorate for the Quality of Medicines & HealthCare. Guide to the Preparation, Use and Quality Assurance of Blood Components. Recommendation No. R (95) 15. 16th Edition.
- Dabadie H, Motta C, Peuchant E, LeRuyet P, Mendy F. Variations in daily intakes of myristic and α -linolenic acids in sn-2 position modify lipid profile and red blood cell membrane fluidity. *Brit J Nutr* 2006; 96:283-289.
- D'Alessandro A, D'Amici GM, Vaglio S, Zolla L. Time-course investigation of SAGM-stored erythrocyte concentrates: from metabolism to proteomics. *Hematologica* 2012;97(1): 107–115.
- D'Alessandro A, Gevi F, Zolla L. A robust high resolution reversed-phase HPLC strategy to investigate various metabolic species in different biological models. *Mol Biosyst*. 2011;7(4):1024-32.
- D'Alessandro A, Liunbruno G, Grazzini G, et al.: Red blood cell storage: the story so far. *Blood Transfus* 2010;8(2):82-88.

- D'Alessandro A, Righetti PG, Zolla L. The red blood cell proteome and interactome: an update. *J Proteome Res.* 2010 Jan;9(1):144-63.
- D'Alessandro A, Zolla L. Metabolomics and cancer drug discovery: let the cells do the talking. *Drug Discov Today.* 2012; 7(1-2):3-9.
- D'Alessandro A, Liumbruno G, Grazzini G, Zolla L. Red blood cell storage: the story so far. *Blood Transfus* 2010; 8: 82-88.
- D'Amici GM, Rinalducci S, Zolla L. Proteomic analysis of RBC membrane protein degradation during blood storage. *J Proteome Res.* 2007;6(8):3242-55.
- Darghouth D, Koehl B, Heilier JF, Madalinski G, Bovee P, Bosman G, et al. Alterations of red blood cell metabolome in overhydrated hereditary stomatocytosis. *Haematologica.* 2011a;96(12):1861-5.
- Darghouth D, Koehl B, Junot C, Roméo PH. Metabolomic analysis of normal and sickle cell erythrocytes. *Transfus Clin Biol.* 2010;17(3):148-50.
- Darghouth D, Koehl B, Madalinski G, Heilier JF, Bovee P, Xu Y, et al. Pathophysiology of sickle cell disease is mirrored by the red blood cell metabolome. *Blood.* 2011b;117(6):e57-66.
- Dinkla S, Wessels K, Verdurmen WP, Tomelleri C, Cluitmans JC, Franssen J, Fuchs B, Schiller J, Joosten I, Brock R, Bosman GJ. Functional consequences of sphingomyelinase-induced changes in erythrocyte membrane structure. *Cell Death Dis.* 2012 Oct 18;3:e410.
- Dodge JT, Phillips GB. Composition of phospholipids and of phospholipid fatty acids and aldehydes in human red cells. *J Lipid Res* 1967;8(6):667-75.
- Donabedian, R. K., and A. Karmen. 1967. Fatty acid transport and incorporation into human erythrocytes in vitro. *J. Clin. Invest.* 46: 1017.
- Dougherty RM, Galli C, Ferro-Luzzi A, Iacono JM. Lipid and phospholipid fatty acid composition of plasma, red blood cells, and platelets and how they are affected by dietary lipids: a study of normal subjects from Italy, Finland, and the USA. *Am J Clin Nutr* 1987;45(2):443-55.
- Dumont LJ, Yoshida T, AuBuchon JP. Anaerobic storage of red blood cells in a novel additive solution improves in vivo recovery. *Transfusion.* 2009;49(3):458-64.
- Ebaugh FG Jr, Ross JF: The radioactive sodium chromate method for erythrocyte survival. *Vox Sang* 1985; 49: 304–307.
- European Directorate for the Quality of Medicines & HealthCare. Guide to the Preparation, Use and Quality Assurance of Blood Components. Recommendation No. R (95) 15. 16th Edition. Council of Europe 2011.
- Fahy E, Subramaniam S, Brown HA et al. A comprehensive classification system for lipids. *J Lipid Res* 2005 May;46(5):839-61.
- Farquhar JW, Ahrens EH Jr. Effects of dietary fats on human erythrocyte fatty acid patterns. *J Clin Invest.* 1963;42:675-85.
- Gallagher PG, Forget BG. Hematologically important mutations: spectrin and ankyrin variants in hereditary spherocytosis. *Blood Cells Mol. Dis.* 1998; 24 (4): 539–43.

- Gehring H, Christen P. A diagonal procedure for isolating sulfhydryl peptides alkylated with N-ethylmaleimide. *Anal Biochem.* 1980;107(2):358-61.
- Gevi F, D'Alessandro A, Rinalducci S, et al.: Alterations of red blood cell metabolome during cold liquid storage of erythrocyte concentrates in CPD-SAGM. *J Proteomics* 2012; 76:168-180.
- Goodman SR, Kurdia A, Ammann L, Kakhniashvili D, Daescu O. The human red blood cell proteome and interactome. *Exp Biol Med (Maywood)*. 2007 Dec;232(11):1391-408.
- Grüllich C, Duvoisin RM, Wiedmann M, van Leyen K. Inhibition of 15-lipoxygenase leads to delayed organelle degradation in the reticulocyte. *FEBS Lett.* 2001 Jan 26;489(1):51-4.
- Han X, Gross RW. Electrospray ionization mass spectroscopic analysis of human erythrocyte plasma membrane phospholipids. *Proc Natl Acad Sci U S A* 1994;91(22):10635-9.
- Hanahan DJ, Watts RM, Papajohn D. Some chemical characteristics of the lipids of human and bovine erythrocytes and plasma. *J Lipid Res.* 1960;1:421-32.
- Hara N, Yamada K, Shibata T, Osago H, Hashimoto T, Tsuchiya M. Elevation of cellular NAD levels by nicotinic acid and involvement of nicotinic acid phosphoribosyltransferase in human cells. *J Biol Chem.* 2007;282(34):24574-82.
- Haradin AR, Weed RI, Reed CF. Changes in physical properties of stored erythrocytes: Relationship to survival in vivo. *Transfusion* 1969; 9:229 – 237.
- Harboe, M. (1959) A method for determination of hemoglobin in plasma by near-ultraviolet spectrophotometry. *Scand J Clin Lab Invest*, 11, 66-70.
- Hess JR, Grazzini G. Blood proteomics and transfusion safety. *J Proteomics* 2010; 73: 365-367.
- Hess JR, Hill HR, Oliver CK, Lippert LE, Greenwalt TJ. Alkaline CPD and the preservation of RBC 2,3-DPG. *Transfusion.* 2002;42(6):747-52.
- Hess JR, Hill HR, Oliver CK, Lippert LE, Rugg N, Joines AD, Gormas JF, Pratt PG, Silverstein EB, Greenwalt TJ. Twelve-week RBC storage. *Transfusion* 2003; 43: 867-872.
- Hess JR, Lippert LE, Derse-Anthony CP, Hill HR, Oliver CK, Rugg N, et al. The effects of phosphate, pH, and AS volume on RBCs stored in saline-adenine-glucose-mannitol solutions. *Transfusion.* 2000;40(8):1000-6.
- Hess JR, Rugg N, Joines AD, Gormas JF, Pratt PG, Silberstein EB, Greenwalt TJ. Buffering and dilution in red blood cell storage. *Transfusion.* 2006;46(1):50-4.
- Hess JR. An update on solutions for red cell storage. *Vox Sang* 2006; 91, 13-19.
- Hess JR. Conventional blood banking and blood component storage regulation: opportunities for improvement. *Blood Transfus.* 2010; 8(3):9-15.
- Hess JR. Improving the predictive value of red blood cell storage trials: lessons from the Biomedical Excellence for Safer Transfusion (BEST) Collaborative Trial 41. *Transfusion.* 2011;51(1):34S-37S. doi:10.1111/j.1537-2995.2010.02961.x.
- Hess JR. Red cell changes during storage. *Transfus Apher Sci.* 2010;43(1):51-9.
- Hess JR. Red cell storage: when is better not good enough? *Blood Transfus.* 2009;7(3):172-3.

- Hogman CF, Hedlund K, Sahlestrom Y: Red cell preservation in protein-poor media. III. Protection against *in vitro* hemolysis. *Vox Sang* 1981; 41:274–281.
- Hogman CF, Hedlund K, Zetterstrom H: Clinical usefulness of red cells preserved in protein-poor media. *N Engl J Med* 1978; 299:1377–1382.
- Högman CF, Löf H, Meryman HT. Storage of red blood cells with improved maintenance of 2,3-bisphosphoglycerate. *Transfusion*. 2006;46(9):1543-52.
- Högman CF, Meryman HT. Storage parameters affecting red blood cell survival and function after transfusion. *Transfus Med Rev*. 1999;13(4):275-96.
- Holmes RP, Mahfouz M, Travis BD, Yoss NL, Keenan MJ. The effect of membrane lipid composition on the permeability of membranes to Ca²⁺. *Ann N Y Acad Sci*. 1983;414:44-56.
- ICSH: International Council for Standardization in Haematology (Expert Panel on Blood Rheology): ICSH recommendations for measurement of erythrocyte sedimentation rate. *J Clin Pathol*, 1993; 46, 198-208.
- Ionescu-Zanetti C, Wang LP, Di Carlo D, Hung P, Di Blas A, Hughey R, Lee LP. Alkaline hemolysis fragility is dependent on cell shape: results from a morphology tracker. *Cytometry A*. 2005;65(2):116-23.
- Ito T, Yamakuchi M, Lowenstein CJ. Thioredoxin Increases Exocytosis by Denitrosylating N-Ethylmaleimide-sensitive Factor. *J Biol Chem*. 2011;286(13):11179-84.
- Ivanova PT, Milne SB, Brown HA. Identification of atypical ether-linked glycerophospholipid species in macrophages by mass spectrometry. *J. Lipid Res*. 2010; 51:1581-1590.
- Jakobik V, Burus I, Decsi T. Fatty acid composition of erythrocyte membrane lipids in healthy subjects from birth to young adulthood. *Eur J Pediatr*. 2009 Feb;168(2):141-7.
- Jarvis HG, Gore DM, Briggs C, Chetty MC, Stewart GW: Cold storage of ‘cryohydrocytosis’ red cells: the osmotic susceptibility of the cold-stored erythrocyte. *Br J Haematol* 2003; 122:859–868.
- Jurado RL. Why shouldn't we determine the erythrocyte sedimentation rate? *Clin Infect Dis* 2001; 33: 548-549.
- Kabagambe EK, Tsai MY, Hopkins PN et al. Erythrocyte Fatty Acid Composition and the Metabolic Syndrome: A National Heart, Lung, and Blood Institute GOLDN Study. *Clin Chem* 2008 January;54(1):154-62.
- Kanias T, Acker JP. Biopreservation of red blood cells--the struggle with hemoglobin oxidation. *FEBS J*. 2010; 277(2):343-56.
- Karon BS, Hoyer JD, Stubbs JR, Thomas DD. Changes in Band 3 oligomeric state precede cell membrane phospholipid loss during blood bank storage of red blood cells. *Transfusion*. 2009 Jul;49(7):1435-42.
- Kates, M., A. C. Allison, and A. T. James. 1961. Phosphatides of human blood cells and their role in spherocytosis. *Biochim. Biophys. Acta*. 48: 571.
- Koch CG, Li L, Sessler DI, Figueroa P, Hoeltge GA, Mihaljevic T, Blackstone EH. Duration of red-cell storage and complications after cardiac surgery. *N Engl J Med*. 2008;358(12):1229-39.
- Kor DJ, Van Buskirk CM, Gajic O. Red blood cell storage lesion. *Bosn J Basic Med Sci* 2009; 9: 21-27.
- Korones D, Pearson HA. Normal erythrocyte osmotic fragility in hereditary spherocytosis. *J Pediatr*. 1989;114(2):264-6.

- Kraus A, Roth HP, Kirchgessner M. Supplementation with vitamin C, vitamin E or beta-carotene influences osmotic fragility and oxidative damage of erythrocytes of zinc-deficient rats. *J Nutr* 1997; 127: 1290-1296.
- Kreuger A, Akerblom O. Adenine consumption in stored citrate-phosphate-dextrose-adenine blood. *Vox Sang*. 1980;38(3):156-60.
- Kriebardis AG, Antonelou MH, Stamoulis KE, Economou-Petersen E, Margaritis LH, Papassideri IS. Progressive oxidation of cytoskeletal proteins and accumulation of denatured hemoglobin in stored red cells. *J Cell Mol Med*. 2007;11(1):148-55.
- Kuchel PW, Philp DJ. Isotopomer subspaces as indicators of metabolic-pathway structure. *J Theor Biol*. 2008;252(3):391-401.
- Kumar, S. (2002) An analogy for explaining erythrocyte fragility: concepts made easy. *Adv Physiol Educ*, 26, 134-135.
- LaCelle PL, Kirkpatrick FH, Udkow MP, Arkin B. Membrane fragmentation and Ca¹¹-membrane interaction: potential mechanism of shape change in the senescent red cell. *Nouv Rev Fr Hemat*. 1972; 12:789-798.
- Lacroix J, Hébert P, Fergusson D, Tinmouth A, Blajchman MA, Callum J, Cook D, Marshall JC, McIntyre L, Turgeon AF; ABLE study group. The Age of Blood Evaluation (ABLE) randomized controlled trial: study design. *Transfus Med Rev*. 2011;25(3):197-205.
- Leidl K, Liebisch G, Richter D, Schmitz G. Mass spectrometric analysis of lipid species of human circulating blood cells. *Biochim Biophys Acta*. 2008 Oct;1781(10):655-64.
- Lelubre C, Piagnerelli M, Vincent JL. Association between duration of storage of transfused red blood cells and morbidity and mortality in adult patients: myth or reality? *Transfusion*. 2009;49(7):1384-94.
- Levine RL, Williams JA, Stadtman ER, Shacter E. Carbonyl assays for determination of oxidatively modified proteins. *Methods Enzymol*. 1994;233:346-57.
- Lewis IA, Campanella ME, Markley JL, Low PS. Role of band 3 in regulating metabolic flux of red blood cells. *Proc Natl Acad Sci U S A*. 2009;106(44):18515-20.
- Lion N, Crettaz D, Rubin O, Tissot JD. Stored red blood cells: a changing universe waiting for its map(s). *J Proteomics*. 2010;73(3):374-85.
- Liumbruno G, D'Alessandro A, Grazzini G, Zolla L. Blood-related proteomics. *J Proteomics*. 2010 Jan 3;73(3):483-507.
- Liumbruno GM, Aubuchon JP. Old blood, new blood or better stored blood? *Blood Transfus*. 2010;8(4):217-9.
- Loutit JF, Mollison PL: Advantages of a disodium-citrate-glucose mixture as a blood preservative. *Br Med J* 1943; 2:744-745.
- Low FM, Hampton MB, Peskin AV, Winterbourn CC. Peroxiredoxin 2 functions as a noncatalytic scavenger of low-level hydrogen peroxide in the erythrocyte. *Blood*. 2007;109(6):2611-7.
- Low PS, Rathinavelu P, Harrison ML. Regulation of glycolysis via reversible enzyme binding to the membrane protein, band 3. *J Biol Chem* 1993; 268:14627-31.
- Messana I, Ferroni L, Misiti F, Girelli G, Pupella S, Castagnola M, Zappacosta B, Giardina B. Blood bank conditions and RBCs: the progressive loss of metabolic modulation. *Transfusion*. 2000;40(3):353-60.

- Messana I, Misiti F, el-Sherbini S, Giardina B, Castagnola M. Quantitative determination of the main glucose metabolic fluxes in human erythrocytes by ^{13}C - and ^1H -MR spectroscopy. *J Biochem Biophys Methods*. 1999;39(1-2):63-84.
- Meyer EK, Dumont DF, Baker S, Dumont LJ. Rejuvenation capacity of red blood cells in additive solutions over long-term storage. *Transfusion*. 2011;51(7):1574-9.
- Mikirova N, Riordan HD, Jackson JA, Wong K, Miranda-Massari JR, Gonzalez MJ. Erythrocyte membrane fatty acid composition in cancer patients. *P R Health Sci J*. 2004 Jun;23(2):107-13.
- Montes LR, López DJ, Sot J, Bagatolli LA, Stonehouse MJ, Vasil ML, Wu BX, Hannun YA, Goñi FM, Alonso A. Ceramide-enriched membrane domains in red blood cells and the mechanism of sphingomyelinase-induced hot-cold hemolysis. *Biochemistry*. 2008 Oct 28;47(43):11222-30.
- Moore GL. Additive solutions for better blood preservation. *CRC Crit Rev Clin Lab Sci* 1987; 25:211–228
- Morera D, Mackenzie SA. Is there a direct role for erythrocytes in the immune response? *Vet Res* 2011; 42:89.
- Muda P, Kampus P, Zilmer M, Zilmer K, Kairane C, Ristimäe T, Fischer K, et al. Homocysteine and red blood cell glutathione as indices for middle-aged untreated essential hypertension patients. *J Hypertens*. 2003;21(12):2329-33.
- Mulder E, de Gier J, Van Deenen LLM. Selective incorporation of fatty acids into phospholipids of mature red cells. *Biochim. Biophys. Acta*. 1962; 70: 94.
- Mulder E, Van Den Berg JWO, Van Deenen LLM. Metabolism of red cell lipids II. Conversions of lysophosphoglycerides. *Biochim. Biophys. Acta*. 1965; 106: 118.
- Nakayama Y, Kinoshita A, Tomita M. Dynamic simulation of red blood cell metabolism and its application to the analysis of a pathological condition. *Theor Biol Med Model*. 2005;2:18.
- Neidlinger NA, Larkin SK, Bhagat A, Victorino GP, Kuypers FA. Hydrolysis of phosphatidylserine-exposing red blood cells by secretory phospholipase A2 generates lysophosphatidic acid and results in vascular dysfunction. *J Biol Chem*. 2006 Jan 13;281(2):775-81.
- Nishino T, Yachie-Kinoshita A, Hirayama A, Soga T, Suematsu M, Tomita M. In silico modeling and metabolome analysis of long-stored erythrocytes to improve blood storage methods. *J Biotechnol*. 2009;144(3):212-23.
- Novgorodtseva TP, Karaman YK, Zhukova NV, Lobanova EG, Antonyuk MV, Kantur TA. Composition of fatty acids in plasma and erythrocytes and eicosanoids level in patients with metabolic syndrome. *Lipids Health Dis*. 2011 May 19;10:82.
- Oliveira, M. M., and M. Vaughn. 1964. Incorporation of fatty acids into phospholipids of erythrocyte membranes. *J. Lipid Res*. 5: 156.
- Olivieri E, Herbert B, Righetti PG. The effect of protease inhibitors on the two-dimensional electrophoresis pattern of red blood cell membranes. *Electrophoresis*. 2001;22(3):560-5.
- Owen JS, Bruckdorfer KR, Day RC, McIntyre N. Decreased erythrocyte membrane fluidity and altered lipid composition in human liver disease. *J Lipid Res* 1982;23(1):124-32.

- Pala V, Krogh V, Muti P, Chajès V, Riboli E, Micheli A, Saadatian M, Sieri S, Berrino F. Erythrocyte membrane fatty acids and subsequent breast cancer: a prospective Italian study. *J Natl Cancer Inst.* 2001 Jul 18;93(14):1088-95.
- Palek J, Stewart G, Lionetti FJ. The dependence of shape of human erythrocyte ghosts on calcium, magnesium and adenosine triphosphate. *Blood* 1974; 44:583- 597.
- Percy AK, Schmell E, Earles BJ, Lennarz WJ. Phospholipid biosynthesis in the membranes of immature and mature red blood cells. *Biochemistry* 1973;12(13):2456–61.
- Perrotta S, Gallagher PG, Mohandas N. Hereditary spherocytosis. *Lancet* 2008; 372 (9647): 1411–26.
- Philips GB, Roome NS. Phospholipids of human red blood cells. *Proc Soc Exp Biol Med.* 1959 Mar;100(3):489-92.
- Pianese P, Salvia G, Campanozzi A, D'Apolito O, Dello Russo A, Pettoello-Mantovani M, Corso G. Sterol profiling in red blood cell membranes and plasma of newborns receiving total parenteral nutrition. *J Pediatr Gastroenterol Nutr.* 2008 Nov;47(5):645-51.
- Pittman, J. G., and Martin, D. B. 1966. Fatty acid biosynthesis in human erythrocytes: Evidence in mature erythrocytes for an incomplete long chain fatty acid synthesizing system. *J. Clin. Invest.* 45: 165.
- Pompeo G, Girasole M, Cricenti A, Boumis G, Bellelli A, Amiconi S. Erythrocyte death *in vitro* induced by starvation in the absence of Ca(2+). *Biochim Biophys Acta.* 2010 Jun;1798(6):1047-55.
- Poppitt SD, Kilmartin P, Butler P, Keogh GF. Assessment of erythrocyte phospholipid fatty acid composition as a biomarker for dietary MUFA, PUFA or saturated fatty acid intake in a controlled cross-over intervention trial. *Lipids Health Dis.* 2005 Dec 5;4:30.
- Pribush, A., Hatskelzon, L., Kapelushnik, J., Meyerstein, N. (2003) Osmotic swelling and hole formation in membranes of thalassemic and spherocytic erythrocytes. *Blood Cells Mol Dis*, 31,43-47.
- Quehenberger O, Armando AM, Brown AH, Milne SB, Myers DS, Merrill AH, Bandyopadhyay S, Jones KN, Kelly S, Shaner RL, Sullards CM, Wang E, Murphy RC, Barkley RM, Leiker TJ, Raetz CR, Guan Z, Laird GM, Six DA, Russell DW, McDonald JG, Subramaniam S, Fahy E, Dennis EA. Lipidomics reveals a remarkable diversity of lipids in human plasma. *J Lipid Res.* 2010 Nov;51(11):3299-305.
- Rinalducci S, D'Amici GM, Blasi B, Vaglio S, Grazzini G, Zolla L. Peroxiredoxin-2 as a candidate biomarker to test oxidative stress levels of stored red blood cells under blood bank conditions. *Transfusion.* 2011;51(7):1439-49.
- Rioux V, Catheline D, Beauchamp E, Le Bloc'h J, Pédrone F, Legrand P. Substitution of dietary oleic acid for myristic acid increases the tissue storage of α -linolenic acid and the concentration of docosahexaenoic acid in the brain, red blood cells and plasma in the rat. *Animal.* 2008 Apr;2(4):636-44.
- Rise P, Eligini S, Ghezzi S et al. Fatty acid composition of plasma, blood cells and whole blood: relevance for the assessment of the fatty acid status in humans. *Prostaglandins Leukot Essent Fatty Acids* 2007 June;76(6):363-9.
- Robertson OH. Transfusion with preserved red blood cells. *Br Med J* 1918; 1:691–695.
- Rocha S, Vitorino RM, Lemos-Amado FM, Castro EB, Rocha-Pereira P, Barbot J, et al. Presence of cytosolic peroxiredoxin 2 in the erythrocyte membrane of patients with hereditary spherocytosis. *Blood Cells Mol Dis.* 2008;41(1):5-9.

- Romero PJ, Romero EA. The role of calcium metabolism in human red blood cell ageing: a proposal. *Blood Cells Mol Dis.* 1999;25(1):9-19.
- Romero PJ. The role of membrane-bound Ca in ghost permeability to Na and K. *J Membrane Biol* 1976; 29:329-343.
- Rouault C. Red cell oxygen delivery. Effect of 2,3-diphosphoglycerate. *Postgrad Med* 1973;53(3):201-3.
- Rous P, Turner JW: The preservation of living red blood cells in vitro. *J Exp Med* 1916; 23:219–237.
- Roux-Dalvai F, Gonzalez de Peredo A, Simó C, Guerrier L, Bouyssié D, Zanella A, et al. Extensive analysis of the cytoplasmic proteome of human erythrocytes using the peptide ligand library technology and advanced mass spectrometry. *Mol Cell Proteomics.* 2008;7(11):2254-69.
- Rubin O, Crettaz D, Tissot JD, Lion N. Microparticles in stored red blood cells: submicron clotting bombs? *Blood Transfus* 2010; 8: s31-38.
- Sadeeh C. The Erythrocyte Sedimentation Rate: Old and New Clinical Applications. http://www.mechatronics.nl/technics/esr/the_erythrocyte_sedimentation_rate_by_c_saadeh_md.pdf Accessed 14 November 2011.
- Saha S, Ramanathan R, Basu A, Banerjee D, Chakrabarti A. Elevated levels of redox regulators, membrane bound globin chains and cytoskeletal protein fragments in hereditary spherocytosis erythrocyte proteome. *Eur J Haematol.* 2011. doi: 10.1111/j.1600-0609.2011.01648.x.
- Schatzmann, HJ. ATP-dependent Ca²⁺-extrusion from human red cells. *Experientia* 1966; 22:364-365.
- Schuster S, Kenanov D. Adenine and adenosine salvage pathways in erythrocytes and the role of S-adenosylhomocysteine hydrolase. A theoretical study using elementary flux modes. *FEBS J.* 2005;272(20):5278-90.
- Shevchenko A, Wilm M, Vorm O, Mann M. Mass spectrometric sequencing of proteins silver-stained polyacrylamide gels. *Anal Chem.* 1996;68(5):850-8.
- Shields CE: Effect of adenine on stored erythrocytes evaluated by autologous and homologous transfusions. *Transfusion* 1969; 9:115–119.
- Shohet SB, Nathan DG, Karnovsky ML. Stages in the incorporation of fatty acids into red blood cells. *J Clin Invest.* 1968 May;47(5):1096-108.
- Simon ER, Chapman RG, Finch CA: Adenine in red cell preservation. *J Clin Invest* 1962; 41:351–359.
- Simons K, Ikonen E. Functional rafts in cell membranes. *Nature.* 1997;387(6633):569-72.
- Siskind LJ, Fluss S, Bui M, Colombini M. Sphingosine forms channels in membranes that differ greatly from those formed by ceramide. *J Bioenerg Biomembr.* 2005 Aug;37(4):227-36.
- Skeaff CM, Hodson L, McKenzie JE. Dietary-induced changes in fatty acid composition of human plasma, platelet, and erythrocyte lipids follow a similar time course. *J Nutr* 2006 March;136(3):565-9.
- Skipski, V. P., R. F. Peterson, and M. Barclay. 1964. Quantitative analysis of phospholipids by thin layer chromatography. *Biochem. J.* 90: 341.
- Smith CA, O'Maille G, Want EJ, Qin C, Trauger SA, Brandon TR, Custodio DE, et al. METLIN: a metabolite mass spectral database. *Ther Drug Monit.* 2005;27(6):747-51.

- Smith EL, Schuchman EH. The unexpected role of acid sphingomyelinase in cell death and the pathophysiology of common diseases. *FASEB J*. 2008 Oct;22(10):3419-31.
- Smith PK, Krohn RI, Hermanson GT, Mallia AK, Gartner FH, Provenzano MD, Fujimoto EK, Goeke NM, Olson BJ, Klenk DC. Measurement of protein using bicinchoninic acid. *Anal Biochem*. 1985;150(1):76-85.
- Smith WL, Murphy RC. The eicosanoids: cyclooxygenase, lipoxygenase, and epoxygenase pathways. Chapter 13 In *Biochemistry of lipids, lipoproteins and membranes* (4th Edition) 2002; Vance DE and Vance JE Eds. Elsevier.
- Spencer DH, Grossman BJ, Scott MG: Red Cell Transfusion Decreases Hemoglobin A1c in Patients with Diabetes. *Clin Chem* 2011; 57(2):344-346.
- Steiner ME, Assmann SF, Levy JH, Marshall J, Pulkrabek S, Sloan SR, Triulzi D, Stowell CP. Addressing the question of the effect of RBC storage on clinical outcomes: the Red Cell Storage Duration Study (RECESS) (Section 7). *Transfus Apher Sci*. 2010;43(1):107-16.
- Stevens VJ, Vlassara H, Abati A, et al.: Nonenzymatic glycosylation of hemoglobin, *J Biol Chem* 1977; 252 2998–3002.
- Suckau D, Resemann A, Schuerenberg M, Hufnagel P, Franzen J, Holle A. A novel MALDI LIFT-TOF/TOF mass spectrometer for proteomics. *Anal Bioanal Chem* 2003;376:952–65.
- Sud M, Fahy E, Cotter D, Brown A, Dennis EA, Glass CK, Merrill AH Jr, Murphy RC, Raetz CR, Russell DW, Subramaniam S. LMSD: LIPID MAPS structure database. *Nucleic Acids Res*. 2007 Jan;35(Database issue):D527-32.
- Szelényi JG, Földi J, Hollàn SR: Enhanced nonenzymatic glycosylation of blood proteins in stored blood. *Transfusion* 1983;23:11–14.
- Tani M, Ito M, Igarashi Y. Ceramide/sphingosine/sphingosine 1-phosphate metabolism on the cell surface and in the extracellular space. *Cell Signal*. 2007 Feb;19(2):229-37.
- Tautenhahn R, Patti GJ, Kalisiak E, Miyamoto T, Schmidt M, Lo FY, et al. MetaXCMS: second-order analysis of untargeted metabolomics data. *Anal Chem*. 2011;83(3):696-700.
- Tautenhahn R, Patti GJ, Rinehart D, Siuzdak G. XCMS Online: a web-based platform to process untargeted metabolomic data. *Anal Chem*. 2012;84(11):5035-9.
- Untucht-Grau R, Schirmer RH, Schirmer I, Krauth-Siegel RL. Glutathione reductase from human erythrocytes: amino-acid sequence of the structurally known FAD-binding domain. *Eur J Biochem* 1981;120(2):407
- Valeri CR, Hirsch NM. Restoration in vivo of erythrocyte adenosine triphosphate, 2,3-diphosphoglycerate, potassium ion, and sodium ion concentrations following the transfusion of acid-citrate-dextrose-stored human red blood cells. *J Lab Clin Med*. 1969;73(5):722-33.
- Valtis DJ, Kennedy AC. Defective gas-transport function of stored red blood cells. *Lancet* 1954;I:119-25.
- Vamvakas EC. Meta-analysis of clinical studies of the purported deleterious effects of "old" (versus "fresh") red blood cells: are we at equipoise? *Transfusion*. 2010;50(3):600-10.
- Van Gastel, C., D. Van Den Berg, J. de Gier, and L. L. M. Van Deenen. 1965. Some lipid characteristics of normal red blood cells of different age. *Brit. J. Haematol*. 11: 193.

- Wallas CH. Sodium and potassium changes in blood bank stored human erythrocytes. *Transfusion*. 1979;19(2):210-5.
- Ways P, Hanahan DJ. Characterization and quantification of red cell lipids in normal man. *J Lipid Res*. 1964;5(3):318-28.
- Weinblatt ME, Kochen JA, Scimeca PG. Chronically transfused patients with increased hemoglobin Alc secondary to donor blood. *Ann Clin Lab Sci* 1986;16:34 –37.
- Whittam R. The high permeability of human red cells to adenine and hypoxanthine and their ribosides. *J Physiol*. 1960;154:614-23.
- Wiley JS, McCulloch KE, Bowden DS. Increased calcium permeability of cold-stored erythrocytes. *Blood*. 1982;60(1):92-8.
- Xu R, Sun W, Jin J, Obeid LM, Mao C. Role of alkaline ceramidases in the generation of sphingosine and its phosphate in erythrocytes. *FASEB J*. 2010 Jul;24(7):2507-15.
- Yoshida T, AuBuchon JP, Dumont LJ, Gorham JD, Gifford SC, Foster KY, Bitensky MW. The effects of additive solution pH and metabolic rejuvenation on anaerobic storage of red cells. *Transfusion*. 2008;48(10):2096-105.
- Yoshida T, AuBuchon JP, Tryzelaar L, Foster KY, Bitensky MW. Extended storage of red blood cells under anaerobic conditions. *Vox Sang*. 2007 Jan;92(1):22-31.
- Yoshida T, Shevkopyas SS. Anaerobic storage of red blood cells. *Blood Transfus*. 2010;8(4):220-36.
- Zimrin AB, Hess JR. Current issues relating to the transfusion of stored red blood cells. *Vox Sang*. 2009; 96(2):93-103.
- Zurbriggen K, Schmutz M, Schmid M, et al.: Analysis of minor hemoglobins by matrix-assisted laser desorption/ionization time-of-flight mass spectrometry. *Clin Chem* 2005;51(6):989-996.

Chapter 6: Cryostorage

Contents

6.1 Monitoring of red blood cells during processing for cryopreservation: from fresh blood to thaw-washing

The contents of this chapter report the contents of the the following publications by the candidate:

1. Pallotta V, D'Amici GM, D'Alessandro A, Rossetti R, Zolla L.
Monitoring of red blood cells during processing for cryopreservation: from fresh blood to thaw-washing
Blood Cells, Molecules and Diseases 2012; 48(4):226-32.
-

In the previous chapter we reported how current guidelines for prolonged hypothermic storage of erythrocyte concentrates do not prevent the accumulation of the so called "storage lesions". Therefore, it is small wonder that Transfusion Medicine experts are continuously pursuing alternative storage strategies. Cryostorage of red blood cells is one of the alternative, already internationally approved, storage strategies that is currently under evaluation. In this chapter, we report the outcome of a preliminary metabolomics approach to evaluate red blood cell quality upon cryostorage, thawing and deglycerolization.

6.1 Monitoring of red blood cells during processing for cryopreservation: from fresh blood to thaw-washing

Overview of this section

Cryostorage of red blood cells represents a valid alternative to liquid storage, since units can be preserved for at least a decade while conserving their safety and viability. While cryostorage has initially attracted a great deal of attention in the clinical field, little is known about the biochemistry and physiology of cryostored erythrocyte concentrates.

In the present study, we investigated cryostorage of red blood cells through monitoring of cell processing steps (from fresh blood, to glycerolization, thawing and deglycerolization/washing) through repeated assays of standard parameters (MCV, RDW-SD) and scanning electron microscopy.

Cell processing for cryostorage resulted in increased red blood cell volumes. Shape alterations caused an increase in osmotic fragility and permeability to ions. A significant pH drop was observed which could not be attributed to a higher metabolic rate, since the levels of lactate did not show substantial fluctuations among the cell processing steps tested in this study. Membrane anomalies could be also related to higher hemolysis, especially of the densest and oldest cell sub-populations, as we could observe by means of discontinuous density gradients.

Our results indicate that cryostorage in presence of glycerol does not significantly affect RBCs. On the other hand, most of the alterations were related to cell processing and, in particular, to the increase of cytosolic glycerol as a consequence of the glycerolization step. Further studies might be thus designed as to replace glycerol with non-penetrating cryoprotectants.

Keywords: Cryopreservation; Red blood cells; Processing; Transfusion.

Introduction

Biopreservation of blood for transfusion purposes has represented a lifesaving practice over the last 90 years (Hess et al., 2000). Separation and liquid storage of red blood cells (RBCs) in plastic bags has a long history as well (Hess, 2010). Currently, RBCs can be stored at 1-6°C (refrigerated liquid storage) for up to 6 weeks. At the dawn of the transfusion era donors and recipients were forced to lay side by side due to the short shelf-life of RBC concentrates. Continuous improvements in biopreservation strategies have progressively prolonged storage duration and thus allowed separating donors and recipients in space and time (Zolla and D'Alessandro, 2010).

The attempts to prolong RBC storage lead to the design of alternative preservation strategies such as cryopreservation. Early studies demonstrated that cryopreservation allowed storing RBCs for years or decades without apparently compromising their safety and viability (Meryman, 1989; Valeri et al., 2000; Lecak et al., 2004). A prolonged shelf-life of RBC concentrates might be pivotal to better cope with seasonal shortages, to face the demand for rare blood groups or to provide adequate supplies to overcome extraordinary events, such as wars or natural calamities (Hess, 2004; Ramsey, 2008). On the other hand, a broader use of cryopreserved RBCs is not economically feasible because of the complicated processing, requiring trained personnel, and high costs of maintenance (Scott et al., 2005).

So far, cryostorage has been mainly performed in military settings: in 2002, the US Department of Defense had more than 50,000 frozen RBC units placed around the world (Fitzpatrick, 2002).

Cryopreservation of mammalian cells can be detrimental, since the freezing and thawing steps trigger physiological changes which are caused by (i) formation of ice crystals and (ii) changes in intra- and extracellular solute concentrations. In order to prevent injuries provoked by exposure to low-temperatures, RBCs are frozen in the presence of a cryoprotective agent. Cryoprotectants such as glycerol prevent the formation of ice-crystals during cold preservation through a process that is known as vitrification. In order to achieve a proper vitrification process, a handful of variables should be constantly monitored, such as: (i) solution effects; (ii) crystallization; (iii) glass fractures; (iv) devitrification and recrystallization; and (v) chilling injury (Yavin and Arav, 2007). The outcome of the vitrification process is influenced by three major factors: i) viscosity of the sample; ii) cooling and warming rates; iii) and sample volume (Yavin and Arav, 2007). While vitrification improves survival of cells upon cryostorage, high concentrations of cryoprotectants in the vitrification solution can damage the cells through chemical toxicity and osmotic shock.

In cryobiology, one of the most diffused cryoprotectants is glycerol, which was at first used for cryopreservation of RBCs and sperm (Yavin and Arav, 2007). Glycerol is an attractive cryoprotectants for RBCs as well, because it is relatively non-toxic at high concentrations and readily permeates the cell at 37°C. Over the years, two different protocols have been proposed for cryostorage of RBCs in presence of glycerol, which differ for glycerol concentrations (either 15-20% or 40% w/v) in relation to the cooling rate (rapid or slow) and the storage temperature (-196 °C or -80 °C, respectively) (Rowe et al., 1968; Meryman and Hornblower, 1972).

Lecak et al. have reported that cryopreservation at -80 °C in presence of glycerol delivers RBCs which are still viable after more than 10 years (Lecak et al., 2004). Although glycerol has low toxicity, at the end of cryostorage it must be removed from thawed RBC units in order to avoid post-transfusion osmotic hemolysis (Kania and Acker,

2010). The removal of glycerol (deglycerolization) is achieved by washing the units in a continuous flow centrifuge. This procedure results in the loss of 15% of the cells (Valeri, 2004). In general, evaluation of RBC recovery is performed at the end of the freeze–thaw washing procedure. Thawed/deglycerolyzed cells are expected to meet the minimum standards for transfusion (hemolysis below the 0.8% threshold in Europe and <1% in the USA, and *in vivo* recovery at 24 h post-transfusion above 75%) (Council of Europe, 2011).

Henkelman and colleagues (2010) have recently reported that RBC processing steps have the largest effect on cryostored RBC quality, while storage duration itself minimally affects rheologic properties of RBCs. In order to ease and standardize cell processing after thawing of glycerolized cryostored RBCs, in 2001 Haemonetics Corp. obtained clearance from the Food and Drug Administration (FDA) for a closed system which permits 14-day storage after thawing (Bandarenko et al., 2007).

Other cryoprotectants have been recently proposed as glycerol substitutes, such as trehalose, a non-reducing disaccharide, and dextran, a carbohydrate polymer. Both these compounds have been shown to protect against freezing injuries during liquid nitrogen storage of RBCs (Pellerin-Mendes, 1997).

A body of evidence has been accumulated which indicates that cryostored RBCs apparently do not show any classic “storage lesion”, in contrast to what observed in RBCs stored hypothermically (1–6 °C) (Hess, 2010). Hemoglobin structure, methemoglobin levels, membrane and cellular energetic behavior are unaffected by extended storage in the frozen state, since very low temperatures suppress molecular motion and arrest metabolic and biochemical reactions (Mazur, 1964).

Storage of RBC concentrates at 1–6 °C is known to trigger a series of biochemical changes, collectively known as “storage lesions”. These lesions include significant ATP or 2,3-DPG loss, accumulation of potassium and free hemoglobin in the supernatant, increased microvesiculation phenomena, CD47 and phosphatidylserine externalization on the outer membrane layer have been observed. None of these phenomena has been observed in cryostored RBCs at 24h after thawing (Lagerberg et al., 2007; Holovati et al., 2008).

On the other hand, it has been reported that thawed RBCs are more fragile than fresh or hypothermically stored RBCs, as they display higher osmotic fragility (Henkelman et al., 2010). Besides, intra-cellular calcium content has been shown to increase in the presence of glycerol and upon freeze/thawing of RBCs, probably due to the blockade of Ca^{2+} pumps or activation of nonspecific cation channels (Kofanova et al., 2008). Freeze-thawing and deglycerolization of RBCs have been thus suggested to compromise ion permeability of the plasma membrane (Kofanova et al., 2008).

While preliminary biochemical observations have already been reported, to the best of authors’ knowledge no study has so far monitored RBCs during cell processing for preparation to cryostorage. In the present study we monitored RBCs during cell processing steps, through the repeated assessment of standard biological indicators such as mean cell volume (MCV), hemoglobin content, pH values (both internal and in the supernatant), lactate levels, osmotic fragility and hemolysis. Besides, by means of density gradient analyses we also tried to understand whether hemolysis was a random phenomenon or it rather targeted a specific sub-population of RBCs during cell processing for cryostorage.

Finally, we performed scanning electron microscope analyses to determine the extent of cell morphology alterations and compared our results with recent literature about cryostorage and hypothermic storage.

Materials and Methods

Sample collection

Whole blood ($450 \text{ mL} \pm 10\%$) was collected at the “Celio” Military Hospital in Rome (Italy) from 10 healthy donor volunteers into CPD anticoagulant (63 mL) and leukodepleted. After separation of plasma by centrifugation, RBCs were suspended in 100 mL of SAG-M (Saline, Adenine, Glucose, Mannitol) additive solution. Ten leukoreduced RBC units were then prepared and cryopreserved, according to the high-glycerol freezing method (Lagerberg et al., 2007).

Briefly, RBC units with a Hct approximately of 60% and fewer than 10^6 white blood cells were obtained from the blood bank and stored at 2 to 6 °C for 2 hours, after which glycerolization and freezing was performed. Glycerolization to a final concentration of 40% glycerol (wt/vol) was obtained using the Haemonetics ACP 215 device. All glycerolized RBC units were frozen and stored at $-80 \pm 10^\circ\text{C}$ in a mechanical freezer for at least 12 months. Frozen RBC units were thawed in a temperature-controlled water bath of 40 °C, until the units reached a temperature between 25 and 30 °C. Thawed RBCs were deglycerolized using the Haemonetics ACP 215 device and resuspended in SAGM.

Thawed deglycerolized RBCs were stored in polypropylene tubes at 2 to 6°C. The supernatant osmolarity of all the thawed deglycerolized units was below 400 mOsm/kg H₂O, indicating an efficient removal of glycerol.

Samples were collected at four sequential stages: (i) fresh blood, within 2 hours from collection; (ii) after glycerolization; (iii) after thawing; and (iv) after deglycerolization through repeated washing cycles (within 2 hours after thawing).

Haemocromocitometric analysis

The RBC mean cell volume (MCV), red cell distribution width-standard deviation (RDW-SD), the mean cell hemoglobin concentration (MCHC), and the hematocrit (Hct) were determined with a hematologic analyzer (CA 530-Oden, Medonic, Stockholm, Sweden).

Determination of intracellular pH, lactate and glycerol

Red cell pellets obtained by centrifuging 600 µl of suspension in a nylon tube at $30,000\times g$ for 10 min, were frozen, thawed during 5 min and then refrozen. To prevent an acid shift, which is observed when samples are kept unfrozen, triplicate measurements of pH were made immediately after a second thawing of each lysate with a Radiometer pH glass capillary electrode maintained at 20°C and linked to a Radiometer PHM acid-base analyzer.

Lactate and glycerol determination was performed upon methanol/chloroform/water sample extraction through rapid-resolution reversed phase high performance liquid chromatography and mass spectrometry, according to the method by D'Alessandro *et al.* (2011). Results were plotted as mass spectra counts, which are proportional to the metabolite concentrations within the linearity range of the instrument, or fold-change variations upon normalization

to the results obtained through testing of fresh RBCs. Rapid resolution reversed phase high performance liquid chromatography (RR-RP-HPLC) was performed to separate low-molecular weight compounds, as previously reported (D'Alessandro et al., 2011). The RR-RP-HPLC directly eluted into an ion trap mass spectrometer (HCT Bruker, Bruker Daltonics, Bremen – Germany), where the compounds were monitored through Multiple Reaction Monitoring (MRM). Mass to charge ratio for precursor and fragment ions to be selected, monitored and quantified were determined as previously reported (D'Alessandro et al., 2011), in agreement with international online available databases (Metlin, Scripps Center for Biotechnology – available at http://metlin.scripps.edu/metabo_info.php?molid=105 – Last accessed on January 30, 2012).

Hemolysis

Hemolysis was calculated following the method by Harboe (1959). Samples were diluted in distilled water and incubated at room temperature for 30 min to lyse RBCs. Samples from lysed RBCs were diluted 1/300 while supernatants were diluted 1/10 in distilled water. After stabilizing during 30 min and vortex mixing (Titramax 100, Heidolph Elektro, Kelheim, Germany), the absorbance of hemoglobin was measured at 380, 415 and 450 nm (PowerWave 200 Spectrophotometer, Bio-Tek Instruments, Winooski, Vermont, USA). The mean blank was subtracted and the corrected OD (OD*) was calculated as follows: $2 \times OD_{415} - OD_{380} - OD_{450}$.

Osmotic fragility

The osmotic fragility of RBCs reflects the ability of the membrane to maintain structural integrity. Osmotic fragility was determined by stepwise dilution through PBS solutions ranging from 0.90% to 0.35%.

RBCs with a Hct of 30% to 40% were diluted 1:100 in each PBS solution, mixed and incubated for 30 minutes at 4 °C, followed by centrifugation for 12 minutes at 1100 x g. The free Hb in the supernatant was measured using a spectrophotometer. The concentration of PBS necessary to induce 50% hemolysis defined the osmotic fragility index of the RBCs (Gyongyossy-Issa et al., 2005). With this method, a larger osmotic fragility index corresponds to more fragile cells.

Density gradients

Density-fractionated RBCs were prepared using Percoll (Sigma-Aldrich, St. Louis, MO, USA) discontinuous gradients, as described by Bosch *et al.* (1992). Briefly, the gradient was built up in five layers of 2 ml containing 80% (1.096 g/mL), 71% (1.087 g/mL), 67% (1.083 g/mL), 64% 1.080 g/mL Percoll, respectively, buffered with buffer A [26.3 g/L bovine serum albumin, 132 mmol/L NaCl, 4.6 mmol/L KCl, and 10 mmol/L HEPES pH 7.1]. RBCs were washed with buffer B [9 mmol/L Na₂HPO₄, 1.3 mmol/L NaH₂PO₄, 140 mmol/L NaCl, 5.5 mmol/L glucose, and 0.8 g/L bovine serum albumin] and diluted with 1 vol of buffer A. One-half milliliter of this suspension was layered on the Percoll gradient and separation was achieved after 15 minutes of centrifugation at 3000 rpm at room temperature. Fractions were collected by careful pipetting and extensively rinsed with buffer B to remove residual Percoll.

Scanning Electron Microscope (SEM)

Scanning electron microscopic studies of RBC were performed by means of a JEOL JSM 5200 electron microscope. Blood samples from each one of the ten subjects were collected (i) soon after withdrawal and separation of RBCs through centrifugation, as specified above (fresh blood); or (ii) upon cryostorage, after thawing, deglycerolization and washing steps. Packed RBCs were then fixed in phosphate-buffered (pH 7.2–7.4) 2.5% glutaraldehyde for 1 h, washed two times in 0.1 M phosphate buffer (pH 7.2–7.4), and mounted on poly-Llysine-coated glass slides. The glass slides were kept in a moist atmosphere for 1 h, washed in phosphate buffer, postfixed in 1% osmium tetroxide for 1 h, rinsed in distilled water, and dehydrated in graded ethanol (50–70–90–100%). After critical-point drying with liquid CO₂ in a vacuum apparatus and covering with a gold-palladium layer, the samples underwent scanning electron microscopic analysis. The different cell shapes were identified using Bessis' classification (1972), as previously reported (D'Alessandro et al., 2012). The percentages of discocytes, echinocytes, spherocytocytes, stomatocytes, spherostomatocytes, and spherocytes were evaluated by counting 1000 to 1500 cells in randomly chosen fields.

Results

Metabolism parameters

In comparison to fresh blood (7.01 ± 0.14 pH units), supernatant pH moderately increased after glycerolization and thawing (7.32 ± 0.34 and 7.46 ± 0.43 , respectively). After deglycerolization through repeated washing cycles, supernatant pH returned to the original levels (6.91 ± 0.11) (**Figure 1.A**).

Cytosolic pH did not show major fluctuations among the various cell processing steps (approximately 6.95 pH units, remaining constant from fresh blood to thawed RBCs), while it significantly decreased after deglycerolization/washing (6.39 ± 0.13 pH units) (**Figure 1.B**).

However, internal pH drop after deglycerolization/washing was not related to lactate accumulation, since no significant fluctuations of lactate levels were observed among samples collected at each cell processing step (**Figure 1.C**).

Glycerol levels

Cytoplasmic glycerol was undetectable (baseline mass spectra counts) in fresh blood controls, while it significantly increased upon glycerolization (p -value < 0.01 ANOVA). After cryostorage, thawing and deglycerolization, cytoplasmic glycerol levels significantly decreased again, although it was still detectable through mass spectrometry (**Figure 2**).

RBC parameters and SEM analysis

Mean cell volume (MCV) increased significantly upon glycerolization (from 89.4 ± 4.5 of fresh RBCs to 126.04 ± 2.3 of glycerolized RBCs), while it remained constant upon cryostorage even after thawing (129.6 ± 3.3). Deglycerolization and washing restored lower MCV values (93.7 ± 5.9), though still higher than controls (**Figure 3.A**).

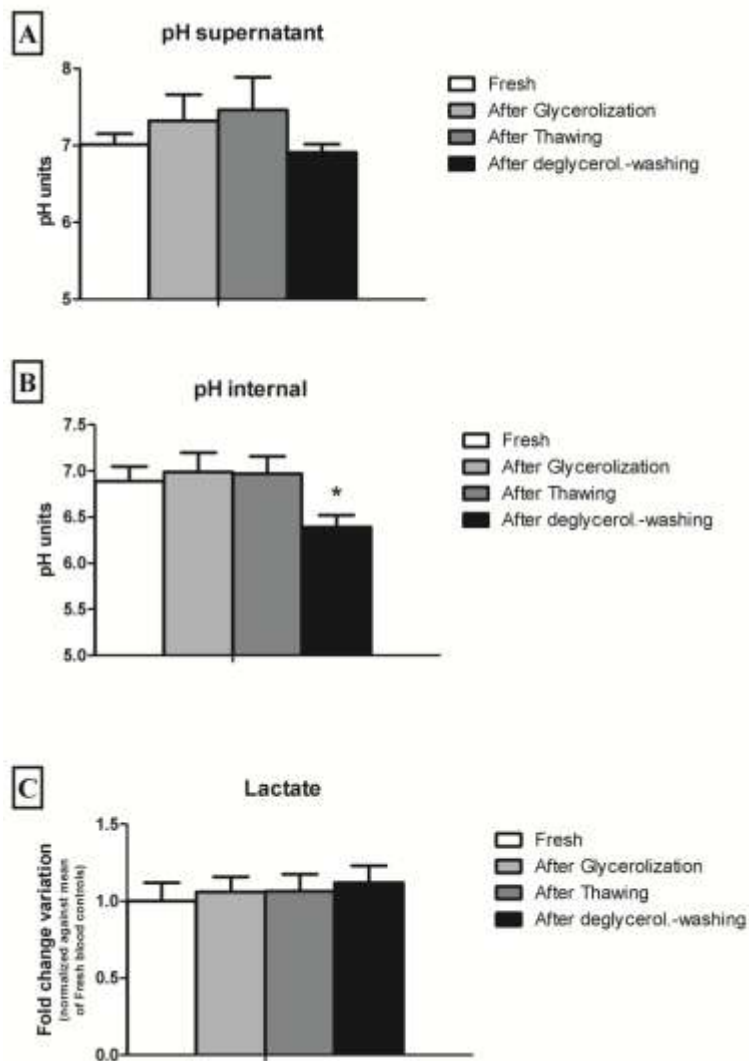


FIGURE 1 Graphs illustrating trends for supernatant pH (A), internal pH (B) and lactate (C), during each one of the tested cell processing steps: fresh red blood cell controls (white column), after glycerolization (light grey), after storage and thawing (dark grey), and after deglycerolization through washing (black). * indicates statistical significance (p -value < 0.05 ANOVA) of variations between groups (columns).

Red cell distribution of width-standard deviation (RDW-SD) followed a similar trend to MCV, since glycerolized RBCs were characterized by higher values (73.92 ± 0.45) than fresh RBC controls (43.15 ± 2.39), even after thawing (73.22 ± 0.56). On the other hand, deglycerolization through multiple washing cycles resulted in a decrease in RDW-SD (48.6 ± 4.71), though final RDW-SD values were still higher than the average reference range (**Figure**

3.B).

The mean corpuscular hemoglobin concentration (MCHC) is a measure of the concentration of hemoglobin in a given volume of packed red blood cells. It is calculated by dividing the hemoglobin by the hematocrit [16]. MCHC values were largely influenced by glycerolization (23.4 ± 1.62 against 33.1 ± 0.57 of fresh RBC controls), while they remained almost identical upon storage and after thawing (23.1 ± 2.32). However, normal values were restored after deglycerolization and thawing (28.1 ± 5.46) (**Figure 3.C**).

Hematocrit (Hct) resulted to be increased by the glycerolization treatment (71.45 ± 2.82) in comparison to fresh RBC concentrates (61.34 ± 3.29). However, it reverted back to lower than control values at the end of cryostorage (57.45 ± 4.19 %) (**Figure 3.D**).

Analogously, osmotic fragility increased after glycerolization (0.78 ± 0.39) and storage/thawing (0.73 ± 0.45) in comparison to fresh RBC controls (0.48 ± 0.1 %), while it was characterized by higher values than in fresh RBC controls after deglycerolization through washing steps (0.69 ± 0.22) (**Figure 3.E**).

Finally, hemolysis increased significantly from 0.23 ± 0.03 % values of fresh RBCs to 2.67 ± 1.95 and 4.73 ± 3.65 of glycerolized and stored/thawed RBCs, respectively. However, after the deglycerolization/washing steps final hemolysis values decreased substantially (0.33 ± 0.05 %) and were thus lower than 0.8%, the maximum allowed threshold for hemolysis as indicated by the European Council guidelines (**Figure 3.F**).

Scanning electron microscope (SEM) micrographs were collected on fresh blood samples (a detail of day 0 discocytes is provided in **Figure 4.A**) and RBCs after cryostorage (**Figure 4.B**). After cryostorage, RBCs showed membrane anomalies (i.e. non-discocyte shape) in almost half of the population (47.3 ± 3.4 %), including a minor echinocyte (**Figure 4.C**) and spherocyte sub-population (5.6 ± 1.2 %) (**Figure 4.E**). In contrast, at the end of the shelf life of hypothermally stored RBCs (42 days at 1-6 °C), approximately 76.3 ± 6.7 % of RBCs showed membrane shape alterations. In particular, at 42 days of liquid storage a greater percentage of RBCs displayed a spherocyte or spherocytic phenotype (approximately 25 %) (**Figure 4.D**).

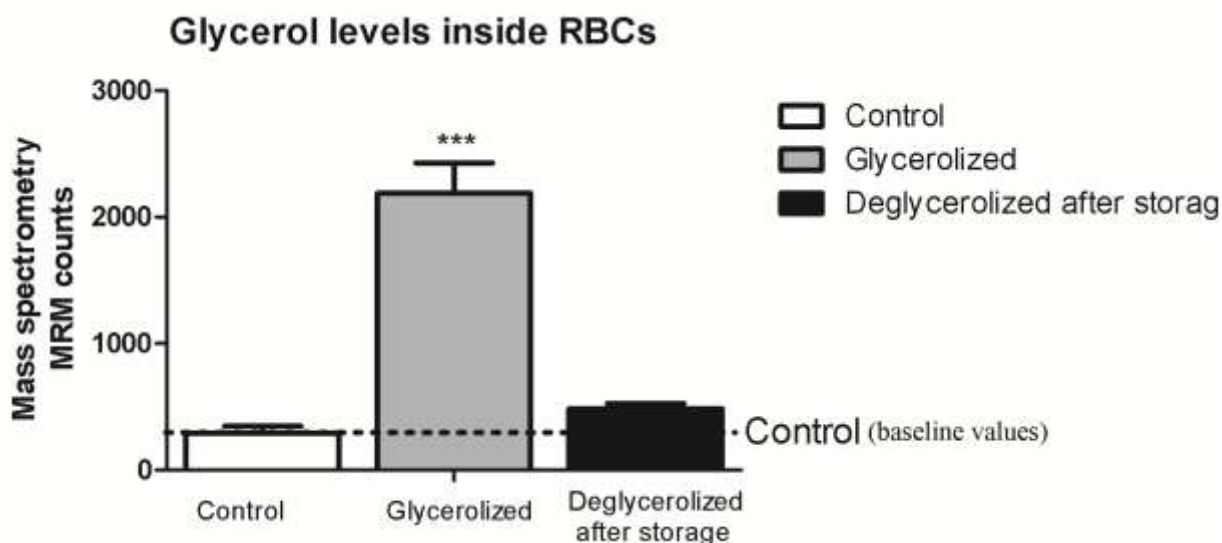


FIGURE 2 Cytoplasmic glycerol levels in freshly withdrawn (white column), glycerolized (grey column), cryostored/thawed, and deglycerolized (black column) red blood cells. Results are reported as mass spectra counts through multiple reaction monitoring (MRM), a mass spectrometric approach which allows detecting, isolating and fragmenting a specific molecular mass to charge ratio (m/z). Glycerol was quantified as 91.04 m/z ($M-H$)⁻ in negative ion mode, in agreement with international databases (METLIN, Scripps Center for Biotechnology – available at http://metlin.scripps.edu/metabo_info.php?molid=105 Last accessed on January 30, 2012).

Discontinuous density gradients

Whole blood samples were collected from ten healthy subjects and centrifuged to separate RBCs. Erythrocyte fractions of varying density were isolated by discontinuous density gradient centrifugation of fresh erythrocytes after withdrawal (**Figure 5.A**) and after cryostorage (**Figure 5.B**). In fresh blood, five different density fractions could be observed (**Figure 5.A**). At the end of cryostorage (after thawing and deglycerolization through washing steps) only 3 bands were still visible, since the 2 densest fractions had disappeared (bands 4 and 5 in **Figure 5**).

Discussions

Biochemical approaches to cryostored RBCs have so far sought to determine the extent of the alterations of a handful of parameters at the end of cryostorage in comparison to fresh blood (Henkelman et al., 2010). In the present study, we tried to investigate the effects of cell processing steps on RBCs.

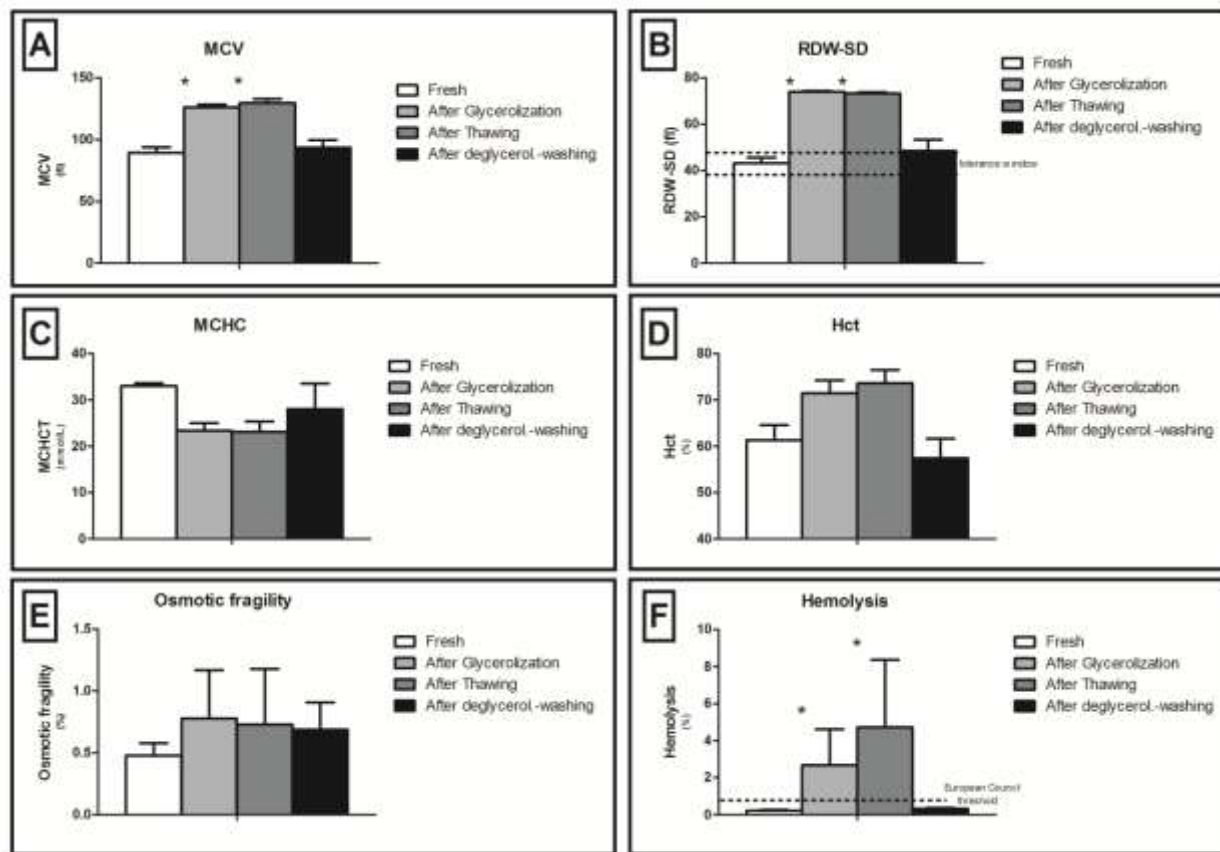


FIGURE 3 Graphs illustrating variations for several parameters including mean cell volume (MCV - A), red cell distribution width-standard deviation (RDW-SD - B), mean cell hemoglobin content (MCHC - C), hematocrit (Hct - D), osmotic fragility (E) and hemolysis percentage (F) during each one of the tested cell processing steps: fresh control red blood cells (white column), after glycerolization (light grey), after storage and thawing (dark grey), and after deglycerolization and washing (black). * indicates statistical significance (p -value < 0.05 ANOVA) of variations between groups (columns).

Metabolism was unaffected by cell processing steps

Metabolic parameters indicated that cryostorage did not significantly affect metabolic activities, since pH was not altered prior to deglycerolization/washing of RBCs and lactate concentration did not significantly vary among the processing steps. These observations are in agreement with previous reports from literature which indicated that no substantial ATP nor 2,3-DPG losses are observed after cryostorage (Holovati et al., 2008; Henkelman et al., 2010).

This is consistent with the assumption that no enzymatic activity should be observed at a storage temperature of -80°C.

While lactate and supernatant pH did not significantly vary during cell processing, internal pH drop was remarkable after deglycerolization through multiple washing steps (**Figure 1**). A tentative explanation might involve the alteration of cation homeostasis. Indeed, changes targeting the RBC membrane might promote the dysregulation of pump activities, as previously proposed by Kofanova and colleagues (2008).

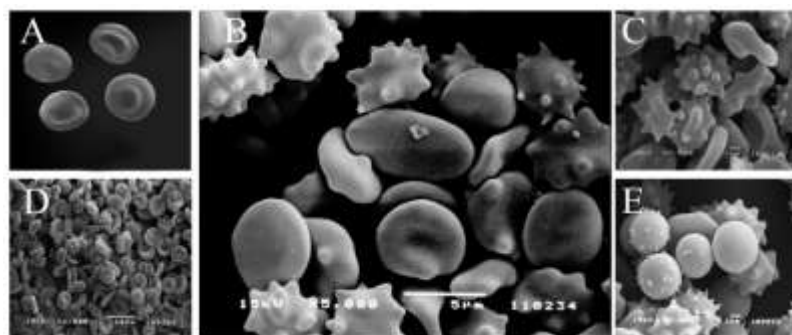


FIGURE 4 Scanning electron micrographs of red blood cells. In (A), a detail is provided of discocytes from fresh blood (detail re-elaborated through Photoshop CS5, Adobe, CA - USA). In (B), a detail of thawed/deglycerolized/washed red blood cells upon cryostorage. In (C)

and (E), a detail is provided of red blood cells showing membrane abnormalities upon cryostorage and, in particular, of echinocytes and spherocytes, respectively. In (D), the micrograph shows red blood cells upon 42 days of liquid (CPD-SAGM) storage under refrigeration (1-6°C). The figure has been composed through Adobe Photoshop CS5.

Alterations to cell morphology and fragility triggered by the glycerolization step were only partially reversible

RBC shape appeared to be significantly altered after the glycerolization step, which promoted significant increases in the MCV and the RDW-SD. This might be due to glycerol penetration inside the cell (**Figure 2**) that results in increased cell volumes.

While cryostorage and the thawing step did not affect these parameters at all, we expected that the washing step would have removed glycerol and thus restored MCV and RDW-SD values within the tolerated range. On the other hand, we could experimentally observe that, despite the washing steps, both MCV and RDW-SD were still higher than in fresh blood controls, especially the latter (11.21 % higher than controls) (**Figure 3**). These observations are in line with the results reported by Henkelman et al. (2010) and are consistent with our observation about an increase of cytoplasmic levels of glycerol, that were detected at the end of the washing steps in comparison to fresh blood controls (**Figure 2**).

Stresses targeting the membrane might not only affect alterations to the internal pH, but the overall osmotic fragility of the cell. Indeed, we could observe that osmotic fragility increased as a consequence of the glycerolization step and remained higher than in fresh blood controls throughout the whole cell processing. This conclusion is further supported by morphological RBC alterations that were evidenced through SEM analyses (**Figure 4**).

Hemolysis mainly involved older cell populations

A decrease in MCHC and Hct is consistent with previous reports about a portion of RBCs from the starting erythrocyte concentrate unit being lost at the end of cryostorage (Holovati et al., 2008; Henkelman et al., 2010). From our results it emerged that this portion could be roughly estimated around 5% of the original Hct. This is confirmed by our results about hemolysis. Although the final washing steps restored hemolysis values within the 0.8% threshold tolerated by the European council guidelines, we could assess a 4.73 ± 3.65 % hemolysis at the end of cryostorage soon after thawing. However, it is worthwhile to stress that hemolysis values were already significantly higher than fresh control RBCs right upon glycerolization (2.67 ± 1.95).

Discontinuous cell density gradients were exploited to understand whether a sub-population of RBCs might represent a privileged target of hemolytic phenomena during cell processing for cryostorage. According to literature (Pierpont et al., 1988; Bosch et al., 1992), the age of a RBC sub-population is directly proportional to its density in a discontinuous Percoll gradient. In other words, older RBC populations are also denser. This is probably due to the loss of both water and hemoglobin over senescence, though the former at a higher rate, which results in an increase in cell density (Pierpont et al., 1988). We hereby observed that, upon cryostorage and deglycerolization via washing steps, the densest RBC sub-populations (bands 4 and 5 in **Figure 5**) disappeared from the density gradient. This observation allowed us to conclude that hemolysis might preferentially involve older sub-populations.

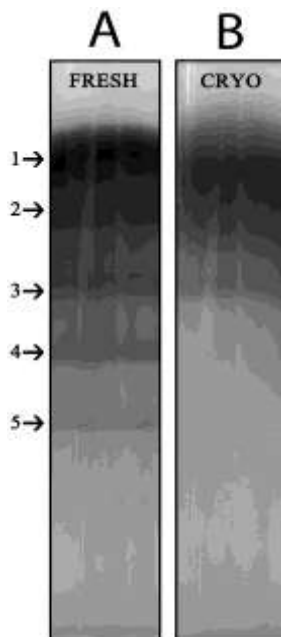


FIGURE 5 Discontinuous density gradients of fresh blood (A – left column) and deglycerolized/washed cryostored blood (B – right column). Bands accounting for populations showing low to high densities are numbered from 1 to 5. Band 1 represent the least dense and youngest population, while band 5 the densest and oldest one.

Conclusion

Cryopreservation of living cells and tissues has become a routine technique in biological and medical laboratories, although cryostorage of RBC concentrates is not as much as widespread. The mechanism of cryoprotection promoted by penetrating agents has been well characterized during the last fifty years, since Lovelock's first analysis (Lovelock, 1953). In brief, the initial concentration and viscosity of protective polymer solutions reduce the extent

and rate of cell water loss to extracellular ice and limit the injurious osmotic stress, which cells face during freezing at moderate rates to $-20\text{ }^{\circ}\text{C}$. Below $-20\text{ }^{\circ}\text{C}$, glass formation prevents further osmotic stress by isolating cells from extracellular ice crystals, virtually eliminating cell water loss at lower temperatures (Takahashi et al., 1988). Cryoprotectants reduce the amount of ice formed at any given temperature, as they contribute to increase the total concentration of all solutes in the system. Cryoprotectants must thus be able to penetrate into the cells and have low toxicity. Many compounds have such properties, including glycerol, dimethyl sulfoxide, ethanediol, and propanediol (Pegg, 2007).

Cryoprotectants have been divided into two categories, namely those which penetrate cell membranes and those which do not. The cryoprotectant glycerol provides a unique window on the mechanism of action of cryoprotectants, since it is a penetrating agent if added at physiological temperatures but it is essentially impermeant if added at 0°C (Pegg, 2007).

In the present study, we could conclude that glycerolization of RBCs resulted in increased cell volumes which were not completely restored back to normal values, even after deglycerolization through washing steps. Shape alterations resulted in an increase in osmotic fragility and permeability to ions. Indeed, the observed pH drop was not to be attributed to metabolism, since lactate did not accumulate over the cell processing steps monitored in this study. Alterations targeting the membrane were assessed indirectly through RBC parameters (MCV, RDW-SD) and directly, through electron microscopy. Membrane anomalies probably lie at the basis of the hemolytic phenomena, which we hereby related to older cell sub-populations by means of discontinuous density gradients.

To conclude, our results indicate that cryostorage in presence of glycerol does not substantially affect RBCs, while most of the alterations were related to cell processing and, in particular, to the penetration of glycerol inside RBCs, as we could observe through mass spectrometry and in agreement with literature (Rowe et al., 1968; Meryman and Hornblower, 1972).

RBC membrane permeability to glycerol has been shown to mainly depend on the presence of aquaporin channels (Wang et al., 2005). When glycerol penetrates inside the cell, on the one hand it protects the erythrocyte from the main damages provoked by freezing, while on the other it may end up triggering alterations of protein-protein interactions in the cytosol and cytoskeleton. Indeed glycerol is a polar molecule which is known to alter ionic strength and dielectric constant in aqueous solutions at high concentrations (Sedgwick et al., 2007; Farnum and Zukoski, 1999). The effects of glycerol penetration inside RBCs might thus result in alterations compromising the cell structure.

Therefore, future studies might be designed as to test the effects of the use of non-penetrating cryoprotectants (such as large molecular-weight polymers - eg, polyvinylpyrrolidone or polyethylene glycol – or the less toxic sucrose and trehalose) (Sedgwick et al., 2007; Farnum and Zukoski, 1999). Trehalose, in particular, is naturally used by plants when facing abiotic stresses such as cold stress (Iordachescu and Imai, 2008), and might represent a natural clue to the clinical challenge posed by cryopreservation.

References

- Bandarenko N, Cancelas J, Snyder EL, Hay SN, Rugg N, Corda T, Joines AD, Gormas JF, Pratt GP, Kowalsky R, Rose M, Rose L, Foley J, Popovsky MA. Successful in vivo recovery and extended storage of additive solution (AS)-5 red blood cells after deglycerolization and resuspension in AS-3 for 15 days with an automated closed system. *Transfusion* 2007;47:680-6.
- Bosch FH, Werre JM, Roerdinkholder-Stoelwinder B, Huls TH, Willekens FL, Halie MR. Characteristics of red blood cell populations fractionated with a combination of counterflow centrifugation and Percoll separation. *Blood*. 1992;79(1):254-60.
- D'Alessandro A, Gevi F, Zolla L. A robust high resolution reversed-phase HPLC strategy to investigate various metabolic species in different biological models. *Mol Biosyst*. 2011;7(4):1024-32.
- European Directorate for the Quality of Medicines & HealthCare. Guide to the Preparation, Use and Quality Assurance of Blood Components. Recommendation No. R (95) 15. 16th Edition. Council of Europe 2011.
- Fitzpatrick GM. Strategic reserves (liquid and frozen). Blood safety transcripts. Department of Health and Human Services, Advisory Committee on Blood Safety and Availability. Seventeenth meeting. Washington (DC): Department of Health and Human Services; September 5, 2002.
- Gyongyossy-Issa MI, Weiss SL, Sowemimo-Coker SO, Garcez RB, Devine DV. Prestorage leukoreduction and low temperature filtration reduce hemolysis of stored red cell concentrates. *Transfusion* 2005;45:90-6.
- Harboe M. A method for determination of hemoglobin in plasma by near-ultraviolet spectrophotometry. *Scand J Clin Lab Invest*. 1959;11(1):66-70.
- Henkelman S, Lagerberg JW, Graaff R, Rakhorst G, Van Oeveren W. The effects of cryopreservation on red blood cell rheologic properties. *Transfusion*. 2010;50(11):2393-401.
- Hess JR (2004) Red cell freezing and its impact on the supply chain. *Transfus Med* 14, 1–8.
- Hess JR, Schmidt PJ. The first blood banker: Oswald Hope Robertson. *Transfusion* 2000;40:110–3.
- Hess JR. Red cell changes during storage. *Transfus Apher Sci*. 2010;43(1):51-9.
- Holovati JL, Wong KA, Webster JM, Acker JP. The effects of cryopreservation on red blood cell microvesiculation, phosphatidylserine externalization, and CD47 expression. *Transfusion* 2008;48:1658-68.
- International Council for Standardization in Haematology (Expert Panel on Blood Rheology): ICSH recommendations for measurement of erythrocyte sedimentation rate. *J Clin Pathol* 1993; 46:198-208.
- Iordachescu M, Imai R. Trehalose biosynthesis in response to abiotic stresses. *J Integr Plant Biol*. 2008;50(10):1223-9.
- Jurado RL. Why shouldn't we determine the erythrocyte sedimentation rate? *Clin Infect Dis*. 2001;33(4):548-9.
- Kanias T, Acker JP. Biopreservation of red blood cells--the struggle with hemoglobin oxidation. *FEBS J*. 2010 Jan;277(2):343-56.
- Kofanova OA, Zemlyanskikh NG, Ivanova L, Bernhardt I. Changes in the intracellular Ca²⁺ content in human red blood cells in the presence of glycerol. *Bioelectrochemistry*. 2008;73(2):151-4.
- Lagerberg JW, Truijens-de Lange R, de Korte D, Verhoeven AJ. Altered processing of thawed red cells to improve the in vitro quality during postthaw storage at 4 degrees C. *Transfusion* 2007;47:2242-9.

- Lecak J, Scott K, Young C, Hannon J & Acker JP (2004) Evaluation of red blood cells stored at -80 °C in excess of 10 years. *Transfusion* 44, 1306–1313.
- Lecak J, Scott K, Young C, Hannon J, Acker JP. Evaluation of red blood cells stored at -80 degrees C in excess of 10 years. *Transfusion* 2004;44:1306-13.
- Lovelock, J. E. 1953b. Het mechanism of the protective action of glycerol against haemolysis by freezing and thawing. *Biochim. Biophys. Acta.* 11:28-36.
- Mazur P: Basic problems in cryobiology, in Timmerhaus KD (ed): *Advances in cryogenic engineering*, vol 9. New York, Plenum Press, 1964, pp 28-37).
- Meryman HT & Hornblower M (1972) A method for freezing and washing red blood cells using a high glycerol concentration. *Transfusion (Paris)* 12, 145–156.
- Pegg DE. Principles of cryopreservation. *Methods Mol Biol.* 2007;368:39-57.
- Pellerin-Mendes C, Million L, Marchand-Arvier M, Labrude P & Vigneron C (1997) In vitro study of the protective effect of trehalose and dextran during freezing of human red blood cells in liquid nitrogen. *Cryobiology* 35, 173–186.
- Pierpont ME, Judd DB, Tukey DP, Smith CM 2nd. Erythrocyte carnitine: a study of erythrocyte fractions isolated by discontinuous density gradient centrifugation. *Biochem Med Metab Biol.* 1988 Dec;40(3):237-46.
- Ramsey G. Frozen red blood cells: cold comfort in a disaster? *Transfusion* 2008;48(10):2053-5.
- Rowe AW, Eyster E & Kellner A (1968) Liquid nitrogen preservation of red blood cells for transfusion: a low glycerol-rapid freeze procedure. *Cryobiology* 5, 119–128.
- Scott KL, Lecak J & Acker JP (2005) Biopreservation of red blood cells: past, present, and future. *Transfus Med Rev* 19, 127–142.
- Shiga T, Maeda N, Kon K. Erythrocyte rheology. *Crit Rev Oncol Hematol* 1990;10:9-48.
- Takahashi T, Hirsh A, Erbe E, Williams RJ. Mechanism of cryoprotection by extracellular polymeric solutes. *Biophys J.* 1988;54(3):509-18.
- Valeri CR (2004) Red cell freezing and its impact on the supply chain. *Transfus Med* 14, 387–388.
- Valeri CR, Ragno G, Pivacek LE, Cassidy GP, Srey R, Hansson-Wicher M, Leavy ME. An experiment with glycerol-frozen red blood cells stored at -80 degrees C for up to 37 years. *Vox Sang* 2000;79:168-74.
- Yavin S, Arav A. Measurement of essential physical properties of vitrification solutions. *Theriogenology.* 2007;67(1):81-9.
- Zolla, L. and D'Alessandro, A. (2011) Proteomic Investigations of Stored Red Blood Cells, in *Chemistry and Biochemistry of Oxygen Therapeutics: From Transfusion to Artificial Blood* (eds A. Mozzarelli and S. Bettati), John Wiley & Sons, Ltd, Chichester, UK. doi: 10.1002/9781119975427.ch18

Chapter 7: Alternative storage strategies

Contents

- 7.1 An efficient and cost-effective apparatus for rapid deoxygenation of blood in erythrocyte concentrates for alternative banking strategies
 - 7.2 Red blood cell metabolism under prolonged anaerobic storage
 - 7.3 Red blood cell storage with vitamin C and N-acetylcysteine prevents oxidative stress-related lesions: a metabolomics overview
-

The contents of this chapter report the contents of the the following publications by the candidate:

1. Zolla L, D'Alessandro A.
An efficient and cost-effective apparatus for rapid deoxygenation of blood in erythrocyte concentrates for alternative banking strategies
J Blood Transfusion 2013; Under review
 2. D'Alessandro A, Gevi F, Zolla L.
Red blood cell metabolism under prolonged anaerobic storage
Molecular Biosystems 2012; accepted
 3. Pallotta V, Gevi F, D'Alessandro A, Zolla L.
Red blood cell storage with vitamin C and N-acetylcysteine prevents oxidative stress-related lesions: a metabolomics overview
2013; under review
-

Since oxidative stress is one of the leading causes promoting the accumulation of storage lesions, alternative storage strategies have been designed as to prevent or tackle the production of reactive oxygen species: anaerobic storage and alternative additive/storage solutions (including antioxidants in the formula, such as ascorbic acid and N-acetyl cysteine). In the present chapter we describe the application of untargeted metabolomics to assess storage quality under anaerobic conditions, or upon the supplementation of anti-oxidants to erythrocyte concentrates. In order to obtain a rapid and efficient deoxygenation, we also describe the set up of a deoxygenation apparatus that was designed and optimized in our laboratory. As a result, we could conclude that deoxygenation promoted energy metabolism, while resulting in the reduced capacity of erythrocyte to cope with oxidative stress (Embden Meyerhof pathway dominance, reduced diversion toward the pentose phosphate pathway, increased nitrogen-NO metabolism and likely impaired activity of the methemoglobin reductase enzyme). On the other hand, ascorbic acid and NAC protected erythrocytes from the accumulation of oxidative stress to proteins, lipids and anti-oxidant metabolites, while partially sacrificing energy metabolism (since ascorbate competes with D-glucose for membrane internalization via GLUT transporters).

7.1 An efficient and cost-effective apparatus for rapid deoxygenation of blood in erythrocyte concentrates for alternative banking strategies

Overview of this section

Erythrocyte concentrates (ECs) stored for transfusion purposes still represent a lifesaving solution in a wide series of clinically occurring circumstances, especially for traumatized and perioperative patients. However, concerns still arise and persist as to whether current criteria for collection and storage of ECs might actually represent the best case scenario or there might rather be still room for improvement.

In particular, prolonged storage of EC has been associated to the accumulation of a wide series of storage lesions, either reversible (metabolism) or irreversible (protein and morphology), although it is still a matter of debate as to whether and to which extent these molecular lesions might relate to the untoward effects which have been documented through controversial retrospective studies.

In this frame, independent laboratories have contributed to propose alternative strategies, among which the introduction of oxygen removal treatments to ECs to the end of eliminating oxidative stress-triggered injury, one of the leading causes of storage lesions. Within this framework, convincing biochemical and preliminary clinical evidences have been produced about the benefits deriving from the introduction of this practice.

We hereby propose a rapid, efficient and time-effective strategy for blood deoxygenation which might fit in current EC production chain. The proposed strategy resulted in the complete deoxygenation of red blood cell hemoglobin ($pO_2 < 0.0021 \text{ mmHg}$). A preliminary small-scale study about the application of the present method resulted in reduced hemolysis, decreased vesiculation and limited alterations to the red blood cell morphology, as gleaned from flow cytometry and scanning electron microscopic analyses. However, further more in-depth and larger scale investigations are encouraged in order to draw any biologically meaningful conclusion.

Keywords: red blood cells; anaerobic storage; blood deoxygenation; hemoglobin;

Introduction

Erythrocyte concentrates (ECs) are still the most widely transfused blood-derived therapeutic worldwide, as many million units of blood are collected, and million units of RBCs are administered to millions of patients every year (Hess, 2010; D'Alessandro et al., 2010). Currently accepted European Council guidelines indicate that ECs may be stored for up to 42 days under controlled conditions before transfusion (Council of Europe, 2011). Nevertheless, recent retrospective and controversial studies have brought about concerns on the suitability of longer stored EC units for transfusion purposes (Koch et al., 2008; Leulubre et al., 2009). It has indeed been stressed that the risk of exposure to long-stored red blood cells (RBCs) is exacerbated when dealing with certain categories of recipients, such as traumatized, post-operative and critically ill patients (Lelubre et al., 2009). However, it should be worth mentioning that early results from randomized double-blind clinical prospective trials have not hitherto indicated any statistically significant disadvantage of the administration of longer stored units in comparison to fresher blood (Fergusson et al., 2012; Flegel et al., 2012).

While the likelihood of untoward effects related to the transfusion of older RBC units is still a matter of debate and of clinical investigations, what is now known for certain is that storage affects biochemical and biological properties of RBCs, and the extent of these accumulating changes, collectively known as “storage lesions”, is proportional to the duration of the storage period (Bennet-Guerrero et al., 2007; Zimrin and Hess, 2009; Lion et al., 2010; Antonelou et al., 2010). Storage lesions include alterations to either morphology (shape changes leading from a discoid to a spherocytic phenotype) or functionality (metabolism, oxygen delivery capacity through an increase in oxygen affinity mediated by a rapid fall in 2,3-diphosphoglycerate concentrations (Valeri et al., 1969; Bennet-Guerrero et al., 2007; D'Amici et al., 2007; Bosman et al., 2008; Rubin et al., 2010; D'Alessandro et al., 2012)). Further lesions occur in stored RBCs which are reversible to some extent, such as potassium leakage to the supernatant, depletion of ATP and DPG stores, while others are not, such as the alteration of lipids and membrane proteins (membrane protein fragmentation and migration to the membrane and/or vesiculation of subsets of structural or anti-oxidant proteins (D'Alessandro et al., 2012)), which results in more rigid cell structures, increased osmotic fragility, higher haemolytic rates, phosphatidylserine exposure to the outer membrane leaflet, increased vesiculation rate and reduced oxygen off-loading capacity (Bennet-Guerrero et al., 2007; Lion et al., 2010; Antonelou et al., 2010; Rinalducci et al., 2011; Antonelou et al., 2010; D'Alessandro et al., 2012).

Membrane protein fragmentation (D'Amici et al., 2007; D'Alessandro et al., 2012), storage time-dependent migration of cytosolic proteins to the membrane (Rinalducci et al., 2011; D'Alessandro et al., 2012) and increased oxidative stress-related parameters (Chaudhary et al., 2011; D'Alessandro et al., 2012) have been also reported to correlate with storage duration. Biochemical studies explicitly suggested that there is considerable room for improvement in the field of RBC biopreservation, especially when considering that the lifespan of RBCs *in vivo* is approximately of 120 days (Shemin and Rittenberg, 1946). One major phenomenon seems to lie at the root of storage lesions to RBCs: oxidative stress (Chaudhary et al., 2011; D'Alessandro et al., 2012). In order to cope with oxidative stress triggering phenomena, alternative RBC storage strategies have been recently proposed, such as the addition of higher loads of anti-oxidants (vitamin E, C and beta-carotene) in additive solutions for storage purposes (Racek et al., 1997) or anaerobic storage (Dumont et al., 2009; Yosida et al., 2008 and 2011). While the former

strategy has been designed as to counteract oxidative stress arising over prolonged storage, the latter has been thought as to prevent over-production of Reactive Oxygen Species (ROS) through the elimination of the main substrate, oxygen.

The anaerobic approach ($pO_2 < 4\%$ - patent WO/1996/039026) has been reported to deliver ECs with hemolysis below 0.8% and *in vivo* survival at 24 h upon transfusion above the 75% threshold (Yoshida et al., 2008 and 2011; Dumont et al., 2009). Independent studies from our group have evidenced that storage under helium also reduced the extent of membrane protein fragmentation or aggregation phenomena of non-leukofiltered erythrocyte concentrates (D'Amici et al., 2007). However, it should be appreciated that these optimistic results are currently undergoing further clinical testing through prospective trials. The clinical milieu has so far looked at the “anaerobic perspective” with diffidence, mainly because the recently proposed protocols implied the introduction of new costly and time-consuming steps in the EC production chain. In other terms, the alternative “anaerobic perspective” appeared not to be optimized for cost/benefits or cost/effectiveness considerations.

In this view, we hereby propose a rapid strategy for cost- and time-effective deoxygenation of ECs and provide details about the likely frame of steps in which this method might be safely and efficiently introduced in clinical routine practice in the future.

Technical design

Blood collection

Whole blood (450 mL + 10%) was collected from healthy volunteer donors into citrate phosphate dextrose - CPD anticoagulant (63 mL; pH 5.6) and leukodepleted. After separation of plasma by centrifugation, RBCs were suspended in 100 mL of SAG-M (Saline, Adenine, Glucose, Mannitol) additive solution. We studied RBC units collected from 8 donors [male = 4, female = 4, age 45 +11.5 (mean + S.D.)]. The present study was approved by the Italian National Blood Centre (Rome, Italy).

Helium cylinders

High purity helium gas cylinders (99.999% of gas purity, 10 m³ each) were obtained from Sol S.p.A. (Pomezia, Italy).

Deoxygenation of red blood cells

EC were stored into CPD-SAGM-containing plastic bags (Fenwal Italy, Milano - Italy).

An illustration of the deoxygenation apparatus is reported in **Figure 1**.

Helium from gas cylinders was regulated for 1 bar output pressure through a common manometer and fluxed into the EC units through sterile connection.

A time valve (standard execution, up to 10 bar; regulation from 1 to 10 seconds) was used to regulate both influx and efflux of helium, through the opening of gas influx for 5 seconds, stabilizing the system for six minutes (in order to allow gas exchange between RBCs in the unit and the gas phase) and the opening of the second valve linked to a vacuum pump aspirating the gas from the unit.

Sterility was further guaranteed by the presence of sterility filters (AcroPak™ 300 – Pall Life Sciences, NY, USA) in between the gas outlet from the cylinder manometer and the inlet tube into the unit and from the unit to the vacuum pump.

Each unit was conditioned with helium through 5 cycles of influx and aspiration via vacuum pump. Each cycle consisted in helium influx, six minutes gas exchange between RBCs in the unit and the gas phase and gas efflux through the opening of the vacuum pump valve.

In order to ease gas exchange, RBC units are placed on a tilting stainless steel plate for gentle agitation, as to prevent hemolysis. The stainless steel surface was thermostated at 37°C, in order to ease oxygen dissociation from hemoglobin (Forbes and Roughton, 1931; Astrup et al., 1965; Glauser and Forster, 1967). Temperature stability was guaranteed by an internal resistance which was used to warm water circulating in within a tunnel in the double-chamber of the stainless steel plate.

The apparatus was optimized to perform deoxygenation on six units simultaneously, by means of a six tap structure (Steroglass; Perugia, Italy) and sterility filters at the end of each tap. Depositories for six independent units were used to block the bags on the stainless steel surface for the duration of the deoxygenation process (30 minutes).

RBC units were stored under standard blood bank conditions (1-6 °C) in a closed chamber conditioned with helium for up to 42 days.

Assessment of conservation of the deoxygenated condition

Prior to storage, hemoglobin oxygenation levels were assayed spectrophotometrically through a double-beam spectrophotometer Cary 4 Varian, and further tested with dissolved oxygen sensors by tryptophan fluorescence quenching (< 0.0021 mmHg) (Steroglass, Perugia, Italy).

Since our goal was to test deoxygenation levels, albeit not hemoglobin concentration, we did not need to establish a precise path length, in agreement with the Lambert-Beer law. Conversely, we were interested in performing the assay directly on the blood unit. The internal architecture of the Cary Varian spectrophotometer allowed us to perform the analysis directly on vertically placed units, where blood was allowed to drip on the lateral surface of the plastic bag and the majority of the unit (labels included) was put below the optic path of the laser beam, in order not to disturb the reading. Any effect of the absorbance and scattering of the plastics was excluded in the range of $500 < \lambda < 600$ nm. When only a film of blood was visible in the lateral wall of the unit (thus excluding any scattering associated with higher volumes of packed RBCs) it was possible to measure hemoglobin absorbance without any significant scattering within a time window of 1 min. **Figure 2** shows hemoglobin absorbance spectra prior to (**A**) and after (**B**) deoxygenation. The (few) inconveniences of such a home-made strategy could be easily overcome by a specifically designed plastic bag with a room of a fixed volume (0.01 cm wide, for example). Further testing with dissolved oxygen sensors by tryptophan fluorescence quenching indicated pO_2 below 1 ppb (< 0.0021 mmHg) (Steroglass, Perugia, Italy), below the limit of detection of the instrument.

No bacterial contamination was observed at the end of the storage period in either control or deoxygenated units, as gleaned through MALDI Biotyper analyses (Elsner et al., 2011).

Hemolysis

Hemolysis was calculated following the method by Harboe (1959). Samples were diluted in distilled water and incubated at room temperature for 30 min to lyse red blood cells. Samples from lysed RBCs were diluted 1/300 while supernatants were diluted 1 / 10 in distilled water. After stabilizing during 30 min and vortex mixing (Titramax 100, Heidolph Elektro, Kelheim, Germany), the absorbance of the hemoglobin was measured at 380, 415 and 450 nm (PowerWave 200 Spectrophotometer, Bio-Tek Instruments, Winooski, Vermont, USA). The mean blank was subtracted and the corrected OD (OD *) was calculated as follows: $2 \times OD_{415} - OD_{380} - OD_{450}$.

Flow cytometry

RBC supernatants of control and deoxygenated units were collected upon 42 days of storage for flow cytometry-based analyses of RBC shed microvesicles. RBC microparticles released during storage were separated from RBCs by centrifugation of RBCs transferred into 50-mL tubes for

10 minutes at 1000 x g at room temperature. The supernatant was recentrifuged for 5 minutes at 2000 x g at room temperature. The resulting supernatant containing RBC microparticles was collected and centrifuged for 30 minutes at 18,000 x g at 4°C. The centrifugation speed of 18,000 x g was selected on the basis of the method optimized by Rubin et al. (2012).

The morphology of the cells and microparticles was assessed by a FACScalibur (Becton-Dickinson, USA). A standard method for approximate quantitation of RBC microparticles on the basis of their relative size and shape was applied (Givan et al., 2011; Rubin et al., 2012). Although the method holds some pitfalls, which could be partly overcome through the use of specific antibodies against microvesicle markers (e.g. CD132 and CD235a) or annexin V (against phosphatidylserine), the presently exploited method still allows obtaining an indicative idea about the relative quantities of microparticles in a given RBC concentrate supernatant. Analyses were conducted using the instrument software by counting events in a 5 minutes time window within the gated area (Givan et al., 2011; Rubin et al., 2012). Events were analysed on the basis of side scatter and forward scatter, as compared against a flow cytometry size calibration kit (Invitrogen, Eugene, OR) containing beads of different diameter, from ~1µm to ~1.4µm (RBC microparticles are smaller than those beads, as previously reported in (Givan et al., 2011)).

Scanning electron microscopy

Scanning electron microscopic studies of RBC were performed by means of an JEOL JSM 5200 electron microscope. Blood samples were fixed in phosphate-buffered (pH 7.2–7.4) 2.5% glutaraldehyde for 1 h, washed two times in 0.1 M phosphate buffer (pH 7.2–7.4), and mounted on poly-Llysine-coated glass slides. The glass slides were kept in a moist atmosphere for 1 h, washed in phosphate buffer, postfixed in 1% osmium tetroxide for 1 h, rinsed in distilled water, and dehydrated in graded ethanol (50–70–90–100%). After critical-point drying with liquid CO₂ in a vacuum apparatus and covering with a gold-palladium layer, the samples underwent scanning electron microscopic analysis and classification between reversible and irreversible phenotypes, as in D'Alessandro et al. (2012). The percentages of discocytes, echinocytes, spherocytocytes, stomatocytes, spherostomatocytes, and spherocytes were evaluated by counting 1000 to 1500 cells in randomly chosen fields. In details, as reported in

D'Alessandro et al., 2012), RBCs manifesting echinocyte and stomatocyte shapes are capable of returning to the discocyte shape under certain conditions. Thus, these RBC shape changes are considered potentially reversible transformations. In contrast, RBCs assuming spherocochinocyte, spherostomatocyte, spherocyte, ovalocyte, and degenerated shapes are irreversibly changed cells.

Results and Discussions

Currently, whole blood withdrawn from a single donor (≈ 450 ml) is collected in a CPD anticoagulant-containing plastic (usually bis(2-ethylhexyl)phthalate - DEHP) multiple blood-pack units. In each system, the main unit (where blood is at first collected during withdrawal) contains 63 ml of CPD solution. Three satellite units (for platelet concentrates, plasma and erythrocyte concentrates) are also present, where cellular components are splitted upon centrifugation at 1500 rpm for 10 min. The satellite unit for erythrocyte concentrates contain 100 ml of SAGM as additive solution. Most commonly available centrifuges can load up to six plastic bags for each run. Plastic bags are then put in a phase separator and RBC present in the bottom of the bag are sterilely transferred through a plastic tube in the final SAGM-containing plastic bag and shipped for hypothermic storage. Before the cycle might start again with six new units, plasma and platelets require additional centrifugation steps, leaving a time frame for additional limited manipulation on EC alone. Any ideal further step to be introduced in the blood components production chain with the goal to reduce storage-induced lesions, eventually including also blood deoxygenation (D'Amici et al., 2007; Yoshida et al., 2008 and 2011; Dumont et al., 2009), should be designed as to fit these preparation cycles. In our opinion, this could be best obtained by performing deoxygenation of erythrocyte concentrates in the time window ranging from separation of blood components through centrifugation of six units, to the next cycle of six units.

The aim of this technical report is to demonstrate the feasibility of a rapid and efficient deoxygenation method to be eventually introduced in clinical routine practice, whether large scale laboratory and clinical trials will outline any significant improvement of deoxygenated RBC concentrate units over current “aerobically”-stored counterparts. The deoxygenation workflow would take place in 30 minutes and does not require any transfer of erythrocytes to additional satellite units nor it compromise safety and effectiveness of the blood therapeutic. The components of the deoxygenation apparatus (**Figure 1**) are relatively inexpensive (less than 2,000 €).

Helium was chosen to perform deoxygenation since it is an inert gas, which can be easily found at highest commercial purity. Attempts to perform deoxygenation were carried on with other gases, including Argon (expensive) and nitrogen. The latter is more difficult to be extracted from air (or commercially obtained) at the highest purity, and was excluded for two main reasons: i) even after performing multiple cycles of deoxygenation we could still observe a 6-10% residual oxyhaemoglobin; ii) after twenty-eight days of storage under nitrogen we could observe a significant haemolysis, which we interpreted as a nitrogen radical species (RNS)-triggered phenomenon.

It could be argued that helium represents a limited resource, other than a rather expensive one. In this view, we care to stress that one single highest purity helium cylinder would theoretically suffice to perform deoxygenation of thousands of units. Although we do understand that this does not solve the issue related to the limitedness of the

helium resource, this is a concern that would involve any other technology that currently adopts helium as the working gas. Just to mention one example that is close to our expertise, most mass spectrometers rely on helium for collision induced dissociation (CID) for tandem mass spectrometry analyses. However, despite decades have passed from the advent of tandem mass spectrometry, while these instruments have become increasingly widespread, helium based CID still represents one key approach to investigate, for example, protein, peptide and metabolic species at the molecular level. Alternative strategies might suggest to rely upon other noble gases for deoxygenation of RBCs (such as Argon) which, however, would not make it any better in terms of availability of the raw material (in this case gas) in the long term and on a larger scale.

As for the deoxygenation procedure, it could be argued that simple flushing with gases would easily replace the timed valve system. We could experience that after one hour flushing we could not obtain full deoxygenation, which was instead rapidly achieved through multiple repeated cycles of gas influx/efflux through timed valves (upon manual optimization of optimal gas exchange rates). Besides, flushing resulted in evaporation of liquid components (additive solution) altering the osmolarity of the solution and influencing RBC physiology and, inevitably, morphology. Conversely, maintenance of temperature homeostasis through the heated stainless steel unit holder and gentle agitation, along with aspiration (without reaching vacuum as RBC would hemolyse) dramatically improved rapidity and efficiency of the deoxygenation protocol without altering RBC integrity and functionality.

It is worthwhile to note that, although the Flick law would suggest to use larger plastic units for storage of EC in order to increase the surface available for gas exchange and thus increase the rapidity of the deoxygenation process, in the hereby proposed method we could obtain rapid deoxygenation with commercially available plastic bags. However, owing to plastic bag permeability to gases, in order to maintain deoxygenation of the units we stored deoxygenated in units in helium chamber under controlled conditions.

One additional parameter that could be implemented in the process would be the acidification of pH in order to reduce haemoglobin oxygen affinity during deoxygenation. This would imply that pH should be buffered towards alkalization later on, since an alkaline pH is known to improve RBC viability via up-modulation of metabolism (ATP and 2,3 DPG are maintained for a longer period in alkaline solutions (Hogman et al., 2006)). Though we also tried to perform deoxygenation at an acidic pH (through buffering via acidic citrate), we did not observe any significant improvement in the workflow except for the rapidity of the deoxygenation process, which was obviously faster. On the other hand, it should be also noted that deoxygenation itself promotes alkalization of the medium, through oxygen and bicarbonate ion removal. While it is beyond the scope of this technical note to propose alternative additive solutions, it could be feasible enough to perform deoxygenation on RBCs collected in acidic pH CPD (or CP2D), centrifuged and leukofiltered, prior to transfer into a satellite units containing a more alkaline pH commercial solutions (such as phosphate-adenine-glucose-guanosine-gluconate-mannitol - PAGGGM (Hogman et al., 2006)).

Besides, gas impermeable plastic bags would have eased storage under deoxygenated conditions, although we could achieve this goal through locating the units in a closed chamber conditioned with helium and stored at refrigerated temperatures (1-6°C). Current plastics, of which commercially available EC storage bags are made of, hold some advantages as well, such as they do not hamper spectrophotometric absorbance assays in the 500-600 nm range, as

they can be adjusted vertically as to screen haemoglobin absorbance curve without any significant scattering or interference (**Figure 2**). Of note, we also tried to adopt oxygen sensors to monitor oxygen levels in the unit upon each deoxygenation cycle. These optic chemosensors detect the presence of oxygen through monitoring the quenched or reduced fluorescence of a specific fluorophore (polydimethylsiloxan) with a long excited-state lifetime upon collision with oxygen molecules (Tusa and Huarui, 2005). The lower the oxygen pressures, the lower is the likelihood of collisions between oxygen molecules and the fluorophore, which is reversely measured through fluorescence detection (Tusas and Huarui, 2005). Unfortunately, these sensors (and the fluorophore-coated surfaces, which are meant to be inserted into the plastic bag where blood is stored) are rather expensive and their safety in the frame of direct contact with transfusable RBCs is yet to be ascertained. Conversely, haemoglobin is totally costless and as much as informative. Within the framework of the present report, when spectrophotometric assays of haemoglobin indicated complete deoxygenation, further testing with dissolved oxygen sensors by tryptophan fluorescence quenching indicated pO_2 below 1 ppb (< 0.0021 mmHg) (Steroglass, Perugia, Italy), below the limit of detection of the instrument.

A small scale study on the effectiveness of deoxygenation on long term storage: preliminary results

While the hereby reported method is only designed as a proof of concept about the feasibility of the deoxygenation approach, we also performed a preliminary small scale study to collect preliminary indicative (albeit not significant, since the power of the study would not allow to draw any biologically meaningful and reliable conclusion) evidences about the effects of deoxygenation on RBCs storage.

In order to determine whether the deoxygenation treatment resulted in alterations of RBC morphology and efficiency, we first tested the rapidity of the re-oxygenation process. We could obtain re-oxygenated haemoglobin after less than one minute of exposure to environmental oxygen conditions. Therefore, re-oxygenation of blood before its usage does not require any additional manipulation, as it would rapidly occur naturally *in vivo* during the slow process of transfusion to the recipient.

As for RBC integrity, no significant haemolysis was observed after deoxygenation treatments (0.17 ± 0.04 % and 0.16 ± 0.04 % in controls and deoxygenated units at day 0, respectively), while haemolysis in 42 days stored ECs under helium was significantly lower than in controls (0.33 ± 0.04 % vs 0.64 ± 0.08 %, respectively – p -value < 0.05 ANOVA) (**Figure 3**).

Hereby reported preliminary results also seem to suggest that storage of ECs under helium results in a reduced vesiculation likelihood (in **Table 1** we report the counted events within the defined 5 minutes time window in the gated area for side scatter and forward scatter for day 42 controls and deoxygenated counterparts). Although further more in depth investigations are mandatory, the observation about an apparent decreased vesiculation rate of deoxygenated RBCs is in agreement with previous reports by Yoshida's group (Yoshida et al., 2008 and 2011; Dumont et al., 2009).

Deoxygenation also apparently resulted in a narrower extent of the morphology alteration phenomena. We could indeed observe that, while 42 days old controls displayed almost 80% of either reversibly (echinocytes and stomatocytes) and irreversibly (spherocochinocyte, spherostomatocyte, spherocyte, ovalocyte, and degenerated

shapes) altered RBCs and only 20.6 ± 2.5 discocytes, the deoxygenated long stored counterparts conserved a greater percentage of unaltered discocytic phenotypes ($\approx 32.1\%$) and of reversibly modified RBCs, and a lower percentage of irreversibly altered erythrocyte shapes (**Table 2**). It is worthwhile to stress that, whether larger scale studies will confirm these results, it would be possible to conclude that shape-based classification of deoxygenated RBCs closely resembles control RBCs stored for a shorter period (28-35 days), in relation to the values that we could previously report for untreated CPD-SAGM control erythrocytes (D'Alessandro et al., 2012; Blasi et al., 2012). We also provide a snapshot of this phenomenon in **Figure 4**, which shows a scanning electron microscope (SEM)-obtained micrograph of RBCs from EC units stored in presence – left panel – or in absence of oxygen – right panel; arrows indicate RBCs showing irreversibly altered morphologies, as previously reported (D'Alessandro et al., 2012)).

An in-depth laboratory investigation is currently in progress which aims to assess of the potential benefits of deoxygenated storage, including the monitoring of several parameters such as RBC morphology, vesiculation, alterations to the membrane proteome (*paper in preparation*). On the other hand, we recently proposed a detailed study about the alterations to the metabolic fluxes upon deoxygenation and over storage duration on a weekly basis (D'Alessandro et al., 2013) and compared the results to our in-depth analyses on CPD-SAGM-stored untreated RBCs (Gevi et al., 2012). From this study, it emerged that deoxygenation of RBCs might result in the alteration of the redox poise by up-modulating the nitric oxide (NO) metabolism, which is known to influence the production of RNS, and by blocking the oxidative stress-triggered metabolic diversion from the Emden Meyerhof classic glycolytic pathway towards the pentose phosphate pathway, which should instead provide reduced coenzymes to regenerate the anti-oxidant battery, such as NADPH (D'Alessandro et al., 2012).

Conclusion

While the clinical improved efficiency of deoxygenated ECs it is yet to be demonstrated, preliminary laboratory evidences (D'Amici et al., 2007, Yoshida et al, 2008 and 2011; Dumont et al., 2009) seem to suggest that deoxygenation might soon become a critical step in the transfusion service pipelines. To this end, we hereby proposed a cheap apparatus for rapid and effective blood deoxygenation for transfusion purposes. We demonstrated its straightforward set up and functioning principles. Also, through a small scale preliminary study we report the effectiveness of this method in delivering deoxygenated RBCs, which do not show any substantial hemolysis after handling while they show improved morphology homeostasis maintenance and reduced vesiculation after 42 days of storage. However, since the hereby presented is but a methodology paper, it is worthwhile to stress that further more in-depth and larger scale investigations are encouraged in order to draw any biologically meaningful conclusion.

Table 1 – RBC-shed microparticles	
Storage day	Microparticles (counted events in the arbitrary time window inside the gated area)
42 (control)	5234 ± 125
42 (deoxygenated)	1865 ± 78

Table 2 – SEM erythrocyte shape classification			
Storage Day	Discocyte (%)	Reversibly* changed RBC (%) (echinocyte and stomatocyte shape)	Irreversibly* changed RBC (%) (spherochinocyte, spherostomatocyte, spherocyte, ovalocyte, and degenerated shapes)
0	76.5±3.1	19.2 ± 5.7	4.3 ± 2.6
42 Control	20.6 ± 2.5	43.2 ± 3.8	36.2 ± 2.9
42 Deoxygenated	32.1 ± 1.9	45.4 ± 2.2	22.5 ± 3.1

* Reversible and irreversible changes were classified based on classification criteria, as previously reported D'Alessandro et al. [12]

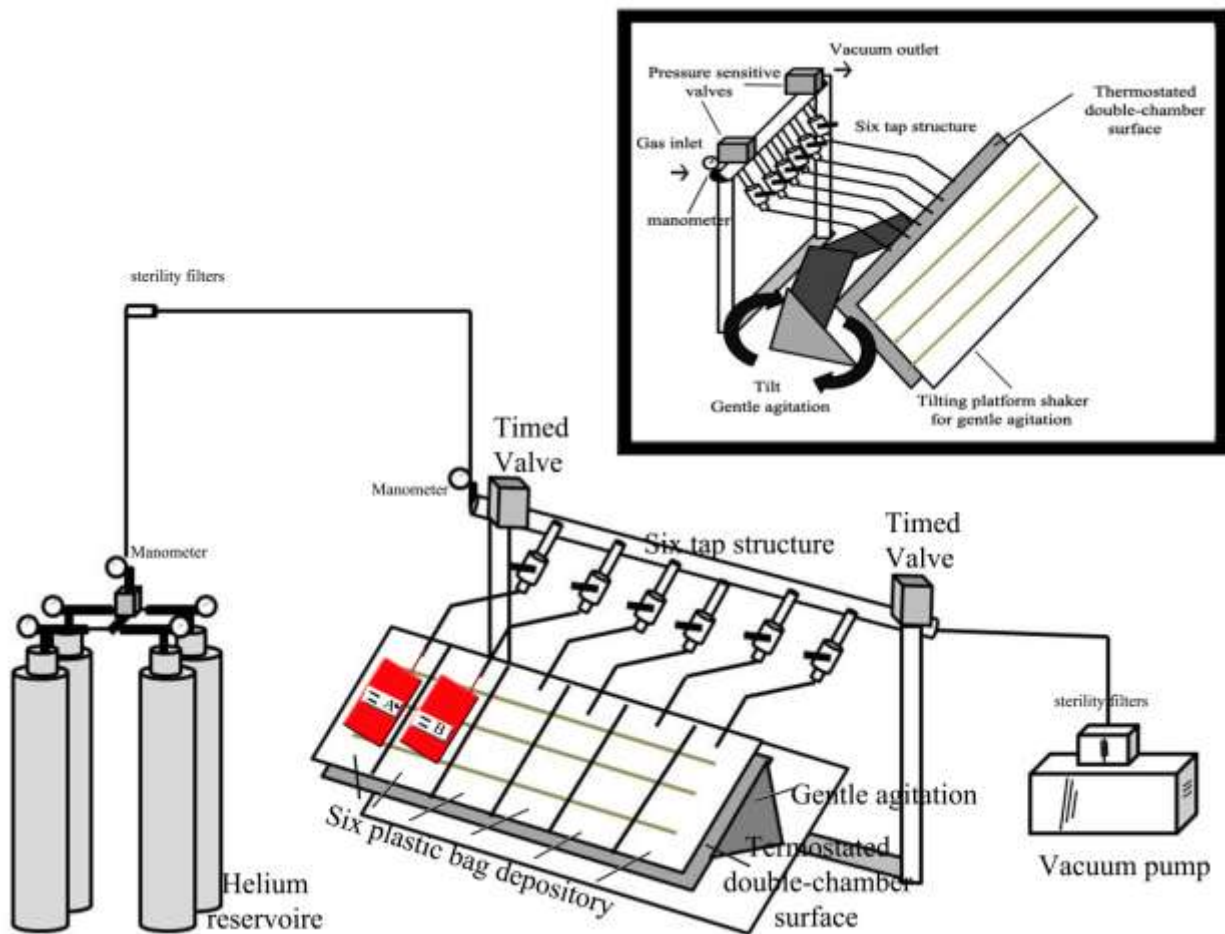


FIGURE 1 A schematization of the blood deoxygenation apparatus. Gas cylinders provide highest purity helium whose pressure is controlled through a manometer. Gas inlet is regulated in a closed system through a time valve which temporizes inlet and outlet towards a vacuum pump after 5 minutes of gas exchange within the plastic bag. Plastic bags are blocked almost horizontally as to favour gas exchange, through gentle agitation and temperature modulation. Sterility filters ensure sterility of the whole system, either in the gas inlet or outlet tubing.

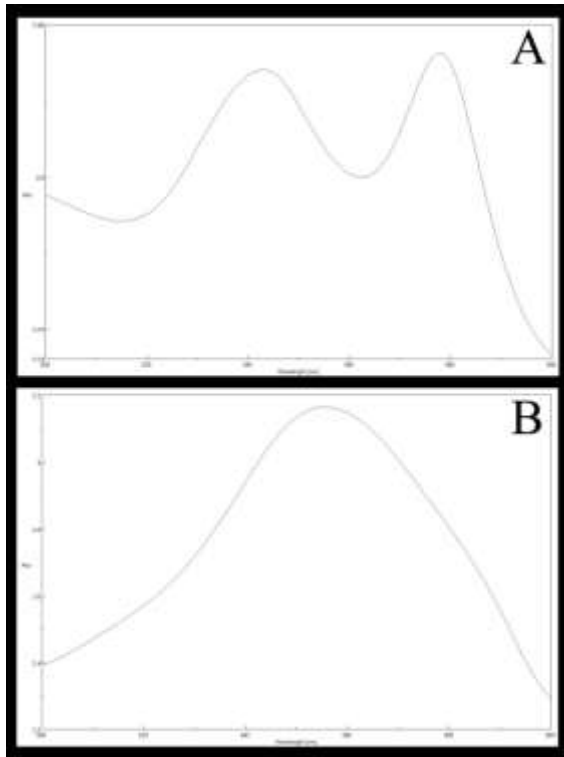


FIGURE 2 Spectrophotometric absorption of hemoglobin in the 500-600 nm range, prior to (A) or after (B) deoxygenation (30 min, 6 cycles of 5 minutes each). The assays were performed directly on red blood cells within the plastic bag, as described in the text. No significant scattering is observed

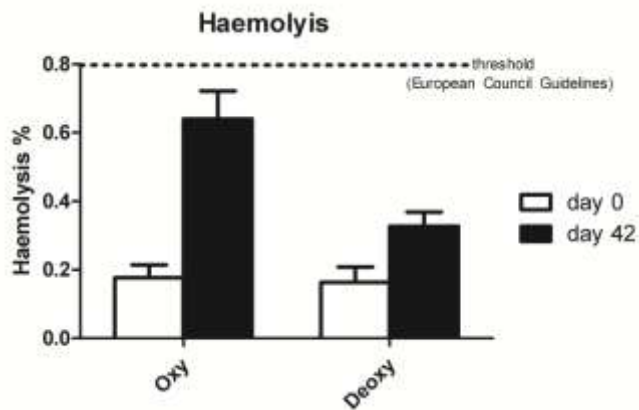


FIGURE 3 Haemolysis levels in control (left columns) red blood cells and red blood cells after deoxygenation (right columns) at day 0 (white columns) or after 42 days (black columns) of refrigerated liquid storage. At day 0, deoxygenated red blood cells do not show any significantly increased haemolysis. On the other hand, haemolysis is lower in deoxygenated red blood cells than in controls after 42 days of storage.

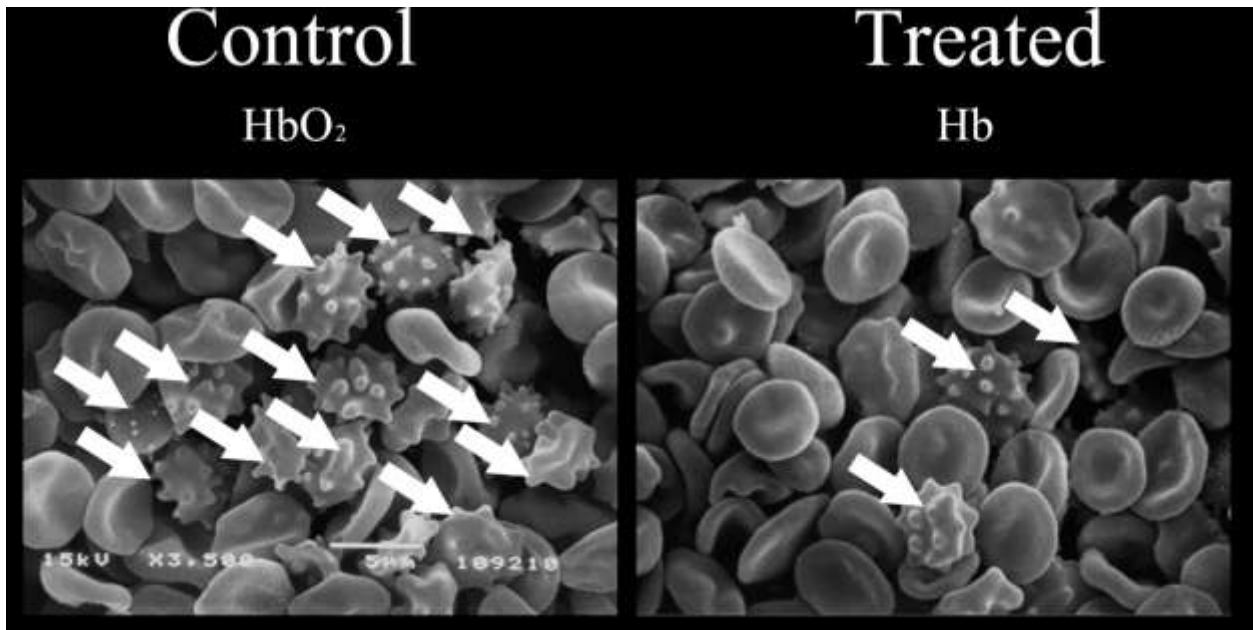


FIGURE 4 The extent of membrane shape alterations is lower in deoxygenated (right panel) than in control (left panel) red blood cells after 42 days of storage, as it emerged from preliminary scanning electron microscope (SEM) analysis.

7.2 Red blood cell metabolism under prolonged anaerobic storage

Overview of this section

Oxygen dependent modulation of red blood cell metabolism is a long investigated issue. However, the recent introduction of novel mass spectrometry-based approaches lends itself to implement our understanding of the effects of red blood cell prolonged exposure to anaerobiosis. Indeed, most of the studies conducted so far have addressed the short term issue, while the limited body of literature covering a 42 days storage period only takes into account a handful of metabolic parameters (ATP, DPG, glucose, glyceraldehyde 3-phosphate, lactate).

We hereby performed a mass spectrometry-based untargeted metabolomics analysis in order to highlight metabolic species in erythrocyte concentrates stored anaerobically in SAGM additive solutions for up to 42 days, by testing cells on a weekly basis.

We could confirm previous evidences about long term anaerobiosis promoting glycolytic metabolism in RBCs and prolonging the conservation of high energy phosphate reservoirs and purine homeostasis. In parallel, we evidenced that, contrarily to aerobic storage, anaerobiosis impairs erythrocyte capacity to cope with oxidative stress by blocking metabolic diversion towards the pentose phosphate pathway, which negatively affects glutathione homeostasis. Therefore, although oxidative stress was less sustained than in aerobically stored counterparts, oxidative stress markers still accumulate over anaerobic storage progression.

Keywords: red blood cell, metabolism, anaerobic storage, mass spectrometry, metabolomics.

1. Introduction

The main biological function of red blood cells (RBCs) is to deliver molecular oxygen (O_2) to tissues, a task that they fulfill through the allosteric regulation of hemoglobin (Hb) (Monod et al., 1965). Allosteric regulation is based upon the transition from a T-state to a relaxed R-state and viceversa, the former displaying lower oxygen affinity that results in oxygen release at the tissue level. The T-state of Hb (deoxygenated Hb) is stabilized by several factors, including low pH, high CO_2 and organic phosphates, including 2,3-diphosphoglycerate (DPG) and ATP (Jensen et al., 2004).

Accelerated glucose consumption, leading to lactate accumulation through the Embden-Meyerhof glycolytic pathway, fuels the generation of DPG and ATP to stabilize the system under hypoxic conditions (Murphy, 1960; Hamasaki et al., 1970), in a Pasteur effect-like phenomenon (Marshall et al., 1973). However, despite a 26% increase of the glycolytic rate upon deoxygenation of RBCs, Rapoport et al. reported that adenine nucleotides and DPG remained constant, as they become increasingly bound to deoxy-Hb (Rapoport et al., 1976).

Oxygenation state of Hb and metabolism are further intertwined, through the indirect modulation of glycolytic enzyme activities via competitive binding to the cytoplasmic domain of band 3 (CDB3) (Low et al., 1986; Chu et al., 2008). Indeed, deoxy-Hb displays a higher affinity for the CDB3 than does oxy-Hb (Walder et al., 1984; Chérite and Cassoly, 1985). The CDB3 is a membrane docking site for several enzymes of the glycolytic pathway, such as phosphofructokinase (PFK), aldolase, glyceraldehyde-3-phosphate dehydrogenase (GAPDH) and lactate dehydrogenase (LDH) (Low et al., 1986; Chu et al., 2008). When bound to the CDB3 these enzymes are inhibited, while their displacement from the membrane in consequence to the binding of deoxy-Hb to the CDB3 results in their activities being restored and thus, in metabolic modulation (Chérite and Cassoly, 1985). Several models have been proposed over the years, out of which the most widely accepted one is the one described into details by Low's (Low et al., 1986; Chu et al., 2008; Lewis et al., 2009) and Giardina's (Messana et al., 1996; Galtieri et al., 2002; Castagnola et al., 2010) groups, both stressing the role of oxygen-linked modulation of erythrocyte metabolism.

More recently, it has been indicated a role for the phosphorylation state of the tyrosine residues of the band 3 protein at position 8 and 21 in modulating the binding of glycolytic enzymes and deoxy-Hb to the CDB3 (Chérite and Cassoly, 1985). Phosphorylation to these residues results in an increased (+45%) glycolytic flux and reduced shift towards the pentose phosphate pathway (PPP) (-66%) than in oxygenated RBCs (Chérite and Cassoly, 1985). The underlying mechanism seems to involve the phosphorylation-dependent increase in the number of negative charges at the N-terminal domain of band 3, which greatly enhances Hb binding to band 3 and thus the displacement of glycolytic enzymes (Lewis et al., 2009). Notably, deoxygenation seems to promote phosphorylation of the CDB3 (Siciliano et al., 2010).

Over the years, several groups have contributed substantial efforts to the continuous improvement of existing mathematical and *in silico* models of RBC metabolism (Moses et al., 1972; Heinrich et al., 1977; Schauer et al., 1981; Ataullakhanov et al., 1981; Werner and Holzthutter et al., 1985; Heinrich, 1985; Nakayama et al., 1985; Mulquiney et al., 1999; Jamshidi et al., 2001; Wiback and Palsson, 2002), towards the achievement of a Systems Biology understanding of RBC metabolic complexity (Jamshidi and Palsson, 2006). In this view, Kinoshita and colleagues recently investigated the role of allostery in hypoxia-induced immediate metabolic alterations (within a 3

minutes framework upon deoxygenation) in RBCs through *in silico* prediction models (E-Cell 3 simulation environment) and experimental testing by means of capillary electrophoresis coupled with mass spectrometry (MS) (Kinoshita et al., 2007).

Over the last decades, several groups have monitored RBC metabolic fluxes under control (aerobic) conditions during a prolonged time span, while exploiting international guidelines for optimized RBC concentrate storage conditions as a model (Messana et al., 1999; Messana et al., 2000; Bennet-Guerrero et al., 2007; Nishino et al., 2009; Gevi et al., 2012). From these studies it emerged that, under control storage conditions (storage in presence of additive solutions such as SAGM (Gevi et al., 2012) and PAGGM (Nishino et al., 2009), under refrigeration at 1-6°C for up to 42 days) RBCs face a rapid fall of the glycolytic rate and undergo an accumulation of glycolysis end products. A shift was observed towards the oxidative phase of PPP (Gevi et al., 2012), in response to an exacerbation of oxidative stress (altered glutathione homeostasis, accumulation of ROS, protein carbonylations, malondialdehyde and peroxidation/inflammatory products in the supernatants) (Gevi et al., 2012; D'Alessandro et al., 2012). Indeed, it is now widely accepted that long stored RBCs under blood bank conditions suffer from oxidative stress-triggered “storage lesions”, a series of either reversible or irreversible modifications to RBC morphology and biochemistry (both at the proteomic and metabolic level) (D'Amici et al., 2007; D'Alessandro et al., 2012). Within this framework, in the transfusion milieu alternative storage strategies for RBC concentrates have been pursued with the goal to improve RBC quality and viability, and to extend the shelf life of erythrocyte concentrates up to 63 days, a goal that might be achieved through deoxygenation of RBC units (Yoshida et al., 2007; Dumont et al., 2009; Yoshida and Shevkoplays, 2010). While these alternative storage strategies are currently under clinical testing (Yoshida and Shevkoplays, 2010), it is yet to be assessed whether the observed alterations of the metabolic fluxes in RBCs upon deoxygenation are persistent throughout a 42 days storage period. Indeed only preliminary, albeit significant, information has been gathered by comparing a handful of metabolic parameters over a 42 days anaerobic storage period, including glucose consumption, glyceraldehydes 3-phosphate accumulation (via glycolysis or PPP) in high versus low oxygen saturated hemoglobin conditions (Galtierei et al., 2002), ATP and 2,3-DPG (Scalbert et al., 2009), and lactate (Galtieri et al., 2002; Scalbert et al., 2009). Taking advantage of recent technical improvements in the field of metabolomics (Scalbert et al., 2009), we hereby investigated the RBC metabolome of deoxygenated RBC units by means of a novel high performance liquid chromatography (HPLC)-micro-time of flight-quadrupole (micro-TOF-Q) mass spectrometry (MS) approach, a workflow that recently contributed precious insights in the understanding of RBC metabolism under control blood banking conditions (Gevi et al., 2012), or in pathological RBCs (e.g. hereditary stomatocytosis, sickle cell disease) (Darghouth et al., 2010, 2011a and 2011b).

Design and Method

Sample collection

Red blood cell units were drawn from healthy donor volunteers according to the policy of the Italian National Blood Centre guidelines (Blood Transfusion Service for donated blood) and upon informed consent in accordance with the declaration of Helsinki. We studied RBC units collected from 10 healthy donor volunteers [male=5, female=5, age

39.4 ± 7.5 (mean \pm S.D.)]. RBC units were stored for up to 42 days under standard conditions (CDP-SAGM, 4°), while samples were removed aseptically for the analysis on a weekly basis (at 0, 7, 14, 21, 28, 35 and 42 days of storage).

Deoxygenation of erythrocyte concentrate units was achieved through 5 repeated gas exchange cycles consisting in bubbling high purity helium (Sol S.p.A. – Pomezia, Italy) under gentle agitation every 10 minutes at room temperature for 50 minutes, while maintaining sterile conditions, as previously reported³⁴. Control counterparts were maintained at the same room temperature conditions in order to exclude any other bias to RBC metabolism than deoxygenation itself. Deoxygenated units were stored under a helium gas atmosphere under standard conditions (4°C). Deoxygenation was confirmed through spectrophotometric assays in the range between 500 – 650 nm.

Materials

Acetonitrile, formic acid, and HPLC-grade water, purchased from Sigma Aldrich (Milano, Italy). Standards (equal or greater than 98% chemical purity) ATP, L-lactic acid, phosphogluconic acid, NADH, D-fructose 1,6-biphosphate, D-fructose 6-phosphate, glyceraldehydes phosphate, phosphoenolpyruvic acid, L-malic acid, L-glutamic acid, oxidized glutathione, a-ketoglutarate were purchased from Sigma Aldrich (Milan). Standards were stored either at -25°C, 4°C or room temperature, following manufacturer's instructions. Each standard compound was weighted and dissolved in nanopure water. Starting at a concentration of 1 mg/ml of the original standard solution, a dilution series of steps (in 18 MΩ, 5% formic acid) was performed for each standard in order to reach the determine the linearity range for relative quantitation using peak areas.

Untargeted Metabolomics Analyses

Metabolite extraction

For each sample, 0.5mL from the pooled erythrocyte stock was transferred into a microcentrifuge tube (Eppendorf® Germany). Erythrocyte samples were then centrifuged at 1000g for 2 minutes at 4°C. Tubes were then placed on ice while supernatants were carefully aspirated, paying attention not to remove any erythrocyte at the interface. Samples were extracted following the protocol by D'Alessandro et al. (2011). The erythrocytes were resuspended in 0.15 mL of ice cold ultra-pure water (18 MΩ) to lyse cell, then the tubes were plunged into a water bath at 37°C for 0.5 min. Samples were mixed with 0.6 mL of -20°C methanol and then with 0.45 mL chloroform. Subsequently, 0.15ml of ice cold ultra-pure water were added to each tube and they were transferred to -20°C freezer for 2-8 h. An equivalent volume of acetonitrile was added to the tube and transferred to refrigerator (4°C) for 20 min. Samples with precipitated proteins were thus centrifuged for 10000 x g for 10 min at 4 °C .

Finally, samples were dried in a rotational vacuum concentrator (RVC 2-18 - Christ GmbH; Osterode am Harz, Germany) and re-suspended in 200 µl of water, 5% formic acid and transferred to glass auto-sampler vials for LC/MS analysis.

Rapid Resolution Reversed-Phase HPLC

An Ultimate 3000 Rapid Resolution HPLC system (LC Packings, DIONEX, Sunnyvale, USA) was used to perform metabolite separation. The system featured a binary pump and vacuum degasser, well-plate autosampler with a six-

port micro-switching valve, a thermostated column compartment. Samples were loaded onto a Reprisil C18 column (2.0mm×150mm, 2.5 µm - Dr Maisch, Germany) for metabolite separation.

Chromatographic separations were achieved at a column temperature of 30°C; and flow rate of 0.2 mL/min. For downstream negative ion mode (-) MS analyses, A 0–100% linear gradient of solvent A (10mM tributylamine aqueous solution adjusted with 15mM acetic acid, pH 4.95) to B (methanol mixed with 10 mM TBA and with 15 mM acetic acid, pH 4.95) was employed over 30 min, returning to 100% A in 2 minutes and a 6-min post-time solvent A hold. For downstream positive ion mode (+) MS analyses, a 0–100% linear gradient of solvent A (ddH₂O, 0.1% formic acid) to B (acetonitrile, 0.1% formic acid) was employed over 30 min, returning to 100% A in 2 minutes and a 6-min post-time solvent A hold.

Mass Spectrometry: Q-TOF settings

Due to the use of linear ion counting for direct comparisons against naturally expected isotopic ratios, time-of-flight instruments are most often the best choice for molecular formula determination. Thus, mass spectrometry analysis was carried out on an electrospray hybrid quadrupole time-of flight mass spectrometer MicroTOF-Q (Bruker-Daltonik, Bremen, Germany) equipped with an ESI-ion source. Mass spectra for metabolite extracted samples were acquired both in positive and in negative ion mode. ESI capillary voltage was set at 4500V (+) (-) ion mode. The liquid nebulizer was set to 27 psi and the nitrogen drying gas was set to a flow rate of 6 L/min. Dry gas temperature was maintained at 200°C. Data were stored in centroid mode. Data were acquired with a stored mass range of m/z 50–1200. Automatic isolation and fragmentation (AutoMSⁿ mode) was performed on the 4 most intense ions simultaneously throughout the whole scanning period (30 min per run).

Calibration of the mass analyzer is essential in order to maintain a high level of mass accuracy. Instrument calibration was performed externally every day with a sodium formate solution consisting of 10 mM sodium hydroxide in 50% isopropanol: water, 0.1 % formic acid. Automated internal mass scale calibration was performed through direct automated injection of the calibration solution at the beginning and at the end of each run by a 6-port divert-valve.

Data elaboration and statistical analysis

In order to reduce the number of possible hits in molecular formula generation, we exploited the SmartFormula3DTM software (Bruker Daltonics, Bremen, Germany), which directly calculates molecular formulae based upon the MS spectrum (isotopic patterns) and transition fingerprints (fragmentation patterns). This software generates a confidence-based list of chemical formulae on the basis of the precursor ions and all fragment ions, and the significance of their deviations to the predicted intact mass and fragmentation pattern (within a predefined window range of 5 ppm). Triplicate runs for each one of the 10 biological replicates over storage duration were exported as mzXML files and processed through XCMS data analysis software (Scripps Centre for Metabolomics) (Tautenhahn et al., 2011) and MAVEN (Melamud et al., 2010). Mass spectrometry chromatograms were elaborated for peak alignment, matching and comparison of parent and fragment ions, and tentative metabolite identification (within a 20 ppm mass-deviation range between observed and expected results against the internal database – METLIN

(Melamud et al., 2010)). XCMS and MAVEN are open-source software that could be freely downloaded from their websites (<http://metlin.scripps.edu/download/> and <http://genomics-pubs.princeton.edu/mzroll/index.php?show=download>). Metabolite assignment was further elaborated in the light of the hydrophobicity/hydrophilicity of the compound and its relative retention time in the RP-HPLC run (as gleaned through database information and, for a subset of metabolites enlisted above in the *Materials* section, against commercial ultra-pure standards – **Supplementary Figure 1**). Relative quantitative variations of intact mass peak areas for each metabolite assigned through MS/MS were determined against day 0 controls and only statistically significant results were considered (ANOVA *p-values* < 0.01). Data were further refined and plotted with GraphPad Prism 5.0 (GraphPad Software Inc.)

Results and Discussions

HPLC-MS runs were performed in triplicate on samples extracted from each donated unit at 0, 7, 14, 21, 28, 35, 42 days of storage. Due to the massive amount of output data, only significant results displaying absolute values for fold-change variations higher than 1.5 (7, 14, 21, 28, 35 or 42 day against day 0) were summarized as in **Supplementary Tables 1-6** (please, refer to D'Alessandro et al., 2013), along with feature number, feature name, *p-value*, mass to charge ratio (m/z), chromatographic retention times, day specific intensities and tentative identification (with isotope description, molecular weight deviation in ppm from database top hit reports, name, presence of K⁺, Na⁺, NH₄⁺ adducts and METLIN identifier), as identified by XCMS (Tautenhahn et al., 2011; Smith et al., 2005). In order to report the main results in a more readable layout, metabolites accounting for the most relevant catabolic pathways in RBCs were grouped and plotted as follows: metabolites involved in (i) glycolysis (**Figure 1**), (ii) adenosine energy metabolism (**Figure 2**), (iii) pentose phosphate pathway (PPP) and glutathione homeostasis (**Figure 3**); (iv) purine salvage pathway (PSP – **Figure 4**), (v) aminoacid transport and fatty acid/lipid metabolism (**Figure 5**); and (vi) oxidative stress markers and vitamins (**Supplementary Figure 2**).

Finally, results were graphed in **Figure 6** as heat maps for the main RBC metabolic pathways (Kinoshita et al., 2007), where a graph is reported for each time point assayed (anaerobic storage weeks 1 to 6) and metabolites are plotted as red or blue circles, in relation to their increase or decrease, respectively, in comparison to day 0 values.

Glycolysis and energy metabolism are sustained throughout anaerobic storage duration

Under control storage conditions, prolonged glycolysis and lactate accumulation result in pH drop and, in turn, this triggers a negative feedback on the glycolysis rate itself. Indeed, glycolytic enzymes (for example the rate limiting enzyme phosphofructokinase) are inhibited by (i) low pH (Burger et al., 2010); (ii) high concentrations of high energy phosphate compounds, such as ATP and DPG; (iii) selective binding to the CDB3 (Weber et al., 2004). All these events are known to occur within the framework of RBC storage (D'Alessandro et al., 2010). The rapid fall of glycolysis over storage duration has been recently detailed by Nishino et al. (2009) for PAGGM-stored RBCs and our group (SAGM-stored RBCs) (Gevi et al., 2012; D'Alessandro et al., 2012). In deoxygenated RBC units, it is to be expected that these phenomena are mitigated to some extent, owing to the following reasons: (i) Hb is forced in the T-state (deoxy-Hb); (ii) free H⁺ ions are bound to deoxy-Hb as a result of the Bohr effect (Jensen et al., 2004);

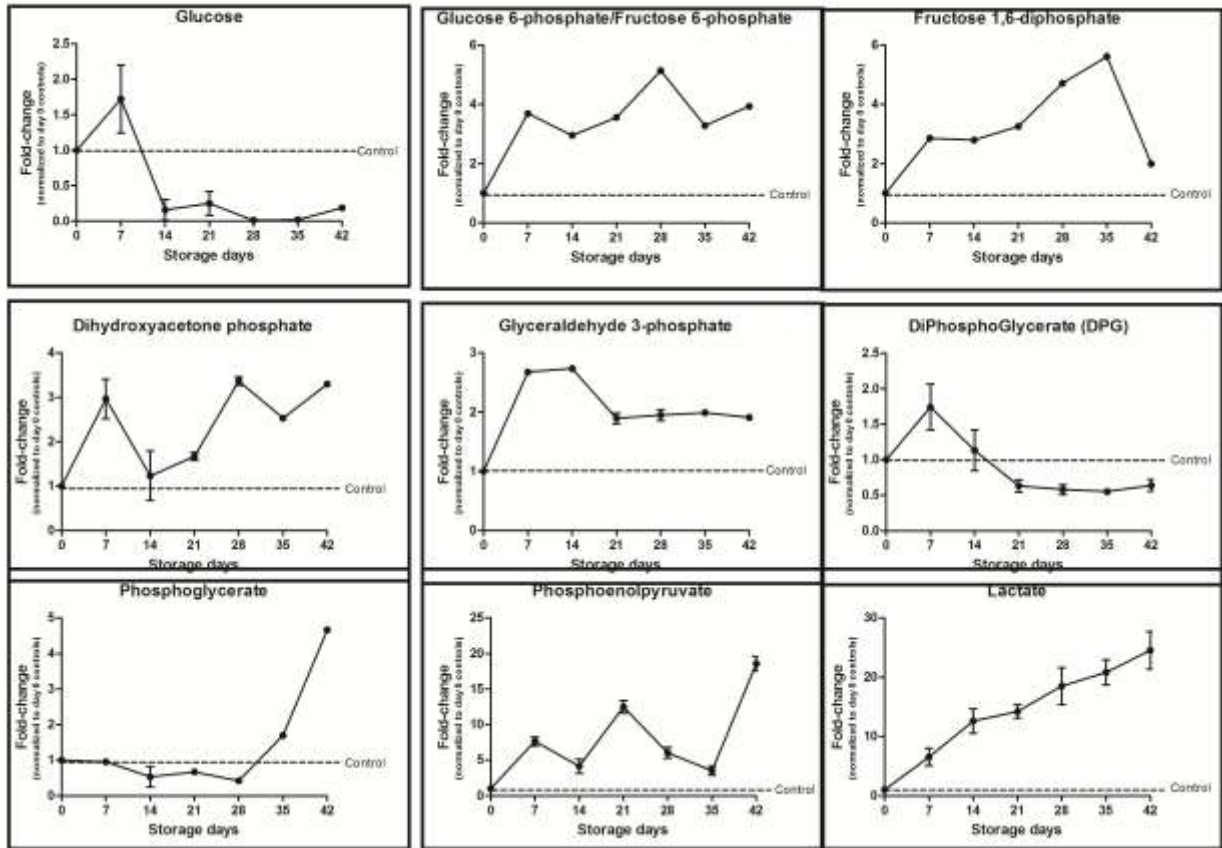


FIGURE 1 Time course metabolomic analyses of RBCs stored under anaerobiosis in SAGM additive solution at 4°C up to 42 days. Results are plotted on a weekly basis (storage day 0, 7, 14, 21, 28, 35, 42) as in [31], as fold-change variations upon normalization against day 0 controls. An overview of the trends for glycolytic metabolites. Averages and standard deviations were calculated on 10 biological replicates, each one assayed in triplicate runs at each storage day.

(iii) high energy phosphates (mainly 2,3-DPG) are sequestered by deoxy-Hb at a near 1:1 stoichiometric ratio (Jensen et al., 2004); (iv) competitive binding of deoxy-Hbs to the CDB3 dislocates and disinhibits glycolytic enzymes (Low et al., 1986; Messana et al., 1996; Galtieri et al., 2002; Chu et al., 2008; Lewis et al., 2009; Castagnola et al., 2010). Consistently with these assumptions, in anaerobically-stored RBCs we could observe a rapid increase in glucose consumption, that was paralleled by the accumulation of all glycolytic intermediates, including: glucose/fructose 6-phosphate (these isobaric species cannot not be distinguished with MS, as previously reported (Darghouth et al., 2011; Gevi et al., 2012)), fructose 1,6-diphosphate, dihydroxyacetone phosphate, glyceraldehyde 3-phosphate, phosphoglycerate (though increasing significantly upon 35 days of anaerobic storage), phosphoenolpyruvate and lactate (**Figure 1**). At the end of the anaerobic storage lactate increased by 24.55 ± 3.17 fold in comparison to day 0 controls, which is consistent with previous reports by Yoshida's group (2007 and 2008) and it is higher in comparison to our previous metabolomic investigation of RBCs stored under control (aerobic conditions) at the end of the storage period (42 days lactate being 20.48 ± 0.31 (Gevi et al., 2012)). Recently,

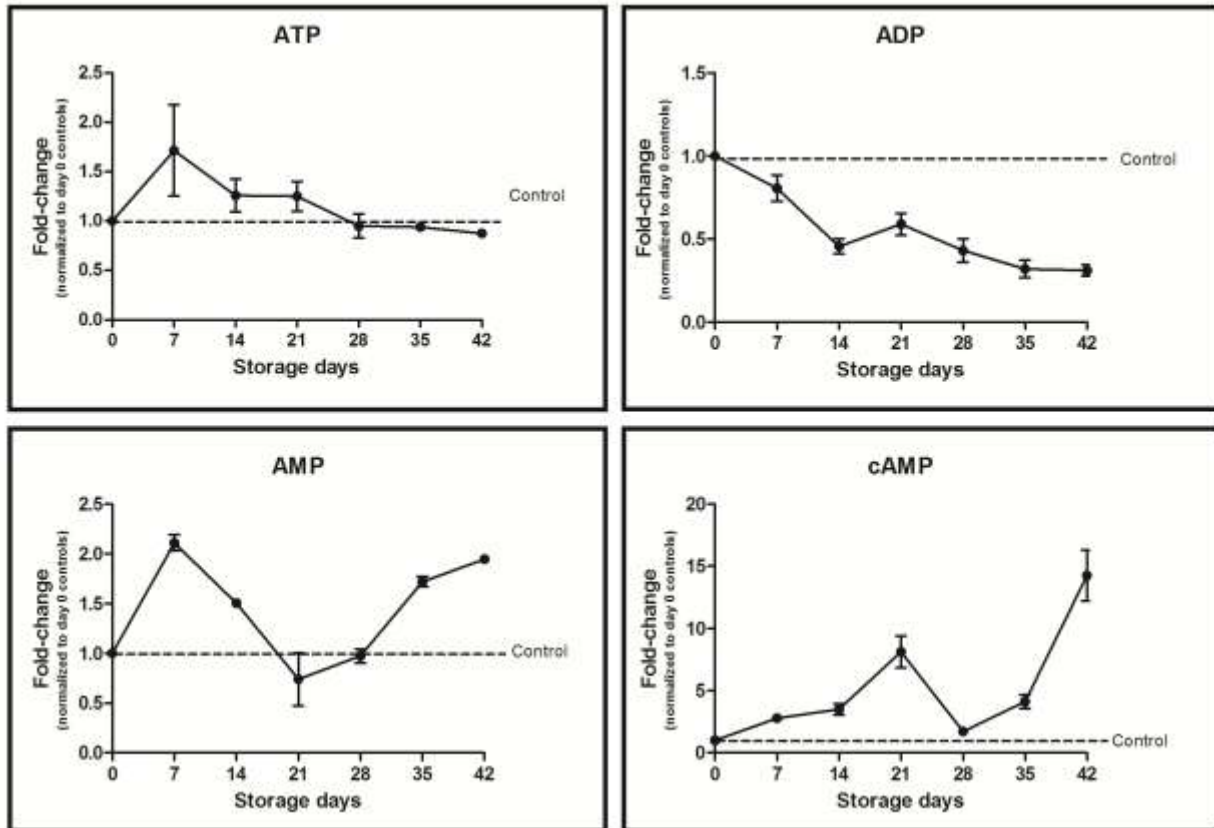


FIGURE 2 An overview of the trends for adenosine energy metabolism and related metabolites in time course analyses of RBC anaerobic storage on a weekly basis. Results are plotted as fold-change variations upon normalization to day 0 controls.

Yoshida and colleagues reported that under anaerobic storage conditions, 2,3-DPG levels are sustained significantly longer than in conventional storage, since 2,3-DPG increased to over 100% of the initial level within the first week and then declined to below the initial concentration only in week 3 (Yoshida and Shevkoplays, 2010). Our results are in agreement with these observations (**Figure 1**).

Glycolysis rate drops under control (aerobic) storage conditions, which results in ATP concentrations reaching a climax at 10-20% above starting level within the first two-three weeks of storage, while they rapidly decline soon afterwards (Gevi et al., 2012; D'Alessandro et al., 2012). This is biologically relevant if we consider that the fall of ATP levels and of the total adenylate content (ATP+ADP+AMP) is associated with poor in vivo survival (Hogman et al., 1985), since the energy-less RBC is rapidly removed from the bloodstream (van Wijk and van Solinge, 2005). While these considerations holds true for aerobic RBC storage, under anaerobic conditions, Yoshida and colleagues reported that ATP peaks at higher levels (50-70% above the initial concentration), and this phase of ATP boost is sustained for a longer period (5-7 weeks) (though their observations also depended on the additive solutions used as a medium for RBC storage) (Dumont et al., 2009; Yoshida and Shevkoplays, 2010). Our results (**Figure 2**) are consistent with these observations. It should be also noted that erythrocytes tend to release ATP as a vasodilator

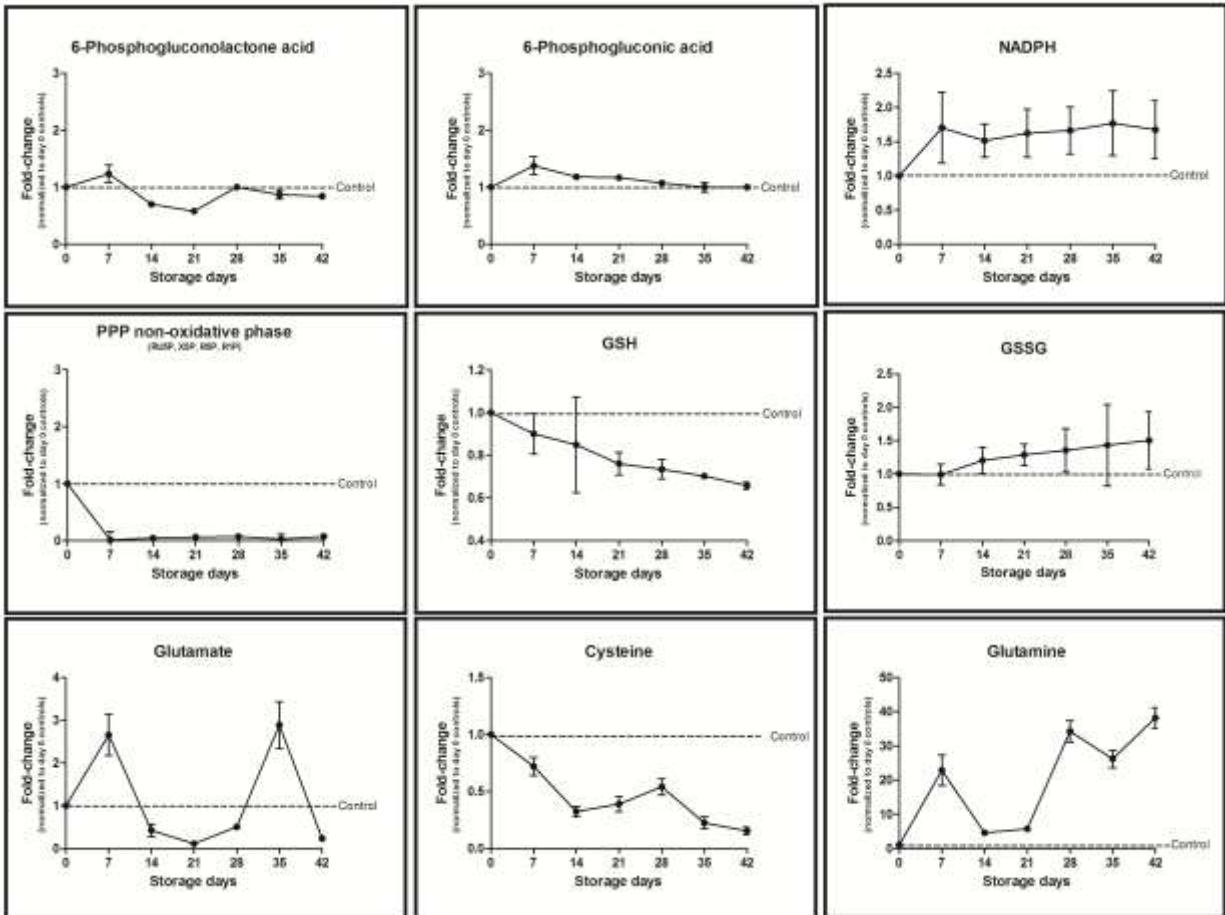


FIGURE 3 An overview of the trends for the pentose phosphate pathway and glutathione homeostasis during time course analyses of RBC anaerobic storage on a weekly basis. Results are plotted as fold-change variations upon normalization to day 0 controls.

molecule in response to hypoxia (Dietrich et al., 2000), and ADP negatively regulates this process by acting on P2Y13 receptors of human RBCs (Wang et al., 2005). In the present study, we could observe that ADP levels decreased over storage duration, while AMP levels suffered from oscillations as they underwent both an early and late increase within the first and the last two weeks of storage (**Figure 2**). On the other hand, cAMP levels increased throughout anaerobic storage duration, reaching an intermediate peak by day 21 and apexing by day 42 of anaerobic storage (**Figure 2**). The increase in cAMP over storage duration is consistent with ATP decrease despite sustained glycolysis in the long term, since cAMP accumulation under hypoxic conditions might trigger ATP release through signalling cascades involving cAMP-dependent protein kinase (PKA) and downstream activated pathways, such as the ones leading to mechanical deformation mediated by the activity of the cystic fibrosis transmembrane conductance regulator (CFTR) (Sprague et al., 2001).

No significant shift towards the pentose phosphate pathway (PPP) despite moderate oxidative stress

PPP accounts only for approximately 8% of glucose metabolism in RBCs under normal steady-state conditions, since 92% of glucose is metabolized through glycolysis (Embden Meyerhof). When faced with oxidative stress, RBCs respond diverting as much as 90% of glucose metabolism toward the PPP (Messana et al., 1999; Misiti et al., 2002). The rationale behind this phenomenon is in part explained by Rogers and colleagues, who envisage a role for the oxygen dependent modulation of glycolytic enzyme activity via competitive binding to the CDB3 and their availability to compete for glucose substrates with the PPP enzymes (Rogers et al., 2009).

Approximately 60% of the total NADPH production in humans relies on the PPP, as obtained through reduction of NADP⁺. This reaction is coupled to the formation of 6-phosphogluconolactone from glucose 6-phosphate and ribulose 5-phosphate from 6-phosphogluconate. The latter end-product of the oxidative phase is represented by ribulose 5-phosphate, that can further react with non-oxidative phase intermediates (carbon chain molecules ranging from 3 to 7 carbon atoms) and re-enter glycolysis at the glyceraldehydes 3-phosphate level, and/or rather be recycled as fructose 6-phosphate, as early glycolytic precursor. Since NADPH is needed to reduce the disulfide form of glutathione (GSSG) to the sulfhydryl form (GSH), oxidative stress modulated increase in the PPP rate is to be considered a natural self-defensive mechanism of erythrocytes to cope with oxidative injury, as also deducible from widespread hereditary anomalies to rate limiting enzymes of this pathways (Efferth et al., 2004; Fico et al., 2004). In 1999, Dumaswala et al. demonstrated that GSH and glutathione peroxidase provide the primary antioxidant defense in stored RBCs, and their decline, concurrent with an increase in oxidative modifications of membrane lipids and proteins, is tied to the destabilization of the membrane skeleton and thus to a compromised RBC survival (Dumaswala et al., 1999). Indeed, GSH is pertinent for maintaining the normal structure of RBCs and for keeping haemoglobin in the ferrous state [Fe(II)]. Recently, we observed that storage of RBC under control aerobic conditions resulted in a metabolic diversion towards the oxidative phase of the PPP in the short term (after the second week of storage), while metabolic end-products of the non-oxidative phase of the PPP appeared to serve as substrates for PSP reactions, rather than for massively re-entering glycolysis (Gevi et al., 2012). This observation was consistent with an early increase of glyceraldehyde 3-phosphate production via the PPP early upon exposure to high oxygen saturation conditions, while differences with erythrocytes exposed to low oxygen saturation conditions were attenuated in the long term (Messana et al., 1999). In the present study, we observed no evident increase of PPP oxidative phase intermediates, while isobaric species in the non-oxidative phase of the PPP suffered from an early decline below control levels yet by anaerobic storage day 7 (ribulose 5-phosphate, Xylose 5-phosphate, ribose 5-phosphate, ribose 1-phosphate - could not be distinguished through the current MS approaches, in agreement with Kinoshita et al., (2007) and Gevi et al. (2012)) (**Figure 3**). The blockade of the storage-dependent metabolic diversion towards the PPP is in line with the observations by Rogers and colleagues about short term RBC exposure to hypoxia (Rogers et al., 2009).

GSH is synthesized through a two step ATP-dependent process: in the first and rate limiting step, the enzyme gamma-glutamylcysteine synthetase exploits the aminoacidic substrates, glutamate and cysteine to generate gamma-glutamylcysteine; in the second step, glycine is added by glutathione synthetase (Lu, 2009). The levels of glutamine (precursor to glutamate – oscillating trend), increased over anaerobic storage (**Figure 3**). Conversely, free cysteine

decreased over anaerobic storage duration (**Figure 3**). It is interesting to note that HEK293 and Hep3B cells exposed to 1.5% O₂ exhibit a time-dependent decrease in cellular glutathione stores and concomitant inhibition of glutathione biosynthesis, which correlates to impaired transport of the substrate cystine (Mansfield et al., 2004). Also, anoxia impairs cysteine-dependent GSH biosynthesis more than hypoxia in hepatocytes owing to lower ATP production via mitochondria (Shan et al., 1989). However, it is worthwhile to stress that, unlike hepatocytes, RBCs do no longer have mitochondria.

Therefore, oxygen removal appeared not to completely eliminate oxidative stress, as suggested by the following observations: (i) the moderate albeit constant decrease of GSH and (ii) increase in GSSG levels (**Figure 3**); (iii) the accumulation of inflammation/oxidative stress-related markers such as prostaglandin D₂/E₂ and thromboxane A₂ (Ibe et al., 1997) (**Supplementary Figure 2**); and (iv) the decrease of antioxidant exogenous compounds such as catechins and epicatechins (D'Alessandro and Zolla, 2012) (**Supplementary Figure 2**). On the other hand, the oxidative stress-marker prostaglandin F_{2α} (8-isoprostane (Karon et al., 2012)) decreased significantly over anaerobic storage duration (**Supplementary Figure 2**). First of all, it is to be excluded that the observed phenomena are to be attributed to partial deoxygenation (hypoxia instead of anoxia), since deoxy-Hb spectrophotometric spectra were assayed and confirmed in the 500–650 nm range. Indeed, enhanced rates for the formation of ROS and RNS occur under hypoxic conditions where an increased fraction of Hb is bound to the RBC membrane (Rifkind et al., 2012). Under normoxic RBC storage conditions, Hb migration to the membrane fraction is accompanied by increased membrane-bound levels of active peroxiredoxin 2 (Rinalducci et al., 2011), which binds to the same membrane docking site (i.e. the CDB3 – Matte et al., 2012) thereby mitigating membrane-targeting oxidative stress. However, peroxiredoxin 2 migration to the membrane does not occur during storage under anaerobic conditions (Rinalducci et al., 2011), which might imply that oxidative stress is not as much sustained as in normoxic counterparts as to activate certain anti-oxidant defensive mechanisms. It should be also noted that, under hypoxic (not anaerobic) conditions, when Hb is partially saturated with oxygen, the oxygen is constantly leaving one Hb molecule and binding to another. Thus, intermediate oxygen pressures and hypoxic conditions in RBCs favour the production of superoxide radical from Hb-bound oxygen, owing to enhanced heme pocket flexibility and higher interactions with distal histidine, which in turn promotes the destabilization of the iron-oxygen bond and in the release of superoxide radicals (Balagopalakrishna et al., 1996). In this view, anaerobic storage strategies failing to achieve complete Hb deoxygenation should take this phenomenon into serious account.

A rationale behind the incomplete elimination of oxidative stress under anaerobic conditions might stem from considerations about the interplay of pro-oxidant/anti-oxidant mechanisms in RBCs (Tsikas et al., 2012). Tsikas et al. (2012) recently reported that GSH promoted the concomitant formation of the current oxidative stress biomarkers malondialdehyde (MDA) and prostaglandins from arachidonic acid via prostaglandin H synthases. On this ground, it emerges that uncommon interplay of enzymatic and chemical reactions might yield species that are considered to be exclusively produced by free-radical-catalysed reactions (Tsikas et al., 2012).

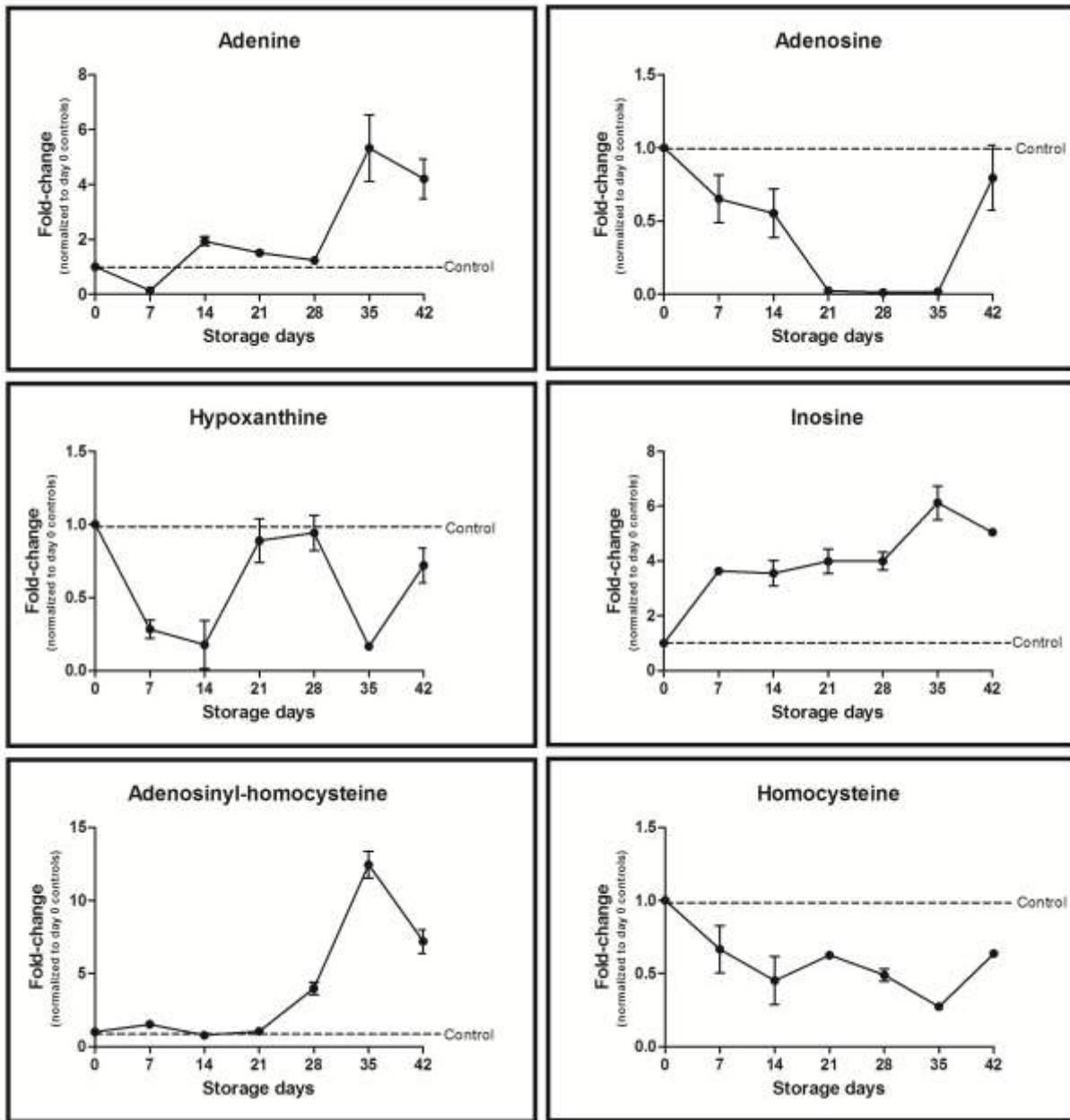


FIGURE 4 Purine salvage pathway main metabolites during RBC anaerobic storage on a weekly basis. Results are plotted as fold-change variations upon normalization to day 0 controls.

Purine Salvage Pathway is activated proportionally to storage progression even under anaerobic conditions

Since mature RBCs are incapable of *de novo* synthesizing 5-phosphoribosylamine, they rely on salvage pathways to restore purine levels (Schuster et al., 2005). Adenine and adenosine are transported through the erythrocyte membranes through the facilitated diffusion (Hess et al., 2010). They are the precursors of adenine nucleotides, accounting for the 70–80% of all free erythrocyte nucleotides (Schuster et al., 2005; Hess, 2010). Anaerobic storage

resulted in increase in intracellular adenine levels, while adenosine followed oscillating trends (despite being comparable to day 0 controls by 42 days of storage – **Figure 4**).

Hypoxanthine and inosine are two major substrates for salvage reactions (Zolla et al., 1977; Schuster et al., 2005). While hypoxanthine levels oscillated throughout anaerobic storage, inosine levels increased significantly, proportionally to anaerobic storage progression. Altered inosine levels in particular might result from deamination of adenosine, which is known to occur under control RBC storage conditions (Hess, 2010). Inosine formed in the adenosine deaminase reaction or supplemented to RBC via storage solutions may enter the erythrocyte and undergo phosphorolysis to form hypoxanthine and ribose 1-phosphate (R1P) (Gabrio et al., 1956).

Through this reaction it is possible to introduce a phosphorylated sugar (PPP non-oxidative phase intermediate) into the erythrocyte without ATP consumption (Gabrio et al., 1956). The use of inosine has received much attention in the field of blood banking since it appears to be the only practical means to obtain ATP production in the cell without first expending ATP to prepare an unphosphorylated substrate for further metabolism (Gabrio et al., 1956).

Adenosine-homocysteine, which serves as a substrate to produce adenosine and homocysteine, accumulated in long anaerobically stored RBCs, while homocysteine decreased (**Figure 4**). Homocysteine is also a precursor to cysteine (also decreasing – **Figure 3**) and thus has an indirect role in GSH synthesis (Filip et al., 2012). Anomalies to homocysteine fine-tuning are known to be related to oxidative stress (Filip et al., 2012) and deficiency B-group vitamins (Curtis et al., 1994). However, no substantial alteration of vitamin intake was observed (retinol – vitamin A, riboflavin vitamin B2 – **Supplementary Figure 2**).

Amino acid transport and lipid homeostasis is affected to some extent under anaerobic storage

Though RBC metabolism has been hitherto supposed to be restricted to pathways enlisted in the previous paragraphs (glycolysis, PPP, PSP, Rapoport-Luebering, methemoglobin reduction pathway), recent advancements in the understanding of the RBC proteome suggested that erythrocytes might also rely on yet undisclosed/uncharacterized pathways (Roux-Dalvai et al., 2008; D'Alessandro et al., 2010). In a recent report, Darghouth et al. (2011) indicated that 30.4% of the RBC metabolome (including 89 validated metabolites) was made up of free aminoacids. The capillary distribution of RBCs through the cardiovascular system allows RBCs to intake aminoacids from plasma, store and deliver them to those districts where they are needed the most. In this view, RBCs might represent active vessels in the inter-organ transport (Elwyn et al., 1972).

Owing to the lack of nuclei and ribosomes, RBCs are devoid of any protein synthesis capacity. Nonetheless, numerous aminoacid transport systems have been found in human RBCs in analogy to other cell types, and anomalies to these RBC aminoacid transport systems have been related to several diseases, including chronic renal failure (Divino Filho et al., 1997; Canepa et al., 2002).

Free arginine levels increased over anaerobic storage, while ornithine decreased (**Figure 5**). While arginase-mediated conversion of arginine to ornithine and urea mainly occurs in liver, arginase is also present in RBCs⁸¹. In circulating RBCs, arginine could be imported from plasma to RBCs through the y⁺ system (Tunncliffe et al., 1994), or might be produced in RBCs from aspartate as demonstrated in analogy to other cell types (Kanehisa et al., 2000). Arginine might be produced from citrulline and argino-succinate, while the metabolic pathway might shift back to citrulline via nitric oxide synthase (which is present and functionally active in RBCs – Kleinbongard et al., 2006),

resulting in the production of NO. This is particularly relevant in the frame of deoxygenated districts, where deoxy-Hb binds to NO[•] thus functioning as a transporter and/or reduces nitrite to generate NO[•] promoting vasodilation (Filip et al., 2012). Consistently, while argino-succinate decreased in like fashion to ornithine, anaerobic storage promoted the accumulation of both arginine and citrulline (**Figure 5**). These results might contribute to justify the observation about oxidative stress in long stored deoxygenated RBC units.

Phosphoglycerate dehydrogenase, a key enzyme in serine metabolism (Locasale et al., 2011), has been reported in the most recently-updated report about the RBC proteome (D'Alessandro et al., 2010). L-serine decreased yet upon 7 days of anaerobic storage, while its concentrations remained apparently unaltered thereon (**Figure 5**).

Tryptophan transport in RBCs has been investigated during the last three decades (Rosenberg et al., 1980), owing to its implications in the pathogenesis of depressive disorders (Jeanningros et al., 1996). Tryptophan uptake increased in the time window range between 21 and 35 days of storage, though at the end of the storage intracellular tryptophan levels were comparable to those in day controls (**Figure 5**).

While mature RBCs are incapable of synthesizing lipids anew (Percy et al., 1973), alterations to lipid homeostasis are strictly tied to membrane blebbing leading to vesiculation and eryptosis (Lang et al., 2012), a phenomenon that is known to be exacerbated by ceramides. Ceramide may be produced from cell membrane sphingomyelin by a sphingomyelinase (Dinkla et al., 2012). At the end of the anaerobic storage we could find that, in comparison to day 0 controls, day 42 RBCs displayed higher levels of sphingomyelins and ceramides, other than sphingosines (SM(d18:1/0:0); CerP(d18:1/24:0); C-2 Ceramide; C-8 Ceramide-1-phosphate; C-8; CerP(d18:1/12:0); Ceramine; D-erythro-Sphingosine C-15; Glucosylsphingosine; Phytosphingosine; Sphinganine - **Supplementary Table 6** – please, refer to D'Alessandro et al., 2013), analogously to day 42 (aerobically stored) control RBCs (Gevi et al., 2012).

Carnitine plays a buffer function in mediating the role of acyl-L-carnitine as a reservoir of activated acyl groups in mature human erythrocytes (Arduini et al., 1992). This might relate to the increased concentrations of cholines in longer (anaerobically) stored RBCs (such as glycerophosphocholine – **Figure 6**; PC(O-18:1(10E)/2:0); PC(O-18:1(11Z)/0:0); PC(P-18:0/0:0); PC(O-16:0/6:0); PC(10:0/4:0) – **Supplementary Table 6** please, refer to D'Alessandro et al., 2013), analogously to RBCs stored under normoxic blood banking conditions (Gevi et al., 2012). Increased concentrations of cholines (especially in the intermediate storage period in within 14 and 28 days of anaerobic storage - **Figure 5**) have been already reported in sickle RBCs, where they have been linked to recycling of phospholipids as to indirectly document the RBC membrane fragility observed in sickle cell disease patients (Darghouth et al., 2011).

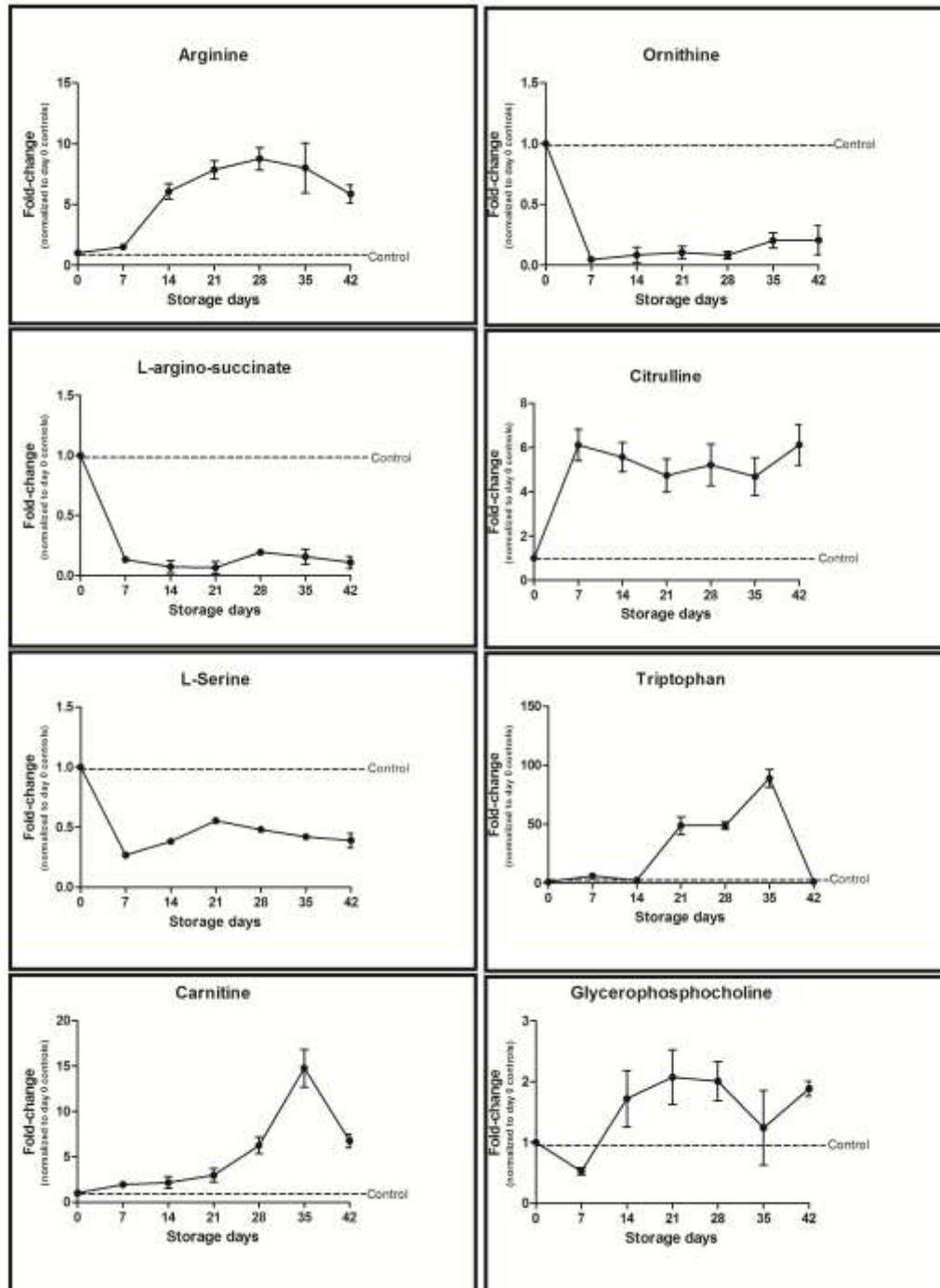


FIGURE 5 A glance at amino acid transport and fatty acid metabolism in anaerobically stored RBCs. Results are plotted as fold-change variations upon normalization to day 0 controls.

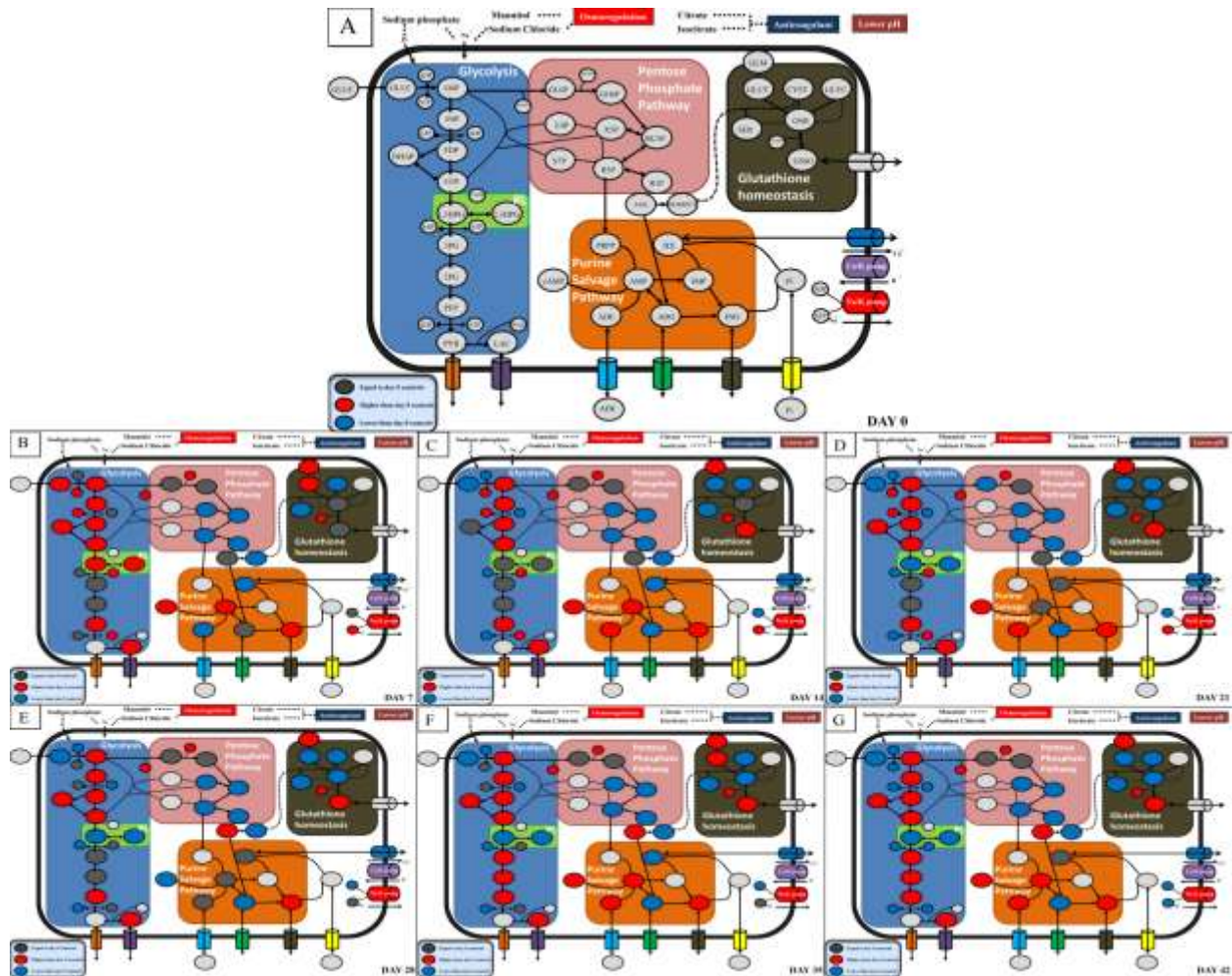


FIGURE 6 An overview of the trends for the main red blood cell metabolic pathways under prolonged anaerobic storage on a weekly basis. The scheme includes glycolysis (Embden Meyerhof pathway), pentose phosphate pathway, purine salvage pathway, glutathione homeostasis and aminoacids that represent cross-talks among multiple pathways. Metabolites are highlighted in circles along with canonical Kegg pathway abbreviations in the day 0 graph (A).

In brief, glycolysis remains overactivated in comparison to day 0 control throughout the whole storage period (red – B-G). The Pentose Phosphate Pathway apparently never activates (blue – B-G), while glutathione homeostasis is altered towards the gradual accumulation of oxidized glutathione from B-G. The Purine Salvage Pathway appears to be comparable with (D, E) or more active than (B, C, F, G) day 0 controls throughout the whole anaerobic storage period.

Colour legend:

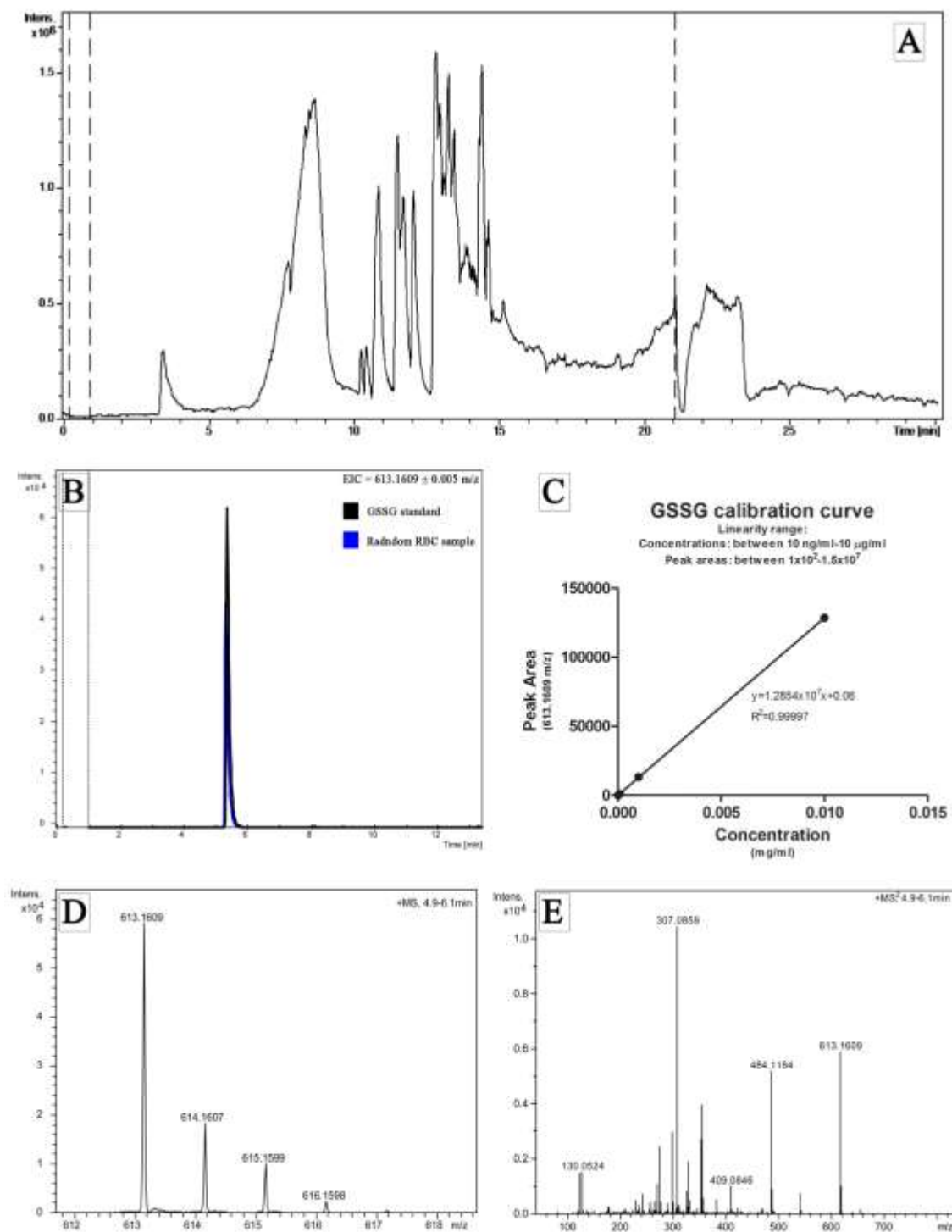
- Blue: decreased against day 0 controls;
- Red: increased against day 0 controls;
- Dark grey: not significantly different from day 0 controls.

Conclusion

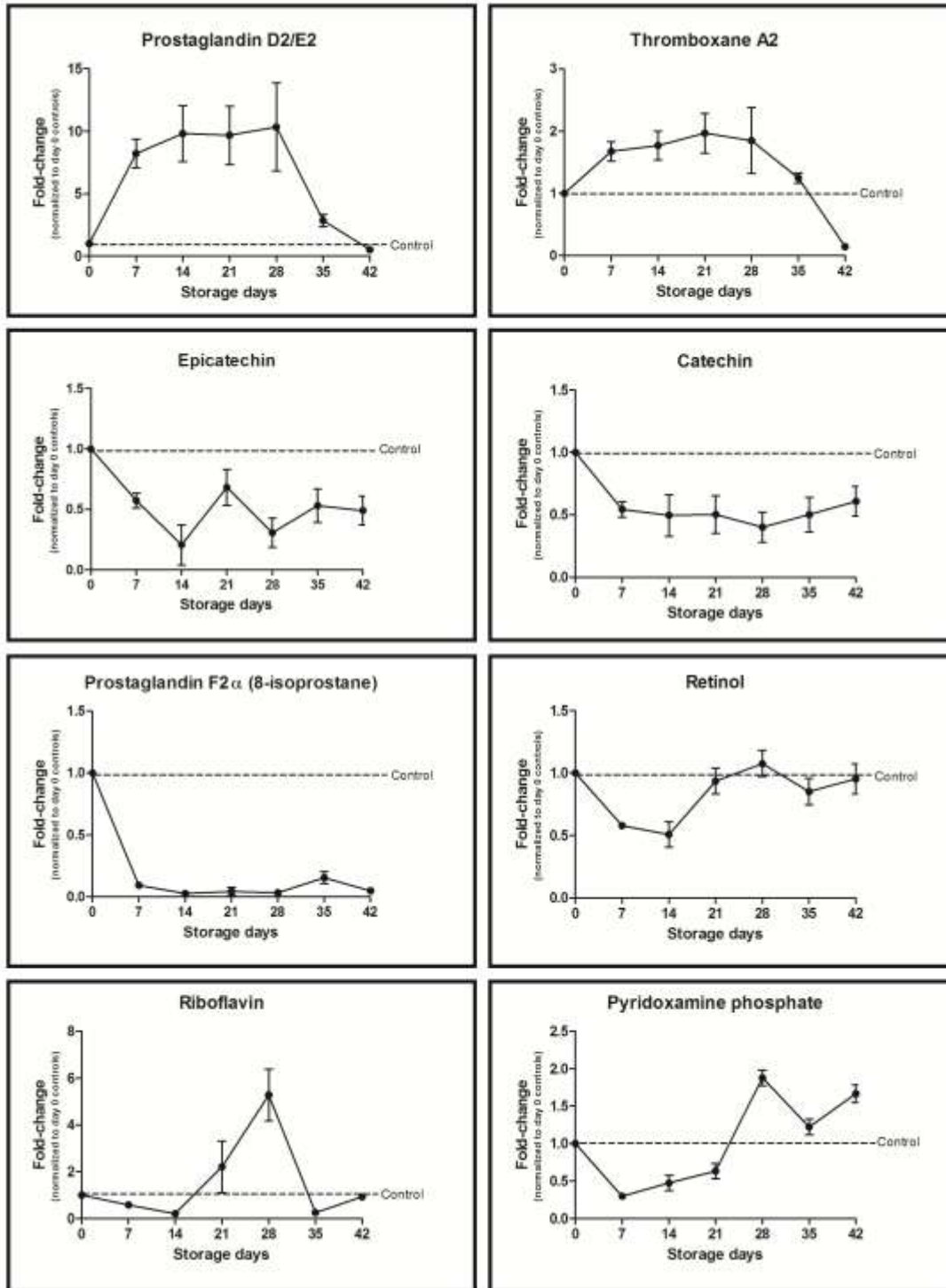
MS-based metabolomics is a promising research endeavour that is gradually complementing decades of accurate biochemical observations with targeted approaches and NMR (Nicholson et al., 2008; Wishart et al., 2009; D'Alessandro and Zolla, 2012). In the present study, the application of novel MS-based metabolomics approaches to the issue of RBC exposure to prolonged anaerobiosis has further shed light on the oxygen-dependent metabolic modulation in RBCs. Long term exposure of RBCs to anaerobic conditions resulted in the exacerbation of all those phenomena observed in the short term (Kinoshita et al., 2007). We hereby confirmed previous evidences about long term anaerobiosis promoting glycolytic metabolism in RBCs and prolonging the conservation of high energy phosphate reservoirs and purine homeostasis (Yoshida et al., 2007 and 2010; Dumont et al., 2009) (**Figure 6**). ATP decrease despite glycolysis being sustained throughout the whole anaerobic storage duration (glycolytic intermediates and lactate accumulate constantly until storage day 42) might not only reflect ATP and DPG sequestering by deoxy-Hb, which should occur early upon deoxygenation, but it might rather reflect cAMP-mediated ATP release by RBCs in response to deoxygenation, a phenomenon that *in vivo* occurs to promote vasodilation in hypoxic districts (Dietrich et al., 2000).

In parallel, we evidenced that, contrarily to aerobic storage (Gevi et al., 2012), anaerobiosis impairs RBC capacity to cope with oxidative stress by blocking metabolic diversion towards the PPP, which negatively affects glutathione homeostasis (**Figure 6**). Therefore, although oxidative stress is less sustained than in aerobically stored RBCs (Gevi et al., 2012), oxidative stress markers still accumulate over anaerobic storage progression, though to a lesser extent. In this view, it should be pointed out that, in the present study, anaerobiosis has been reached in SAGM-stored RBCs (pH_{22°C} 5.7), while higher pH additive solutions should in part counteract PPP blockade by increasing glucose 6-phosphate dehydrogenase activity (Cohen and Rosemeyer, 1968). Indeed, neutral or alkaline storage solutions have been already proposed with encouraging results (higher DPG and ATP levels at the end of the shelf-life, higher *in vivo* survival upon transfusion), both in the frame of aerobic (Hess et al., 2002; Veale et al., 2011) and anaerobic storage of RBCs (Yoshida et al., 2007 and 2008).

While metabolomics is one key area of biological investigations, further clues about the effects of prolonged exposure of RBCs to anaerobiosis will soon derive from the application of other Omics disciplines, above all proteomics, to this delicate topic.



Supplementary FIGURE 1 In A, A representative total ion current (TIC) mass spectrum chromatogram of a red blood cell sample. In B, a detail of the extract ion current (EIC) mass spectrum chromatogram for oxidized glutathione (GSSG) of a standard (black spectrum) and random red blood cell sample (blue chromatogram). In C, D and E, the calibration curve to determine the linearity range, the intact accurate mass isotopic pattern and the fragmentation pattern for a sample metabolite (GSSG), respectively.



Supplementary FIGURE 2 Inflammation/oxidative stress markers (prostaglandins and thromboxane), exogenous anti-oxidant metabolites (epicatechin and catechin) and vitamins/vitamin related metabolites in anaerobically stored RBCs. Results are plotted as fold-change variations upon normalization to day 0 controls.

7.3 Red blood cell storage with vitamin C and N-acetylcysteine prevents oxidative stress-related lesions: a metabolomics overview

Overview of this section

Mass spectrometry-based metabolomics has recently proven its worth, as an innovative and highly sensitive tool to dissect red blood cell metabolism and enable a wide series of translational applications in the field of erythrocyte biology and transfusion medicine.

In the present study, we exploited a validated HPLC-MS analytical workflow to determine the effects of vitamin C and NAC supplementation (antioxidants) on the metabolome of CPD-SAGM erythrocyte concentrates stored under blood bank conditions.

As a result, we could observe decreased energy metabolism fluxes (glycolysis and PPP), depressed by the competitive uptake of ascorbate and glucose.

Supplementation of anti-oxidants was indeed effective in positively modulating the redox poise, through the promotion of glutathione homeostasis, which resulted in decreased haemolysis, lower accumulation of malondialdehyde and oxidation byproduct metabolites (including GSSG and prostaglandins).

Antioxidants did not help preserving erythrocyte morphology, as gleaned through scanning electron microscopy. Through these results, we could confirm a central role for energy metabolism, rather than oxidative stress, in the accumulation of the most evident RBC storage lesions (such as those targeting the erythrocyte phenotype).

Keywords: red blood cell; metabolism; vitamin C; N-acetyl cysteine mass spectrometry; metabolomics.

Introduction

Upon decades of significant technological improvements, red blood cell (RBC) storage under blood bank conditions is still accompanied by the exacerbation of *in vivo* ageing phenomena, a process that is often referred to as “storage lesions” (Hess, 2010; D’Alessandro et al., 2010; Lion et al., 2010; Karon et al., 2012). Storage lesions include a well documented list of either reversible or irreversible modifications to RBC morphology and biochemistry (Hess, 2010; D’Alessandro et al., 2010; Lion et al., 2010; Karon et al., 2012), including alterations to RBC metabolism and ion homeostasis (Gevi et al., 2012), accumulation of oxidative stress, especially to the lipid (malondialdehyde accumulation) and protein fractions (carbonylations, protein fragmentation) (D’Alessandro et al., 2012; Antonelou et al., 2012), increased vesiculation rate (Bosman et al., 2008) utterly resulting in compromised shape morphology, which promotes osmotic fragility (Blasi et al., 2012). From this accumulating body of laboratory science literature in the field of RBC biopreservation, it clearly emerges that hypothermic storage represents a significant hurdle for the maintenance of RBC metabolism (Gevi et al., 2012), and especially of high energy phosphate compounds, such as adenosine triphosphate (ATP) and 2,3-diphosphoglycerate (DPG) (Hogman et al., 1985; Hess, 2010; D’Alessandro et al., 2010; Lion et al., 2010; Karon et al., 2012; Blasi et al., 2012;). These metabolic anomalies, although reversible to some extent, are indeed tied to the promotion of apoptosis-like phenomena compromising RBC survival *in vitro* and, upon transfusion, *in vivo*, since the energy-less RBC is rapidly lost in the bloodstream of the recipient (van Wijk and van Solinge, 1985). Furthermore, other than targeting energy metabolism, storage lesions end up impairing RBC anti-oxidant defenses (Dumaswala et al., 1999; D’Alessandro et al., 2012; Antonelou et al., 2012; Gevi et al., 2012). Indeed, progressive accumulation of oxidized proteins and lipids represents one key feature of RBC ageing *in vitro* (Dumaswala et al., 1999; Kriebardis et al., 2007; Antonelou et al., 2010; Delobel et al., 2012). In the light of these considerations, RBC biopreservation experts are continuously struggling to find alternative storage strategies to improve the quality, safety and efficacy of long-stored RBC concentrates, mainly by addressing metabolic modulation through alternative storage strategies that could tackle the alteration of both energy and anti-oxidant metabolism.

In this view, two main intervention scenarios have been described: (i) oxygen removal in order to pursue anaerobic storage and (ii) the formulation of alternative additive/rejuvenation solutions.

Anaerobic storage of RBCs through deoxygenation of erythrocyte concentrate units has been demonstrated to potentially extend the shelf life of erythrocyte concentrates up to 63 days (Yoshida et al., 2007). Anaerobic storage efficacy was demonstrated to be tied to the increased glycolytic rate, resulting in a more efficient preservation of ATP and DPG throughout storage duration (Yoshida et al., 2007). This is due to the oxygen-linked modulation of hemoglobin allostery (Kinoshita et al., 2007). Indeed, the N-terminal cytosolic domain of band 3 represents a membrane docking site for several enzymes of the glycolytic pathway (e.g. phosphofructokinase, aldolase, glyceraldehyde-3-phosphate dehydrogenase and lactate dehydrogenase), which are thereby sequestered and bound/inactivated (Low et al., 1986; Messana et al., 1996). Deoxygenation of RBCs promotes deoxy-hemoglobin binding to the cytosolic domain of band 3 and thus the displacement of glycolytic enzymes, which boosts glycolytic activity (Low et al., 1986; Messana et al., 1996).

Accelerated glucose consumption promotes lactate accumulation through the Embden-Meyerhof glycolytic pathway, and fuels the generation of DPG and ATP to stabilize the T-state of hemoglobin under hypoxic conditions, in a Pasteur effect-like phenomenon (Low et al., 1986; Messana et al., 1996; Kinoshita et al., 2007; Rogers et al., 2009; D'Alessandro et al., 2013).

However, almost counterintuitively, oxygen removal does not result in lower levels of oxidative stress (Rogers et al., 2009; D'Alessandro et al., 2013). Conversely, hypoxia limits antioxidant capacity of RBCs as it blocks the metabolic shift towards the pentose phosphate pathway (PPP) (Rogers et al., 2009; D'Alessandro et al., 2013), which is responsible for the production of the reducing coenzyme NADPH, that in turn is essential to maintain the homeostasis of several anti-oxidant enzymes and pathways (glutathione homeostasis, for example).

In parallel, alternative storage strategies envisaged the formulation of novel additive/rejuvenation solutions, which are mostly based upon pH modulation (affecting glycolytic enzyme activity which in turn benefits the replenishing of ATP and DPG reservoirs (Hess et al., 2002; Burger et al., 2010; Veale et al., 2011)) and/or supplementation of carbon substrates to refuel energy production (Yoshida et al., 2008).

Blood preservation studies have been also conducted to understand the potential benefits arising from the addition of antioxidants to storage solutions, such as vitamin C – ascorbate (Dawson et al., 1980 and 1981; May et al., 1998). Ascorbate levels in RBCs *in vivo* are the same as in plasma (May, 1998), although RBCs also display a high capacity to regenerate the vitamin from its two electron-oxidized form, dehydroascorbic acid (Johnston et al., 1993). Besides, ascorbate helps to preserve from oxidation alpha-tocopherol (vitamin E), which is found in lipoproteins and in the RBC membrane.

While thiol compounds are known to directly defend against oxidative stress and their permeability into RBC membranes has already been demonstrated (Mazor et al., 1996; Dumaswala et al., 2000), only glutathione loading has been so far proposed as a potential additive to storage solution formulations (Dumaswala et al., 2000). N-acetylcysteine (NAC), for example, is a precursor to the tripeptide glutathione (GSH). NAC plays an important anti-oxidant activity, as it has been demonstrated to reduce oxidative stress in sickle cell patients (Nur et al., 2012).

Decades of investigations in the field of RBC biochemistry (Murphy, 1960; Heinrich et al., 1977; Schauer et al., 1981) have paved the way for a “Systems biology” (Wiback and Palsson, 2002; Jamshidi and Palsson, 2006; Nicholson and Lindon, 2008)-oriented understanding of RBC physiology and metabolism. These *in silico* models have allowed dissecting RBC metabolism under *in vitro* ageing (storage under blood bank conditions), enabling spectrophotometry (Bennet-Guerrero et al., 2007), nuclear magnetic resonance (NMR) (Messana et al., 1999 and 2000) or, more recently, mass spectrometry (MS)-based metabolomics investigations (Nishino et al., 2009; Darghouth et al., 2011a and 2011b; D'Alessandro et al., 2012; Gevi et al., 2012; D'Alessandro et al., 2013). MS-based metabolomics (the comprehensive quali-quantitative analysis of low molecular weight compounds below 1.5k Da) holds several advantages over NMR, owing to the higher sensitivity and specificity of MS instruments, other than the possibility to rely upon recently introduced novel software platforms and databases (Scalbert et al., 2009).

Therefore, taking advantage of a novel high performance liquid chromatography (HPLC)- micro-time of flight-quadrupole (micro-TOF-Q) mass spectrometry (MS) approach, a workflow that recently contributed precious insights in the understanding of RBC metabolism under control and anaerobic blood banking conditions

(D'Alessandro et al., 2012; Gevi et al., 2012; D'Alessandro et al., 2013), we hereby investigated the RBC metabolome of RBC units stored in presence of CPD-SAGM supplemented with vitamin C and NAC. Results are thus discussed in the light of our recent reports about RBC metabolism under standard blood bank conditions (in presence of CPD-SAGM) (Gevi et al, 2012) and upon deoxygenation (D'Alessandro et al., 2013).

Materials and Method

Sample collection

Red blood cell units were drawn from healthy donor volunteers according to the policy of the Italian National Blood Centre guidelines (Blood Transfusion Service for donated blood) and upon informed consent in accordance with the declaration of Helsinki. We studied RBC units collected from 10 healthy donor volunteers [age 39.4 ± 7.5 (mean \pm S.D.)]. RBC units were stored either under standard conditions at 4° for up to 42 days in presence of CDP-SAGM, or in CPD-SAGM with the addition of ascorbic acid (SIGMA Aldrich, Milan, Italy) and N-acetyl cysteine (SIGMA Aldrich, Milan, Italy).

Samples were removed aseptically for the analysis on a weekly basis (at 0, 7, 14, 21, 28, 35 and 42 days of storage). Samples for metabolomics analyses were collected at 0, 7, 21, 28 and 42 days of storage, while SEM analyses were performed at day 0 and 42.

Materials

Acetonitrile, formic acid, and HPLC-grade water, purchased from Sigma Aldrich (Milano, Italy). Standards (equal or greater than 98% chemical purity) ATP, L-lactic acid, phosphogluconic acid, NADH, D-fructose 1,6-biphosphate, D-fructose 6-phosphate, glyceraldehydes phosphate, phosphoenolpyruvic acid, L-malic acid, L-glutamic acid, oxidized glutathione, a-ketoglutarate were purchased from Sigma Aldrich (Milan). Standards were stored either at -25°C, 4°C or room temperature, following manufacturer's instructions. Each standard compound was weighted and dissolved in nanopure water. Starting at a concentration of 1 mg/ml of the original standard solution, a dilution series of steps (in 18 MΩ, 5% formic acid) was performed for each standard in order to reach the determine the linearity range for relative quantitation using peak areas.

Determination of haemolysis, intracellular pH and malondialdehyde

Hemolysis was calculated following the method by Harboe. (1959) Samples were diluted in distilled water and incubated at room temperature for 30 min to lyse red blood cells. Samples from lysed RBCs were diluted 1/300 while supernatants were diluted 1 / 10 in distilled water. After stabilizing during 30 min and vortex mixing (Titramax 100, Heidolph Elektro, Kelheim, Germany), the absorbance of the hemoglobin was measured at 380, 415 and 450 nm (PowerWave 200 Spectrophotometer, Bio-Tek Instruments, Winooski, Vermont, USA). The mean blank was subtracted and the corrected OD (OD) was calculated as follows: $2 \times OD_{415} - OD_{380} - OD_{450}$.

Red cell pellets obtained by centrifuging 600 µl of suspension in a nylon tube at 30,000×g for 10 min, were frozen, thawed during 5 min and then refrozen. To prevent an acid shift observed when samples are kept unfrozen, triplicate measurements of pH were made immediately after a second thawing of each lysate with a Radiometer pH glass capillary electrode maintained at 20°C and linked to a Radiometer PHM acid-base analyzer.

Malondialdehyde (MDA) levels were estimated in RBCs following the Stocks and Dormandy's method (1971), as previously reported (D'Alessandro et al., 2012).

Untargeted Metabolomics Analyses

Metabolite extractions and metabolomics analyses were performed as previously reported (D'Alessandro et al., 2011). Analyses were performed through an Ultimate 3000 Rapid Resolution HPLC system (LC Packings, DIONEX, Sunnyvale, USA) and an electrospray hybrid quadrupole time-of flight mass spectrometer MicroTOF-Q (Bruker-Daltonik, Bremen, Germany) equipped with an ESI-ion source. Procedures and technical settings are consistent with our previous investigations (**Chapter 3**) (D'Alessandro et al., 2012; Gevi et al., 2012; D'Alessandro et al., 2013). Mass spectra analyses were performed with the software MAVEN (Princeton, USA) (Melamud et al., 2010)), which allows to interrogate the KEGG (Kanehisa and Goto, 2000) database for metabolite identification. Results were plotted through GraphPad Prism 5.03 as fold-change variations against day 0 controls.

Scanning Electron Microscopy

Scanning electron microscopy (SEM) studies of RBC were performed at day 0 and 42 for control and (vitamin C + NAC) supplemented erythrocyte concentrates by means of an JEOL JSM 5200 electron microscope, as previously reported (Bessis et al., 1972; Blasi et al., 2012). Blood samples were fixed in phosphate-buffered (pH 7.2–7.4) 2.5% glutaraldehyde for 1 h, washed two times in 0.1 M phosphate buffer (pH 7.2–7.4), and mounted on poly-L-lysine-coated glass slides. The glass slides were kept in a moist atmosphere for 1 h, washed in phosphate buffer, postfixed in 1% osmium tetroxide for 1 h, rinsed in distilled water, and dehydrated in graded ethanol (50–70–90–100%). After critical-point drying with liquid CO₂ in a vacuum apparatus and covering with a gold-palladium layer, the samples underwent scanning electron microscopic analysis.

The percentages of discocytes, echinocytes, spherocytocytes, stomatocytes, spherostomatocytes, and spherocytes were evaluated by counting 1000 to 1500 cells in randomly chosen fields. Classification was indeed performed as previously reported (Blasi et al., 2012), since RBCs manifesting echinocyte and stomatocyte shapes are capable of returning to the discocyte shape under certain conditions. Thus, these RBC shape changes are considered potentially reversible transformations. In contrast, RBCs assuming spherocytocyte, spherostomatocyte, spherocyte, ovalocyte, and degenerated shapes are irreversibly changed cells.

Results and Discussions

The addition of ascorbic acid and NAC influenced pH by demodulating glycolysis

The addition of ascorbic acid (and NAC) did not provoke major fluctuation of additive solution (CPD-SAGM) pH, which was decreased by 0.2 immediately upon addition, but did not show any major deviation from the control upon introduction of packed RBCs (**Figure 1.A-B**). In particular, pH (both internal – **Figure 1.A** and external – **Figure 1.B**) were consistently higher (especially the latter) throughout the whole storage duration, while the former showed higher levels than control counterparts starting from storage day 21 onwards.

The supplementation of vitamin C and NAC had measurable positive effects on haemolysis (**Figure 1.C**), especially within storage day 28 and, in particular, in between storage day 0 and 21.

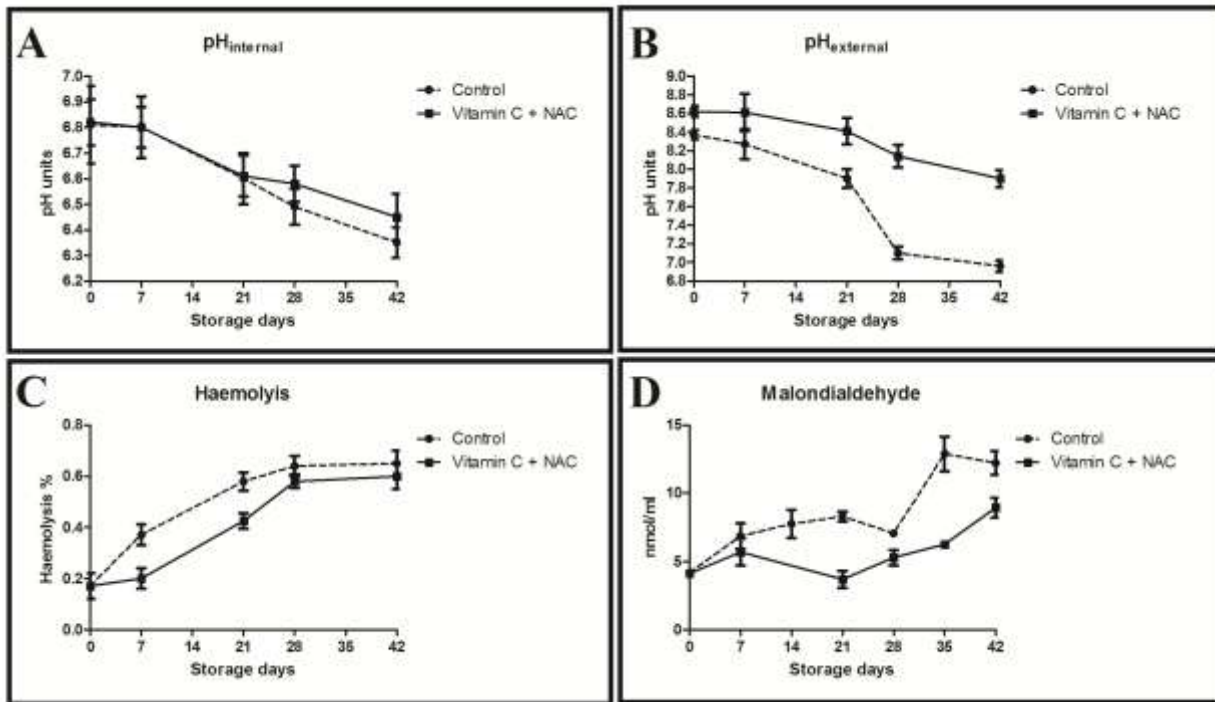


FIGURE 1 A time course overview of internal pH, external pH, haemolysis and malondialdehyde accumulation for control (gapped line) and vitamin C + NAC-supplemented (continuous line) CPD-SAGM erythrocyte concentrates stored at 4°C for up to 42 days.

Malondialdehyde showed a progressive increment both in control and supplemented erythrocyte concentrates, although control units showed constantly higher levels than the supplemented counterparts (**Figure 1.D**).

Upon three hours from the supplementation of vitamin C and NAC (day 0), we could observe the intracellular accumulation of NAC (1.5 ± 0.04 fold-change variation against controls), ascorbate (1.67 ± 0.24), dehydroascorbate (35.00 ± 2.14), GSH (2.24 ± 0.41) and α -tocopherol (205.48 ± 4.73), apparently unaltered levels of oxidized glutathione (GSSG - 1.02 ± 0.09), while intracellular glucose levels were apparently decreased (0.62 ± 0.11), as reported in **Figure 2**. The decreased levels of glucose are consistent with the documented competition between ascorbate and D-glucose for GLUT transporters for membrane transport (internalization) in human RBCs (May, 1998). Immediate benefits on the levels of GSH and α -tocopherol were expected as well, on the basis of the NAC-promoted biosynthesis of the former (Mazor et al., 1996), and the antioxidant and protective action of ascorbic acid on the latter (May et al., 1998). Slower internalization of glucose in supplemented erythrocyte concentrates (**Figure 2**) might also justify the influence on the slope of the pH decrease curves (**Figure 1.A-B**), as described above. Indeed, a slower glycolytic rate might result in lower lactate accumulation and reduced pH decrease. In order to underpin this hypothesis, MS-based metabolomics analyses were performed to assay metabolic fluxes for glucose consumption.

HPLC-MS runs were performed in triplicate on samples extracted from each donated unit at 0, 7, 21, 28, and 42 days of storage. In order to report the main results in a more readable layout, metabolites accounting for the most

relevant catabolic pathways in RBCs were grouped and plotted as fold-change variation of time course measurements in each group, normalized against day 0 controls (in this view, it is worthwhile stressing that the day 0 levels of specific metabolites already differed upon 3 hours from supplementation, as also reported in **Figure 2** for a subset of redox poise-related metabolites). The analysed pathways could be enlisted as follows: (i) glycolysis (**Figure 3**), (ii) PPP (**Figure 4**), (iii) glutathione homeostasis (**Figure 5**); (iv) lipid peroxidation (**Figure 6**), (v) purine metabolism (**Figure 7**).

In **Figure 3**, we report how glycolytic intermediates, including glucose 6-phosphate (G6P), fructose 6-phosphate (F6P), glyceraldehyde 3-phosphate (G3P), pyruvate, and byproducts of lactic fermentation (lactate), consistently decreased upon supplementation of vitamin C and NAC.

On the other hand, DPG levels followed a peculiar trend, with a rapid decrease in supplemented units within the first week of storage, while day 21 levels in supplemented units were higher than in controls (**Figure 3**), suggesting a long-term positive effect of NAC-vitamin C supplementation to RBCs, in agreement with previous studies on ascorbate (Dawson et al., 1980 and 1981).

Higher levels of NADH in vitamin C + NAC-supplemented erythrocyte concentrates might be explained in the light of two considerations: (i) a reduced glycolytic rate and slower lactate production rate is accompanied by a slower oxidation rate of NADH back to NAD^+ ; (ii) NADH is also an essential cofactor for the cytochrome b5 reductase – methemoglobin reductase, which is responsible for the reduction of oxidized iron in methemoglobin back to ferrous state. Therefore, higher NADH levels might represent an indirect proof of a lower necessity of RBCs to cope with hemoglobin oxidation in vitamin C + NAC-supplemented units.

ATP higher levels in supplemented units are consistent with the positive effect on ATP preservation observed during whole blood storage in presence of ascorbic acid (Zan et al., 2005), and with early blood preservation studies on the effects of ascorbic acid and dehydroascorbate (Dawson et al., 1980 and 1981).

A tentative explanation to this phenomenon is tied to the relative concentrations of cyclic AMP (cAMP – **Figure 3**), which constantly increases in control RBCs (and deoxygenated units, as we observed in our recent study – D'Alessandro et al., 2013) over storage duration, while it remains constant and slowly decreases in vitamin C-NAC supplemented units. Indeed, while it has been reported that long term anaerobiosis promoted glycolytic metabolism in RBCs and prolonging the conservation of high energy phosphate reservoirs and purine homeostasis (Yoshida et al., 2007), it is nonetheless true that ATP decreases (though slowly than in “oxygenated” controls) despite glycolysis being sustained throughout the whole anaerobic storage duration (glycolytic intermediates and lactate accumulate constantly until storage day 42 – D'Alessandro et al., 2013). In our previous research, we could thus hypothesized that progressive decrease of high energy phosphate compounds in deoxygenated units might not only reflect ATP and DPG sequestering by deoxy-Hb, which should occur early upon deoxygenation, but it might rather reflect cAMP-mediated ATP release by RBCs in response to deoxygenation (D'Alessandro et al., 2013), a phenomenon that *in vivo* occurs to promote vasodilation in hypoxic districts (Sprague et al., 2001). Therefore, in the present study, slower glycolytic rates albeit higher ATP and DPG levels might be likely explained by the lower cAMP levels in supplemented units (**Figure 3**), in comparison to complemented counterparts, which would in turn decrease cAMP-mediated ATP release from RBCs.

The observed decrease in cAMP levels is also relevant in the light of the role of this molecule in modulating second messenger cascades, such as the activation of cAMP-dependent kinases, which in turn affect regulation and post-translational modifications (i.e. phosphorylations) of erythrocyte membrane and membrane-skeletal proteins (Cohen et al., 1992).

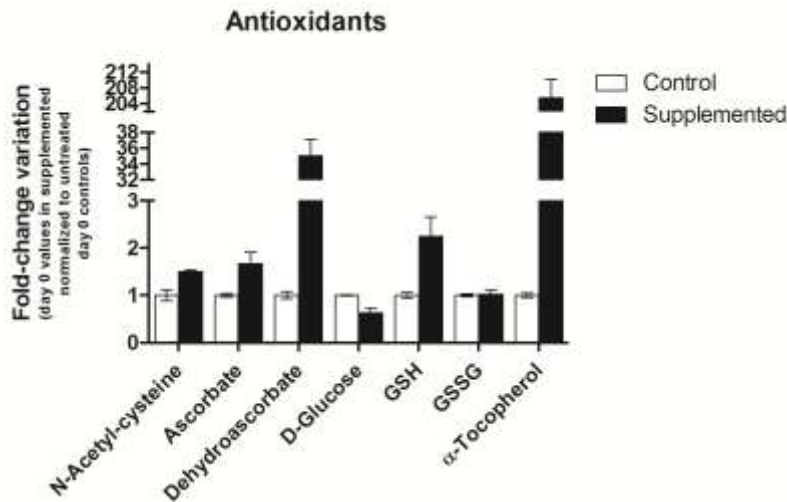


FIGURE 2 An overview of relative quantities for a subset of metabolites involved in redox metabolism poised at day 0, after three hours from supplementation with vitamin C and NAC. Results are plotted as fold-change variations (mean \pm SD) against untreated controls.

Glycolytic fluxes were not redirected towards the pentose phosphate pathway

On the basis of the aforementioned evidences, we wondered whether the observed lower levels of lactate were to be attributed to a slower rate of glucose consumption via the Embden-Meyerhof pathway or they rather hid a metabolic diversion toward the PPP, a pathway devoted to RBC protection from oxidative stress (Fico et al., 2004), in likewise fashion to control RBCs upon the second week of storage, as previously reported (D'Alessandro et al., 2012; Gevi et al., 2012).

In **Figure 4** we report the result for flux analyses of RBCs PPP intermediate metabolites, including 6-phosphogluconolactone, 6-phosphogluconate, erythrose 4-phosphate (E4P), ribulose 5-phosphate (RU5P), sedueptulose 7-phosphate and the byproduct NADPH. For all the tested metabolites we could observe lower relative levels of each compound in comparison to untreated controls, except for sedueptulose 7-phosphate and NADPH, where the levels were similar to untreated counterparts.

For NADPH, in particular, we could observe a 4-fold increase after 7 days of storage in supplemented units, while later on the detected levels were similar to those detected in untreated counterparts. Since NADPH is an essential coenzyme in antioxidant reactions, including GSSG reduction to GSH, the observed result could be due to a reduced consumption of NADPH, promoted by decreased oxidative stress levels in supplemented units (also confirmed by lower accumulation of malondialdehyde – **Figure 1.D**), rather than to an actual increased production of this metabolite.

Increased relative levels of sedueptulose 7-phosphate in vitamin C + NAC supplemented units might result from a regular carbon flux from the oxidative to the non-oxidative phase of the PPP, that results in metabolic fluxes re-

entering glycolysis, while in control RBCs prolonged storage results in the progressive flux towards the purine salvage pathway (PSP), as previously reported (Gevi et al., 2012).

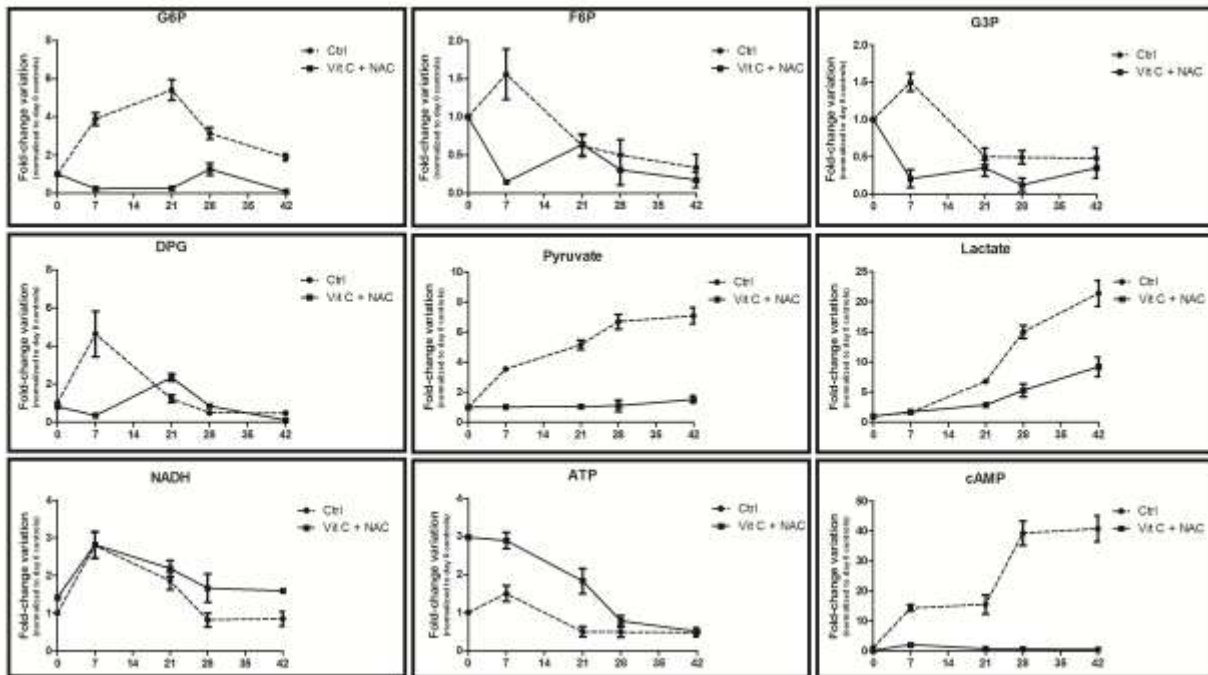


FIGURE 3 Time course metabolomic analysis of glycolysis in RBCs stored under control conditions (gaped line) or in CPD-SAGM supplemented with vitamin C and NAC (continuous line) at 4°C for up to 42 days. Results are plotted on a weekly basis (storage day 0, 7, 21, 28 and 42), as fold-change variations (means \pm SD) upon normalization against day 0 controls.

Abbreviations: G6P: glucose 6-phosphate; F6P: fructose 6-phosphate; G3P: glyceraldehyde 3-phosphate; DPG: diphosphoglycerate; cAMP: cyclic AMP.

Additives promoted anti-oxidant responses related to the glutathione system and homeostasis

Vitamin C and NAC were carefully selected for their expected potential benefits on the anti-oxidant defense systems, including glutathione homeostasis (Dawson et al., 1980 and 1981; Mazor et al., 1996; Dumaswala et al., 2000; Nur et al., 2012).

In **Figure 5** we report the results for the main metabolites involved in the maintenance of glutathione homeostasis and biosynthesis (Lu, 2009), including GSH, GSSG, glutamic acid, γ -glutamyl cysteine, acetyl-cysteine, cysteine, cysteine-glycine, methionine, ascorbate and dehydroascorbate.

First of all, it is worthwhile to recall that day 0 levels of GSH, acetyl-cysteine, ascorbate and dehydroascorbate were different between controls and supplemented units (**Figure 2, Figure 5**). Also, it should be considered that results in **Figure 5** are plotted as fold change variations against day 0 control values, which further stresses the significance of the observed trends towards increase (GSH, acetyl-cysteine, ascorbate) and decrease (dehydroascorbate – the oxidized form of ascorbic acid) of the graphed metabolites in supplemented units. Furthermore, cysteine (one key

aminoacid precursor of the tripeptide GSH) and thiol metabolism was up-regulated (cysteine, cysteine-glycine, methionine) in supplemented units (**Figure 5**).

These results are indicative that vitamin C and NAC supplementation are more effective than anaerobic storage in protecting RBCs from oxidative stress. Indeed, while anaerobiosis results in deoxy-hemoglobin-dependent blockade of metabolic diversion towards the PPP (Rogers et al., 2009; D'Alessandro et al., 2013), it also impairs RBC capacity to cope with oxidative stress by negatively affecting glutathione homeostasis (D'Alessandro et al., 2013), which is instead boosted by vitamin C and NAC supplementation, as hereby observed (**Figure 5**).

It should be also noted that preservation of thiol groups by improved glutathione homeostasis should also affect the activity of several key metabolic enzymes that rely upon thiol groups in functional active sites, such as glyceraldehyde 3-phosphate dehydrogenase (glycolysis) (Li et al., 1991) and peroxiredoxin 2 (antioxidant defenses – (Rinalducci et al., 2011)), the latter becoming oxidized and progressively migrating to the membrane over storage duration under blood bank conditions (Rinalducci et al., 2011; D'Alessandro et al., 2012).

The beneficial effects of vitamin C + NAC supplementation are evident at the glutathione homeostasis level, but also when focusing on lipid oxidation. In the light of malondialdehyde decrease in supplemented units (**Figure 1.D**), we further focused on prostaglandin metabolism (**Figure 6**), in particular on prostaglandin B1, D1, F1 α and F2 α (8-isoprostane). The latter metabolite, in particular, is a widely accepted marker of lipid peroxidation (Tsikas et al., 2012), and has been demonstrated to accumulate (especially in the supernatant) over storage duration (Hess et al., 2010; D'Alessandro et al., 2010; Karon et al., 2012). Concomitantly to the tested hypothesis, supplemented units displayed lower levels of prostaglandins throughout the whole 42 days tested time span.

Supplementation of vitamin C and NAC promoted the purine salvage pathway (in analogy to untreated controls)

RBCs cannot *de novo* synthesize 5-phosphoribosylamine and thus rely upon salvage reactions to replenish purine reservoirs which serve as substrates for high energy phosphate purine compounds (such as ATP and adenine nucleotides, accounting for 70-80% of cellular nucleotides) (Schuster and Kenanov, 2005). Erythrocyte membranes allow adenine and adenosine transport via facilitated diffusion, which allowed introducing adenine in additive solutions (such as in SAGM) without any major technical caveat (Zolla et al., 1977).

In like fashion to standard (Gevi et al., 2012) and anaerobic (D'Alessandro et al., 2013) storage, storage of vitamin C and NAC supplemented RBCs resulted in the progressive accumulation of both adenine and adenosine (although the accumulation rate of the latter was, from day 21 onwards, lower than in untreated controls – **Figure 7**).

Inosine, a major substrate for salvage reactions (Zolla et al., 1977), increased significantly over storage duration (**Figure 6**), in analogy to standard (Gevi et al., 2012) and anaerobic storage (D'Alessandro et al., 2013). Inosine accumulation might stem from deamination of adenosine, a documented process within the framework of RBC storage (Hess, 2010). Inosine has attracted a great deal of attention in the field of blood preservation, since it may further undergo phosphorolysis to form hypoxanthine (increasing both in controls and supplemented units – **Figure 7**) and ribose 1-phosphate (R1P), a reaction that enables the introduction of a phosphorylated sugar (through non-oxidative phase PPP intermediates) into the RBC without ATP consumption.

ADP levels were higher in supplemented units in comparison to untreated controls (**Figure 7**), almost paralleling relative quantitative trends observed for ATP.

While inosine monophosphate (IMP) accumulation has been reported for standard (Strauss et al., 1980; Gevi et al., 2012) and deoxygenated (D'Alessandro et al., 2013) erythrocyte concentrates over storage duration, vitamin C and NAC supplementation resulted in higher than controls levels until storage day 21, while they decreased back to control levels by storage day 28 and 42 (**Figure 7**). However, it is worthwhile to stress that optimum biopreservation strategies of RBCs should pursue the conservation of control like levels of IMP (Sidi et al., 1989), as we could observe hereby (control like levels of IMP were detected at the end of the shelf-life – **Figure 7**).

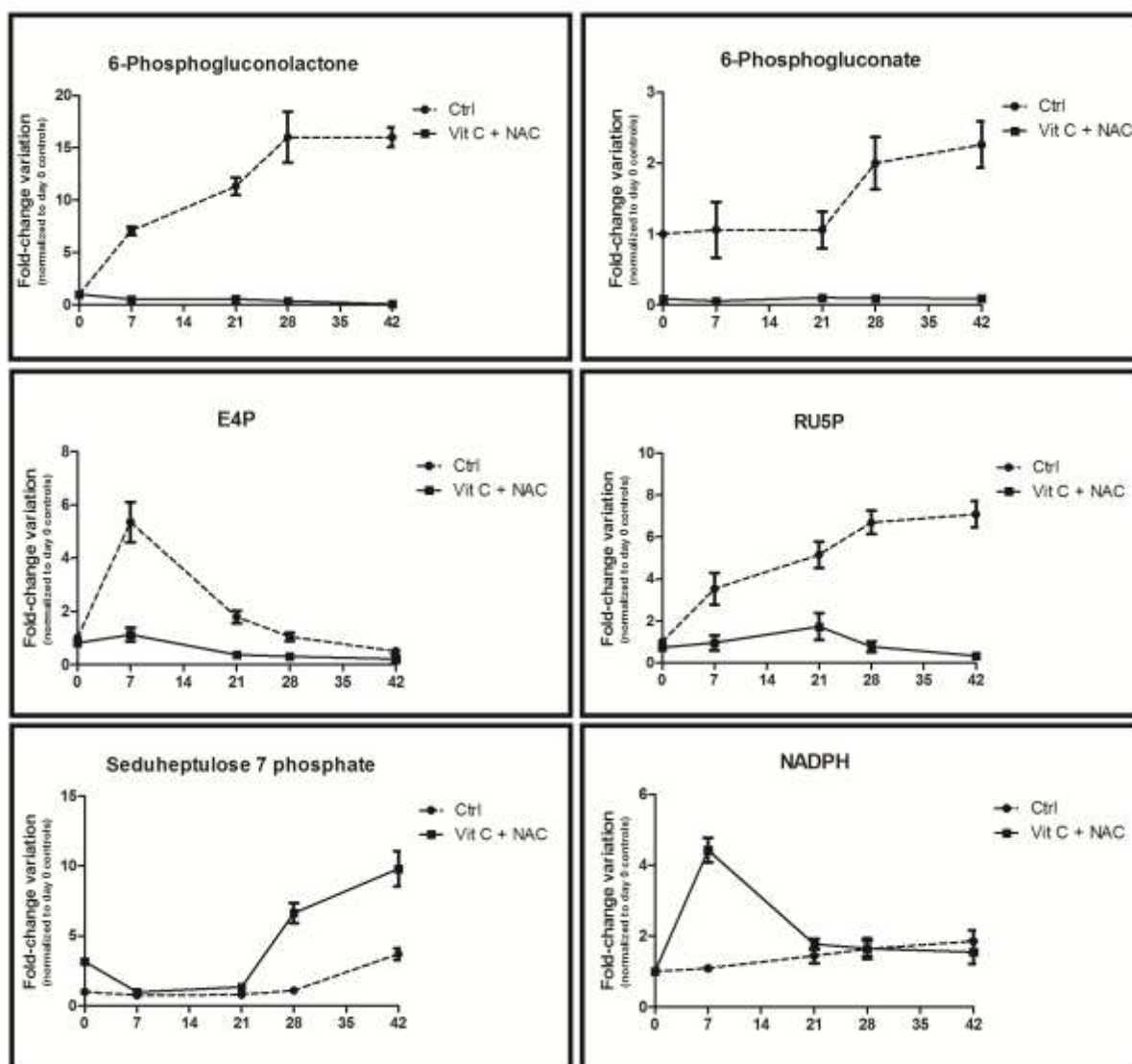


FIGURE 4 Time course metabolomic analysis of the pentose phosphate pathway in RBCs stored under control conditions (gapped line) or in CPD-SAGM supplemented with vitamin C and NAC (continuous line) at 4°C for up to 42 days. Results are plotted on a weekly basis (storage day 0, 7, 21, 28 and 42), as fold-change variations (means \pm SD) upon normalization against day 0 controls.

Abbreviations: E4P: erythrose 4-phosphate; RU5P: ribulose 5-phosphate.

Electron microscopy analyses did not evidence substantial improvements about RBC morphology parameters

Storage in presence of vitamin C and NAC did not improve the score related to morphology alterations (**Table 1**). Indeed, at the end of the tested storage period (42 days), the percentage of discocytes in supplemented units was not significantly higher than in untreated controls (24.2 ± 2.1 vs $21.8 \pm 1.6\%$ - **Table 1**), while the percentage of irreversibly altered RBCs (including spherocinocytes, spherostomatocytes, spherocytes and degenerated shapes) was lower than controls ($29.5\% \pm 3.6$ vs 34.6 ± 3.2), and comparable to 35 days controls, as gleaned from direct comparison against the results from our recent investigations on RBC storage-triggered alterations to morphology (D'Alessandro et al., 2012; Blasi et al., 2012).

In **Figure 8**, we report a mosaic of SEM images, including day 0 control discocyte RBCs (**Figure 8.A**), a detail of a discocyte and irreversibly altered spherocinocytes and degenerated shapes from day 42 RBCs supplemented with vitamin C and NAC (**Figure 8.B**), while in **Figure 8.C** we report a panoramic overview of a x2,000 field of RBCs stored for 42 days in vitamin C + NAC-supplemented CPD-SAGM. Panels **D** and **E** of **Figure 8** report a detail for SEM micrographs of 42 days-stored control RBCs, whereby unaltered discocytes represented a minoritarian percentage of the population and perfectly disc-shaped phenotypes are almost totally absent (in **D**, for example, the represented discocyte tends towards the acquisition of the echinocyte morphology) (Lim et al., 2002).

A direct comparison of these results against a recent short report on RBC morphology changes arising upon deoxygenation (Zolla and D'Alessandro, 2013) suggests that oxygen removal might preserve RBC morphology better than the hereby discussed supplementation of anti-oxidants. In the light of this consideration, it could be confirmed (Clark et al., 1981; Li et al., 2007; Park et al., 2010 and 2011) that ATP maintenance plays a key role in membrane structure homeostasis, and, although oxidative stress represents a critical challenge for RBCs under blood bank storage conditions, boosting redox metabolism instead of energy metabolism might not be sufficient to prevent and cope with those lesions targeting membrane morphology.

Conclusion

Recent strides in the field of MS-based metabolomics have prompted a thorough update and integration to decades of accurate biochemical observations with spectrophotometry and NMR. In particular, it is rapidly emerging a role for MS-based metabolomics in the fields of RBC research, transfusion medicine and clinical biochemistry (D'Alessandro et al., 2012; Sparrow, 2012; Cluitmans et al., 2012).

In the present study, we could apply a validated HPLC-MS-metabolomics workflow to determine the effects of vitamin C and NAC supplementation (antioxidants) to CPD-SAGM erythrocyte concentrates stored under blood bank conditions.

As a result, we could observe decreased energy metabolism fluxes (glycolysis and PPP), depressed by the diminished uptake of glucose and increased internalization of ascorbate. On the other hand, anti-oxidant defenses were boosted, above all glutathione homeostasis, resulting in decreased haemolysis, lower accumulation of malondialdehyde and oxidation byproduct metabolites (including GSSG and prostaglandins).

However, replenishing the RBC antioxidant battery through vitamin C and NAC did not help preserving RBC morphology, as gleaned through SEM analyses, thus confirming a central role for energy metabolism, rather than

oxidative stress, in the accumulation of the most evident RBC storage lesions (such as those targeting RBC phenotype).

Although metabolomics provides an exhaustive description of the biochemical scenario arising upon vitamin C and NAC supplementation, further clues will be soon collected through the application on this topic of other Omics disciplines, above all proteomics.

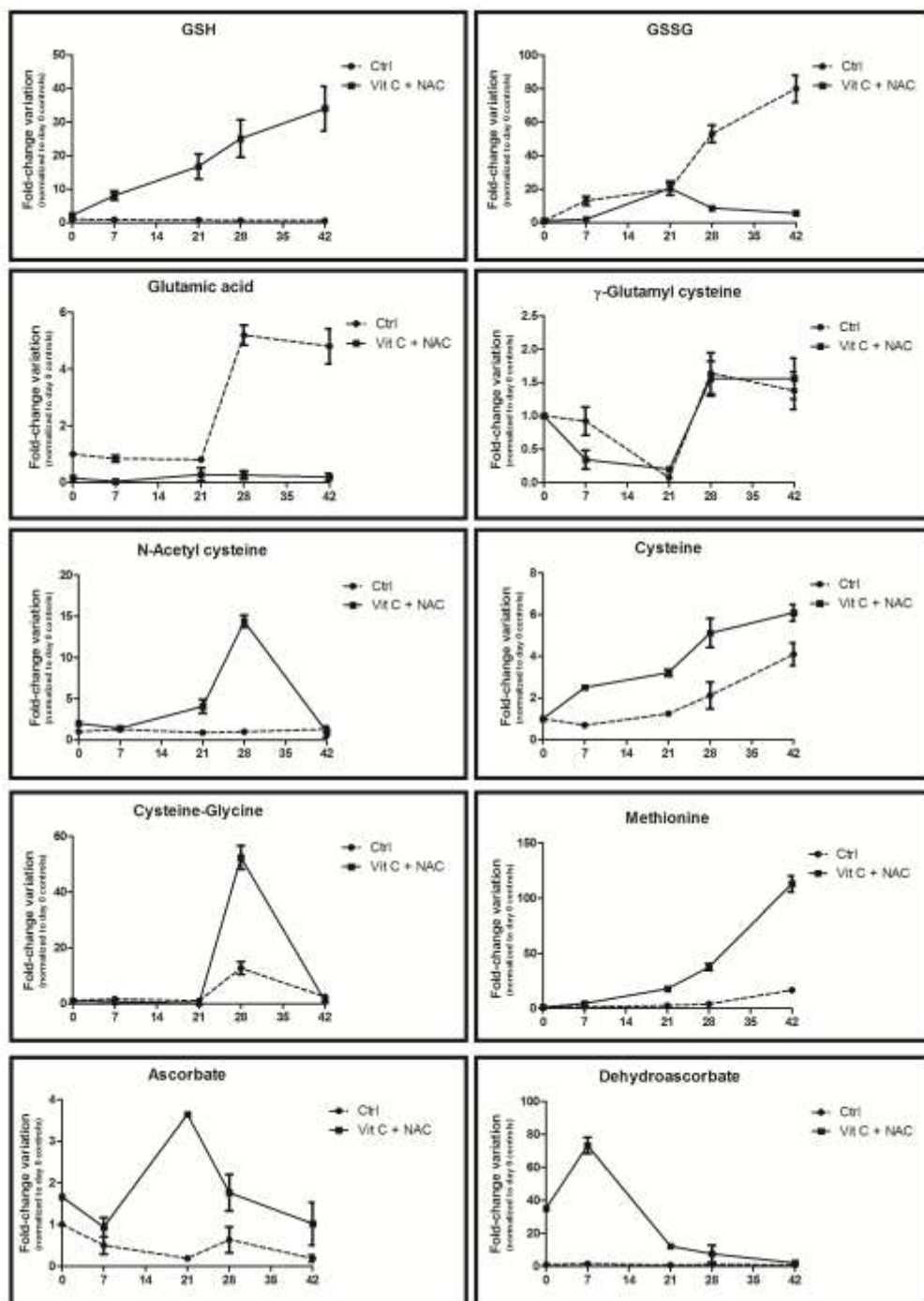


FIGURE 5 Time course metabolomic analysis of glutathione homeostasis-related metabolites in RBCs stored under control conditions (gaped line) or in CPD-SAGM supplemented with vitamin C and NAC (continuous line) at 4°C for up to 42 days. Results are plotted on a weekly basis (storage day 0, 7, 21, 28 and 42), as fold-change variations (means \pm SD) upon normalization against day 0 controls.

Abbreviations:
GSH: reduced glutathione; GSSG: oxidized glutathione.

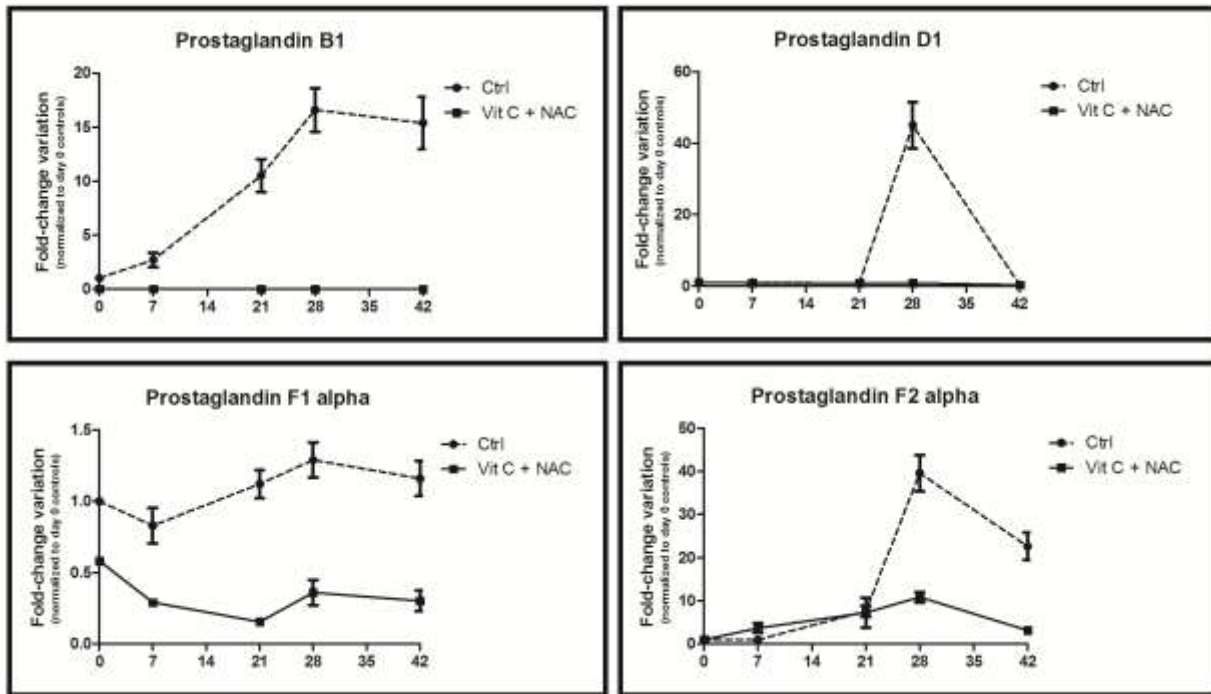


FIGURE 6 Time course metabolomic analysis of prostaglandins in RBCs stored under control conditions (gaped line) or in CPD-SAGM supplemented with vitamin C and NAC (continuous line) at 4°C for up to 42 days. Results are plotted on a weekly basis (storage day 0, 7, 21, 28 and 42), as fold-change variations (means \pm SD) upon normalization against day 0 controls.

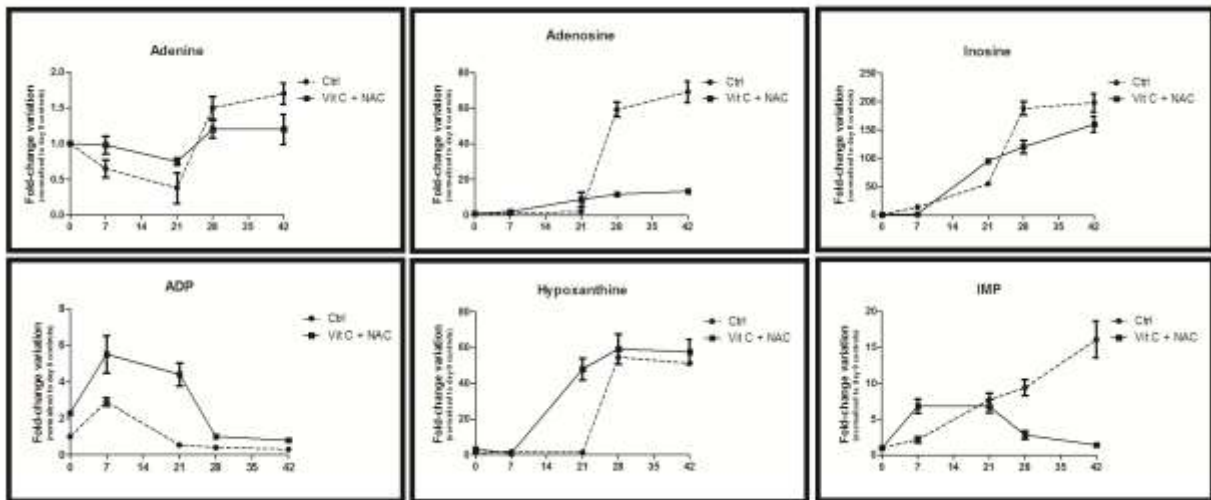


FIGURE 7 Time course metabolomic analysis of the purine metabolism in RBCs stored under control conditions (gaped line) or in CPD-SAGM supplemented with vitamin C and NAC (continuous line) at 4°C for up to 42 days. Results are plotted on a weekly basis (storage day 0, 7, 21, 28 and 42), as fold-change variations (means \pm SD) upon normalization against day 0 controls.

Abbreviations: ADP: adenosine diphosphate; IMP: inosine monophosphate.

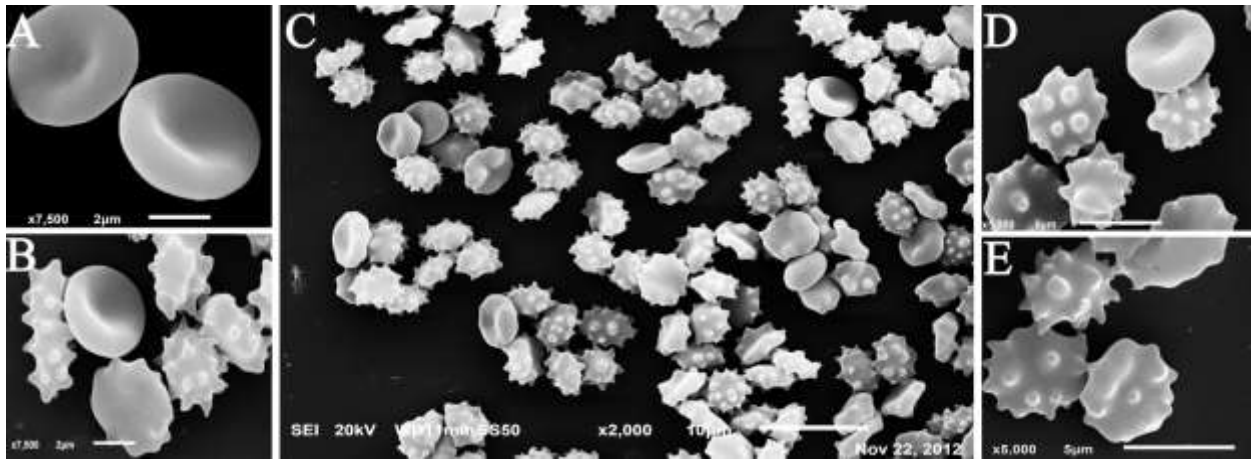


FIGURE 8 Scanning electron micrograph of day 0 control red blood cells (discocytes – **A**), 42 days discocyte and echinocytes in vitamin C + NAC-supplemented red blood cells (**B**). In **C**, a x2,000 magnification of 42 days vitamin C + NAC-supplemented red blood cells. In **D** and **E**, a detail of echinocytes of different degrees from 42 days-stored control erythrocyte concentrates.

References

- Antonelou M, Kriebardis A, Stamoulis K, Margaritis L, Trougakos I, Papassideri I. Secretory apolipoprotein J/Clusterin is an integral component of human erythrocytes and a novel biomarker of vesiculation and senescence in vivo and in stored red cells. XXXIst International Congress of the International Society of Blood Transfusion (ISBT), Berlin, Germany. *Vox Sanquinis* 2010; 99(s1):213.
- Antonelou MH, Kriebardis AG, Stamoulis KE, Economou-Petersen E, Margaritis LH, Papassideri IS. Red blood cell aging markers during storage in citrate-phosphate-dextrose-saline-adenine-glucose-mannitol. *Transfusion*. 2010;50(2):376-89.
- Antonelou MH, Tzounakas VL, Velentzas AD, Stamoulis KE, Kriebardis AG, Papassideri IS. Effects of pre-storage leukoreduction on stored red blood cells signaling: a time-course evaluation from shape to proteome. *J Proteomics*. 2012; 76:220-38.
- Arduini A, Mancinelli G, Radatti GL, Dottori S, Molajoni F, Ramsay RR. Role of carnitine and carnitine palmitoyltransferase as integral components of the pathway for membrane phospholipid fatty acid turnover in intact human erythrocytes. *J Biol Chem*. 1992;267(18):12673-12681.
- Astrup P, Engel K, Severinghaus JW, Munson E. The influence of temperature and pH on the dissociation curve of oxyhemoglobin of human blood. *Scand J Clin Lab Invest*. 1965;17(6):515-23.
- Ataullakhanov FI, Vitvitsky VM, Zhabotinsky AM, Pichugin AV, Platonova OV, Kholodenko BN, Ehrlich LI. The regulation of glycolysis in human erythrocytes. The dependence of the glycolytic flux on the ATP concentration. *Eur J Biochem*. 1981;115(2):359-65
- Balagopalakrishna C, Manoharan PT, Abugo OO, Rifkind JM. Production of superoxide from hemoglobin-bound oxygen under hypoxic conditions. *Biochemistry*. 1996;35(20):6393-8.
- Bennett-Guerrero E, Veldman TH, Doctor A, Telen MJ, Ortel TL, Reid TS, et al. Evolution of adverse changes in stored RBCs. *Proc. Natl. Acad. Sci. U S A*. 2007;104:17063-17068.
- Bessis M. Red cell shapes. An illustrated classification and its rationale. *Nouv Rev Fr Hematol*. 1972;12(6):721-45.
- Blasi B, D'Alessandro A, Ramundo N, Zolla L. Red blood cell storage and cell morphology. *Transfus Med* 2012; 22(2):90-6.
- Bosman GJ, Lasonder E, Luten M, Roerdinkholder-Stoelwinder B, Novotný VM, Bos H, De Grip WJ. The proteome of red cell membranes and vesicles during storage in blood bank conditions. *Transfusion*. 2008;48(5):827-35.
- Burger P, Korsten H, De Korte D, Rombout E, Van Bruggen R, Verhoeven AJ. An improved red blood cell additive solution maintains 2,3-diphosphoglycerate and adenosine triphosphate levels by an enhancing effect on phosphofructokinase activity during cold storage. *Transfusion*. 2010;50(11):2386-2392.
- Canepa A, Filho JC, Gutierrez A, Carrea A, Forsberg AM, Nilsson E, Verrina E, Perfumo F, Bergström J. Free amino acids in plasma, red blood cells, polymorphonuclear leukocytes, and muscle in normal and uraemic children. *Nephrol Dial Transplant*. 2002;17(3):413-21.
- Castagnola M, Messana I, Sanna MT, Giardina B. Oxygen-linked modulation of erythrocyte metabolism: state of the art. *Blood Transfus*. 2010 Jun;8 Suppl 3:s53-8.

- Chaudhary R, Katharia R. Oxidative injury as contributory factor for red cells storage lesion during twenty eight days of storage. *Blood Transfus.* 2011;1-4.
- Chétrite G, Cassoly R. Affinity of hemoglobin for the cytoplasmic fragment of human erythrocyte membrane band 3. Equilibrium measurements at physiological pH using matrix-bound proteins: the effects of ionic strength, deoxygenation and of 2,3-diphosphoglycerate. *J Mol Biol.* 1985 Oct 5;185(3):639-44.
- Chu H, Breite A, Ciraolo P, et al. Characterization of the deoxyhemoglobin binding site on human erythrocyte band 3: implications for O₂ regulation of erythrocyte properties. *Blood* 2008; 111: 932-8.
- Clark MR, Mohandas N, Feo C, Jacobs MS, Shohet SB. Separate mechanisms of deformability loss in ATP-depleted and Ca-loaded erythrocytes. *J Clin Invest.* 1981;67(2):531-9.
- Cluitmans JC, Hardeman MR, Dinkla S, Brock R, Bosman GJ. Red blood cell deformability during storage: towards functional proteomics and metabolomics in the Blood Bank. *Blood Transfus.* 2012;10 Suppl 2:s12-8.
- Cohen C. M., Gascard P. Regulation and post-translational modification of erythrocyte membrane and membrane-skeletal proteins. *Semin. Hematol.* 1992; 29:244–292.
- Cohen P, Rosemeyer MA. Human glucose 6 –phosphate dehydrogenase: purification of the erythrocyte enzyme and the influence of ions in its activity. *European J Biochem* 1968; 8:1-7.
- Curtis D, Sparrow R, Brennan L, Van der Weyden MB. Elevated serum homocysteine as a predictor for vitamin B12 or folate deficiency. *Eur J Haematol.* 1994;52(4):227-32.
- D'Alessandro A, D'Amici GM, Vaglio S, Zolla L. Time-course Investigation of SAGM-Stored Erythrocyte Concentrates: from Metabolism to Proteomics. *Hematologica* 2012; 97:107-115.
- D'Alessandro A, Gevi F, Zolla L. Red blood cell metabolism under prolonged anaerobic storage. *Molecular Biosystems* 2013; doi:
- D'Alessandro A, Gevi F, Zolla L. A robust high resolution reversed-phase HPLC strategy to investigate various metabolic species in different biological models. *Mol Biosyst.* 2011; 7:1024-1032.
- D'Alessandro A, Giardina B, Gevi F, Timperio AM, Zolla L. Clinical metabolomics: the next stage of clinical biochemistry. *Blood Transfus.* 2012;10 Suppl 2:s19-24.
- D'Alessandro A, Liumbruno G, Grazzini G, Zolla L. Red blood cell storage: the story so far. *Blood Transfus.* 2010;8(2):82-8.
- D'Alessandro A, Righetti PG, Zolla L. The red blood cell proteome and interactome: an update. *J Proteome Res.* 2010;9(1):144-63.
- D'Alessandro A, Zolla L. Metabolomics and cancer drug discovery: let the cells do the talking. *Drug Discov Today.* 2012; 7(1-2):3-9.
- D'Alessandro A, Zolla L. We are what we eat: food safety and proteomics. *J Proteome Res.* 2012;11(1):26-36.
- D'Amici GM, Rinalducci S, Zolla L. Proteomic analysis of RBC membrane protein degradation during blood storage. *J Proteome Res.* 2007;6(8):3242-55.
- Darghouth D, Koehl B, Heilier JF, Madalinski G, Bovee P, Bosman G. Alterations of red blood cell metabolome in overhydrated hereditary stomatocytosis. *Haematologica.* 2011a; 96:1861-1865.

- Darghouth D, Koehl B, Junot C, Roméo PH. Metabolomic analysis of normal and sickle cell erythrocytes. *Transfus Clin Biol*. 2010;17(3):148-50.
- Darghouth D, Koehl B, Madalinski G, Heilier JF, Bovee P, Xu Y, et al. Pathophysiology of sickle cell disease is mirrored by the red blood cell metabolome. *Blood*. 2011b;117(6):e57-66.
- Dawson RB, Dabezies M, Hershey RT, Myers CS, Miller RM. Blood preservation. XLIII. Studies on the ascorbate mechanisms of maintaining red cell 2,3-DPG. *Transfusion*. 1980;20(3):316-20.
- Dawson RB, Hershey RT, Myers CS, Eaton JW. Blood preservation XLIV. 2,3-DPG maintenance by dehydroascorbate better than D-ascorbic acid. *Transfusion*. 1980;20(3):321-3.
- Dawson RB, Hershey RT, Myers CS, Miller RM. Blood preservation 35. Red cell 2,3-DPG and ATP maintained by DHA-ascorbate-phosphate. *Transfusion*. 1981;21(2):219-23.
- Delobel J, Prudent M, Rubin O, Crettaz D, Tissot JD, Lion N. Subcellular fractionation of stored red blood cells reveals a compartment-based protein carbonylation evolution. *J Proteomics*. 2012;76:181-93.
- Dietrich HH, Ellsworth ML, Sprague RS, Dacey RG Jr. Red blood cell regulation of microvascular tone through adenosine triphosphate. *Am J Physiol Heart Circ Physiol*. 2000 Apr;278(4):H1294-8.
- Dinkla S, Wessels K, Verdurmen WP, Tomelleri C, Cluitmans JC, Franssen J, Fuchs B, Schiller J, Joosten I, Brock R, Bosman GJ. Functional consequences of sphingomyelinase-induced changes in erythrocyte membrane structure. *Cell Death Dis*. 2012;3:e410.
- Divino Filho JC, Barany P, Stehle P, Fuhrst P, Bergström J. Free amino-acid levels simultaneously collected in plasma, muscle and erythrocytes of uraemic patients. *Nephrol Dial Transplant* 1997;12: 2339–2348
- Dumaswala UJ, Wilson MJ, Wu YL, Wykle J, Zhuo L, Douglass LM, Daleke DL. Glutathione loading prevents free radical injury in red blood cells after storage. *Free Radic Res*. 2000 Nov;33(5):517-29.
- Dumaswala UJ, Zhuo L, Jacobsen DW, et al. Protein and lipid oxidation of banked human erythrocytes: role of glutathione. *Free Radic Biol Med* 1999; 27: 1041-9.
- Dumont LJ, Yoshida T, AuBuchon JP. Anaerobic storage of red blood cells in a novel additive solution improves in vivo recovery. *Transfusion*. 2009;49(3):458-64.
- Efferth T, Bachli EB, Schwarzl SM, Goede JS, West C, Smith JC, Beutler E. Glucose-6-phosphate dehydrogenase (G6PD) deficiency-type Zurich: a splice site mutation as an uncommon mechanism producing enzyme deficiency. *Blood*. 2004;104(8):2608.
- Elsner T, Kostrezewa M, Maier T, Kruppa G. Microorganism Identification Based On MALDI-TOF-MS Fingerprints. In *Detection of Biological Agents for the Prevention of Bioterrorism NATO Science for Peace and Security Series A: Chemistry and Biology* 2011, pp 99-113
- Elwyn DH, Launder WJ, Parikh HC, Wis EM, Jr. Roles of plasma and erythrocytes in interorgan transport of amino acids in dogs. *Am J Physiol* 1972; 222: 1333–1342
- European Directorate for the Quality of Medicines & HealthCare. *Guide to the Preparation, Use and Quality Assurance of Blood Components*. Recommendation No. R (95) 15.16th Edition. Council of Europe 2011.7
- Fergusson DA, Hébert P, Hogan DL, LeBel L, Rouvinez-Bouali N, Smyth JA, Sankaran K, Tinmouth A, Blajchman MA, Kovacs L, Lachance C, Lee S, Walker CR, Hutton B, Ducharme R, Balchin K, Ramsay T, Ford JC,

- Kakadekar A, Ramesh K, Shapiro S. Effect of fresh red blood cell transfusions on clinical outcomes in premature, very low-birth-weight infants: the ARIPI randomized trial. *JAMA*. 2012;308(14):1443-51.
- Fico A, Paglialunga F, Cigliano L, Abrescia P, Verde P, Martini G, Iaccarino I, Filosa S. Glucose-6-phosphate dehydrogenase plays a crucial role in protection from redox-stress-induced apoptosis. *Cell Death Differ*. 2004;11(8):823-31.
- Filip C, Zamosteanu N, Albu E. Homocysteine in red blood cell metabolism – pharmacological approaches. 2012; Chapter 3 in “Blood Cell – An overview of Studies in Hematology”. Edited by Terry E. Moschandreou, ISBN 978-953-51-0753-8. doi:10.5772/47795
- Flegel WA. Fresh blood for transfusion: how old is too old for red blood cell units? *Blood Transfus*. 2012;10(3):247-51.
- Forbes WH, Roughton FJ. The equilibrium between oxygen and haemoglobin: I. The oxygen dissociation curve of dilute blood solutions. *J Physiol*. 1931;71(3):229-60.
- Gabrio BW, Finch CA, Huennekens FM: Erythrocyte preservation: a topic in molecular biochemistry. *Blood* 11:103, 1956.
- Galtieri A, Tellone E, Romano L, Misiti F, Bellocco E, Ficarra S, Russo A, Di Rosa D, Castagnola M, Giardina B, Messina I. Band-3 protein function in human erythrocytes: effect of oxygenation-deoxygenation. *Biochim Biophys Acta*. 2002 Aug 19;1564(1):214-8.
- Gevi F, D'Alessandro A, Rinalducci S, Zolla L. Alterations of red blood cell metabolome during cold liquid storage of erythrocyte concentrates in CPD-SAGM. *J Proteomics*. 2012; 76:10-27.
- Givan A. Flow cytometry. *Methods in Molecular Biology: Flow Cytometry Protocols* 2011; 699, pp1-29. Edited by: T. S. Hawley and R. G. Hawley © Humana Press Inc., Totowa, NJ
- Glauer SC, Forster RE 2nd. pH dependence of the oxyhemoglobin dissociation curve at high oxygen tension. *J Appl Physiol*. 1967 Jan;22(1):113-6.
- Hamasaki N, Asakura T, Minakami S. Effect of oxygen tension on glycolysis in human erythrocytes. *J Biochem*. 1970;68(2):157-61.
- Harboe M. A method for determination of hemoglobin in plasma by near-ultraviolet spectrophotometry. *Scand J Clin Lab Invest*. 1959;11(1):66-70.
- Heinrich R, Rapoport SM, Rapoport TA. Metabolic regulation and mathematical models, *Prog. Biophys. Mol. Biol*. 1977; 32 (1): 1–82.
- Hess JR, Hill HR, Oliver CK, Lippert LE, Greenwalt TJ. Alkaline CPD and the preservation of RBC 2,3-DPG. *Transfusion* 2002, 42: 747–752.
- Hess JR. Red cell changes during storage. *Transfus Apher Sci*. 2010;43(1):51-9.
- Hess JR. Red cell storage. *J Proteomics*. 2010;73(3):368-73.
- Hogman CF, de Verdier CH, Ericson A, et al. Studies on the mechanism of human red cell loss of viability during storage at +4 degrees C in vitro. I. Cell shape and total adenylate concentration as determinant factors for posttransfusion survival. *Vox Sang* 1985; 48: 257-268.

- Högman CF, Löf H, Meryman HT. Storage of red blood cells with improved maintenance of 2,3-bisphosphoglycerate. *Transfusion*. 2006;46(9):1543-52.
- Holzhtutter HG, Jacobasch G, Bisdorff A. Mathematical modelling of metabolic pathways affected by an enzyme deficiency. A mathematical model of glycolysis in normal and pyruvate-kinase-deficient red blood cells, *Eur. J. Biochem*. 1985; 149(1): 101–111.
- Ibe BO, Morris J, Kurantsin-Mills J, Raj JU. Sickle erythrocytes induce prostacyclin and thromboxane synthesis by isolated perfused rat lungs. *Am J Physiol*. 1997;272(4 Pt 1):L597-602.
- Jamshidi N, Edwards JS, Fahland T, Church GM, Palsson BO. Dynamic simulation of the human red blood cell metabolic network. *Bioinformatics*. 2001;17(3):286-7.
- Jamshidi N, Palsson BØ. Systems biology of the human red blood cell. *Blood Cells Mol Dis*. 2006;36(2):239-47.
- Jeanningros R, Serres F, Dassa D, Azorin JM, Grignon S. Red blood cell L-tryptophan uptake in depression: kinetic analysis in untreated depressed patients and healthy volunteers. *Psychiatry Res*. 1996;63(2-3):151-9.
- Jensen FB. Red blood cell pH, the Bohr effect, and other oxygenation-linked phenomena in blood O₂ and CO₂ transport. *Acta Physiol Scand*. 2004 Nov;182(3):215-27.
- Johnston CS, Meyer CG, Srilakshmi JC. Vitamin C elevates red blood cell glutathione in healthy adults. *Am J Clin Nutr*. 1993;58(1):103-5.
- Kanehisa M, Goto S. KEGG: kyoto encyclopedia of genes and genomes. *Nucleic Acids Res*. 2000; 28(1):27-30.
- Karon BS, Van Buskirk CM, Jaben EA, Hoyer JD, Thomas DD. Temporal sequence of major biochemical events during Blood Bank storage of packed red blood cells. *Blood Transfus*. 2012; 28:1-9.
- Kim PS, Iyer RK, Lu KV, et al. Expression of the liver form of arginase in erythrocytes. *Mol Genet Metab*. 2002;76(2):100-110.
- Kinoshita A, Tsukada K, Soga T, et al. Roles of hemoglobin. Allosterity in hypoxia-induced metabolic alterations in erythrocytes: simulation and its verification by metabolome analysis. *J Biol Chem* 2007; 282: 10731-41.
- Kleinbongard P, Schulz R, Rassaf T, Lauer T, Dejam A, Jax T, Kumara I, Gharini P, Kabanova S, Ozüyanan B, Schnürch HG, Gödecke A, Weber AA, Robenek M, Robenek H, Bloch W, Rösen P, Kelm M. Red blood cells express a functional endothelial nitric oxide synthase. *Blood*. 2006 Apr 1;107(7):2943-51.
- Koch CG, Li L, Sessler DI, Figueroa P, Hoeltge GA, Mihaljevic T, Blackstone EH. Duration of red-cell storage and complications after cardiac surgery. *N Engl J Med* 2008; 358:1229-39.
- Kriebardis AG, Antonelou MH, Stamoulis KE, Economou-Petersen E, Margaritis LH, Papassideri IS. Progressive oxidation of cytoskeletal proteins and accumulation of denatured hemoglobin in stored red cells. *J Cell Mol Med* 2007;11:148-55.
- Lang E, Qadri SM, Lang F. Killing me softly - suicidal erythrocyte death. *Int J Biochem Cell Biol*. 2012 Aug;44(8):1236-43.
- Lelubre C, Piagnerelli M, Vincent JL. Association between duration of storage of transfused red blood cells and morbidity and mortality in adult patients: myth or reality? *Transfusion*. 2009;49(7):1384-94.
- Lewis IA, Campanella ME, Markley JL, et al. Role of band 3 in regulating metabolic flux of red blood cells. *Proc Natl Acad Sci U S A* 2009; 106: 18515-20.

- Li J, Lykotrafitis G, Dao M, Suresh S. Cytoskeletal dynamics of human erythrocyte. *Proc Natl Acad Sci U S A*. 2007;104(12):4937-42.
- Li YK, Boggaram J, Byers LD. Alkylation of glyceraldehyde-3-phosphate dehydrogenase with haloacetylphosphonates. An unusual pH-dependence. *Biochem J*. 1991;275 (Pt 3):767-73.
- Lim GHW, Wortis M, Mukhopadhyay R. Stomatocyte-discocyte-echinocyte sequence of the human red blood cell: evidence for the bilayer-couple hypothesis from membrane mechanics. *Proc Natl Acad Sci* 2002; 99(26):16766-9.
- Lion N, Crettaz D, Rubin O, Tissot JD. Stored red blood cells: a changing universe waiting for its map(s). *J Proteomics*. 2010;73(3):374-85.
- Locasale JW, Grassian AR, Melman T, Lyssiotis CA, Mattaini KR, Bass AJ, Heffron G, Metallo CM, Muranen T, Sharfi H, Sasaki AT, Anastasiou D, Mullarky E, Vokes NI, Sasaki M, Beroukhim R, Stephanopoulos G, Ligon AH, Meyerson M, Richardson AL, Chin L, Wagner G, Asara JM, Brugge JS, Cantley LC, Vander Heiden MG. Phosphoglycerate dehydrogenase diverts glycolytic flux and contributes to oncogenesis. *Nat Genet*. 2011 Jul 31;43(9):869-74.
- Low PS. Structure and function of the cytoplasmic domain of band 3: center of erythrocyte membrane-peripheral protein interactions. *Biochim. Biophys Acta*. 1986; 864:145-167.
- Lu SC. Regulation of glutathione synthesis. *Mol. Aspects. Med*. 2009; 30:42-59.
- Mansfield KD, Simon MC, Keith B. Hypoxic reduction in cellular glutathione levels requires mitochondrial reactive oxygen species. *J Appl Physiol*. 2004;97(4):1358-66.
- Marshall WE, Goldinger JM, Omachi A. The influence of anaerobiosis on human erythrocyte metabolism. *Proc Soc Exp Biol Med*. 1977 Mar;154(3):356-9.
- Matte A, Bertoldi M, Mohandas N, An X, Bugatti A, Maria Brunati A, Rusnati M, Tibaldi E, Siciliano A, Turrini F, Perrotta S, De Franceschi L. Membrane association of peroxiredoxin-2 in red cells is mediated by n-terminal cytoplasmic domain of band 3. *Free Radic Biol Med*. 2012 Oct 30. doi:pil:S0891-5849(12)01774-1.
- May JM, Qu ZC, Mendiratta S. Protection and recycling of alpha-tocopherol in human erythrocytes by intracellular ascorbic acid. *Arch Biochem Biophys*. 1998;349(2):281-9.
- May JM. Ascorbate function and metabolism in the human erythrocyte. *Front Biosci*. 1998;3:d1-10.
- Mazor D, Golan E, Philip V, Katz M, Jafe A, Ben-Zvi Z, Meyerstein N. Red blood cell permeability to thiol compounds following oxidative stress. *Eur J Haematol*. 1996 Sep;57(3):241-6.
- Melamud E, Vastag L, Rabinowitz JD. Metabolomic analysis and visualization engine for LC-MS data. *Anal Chem*. 2010; 82(23):9818-9826.
- Messana I, Ferroni L, Misiti F, Girelli G, Pupella S, Castagnola M, et al. Blood bank conditions and RBCs: the progressive loss of metabolic modulation. *Transfusion*. 2000;40(3):353-60.
- Messana I, Misiti F, el-Sherbini S, Giardina B, Castagnola M. Quantitative determination of the main glucose metabolic fluxes in human erythrocytes by ¹³C- and ¹H-MR spectroscopy. *J Biochem Biophys Methods*. 1999; 39:63-84.

- Messana I, Orlando M, Cassiano L, Pennacchietti L, Zuppi C, Castagnola M, Giardina B. Human erythrocyte metabolism is modulated by the O₂-linked transition of hemoglobin. *FEBS Lett.* 1996;390(1):25-28.
- Misiti F, Meucci E, Zuppi C, Vincenzoni F, Giardina B, Castagnola M, Messana I. O(2)-dependent stimulation of the pentose phosphate pathway by S-nitrosocysteine in human erythrocytes. *Biochem Biophys Res Commun.* 2002;294(4):829-34.
- Monod J, Wyman J, Changeux JP. On the nature of allosteric transitions: a plausible model. *J Mol Biol.* 1965;12:88-118.
- Moses SW, Bashan N, Gutman A. Glycogen metabolism in the normal red blood cell. *Blood.* 1972 Dec;40(6):836-43.
- Mulquiney PJ, Bubb WA, Kuchel PW. Model of 2,3-bisphosphoglycerate metabolism in the human erythrocyte based on detailed enzyme kinetic equations: in vivo kinetic characterization of 2,3-bisphosphoglycerate synthase/phosphatase using ¹³C and ³¹P NMR. *Biochem. J.* 1999; 342 (Pt. 3):567-580
- Murphy JR. Erythrocyte metabolism. II. Glucose metabolism and pathways. *J. Lab. Clin. Med.* 1960; 55:286-302.
- Nakayama Y, Kinoshita A, Tomita M. Dynamic simulation of red blood cell metabolism and its application to the analysis of a pathological condition. *Theor Biol Med Model.* 2005;2:18.
- Nicholson JK, Lindon JC. Systems biology: Metabonomics. *Nature* 2008; 455 (7216): 1054-6.
- Nishino T, Yachie-Kinoshita A, Hirayama A, Soga T, Suematsu M, Tomita M. In silico modeling and metabolome analysis of long-stored erythrocytes to improve blood storage methods. *J Biotechnol.* 2009; 144: 212-223.
- Nur E, Brandjes DP, Teerlink T, Otten HM, Oude Elferink RP, Muskiet F, Evers LM, ten Cate H, Biemond BJ, Duits AJ, Schnog JJ; CURAMA study group. N-acetylcysteine reduces oxidative stress in sickle cell patients. *Ann Hematol.* 2012;91(7):1097-105.
- Park Y, Best CA, Auth T, Gov NS, Safran SA, Popescu G, Suresh S, Feld MS. Metabolic remodeling of the human red blood cell membrane. *Proc Natl Acad Sci U S A.* 2010;107(4):1289-94.
- Park Y, Best-Popescu CA, Dasari RR, Popescu G. Light scattering of human red blood cells during metabolic remodeling of the membrane. *J Biomed Opt.* 2011;16(1):011013.
- Percy AK, Schmell E, Earles BJ, Lennarz WJ. Phospholipid biosynthesis in the membranes of immature and mature red blood cells. *Biochemistry.* 1973;12(13):2456-61.
- Racek J, Herynková R, Holecek V, Jerábek Z, Sláma V. Influence of antioxidants on the quality of stored blood. *Vox Sang.* 1997;72(1):16-9.
- Rapoport I, Berger H, Rapoport SM, Elsner R, Gerber G. Response of the glycolysis of human erythrocytes to the transition from the oxygenated to the deoxygenated state at constant intracellular pH. *Biochim Biophys Acta.* 1976 Mar 25;428(1):193-204
- Rifkind JM, Nagababu E. Hemoglobin Redox Reactions and Red Blood Cell Aging. *Antioxid Redox Signal.* 2012; doi:10.1089/ars.2012.4867.
- Rinalducci S, D'Amici GM, Blasi B, Vaglio S, Grazzini G, Zolla L. Peroxiredoxin-2 as a candidate biomarker to test oxidative stress levels of stored red blood cells under blood bank conditions. *Transfusion.* 2011;51(7):1439-49.

- Rizvi SI, Pandey KB, Jha R, Maurya PK. Ascorbate recycling by erythrocytes during aging in humans. *Rejuvenation Res.* 2009;12(1):3-6.
- Rogers SC, Said A, Corcuera D, McLaughlin D, Kell P, Doctor A. Hypoxia limits antioxidant capacity in red blood cells by altering glycolytic pathway dominance. *FASEB J.* 2009; 23: 3159-3170.
- Rogers SC, Said A, Corcuera D, McLaughlin D, Kell P, Doctor A. Hypoxia limits antioxidant capacity in red blood cells by altering glycolytic pathway dominance. *FASEB J.* 2009;23(9):3159-70.
- Rosenberg R, Young JD, Ellory JC. L-Tryptophan transport in human red blood cells. *Biochim Biophys Acta.* 1980;598(2):375-84.
- Roux-Dalvai F, Gonzalez de Peredo A, Simó C, Guerrier L, Bouyssié D, Zanella A, Citterio A, Burlet-Schiltz O, Boschetti E, Righetti PG, Monsarrat B. Extensive analysis of the cytoplasmic proteome of human erythrocytes using the peptide ligand library technology and advanced mass spectrometry. *Mol Cell Proteomics.* 2008;7(11):2254-69.
- Rubin O, Crettaz D, Tissot JD, Lion N. Microparticles in stored red blood cells: submicron clotting bombs? *Blood Transfus.* 2010;8 Suppl 3:s31-8.
- Rubin O, Delobel J, Prudent M, Lion N, Kohl K, Tucker EI, Tissot JD, Angelillo-Scherrer A. Red blood cell-derived microparticles isolated from blood units initiate and propagate thrombin generation. *Transfusion.* 2012; doi: 10.1111/trf.12008.
- Scalbert A, Brennan L, Fiehn O, Hankemeier T, Kristal BS, van Ommen B, Pujos-Guillot E, Verheij E, Wishart D, Wopereis S. Mass-spectrometry-based metabolomics: limitations and recommendations for future progress with particular focus on nutrition research. *Metabolomics.* 2009;5:435-458.
- Schauer M, Heinrich R, Rapoport SM. Mathematical modelling of glycolysis and adenine nucleotide metabolism of human erythrocytes: I. Reaction-kinetic statements, analysis of in vivo state and determination of starting conditions for in vitro experiments, *Acta Biol. Med. Ger.* 1981; 12: 1659–1682.
- Schuster S, Kenanov D. Adenine and adenosine salvage pathways in erythrocytes and the role of S-adenosylhomocysteine hydrolase. A theoretical study using elementary flux modes. *FEBS J.* 2005, 272:5278-5290.
- Shan X, Aw TY, Shapira R, Jones DP. Oxygen dependence of glutathione synthesis in hepatocytes. *Toxicology and Applied Pharmacology* 1989; 101:261-270.
- Shemin D, Rittenberg D. The life span of the human red blood cell. *J Biol Chem.* 1946;166(2):627-36.
- Siciliano A, Turrini F, Bertoldi M, Matte A, Pantaleo A, Olivieri O, De Franceschi L. Deoxygenation affects tyrosine phosphoproteome of red cell membrane from patients with sickle cell disease. *Blood Cells Mol Dis.* 2010;44(4):233-42.
- Sidi Y, Gelvan I, Brosh S, Pinkhas J, Sperling O. Guanine ribonucleotide metabolism in human red blood cells: evidence for a high rate of GMP dephosphorylation. *Biochem Med Metab Biol.* 1989 Apr;41(2):149-54.
- Smith CA, O'Maille G, Want EJ, Qin C, Trauger SA, Brandon TR, Custodio DE, et al. METLIN: a metabolite mass spectral database. *Ther Drug Monit.* 2005;27(6):747-51.

- Sparrow RL. Time to revisit red blood cell additive solutions and storage conditions: a role for "omics" analyses. *Blood Transfus.* 2012;10 Suppl 2:s7-11.
- Sprague RS, Ellsworth ML, Stephenson AH, Lonigro AJ. Participation of cAMP in a signal-transduction pathway relating erythrocyte deformation to ATP release. *Am J Physiol Cell Physiol.* 2001;281(4):C1158-64.
- Stocks J, Dormandy TL. The autoxidation of human red cell lipids induced by hydrogen peroxide. *Br J Haematol.* 1971;20(1):95-111.
- Strauss D, de Verdier CD. Preservation of red blood cells with purines and nucleosides. III. Synthesis of adenine, guanine, and hypoxanthine nucleotides. *Folia Haematol Int Mag Klin Morphol Blutforsch.* 1980;107(3):434-53.
- Tautenhahn R, Patti GJ, Kalisiak E, Miyamoto T, Schmidt M, Lo FY, et al. MetaXCMS: second-order analysis of untargeted metabolomics data. *Anal Chem.* 2011;83(3):696-700.
- Tsikas D, Suchy MT, Niemann J, Tossios P, Schneider Y, Rothmann S, Gutzki FM, Frölich JC, Stichtenoth DO. Glutathione promotes prostaglandin H synthase (cyclooxygenase)-dependent formation of malondialdehyde and 15(S)-8-iso-prostaglandin F(2 α). *FEBS Lett.* 2012; 586: 3723-3730.
- Tunncliffe G. Amino acid transport by human erythrocyte membranes. *Comp Biochem Physiol Comp Physiol.* 1994;108(4):471-478.
- Tusa JK, Huarui H. Critical care analyzer with fluorescent optical chemosensors for blood analytes. *J Mater Chem* 2005; 15:2640-2647.
- Valeri CR, Hirsch NM. Restoration in vivo of erythrocyte adenosine triphosphate, 2,3-diphosphoglycerate, potassium ion, and sodium ion concentrations following the transfusion of acid-citrate-dextrose-stored human red blood cells. *J Lab Clin Med.* 1969;73(5):722-33.
- van Wijk R, van Solinge WW. The energy-less red blood cell is lost: erythrocyte enzyme abnormalities of glycolysis. *Blood.* 2005;106:4034-4042.
- Veale MF, Healey G, Sparrow RL. Effect of additive solutions on red blood cell (RBC) membrane properties of stored RBCs prepared from whole blood held for 24 hours at room temperature. *Transfusion.* 2011;51(1):25S-33S.
- Walder JA, Chatterjee R, Steck TL, Low PS, Musso GF, Kaiser ET, Rogers PH, Arnone A. The interaction of hemoglobin with the cytoplasmic domain of band 3 of the human erythrocyte membrane. *J Biol Chem.* 1984 Aug 25;259(16):10238-46.
- Wang L, Olivecrona G, Götberg M, Olsson ML, Winzell MS, Erlinge D. ADP acting on P2Y₁₃ receptors is a negative feedback pathway for ATP release from human red blood cells. *Circ Res.* 2005 Feb 4;96(2):189-96.
- Weber RE, Voelter W, Fago A, Echner H, Campanella E, Low PS. Modulation of red cell glycolysis: interactions between vertebrate hemoglobins and cytoplasmic domains of band 3 red cell membrane proteins. *Am J Physiol Regul Integr Comp Physiol.* 2004;287(2):R454-64.
- Werner A, Heinrich R. A kinetic model for the interaction of energy metabolism and osmotic states of human erythrocytes. Analysis of the stationary "in vivo" state and of time dependent variations under blood preservation conditions, *Biomed. Biochim. Acta* 1985; 44(2):185-212.

- Wiback SJ, Pålsson BØ. Extreme pathway analysis of human red blood cell metabolism. *Biophys J.* 2002; 83:808-818.
- Wishart DS, Knox C, Guo AC, Eisner R, Young N, Gautam B, Hau DD, Psychogios N, Dong E, Bouatra S, Mandal R, Sinelnikov I, Xia J, Jia L, Cruz JA, Lim E, Sobsey CA, Shrivastava S, Huang P, Liu P, Fang L, Peng J, Fradette R, Cheng D, Tzur D, Clements M, Lewis A, De Souza A, Zuniga A, Dawe M, Xiong Y, Clive D, Greiner R, Nazzyrova A, Shaykhtudinov R, Li L, Vogel HJ, Forsythe I. HMDB: a knowledgebase for the human metabolome. *Nucleic Acids Res.* 2009 Jan;37(Database issue):D603-10.
- Yoshida T, AuBuchon JP, Dumont LJ, Gorham JD, Gifford SC, Foster KY, Bitensky MW. The effects of additive solution pH and metabolic rejuvenation on anaerobic storage of red cells. *Transfusion* 2008; 48: 2096-1205.
- Yoshida T, AuBuchon JP, Tryzelaar L, Foster KY, Bitensky MW. Extended storage of red blood cells under anaerobic conditions. *Vox Sang.* 2007;92(1):22-31.
- Yoshida T, Shevkopyas SS. Anaerobic storage of red blood cells. *Blood Transfus.* 2011;8(4):220-36.
- Zan T, Tao J, Tang RC, Liu YC, Liu Y, Huang B, Zhou JY, Wu MH, Liu HL. [Effect of vitamin C antioxidative protection on human red blood cells]. *Zhongguo Shi Yan Xue Ye Xue Za Zhi.* 2005;13(6):1106-8.
- Zimrin AB, Hess JR. Current issues relating to the transfusion of stored red blood cells. *Vox Sang.* 2009; 96(2):93-103.
- Zolla L, D'Alessandro A. An efficient apparatus for rapid deoxygenation of erythrocyte concentrates for alternative banking strategies. *J Blood Transfusion* 2013; doi:
- Zolla L, Ioppolo C, Amiconi G, Benaglia A, Antonini E. Changes in rate of methemoglobin reduction and oxygen affinity of erythrocytes incubated with inosine, pyruvate and phosphate. *Experientia.* 1977; 33:1524-1526.
- Zolla L, Ioppolo C, Amiconi G, Benaglia A, Antonini E. Changes in rate of methemoglobin reduction and oxygen affinity of erythrocytes incubated with inosine, pyruvate and phosphate. *Experientia.* 1977;33(11):1524-6.

Chapter 8: *Translational applications*

Contents

8.1 Red blood cell populations and membrane levels of peroxiredoxin 2 as candidate biomarkers to reveal blood doping

The contents of this chapter report the contents of the the following publications by the candidate:

1. Marrocco Cristina, Pallotta Valeria, D'Alessandro Angelo, Gilda Alves, Zolla Lello
Red blood cell populations and membrane levels of peroxiredoxin 2 as candidate biomarkers to reveal blood doping
Blood Transfusion 2012; 10 Suppl 2:s71-7.
-

In the previous chapters, we dissected red blood cell storage lesions through Integrated Omics approaches and we compared the obtained results with analogous investigations on senescent (*in vivo* aged) erythrocytes. From these basic science/transfusion medicine-oriented investigations, we could build up a significant body of knowledge that could hold unexpected translational applications. Biomarkers of *in vitro* aged red blood cells, as determined in the previous chapters, might indeed represent a key strategy to challenge the increasingly widespread doping practice of autologous blood transfusions, a phenomenon that is deeply rooted in fatigue sports, such as cycling (many cases are now worldwide famous, such as the recent cases of the former cycling professionals Armstrong and Hincapie, or the Italian Riccardo Riccò) and might as well represent a diffused illicit practice in many other disciplines, including soccer (according to the shocking declaration of the Dr. Eufemiano Fuentes within the framework of the Operacion Puerto - <http://11x2.com/news/1167678/fuentes-if-i-would-talk-the-spanish-football-team-would-be-stripped-of-the-2010-world-cup>).

8.1 Red blood cell populations and membrane levels of peroxiredoxin 2 as candidate biomarkers to reveal blood doping

Overview of this section

Blood doping represents one main trend in doping strategies. Blood doping refers to the practice of boosting the number of red blood cells (RBCs) in the bloodstream in order to enhance athletic performance, by means of blood transfusions, administration of erythropoiesis-stimulating substances, blood substitutes, natural or artificial altitude facilities, and innovative gene therapies. While detection of recombinant EPO and homologous transfusion is already feasible through electrophoretic, mass spectrometry or flow cytometry-based approaches, no method is currently available to tackle doping strategies relying on autologous transfusions.

We exploited an *in vitro* model of autologous transfusion through a 1:10 dilution of concentrated RBCs after 30 days of storage upon appropriate dilution in freshly withdrawn RBCs from the same donor. Western blot towards membrane Prdx2 and Percoll density gradients were exploited to assess their suitability as biomarkers of transfusion.

Membrane Prdx2 was visible in day 30 samples albeit not in day 0, while it was still visible in the 1:10 dilution of day 30 in day 0 RBCs. Cell gradients also highlighted changes in the profile of the RBC subpopulations upon dilution of stored RBCs in the fresh ones.

From this preliminary *in vitro* investigation it emerges that Prdx2 and RBC populations might be further tested as candidate biomarkers of blood doping through autologous transfusion, though it is yet to be assessed whether the kinetics *in vivo* of Prdx2 exposure in the membrane of transfused RBCs will endow a sufficient time-window to allow reliable anti-doping testing.

Keywords: blood doping; red blood cell; population; peroxiredoxin 2.

Introduction

One recent trend in illicit doping practices regards the adoption of blood doping, which is forbidden by the World Anti-Doping Agency (WADA) (Segura et al., 2012). Blood doping refers to the practice of boosting the number of red blood cells (RBCs) in the bloodstream in order to enhance athletic performance, by means, for example, of transfusions. A wide group of illicit practices goes under the name of blood doping, including blood transfusions, administration of erythropoiesis-stimulating substances, blood substitutes, natural or artificial altitude facilities, and innovative gene therapies (Lippi and Banfi, 2006). Blood transfusion for doping purposes is an extremely straightforward, practical and effective means of increasing an athlete's red blood-cell supply in advance of competition, which became rather popular in the 1970s. Nonetheless it has suddenly declined upon the introduction and widespread diffusion of recombinant human erythropoietin (rEPO) among elite endurance athletes in late 80's (Giraud et al., 2010). As RBCs carry oxygen from the lungs to the muscles, an increase in the overall number of circulating RBCs might result in the improvement of an athlete's aerobic capacity (VO_2 max) and endurance (Ashenden, 2002). Blood doping has become rather widespread especially in those sports where other doping strategies based on hormone stimulation (erythropoietins) (Baumann et al., 2012) or other drugs are no longer feasible, due to the rise of new anti-doping approaches. Most recently, following implementation of reliable tests to screen for erythropoiesis-stimulating substances in 2001 (Giraud et al., 2010), trends in blood doping have come back to origins, with blood transfusions making a strong resurgence. Doping by blood transfusion can be classified as homologous, where the blood is infused into someone other than the donor, and autologous, where the blood donor and transfusion recipient are the same. The former case produces more clinically relevant side effects, while it is easily detectable using current antidoping protocols based on erythrocyte phenotyping by flow cytometry (Arndt and Kumpel, 2008).

Since the donor and recipient blood are identical in autologous blood doping, this is less risky, though much more challenging to detect. Indirect strategies, relying on significant deviations from individual hematological profiles following autologous blood donation and reinfusion, are currently being investigated.

Other than in the modalities of collection (homologous versus autologous), RBCs could also be differentially stored at 4°C (hypothermique storage) or glycerolized and thus frozen in order to be cryostored. RBCs uniquely suited to this process because they can be concentrated, frozen and later thawed with little loss of viability (haemolysis below 1% and 24h *in vivo* survival above the 75% thresholds), though both procedures hold different biological drawbacks (D'Alessandro et al., 2010; D'Alessandro et al., 2012; Pallotta et al., 2012). In an autologous transfusion, the athlete's own RBCs are harvested well in advance of competition and then re-introduced before a critical event. For some time after the harvesting the athlete may be anemic. However, cryostorage is rather expensive and thus only top athletes are thought to be able to afford such a technology, while hypothermique storage is thought to be more diffused.

From a logistical standpoint, either type of transfusion requires the athlete to surreptitiously transport cold or frozen RBCs, thaw (for the latter) and re-infuse them in a non-clinical setting and then dispose of the medical paraphernalia.

However, also other blood doping approaches are not free of health hazards. Excessive use of the rEPO hormone, for example, can raise hematocrit above 70% which can cause polycythemia, increase blood viscosity and raise the likelihood of heart suffering from excessive stress, which could result in fatal outcomes. Indeed, rEPO use is a suspect in nearly 20 deaths in 4 years in European cyclists. In the 1998 Tour de France, a team was ejected for using rEPO and six other teams quit the race, while in recent years, diverse endurance and sprint athletes have been caught or accused of using rEPO (Eichner, 2007).

While rEPO could be now easily detected through electrophoretic and MS approaches (Tsitsimpikou et al., 2011), indirect testing might allow also monitoring of indirect effects of rEPO in order to reveal doping in athletes long time after assumption of the drug. Such a detection strategy focuses on the monitoring of RBC-related parameters, including hematocrit (HCT) and the concentration of hemoglobin (Hb).

On the other hand, at the moment there is no official methodology available to detect autologous blood transfusions. Total haemoglobin mass measurements (ASHenden and Morkeberg, 2011) and the detection of metabolites of blood bags plasticizers (di(2-ethylhexyl) phthalate - DEHP) in urine (Solymos et al., 2011) have been recently proposed as valid strategies to tackle blood doping episodes.

However, no definitive approach is currently available and the search for alternative strategies is still an open issue. Literature has provided a great deal of data about hypothermically stored blood (Bosman et al., 2008; Lion et al., 2010; Blasi et al., 2012; Pallotta et al., 2012). Recent publications from our group have documented irreversible modifications taking place at the protein level as storage progresses at 4°C degrees, such as the accumulation of membrane protein fragments or aggregates (D'Alessandro et al., 2012), the accumulation at the membrane level of oxidative stress-related proteins such as peroxiredoxin (Prdx) 2 (Rinalducci et al., 2011a) and the alteration of its oligomeric state (Rinalducci et al., 2011). The goal of the present paper is to provide preliminary results about testing of the hypothesis whether the anomalous and irreversible changes in protein patterns (in particular Prdx2), which we could outline in our previous investigations on blood storage (Rinalducci et al., 2011a and 2011b; Pallotta et al., 2012), might also represent a suitable marker for *in vitro* aging of RBCs could be hopefully adopted also as markers of doping transfusion practices in athletes.

Materials and Methods

Sample collection Whole blood ($56.25 \text{ mL} \pm 10\%$) was collected from healthy volunteer donors into CPD anticoagulant (7.875 mL). After separation of plasma and buffy coat by centrifugation, RBCs were suspended in 12.5 mL of SAG-M (Saline, Adenine, Glucose, Mannitol) additive solution. We studied RBC units collected from 4 donors [male = 2, female = 2, age 35 ± 8.5 (mean \pm S.D.)] in Rome (Italy), upon signing of informed consent according to the declaration of Helsinki. It is worthwhile to stress that the experiment was a scale-down of a routine donation/transfusion workflow, since only 1/8 of the volume of a routine donation (56.25 mL vs 450 mL) was collected from the same donor twice, once at day 0 (which would be stored for 30 days), and the second time at 30 days after the first withdrawal, in order to obtain a fresh day 0 control to be exploited in 1:10 dilutions, as specified below, without any complication to the donor.

RBC units were stored under standard blood bank conditions (4 ± 2 °C) and samples were removed aseptically for the analysis at day 0 or upon 30 days of storage.

RBC dilution: *in vitro* model for blood transfusion. An *in vitro* model for dilution 1:10 of 30 days old RBCs in day 0 RBCs from the same donor has been designed as to simulate dilutions of RBCs in the bloodstream of the recipient/transfusing athlete. Indeed the final HCT of RBCs from processed whole blood and stored in CPD-SAGM is approximately 60 percent. A unit of packed RBCs contains approximately 150-200 ml of RBCs. Since the average whole blood volume in an adult male is approximately 5 liters, with hematocrit around 45%, the approximate volume of circulating RBCs is around 2.250 liters. Thus, a reliable *in vitro* model would be designed as to perform a 1:10 dilution as follows: after 30 days of storage RBCs will be concentrated (through removal of the additive solution via centrifugation) and diluted in 10 volumes of day 0 RBCs enriched from whole blood.

RBC protein extraction Extraction of membrane and cytosol proteins from human erythrocyte has been performed following the conventional method as described by Olivieri et al. (2001) with minor modifications. Erythrocytes were isolated by centrifuging twice at $1000\times g$ for 10 min. Packed cells were washed three times in 5 mM phosphate buffer pH 8.0, containing 0.9% w/v NaCl; then, they were centrifuged at $300\times g$ for 10 min, at 4 °C. Erythrocytes were resuspended in 1 mL PBS containing 100 mM N-ethylmaleimide (NEM), to avoid possible oxidation artifacts during cell preparation (Low et al., 2007). After 15 min of incubation at room temperature, cells were pelleted and then lysed with 9 vol of cold 5 mM phosphate buffer pH 8.0 containing 1 mM EDTA, 1 mM phenylmethanesulfonyl fluoride (PMSF) and 100 mM NEM. Cytosol was collected after centrifugation at $17,000\times g$ for 20 min at 4 °C and its protein content was estimated by the DC protein assay method (Bio-Rad, Hercules, CA, USA). Membranes were washed with the same buffer until free of hemoglobin: in order to remove non-specifically membrane-bound cytosolic proteins, membranes were further washed for three times with 0.9% w/v NaCl and collected at $17,000\times g$, for 20 min at 4 °C. Protein content was estimated by the bicinchoninic acid method²¹ and the membrane samples were exploited for the subsequent analyses.

1D-SDS-PAGE gel electrophoresis Electrophoretic analyses of the RBC membrane proteins were carried out on a continuous system of polyacrylamide gels in the presence of sodium dodecyl sulphate (SDS-PAGE) using a non-reducing 14% acrylamide gel (30 µg protein/lane) according to Laemmli (1970). To prepare RBC membranes for electrophoresis, membrane suspensions were treated with an equal volume of solubilization buffer (0.125M Tris HCl pH 6.8, 4% SDS, 20% glycerol, 0.053% bromophenol blue) containing either 200 mM DTT when working under reducing conditions, or 100 mM NEM in oxidizing conditions. Proteins were thus blotted for western blot analysis towards Prdx2, as specified below.

Western blot analysis against Prdx2 in 1:10 diluted long-stored (30 days) RBCs in day 0 RBC concentrates

Proteins separated through 1D-SDS-PAGE were electrophoretically transferred to a polyvinylidene difluoride membrane. To reduce the likelihood of false positives, blocking has been performed for 2 hours at room temperature

in 5% (wt/vol) non-fat dried milk in Tris-buffered saline. Incubation with antibodies anti-human Prdx2 was performed overnight at 4°C in 1% (wt/vol) bovine serum albumin in Tris-buffered saline/0.1% Tween 20. Bands were detected with goat anti-rabbit horseradish peroxidase using enhanced chemiluminescence reagents and digitized with a high-resolution scanner (ImageScanner II, GE Healthcare). Quantification of band intensities was performed with an *ad hoc* analytic software (Quantity One 4.6.3, Bio-Rad), using an internal control of human recombinant Prdx2 protein. The amount of Prdx2 of each sample was determined as a ratio between the sample value and the internal control.

Separation of RBC populations. Density-fractionated RBCs were prepared as previously reported (Cryo e Blood Transfusion nostro), using Percoll (Sigma-Aldrich, St. Louis, MO, USA) discontinuous gradients as described by Bosch et al. (1992). Briefly, the gradient was built up in five layers of 2 ml containing 80% (1.096 g/mL), 71% (1.087 g/mL), 67% (1.083 g/mL), 64% 1.080 g/mL Percoll, respectively, buffered with buffer A [26.3 g/L bovine serum albumin, 132 mmol/L NaCl, 4.6 mmol/L KCl, and 10 mmol/L HEPES pH 7.1]. RBCs were washed with buffer B [9 mmol/L Na₂HPO₄, 1.3 mmol/L NaH₂PO₄, 140 mmol/L NaCl, 5.5 mmol/L glucose, and 0.8 g/L bovine serum albumin] and diluted with 1 vol of buffer A. One-half milliliter of this suspension was layered on the Percoll gradient and separation was achieved after 15 minutes of centrifugation at 3000 rpm at room temperature. Fractions were collected by careful pipetting and extensively rinsed with buffer B to remove any residual Percoll.

Results and discussions

Blood doping through rEPO could be now assessed rather easily through electrophoretic approaches (Tsitsimpikou et al., 2011) or monitoring of HCT and Hb. Indeed, normal HCT values are within the range of 41-50% in adult men and 36-44% in adult women, while normal Hb levels are 14-17 g/dL of blood in men and 12-15 g/dL in women. Although for most healthy persons the two measurements are in close agreement, in athletes assuming rEPO as blood doping two cases might occur: both the values anomalously increase as a result of doping, or the athletes are biologically prone to have higher-than-normal values for both the parameters. The Union Cycliste Internationale (UCI), for example, imposes a 15-day suspension from racing on any male athlete found to have an HCT above 50% and hemoglobin concentration above 17 grams per deciliter (g/dL). A few athletes naturally have high RBC concentrations (polycythemia), which they must demonstrate through a series of consistently high HCT and Hb results over an extended period of time. All these parameters are routinely included in the biological passport of each cycling professional, and their fluctuations monitored in order to identify eventual assumption of illicit substances.

A recent, more sophisticated method of analysis against doping through rEPO, which has not yet reached the level of an official standard, is to compare the numbers of mature and immature RBCs in an athlete's circulation. If a high number of mature RBCs is not accompanied by a high number of immature RBCs (reticulocytes) it suggests that the mature RBCs were artificially introduced by transfusion (Tsitsimpikou et al., 2011). rEPO use can also lead to a similar RBC profile because a preponderance of mature RBCs tends to suppress the formation of reticulocytes. A measure known as the "stimulation index" or "off-score" has been proposed based on an equation involving

hemoglobin and reticulocyte concentrations. A normal score is 85-95 and scores over 133 are considered evidence of doping. The stimulation index is defined as Hb (g/L) minus sixty times the square root of the percentage of RBCs identified as reticulocytes.

Doping through homologous blood transfusion is easily detectable using current antidoping protocols based on erythrocyte phenotyping by flow cytometry (Arndt and Kumpel, 2008). On the other hand, detection of blood doping through autologous blood transfusion is still challenging and no definitive method currently exists, while two approaches have been recently proposed including total Hb mass measurement and urine DEHP levels (Ashenden and Morkeberg, 2011; Solymos et al., 2011). Therefore, novel biomarkers which could be suitable to detect autologous transfusions might be individuated through the translation of the ongoing in-depth investigations on RBC storage.

The introduction of plastic bags, the diffusion of new collection and additive solutions other than the introduction of leukocyte filtering strategies have dramatically improved safety and efficacy of RBC concentrates for transfusion purposes (Hess, 2006). However, despite these notable advancements, current European Council guidelines suggest that RBC concentrates may be stored for up to 42 days under controlled conditions before transfusion (Council of Europe, 2011).

It is now widely accepted that storage affects a wide array of biochemical and biological properties of RBCs to a significant extent, a phenomenon which goes by the name of storage lesions. Storage lesions include (i) alterations to RBC morphology (shape changes leading from a discoid to a spherocytic phenotype) or (ii) RBC functionality (metabolism and oxygen delivery capacity, through an increase in oxygen affinity mediated by a rapid fall in 2,3-diphosphoglycerate concentrations), as it has been recently reviewed (Bosman et al., 2008; Lion et al., 2010; D'Alessandro et al., 2010).

While some changes are reversible to some extent, such as restoring of 2,3-DPG reservoirs after transfusion (Valeri et al., 1971), others are not, especially those targeting the protein compartment (i.e. the proteome). Under a biochemical point of view, these irreversible changes to the proteome are best visualized when considering the variation of 2-dimensional electrophoretic (2DE) patterns of long-stored RBCs, which change dramatically as storage progresses with the presence of new spots in the RBC membrane protein profile (D'Alessandro et al., 2012). Since RBCs are devoid of any new protein synthesis capacity, these newly appearing spots are represented by:

- i) Cytosolic proteins which are relocated at the membrane level as storage progresses;
- ii) Protein fragments in the low molecular weight (MW) range;
- iii) Protein aggregates in the high MW range.

These three categories of newly appearing protein spots either represent protein fragments, aggregates or cytosolic proteins relocating to the membrane (yet by storage day 21 (Rinalducci et al., 2011a and 2011b; D'Alessandro et al., 2012)).

The first category of newly appearing spots might represent a realistic marker for blood doping upon transfusion, through direct targeted analyses. In a set of recent investigations (Rinalducci et al., 2011a and 2011b), we performed detailed analyses of RBC membrane protein changes to determine whether some of the cytosolic proteins relocating at the membrane could represent a suitable age-dependent biomarker of long-stored RBCs and their oxidation level.

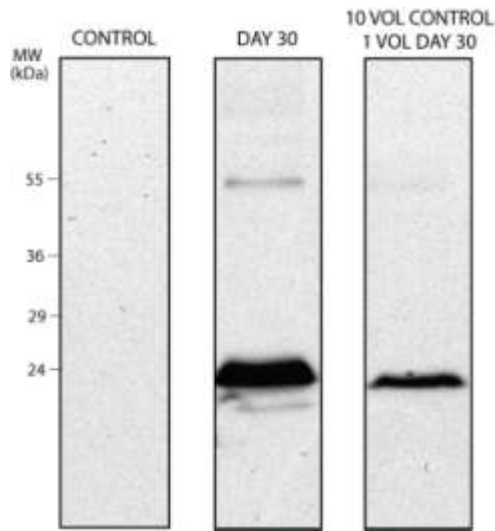
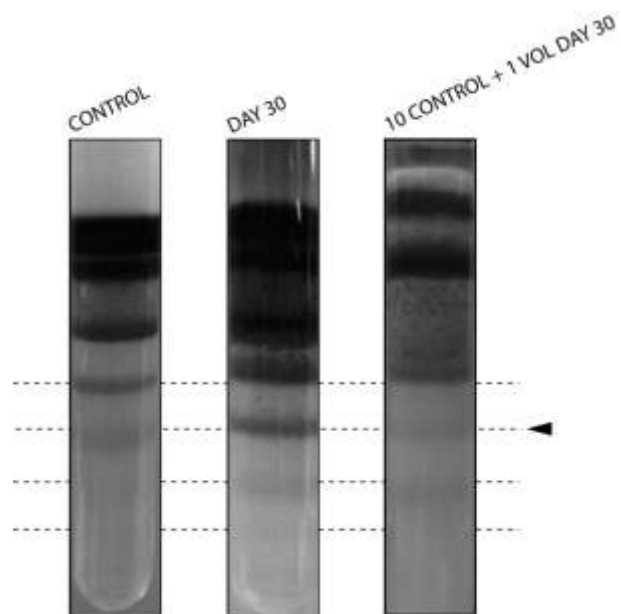


FIGURE 1 - Peroxiredoxin 2 levels in day 0, day 30 and 1:10 dilution of day 30 in day 0 membrane protein extracts from RBC concentrates. Although less intensely, Prdx2 immunopositivity could be observed also upon dilution (right lane) under non-reducing conditions with two bands corresponding to the monomer and the dimer.

FIGURE 2 - Density gradient of day 0 (left column), day 30 (right column) and 10(day 0):1 (day 30) mixed RBC concentrates (center). The intensity from band 6 down (from top to bottom) increases in day 30 hypothermally stored RBCs and are still evident upon 10:1 mixing.



One of these relevant biomarkers was identified as the oxidative stress-related protein peroxiredoxin 2 (Prdx2) (Rinalducci et al., 2011a and 2011b).

In RBCs from healthy individuals, Prdx2 is normally located in the cytosol and thus western blot analyses toward Prdx2 in RBC membranes from day 0 units do not show Prdx2 immunoreactivity (Rinalducci et al., 2011a). On the other hand, older units display immunopositivity for Prdx2 at the membrane (Rinalducci et al., 2011a). On this basis, we concluded that, immunopositivity for Prdx2 in RBC membranes could be also a biomarker of RBC transfusion, as long as RBCs have been stored at least longer than three weeks (which is actually the case of transfusing athletes). Indeed, membranes of freshly withdrawn RBCs should be Prdx2-free, unless the athlete does not suffer from hereditary anomalies such as hereditary spherocytosis (Rocha et al., 2008), which is very infrequent (the incidence of hereditary spherocytosis is about 200 to 300 per million in northern European populations (Eber et al., 1992)) and also unlikely for professional athletes for obvious reasons.

To understand whether this marker could be suitable for blood doping testing, we designed an *in vitro* model for autologous blood transfusion through diluting in a 1:10 ratio long-stored packed RBCs into freshly withdrawn concentrated RBCs (day 0 from the same donor) (the rationale behind this dilution ratio is further explained in the *Methodologies* section, and stems from a rough estimation of the actual dilution of transfused RBCs in the bloodstream of a healthy recipient, such as in the case of an athlete undergoing an autologous transfusion). This model has been thought as to mimic autologous transfusion in transfusing athletes through maintaining a 1:10 approximate ratio which is obtained upon transfusion of a whole unit of refrigerated packed RBCs in an adult male (5 liters of whole blood, hematocrit 45%). We chose 30 day-stored RBC as a long-stored RBC counterpart, which should represent a realistic model for athletes collecting blood at least one month and a half before a competition and transfusing ten days before. Through western blot against Prdx2 we could identify immunopositivity in RBC membranes from 30 day-stored concentrates while not in day 0 counterparts (**Figure 1**). Immunopositivity was still visible in the 1:10 dilution (though with a reduced intensity – **Figure 1**).

Using fluctuations in RBC population as an indicator of blood transfusion

While it has been evidenced the linkage between the rEPO-induced modulation of erythropoiesis and the alteration in the RBC population pattern (increased reticulocyte/mature RBC ratio) (Tsitsimpikou et al., 2011), it has been so far only partially demonstrated that transfusion of long-stored RBCs (either stored hypothermically or cryostored) would result in anomalously biasing of the physiological percentage distribution in RBC subpopulations (Pottgiesser et al., 2011).

To this end, we conducted preliminary investigations with discontinuous density gradients to understand whether this approach might reveal precious insights for further development of anti-doping strategies. In particular, long stored RBCs (day 30 – again, as a realistic model for an athlete auto-transfusing one week before the beginning of a competition a unit withdrawn one month and a half before) were mixed in a dilution 1:10 with freshly drawn (day 0 from the same donor) erythrocyte concentrates. As a result (**Figure 2**), newly detectable higher density bands (as older RBCs are also denser (D'Alessandro et al., 2012b)) at day 30 appeared, which could still be visible upon dilution in 1:10 (day 30: day 0 RBCs).

Conclusion

These preliminary results suggest for further experimenting in this direction, with the planning of larger scale *in vivo* studies to understand the robustness of the reported phenomena (Prdx2 membrane-immunopositivity and alteration of RBC populations upon transfusion of RBC concentrates which had been stored for longer than four weeks). Full automation of the RBC population analysis might be provided by the application of haemocromocitometric analyses on blood samples collected from transfused recipients. If results from further studies will confirm our preliminary results (**Figure 1-2**), it will be also necessary to monitor the kinetics of these changes *in vivo* (it is indeed difficult to postulate *a priori* how long would the membrane Prdx2 marker be still visible in RBC samples from recipients transfused with RBC stored longer than four weeks). This additional information would be pivotal to assess whether the Prdx2 biomarker would be detectable for a period long enough to allow for blood testing as a suitable anti-doping strategy.

References

- Arndt PA, Kumpel BM. Blood doping in athletes--detection of allogeneic blood transfusions by flow cytometry. *Am J Hematol*. 2008;83(8):657-67.
- Ashenden M, Mørkeberg J. Net haemoglobin increase from reinfusion of refrigerated vs. frozen red blood cells after autologous blood transfusions. *Vox Sang*. 2011;101(4):320-6.
- Ashenden M. A strategy to deter blood doping in sport. *Haematologica* 2002; 87:225-34.
- Baumann GP. Growth Hormone Doping in Sports: A Critical Review of Use and Detection Strategies. *Endocr Rev*. 2012; doi: 10.1210/er.2011-1035
- Blasi B, D'Alessandro A, Ramundo N, Zolla L. Red blood cell storage and cell morphology. *Transfus Med*. 2012 Apr;22(2):90-6.
- Bosch FH, Werre JM, Roerdinkholder-Stoelwinder B, Huls TH, Willekens FL, Halie MR. Characteristics of red blood cell populations fractionated with a combination of counterflow centrifugation and Percoll separation. *Blood*. 1992;79(1):254-60.
- Bosman GJ, Werre JM, Willekens FL, Novotný VM. Erythrocyte ageing in vivo and in vitro: structural aspects and implications for transfusion. *Transfus Med*. 2008;18(6):335-47.
- Council of Europe. Guide to the Preparation, Use and Quality Assurance of Blood Components (16th edn). Recommendation No. R (95) 15. European Directorate for the Quality of Medicines & HealthCare 2011; Strasbourg, France.
- D'Alessandro A, Blasi B, D'Amici GM, Marrocco C, Zolla L. Red blood cell populations in freshly drawn blood: application of proteomics and metabolomics to a decades-long biological issue *Blood Transfusion* 2012; doi: 10.1016/j.blot.2012.02.004
- D'Alessandro A, D'Amici GM, Vaglio S, Zolla L. Time-course investigation of SAGM-stored leukocyte-filtered red blood cell concentrates: from metabolism to proteomics. *Haematologica*. 2012;97(1):107-15.
- D'Alessandro A, Liumbruno G, Grazzini G, Zolla L. Red blood cell storage: the story so far. *Blood Transfus*. 2010 Apr;8(2):82-8.
- Eber SW, Pekrun A, Neufeldt A, Schröter W. Prevalence of increased osmotic fragility of erythrocytes in German blood donors: screening using a modified glycerol lysis test. *Ann Hematol* 1992; 64:88.
- Eichner ER. Blood doping : infusions, erythropoietin and artificial blood. *Sports Med*. 2007;37(4-5):389-91.
- Giraud S, Sottas PE, Robinson N, Saugy M. Blood transfusion in sports. *Handb Exp Pharmacol*. 2010;(195):295-304.
- Hess, J.R. An update on solutions for red cell storage. *Vox Sanguinis* 2006; 91: 13–19.
- Laemmli UK. Cleavage of structural proteins during the assembly of the head of bacteriophage T4. *Nature*. 1970 Aug 15;227(5259):680-5.
- Lion N, Crettaz D, Rubin O, Tissot JD. Stored red blood cells: a changing universe waiting for its map(s). *J Proteomics*. 2010;73(3):374-85.
- Lippi G, Banfi G. Blood transfusions in athletes. Old dogmas, new tricks. *Clin Chem Lab Med*. 2006;44(12):1395-402.
- Low FM, Hampton MB, Peskin AV, Winterbourn CC. Peroxiredoxin 2 functions as a noncatalytic scavenger of low-level hydrogen peroxide in the erythrocyte. *Blood*. 2007;109(6):2611-7.
- Olivieri E, Herbert B, Righetti PG. The effect of protease inhibitors on the two-dimensional electrophoresis pattern of red blood cell membranes. *Electrophoresis*. 2001;22(3):560-5.
- Pallotta V, D'Amici GM, D'Alessandro A, Rossetti R, Zolla L. Red blood cell processing for cryopreservation: from fresh blood to deglycerolization. *Blood Cells Mol Dis*. 2012; doi: 10.1016/j.bcmd.2012.02.004
- Pottgiesser T, Sottas PE, Echter T, Robinson N, Umhau M, Schumacher YO. Detection of autologous blood doping with adaptively evaluated biomarkers of doping: a longitudinal blinded study. *Transfusion*. 2011;51(8):1707-15.
- Rinalducci S, D'Amici GM, Blasi B, Vaglio S, Grazzini G, Zolla L. Peroxiredoxin-2 as a candidate biomarker to test oxidative stress levels of stored red blood cells under blood bank conditions. *Transfusion* 2011a; 51(7):1439-49.
- Rinalducci S, D'Amici GM, Blasi B, Zolla L. Oxidative stress-dependent oligomeric status of erythrocyte peroxiredoxin II (PrdxII) during storage under standard blood banking conditions. *Biochimie*. 2011b; 93: 845-85.
- Rocha S, Vitorino RM, Lemos-Amado FM, Castro EB, Rocha-Pereira P, Barbot J, Cleto E, Ferreira F, Quintanilha A, Belo L, Santos-Silva A. Presence of cytosolic peroxiredoxin 2 in the erythrocyte membrane of patients with hereditary spherocytosis. *Blood Cells Mol Dis*. 2008;41(1):5-9.
- Segura J, Monfort N, Ventura R. Detection methods for autologous blood doping. *Drug Test Anal*. 2012 doi: 10.1002/dta.405.

- Solymos E, Guddat S, Geyer H, Thomas A, Thevis M, Schänzer W. Di(2-ethylhexyl) phthalate metabolites as markers for blood transfusion in doping control: intra-individual variability of urinary concentrations. *Drug Test Anal.* 2011;3(11-12):892-5.
- Tsitsimpikou C, Kouretas D, Tsarouhas K, Fitch K, Spandidos DA, Tsatsakis A. Applications and biomonitoring issues of recombinant erythropoietins for doping control. *Ther Drug Monit.* 2011;33(1):3-13.
- Valeri, C.R. and Collins, F.B. Physiologic effects of 2,3-DPG-depleted red cells with high affinity for oxygen. *J. Appl. Physiol.* 1971; 31: 823–827.

Chapter 9: *Conclusions*

Contents

9.1 Biochemistry of red cell aging in vivo and storage lesions

The contents of this chapter report the contents of the the following publications by the candidate:

1. D'Alessandro A, Zolla L.
Biochemistry of red cell aging in vivo and storage lesions
Haematologica 2013; (Invited review – 18 European Haematology Association EHA18 – invited speaker)
-

In this concluding chapter, we review the presented results and critically complement the gathered information with existing literature, in order to delineate the most comprehensive possible updated portrait of red blood cell ageing *in vivo* (senescence) and *in vitro* (storage of erythrocyte concentrates).

9.1 Biochemistry of red cell aging in vivo and storage lesions

Overview of this section

The study of *in vivo* and *in vitro* (storage conditions) ageing of red blood cells (RBCs) has recently taken advantage of the introduction of mass spectrometry-based Omics disciplines, such as proteomics, metabolomics and lipidomics.

In vivo and *in vitro* ageing are characterized by shared features, including altered cation homeostasis, alteration of metabolic fluxes via decreased enzymatic activity and progressive depletion of high energy phosphates, increased susceptibility to oxidative stress, which in turn promotes oxidative-lesions to proteins (carbonylation, fragmentation, hemoglobin glycation) and lipids (peroxidation), morphological changes (membrane blebbing, vesiculation). Most of these mechanisms closely resemble apoptosis-like phenomena.

On the other hand, the closed system of blood bank-storage in plastic bags and additive solutions results in peculiar *in vitro* alterations to RBCs, such as hypothermally-depressed metabolism, the exacerbation of oxidative stress-related phenomena, the progressive leakage of DEHP-plasticizers, the accumulation of RBC-shed microvesicles in the supernatant. These phenomena underlie the difficulties related to the extension of the shelf-life of RBC concentrates *in vitro* from the currently allowed threshold(42days) up to the actual life-span of RBCs *in vivo*(120days).

Meanwhile, retrospective clinical and basic science evidences suggest that RBCs stored longer than 14days might not be as safe and effective as the fresh ones.

Keywords: red blood cell; ageing; storage; mass spectrometry; proteomics; metabolomics.

Learning goals:

- Mass spectrometry-based Omics (such as proteomics and metabolomics) strategies have contributed the latest strides in this field of research.
- Ageing of red blood cells *in vitro* and *in vitro* promotes the accumulation of reversible and irreversible lesions;
- *In vitro* storage of red blood cells (closed plastic bag system, hypothermia, additive solutions) exacerbates oxidative stress and accelerates ageing;
- Storage lesions accumulating *in vitro* soon after 14 days of storage are only reversible to some extent.

Introduction

Ageing of red blood cells (RBCs) *in vivo* and *in vitro* represents a key biomedical issue.

Human RBCs are characterized by an approximate lifespan of 120days in the peripheral circulation, while the shelf-life of RBC concentrates stored under blood bank conditions is in most countries limited to 42days.

In vivo, since RBCs number is approximately 4×10^{12} /L circulating blood, on the basis of their average lifespan, in an individual with 5L of blood, more than 10^{11} erythrocytes are newly formed and removed each single day (Shinozuka et al., 1994; Bosman et al., 2010; Lang et al., 2012).

Normal human RBCs all survive to about the same age, which implies the likely existence of a molecular countdown that triggers, at the proper time, a series of changes leading to removal by the reticuloendothelial system (**Table1, Figure1**) (Shinozuka et al., 1994; Bosman et al., 2010). As it has been noted over the years, the mechanisms underlying these changes share some distinct features with programmed cell death of nucleated cells, which prompted Lang's group to coin the term "eryptosis", that refers to erythrocyte-specific apoptosis (Lang et al., 2012).

At the same time, storage under blood bank conditions results in the exacerbation of most of these changes and shortening of RBC lifespan, a phenomenon which goes by the name of "storage lesions" that is mainly attributable to storage conditions (closed plastic bag storage system, additive/storage solutions and hypothermia) (D'Alessandro et al., 2010; Lion et al., 2010; Karon et al., 2012). Nonetheless, it should be also considered that a RBC concentrate unit already contains normally distributed (partly aged) RBC populations.

From a transfusion medicine standpoint, while no definitive evidence has been so far provided and controversial hints from retrospective studies have been collected (Koch et al., 2008; Lelubre et al., 2009), it is still matter of debate as to whether and to which extent transfusion of RBC concentrate units older than 14days might be tied to actual untoward effects in certain categories of recipients (e.g. traumatized, peri-operative and critically ill patients). Meanwhile, prospective clinical trials (summarized by Grazzini and Vaglio (2012)) are currently underway to shed light on this delicate issue, though early results seem to confute any statistically significant effect of older RBC transfusions on clinical outcomes in premature, very low-birth-weight infants (Fergusson et al., 2012).

From a biochemical standpoint, storage lesions are only reversible to some extent and might thus in theory affect RBC viability and functionality upon transfusion and thus, at least theoretically, also safety and effectiveness of the transfusion therapy with older units (D'Alessandro et al., 2010; Lion et al., 2010; Karon et al., 2012).

In this review, we will face the challenging task to encompass the major aspects of RBC ageing *in vivo* and *in vitro*, while focusing on recent strides that have been favored by the introduction of novel technologies, such as mass spectrometry (MS)-based metabolomics, proteomics, and lipidomics. These disciplines fit within the framework of Omics technologies, whereby specific classes of biomolecules (e.g. metabolites, proteins and lipids) are qualitatively/quantitatively investigated as a whole, and subsequently related to RBC biology and functionality.

RBC senescence has so far been investigated through the isolation of cell populations of different mean ages. Since ageing RBCs have been shown to undergo dehydration with increased density and decreased size, most of the investigations have been performed by means of centrifugation (either plain, angle-head or counterflow), or through the use of several discontinuous gradients, including albumin, stractan and Percoll (Bosch et al., 1992). However, it has been also argued that density might not represent a good criterion to determine RBC age and thus alternative approaches have been proposed, such as biotin labeling, which allows age-dependent separation of normal RBCs in animals (Suzuki and Dale, 1987).

RBC ageing and physiology *in vivo* and *in vitro*

The main biological role of RBCs is to deliver oxygen to peripheral tissues. Therefore, since earliest times, investigators were concerned about determining whether senescent human erythrocytes could still handle oxygen delivery efficiently (Valtis, 1954). Among crucial factors determining haemoglobin-oxygen affinity *in vivo*, aged erythrocytes showed a decreased content of organic phosphate compounds (namely, adenosine triphosphate-ATP and 2,3-diphosphoglycerate-DPG) (Samaja et al., 1990) and an internal pH of about 0.2 pH units more alkaline than the younger cells (Romero and Romero, 2004). These results suggested that *in vivo* aged RBCs display an apparent increase in haemoglobin-oxygen affinity and a deficient oxygen release (Romero and Romero, 2004).

Analogous observations were reported for *in vitro* stored RBCs (Bennet-Guerrero et al., 2007), whereby pO_2 was essentially unchanged between 3h and 14days, whereas hemoglobin O_2

saturation increased steadily during this period (reaching 99% levels by storage day 42), possibly reflecting the concomitant decline in the negative allosteric effector DPG (98% decline by 2 weeks). Since pH is inversely related to oxygen off-loading capacity (Bohr effect), it is relevant to note that RBC storage under blood bank conditions also results in constant pH lowering (Romero and Romero, 2004), as a result of ongoing glycolysis in a closed system. On the other hand, excessive pH lowering has a negative feedback on glycolysis itself (Burr, 1972). Recent evidences indicated that RBC storage corresponds to a rapid decrease of S-nitrosylation of $\beta 93\text{cys}$ of hemoglobin, seem to further support a partially compromised “hypoxic vasodilation” capacity of longer stored RBCs (Bennet-Guerrero et al., 2007).

Besides, cation transport is negatively influenced by RBC age *in vivo* (Hentschel et al., 1986) and *in vitro* (Wallas, 1979). In details, older RBCs display altered Na^+/K^+ fluxes (Burr, 1972), since sodium influx and potassium efflux become dysregulated in senescent RBCs and longer stored erythrocyte concentrates, a phenomenon further stressed by hypothermia in the latter case (Bennet-Guerrero et al., 2007; Wallas, 1979). Supernatant accumulation of potassium has been long considered to hold pitfalls in relation to transfusion to paediatric patients.

Altered potassium homeostasis is also tied to progressive increase in intracellular ionic calcium (Romero and Romero, 1982). Indeed, *in vivo* (Romero and Romero, 1982) and *in vitro* (Wiley et al., 1982; Antonelou et al., 2012; Gevi et al., 2012) ageing of RBCs have been related to intracellular increases of Ca, which in turn determines a series of events such as Ca^{2+} pump proteolysis and opening of the Ca^{2+} -dependent K^+ channel. Increases in intracellular calcium levels are consistent with activation of calcium-activated proteases (i.e. μ -calpain) and apoptosis-like phenomena (Lang et al., 2012), though *in vitro* eryptosis mechanisms can still be triggered by starvation (high energy phosphate consumption) in the absence of calcium (Pompeo et al., 2010). Also, calcium loading in rabbit erythrocytes results in dose-dependent decreases in reduced glutathione (GSH) levels (Kurata and Suzuki, 1994).

In the light of the considerations above, it has thus been concluded that cation perturbation, metabolic decay and oxidative damage are all interrelated in the erythrocyte aging process (Kurata and Suzuki, 1994).

However, it is also worthwhile to stress that, although ATP levels influence membrane stability and thus RBC survival (Nakao et al., 1962), *in vitro* alterations to DPG, ATP and cation

imbalances are rapidly restored upon transfusion of RBCs in the bloodstream of the recipients (Valeri et al., 1969).

From physiology to metabolism

Owing to the lack of nuclei and organelles, including mitochondria, mature RBCs are incapable of generating energy via the (oxidative) Krebs cycle. Nonetheless, they rely upon a limited network of intertwined metabolic pathways for energy production and redox homeostasis (Messana et al., 1999; Jamshidi and Palsson, 2006):

- (i) the Embden-Meyerhof pathway (glycolysis), in which 90% of the ATP is generated (under control conditions) through the anaerobic breakdown of glucose;
- (ii) the pentose phosphate pathway, which is responsive to oxidative stress;
- (iii) the Rapoport-Lubering shunt, for DPG production;
- (iv) the purine salvage pathway, to salvage purine substrates for replenishing high energy purine reservoirs (*de novo* synthesis of purines is not present in RBCs);
- (v) Glutathione (GSH) homeostasis;
- (vi) the methemoglobin (met-Hb) reduction pathway, which reduces ferric heme iron to the ferrous form to prevent Hb denaturation via the enzyme NADH-cytochrome b5 reductase.

Energy metabolism

RBC ageing *in vivo* corresponds to a progressive steep decline in the activity of key metabolic enzymes, including hexokinase and pyruvate kinase (Embden Meyerhof) (Jansen et al., 1985). By exploiting a novel MS-based metabolomics set up, optimized for RBC-targeting investigations (D'Alessandro et al., 2011), we could recently confirm and expand these data by directly assessing a decrease in the levels of the main glycolytic intermediate metabolites (glucose 6-phosphate, glyceraldehyde 3-phosphate, phosphoenolpyruvate and lactate) in density gradient-separated senescent RBCs (D'Alessandro et al., 2013).

Analogously, RBC storage under blood bank conditions also results in the progressive loss of metabolic modulation, through the decrease in the rates of ATP and DPG production, also favored by hypothermic storage temperature negatively affecting enzyme activity rates, constant lactate accumulation in the supernatants and altered glycolysis/pentose phosphate fluxes (Messana et al., 2000; Romero and Romero, 2004). In this respect, MS-based approaches revealed consistent trends for RBCs stored in two different storage solutions, namely mannitol-

adenine-phosphate(MAP) (Nishino et al., 2009) and citrate-phosphate-dextrose–saline-adenine-glucose-mannitol(CPD-SAGM) (Gevi et al., 2012; D’Alessandro et al., 2012). In particular, in CPD-SAGM-stored erythrocyte concentrates we could evidence increased levels of glycolytic metabolites over the first 2weeks of storage, while from day14 onwards, we observed a significant consumption of all metabolic species, and diversion towards the oxidative phase of the pentose phosphate (NADPH and 6-phosphogluconic acid), in response to an exacerbation of oxidative stress (Gevi et al., 2012; D’Alessandro et al., 2012).

Redox metabolism

Senescent RBCs display increased susceptibility to oxidative stress and altered glutathione homeostasis (Sass et al., 1965), despite the activity of key enzymes such as glutathione S-transferase being independent from erythrocyte age (Strange et al., 1982). On the other hand, aged erythrocytes are characterized by decreased activities of the rate limiting enzyme for the oxidative phase of the pentose phosphate pathway, glucose 6-phosphate dehydrogenase, and of NADH-cytochrome b5 reductase (Brajovich et al., 2009).

Decreased GSH levels in senescent RBCs (Ghashghaenia et al., 2012) and accumulation of GSSG (D’Alessandro et al., 2013) *in vivo* are paralleled by significant decreases of the rate of GSH synthesis ($-45\pm 8\%$) (Low et al., 1993) and increased GSSG (Gevi et al., 2012; D’Alessandro et al., 2012) levels under *in vitro* blood bank conditions, both being largely attributable to reduced amino acid transport (reduced levels of glutamate, glutamate-precursor glutamine, glycine and cysteine), secondary to decreased ATP concentration (D’Alessandro et al., 2013; Whillier et al., 2011).

Direct measurement of reactive oxygen species (ROS) during RBC storage under blood bank conditions evidenced a significant increase of oxidative stress after 14days of storage of either leukofiltered or non-leukofiltered erythrocyte concentrates (Antonelou et al., 2012; D’Alessandro et al., 2012).

From metabolism to proteomics: the transport metabolon

Both *in vivo* and *in vitro*, cation and metabolic modulation of RBCs is largely dependent on ultra-structural complexes of cytosolic enzymes and protein-protein interactions, whereof those involving the anion exchanger 1-band 3(AE1) membrane protein represent a paradigmatic example.

AE1, the major integral membrane protein of RBCs, is involved in the “chloride shift”(exchange of cellular HCO_3^- with plasma Cl^-), a process that promotes the conversion of the weak acid H_2CO_3 to the strong acid HCl , thereby rendering the intracellular pH acidic. Acidification triggers dissociation of O_2 from oxyhemoglobin, and the dissociated O_2 is supplied to tissues that metabolically produce CO_2 . Protons formed in RBCs are accepted by the groups of deoxy-hemoglobin participating in the ‘Bohr Effect’, and the pH within the RBCs is restored in order to prevent further dissociation of oxygen from oxy-hemoglobin. By means of the transient acidification triggered by the anion exchange activity, tissues producing more CO_2 are supplied with more O_2 from oxy-hemoglobin.

Moreover, the N-terminal cytosolic domain of AE1 represents a membrane docking site for several enzymes of the glycolytic pathway, such as phosphofructokinase, aldolase, glyceraldehyde-3-phosphate dehydrogenase and lactate dehydrogenase (Low et al., 1993; Lewis et al., 2009), other than for deoxy-hemoglobin (Low et al., 1993; Lewis et al., 2009; Castagnola et al., 2010) and the anti-oxidant enzyme peroxiredoxin 2 (Matte et al., 2012), a noncatalytic scavenger of low-level hydrogen peroxide in the erythrocyte (Low et al., 2007). Competitive binding of deoxy-hemoglobin to the cytosolic domain of AE1 results in the displacement of glycolytic enzymes from the RBC membrane and promotes their activation. In so doing, RBCs are able to undergo an oxygen-linked modulation of metabolism (Low et al., 1993; Lewis et al., 2009; Castagnola et al., 2010).

More recently, it has been observed that phosphorylation of the tyrosine residues of the AE1 protein at position 8 and 21 in modulating the binding of glycolytic enzymes and deoxy-hemoglobin to the N-terminal domain (Lewis et al., 2009). Phosphorylation to these residues results in an increased (+45%) glycolytic flux and reduced shift towards the pentose phosphate pathway (-66%) (Lewis et al., 2009). The underlying mechanism seems to involve the phosphorylation-dependent increase in the number of negative charges at the N-terminal domain of AE1, which affects deoxy-hemoglobin binding to AE1 (in a likewise fashion to negatively charged DPG stabilizing T-state of deoxy-Hb) and thus the displacement of otherwise bound/inhibited glycolytic enzymes (Lewis et al., 2009). Notably, deoxygenation seems to promote phosphorylation of the N-terminal domain of AE1 (Matte et al., 2012).

This brief introduction about the central role of AE1 as an actual “transport metabolon” in the physiology of RBCs paves the way for a better understanding of the importance of the long-time

documented *in vivo* and *in vitro* ageing-triggered lesions to AE1 (Lutz et al., 1988; Rinalducci et al., 2012). In details, the most widely accepted models for RBC senescence *in vitro* and *in vivo* imply either (i) enzyme and oxidative stress-mediated proteolysis of AE1 (promoting the formation of a 24 and 34kDa fragment, respectively – Rinalducci et al., 2012) or (ii) the formation of AE1 oligomeric clusters (Lutz et al., 1988; Karon et al., 2009), which display pro-immunogenic properties and mediate recognition through naturally-occurring antibodies and RBC removal by resident spleen and liver macrophages.

While the involvement of calcium-modulated proteases represents a long-investigated aspect of RBC ageing and strengthens its resemblance to apoptosis (Lang et al., 2012), the involvement of oxidative stress-mediated proteolysis of the cytosolic domain of AE1 is but a recent finding, which better fits in the rapidly evolving scenario depicting a central role for oxidative stress in RBC-storage lesions, at least in the blood bank (D'Alessandro et al., 2013). However, also clusterization of AE1 proteins might be indirectly dependent upon oxidative stress, since oxidized and poorly-glycosylated AE1 is selectively phosphorylated by Syk kinase to form large membrane clusters in normal and glucose 6-phosphate dehydrogenase-deficient RBCs (Pantaleo et al., 2009). RBC protein phosphorylations need a special mention and should deserve, in the near future, further investments through innovative techniques (such as electron transfer dissociation MS), in the light of their modulatory role and their dependency upon second messenger-dependent kinases (such as PKC and AMPK).

Recent evidences about increased levels of membrane peroxiredoxin-2 in longer stored RBCs (Rinalducci et al., 2011; D'Alessandro et al., 2012) further support the rationale above, since membrane levels of peroxiredoxin-2 are increased in certain categories of patients, such as in the case of hereditary spherocytosis (Rocha et al., 2008). In this view, we recently proposed to design targeted assays that could take advantage of this phenomenon as to realize quality control tests for long stored erythrocyte concentrates (Marrocco et al., 2012). Unexpected applications of these tests might stem from the compelling need for anti-doping agencies worldwide to detect autologous transfusion, an increasingly diffused illicit blood doping practice especially in endurance sports (Marrocco et al., 2012).

Oxidative stress to proteins: proteomics of RBC ageing *in vivo* and *in vitro*

Ageing of RBCs results in the accumulation of oxidative stress modifications to RBC proteins. So far, two main oxidative stress-mediated modifications to RBC proteins have been investigated: glycation of hemoglobin and carbonylation of RBC proteins.

Glycation of hemoglobin (HbA1c) is a non-enzymatic irreversible process that is promoted by the prolonged exposure of erythrocytes to high glucose concentrations (Bunn et al., 1976), a condition that is known to occur in diabetic patients or under blood banking conditions, where additive solutions (such as SAGM) expose RBCs to higher than normal glycemic levels (e.g. 50 mM). While the process has been widely documented for senescent erythrocytes *in vivo* (Bunn et al., 1976), experiments on *in vitro* stored RBCs indicate controversial results (Whillier et al., 2011; Szelényi et al., 1983), although recent MS-based evidences from our group (D'Alessandro et al., 2013b) seem to support early observations about a likely increase in the levels of HbA1C in longer stored RBCs in the blood bank.

Other than glycation, (enzyme-mediated) glycosylations might play a role in the alteration of rheological properties and RBC recognition by macrophages during RBC ageing *in vivo* and *in vitro* (Sparrow et al., 2007). Indeed, membrane-associated carbohydrate changes act as signals for removal of senescent and damaged RBCs from the circulation and could play a role in the RBC storage lesion and RBC survival after transfusion. A recent experiment with fluorescein-labeled lectins in young and senescent RBC populations and long stored RBCs, indicated that both *in vivo* and *in vitro* ageing corresponded to progressively increased binding of lectins specific for galactose and N-acetylglucosamine residues (Sparrow et al., 2007).

Carbonylation is a hallmark of protein oxidative lesions. There is a substantial agreement among laboratories involved in RBC storage carbonylation studies, since carbonylations in the cytoskeletal membrane fraction appear to significantly increase after the third week of storage in CPD-SAGM (Kriebardis et al., 2007; D'Alessandro et al., 2012), and in particular between day29 of storage and the expiration date of the erythrocyte concentrate unit (Delobel et al., 2012). Of note, leukodepletion of erythrocyte concentrate in the production chain ameliorates oxidative stress-related parameters and mitigates, albeit not eliminates, carbonylation phenomena (Kriebardis et al., 2007; D'Amici et al., 2008; D'Alessandro et al., 2012).

Ageing of RBCs *in vivo* is characterized by alternative oxidation and post-translational modification phenomena, such as desialiation (Jakubowska-Solarska and Solski, 2000) or the

progressive deamidation of Asn478 and 502 of the band 4.1b protein which results in altered electrophoretic mobility and thus different apparent molecular weight in SDS-PAGE runs (D'Alessandro et al., 2013).

Especially *in vitro*, the exacerbation of oxidative stress also triggers a wide series of additional alterations to the RBC proteome, among which protein fragmentation and aggregation have attracted the bulk of interest.

During the last five years, great strides in the field of proteomics and sample pre-fractionation strategies have enabled the simultaneous identification of 1578 distinct cytosolic proteins (Roux-Dalvai et al., 2008), that could be complemented with the previously documented membrane entries as to compile a non-redundant list of 1989 RBC proteins (D'Alessandro et al., 2010). Bioinformatic *in silico* elaborations have helped translating this immense background knowledge into actual applications (Goodman et al., 2007; D'Alessandro et al., 2012).

Alterations of the RBC membrane and cytosol proteome during *in vitro* storage have been analyzed by several groups (Bosman et al., 2008; Antonelou et al., 2010; D'Alessandro et al., 2012; Walpurgis et al., 2012), as to conclude that storage-induced changes to the proteome included fragmentation of membrane structural proteins (spectrin, ankyrin, AE1, band 4.1), membrane accumulation of hemoglobin, antioxidant enzymes (peroxiredoxin-2) and chaperones, other than cytosolic decrease of transglutaminase-2, beta actin, and copper chaperone for superoxide dismutase. Also, proteomics could provide a snapshot of cytoskeletal reorganization, by highlighting the relocation of SNAP proteins (D'Alessandro et al., 2012) and the decrease in RBC membrane content of lipid raft-associated proteins flotillins and stomatin (Bosman et al., 2008).

Alterations to the RBC membrane proteome were also found to be dependent on the tested additive solution, since AS-3 ameliorated the storage induced increase in the overall spot number of 2D-gel electrophoresis analyses (which is tied to the amplitude of protein fragmentation events) in comparison to SAGM-stored counterparts (D'Amici et al., 2012).

On the other hand, it is worthwhile to stress that RBC have a functional protein degradation system via the proteasome (Geng et al., 2009), whereas this is affected by cell age. Indeed, membrane remodeling results in the impairment of proper ubiquitination of specific structural proteins, such as spectrin (Corsi et al., 1999; Park et al., 2010), a phenomenon that might be affected to some extent by phosphorylation of spectrin and band 4.1 (Manno et al., 2005).

Oxidative stress: effects on the lipidome

Ageing of RBCs results in the progressive accumulation of oxidative stress markers also in the lipid fraction. Thiobarbituric acid-reactivity assays have helped individuating malondialdehyde accumulation in senescent RBCs *in vivo* (Jain, 1988), and *in vitro* (Dumaswala et al., 1999). Excess of glucose and thus glucose autoxidation, like in RBC storage solutions, might contribute to the promotion of oxidative stress-induced malondialdehyde accumulation (Virgili et al., 1996). In line with this assumption, we could recently detect ferrous-conjugated lactone dimer derivatives of glucose autoxidation in the supernatants of longer stored RBC concentrates (Gevi et al., 2012).

Indirectly, oxidative stress under prolonged storage *in vitro* also promoted the accumulation of peroxidized lipids in the supernatant, in the form of prostaglandins (such as 8-isoprostane, PGF_{2α}) (Gevi et al., 2012; Karon et al., 2012).

Oxidative stress-induced alterations to the RBC lipidome are relevant in that mature erythrocytes are devoid of any *de novo* lipid synthesis capacity, owing to an incomplete long chain fatty acid synthesizing system (Pittman and Martin, 1966).

RBC membrane properties are largely affected by lipid composition, which in turn is influenced by diet. Earliest approaches to the RBC lipidome relied on thin layer chromatography analytical methods (Ways and Hanahan, 1964), while recent advancements in the field of MS have favored the diffusion of gas/liquid chromatography coupled with MS-analyses.

Studies over the years (Van Gestel et al., 1965; Percy et al., 1973; Schroit et al., 1985) pointed out that senescent RBCs suffer from membrane phospholipid asymmetry, owing to ATP reservoirs consumption, which results in the externalization of phosphatidylserine (PS) in the outer leaflet of the plasma membrane. Externalization of PS is another peculiar aspect of RBC ageing which recalls apoptosis-like phenomena (Lang et al., 2012).

While over the years this observations was also confirmed for longer stored RBCs *in vitro* (Bosman et al., 2011), a recent study seems to question this concept in the light of the absence of any evidence for elevated external PS in senescent RBCs, even though older RBC had significantly lower activity of aminophospholipid translocase (Franco et al., 2013).

Like apoptotic cells,³ senescent RBCs and long-stored RBCs display higher levels of ceramides, which can be produced from cell membrane sphingomyelins by an acid sphingomyelinase (Dinkla et al., 2012; Bicalho et al., 2013). The sphingomyelinase is stimulated by platelet-

activating factor PAF, which is in turn generated from cell membrane lipids by a phospholipase, that is in turn activated during osmotic erythrocyte shrinkage (reviewed in Lang et al. (2012)). Ceramides and sphingosines might also be responsible for the formation of specific rafts/membrane domains, which underlie hot cold-hemolysis (preincubated at 37°C in the presence of certain agents, undergo rapid hemolysis when transferred to 4°C) (Montes et al., 2008).

Osmotic fragility, morphology changes and vesiculation

Senescent RBCs are characterized by increased osmotic fragility, which results in impaired deformability, as measured through viscoelastic time constant indexes (Linderkamp and Meiselman, 1982). In other terms, shape recovery following membrane deformation is delayed in old RBC, which compromises their functionality *in vivo*, where they should be able to traverse passage ways as narrow as 1 µm in diameter, capillaries and splenic slits, periodic high turbulences and high shear stresses, along with extremely hypertonic conditions. Increased osmotic fragility have been also reported for long stored RBCs under blood bank conditions (Blasi et al., 2012).

Prolonged RBC storage in plastic bags under blood bank conditions is also accompanied by the progressive leaching of the plasticizer di-2-ethylhexyl phthalate (DEHP), a common component in medical plastics. Although there is motivation to replace this component, owing to its potential toxicity, and novel plasticizers are continuously under evaluation, DEHP is necessary to prevent excessive hemolysis in stored RBCs as it intercalates erythrocyte membranes and serves as a stabilizer (Dumont et al., 2012), though on the other hand, it might affect membrane deformability and thus osmotic fragility.

Osmotic fragility is undoubtedly tied to shape changes from a biconcave disc, towards an echinocyte, spherocochinocyte and utterly spherocytic phenotype, proportionally to RBC age (Bessis et al., 1972; Nash and Wyard, 1980; Berezina et al., 2002; Gifford et al., 2006; Blasi et al., 2012;). Data acquired on tens of thousands of red cells showed that nearly as much membrane area is lost during the 1-2 d of reticulocyte maturation (10-14%) as in the subsequent 4 months of erythrocyte ageing (c. 16-17%) (Gifford et al., 2006). Surface/volume ratio constantly increases as RBCs shed one microvesicle per hour during their lifespan *in vivo* (Sens and Gov, 2007). *In vitro*, irreversible morphology phenotypes accumulate significantly after the

first two weeks of storage (Berezina et al., 2002; Blasi et al., 2012). By storage day 21 more than 50% of RBCs displayed non-discocyte phenotypes (Berezina et al., 2002; Blasi et al., 2012).

Other than representing the most evident age-related change of RBCs, alterations to RBC morphology also underpin the first sight resemblance of erythrocyte senescence with apoptosis-like phenomena, whereby membrane blebbing and vesiculation represent the conclusive step (Lang et al., 2012).

Decades of research in the field have highlighted a role for biological inputs (e.g. calcium signaling, ATP depletion, ceramide accumulation) and physico-chemical constraints (e.g. alterations to surface charge density and surface/volume ratio minimization in the model proposed by Gov (Sens and Gov, 2007)) in the acquisition of the spherocytic phenotype (Palek et al., 1974; Sens and Gov, 2007; Huang et al., 2011).

Over the years, concerns have arisen and persisted about the relation of exocytic micro- and nano-vesicles (180 and 80 nm, respectively) to untoward consequences in the recipients (Greenwalt and Dumaswala, 1988). In this view, during the last decade many research groups have focused their research activity on the determination of the rheological properties and molecular content of these vesicles, mainly through flow-cytometry and proteomics approaches (Greenwalt and Dumaswala, 1988; Annis et al., 2005; Bosman et al., 2012; Canellini et al., 2012).

First of all, leukofiltration affects RBC-shed vesicles quantity and content (Annis et al., 2005; Antonelou et al., 2012), and RBC-derived vesicles can be separated from white blood cell counterparts, and expose a long series of membrane biomarkers, including blood group antigens from the RH, KEL, JK, FY, MNS, LE and LU systems and PS (Canellini et al., 2012). On the other hand, the presence of M(MNS1), N(MNS2) and s(MNS4) antigens could not be demonstrated by flow-cytometry, despite that glycophorin A and B were identified on microparticles using anti-CD235a and anti-MNS3 (Canellini et al., 2012).

Generation of vesicles during blood bank storage accounts for a considerable part of the cellular hemoglobin loss (Greenwalt et al., 1991). These vesicles, that not only expose PS but also contain immunoglobulins and various complement proteins, which may contribute to the adverse effects upon transfusion. Vesicles are also enriched in ankyrin, AE1, spectrin beta, lipid raft-associated proteins (flotilin and stomatin) while relatively low amounts of glyceraldehyde 3-phosphate dehydrogenase have been detected (Bosman et al., 2012). Proteomics analyses of

RBC-shed vesicles have elucidated a compositional resemblance with older RBC membranes, which prompted considerations about the likely role of vesiculation as a self-defensive mechanism to remove irreversibly-damaged or no-longer functional proteins. In this view, extracellular 20S proteasome subunits have been found to accumulate in the supernatants of packed RBC units (Geng et al., 2009).

miRNAs

Though still being underinvestigated, differential profiling of RBCs for 52 micro-RNAs(miRNAs, negative regulators of mRNAs)revealed that miR-96, miR-150, miR-196a, and miR-197, demonstrated an increase up to day20 and subsequently decreased during storage *in vitro* (Kannan et al., 2010).

Ageing *in vitro* under alternative storage conditions

Ageing under alternative storage conditions (such as cryoconservation (Pallotta et al., 2012), anaerobic storage (D'Alessandro et al., 2013) and alternative additive/storage solutions (vitamin C and NAC – Pallotta et al., 2013)) has been thoroughly discussed in **Chapter 6** and **Chapter 7**, respectively. Cryostorage of RBCs results in increased cell volumes, owing to glycerol entrance during the glycerolization steps, which cannot be fully reverted back to normal values even upon thawing, deglycerolization and washing steps (Pallotta et al., 2012). Shape alterations caused an increase in osmotic fragility and permeability to ions. A significant pH drop was observed which could not to be attributed to a higher metabolic rate, since the levels of lactate did not show substantial fluctuations among the cell processing steps (Pallotta et al., 2012). Membrane anomalies could be also related to higher hemolysis, especially of the densest and oldest cell sub-populations, as we could observe by means of discontinuous density gradients.

Overall, cryostorage in presence of glycerol seems not to significantly affect RBCs, since most of the observed cyrostorage-triggered alterations were related to cell processing and, in particular, to the increase of cytosolic glycerol as a consequence of the glycerolyzation step. Further studies might be thus designed as to replace glycerol with non-penetrating cryoprotectants.

Since oxidative stress is one of the leading causes promoting the accumulation of storage lesions, alternative storage strategies have been designed as to prevent or tackle the production of

reactive oxygen species: anaerobic storage and alternative additive/storage solutions (including antioxidants in the formula, such as ascorbic acid and N-acetyl cysteine) (D'Alessandro et al., 2013; Pallotta et al., 2013). Deoxygenation promoted energy metabolism, while resulting in the reduced capacity of erythrocyte to cope with oxidative stress (Embden Meyerhof pathway dominance, reduced diversion toward the pentose phosphate pathway, increased nitrogen-NO metabolism and likely impaired activity of the methemoglobin reductase enzyme). On the other hand, ascorbic acid and NAC protected erythrocytes from the accumulation of oxidative stress to proteins, lipids and anti-oxidant metabolites, while partially sacrificing energy metabolism (since ascorbate competes with D-glucose for membrane internalization via GLUT transporters).

Conclusion

In the present PhD thesis project, we summarized the major biochemical changes related to RBC ageing *in vivo* and *in vitro*.

Future improvements in the field, at least from a molecular standpoint, will be soon fueled by the introduction of novel storage strategies (new additive or rejuvenation solutions, anaerobiosis, pathogen inactivation protocols), other than from the application of integrated omics approaches and mathematical models, as envisaged by systems biology (Jamshidi and Palsson, 2006), and the diffusion of nanotechnology-based assays, such as atomic force microscopy.

Table 1 – List of the main biochemical changes of ageing red blood cells *in vivo* and *in vitro*

- potassium leakage to the supernatant;
- loss of metabolic modulation and depletion of DPG and ATP stores and pH lowering;
- accumulation of intracellular calcium and activation of Ca²⁺-mediated signaling cascades (e.g. kinases, calpains);
- reduced oxygen off-loading capacity;
- decreased S-nitrosothiohaemoglobin;
- increased susceptibility to oxidative stress and alteration to the GSH homeostasis and Pentose Phosphate Pathway metabolism;
- alteration of lipids (phospholipid loss, phosphatidylserine exposure to the outer membrane leaflet, accumulation of ceramide);
- alteration of membrane proteins (membrane protein fragmentation and migration to the membrane and/or vesiculation of subsets of structural or cytosolic antioxidant proteins);
- miR-96, miR-150, miR-196a, and miR-197 increase up to day 20 and subsequently decreased during storage *in vitro*
- decreased desialiation, increased glycosylation and carbonylation of proteins; increased non-enzymatic glycation of hemoglobin (HbA1c)
- increased lipid oxidation (storage duration-dependent accumulation of malondialdehyde and 8-isoprostane);
- increased non-enzymatic glycation of hemoglobin and protein carbonylations;
- oligomerisation of band 3 and enzyme/ROS-mediated fragmentation;
- accumulation/ decrease through vesiculation of protein biomarkers at the membrane level (CD47, Apo-J/Clusterin, peroxiredoxin 2, RH and rheology markers);
- progressive leaching of DEHP plasticizers (*in vitro*) that intercalates into the membrane;
- more rigid cell structures (reduced deformability and increased osmotic fragility);
- increased vesiculation rate (shedding of nano- and micro-vesicles);
- loss of the discocytic shape towards the acquisition of the echinocytic, spherocytic and utterly echinocytic phenotype;

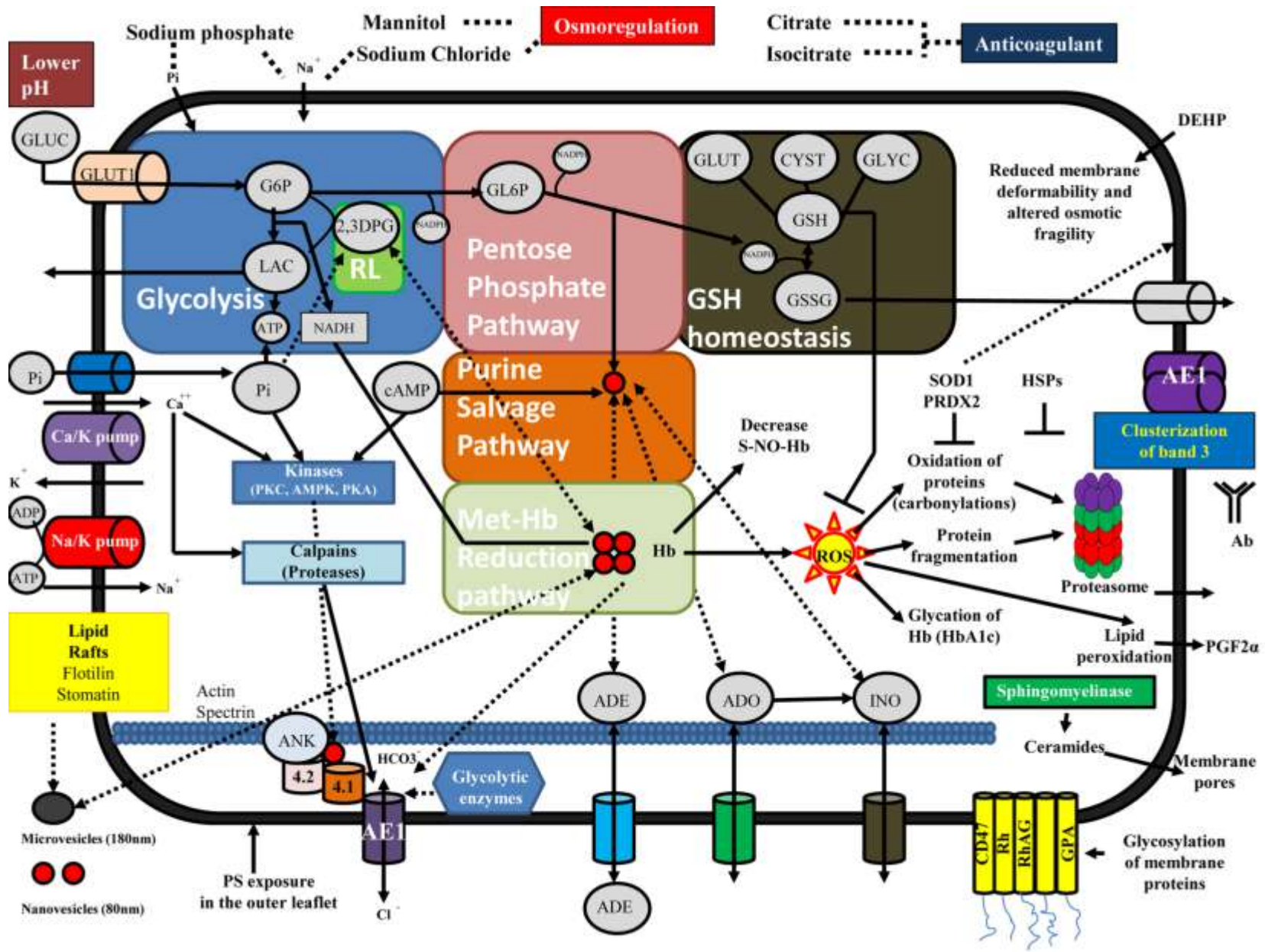


FIGURE 1 – The figure can be read from the upper-left corner in a counter-clockwise direction.

An overview of the main biochemical changes of *in vitro* ageing red blood cells (RBCs) under blood bank conditions. Cation homeostasis dysregulation (K^+ , Ca^{2+}) is influenced by low temperatures and progressive depletion of high energy phosphate reservoirs (adenosine triphosphate – ATP and 2,3-diphosphoglycerate - DPG). Glucose (additive solution) is internalized through GLUT transporters and consumed through the Emden-Meyerhof glycolytic pathway, as to produce ATP, lactate (LAC) and promote pH lowering. Besides, storage results in progressive decrease of S-nitrosothiol-Hemoglobin (Hb). However, low temperatures and the progressive accumulation of oxidative stress (likely triggered by Hb-mediated Fenton reactions) promote a metabolic diversion towards the pentose phosphate pathway, as to produce oxidized glutathione (GSSG)-reducing NADPH from glucose 6-phosphate (G6P). Pentose phosphate pathway intermediates can re-enter glycolysis or rather proceed towards the purine salvage pathway (also influenced by adenosine and inosine in the additive/rejuvenation solution).

Alterations to calcium (Ca^{2+}) homeostasis (and of other second messenger signaling molecules, such as cAMP and AMP) promote the activation of specific kinases (e.g. PKC, PKA, AMPK) or rather activate proteolytic enzymes (such as calpains) that start digesting structural and functional proteins at the cytosol and membrane level, above all band 3 (AE1). Anion exchanger 1/band 3 (AE1) is indeed responsible for the chloride shift, whereby bicarbonate (HCO_3^-) is exchanged for chloride (Cl^-), thus modulating anion homeostasis, intracellular pH and, indirectly, Hb-oxygen affinity and thus gas exchanges. Fragmentation of the cytosolic domain of AE1 (also mediated by reactive oxygen species – ROS) promotes displacement of glycolytic enzymes (thereby bound/inhibited) and structural proteins (ankyrin – ANK, band 4.2 and 4.1). Enhanced oxidation of cytosolic proteins is partly challenged by antioxidant defenses (SOD1, PRDX2) and chaperone molecules (heat shock proteins – HSPs), while they progressively result in the accumulation of redox modifications to proteins (carbonylations, glycation of hemoglobin – HbA1c, protein fragmentation) and lipids (lipid peroxidation, accumulation of prostaglandins in the supernatant).

A role in the process is also mediated by alternative degradation strategies to proteins (proteasome, eventually extruded in the supernatant) and lipids (sphingomyelinase-dependent accumulation of ceramides). Progressive leaching of plasticizers (DEHP) from the plastic bag results in the local accumulation at the membrane. At the membrane level, AE1 clusters, exposure of phosphatidylserine (PS) in the outer leaflet, lipid raft formation alter RBC pro-immunogenic potential. Taken together, these alterations affect membrane deformability, increase osmotic fragility and promote vesiculation events, a process where micro- and nanovesicles are shed as to eliminate irreversibly altered proteins (among which traces of glycolytic enzymes), enriched with hemoglobin and lipid raft proteins, membrane portions (also exposing common rheological antigens – CD47, Rh, RhAG, glycophorin A-GPA).

References

- Annis AM, Glenister KM, Killian JJ, Sparrow RL. Proteomic analysis of supernatants of stored red blood cell products. *Transfusion*. 2005;45(9):1426-33.
- Antonelou MH, Kriebardis AG, Stamoulis KE, Economou-Petersen E, Margaritis LH, Papassideri IS. Red blood cell aging markers during storage in citrate-phosphate-dextrose-saline-adenine-glucose-mannitol. *Transfusion*. 2010; 50(2):376-89.
- Antonelou MH, Tzounakas VL, Velentzas AD, Stamoulis KE, Kriebardis AG, Papassideri IS. Effects of pre-storage leukoreduction on stored red blood cells signaling: a time-course evaluation from shape to proteome. *J Proteomics*. 2012;76.:220-38.
- Bennett-Guerrero E, Veldman TH, Doctor A, Telen MJ, Ortel TL, Reid TS, et al. Evolution of adverse changes in stored RBCs. *Proc Natl Acad Sci U S A*. 2007;104(43):17063-8.
- Berezina TL, Zaets SB, Morgan C, Spillert CR, Kamiyama M, Spolarics Z, et al. Influence of storage on red blood cell rheological properties. *J Surg Res*. 2002;102(1):6-12.
- Bessis M. Red cell shapes. An illustrated classification and its rationale. *Nouv Rev Fr Hematol*. 1972;12(6):721-45.
- Bicalho B, Holovati JL, Acker JP. Phospholipidomics reveals differences in glycerophosphoserine profiles of hypothetically stored red blood cells and microvesicles. *Biochim Biophys Acta*. 2013;1828(2):317-26.
- Blasi B, D'Alessandro A, Ramundo N, Zolla L. Red blood cell storage and cell morphology. *Transfus Med*. 2012;22(2):90-6.
- Bosch FH, Werre JM, Roerdinkholder-Stoelwinder B, Huls TH, Willekens FL, Halie MR. Characteristics of red blood cell populations fractionated with a combination of counterflow centrifugation and Percoll separation. *Blood*. 1992; 79(1):254-60.
- Bosman GJ, Cluitmans JC, Groenen YA, Werre JM, Willekens FL, Novotný VM. Susceptibility to hyperosmotic stress-induced phosphatidylserine exposure increases during red blood cell storage. *Transfusion*. 2011;51(5):1072-8.
- Bosman GJ, Lasonder E, Groenen-Döpp YA, Willekens FL, Werre JM, Novotný VM. Comparative proteomics of erythrocyte aging in vivo and in vitro. *J Proteomics*. 2010; 73(3):396-402.
- Bosman GJ, Lasonder E, Groenen-Döpp YA, Willekens FL, Werre JM. The proteome of erythrocyte-derived microparticles from plasma: new clues for erythrocyte aging and vesiculation. *J Proteomics*. 2012;76 Spec No.:203-10.
- Bosman GJ, Lasonder E, Lutten M, Roerdinkholder-Stoelwinder B, Novotný VM, Bos H, et al. The proteome of red cell membranes and vesicles during storage in blood bank conditions. *Transfusion*. 2008;48(5):827-35
- Brajovich ML, Rucci A, Acosta IL, Cotorruelo C, García Borrás S, Racca L, et al. Effects of aging on antioxidant response and phagocytosis in senescent erythrocytes. *Immunol Invest*. 2009; 38(6):551-9.
- Bunn HF, Haney DN, Kamin S, Gabbay KH, Gallop PM. The biosynthesis of human hemoglobin A_{1c}. Slow glycosylation of hemoglobin in vivo. *J Clin Invest* 1976; 57:1652-9.
- Burr MJ. The relationship between pH and aerobic glycolysis in human and canine erythrocytes. *Comp Biochem Physiol B* 1972;41(4):687-94.
- Canellini G, Rubin O, Delobel J, Crettaz D, Lion N, Tissot JD. Red blood cell microparticles and blood group antigens: an analysis by flow cytometry. *Blood Transfus*. 2012;10(2):s39-45.
- Castagnola M, Messana I, Sanna MT, Giardina B. Oxygen-linked modulation of erythrocyte metabolism: state of the art. *Blood Transfus*. 2010;8(3): 53-58.
- Corsi D, Paiardini M, Crinelli R, Bucchini A, Magnani M. Alteration of α -spectrin ubiquitination due to age-dependent changes in the erythrocytes membrane. *Eur. J. Biochem* 1999; 261:775-783.
- D'Alessandro A, Mirasole C, Zolla L. Hemoglobin alpha glycation (Hb1Ac) increases during red blood cell storage: a MALDI-TOF mass spectrometry-based investigation. *Vox Sanguinis* 2013; DOI: 10.1111/vox.12029
- D'Alessandro A, Blasi B, D'Amici GM, Marrocco C, Zolla L. Red blood cell subpopulations in freshly drawn blood: application of proteomics and metabolomics to a decades-long biological issue. *Blood Transfus*. 2013; 11:1-13.
- D'Alessandro A, Gevi F, Zolla L. Red blood cell metabolism under prolonged anaerobic storage. *Mol Biosyst* 2013; doi:
- D'Alessandro A, D'Amici GM, Vaglio S, Zolla L. Time-course investigation of SAGM-stored leukocyte-filtered red blood cell concentrates: from metabolism to proteomics. *Haematologica*. 2012;97(1):107-15.
- D'Alessandro A, Gevi F, Zolla L. A robust high resolution reversed-phase HPLC strategy to investigate various metabolic species in different biological models. *Mol Biosyst*. 2011;7(4):1024-32.
- D'Alessandro A, Liunbruno G, Grazzini G, Zolla L. Red blood cell storage: the story so far. *Blood Transfus*. 2010;8(2):82-8.

- D'Alessandro A, Righetti PG, Zolla L. The red blood cell proteome and interactome: an update. *J Proteome Res.* 2010;9(1):144-63.
- D'Amici GM, Mirasole C, D'Alessandro A, Yoshida T, Dumont LJ, Zolla L. Red blood cell storage in SAGM and AS3: a comparison through the membrane two-dimensional electrophoresis proteome. *Blood Transfus.* 2012;10(2):46-54.
- D'Amici GM, Rinalducci S, Zolla L. Proteomic analysis of RBC membrane protein degradation during blood storage. *J Proteome Res.* 2007;6(8):3242-55.
- Delobel J, Prudent M, Rubin O, Crettaz D, Tissot JD, Lion N. Subcellular fractionation of stored red blood cells reveals a compartment-based protein carbonylation evolution. *J Proteomics.* 2012;76:181-93.
- Dinkla S, Wessels K, Verdurmen WP, Tomelleri C, Cluitmans JC, Franssen J, et al. Functional consequences of sphingomyelinase-induced changes in erythrocyte membrane structure. *Cell Death Dis.* 2012;3:e410.
- Dumaswala UJ, Zhuo L, Jacobsen DW, Jain SK, Sukalski KA. Protein and lipid oxidation of banked human erythrocytes: role of glutathione. *Free Radic Biol Med.* 1999;27(9-10):1041-9.
- Dumont LJ, Baker S, Dumont DF, Herschel L, Waters S, Calcagni K, et al. Exploratory in vitro study of red blood cell storage containers formulated with an alternative plasticizer. *Transfusion.* 2012;52(7):1439-45.
- Fergusson DA, Hébert P, Hogan DL, LeBel L, Rouvinez-Bouali N, Smyth JA, Sankaran K, et al. Effect of fresh red blood cell transfusions on clinical outcomes in premature, very low-birth-weight infants: the ARIPI randomized trial. *JAMA.* 2012;308(14):1443-51.
- Franco RS, Puchulu-Campanella ME, Barber LA, Palascak MB, Joiner CH, Low PS, Cohen RM. Changes in the properties of normal human red blood cells during in vivo aging. *Am J Hematol.* 2013;88(1):44-51.
- Geng Q, Romero J, Saini V, Patel MB, Majetschak M. Extracellular 20S proteasomes accumulate in packed red blood cell units. *Vox Sang.* 2009;97(3):273-4.
- Gevi F, D'Alessandro A, Rinalducci S, Zolla L. Alterations of red blood cell metabolome during cold liquid storage of erythrocyte concentrates in CPD-SAGM. *J Proteomics.* 2012;76:168-80.
- Ghashghaieina M, Cluitmans JC, Akel A, Dreischer P, Toulany M, Köberle M, et al. The impact of erythrocyte age on eryptosis. *Br J Haematol.* 2012;157(5):606-14.
- Gifford SC, Derganc J, Shevkopyas SS, Yoshida T, Bitensky MW. A detailed study of time-dependent changes in human red blood cells: from reticulocyte maturation to erythrocyte senescence. *Br J Haematol.* 2006;135(3):395-404.
- Goodman SR, Kurdia A, Ammann L, Kakhniashvili D, Daescu O. The human red blood cell proteome and interactome. *Exp Biol Med (Maywood).* 2007;232(11):1391-408.
- Grazzini G, Vaglio S. Red blood cell storage lesion and adverse clinical outcomes: post hoc ergo propter hoc? *Blood Transfus.* 2012;10(2):4-6.
- Greenwalt TJ, Dumaswala UJ. Effect of red cell age on vesiculation in vitro. *Br J Haematol.* 1988; 68(4):465-7.
- Greenwalt TJ, McGuinness CG, Dumaswala UJ. Studies in red blood cell preservation: 4. Plasma vesicle hemoglobin exceeds free hemoglobin. *Vox Sang* 1991;61:14-7.
- Hentschel WM, Wu LL, Tobin GO, Anstall HB, Smith JB, Williams RR, et al. Erythrocyte cation transport activities as a function of cell age. *Clin Chim Acta.* 1986; 157(1):33-43.
- Huang YX, Wu ZJ, Mehrishi J, Huang BT, Chen XY, Zheng XJ, et al. Human red blood cell aging: correlative changes in surface charge and cell properties. *J Cell Mol Med.* 2011;15(12):2634-42.
- Jain SK. Evidence for membrane lipid peroxidation during the in vivo aging of human erythrocytes. *Biochim Biophys Acta.* 1988; 937(2):205-10.
- Jakubowska-Solarska B, Solski J. Sialic acids of young and old red blood cells in healthy subjects. *Med Sci Monit.* 2000;6(5):871-4.
- Jamshidi N, Palsson BØ. Systems biology of the human red blood cell. *Blood Cells Mol Dis.* 2006; 36:239-47.
- Jansen G, Koenderman L, Rijkssen G, Cats BP, Staal GE. Characteristics of hexokinase, pyruvate kinase, and glucose-6-phosphate dehydrogenase during adult and neonatal reticulocyte maturation. *Am J Hematol.* 1985; 20(3):203-15.
- Kannan M, Atreya C. Differential profiling of human red blood cells during storage for 52 selected microRNAs. *Transfusion.* 2010 Jul;50(7):1581-8.
- Karon BS, Hoyer JD, Stubbs JR, Thomas DD. Changes in Band 3 oligomeric state precede cell membrane phospholipid loss during blood bank storage of red blood cells. *Transfusion* 2009;49:1435-42.
- Karon BS, Van Buskirk CM, Jaben EA, Hoyer JD, Thomas DD. Temporal sequence of major biochemical events during Blood Bank storage of packed red blood cells. *Blood Transfus.* 2012; 28:1-9.
- Koch CG, Li L, Sessler DI, Figueroa P, Hoeltge GA, Mihaljevic T, et al. Duration of red-cell storage and complications after cardiac surgery. *N Engl J Med* 2008; 358:1229-39.

- Kriebardis AG, Antonelou MH, Stamoulis KE, Economou-Petersen E, Margaritis LH, Papassideri IS. Progressive oxidation of cytoskeletal proteins and accumulation of denatured hemoglobin in stored red cells. *J Cell Mol Med* 2007;11:148-55.
- Kurata M, Suzuki M. Glutathione regeneration in calcium-loaded erythrocytes: a possible relationship among calcium accumulation, ATP decrement and oxidative damage. *Comp Biochem Physiol B Biochem Mol Biol*. 1994;109(2-3):305-12.
- Lang E, Qadri SM, Lang F. Killing me softly - suicidal erythrocyte death. *Int J Biochem Cell Biol*. 2012; 44(8):1236-43.
- Lelubre C, Piagnerelli M, Vincent JL. Association between duration of storage of transfused red blood cells and morbidity and mortality in adult patients: myth or reality? *Transfusion*. 2009;49(7):1384-94.
- Lewis IA, Campanella ME, Markley JL, Low PS. Role of band 3 in regulating metabolic flux of red blood cells. *Proc Natl Acad Sci U S A* 2009;106(44):18515–20.
- Linderkamp O, Meiselman HJ. Geometric, osmotic, and membrane mechanical properties of density-separated human red cells. *Blood*. 1982; 59(6):1121-7.
- Lion N, Crettaz D, Rubin O, Tissot JD. Stored red blood cells: a changing universe waiting for its map(s). *J Proteomics*. 2010;73(3):374-85.
- Low FM, Hampton MB, Peskin AV, Winterbourn CC. Peroxiredoxin 2 functions as a noncatalytic scavenger of low-level hydrogen peroxide in the erythrocyte. *Blood*. 2007;109(6):2611-7.
- Low PS, Rathinavelu P, Harrison ML. Regulation of glycolysis via reversible enzyme binding to the membrane protein, band 3. *J Biol Chem* 1993; 268:14627-31.
- Lutz HU, Fasler S, Stammler P, Bussolino F, Arese P. Naturally occurring anti-band 3 antibodies and complement in phagocytosis of oxidatively-stressed and in clearance of senescent red cells. *Blood Cells*. 1988; 14(1):175-203.
- Manno S, Takakuwa Y, Nagao K, Mohandas N. Modulation of erythrocyte membrane mechanical function by protein 4.1 phosphorylation. *J Biol Chem*. 2005;280:7581–7.
- Marrocco C, Pallotta V, D'Alessandro A, Alves G, Zolla L. Red blood cell populations and membrane levels of peroxiredoxin 2 as candidate biomarkers to reveal blood doping. *Blood Transfus*. 2012;10(2):s71-7.
- Matte A, Bertoldi M, Mohandas N, An X, Bugatti A, Brunati AM, et al. Membrane association of peroxiredoxin-2 in red cells is mediated by the N-terminal cytoplasmic domain of band 3. *Free Radic Biol Med*. 2012;55C:27-35.
- Messana I, Ferroni L, Misiti F, Girelli G, Pupella S, Castagnola M, et al. Blood bank conditions and RBCs: the progressive loss of metabolic modulation. *Transfusion*. 2000;40(3):353-60.
- Messana I, Misiti F, el-Sherbini S, Giardina B, Castagnola M. Quantitative determination of the main glucose metabolic fluxes in human erythrocytes by ¹³C- and ¹H-MR spectroscopy. *J Biochem Biophys Methods* 1999;39(1-2):63–84.
- Montes LR, López DJ, Sot J, Bagatolli LA, Stonehouse MJ, Vasil ML, Wu BX, Hannun YA, Goñi FM, Alonso A. Ceramide-enriched membrane domains in red blood cells and the mechanism of sphingomyelinase-induced hot-cold hemolysis. *Biochemistry*. 2008;47(43):11222-30.
- Nakao K, Wada T, Kamiyama T, Nakao M, Nagano K. A direct relationship between adenosine triphosphate-level and in vivo viability of erythrocytes. *Nature* 1962; 194:877-87852.
- Nash GB, Wyard SJ. Changes in surface area and volume measured by micropipette aspiration for erythrocytes ageing in vivo. *Biorheology*. 1980;17(5-6):479-84.
- Nishino T, Yachie-Kinoshita A, Hirayama A, Soga T, Suematsu M, Tomita M. In silico modeling and metabolome analysis of long-stored erythrocytes to improve blood storage methods. *J Biotechnol*. 2009;144(3):212-23.
- Palek J, Stewart G, Lionetti FJ. The dependence of shape of human erythrocyte ghosts on calcium, magnesium and adenosine triphosphate. *Blood* 1974; 44:583- 597.
- Pallotta V, Gevi F, D'Alessandro A, Zolla L. Red blood cell storage with vitamin C and N-acetylcysteine prevents oxidative stress-related lesions: a metabolomics overview. *To be submitted* 2013;
- Pallotta V, D'Amici GM, D'Alessandro A, Rossetti R, Zolla L. Red blood cell processing for cryopreservation: from fresh blood to deglycerolization. *Blood Cells Mol Dis*. 2012;48(4):226-32.
- Pantaleo A, Ferru E, Giribaldi G, Mannu F, Carta F, Matte A, et al. Oxidized and poorly glycosylated band 3 is selectively phosphorylated by Syk kinase to form large membrane clusters in normal and G6PD-deficient red blood cells. *Biochem J*. 2009;418(2):359-67.
- Park Y, Best CA, Auth T, Gov NS, Safran SA, Popescu G, Suresh S, Feld MS. Metabolic remodeling of the human red blood cell membrane. *Proc Natl Acad Sci U S A*. 2010;107(4):1289-94.

- Percy AK, Schmell E, Earles BJ, Lennarz WJ. Phospholipid biosynthesis in the membranes of immature and mature red blood cells. *Biochemistry* 1973;12(13):2456–61.
- Pittman JG, Martin DB. Fatty acid biosynthesis in human erythrocytes: evidence in mature erythrocytes for an incomplete long chain fatty acid synthesizing system. *J Clin Invest.* 1966;45(2):165-72.
- Pompeo G, Girasole M, Cricenti A, Boumis G, Bellelli A, Amiconi S. Erythrocyte death in vitro induced by starvation in the absence of Ca(2+). *Biochim Biophys Acta.* 2010;1798(6):1047-55.
- Rinalducci S, D'Amici GM, Blasi B, Vaglio S, Grazzini G, Zolla L. Peroxiredoxin-2 as a candidate biomarker to test oxidative stress levels of stored red blood cells under blood bank conditions. *Transfusion.* 2011;51(7):1439-49.
- Rinalducci S, Ferru E, Blasi B, Turrini F, Zolla L. Oxidative stress and caspase-mediated fragmentation of cytoplasmic domain of erythrocyte band 3 during blood storage. *Blood Transfus.* 2012;10 Suppl 2:s55-62.
- Rocha S, Vitorino RM, Lemos-Amado FM, Castro EB, Rocha-Pereira P, Barbot J, et al. Presence of cytosolic peroxiredoxin 2 in the erythrocyte membrane of patients with hereditary spherocytosis. *Blood Cells Mol Dis.* 2008;41(1):5-9.
- Romero PJ, Romero EA. Determinant factors for an apparent increase in oxygen affinity of senescent human erythrocytes. *Acta Cient Venez.* 2004; 55(1):83-5.
- Romero PJ, Romero EA. The role of calcium metabolism in human red blood cell ageing: a proposal. *Blood Cells Mol Dis.* 1999;25(1):9-19.
- Roux-Dalvai F, Gonzalez de Peredo A, Simó C, Guerrier L, Bouyssié D, Zanella A, et al. Extensive analysis of the cytoplasmic proteome of human erythrocytes using the peptide ligand library technology and advanced mass spectrometry. *Mol Cell Proteomics* 2008;7(11):2254–69.
- Samaja M, Rovida E, Motterlini R, Tarantola M, Rubinacci A, diPrampetro PE. Human red cell age, oxygen affinity and oxygen transport. *Respir Physiol.* 1990; 79(1):69-79.
- Sass MD, Caruso CJ, O'Connell DJ. Decreased glutathione in aging red cells. *Clin Chim Acta* 1965; 11: 334.
- Schroit AJ, Madsen JW, Tanaka Y. In vivo recognition and clearance of red blood cells containing phosphatidylserine in their plasma membranes. *J Biol Chem.* 1985; 260(8):5131-8.
- Sens P, Gov N. Force balance and membrane shedding at the red-blood-cell surface. *Phys Rev Lett.* 2007; 98(1):018102.
- Shinozuka T. Changes in human red blood cells during aging in vivo. *Keio J Med.* 1994; 43(3):155-63.
- Sparrow RL, Veale MF, Healey G, Payne KA. Red blood cell (RBC) age at collection and storage influences RBC membrane-associated carbohydrates and lectin binding. *Transfusion.* 2007 Jun;47(6):966-8.
- Strange RC, Johnson PH, Lawton A, Moulton JA, Tector MJ, Tyminski RJ, et al. Studies on the variability of glutathione S-transferase from human erythrocytes. *Clin Chim Acta.* 1982; 120(2):251-60.
- Suzuki T, Dale GL. Biotinylated erythrocytes: In vivo survival and in vitro recovery. *Blood* 1987; 791–795.
- Szelényi JG, Földi J, Hollán SR: Enhanced nonenzymatic glycosylation of blood proteins in stored blood. *Transfusion* 1983;23:11–14.
- Valeri CR, Hirsch NM. Restoration in vivo of erythrocyte adenosine triphosphate, 2,3-diphosphoglycerate, potassium ion, and sodium ion concentrations following the transfusion of acid-citrate-dextrose-stored human red blood cells. *J Lab Clin Med.* 1969;73(5):722-33.
- Valtis DJ. Defective gas-transport function of stored red blood-cells. *Lancet.* 1954;266(6803):119-24.
- Van Gestel C, Van Den Berg D, de Gier J, Van Deenen LLM. Some lipid characteristics of normal red blood cells of different age. *Brit J Haematol.* 1965;11: 193-9.
- Virgili F, Battistini N, Canali R, Vannini V, Tommasi A. High glucose-induced membrane lipid peroxidation on intact erythrocytes and on isolated erythrocyte membrane (ghosts). *J Nutr Biochem* 1996; 151-161.
- Wallas CH. Sodium and potassium changes in blood bank stored human erythrocytes. *Transfusion.* 1979;19(2):210-5.
- Walpurgis K, Kohler M, Thomas A, Wenzel F, Geyer H, Schänzer W, Thevis M. Storage-induced changes of the cytosolic red blood cell proteome analyzed by 2D DIGE and high-resolution/high-accuracy MS. *Proteomics.* 2012 Nov;12(21):3263-72.
- Ways P, Hanahan DJ. Characterization and quantification of red cell lipids in normal man. *J Lipid Res.* 1964;5(3):318-28.
- Whillier S, Raftos JE, Sparrow RL, Kuchel PW. The effects of long-term storage of human red blood cells on the glutathione synthesis rate and steady-state concentration. *Transfusion.* 2011;51(7):1450-9.
- Wiley JS, McCulloch KE, Bowden DS. Increased calcium permeability of cold-stored erythrocytes. *Blood* 1982;60(1): 92–8.

D'Alessandro Angelo**CV****General Data**

Last name	D'Alessandro		
First name	Angelo		
Street and number	Via Occorsio, 1		
City	Canino (VT)	Nationality	Italian
Postcode	01011		
Country	Italy		
Phone nr (work)	+39 3332310064		
Phone nr, (home)	+39 0761438259		
E-mail	a.dalessandro@unitus.it ; angel1025@hotmail.it ;		
Skype	angelo.dalessandro.1984		
Date and place of birth	25/04/1984 Tarquinia (VT) - Italy		

Currently:**PhD Student in Genetics and Cell Biology (Last year)****Subject Expert (“Cultore della Materia”) in Molecular Biology**

at Department of Ecological and Biological Sciences - Tuscia University – Viterbo (Italy)

Associated Editor of Journal of Integrated Omics (since October 2012) - ISSN 2182-0287**Guest Editor of the Special Issue: “Integrated Omics” of Journal of Proteomics** – (2012) co-guest edited with Prof. Lello Zolla – Volume 76 - ISSN: 1874-3919

List of Publications

1. D'Alessandro A, Gevi F, Zolla L.
Red blood cell metabolism under prolonged anaerobic storage
Molecular Biosystems 2013; Accepted Waiting for doi
2. Zolla L, D'Alessandro A.
An efficient apparatus for rapid deoxygenation of erythrocyte concentrates for alternative banking strategies.
J Blood Transfusion 2013; Accepted Waiting for doi
3. D'Alessandro A, Mirasole C, Zolla L.
Hemoglobin alpha glycation (Hb1Ac) increases during red blood cell storage: a MALDI-TOF mass spectrometry-based investigation.
Vox Sanguinis 2013; DOI: 10.1111/vox.12029
4. Marrocco C, D'Alessandro A, Rinalducci S, Rebulli P, Zolla L.
The IPTAS study: the effects of pathogen inactivation technology Mirasol on apheresis platelet concentrates.
Transfusion 2013; DOI: 10.1111/trf.12060.
5. D'Alessandro A, Zolla L.
Meat science: from Proteomics to Integrated Omics towards System biology
Journal of Proteomics 2013; 78:558-577.
6. D'Alessandro A, Blasi B, D'Amici GM, Marrocco C, Zolla L.
Red blood cell populations in freshly drawn blood: application of proteomics and metabolomics to a decades-long biological issue
Blood Transfusion; 2013;11: 75-87.
7. Murgiano L, D'Alessandro A, Zolla L, Valentini A, Pariset L.
Comparison of Milk Fat Globule Membrane (MFGM) Proteins in Milk Samples of Chianina and Holstein Cattle Breeds across three Lactation Phases through 2D IEF SDS PAGE – a preliminary study.
Food Research International 2012; doi: 10.1016/j.foodres.2012.10.035
8. Zolla L, D'Alessandro A.
Response to "Platelets proteomics in Transfusion Medicine: a reality with challenging but promising future"
Blood Transfusion 2012; doi: 10.2450/2012.0175-12
9. Zolla L, D'Alessandro A.
Preface to the Special Issue Integrated Omics.
J Proteomics 2012; 76:3-9.
10. Rita Polati, Annalisa Castagna, Alessandra Maria Bossi, Tiziana Alberio, Ivana De Domenico, Jerry Kaplan, Anna Maria Timperio, Lello Zolla, Gevi Federica, Angelo D'Alessandro, Ryan Brunch, Oliviero Olivieri, Domenico Girelli
Murine macrophages response to iron
J Proteomics 2012; 76:10-27.
11. Zolla L, D'Alessandro.
Shaking hands with the future through Omics application in Transfusion Medicine and Clinical Biochemistry. Preface
Blood Transfusion 2012; 10(2):s1-3.
12. D'Alessandro A, Gevi F, Timperio AM, Giardina B, Zolla L.
Clinical Metabolomics: the next stage of clinical biochemistry
Blood Transfusion 2012; 10 Suppl 2:s19-24.
13. D'Amici GM, Mirasole C, D'Alessandro A, Yoshida T, Dumont LJ, Zolla L.

- Red blood cell storage in SAGM and AS3: a comparison through the membrane two-dimensional electrophoresis proteome**
Blood Transfusion 2012; 10 Suppl 2:s46-54.
14. Marrocco Cristina, Pallotta Valeria, D'Alessandro Angelo, Gilda Alves, Zolla Lello
Red blood cell populations and membrane levels of peroxiredoxin 2 as candidate biomarkers to reveal blood doping
Blood Transfusion 2012; 10 Suppl 2:s71-7.
15. D'Alessandro A, Marrocco C, Rinalducci S, Mirasole C, Failla S, Zolla L.
Chianina beef tenderness investigated through integrated Omics.
Journal of Proteomics 2012; 75(14):4381-98.
16. D'Alessandro A, Zolla L.
Food safety and quality control: hints from proteomics
Food Technology and Biotechnology 2012; 50(3):275-85.
17. Peschiaroli A, Giacobbe A, Formosa A, Markert EK, Bongiorno-Borbone L, Levine AJ, Candi E, D'Alessandro A, Zolla L, Finazzi Agrò A, Melino G.
MIR-143 REGULATES HEXOKINASE 2 EXPRESSION IN CANCER CELLS
Oncogene 2012; doi:10.1038/onc.2012.100
18. Gevi F*, D'Alessandro A*, Rinalducci S, Zolla L. (* = shared first authorship)
Alterations of Red Blood Cell metabolome during cold liquid storage of erythrocyte concentrates in CPD-SAGM.
Journal of Proteomics. 2012; 76:168-180.
19. D'Alessandro A, Rinalducci S, Marrocco C, , Zolla V, Napolitano F, Zolla L.
Love me tender: an omics window on the Maremmana meat tenderness network.
J Proteomics 2012; 75(14):4360-80.
20. Blasi B, D'Alessandro A, Nicola Ramundo, Zolla L.
Red blood cell storage and cell morphology
Transfusion Medicine 2012; 22(2):90-6.
21. Blasi B, D'Amici GM, D'Alessandro A, Zolla L.
Native analysis of Plasma-derived clotting factor VIII concentrates: "sponge effect" and contaminants
Electrophoresis 2012; 33:1-7.
22. Pallotta V, D'Amici GM, D'Alessandro A, Rossetti R, Zolla L.
Monitoring of red blood cells during processing for cryopreservation: from fresh blood to thaw-washing
Blood Cells, Molecules and Diseases 2012; 48(4):226-32.
23. D'Alessandro A, Zolla L.
We are what we eat: food safety and proteomics
Journal of proteome research 2012; 11(1):26-36.
24. D'Alessandro A, Gevi F, Palini S, Bulletti C, Zolla L.
A targeted mass spectrometry-based metabolomics strategy of human blastocoele fluid: a promising tool in fertility research
Mol Biosystems; 2012; 8(4):953-8.
25. D'Alessandro A, D'Amici GM, Vaglio S, Zolla L.
Time-course Investigation of SAGM-Stored Erythrocyte Concentrates: from Metabolism to Proteomics.
Hematologica 2012 ;97(1):107-15.
26. D'Alessandro A, Zolla L.
Metabolomics and cancer drug discovery: let the cells do the talking
Drug Discov Today 2012; 17(1-2):3-9.
27. Timperio AM, D'Alessandro A, Fagioni M, Zolla L.

- Production of the phytoalexin trans-resveratrol and delta-viniferin in two economy-relevant grape cultivars upon infection with *Botrytis cinerea* in field conditions.**
Plant Physiology Biochemistry 2012; ;50(1):65-71.
- 28.D'Alessandro A, Gevi F, Zolla L.
Targeted mass spectrometry-based metabolomic profiling through Multiple Reaction Monitoring of Liver and other biological matrices.
Methods Mol Biol. 2012; In Liver Proteomics. In Methods and Protocols Series: Methods in Molecular Biology. 2012; vol. 909. Josic, Djuro; Hixson, Douglas C. (Eds.)
- 29.D'Alessandro A, Marrocco C, Zolla V, D'Andrea MS, Zolla L.
Meat quality and the Longissimus lumborum muscle of Casertana and Large White pigs: metabolomics and proteomics intertwined
Journal of Proteomics 2011;75(2):610-27.
- 30.D'Amici GM, Blasi B, D'Alessandro A, Vaglio S, Zolla L.
Plasma-derived clotting factor VIII: heterogeneity evaluation in the quest for potential inhibitory-antibody stimulating factors
Electrophoresis 2011; 32: 1-10.
- 31.D'Alessandro A, D'Amici GM, Timperio AM, Merendino N, Zolla L.
Docosohaexanoic acid-treated PACA44 cell lines and over-activation of Krebs cycle: an integrated proteomics, metabolomics and interactomics overview
J Proteomics. 2011;74(10):2138-58.
- 32.Basco D, Nicchia GP, D'Alessandro A, Zolla L, Svelto M, Frigeri A.
Absence of AQP4 in skeletal muscle alters proteins involved in bioenergetic pathways and calcium handling.
PLOS ONE 2011; 6(4):e19225.
- 33.D'Alessandro A, Zolla L.
The SODyssey – Superoxide dismutases: from biochemistry, through proteomics, to oxidative stress, ageing and nutraceuticals.
Exp Rev Proteomics. 2011; 8(3):405-21.
- 34.D'Alessandro A, Gevi F, Zolla L.
A robust high resolution reversed-phase HPLC strategy to investigate various metabolic species in different biological models.
Mol Biosyst. 2011; 7(4):1024-32.
- 35.D'Alessandro A, Rinalducci S, Zolla L.
Redox proteomics and drug development.
J Proteomics. 2011; 74(12):2575-95
- 36.D'Alessandro A, Zolla L, Scaloni A.
The bovine milk proteome: cherishing, nourishing and fostering molecular complexity. An interactomics and functional overview.
Mol Biosyst. 2011;7(3):579-97.
- 37.D'Alessandro A, Zolla L.
Pharmacoproteomics: a chess game on a protein field.
Drug Discov Today. 2010;15(23-24):1015-23.
- 38.Murgiano L, D'Alessandro A, Egidi MG, Crisà A, Prosperini G, Timperio AM, Valentini A, Zolla L.
Proteomics and transcriptomics investigation on longissimus muscles in Large White and Casertana pig breeds.
J Proteome Res. 2010;9(12):6450-66.
- 39.D'Alessandro A, Grazzini G, Giardina B, Zolla L.
In silico analyses of proteomic data suggest a role for heat shock proteins in umbilical cord blood hematopoietic stem cells.
Stem Cell Rev. 2010;6(4):532-47.
- 40.Egidi MG, D'Alessandro A, Mandarello G, Zolla L.

Troubleshooting in platelet storage temperature and new perspectives through proteomics.*Blood Transfus.* 2010;8 Suppl 3:s73-81

41.D'Alessandro A, Zolla L.

Proteomics for quality-control processes in transfusion medicine.*Anal Bioanal Chem.* 2010;398(1):111-24.

42.D'Alessandro A, Scaloni A, Zolla L.

Human milk proteins: an interactomics and updated functional overview.*J Proteome Res.* 2010;9(7):3339-73.

43.D'Alessandro A, Liumbruno G, Grazzini G, Zolla L.

Red blood cell storage: the story so far.*Blood Transfus.* 2010;8(2):82-8.

44.Liumbruno G, D'Alessandro A, Grazzini G, Zolla L.

How has proteomics informed transfusion biology so far?*Crit Rev Oncol Hematol.* 2010;76(3):153-72.

45.Liumbruno GM, D'Alessandro A, Rea F, Piccinini V, Catalano L, Calizzani G, Pupella S, Grazzini G.

The role of antenatal immunoprophylaxis in the prevention of maternal-foetal anti-Rh(D) alloimmunisation.*Blood Transfus.* 2010;8(1):8-16.

46.D'Alessandro A, Righetti PG, Fasoli E, Zolla L.

The egg white and yolk interactomes as gleaned from extensive proteomic data.*J Proteomics.* 2010;73(5):1028-42.

47.D'Alessandro A, Righetti PG, Zolla L.

The red blood cell proteome and interactome: an update.*J Proteome Res.* 2010;9(1):144-63.

48.Timperio AM, D'Alessandro A, Pariset L, D'Amici GM, Valentini A, Zolla L.

Comparative proteomics and transcriptomics analyses of livers from two different Bos taurus breeds: "Chianina and Holstein Friesian".*J Proteomics.* 2009;73(2):309-22.

49.Liumbruno G, D'Alessandro A, Grazzini G, Zolla L.

Blood-related proteomics.*J Proteomics.* 2010;73(3):483-507.

50.D'Alessandro A, Liumbruno G, Grazzini G, Pupella S, Lombardini L, Zolla L.

Umbilical cord blood stem cells: towards a proteomic approach.*J Proteomics.* 2010;73(3):468-82.**Book chapters:**

51.Zolla L, D'Alessandro A. Proteomic Investigations on Stored Red Blood Cells. *In* Chemistry and Biochemistry of Oxygen Therapeutics: From Transfusion to Artificial Blood. Mozzarelli A. Editor; John Wiley and Sons Ltd The Atrium, Southern Gate Chichester, West Sussex, PO19 8SQ

Encyclopedia Chapters

52.Zolla L, D'Alessandro A. Chromatography of Membrane Proteins and Lipoproteins. *Encyclopedia of Analytical Chemistry.* 2011. R.A. Meyers (Ed.) Copyright John Wiley & Sons Ltd. DOI: 10.1002/9780470027318.a1607.pub2

53.Angelo D'Alessandro, Andrea Scaloni, Lello Zolla

Human milk proteins: strides in proteomics and benefits in nutrition research

In “Dietary and Nutritional Aspects of Human Breast Milk” – Book Chapter – cured by Dr Sherma Zibadi, Prof Ronald R Watson and Prof Victor R Preedy; Human health handbooks - 2212-375X, Volume 5. Wageningen Academic Publisher ISBN: 978-90-8686-209-2

Under review

54. Timperio AM, Mirasole C, D’Alessandro A, Zolla L.

Red Blood Cell Lipidomics analysis through HPLC-ESI-qTOF: application to red blood cell storage

J Integrated Omics 2013; Minor revisions

55. Zolla L, D’Alessandro A, Parguina A, Garcia A.

In reply to “Response to reply –response “Platelet Proteomics in Transfusion Medicine: a reality with a challenging but promising future”

Blood Transfusion 2013; Minor revisions

56. Dando I, Donadelli M, Costanzo C, Dalla Pozza E, D’Alessandro A, Zolla L, Palmieri M.

Cannabinoids inhibit energetic metabolism and induce AMPK-dependent autophagy in pancreatic cancer cells

Cell Death and Diseases 2013; Minor revisions

57. D’Alessandro A, Zolla L.

Biochemistry of red cell aging in vivo and storage lesions

Haematologica 2013; Under review

58. Pallotta V, D’Alessandro A, Rinalducci S, Zolla L.

Native protein complexes in the cytoplasm of Red Blood Cells

J Proteomics 2013; Under review

59. D’Alessandro A, Cervia D, Catalani E, Gevi F, Zolla L, Casini G.

A metabolomic analysis of the protective effects of neuropeptides in retinal ischemia

Neurobiology of Disease 2013; to be submitted

60. Pallotta V, Gevi F, D’Alessandro A, Zolla L.

Red blood cell storage with vitamin C and N-acetylcysteine prevents oxidative stress-related lesions: a metabolomics overview

Brit J Haematol 2013; to be submitted

61. D’Alessandro A, Marrocco C, Rinalducci S, Timperio AM, Peschiaroli A, Melino G, Finazzi Agrò A, Zolla L.

Integrated Omics suggest a role for PTEN and mTOR-mediated pathways in p73 alpha-induced apoptosis of SAOS cell lines

2013; to be submitted

Oral presentations

1. (*upcoming*) D'Alessandro A. Biochemistry of red cell aging in vivo and storage lesions. *Invited VIP speaker at the 18th congress of the European Haematology Association (EHA 18)* – Stockholm, Sweden. June 13-16, 2013.
2. D'Alessandro A, Zolla L. Meat tenderness and Integrated Omics. *LMC Food Science Network*. Technical University of Denmark, Copenhagen. August 29-30, 2012.
3. D'Alessandro A, D'Amici GM, Vaglio S, Zolla L. Red blood cell storage: Omics intertwined. VII ItPA Annual Congress. Session: *Technological Innovations*. Viterbo June 12-15, 2012.
4. D'Alessandro A, D'Amici GM, Vaglio S, Zolla L. Conservazione dei concentrati eritrocitari ad uso trasfusionale: analisi integrata di proteomica e metabolomica. In *Nuove Tecnologie in Medicina Trasfusionale*. 40° Congresso SIMTI – Rimini. May 23-26, 2012.
5. D'Alessandro A. Omics techniques: application to red blood cell storage for transfusion purposes. Viterbo December 12, 2011.
6. D'Alessandro A, Egidi MG, Zolla L. Proteomics and platelet research. Rome May 5, 2011.
7. D'Alessandro A, Righetti PG, Zolla L. The red blood cell proteome and interactome: an update. 5th ItPA Congress; Firenze June 10, 2010.
8. D'Alessandro A, D'Amici GM, Rinalducci S, Zolla L. Proteomics of the red blood cell membrane. New perspectives on red cell membrane research Rome. June 4, 2010
9. D'Alessandro A, Grazzini G, Giardina B, Zolla L. Umbilical cord blood stem cells: towards a proteomics approach. 1st Stem Cell Research Italy congress; Certosa di Pontignano (Siena) May 17-18, 2010.
10. Liunbruno GM, D'Alessandro A. La proteomica in Medicina Trasfusionale. Arezzo, November 25-26, 2009
11. D'Alessandro A, Zolla L. The Red Blood Cell proteome and interactome: an update. Blood and Proteomics in Viterbo. October 13, 2009.
12. Liunbruno GM, D'Alessandro A. La proteomica nello studio della conservazione degli emocomponenti labili. Firenze, September 25, 2009.
13. D'Alessandro A, Liunbruno G, Grazzini G, Zolla L. Anaerobic storage of red blood cells. Parma. August 25, 2009.

Congress: abstracts and posters (14 out of 40)**With ISBN**

1. Angelo D'Alessandro, Gian Maria D'Amici, Stefania Vaglio, Lello Zolla. Red blood cell storage: Omics intertwined. VII ItPA Annual Congress 2012; Book of abstracts. ISBN: 88-903318-5-5
2. Angelo D'Alessandro, Gian Maria D'Amici, Anna Maria Timperio, Niccolò Merendino, Lello Zolla. Docosohaexanoic acid-supplemented PACA44 cell lines and over-activation of Krebs cycle: an integrated proteomic, metabolomic and interactomic overview. VII ItPA Annual Congress 2012; Book of abstracts. ISBN: 88-903318-5-5
3. Valeria Pallotta, Gian Maria D'Amici, Angelo D'Alessandro, Roberto Rossetti, Lello Zolla. Red blood cell processing for cryopreservation: from fresh blood to deglycerolization. VII ItPA Annual Congress 2012; Book of abstracts. ISBN: 88-903318-5-5
4. Barbara Blasi, Gian Maria D'Amici, Angelo D'Alessandro, Giuliano Grazzini, Lello Zolla. Native analysis of Plasma-derived clotting factor VIII concentrates: "sponge effect" and contaminants. VII ItPA Annual Congress 2012; Book of abstracts. ISBN: 88-903318-5-5
5. Gian Maria D'Amici, Barbara Blasi, Angelo D'Alessandro, Stefania Vaglio, Lello Zolla. Plasma-derived clotting factor VIII: heterogeneity evaluation in the quest for potential inhibitory-antibody stimulating factors. VII ItPA Annual Congress 2012; Book of abstracts. ISBN: 88-903318-5-5
6. Rita Polati, Annalisa Castagna, Alessandra Maria Bossi, Tiziana Alberio, Ivana De Domenico, Jerry Kaplan, Anna Maria Timperio, Lello Zolla, Gevi Federica, Angelo D'Alessandro, Ryan Brunch, Oliviero Olivieri, and Domenico Girelli. Murine macrophages response to iron. VII ItPA Annual Congress 2012; Book of abstracts. ISBN: 88-903318-5-5
7. Angelo D'Alessandro, Barbara Blasi, Gian Maria D'Amici, Cristina Marrocco, Giuliano Grazzini, Lello Zolla. Red blood cell populations in freshly drawn blood: application of proteomics and metabolomics to a decades-long biological issue. VII ItPA Annual Congress 2012; Book of abstracts. ISBN: 88-903318-5-5
8. Cristina Marrocco, Valeria Pallotta, Angelo D'Alessandro, Gilda Alves, Lello Zolla. Red blood cell populations and membrane levels of peroxiredoxin 2 as candidate biomarkers to reveal blood doping. VII ItPA Annual Congress 2012; Book of abstracts. ISBN: 88-903318-5-5
9. Federica Gevi, Angelo D'Alessandro, Sara Rinalducci, Lello Zolla. Alterations of Red Blood Cell metabolome during storage of erythrocyte concentrates in CPD-SAGM. VII ItPA Annual Congress 2012; Book of abstracts. ISBN: 88-903318-5-5
10. Angelo D'Alessandro, Cristina Marrocco, Sara Rinalducci, Cristiana Mirasole, Sebastiana Failla, Lello Zolla. Chianina beef tenderness investigated through integrated Omics. VII ItPA Annual Congress 2012; Book of abstracts. ISBN: 88-903318-5-5
11. Angelo D'Alessandro, Sara Rinalducci, Cristina Marrocco, Valerio Zolla, Francesco Napolitano, Lello Zolla. Love me tender: An Omics window on the bovine meat tenderness network. VII ItPA Annual Congress 2012; Book of abstracts. ISBN: 88-903318-5-5
12. Angelo D'Alessandro, Cristina Marrocco, Valerio Zolla, Maria Silvia D'Andrea, Lello Zolla. Meat quality of the longissimus lumborum muscle of Casertana and Large White pigs: Metabolomics and proteomics intertwined. VII ItPA Annual Congress 2012; Book of abstracts. ISBN: 88-903318-5-5
13. Leonardo Murgiano, Angelo D'Alessandro, Maria Giulia Egidi, Alessandra Crisà, Gianluca Prosperini, Anna Maria Timperio, Alessio Valentini, Lello Zolla. An interactomics overview of proteomics and transcriptomics data upon comparison of Large White and Casertana pig breeds. VII ItPA Annual Congress 2012; Book of abstracts. ISBN: 88-903318-5-5
14. Casini G, Dal Monte M, Martini D, D'Alessandro A, Bagnoli P. The somatostatinergetic system contributes to the severity of angiogenetic responses to hypoxia in the mouse retina. *Acta Physiologica* 2008; Volume 194, Supplement 665 :OC36

Without ISBN

1. D'Alessandro A, Zolla L. Meat tenderness and integrated Omics. Technical University of Denmark (DTU) – Copenhagen – August 28-30, 2012
2. D'Alessandro A, Marrocco C, Rinalducci S, Mirasole C, Zolla V, Failla S, Napolitano F, Zolla L. Love me tender: an omics window on bovine meat tenderness. VII Annual ItPA Congress, Viterbo June 12-15, 2012.
3. D'Alessandro A, Marrocco C, Zolla V, Mirasole C, D'Andrea MS, Zolla L. Meat quality of the *longissimus lumborum* muscle of Casertana and Large White pigs: metabolomics and proteomics intertwined. VII Annual ItPA Congress, Viterbo June 12-15, 2012.
4. D'Alessandro A, Blasi B, D'Amici GM, Marrocco C, Zolla L. Red blood cell populations in freshly drawn blood: application of proteomics and metabolomics to a decades-long biological issue. SIMTI annual congress. Rimini, May 23-26 2012.
5. D'Alessandro A, Gevi F, Rinalducci S, Zolla L. Alterations of Red Blood Cell metabolome during cold liquid storage of erythrocyte concentrates in CPD-SAGM. SIMTI annual congress. Rimini, May 23-26 2012.
6. Palini S, Zolla L, De Stefani S, Scala V, D'Alessandro A, Polli V, Rocchi P, Tiezzi A, Pelosi E, Dusi L and Bulletti C. Omics in blastocoele. Hum. Reprod. (2011) 26 (suppl 1): i160-i202. Abstracts of the 27th Annual Meeting of the European Society of Human Reproduction and Embryology, Stockholm, Sweden, 3-6 July 2011
7. D'Alessandro A, D'Amici GM, Blasi B, Marrocco C, Zolla L. Time-course investigation of SAGM-stored Erythrocyte Concentrates: from metabolism to proteomics. Torino, June 21-24 2011.
8. D'Alessandro A, Grazzini G, Giardina B, Zolla L. *In silico* analyses of proteomic data suggest a role for heat shock proteins in umbilical cord blood hematopoietic stem cells. 5th annual ItPA congress; Firenze, June 9-12 2010.
9. D'Alessandro A, D'Amici GM, Zolla L. Proteomics investigation of stored red blood cells. XII ISBS; Parma, August 2009
10. Fasoli E, D'Alessandro A, Righetti PG, Zolla L. Proteomics and interactomics of red blood cells: an update. Blood and Proteomics in Viterbo, October 12-14th, 2009

Congress organization:

2013 – XII corso di Spettrometria di Massa – Viterbo – Organizing committee

2012 – VII Italian Proteomics Association (ItPA) congress – Viterbo - Organizing committee

2011 – XI corso di Spettrometria di Massa – Viterbo/Vitorchiano – Organizing committee

2010 – X corso di Spettrometria di Massa – Viterbo/Vitorchiano – Organizing committee

2009 – BPV: Blood and Proteomics in Viterbo – Viterbo – Organizing committee

Education. Part 1**CIB (Italian Consortium of Biotechnologies) mobility program 2012**

Granted	Mass spectrometry-based Metabolomics
Date	May 2012 – May 2013
Granted by	Italian Consortium of Biotechnologies (CIB)
Subject area of study	Metabolomics and Mass Spectrometry

ItPA mobility program 2012

University/college	Bruker Daltonics, Brehmen (Germany)
Period	May 2012
Class	MALDI TOF TOF: PTMs and Biotyper
Date	May 2012
Granted by	Italian Proteomics Association (ItPA)
Subject area of study	Clinical Proteomics and Mass Spectrometry

Bruker specialization training on MALDI TOF and Imaging Applications

University/college	Bruker Daltonics, Brehmen Germany
Period	May 2011
Class	Specialization training on basic MALDI TOF TOF and imaging applications
Date	One week
Organized by	Bruker Daltonics, Brehmen Germany
Subject area of study	Proteomics, Statistics and Bioinformatics

Summer School

University/college	European Proteomics Association (EuPA) – Brixen (Italy)
Period	August 2010
Class	High-throughput data analysis and statistics
Date	1/08/2010 to 7/8/2010
Organized by	Max-Planck-Institute for Biophysical Chemistry
Granted by	Italian Proteomics Association (ItPA)
Subject area of study	Proteomics, Statistics and Bioinformatics

ItPA mobility program 2009

University/college	Proteomics Laboratory – Prof. Urbani Andrea – Rome, Italy
Period	Three months
Class	Applications of MALDI TOF TOF
Date	1/08/2009 to 1/12/2009
Granted by	Italian Proteomics Association (ItPA)
Subject area of study	Proteomics, Statistics and Bioinformatics

Specialization course (Granted)

University/college	University of Tuscia – Viterbo, Italy Italian National Blood Centre (CNS)
From	January 2009
To	January 2010
Class	Proteomics application to transfusion medicine
Date	Officially 1/03/2009 – Actually (1/1/2009)

Name of Advisor	Prof. Zolla Lello
Subject area of study	Blood-related Proteomics

Second degree (Master)

University/college	Università degli Studi della Tuscia – Viterbo, Italy
From	2006
To	2008
Class	Cellular and Molecular Biology
Date	16/07/2008
Degree/Grade	110/110 <i>cum laude</i>
Name of Advisor	Prof. Casini Giovanni
Subject area of study	Molecular and developmental neurophysiology

First degree (Bachelor)

University/college	Università degli Studi della Tuscia – Viterbo, Italy
From	2003
To	2006
Class	Biology
Date	19/07/2006
Degree/Grade	110/110 <i>cum laude</i>
Name of Advisor	Prof. Casini Giovanni
Subject area of study	Neurophysiology

Education Part 2

Working Experience during my studies

Special Issue of Journal of Proteomics: Blood Proteomics – Guest Editor collaborator

Website building: <http://www.unitus.it/bloodprot/imagemenu/index.html>

Receptionist by night – Camping Europing 2000 srl – from April to September 2005;

Receptionist by night – Camping Europing 2000 srl – from April to September 2006;

Receptionist and foreign tourist coordinator– Camping Europing 2000 srl – from April to September 2007;

Interpreter for neuromedical visit/expertise at Stanford, California (USA) for an Italian businessman – February 2007

Summary: Academic workplaces

Proteomics core - Department of Environmental Sciences/Department of Biological and Ecological Sciences, Tuscia University – Viterbo (Italy) (March 2009-2012 - ongoing)

Italian National Blood Centre – Via Giano della Bella, 27 – Rome (Italy) (January 2008 to March 2009)

Laboratory of Medical Analysis – ASL Tarquinia (VT), Italy – Stage – from November 2005 to May 2006

Laboratory of Molecular Biology and Biochemistry – Prof. Caruso, DABAC, Università degli Studi della Tuscia, VT, Italy – from October to December 2008

BEST 2008 – a selection of the 50 BEST Italian Graduates of 2008 – Alma Graduate School of Bologne under the patronage of the Presidency of the Italian Republic

Research Experience

I attended several laboratories during my first and second degree academic career: Laboratory of Immunology, Molecular Biology, Proteomics and Mass Spectrometry (theoretical basis of HPLC-MS, ESI-MS, QTOF, 2-DE, Western blot), Optical Microscopy, Confocal and Electronic Microscopy both TEM and SEM, Biophysics and Nanosciences (AFM, RAMAN, light scattering, spectroscopy), Microbiology, Bioinformatics (Sequence homology, Database query, Molecular modeling and docking). My second-degree experimental thesis was about Neurophysiology ("The somatostatinergic system is directly involved in the regulation of the neovascularization processes in the diseased retina"). I have been working for 1 year (from July 2007 to July 2008) in the Laboratory of Neurobiology of Professor Casini at the University of Tuscia - Viterbo, Italy. We focused our attention on the retina and, in particular, on

the alteration of the vasculogenesis and the neovascularization during the early stages of development in a mouse model of hypoxia-induced retinopathy (Smith et al, 1994) that mimics several pathological conditions (diabetic macular and proliferative retinopathy, ischaemia and hypoxia). In this regard, we tried to determine whether somatostatin, acting on its GPCRs (G-protein coupled receptors) could play an anti-angiogenic role. I practiced numerous techniques, in particular immunofluorescence techniques (single, double, triple staining; whole mount; DAPI, TUNEL) and immunoenzymatic techniques (ABC-immunoperoxidase). I had the opportunity to practice with cryostat, microtome and ultramicrotome. Moreover I experienced several hundreds of hours with fluorescence microscope and confocal microscope whose Professor Casini was the responsible. Image analysis and elaboration, along with the statistical analysis of the obtained data took several hundreds of hours too. Western blot and Semiquantitative RT-PCR were used as proteomic and genomic techniques. In order to widen my practical knowledge I attended the Laboratory of Biochemistry and Molecular Biology of Prof. Caruso at the University of Tuscia - Viterbo, Italy. There I experienced several proteomic approaches, such as electrophoresis (agarose gel, acrilamide gel - SDS, Tris-Tricine) and genetic approaches (PCR, RT-PCR, Colony-PCR). Moreover, I practiced several kinds of extractions (plasmidic DNA, genomic DNA, protein precipitation, total RNA), The leading issue faced in this laboratory during my staying dealt with bioremediation by means of several Pseudomonaceae digesting aromatic compounds and their aromatic and methylated derivatives (phenol, o-xylene, toluene, o-cresol).

During the bachelor's degree, class of Biology, I attended a compulsory stage in an Analytic Laboratory where I had the opportunity to actively work from November 2005 until May 2006 in the Laboratory of Medical Microbiology, Immunology, Urine analysis, urinoculture and urinary sediment analysis, nephelometry, electrophoresis, spectroscopy, emochrome, eritrosedimentation speed and blood typing.

During the last 36 months I helped Prof. Zolla, guest-editor of the prestigious and successful Special Issue of Journal of Proteomics: Blood Proteomics, Redox Proteomics and Proteomics and Integrated Omics. I actively participated in the main phases of the organization of the BPV: Blood and Proteomics in Viterbo congress (October 12-14, 2009) and Italia Proteomics Association annual congress (Viterbo June 12-15, 2012). During the first year and a half, I personally set up metabolomics (RR-RP-HPLC Dionex Ultra 3000, online with MS-ESI-ion trap HCT Bruker; or Dionex Ultra HPLC online with MicroTOFq Bruker) in our laboratory. Eventually, I worked on the automatization of protein identification (either via PMF or LIFT) through MALDI TOF TOF (Autoflex III – Bruker Daltonics). My research activity in Prof. Zolla's laboratory has been focused on the application of OMICS techniques to blood, meat and tumour research (please, refer to the "List of publications" section for further details). Indeed, I had the opportunity to handle and interpret massive amounts of data from either metabolomics, proteomics or microarray analyses, and elaborated them in agreement with approaches from System Biology (Skyrails, Interactorium, Igraph, UniHi, Ingenuity Pathway Analysis from Ingenuity Systems, Cytoscape, Ariadne Pathway Studio Enterprise; String; Gene Ontology FatiGO, AmiGO, Babelomics; Excel; GraphPad; PermutMatrix for statistical analyses).

Honours, scholarships, prizes and awards

Granted by the Italian Proteomics Association (ItPA) a scholarship for the European Summer School of Proteomics 2010 (Brixen, Italy).

Granted by the Italian Proteomics Association (ItPA) a scholarship for the “student mobility” project in the laboratory of Prof. Urbani Andrea, Università di Torvergata, Rome (ITALY).

Granted by the Italian National Blood Centre (CNS – ISS) for the Specialization Course in “Proteomics application to transfusion Medicine”.

Awarded as one of the Best 50 Italian graduates of 2008 by the Alma Graduate School of Bologna under the patronage of the Presidency of the Italian Republic (2008).

Awarded as one of the best 100 Italian Secondary school (Highschool) students by the Scuola Normale Superiore di Pisa (2002-2003); Winner of “David Donatello - Junior section” for critical reviewers of Italian Movies (2003); FILPIK Judo black belt (2000); Youngest sonnetist of the Italian Academy of the Contemporary Sonnet – ORION, First Edition (2005) and Second Edition (2009); Winner of several national poetry awards (Civitavecchia, Rome 2004, 2005, 2006); “Path through the Dark cLOUDS” is my first book of poems (sonnets, ballads, iambic pentameter, metrical studies, chansons provençales, free style) (2004); Correspondent for the daily newspaper “Corriere di Viterbo” during the monthly magazine “Il Secchio Matto” of the Scientific Highschool (2002-2003); Cambridge First Certificate of English (A/A+) (2002); Alliance française A1. A2. A3. A4 (2002);

Outside Interests

Neural networks (Penrose, Kurtzweil, Hofstadter), fractal geometry (Mandelbrot, Peitgen), chaos theory (Buchanan), nanobiology/nanobiotechnology (Goodsell);

Phylosophy (classic period: Socrate, Eraclito, Democrito; Catullo, Lucrezio, Orazio; ‘600-’700 UK: Locke, Hume; ‘800 Germany: Kant, Hegel, Schopenhauer, Nietzsche; Eastern phylosophy: Chuang-Tzu, Lao-Tzu, Osho)

Table of contents

Summary

Chapter 1: Introduction.....3

1.1 Introduction to Red Blood Cell storage: the clinical/biological question about storage quality and compromised safety and efficacy of long-stored erythrocyte concentrates4

1.2 Introduction to the field of “Integrated Omics”: Proteomics, Metabolomics, Lipidomics and Interactomics and their application to Transfusion Medicine and Red Blood cell Biology relevant issues29

References.....55

Chapter 2: *In silico* analyses and protein-protein interactions.....75

2.1 The red blood cell proteome and interactome: an update76

2.2 Native protein complexes in the cytoplasm of Red Blood Cells.....96

References.....125

Chapter 3: Set up of the metabolomics methods.....131

3.1 A robust high resolution reversed-phase HPLC strategy to investigate various metabolic species in different biological models.....132

3.2 Targeted mass spectrometry-based metabolomic profiling through Multiple Reaction Monitoring of Liver and other biological matrices.....148

References.....163

Chapter 4: *In vivo* ageing of red blood cells167

4.1 Red blood cell populations in freshly drawn blood: application of proteomics and metabolomics to a decades-long biological issue.....168

References.....183

Chapter 5: *In vitro* ageing of red blood cells: storage under blood bank conditions.....186

5.1 Time-course Investigation of SAGM-Stored Erythrocyte Concentrates: from Metabolism to Proteomics.....187

5.2 Alterations of Red Blood Cell metabolome during cold liquid storage of erythrocyte concentrates in CPD-SAGM.....205

5.3 Red blood cell storage and cell morphology222

5.4 Red blood cell storage in SAGM and AS3: a comparison through the membrane two-dimensional electrophoresis proteome	232
5.5 Hemoglobin alpha glycation (Hb1Ac) increases during red blood cell storage: a MALDI-TOF mass spectrometry-based investigation	242
5.6 Red Blood Cell Lipidomics analysis through HPLC-ESI-qTOF: application to red blood cell storage.....	247
<i>References</i>	261

Chapter 6: Cryostorage.....272

6.1 Monitoring of red blood cells during processing for cryopreservation: from fresh blood to thaw-washing..	273
<i>References</i>	285

Chapter 7: Alternative storage strategies.....287

7.1 An efficient and cost-effective apparatus for rapid deoxygenation of blood in erythrocyte concentrates for alternative banking strategies	288
7.2 Red blood cell metabolism under prolonged anaerobic storage	300
7.3 Red blood cell storage with vitamin C and N-acetylcysteine prevents oxidative stress-related lesions: a metabolomics overview.....	319
<i>References</i>	334

Chapter 8: Translational applications.....344

8.1 Red blood cell populations and membrane levels of peroxiredoxin 2 as candidate biomarkers to reveal blood doping.....	345
<i>References</i>	353

Chapter 9: Conclusions.....355

9.1 Biochemistry of red cell aging in vivo and storage lesions.....	356
<i>References</i>	374

***Curriculum vitae* of the candidate.....378**
